INTERNATIONAL REVIEW OF CYTOLOGY

A SURVEY OF CELL BIOLOGY

Edited by
Kwang W. Jeon

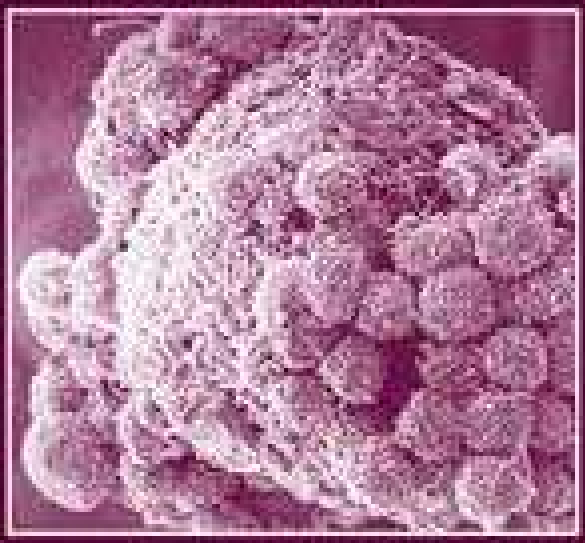

Volume 249

International Review of
Cytology

A Survey of
Cell Biology

VOLUME 249

International Review of Cytology
A Survey of Cell Biology

Edited by

Kwang W. Jeon
Department of Biochemistry
University of Tennessee
Knoxville, Tennessee

VOLUME 249

AMSTERDAM • BOSTON • HEIDELBERG • LONDON
NEW YORK • OXFORD • PARIS • SAN DIEGO
SAN FRANCISCO • SINGAPORE • SYDNEY • TOKYO
Academic Press is an imprint of Elsevier

Front Cover Photograph: Image courtesy of Giuseppe Familiari
University of Rome "La Sapienza"

Academic Press is an imprint of Elsevier
525 B Street, Suite 1900, San Diego, California 92101-4495, USA
84 Theobald's Road, London WC1X 8RR, UK

This book is printed on acid-free paper. ♾

For all information on all Elsevier Academic Press publications
visit our Web site at www.books.elsevier.com

ISBN-13: 978-0-12-364653-8
ISBN-10: 0-12-364653-7

PRINTED IN THE UNITED STATES OF AMERICA
06 07 08 09 9 8 7 6 5 4 3 2 1

CONTENTS

Ultrastructural Dynamics of Human Reproduction, from Ovulation to Fertilization and Early Embryo Development

Giuseppe Familiari, Rosemarie Heyn, Michela Relucenti, Stefania A. Nottola, and A. Henry Sathananthan

Chromosomal Variation in Mammalian Neuronal Cells: Known Facts and Attractive Hypotheses

Ivan Y. Iourov, Svetlana G. Vorsanova, and Yuri B. Yurov

Automated Interpretation of Protein Subcellular Location Patterns

Xiang Chen and Robert F. Murphy

Cell and Molecular Biology of Human Lacrimal Gland and Nasolacrimal Duct Mucins

Friedrich Paulsen

This page intentionally left blank

CONTRIBUTORS

Numbers in parentheses indicate the pages on which the authors' contributions begin.

Xiang Chen (193), *Department of Biological Sciences, Center for Automated Learning and Discovery and Center for Bioimage Informatics, Carnegie Mellon University, Pittsburgh, Pennsylvania 15213*

Maria Teresa Conconi (1), *Department of Pharmaceutical Sciences, School of Pharmacy, University of Padua, I-35121 Padua, Italy*

Giuseppe Familiari (53), *Laboratory of Electron Microscopy, Pietro M. Motta Department of Anatomy, University of Rome, "La Sapienza," 00161, Rome, Italy*

Rosemarie Heyn (53), *Laboratory of Electron Microscopy, Pietro M. Motta Department of Anatomy, University of Rome, "La Sapienza," 00161, Rome, Italy*

Ivan Y. Iourov (143), *National Research Center of Mental Health, Russian Academy of Sciences, Moscow, Russia 119152*

Robert F. Murphy (193), *Department of Biological Sciences, Center for Automated Learning and Discovery and Center for Bioimage Informatics, Carnegie Mellon University, Pittsburgh, Pennsylvania 15213; Department of Biomedical Engineering, Carnegie Mellon University, Pittsburgh, Pennsylvania 15213*

Stefania A. Nottola (53), *Laboratory of Electron Microscopy, Pietro M. Motta Department of Anatomy, University of Rome, "La Sapienza," 00161, Rome, Italy*

Gastone G. Nussdorfer (1), *Department of Human Anatomy and Physiology, School of Medicine, University of Padua, I-35121 Padua, Italy*

Friedrich Paulsen (229), *Department of Anatomy and Cell Biology, Martin Luther University, Halle-Wittenberg, 06097 Halle, Germany*

Michela Relucenti (53), *Laboratory of Electron Microscopy, Pietro M. Motta Department of Anatomy, University of Rome, "La Sapienza," 00161 Rome, Italy*

A. Henry Sathananthan (53), *Monash Institute of Reproduction and Development, Monash University, Melbourne, Australia 3168*

Raffaella Spinazzi (1), *Department of Human Anatomy and Physiology, School of Medicine, University of Padua, I-35121 Padua, Italy*

Svetlana G. Vorsanova (143), *National Research Center of Mental Health, Russian Academy of Sciences, Moscow, Russia 119152; Institute of Pediatrics and Pediatric Surgery, Roszdrav, Moscow, Russia 127412*

Yuri B. Yurov (143), *National Research Center of Mental Health, Russian Academy of Sciences, Moscow, Russia 119152; Institute of Pediatrics and Pediatric Surgery, Roszdrav, Moscow, Russia 127412*

Endogenous Ligands of PACAP/VIP Receptors in the Autocrine–Paracrine Regulation of the Adrenal Gland

Maria Teresa Conconi,* Raffaella Spinazzi,† and Gastone G. Nussdorfer†
*Department of Pharmaceutical Sciences, School of Pharmacy
University of Padua, I-35121 Padua, Italy
†Department of Human Anatomy and Physiology, School of Medicine
University of Padua, I-35121 Padua, Italy

Vasoactive intestinal peptide (VIP) and pituitary adenylate cyclase-activating polypeptide (PACAP) are the main endogenous ligands of a class of G protein-coupled receptors (Rs). Three subtypes of PACAP/VIP Rs have been identified and named PAC_1-Rs, $VPAC_1$-Rs, and $VPAC_2$-Rs. The PAC_1-R almost exclusively binds PACAP, while the other two subtypes bind with about equal efficiency VIP and PACAP. VIP, PACAP, and their receptors are widely distributed in the body tissues, including the adrenal gland. VIP and PACAP are synthesized in adrenomedullary chromaffin cells, and are released in the adrenal cortex and medulla by VIPergic and PACAPergic nerve fibers. PAC_1-Rs are almost exclusively present in the adrenal medulla, while $VPAC_1$-Rs and $VPAC_2$-Rs are expressed in both the adrenal cortex and medulla. Evidence indicates that VIP and PACAP, acting via $VPAC_1$-Rs and $VPAC_2$-Rs coupled to adenylate cyclase (AC)- and phospholipase C (PLC)-dependent cascades, stimulate aldosterone secretion from zona glomerulosa (ZG) cells. There is also proof that they can also enhance aldosterone secretion indirectly, by eliciting the release from medullary chromaffin cells of catecholamines and adrenocorticotropic hormone (ACTH), which in turn may act on the cortical cells in a paracrine manner. The involvement of VIP and PACAP in the regulation of glucocorticoid secretion from inner adrenocortical cells is doubtful and surely of minor relevance. VIP and PACAP stimulate the synthesis and release of adrenomedullary catecholamines, and all three subtypes of PACAP/VIP Rs mediate this effect, PAC_1-Rs being coupled to AC, $VPAC_1$-Rs to both AC and PLC, and $VPAC_2$-Rs only to PLC. A privotal role in the catecholamine secretagogue action of VIP and PACAP is played by Ca^{2+}. VIP and PACAP may

International Review of Cytology, Vol. 249

0074-7696/06 $35.00
DOI: 10.1016/S0074-7696(06)49001-X

also modulate the growth of the adrenal cortex and medulla. The concentrations attained by VIP and PACAP in the blood rule out the possibility that they act as true circulating hormones. Conversely, their adrenal content is consistent with a local autocrine–paracrine mechanism of action.

KEY WORDS: Vasoactive intestinal polypeptide (VIP), Pituitary adenylate cyclase-activating polypeptide (PACAP), PACAP/VIP receptors, Adrenal gland, Aldosterone secretion, Catecholamine secretion.

I. Introduction

The endogenous ligands of PACAP/VIP receptors (Rs) are two regulatory peptides, widely distributed in the body and exerting pleiotropic actions, named vasoactive intestinal polypeptide (VIP) and pituitary adenylate cyclase-activating polypeptide (PACAP). VIP and PACAP are members of a superfamily of structurally related peptides that includes secretin, glucagon, glucagon-like peptides, growth hormone-releasing hormone, gastric inhibitory peptide, parathyroid hormone, and exendins (Nussdorfer and Malendowicz, 1998b; Nussdorfer *et al.*, 2000; Sherwood *et al.*, 2000).

Many review articles have been published on the involvement of VIP and PACAP in the regulation of neuroendocrine functions and adrenal secretion (Arimura, 1998, 2003; Arimura and Shioda, 1995; Delarue *et al.*, 2001; Gonzalez *et al.*, 1998; Nussdorfer, 1996, 2003; Nussdorfer and Malendowicz, 1998b; Sherwood *et al.*, 2000; Toth and Hinson, 1995; Vaudry *et al.*, 2000; Vinson *et al.*, 1994), but none of them specifically dealt with the role played by these peptides in the autocrine–paracrine control of the adrenal gland as a functional unit. In fact, in the mammalian adrenal gland the intimate morphological interrelationships between cortex and medulla allow multiple and relevant reciprocal paracrine interactions (Nussdorfer, 1996), among which are the induction and stimulation of the enzymes involved in epinephrine (E) synthesis by corticosteroid hormones (Cryer, 1992) and the stimulation of steroid hormone secretion from cortical cells by catecholamines (Bornstein *et al.*, 1997).

After a concise description of the general biological characteristics of VIP, PACAP, and their Rs, we survey findings indicating that these regulatory peptides and PACAP/VIP Rs are expressed in the adrenal gland, and VIP and PACAP control secretion and growth of the adrenal cortex and medulla. The Rs and signaling mechanisms involved in the actions of VIP and PACAP are reviewed, and a brief account is provided of the possible role played by the VIP/PACAP system in the functional regulation of tissues that, like the adrenal cortex, are able to secrete steroid hormones, i.e., endocrine gonads.

Finally, the relevance of the endogenous VIP and PACAP in adrenal regulation under physiological and pathological conditions will be discussed.

II. Biology of PACAP/VIP Receptors and Their Endogenous Ligands

A. VIP, PACAP, and Related Peptides

VIP is a highly basic 28-amino acid peptide, originally isolated from the gastrointestinal tract (Said and Mutt, 1970), that derives, along with peptide histidine–methionine (PHM), from the posttranslational proteolytic cleavage of the 170-amino acid prepro (pp) VIP (Fig. 1). Human ppVIP is encoded from a single copy gene, located on chromosome 6q26–q27 (Gotoh *et al.*, 1988), consisting of seven exons: exon 4 codes for PHM and exon 5 for VIP (Tsukada *et al.*, 1985). The primary sequence of VIP is identical in most mammals (humans, cow, pig, goat, dog, and rat); the only exception is the guinea pig, in which VIP displays four substitutions in the 5, 9, 19, and 26 positions (Fig. 2). Human PHM differs from its rat counterpart by four substitutions in the 10, 12, 17, and 27 positions; the C-terminal 27 methionine is replaced by isoleucine, and therefore PHM in rats is named peptide histidine–isoleucine (PHI) (Fig. 2).

PACAP is a basic 38-amino acid C-terminally α-amidated peptide, originally isolated from the ovine hypothalamus (Miyata *et al.*, 1989), which derives, along with PACAP-related peptide (PRP), from the cleavage of the 176-amino acid ppPACAP (Fig. 1). Human ppPACAP is encoded by a single gene, located on chromosome 18p11 (Hosoya *et al.*, 1992), composed of five exons; exon 4 codes for PRP and exon 5 for PACAP. Exon 5 codes both for PACAP38 and its alternative form possessing the N-terminal 27-amino acid sequence of PACAP38, indicating that PACAP38 and PACAP27 are not encoded by mRNA generated by alternative splicing (Arimura, 2003). The primary sequence of PACAP is identical in humans and other mammals, and displays elevated homology with that of VIP (Miyata *et al.*, 1990). Human and rat PRP sequences differ by four substitutions in the 5, 21, 23, and 27 positions (Fig. 2).

B. PACAP/VIP Receptors

PACAP/VIP-Rs are glycoproteins with a large hydrophilic extracellular domain followed by seven highly conserved hydrophobic transmembrane helices. Three subtypes of Rs have been identified, and according to the

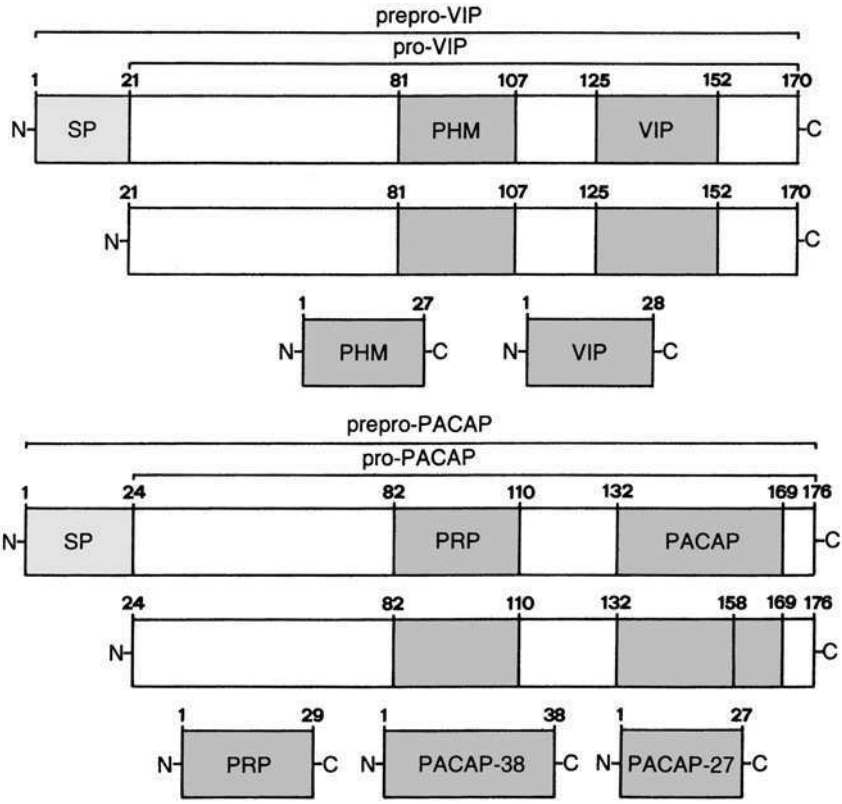

FIG. 1 Scheme illustrating the posttranslational processing of ppVIP and ppPACAP. SP, signal peptide.

International Union of Pharmacology they are named PAC_1-R, $VPAC_1$-R, and $VPAC_2$-R (Harmar *et al.*, 1998). For convenience, we indicate an alternative nomenclature that is sometimes still used: (1) PAC_1-R, PVR_1, PACAP type I-R, or PACAP-R; (2) $VPAC_1$-R, PVR_2, PACAP type II-R, VIP/PACAP type II-R, or classic VIP-R; and (3) $VPAC_2$-R, PVR_3, VIP_2-R, or PACAP-3-R. The three R subtypes have been cloned. The human PAC_1-R gene is located on chromosome 7p15 (Brabet *et al.*, 1996), the $VPAC_1$-R gene on chromosome 3p22 (Sreedharan *et al.*, 1995), and the $VPAC_2$-R gene on chromosome 7q36.3 (Mackay *et al.*, 1996). They display a high degree of homology among the various vertebrate species (Nussdorfer and Malendowicz, 1998b). The binding potency of human PACAP/VIP-Rs for their endogenous ligands is as follows: (1) PAC_1-R, PACAP38 = PACAP27 >> VIP = PHM; (2) $VPAC_1$-R, VIP = PACAP27 $\geq$ PACAP38

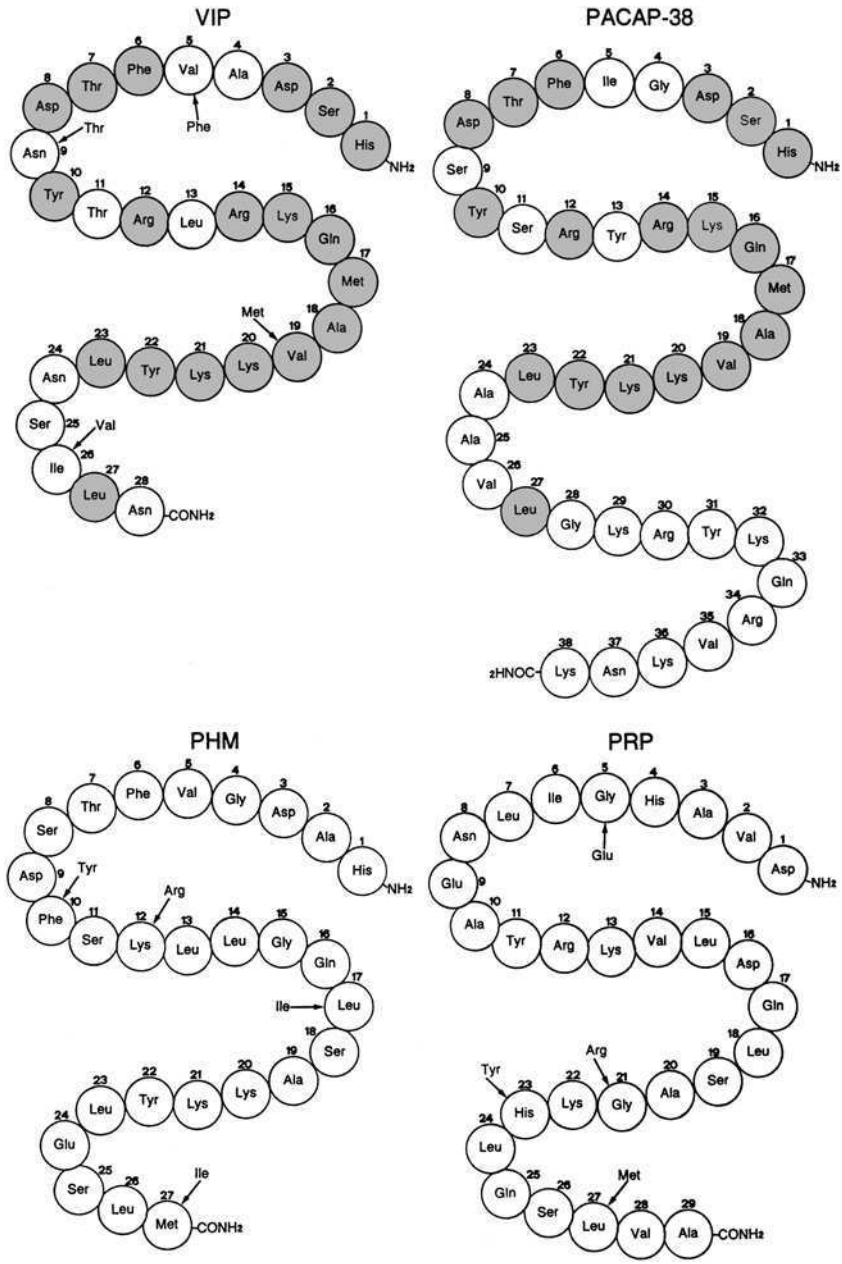

FIG. 2 Amino acid sequence of human PACAP/VIP-R endogenous ligands. Human VIP, PHM, and PRP differ from rat peptides for four amino acid substitutions, which are indicated by arrows. Identical amino acids between VIP and PACAP are shadowed.

>> PHM; and (3) $VPAC_2$-R, VIP = PHM = PACAP27 = PACAP38 (Harmar *et al.*, 1998). Two subtypes of PAC_1-Rs have been identified: subtype A has about equal affinity for PACAP38 and PACAP27, whereas subtype B possesses about 100 times more affinity for PACAP38 than PACAP27 (Van Rampelbergh, 1996). Selective antagonists of PAC_1-R and $VPAC_1$-R are PACAP(6–38) and [Ac-His[1], D-Phe[2], Lys[15], Arg[16]]VIP(3–7) GRF(8–27)-NH_2, respectively. No selective antagonists of the $VPAC_2$-R are available, but two agonists have been identified (Ro 25–1553 and Ro 25–1392). However, PACAP(6–38) has a significant affinity for $VPAC_2$-Rs (Harmar *et al.*, 1998; Robberecht *et al.*, 2003). PACAP/VIP-Rs are G protein-coupled Rs: the PAC_1-R and $VPAC_1$-R activate both adenylate cyclase (AC) and phospholipase-C (PLC)-dependent cascades, whereas the $VPAC_2$-R seems to activate PLC almost exclusively (Shioda *et al.*, 2003). The main pathways involved in PACAP/VIP-R signaling are depicted in Fig. 3.

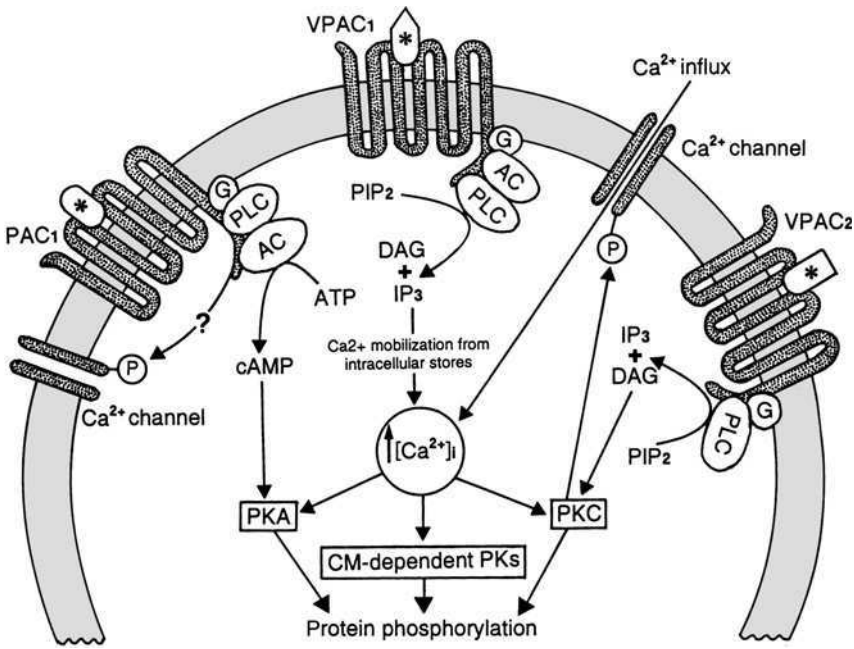

FIG. 3 Schematic drawing of the main signaling pathways of PACAP/VIP Rs upon activation by their endogenous ligands. ATP, adenosine 5′-triphosphate; CM, calmodulin; DAG, diacylglycerol; G, G protein; P, phosphorylation site; PIP_2, phosphatidylinositol biphosphate. Other abbreviations are indicated in the text. Asterisks mark the VIP- and PACAP-recognizing sites of PACAP/VIP Rs.

III. Expression of PACAP/VIP Receptors and Their Endogenous Ligands in the Adrenal Gland

A. Biosynthesis and Localization of the Endogenous Ligands of PACAP/VIP Receptors

1. VIP and Related Peptides

Reverse transcription (RT)-polymerase chain reaction (PCR) detected VIP mRNA in the human adrenal medulla (Mazzocchi *et al.*, 2002b), cultured bovine adrenomedullary cells (Lee *et al.*, 1999a), and newborn rat adrenals (Bodnar *et al.*, 1997), as well as in human pheochromocytomas (Isobe *et al.*, 2003) and rat PC12 pheochromocytoma cells (Tsukada *et al.*, 1995). PHM/VIP mRNA has also been demonstrated by *in situ* hybridization (ISH) in human pheochromocytomas (Fahrenkrug *et al.*, 1995) and a few neuroblastomas (Isobe *et al.*, 2004). VIP mRNA expression has been reported to be up-regulated by VIP in PC12 cells, via a cyclic adenosine 3′,5′-monophosphate (cAMP)-dependent mechanism (Tsukada *et al.*, 1995), and PACAP27 in cultured bovine adrenomedullary cells, via the activation of both Ca^{2+} channels and calcineurin (Lee *et al.*, 1999a).

Radioimmunoassay (RIA) demonstrated a sizable VIP content in the human adrenal medulla (about 80 fmol/mg protein) (Mazzocchi *et al.*, 2002b), and abundant VIP immunoreactivity (ir), and PHM-ir in human pheochromocytomas (Said, 1976; Sasaki *et al.*, 1990; Yiangou *et al.*, 1987), and especially those associated with neurofibromatosis type 1 (Quarles Van Ufford-Mannesse *et al.*, 1999) and multiple endocrine neoplasia (Moreno *et al.*, 1999). In the pig, the adrenal VIP-ir content was about 9 pmol/g (Ehrhart-Bornstein *et al.*, 1991), and in the sheep, it rose from day 80 to day 110–130 of gestation and fell at day 140 immediately prior to term (Cheung, 1988; Cheung and Holzwarth, 1986). An elevated VIP-ir content was shown in the rat adrenals (Cauvin *et al.*, 1989; Hinson and Kapas, 1996; Hinson *et al.*, 1996), where the VIP concentration ranged from 4 to 28 pmol/g (Tsuchiya *et al.*, 1990; Wakade *et al.*, 1991) and appeared to be regulated by the histaminergic system (Tsuchiya *et al.*, 1990). In rats, splanchnic-nerve section was found to decrease VIP-ir content in the inner adrenocortical zone and adrenal medulla (about 70%), but not in the zona glomerulosa (ZG); unilateral adrenalectomy did not alter VIP-ir content in the contralateral gland (Hinson and Kapas, 1996; Hinson *et al.*, 1996). Of interest, low-sodium and high-sodium diets have been reported to increase and to decrease, respectively, VIP-ir concentrations in rat capsular ZG, but not the adrenal medulla (Hinson *et al.*, 2001). This suggests that VIP biosynthesis is up-regulated and down-regulated in stimulated and inhibited ZG cells, respectively.

Immunocytochemistry (ICC) evidenced the prevalence of VIP-ir in the adrenal medulla. VIP-positive cells are mainly voluminous ganglion neurons, which originate in fibers reaching the cortex and a few catecholamine-storing cells. These latter cells are frequently grouped in small islets intermingled with cortical cells, so that they can release VIP in close proximity to steroid-secreting cells. VIPergic nerve fibers can be traced in the capsule-ZG and adrenal medulla, as well as in the juxtamedullary inner cortex. There is evidence that in mammals VIP-positive fibers reaching the outer cortex originate from the splanchnic nerve (extrinsic), whereas those ending in the inner cortex and medulla largely originate from VIP-positive medullary ganglion cells. This pattern of VIP-ir distribution seems to apply to the adrenal glands of humans (Bryant *et al.*, 1976; Hakanson *et al.*, 1982; Heym, 1997; Li *et al.*, 1999; Linnoila *et al.*, 1980), monkeys (Berghorn *et al.*, 2000), cows (Yoshikawa *et al.*, 1990), pigs (Ehrhart-Bornstein *et al.*, 1991; Kong *et al.*, 1989), sheep fetuses (Berghorn *et al.*, 2000; Cheung and Holzwarth, 1986), and rats (Hakanson *et al.*, 1982; Hokfelt *et al.*, 1981; Holzwarth, 1984; Kondo, 1985; Kondo *et al.*, 1986; Maubert *et al.*, 1990; Oomori *et al.*, 1994; Wakade *et al.*, 1991; Yoshikawa *et al.*, 1990). ICC showed abundant VIP-ir and PHI-ir in human pheochromocytoma cells (Hacker *et al.*, 1988; Hassoun *et al.*, 1984; Viale *et al.*, 1985), and VIP-positive nerve fibers in human adrenal hyperplasias, adenomas, and carcinomas (Li *et al.*, 1999). VIP-ir was also detected in chromaffin cells of frog (De Falco *et al.*, 2002; Leboulenger *et al.*, 1983a,b) and lizard adrenals (De Falco *et al.*, 2003), and VIPergic nerve fibers were detected in the interrenals of teleosts (Reid *et al.*, 1995) and lizards (De Falco *et al.*, 2003).

A sizable VIP-ir release from perfused adrenals has been reported in dogs (Gaspo *et al.*, 1995), cows (Bloom *et al.*, 1988; Yoshikawa *et al.*, 1990), pigs (Ehrhart-Bornstein *et al.*, 1991), and rats (Wakade *et al.*, 1991), and there is general agreement that it dramatically increases upon splanchnic nerve stimulation. This accords well with the fact that the majority of VIPergic fibers originate from the splanchnic nerve, and with the observed lowering of adrenal VIP-ir content after bilateral splanchnotomy.

It has been suggested that during the early phases of postnatal maturation, rat adrenocortical cells are able to produce VIP (Bodnar *et al.*, 1997). Capsular-ZG VIP staining was most abundant from day 2 to day 18, whereas adrenomedullary staining was appreciable only at day 18. VIP-ir was also observed in the cells of the cortex at all stages of maturation, the staining intensity shifting from the outer to the inner cortex. By day 8, VIP-positive nerve fibers were observed not only in the capsular region, but also in the entire cortex. The possible involvement of VIP in the maturation of fetal sheep adrenals has also been suggested (Berghorn *et al.*, 2000).

2. PACAP and Related Peptides

RT-PCR showed the expression of PACAP mRNA in the human adrenal medulla (Mazzocchi *et al.*, 2002b) and human pheochromocytomas, where real-time PCR demonstrated a positive correlation between PACAP mRNA and tyrosine hydroxylase (TH)/phenylethanolamine *N*-methyltransferase (PNMT) expression (Isobe *et al.*, 2003). PACAP mRNA has also been detected in the rat adrenal medulla (Ghatei *et al.*, 1993; Mazzocchi *et al.*, 2002a) and rat pheochromocytoma PC12 cells (Sakai *et al.*, 2001, 2004). Evidence has been provided that PACAP up-regulates its own expression in rat adrenomedullary cells, via a mechanism involving the activation of AC- and PLC-dependent cascades and an increase in the intracellular Ca^{2+} concentration ($[Ca^{2+}]_i$) (MacArthur and Eiden, 1996). Likewise, in the presence of nerve growth factor (NGF), PACAP38 has been shown to enhance PACAP mRNA in PC12 cells, through the activation of a p38 mitogen-activated protein kinase (MAPK) cascade (Sakai *et al.*, 2004).

The presence of PACAP-ir has been demonstrated by RIA in the mammalian adrenal medulla (Arimura *et al.*, 1991; Tabarin *et al.*, 1994; Watanabe *et al.*, 1992), but its concentration varied greatly among species and among different assays. In the human adult and fetal adrenals the concentrations were 4 and 20 pmol/g, respectively (Breault *et al.*, 2000; Takahashi *et al.*, 1993), in the human adult adrenal medulla the concentration was 110 fmol/mg protein (Mazzocchi *et al.*, 2002b), and in human pheochromocytomas a concentration of 25 pmol/g was measured (Takahashi *et al.*, 1993). In the pig adrenal medulla the estimated concentration of PACAP38 was 14 pmol/g (Tornøe *et al.*, 2000) and in the rat 24 pmol/g or 9 fmol/mg protein (Frodin *et al.*, 1995; Ginda *et al.*, 1999; Mazzocchi *et al.*, 2002a). According to Tabarin *et al.* (1994), PACAP27 concentrations were 0.7–0.8 pmol/g in cows and pigs, 2 pmol/g in rats, 9 pmol/g in hamsters, and 12 pmol/g in mice. It must be noted that in mammalian adrenals the concentration of PACAP38 is always higher than that of PACAP27 (Arimura *et al.*, 1991). PACAP38 is also the predominant peptide in frog interrenals (about 0.15 pmol/mg protein) (Yon *et al.*, 1994a,b).

ICC showed the presence of PACAP38-ir and PACAP27-ir in the norepinephrine (NE)-storing cells of the cow, pig, hamster, and rat adrenal medulla (Shiotani *et al.*, 1995; Tabarin *et al.*, 1994). Likewise, in VIP-secreting human pheochromocytomas PACAP38-ir, PACAP27-ir, and PRP-ir have been demonstrated, and double-staining experiments revealed the coexistence of PHM/VIP mRNA and PACAP-ir in the same tumor cells (Fahrenkrug *et al.*, 1995). PACAP38-ir has also been detected in a few E-storing cells of the rat adrenal medulla (Holgert *et al.*, 1996), although other studies were unable to find PACAP-positive cells in rat and guinea pig adrenal medulla (Inoue *et al.*,

2000; Moller and Sundler, 1996). A dense network of PACAP-positive nerve fibers, mainly of splanchnic nerve origin, has been observed to transverse the cortex and to end in close apposition to chromaffin cells in the adrenal of pigs (Tornøe *et al.*, 2000), guinea pigs (Inoue *et al.*, 2000), and rats (Dun *et al.*, 1996; Frodin *et al.*, 1995; Hamelink *et al.*, 2002; Holgert *et al.*, 1996; Moller and Sundler, 1996; Shiotani *et al.*, 1995). In the calf adrenals, the administration of capsaicin was found to markedly reduce the number of PACAP-positive fibers, thereby suggesting that they are primarily sensory in origin (Edwards and Jones, 1993b). Few sensory PACAPergic fibers have been observed to end in the subcapsular region of rat adrenals (Holgert *et al.*, 1996). In the frog interrenals, two types of PACAP-positive fibers have been traced: thick varicose fibers running between adrenal cells and thin fibers ending on the blood vessel walls (Yon *et al.*, 1993a,b, 1994a,b).

Consistent with the view that several PACAP-positive nerve fibers have a splanchnic nerve origin, bilateral splanchnotomy was found to lower the PACAP38 content in the rat adrenal medulla by about 50% (Ginda *et al.*, 1999). Moreover, evidence indicates that PACAP38 is released from perfused dog (Lamouche and Yamaguchi, 2003), pig (Tornøe *et al.*, 2000), and rat adrenals following splanchnic nerve stimulation (Przywara *et al.*, 1996; Wakade, 1998).

B. Expression of PACAP/VIP Receptors

The existence of VIP-binding sites was demonstrated about 25 years ago in the mouse Y-1 cell line (Birnbaum *et al.*, 1980; Morera *et al.*, 1979). Subsequently, high-affinity ^{125}I-labeled VIP-binding sites have been identified by autoradiography in the rat adrenals, and especially in the ZG (Cunnigham and Holzwarth, 1989; Magistretti *et al.*, 1988). In the rat capsule ZG preparations saturation and inhibition binding experiments showed the presence of a single class of VIP-binding sites with an apparent dissociation constant (K_d) of 2–3 pM and a maximal binding capacity (B_{max}) of about 850 fmol/mg protein (Hinson *et al.*, 1999). ^{125}I-labeled VIP binding has also been detected in the membranes of the bovine adrenal cortex, where it was displaced by both cold VIP and adrenocorticotropic hormone (ACTH) (Li *et al.*, 1990). This finding is in contrast to the reported ineffectiveness of ACTH in displacing VIP binding in the rat capsule ZG (Hinson *et al.*, 1999). Studies carried out in newborn rat adrenals showed that VIP-binding sites were more abundant in the cortex than in the medulla, their density being maximum between day 8 and day 12, i.e., at a time coinciding with the onset of functional splanchnic innervation of the medulla (Bodnar *et al.*, 1997). ^{125}I-labeled PACAP-binding sites were found in the rat adrenal medulla, and to a lesser extent in the cortex (Moller and Sundler, 1996; Watanabe *et al.*, 1992).

1. PAC_1 Receptors

The bulk of evidence clearly shows that PAC_1-Rs are almost exclusively present in adrenal medulla. RT-PCR and ISH detected PAC_1-R mRNA expression only in the medullary chromaffin cells of human adult and fetal (Mazzocchi *et al.*, 2002b; Payet *et al.*, 2003; Yon *et al.*, 1998), bovine (Bodart *et al.*, 1997; Spengler *et al.*, 1993; Tanaka *et al.*, 1998), and rat adrenals (Hashimoto *et al.*, 1993; Mazzocchi *et al.*, 2002a; Moller and Sundler, 1996; Muroi *et al.*, 1999; Nogi *et al.*, 1997; Shioda *et al.*, 2000; Shivers *et al.*, 1991; Spengler *et al.*, 1993; Watanabe *et al.*, 1992). This contention has been confirmed in the guinea pig (Inoue *et al.*, 2000) and mouse adrenal medulla (Harmar *et al.*, 2004), as well as in chromaffin cells of the frog interrenals (Alexandre *et al.*, 2002; Yon *et al.*, 1994a). PAC_1-R mRNA has also been found in human pheochromocytomas (Isobe *et al.*, 2003) and some neuroblastomas (Isobe *et al.*, 2004), as well as in the rat pheochromocytoma PC12 cell line (Onoue *et al.*, 2002).

2. $VPAC_1$ and $VPAC_2$ Receptors

RT-PCR studies indicated that $VPAC_1$-R and $VPAC_2$-R mRNAs are expressed in both adrenal cortex and medulla of adult humans (Mazzocchi *et al.*, 2002b; Payet *et al.*, 2003) and rats (Mazzocchi *et al.*, 2002a). Coupled molecular biology and autoradiographic findings showed that these Rs are mainly expressed in the ZG (Mazzocchi *et al.*, 2002a,b). The expression of both $VPAC_1$-Rs and $VPAC_2$-Rs has also been detected in the human carcinoma-derived cell line H-295 (Bodart *et al.*, 1997; Haidan *et al.*, 1998; Nicol *et al.*, 2004). $VPAC_1$-R mRNA was present in cultured guinea pig zona fasciculata (ZF) cells (Fang *et al.*, 2001), and in the chromaffin cells of the posterior cardinal vein of teleosts (Montpetit and Perry, 2000; Montpetit *et al.*, 2003), as well as, along with less abundant $VPAC_2$-R expression, in human pheochromocytomas (Isobe *et al.*, 2003) and neuroblastomas (Isobe *et al.*, 2004).

IV. Effects of Endogenous Ligands of PACAP/VIP Receptors on Adrenal Cortex Secretion

A. Zona Glomerulosa and Aldosterone Secretion

1. VIP

a.* In Vivo *Studies The *bolus* intraperitoneal (ip) administration of VIP was found to raise aldosterone plasma concentration in rats, whose hypothalamic–pituitary–adrenal axis and renin–angiotensin system had been

pharmacologically interrupted (Nussdorfer and Mazzocchi, 1987). Likewise, VIP has been shown to exert an acute aldosterone secretagogue action on 9- and 12-day-old rats, which was only partially prevented by corticotropin-releasing hormone (CRH) immunoneutralization (Bodnar *et al.*, 1997). In contrast, in short-term (24 h) dexamethasone-suppressed rats, VIP did not raise the level of circulating aldosterone, whereas a *bolus* subcutaneous (sc) injection of a VIP-receptor antagonist (VIP-A) lowered it (Nowak *et al.*, 1994). The prolonged (7-day) ip infusion of VIP evoked a marked increase in the blood level of aldosterone in both normal or bilaterally adrenalectomized rats bearing adrenocortical autotransplants (Mazzocchi *et al.*, 1987; Rebuffat *et al.*, 1994). The simultaneous infusion of VIP-A annulled the effect of VIP, and the administration of VIP-A alone resulted in a significant decrease in plasma aldosterone concentration in sham-operated but not autotransplanted animals (Rebuffat *et al.*, 1994). VIP was also found to acutely increase aldosterone release from *in situ* perfused adrenals of rats (Hinson *et al.*, 1992, 1996) and pigs (Ehrhart-Bornstein *et al.*, 1991). Collectively, *in vivo* studies suggest that VIP possesses an acute direct adrenoglomerulotropic action, that, however, requires a normal level of circulating ACTH to become manifest, and that endogenous VIP exerts a tonic stimulating action on the secretory activity of ZG.

b.* In Vitro *Studies

i. Dispersed ZG Cells Earlier studies were unable to find any effect of VIP on basal aldosterone secretion from freshly dispersed rat ZG cells over a concentration range from 10^{-11} to 10^{-5} *M* (Enyedi *et al.*, 1983; Hinson *et al.*, 1992). Subsequent investigations, however, reported a clear stimulating effect of VIP (from 10^{-8} to 10^{-6} *M*) (Hinson and Kapas, 1995; Mazzocchi *et al.*, 1994c; Nowak *et al.*, 1999). The VIP effect was much more potent when ZG cells were obtained from rats maintained on a low-sodium diet, suggesting that sodium depletion up-regulates the expression of VIP Rs (Hinson and Kapas, 1995). VIP (10^{-8} and 10^{-7} *M*) has been shown to enhance aldosterone production from dispersed human ZG cells (Mazzocchi *et al.*, 2002b). The response was decreased by a $VPAC_1$-R antagonist, but not only by a PAC_1-R antagonist, suggesting that it is mediated by the $VPAC_1$-R and $VPAC_2$-R of which ZG cells are provided (see Section III.B). VIP has also been reported to enhance aldosterone secretion from dispersed Conn's adenoma cells (Glaz *et al.*, 1988).

ii. Capsule ZG and Adrenal Slices There is a general consensus that these preparations obtained from rat adrenals exhibit a sizable aldosterone response to VIP, the minimal effective concentration of VIP ranging from 10^{-10} to 10^{-5} *M* (Bernet *et al.*, 1994; Cunningham and Holzwarth, 1988; Hinson *et al.*, 1992, 1996, 1999; Mazzocchi *et al.*, 1993a). It was also shown that this response to VIP was blunted by antagonists of β-adrenoceptors,

thereby making it likely that it may be partly mediated by VIP-induced catecholamine secretion from chromaffin cells (see Section IV.D.2). The aldosterone response to VIP is enhanced in capsule ZG preparations from rats maintained on a low-sodium diet (Hinson *et al.*, 1999): of interest, in this case the response was not hampered by β-adrenoceptor antagonists, confirming that sodium depletion up-regulates the expression of VIP Rs (see above).

iii. In Vitro *Cultures* VIP did not exert any effect on aldosterone production from primary culture of bovine ZG cells (Bodart *et al.*, 1997), but it did elicit a marked response from human adrenocortical cell cultures (Bornstein *et al.*, 1996). A significant aldosterone secretagogue effect of VIP (from 10^{-9} to 10^{-6} *M*) has also been shown in the human H295 cell line (Bodart *et al.*, 1997; Haidan *et al.*, 1998).

2. PACAP

Only *in vitro* studies on the effect of PACAP on ZG secretion are available.

a. Dispersed ZG Cells Earlier studies did not report any effect of PACAP38 (from 10^{-14} to 10^{-4} *M*) on aldosterone secretion from dispersed rat and human adrenocortical cells (Andreis *et al.*, 1995; Neri *et al.*, 1996). However, subsequent investigations clearly showed that PACAP38 (from 10^{-9} to 10^{-7} *M*) exerted a sizable aldosterone secretagogue effect (Mazzocchi *et al.*, 2002a,b). In both species, $VPAC_1$-R, but not PAC_1-R, antagonists blunted the aldosterone response, and in the rat a $VPAC_2$-R agonist mimicked the PACAP effect, suggesting that the aldosterone secretagogue effect of PACAP, as that of VIP (see above), is mediated by both $VPAC_1$-Rs and $VPAC_2$-Rs.

b. Adrenal Quarters PACAP38 concentration dependently raised aldosterone secretion from adrenal quarters containing medullary chromaffin tissue, the minimal and maximal concentrations being 10^{-12} *M* (34% increase) and 10^{-8} *M* (3.7-fold increase) (Andreis *et al.*, 1995; Neri *et al.*, 1996). Quarters of regenerated rat adrenocortical autotransplants that are deprived of chromaffin cells were insensitive to PACAP38 (Andreis *et al.*, 1995). As discussed for VIP, collectively these findings suggest that the aldosterone secretagogue effect of PACAP is, at least partly, mediated by medullary chromaffin cells (see Section IV.D.2).

c.* In Vitro *Cultures Both PACAP38 and PACAP27 were found to enhance cAMP production and aldosterone secretion from cultured bovine ZG cells in a concentration-dependent manner, as well as from the H295 cell line (Bodart *et al.*, 1997). It was suggested that H295 cells are provided with both

PAC_1-Rs and $VPAC_1$-Rs, and bovine ZG cells only with PAC_1-Rs (Bodart *et al.*, 1997).

B. Zonae Fasciculata-Reticularis and Glucocorticoid Secretion

1. VIP and Related Peptides

a.* In Vivo *Studies The bulk of *in vivo* studies indicated that the systemic administration of VIP, either acute or prolonged, was unable to change the plasma corticosterone concentration in adult rats (Bodart *et al.*, 1997; Itoh and Hirota, 1983; Itoh *et al.*, 1982; Mazzocchi *et al.*, 1987; Nowak *et al.*, 1994; Nussdorfer and Mazzocchi, 1987; Rebuffat *et al.*, 1994). In contrast, the sc administration of VIP for 7 or 14 days was found to cause a marked decrease in the level of circulating corticosterone in female rats (Malendowicz and Nussdorfer, 1993). Likewise, VIP and PHM did not alter the basal cortisol plasma concentration in healthy human volunteers (Ambrosi *et al.*, 1987; Ottesen *et al.*, 1986; Sasaki *et al.*, 1987). However, they elicited a significant increase in blood cortisol in patients with Cushing's disease, which was probably due to the hyperresponsiveness of adenomatous pituitary corticotrophs to VIP (Ambrosi *et al.*, 1987; Watanabe and Tamura, 1994). The intracerebroventricular administration of VIP and PHI via a hypothalamic cannula was found to markedly increase the blood corticosterone level in freely moving male rats, which can be ascribed to the stimulating effect of the peptides on the hypothalamic–pituitary CRH/ACTH system (Alexander and Sander, 1994, 1995a,b; Alexander *et al.*, 1994). Hence, the discrepancies in the results of *in vivo* experiments could conceivably be ascribed to the difficulty of systemically administered VIP and related peptides to reach effective concentrations in the hypothalamic–pituitary complex.

However, some *in vivo* investigations suggest a direct adrenal effect of VIP. VIP was found to enhance the plasma concentration of cortisol in conscious hypophysectomized ACTH-replaced calves (Bloom *et al.*, 1987; Edwards and Jones, 1993a), and dexamethasone-administered ACTH-replaced palm squirrels (Firoz-Ahmad *et al.*, 2000). VIP raised the blood level of corticosterone in 9- to 12-day-old rats, and the effect was not completely prevented by ACTH immunoneutralization (Bodnar *et al.*, 1997). By means of *in situ* perfusion of isolated adrenals, a marked glucocorticoid response to VIP was observed in rats (Hinson *et al.*, 1992, 1994b, 1996) and pigs (Ehrhart-Bornstein *et al.*, 1991). Bornstein *et al.* (1992) also demonstrated that 10^{-8} *M* VIP elicited a 3-fold rise in androstenedione output, a response comparable to that of ACTH (10^{-10} *M*).

b.* In Vitro *Studies

i. Dispersed Cells VIP (10^{-8} *M*) was found to elicit a moderate stimulation of basal corticosterone production from dispersed rat zona fasciculata-reticularis (ZF/R) cells (Mazzocchi *et al.*, 1994c; Nowak *et al.*, 1999). Submaximally, ACTH (10^{-10} *M*)-stimulated corticosterone output was also enhanced, and the responses to VIP were blocked by both VIP-A and the ACTH-receptor antagonist corticotropin-inhibiting peptide (CIP) (Mazzocchi *et al.*, 1994c). A weak but significant stimulating effect of VIP on dispersed bovine inner ZF/R cells has been reported, the minimal and maximal effective concentrations being 10^{-10} and 10^{-8} *M* (Li *et al.*, 1990). Maximal cortisol production in response to VIP was only about half that to ACTH. VIP and ACTH exerted additive effects when added at a concentration of 10^{-10} *M*, but not at their maximal effective concentration of 10^{-8} *M*, thereby suggesting that the two peptides interact with a common R. However, more recent studies failed to show any sizable effect of VIP on dispersed human ZF/R cells (Mazzocchi *et al.*, 2002b).

ii. Adrenal Quarters A corticosterone response to 10^{-10} and 10^{-8} *M* VIP of rat adrenal slice preparations was demonstrated (Mazzocchi *et al.*, 1993a), but adrenal quarters obtained from rats treated for 1 or 2 weeks with daily sc injections of VIP secreted less corticosterone than the control ones (Malendowicz and Nussdorfer, 1993).

iii. In Vitro *Cultures* In the presence of VIP, cultures of rat ZF/R cells displayed a sustained high level of voltage-dependent T-type current, which is known to be associated with increased cell excitability and steroid secretion (Barbara and Takeda, 1995). VIP increased cAMP and steroid production from the Y-1 murine cell line (Birnbaum *et al.*, 1980; Kowal *et al.*, 1977; Morera *et al.*, 1979) and cortisol release from cultured guinea pig ZF/R cells, the effect being counteracted by a $VPAC_1$-R antagonist (Fang *et al.*, 2001). VIP stimulated the secretion of cortisol, testosterone, androstenedione, and dehydroisoandrosterone from primary cultures of human adrenocortical cells (Bornstein *et al.*, 1996). Likewise, VIP (from 10^{-10} to 10^{-6} *M*) was found to increase basal cortisol, dehydroepiandrosterone (DHEA), and cAMP release, and ACTH-stimulated cortisol secretion from the human H-295 cell line (Cobb *et al.*, 1997; Haidan *et al.*, 1998; Nicol *et al.*, 2004). A $VPAC_1$-R agonist mimicked and a $VPAC_1$-R antagonist abrogated cortisol and cAMP responses to VIP, whereas a $VPAC_2$-R agonist was ineffective (Nicol *et al.*, 2004), thereby indicating the involvement of $VPAC_1$-R of which H-295 cells are provided (see Section III.B).

2. PACAP

a.* In Vivo *Studies The intraaortic infusion of PACAP38 into conscious chemically (dexamethasone) hypophysectomized calves evoked a

dose-related increase in adrenal cortisol output (Edwards and Jones, 1994). The intravenous (iv) administration of PACAP27 increased the plasma concentration of cortisol in dogs (Kawai *et al.*, 1994), but the PACAP38 infusion did not alter plasma cortisol in humans, although blunting the diurnal decline of blood cortisol concentration (Murakami *et al.*, 1996). Using perfused isolated pig adrenals, Tornøe *et al.* (2000) showed that PACAP38 (from 2% 10^{-10} to 10^{-9} *M*) elicited a 12-fold increase in cortisol release, associated with a marked decrease in vascular resistances. Of interest, the PAC_1-R antagonist PACAP(6–38) blocked the cortisol response to PACAP38 without affecting vascular resistance, which indicates that increased glucocorticoid secretion does not ensue from enhanced intraadrenal blood flow (see Section IV.D.2).

b.* In Vitro *Studies

i. Dispersed Cells PACAP38 (up to 10^{-4} *M*) did not affect basal glucocorticoid secretion from dispersed rat and human ZF/R cells (Andreis *et al.*, 1995; Mazzocchi *et al.*, 2002a,b; Neri *et al.*, 1996). However, PACAP27 has been reported to evoke a moderate increase in corticosterone output from rat ZF/R cells, which was not blocked by CIP (Nowak *et al.*, 1999).

ii. Adrenal Quarters Rat adrenal slices, containing medullary chromaffin cells, were found to secrete corticosterone in response to 10^{-6} *M* PACAP38, and the effect was abrogated by both a PAC_1-R antagonist and CIP (Andreis *et al.*, 1995). In contrast, a cortisol response to 10^{-8} *M* PACAP38 was not observed in human adrenal slices (Neri *et al.*, 1996).

iii. In Vitro *Cultures* PACAP38 (10^{-7} *M*) has been reported to increase cortisol and DHEA secretion from primary cultures of fetal human adrenocortical cells, and the effect was blocked by a β_1-adrenoceptor antagonist (Breault *et al.*, 2000). PACAP38 also evoked a moderate cortisol response from human H-295 cells (Nicol *et al.*, 2004).

C. Interrenal Cells of Lower Vertebrates

1. VIP

The ip injection of VIP was found to increase the plasma concentration of corticosterone in the lizard *Podarcis sicula*. ACTH blood level was not affected, suggesting a direct effect of the peptide on adrenocortical cells (De Falco *et al.*, 2003).

VIP increased both aldosterone and corticosterone secretion from perfused frog interrenal slices in a concentration-dependent manner, with the aldosterone response being significantly more intense than that of corticosterone (Feuilloley *et al.*, 1992; Larcher *et al.*, 1992; Leboulenger *et al.*, 1983a,

1984, 1988). The secretory response to VIP of these preparations was blocked by the microfilament disruptor cytochalasin-B (Netchitailo *et al.*, 1985).

2. PACAP

Frog (f) PACAP38 has been shown to evoke a rapid and transient rise in aldosterone and corticosterone release from freshly dispersed interrenal cells of *Rana ridibunda*. The application of a second pulse of fPACAP38, after a resting period of 120 min, elicited a secretory response from two to three times less intense than the first one, indicating strong desensitization of PACAP Rs (Yon *et al.*, 1994a). fPACAP38 (from 10^{-7} to 10^{-5} *M*) concentration-dependently increased aldosterone and to a lesser extent corticosterone output from perfused frog adrenal slices (Yon *et al.*, 1993a,b, 1994a, 1996). The exposure of cultured frog interrenal cells to fPACAP38 provoked a marked increase in $[Ca^{2+}]_i$, no correlation existing between the peptide concentration and the percentage of responding cells or the profile of the Ca^{2+} response. Similar effects were observed in cultured frog chromaffin cells (Yon *et al.*, 1994a).

PACAP38 did not affect secretion of dispersed fowl interrenal cells, but it did raise aldosterone and corticosterone output from interrenal quarters in a concentration-dependent manner (Mazzocchi *et al.*, 1997a). Minimal and maximal effective concentrations were 10^{-8} and 10^{-7} *M*, and the maximum response was about 3-fold for both aldosterone and corticosterone. PACAP(6–38) abolished the secretory response, suggesting the involvement of PAC_1-Rs.

D. Mechanism of Action

1. Direct Mechanisms

In Section III evidence was reviewed strongly suggesting that PAC_1-Rs are exclusively located in the adrenal medulla, whereas $VPAC_1$-Rs and $VPAC_2$-Rs are present in both medullary and cortical cells, and especially ZG cells. Hence, the direct aldosterone secretagogue effect of VIP and PACAP (see Section IV.A) is conceivably mediated by both $VPAC_1$-Rs and $VPAC_2$-Rs. VIP and PACAP were found to increase both cAMP and inositol-triphosphate (IP_3) production in human, bovine, and rat ZG cells (Bodart *et al.*, 1997; Mazzocchi *et al.*, 2002a,b). The cAMP and IP_3 responses were decreased by a $VPAC_1$-R antagonist, whereas a $VPAC_2$-R agonist increased only IP_3 accumulation. As expected, a PAC_1-R antagonist was ineffective. The aldosterone response to PACAP38 was decreased by exposing ZG cells to inhibitors of AC and protein kinase (PK)A or PLC and PKC, whereas that

to the $VPAC_2$-R agonist was hampered only by PLC inhibitors (Mazzocchi *et al.*, 2002a,b). In light of these findings, it was concluded that VIP and PACAP stimulate aldosterone secretion from ZG cells via the activation of either $VPAC_1$-Rs coupled to the AC- and PLC-dependent cascades, or $VPAC_2$-Rs coupled to only the PLC-dependent pathway.

Although the bulk of evidence indicates that ZF/R cells are not provided with PACAP/VIP Rs (see Section III), sporadic studies showed that VIP and PACAP are able to directly enhance glucocorticoid production from dispersed or cultured adrenocortical cells (see Section IV.A). These studies were largely carried out on primary cultures of adrenocortical cells, where the presence of contaminating medullary chromaffin cells cannot be ruled out (Barbara and Takeda, 1995; Bornstein *et al.*, 1996; Breault *et al.*, 2000; Fang *et al.*, 2001), or on adrenocortical tumor-derived cell lines, whose physiology could not completely reflect that of normal inner adrenocortical cells (Birnbaum *et al.*, 1980; Cobb *et al.*, 1997; Haidan *et al.*, 1998; Nicol *et al.*, 2004). Li *et al.* (1990) reported that VIP binds ACTH-Rs, and specifically the subtype recognizing the ACTH(11–24) sequence. Mazzocchi *et al.* (1993a, 1994c) obtained findings indicating that the nonspecific activation of ACTH Rs may, at least partly, underlie the direct stimulating effect of VIP on dispersed rat adrenocortical cells. CIP partially blocked the secretagogue action of VIP on ZG cells and completely annulled that on ZF/R cells, suggesting that VIP-induced aldosterone secretion is mediated by both ACTH and VIP Rs, whereas the corticosterone response occurs exclusively via the activation of ACTH Rs. A selective VIP-A completely reversed the weak direct glucocorticoid secretagogue action of VIP, but only partially blunted that of ACTH, which in contrast was abolished by CIP. This last observation is in keeping with the contention that VIP competes only with a subtype of ACTH Rs (Li *et al.*, 1990), and could explain why VIP raises the level of circulating glucocorticoid in hypophysectomized, but not in intact, animals (Bloom *et al.*, 1987; Edwards and Jones, 1993a): in fact, the tonic activation of adrenal ACTH Rs by circulating ACTH may mask *in vivo* their VIP-induced nonspecific activation, which can manifest itself only when the pituitary release of ACTH is abolished by hypophysectomy. These findings were confirmed by Mazzocchi *et al.* (1998c), who additionally showed that the nonspecific binding of VIP to ACTH Rs was coupled to the activation of the AC/PKA signaling pathway. In keeping with this contention, VIP was found to enhance basal cAMP accumulation in the human H-295 cell line (Cobb *et al.*, 1997; Nicol *et al.*, 2004).

2. Indirect Mechanisms

VIP and PACAP are able to stimulate hypothalamic–pituitary CRH/ACTH release, thereby increasing both mineralo- and glucocorticoid blood levels

(Nussdorfer and Malendowicz, 1998b). However, the aldosterone response is stronger than the glucorticoid one, which could be due to the fact that the direct effect of these peptides is mainly related to the ZG and/or that they stimulate arginine–vasopressin (AVP) release (Chiodera *et al.*, 1995; Murase *et al.*, 1993), which is an important agonist of aldosterone secretion in mammals (Nussdorfer, 1996).

a. Via Medullary Catecholamines There is evidence that adrenocortical cells are provided with β-adrenoceptors, whose activation by catecholamines and other agonists enhances steroid secretion (Nussdorfer, 1996). This occurs in both mammals (Lightly *et al.*, 1990) and lower vertebrates (Lesouhaitier *et al.*, 1995; Mazzocchi *et al.*, 1997b, 1998a). Adrenal catecholamine secretion is stimulated by VIP and PACAP in mammals and lower vertebrates (see Section VI.A). Evidence has been provided that VIP and PACAP may enhance steroid secretion by eliciting the release of catecholamines from chromaffin cells, which in turn stimulate adrenocortical cells acting in a paracrine manner. The β-adrenoceptor antagonists *l*-alprenolol, propanolol, and atenolol were found to block the aldosterone response not only to the β-adrenoceptor agonists, but also to VIP and PACAP in rats (Andreis *et al.*, 1995; Bernet *et al.*, 1994; Hinson *et al.*, 1992; Mazzocchi *et al.*, 1993a) and humans (Bornstein *et al.*, 1996; Neri *et al.*, 1996). Moreover, β-adrenoceptor antagonists abolished the cortisol and androgen response to VIP of human adrenocortical cells in primary cultures (that also contain a number of chromaffin medullary cells) (Bornstein *et al.*, 1996), as well as the aldosterone and corticosterone response to PACAP of frog (Yon *et al.*, 1994a) and fowl interrenal cells (Mazzocchi *et al.*, 1997a). Of interest, an analogous mechanism seems to underlie the aldosterone secretagogue effect of other regulatory peptides, including neuropeptide-Y (Bernet *et al.*, 1994; Mazzocchi *et al.*, 1996a; Renshaw *et al.*, 2000; Spinazzi *et al.*, 2005), substance-P (Mazzocchi *et al.*, 1995a; Nussdorfer and Malendowicz, 1998a), neuropeptide-K (Mazzocchi *et al.*, 1994a), endothelins (Nussdorfer *et al.*, 1997a, 1999; Rebuffat *et al.*, 1999, 2000), calcitonin gene-related peptide and adrenomedullin (Andreis *et al.*, 1997; Mazzocchi *et al.*, 1996b; Nussdorfer, 2001; Nussdorfer *et al.*, 1997b), and cerebellin (Albertin *et al.*, 2000; Mazzocchi *et al.*, 1999).

b. Via Medullary CRH/ACTH System Compelling evidence indicates that at least in the rat, a CRH/ACTH system is operative in the adrenal gland and can modulate glucocorticoid secretion in a paracrine manner (Vrezas *et al.*, 2003): (1) the adrenal medulla contains CRH-ir and ACTH-ir (Andreis *et al.*, 1992; Bagdy *et al.*, 1990; Hashimoto *et al.*, 1984; Mazzocchi *et al.*, 1993b, 1994b); (2) medullary chromaffin cells are provided with CRH Rs (Aguilera *et al.*, 1987; Dave *et al.*, 1985); (3) CRH can evoke a sizable release

of ACTH-ir from medullary-tissue fragments (Andreis *et al.*, 1992; Mazzocchi *et al.*, 1994b); and finally (4) CRH does not enhance corticosterone release from dispersed ZF/R cells, but stimulates corticosterone production from adrenal slices containing medullary chromaffin cells, the effect being abolished by CIP (Andreis *et al.*, 1991a, 1992; Mazzocchi *et al.*, 1993b, 1994b). PACAP38 has been reported to induce CRH-ir release from the adrenal medulla of hypophysectomized calves (Edwards and Jones, 1994), and both the CRH-R antagonist α-helical CRH and CIP were found to abolish the corticosterone response of rat adrenals to PACAP38, without per se evoking any appreciable effect on basal glucocorticoid secretion (Andreis *et al.*, 1995). Of interest, an analogous mechanism appears to underlie the glucocorticoid secretagogue action of tachykinins (Mazzocchi *et al.*, 1994a; Nussdorfer and Malendowicz, 1998a), neuromedin-U8 (Malendowicz *et al.*, 1994), neurotensin (Mazzocchi *et al.*, 1997c), AVP (Mazzocchi *et al.*, 1995b, 1997d), and interleukin-1β (Andreis *et al.*, 1991b; Mazzocchi *et al.*, 1993b, 1994b; Nussdorfer and Mazzocchi, 1998).

c. Rise in Adrenal Blood Flow A close direct correlation between the rates of blood flow and glucocorticoid release exists in the mammalian adrenal gland (Vinson and Hinson, 1992). Hence, any regulatory peptide that modulates adrenal blood flow may indirectly enhance glucocorticoid secretion. Findings indicate that VIP and PACAP reduce adrenal vascular resistances. Although denied by Huffman *et al.* (1988), Hinson *et al.* (1992, 1994a,b) clearly showed that the *bolus* injection of VIP increased the perfusion medium flow rate in the *in situ* perfused rat adrenals. PACAP38 and PACAP27 were found to increase adrenal blood flow in the rabbit (Nilsson, 1994). Finally, both VIP and PACAP38 enhanced adrenal blood flow in hypophysectomized calves (Edwards and Jones, 1993a, 1994). PACAP38 was found to decrease vascular resistance in perfused pig adrenals. However, this effect did not appear to be connected to steroid release, because a PAC_1-R antagonist blocked the cortisol response, without affecting the increase in blood flow (Tornøe *et al.*, 2000). Such a mechanism has been documented for substance-P (Hinson *et al.*, 1994a,b), endothelins (Nussdorfer *et al.*, 1997a, 1999; Mazzocchi *et al.*, 1998b), and calcitonin gene-related peptide (CGRP) and adrenomedullin (Mazzocchi *et al.*, 1996b; Nussdorfer *et al.*, 1997b, 2000).

E. Other Steroid–Secreting Cells

Endogenous ligands of PACAP/VIP Rs appear to play a role in the local regulation of steroid-secreting cells other than adrenocortical ones, namely those of endocrine gonads.

1. Testis

RT-PCR showed the expression of $VPAC_2$-R, but not $VPAC_1$-R, mRNA in the rat testis, and the expression increased with age from fetal to newborn to adult animals. However, PACAP38-ir was elevated in the rat testis, but apparently only in the germ cells (Hurley *et al.*, 1995; Shioda *et al.*, 1994; Yanaihara *et al.*, 1998).

VIP (from 10^{-9} to 10^{-7} *M*) was found to raise testosterone secretion from dispersed and cultured rat Leydig cells (El-Gehani *et al.*, 1998a,b; Kasson *et al.*, 1986; Romanelli *et al.*, 1997). However, other studies failed to show any effect of VIP (Rossato *et al.*, 1997).

PACAP38 (from 10^{-10} to 10^{-7} *M*), but not PACAP27, was shown to enhance testosterone production from dispersed rat Leydig cells (Romanelli *et al.*, 1997; Rossato *et al.*, 1997). Using PACAP/VIP R antagonists, Romanelli *et al.* (1997) demonstrated that PACAP38 exerted its secretagogue effect acting via PAC_1-Rs coupled to both AC- and PLC-dependent cascades, inasmuch as it raised both cAMP and IP_3 production. However, Rossato *et al.* (1997) did not find any effect of PACAP38 on either cAMP production or $[Ca^{2+}]_i$, and provided evidence that this peptide enhanced testosterone secretion via an R coupled to a pertussis toxin (PTX)-sensitive G protein, whose activation induced Na^+-dependent depolarization of the plasma membrane. Before concluding, we recall that the intratesticular injection of VIP or PACAP38 has been shown to decrease basal testosterone secretion in 9-day-old hemicastrated rats (Csaba *et al.*, 1997). Moreover, PACAP38 has been reported to lower testosterone secretion from newt gonads (Gobbetti and Zerani, 2002).

2. Ovary

VIP expression, as mRNA and protein, was found in rat preovulatory ovary (Gozes and Tsafriri, 1986; Schmidt *et al.*, 1990), and ICC traced VIPergic fibers around the thecal layer of rat developing follicles (Ahmed *et al.*, 1986). Several studies demonstrated the expression of PACAP mRNA in rat ovary follicles (Gräs *et al.*, 1996; Scaldaferri *et al.*, 1996), cultured rat granulosa cells (Lee *et al.*, 1999b; Koh *et al.*, 2000), rat corpus luteum (Kotani *et al.*, 1997a,b), and cultured newt ovarian cells (Gobbetti *et al.*, 1997). ISH showed that PACAP mRNA was contained in both granulosa and theca interstitial cells of rat follicles, and that gonadotropins or human chorionic gonadotropin (hCG) enhanced PACAP expression (Lee *et al.*, 1999b; Koh *et al.*, 2000). Coupled RIA and ICC studies demonstrated that cultured preovulatory rat granulosa-lutein cells accumulated and secreted PACAP-ir (Gräs *et al.*, 1999). PAC_1-R, $VPAC_1$-R, and $VPAC_2$-R expression has been detected in rat granulosa and theca-interstitial cells (Gräs *et al.*, 2000; Ko and Park-Sarge,

2000; Koh *et al.*, 2000; Kotani *et al.*, 1997c, 1998; Scaldaferri *et al.*, 1996), and PAC_1-R expression in the rat corpus luteum (Kotani *et al.*, 1997c, 1998). Evidence has been provided that hCG exposure markedly increased PAC_1-R expression within 6 h (Ko and Park-Sarge, 2000; Koh *et al.*, 2000).

VIP (from 10^{-10} to 10^{-6} *M*) increased estrogen and progesterone secretion from *in vitro* incubated rat ovary (Ahmed *et al.*, 1986), isolated rat follicles (George and Ojeda, 1987; Törnell *et al.*, 1988), dispersed (Gräs *et al.*, 2000) or cultured rat granulosa-lutein cells (Davoren and Hsueh, 1985), and cultured human granulosa-lutein cells (Gräs *et al.*, 1994; Ojeda *et al.*, 1989; Ottesen and Fahrenkrug, 1995), but not cultured bovine granulosa cells (Spicer *et al.*, 1992). VIP enhanced steroidogenesis in the chicken ovary (Johnson and Tilly, 1988). A steroidogenic effect of PHI and PHM, less intense than that of VIP, has also been reported in rats (Ahmed *et al.*, 1986) and humans (Gräs *et al.*, 1994; Ojeda *et al.*, 1989; Ottesen and Fahrenkrug, 1995), respectively. According to its secretagogue action, VIP was shown to stimulate aromatase activity (Davoren and Hsueh, 1985) and to up-regulate cytochrome P450scc mRNA expression in the rat ovary (Trzeciak *et al.*, 1986, 1987). VIP increased cAMP production from rat follicles (Davoren and Hsueh, 1985; Gräs *et al.*, 2000; Törnell *et al.*, 1988), and this finding, coupled with the demonstration that the PKA inhibitor H-89 blocked progesterone response to VIP of dispersed granulosa-lutein cells, strongly suggests that the mechanism underlying the secretagogue action of this peptide involves the stimulation of the AC/PKA cascade (Gräs *et al.*, 2000).

PACAP (from 10^{-9} to 10^{-6} *M*) increased estrogen and progesterone production from dispersed (Gräs *et al.*, 2000) and cultured rat granulosa-lutein cells (Apa *et al.*, 1997; Gräs *et al.*, 1996, 1999; Heindel *et al.*, 1996; Kotani *et al.*, 1997c, 1998; Zhong and Kasson, 1994) as well as cultured newt ovarian cells (Gobbetti *et al.*, 1997). Of interest, PACAP immunoneutralization was found to lower basal progesterone secretion from cultured preovulatory rat granulosa cells and to hamper their luteinization (Gräs *et al.*, 1999), suggesting an autocrine–paracrine role of endogenous PACAP in the functional maintenance of follicles before ovulation. In this connection, we recall that other evidence indicates that an hCG-induced PACAP expression surge (see above) could favor follicle survival during the preovulatory period in rats. In fact, PACAP38 was found to lower the follicle apoptosis rate and a PAC_1-R antagonist to partially prevent luteinizing hormone-induced inhibition of follicle apoptosis (Lee *et al.*, 1999b). Before concluding, it must be stressed that the effects of PACAP on rat follicle appear to be mediated, as in the case of VIP, by the AC/PKA signaling pathway (Gräs *et al.*, 2000).

Taken together, the findings surveyed clearly indicate that the endogenous ligands of PACAP/VIP Rs play a role in the local regulation of the adrenal cortex, and especially of ZG and aldosterone secretion. VIP and PACAP, acting via $VPAC_1$-Rs and $VPAC_2$-Rs coupled to both AC/PKA and

PLC/PKC cascades, exert a direct stimulating effect on ZG secretion. There is also proof that VIP and PACAP may also enhance the secretory activity of adrenocortical cells indirectly, through the stimulation of catecholamine and CRH/ACTH release from medullary chromaffin cells. The involvement of VIP and PACAP in the local regulation of glucocorticoid secretion from the inner adrenal cortex is doubtful, but there is evidence that these peptides may be involved in the autocrine–paracrine regulation of the secretory activity of other steroid-secreting cells, namely those of the endocrine gonads.

V. Effects of Endogenous Ligands of PACAP/VIP Receptors on Adrenal Medulla Secretion

A. Catecholamine Secretion in Mammals

Consistent findings show that VIP and PACAP are able to raise catecholamine secretion from mammalian adrenal chromaffin cells either *in vivo* or *in vitro* in a concentration-dependent manner.

1. VIP and Related Peptides

a.* In Vivo *Studies The intraaortic infusion of VIP was found to increase NE and E blood concentrations in chemically hypophysectomized ACTH-replaced cows (Edwards and Jones, 1993a). Likewise, VIP infusion increased catecholamine release from *in situ* perfused dog (Gaspo *et al.*, 1997; Lamouche and Yamaguchi, 2001; Yamaguchi, 1993) and rat adrenals (Malhotra and Wakade, 1987; Malhotra *et al.*, 1988, 1989), and the involvement of $VPAC_1$-Rs has been suggested (Gaspo *et al.*, 1997). Splanchnic nerve stimulation enhanced the release of both catecholamine and VIP from perfused dog and rat adrenals (Gaspo *et al.*, 1995; Wakade *et al.*, 1991). In rats, catecholamine response to splanchnic nerve stimulation was hampered by either acetylcholine (ACh)-R or VIP R antagonists. Since ACh raised catecholamine, but not VIP release, the conclusion was drawn that VIP acts as a neurotransmitter in the adrenal medulla via ACh Rs (Wakade *et al.*, 1991).

b.* In Vitro *Studies VIP (from 10^{-8} to 10^{-6} *M*) was found to increase basal NE and E secretion from cultured human (Mazzocchi *et al.*, 2002b) and bovine adrenomedullary cells (Houchi *et al.*, 1987; Malhotra *et al.*, 1989; Olasmaa *et al.*, 1992; Waymire *et al.*, 1991; Wilson, 1987), as well as from dispersed guinea pig (Misbahuddin *et al.*, 1988) and rat medullary chromaffin

cells (Anderova *et al.*, 1998). PHI was ineffective (Waymire *et al.*, 1991). Using PACAP/VIP R selective antagonists, evidence indicates that in humans VIP acts via both the $VPAC_1$-R and the $VPAC_2$-R (Mazzocchi *et al.*, 2002b). Of interest, evidence has been provided that VIP enhanced agonist (K^+, veratridine, and nicotine)-stimulated, but not basal, catecholamine secretion from cultured bovine adrenomedullary cells (Wilson, 1988). Likewise, VIP was found to potentiate K^+-, ACh-, and muscarine-induced catecholamine release from dispersed rat chromaffin cells (Anderova *et al.*, 1998). Collectively, these observations may suggest that VIP acts a *trans*-synaptic modulator of catecholamine release.

2. PACAP

a.* In Vivo *Studies PACAP was found to stimulate basal catecholamine release from *in situ* perfused dog (Geng *et al.*, 1997; Lamouche and Yamaguchi, 2001; Lamouche *et al.*, 1999) and rat adrenals (Fukushima *et al.*, 2001b, 2002; Watanabe *et al.*, 1995). PACAP38 also increased chromogranin-A secretion from the perfused pig adrenal gland (Tornøe *et al.*, 2000). In contrast to VIP (Wakade *et al.*, 1991), the response of E to PACAP was not blocked in the rat by either nicotinic-R or muscarinic-R antagonists, indicating that PACAP did not act via cholinergic Rs (Watanabe *et al.*, 1995). There is a general consensus that all these adrenomedullary effects of PACAP are mediated by PAC_1-R (Fukushima *et al.*, 2001b; Lamouche and Yamaguchi, 2001; Tornøe *et al.*, 2000). PACAP potentiated the catecholamine response to splanchnic nerve stimulation (Lamouche and Yamaguchi, 2001; Lamouche *et al.*, 1999), and PAC_1-R antagonists blocked splanchnic nerve-induced catecholamine release (Fukushima *et al.*, 2001b), thereby making it likely that endogenous PACAP, released by splanchnic nerves, mediates and potentiates reflex-induced catecholamine release, acting as a postsynaptic neuromodulator (Lamouche and Yamaguchi, 2003). In keeping with a physiological role for PACAP, it has been observed that PACAP-deficient mice, although displaying normal basal catecholamine secretion, exhibit a blunted catecholamine response to splanchnic nerve stimulation elicited by insulin-induced hypoglycemia. Hence, their counter-regulatory mechanisms by which catecholamines, by stimulating hepatic gluconeogenesis, counteract hypoglycemia are impaired (Hamelink *et al.*, 2002, 2003).

b.* In Vitro *Studies Although a recent study reported that PACAP (10^{-6} *M*) inhibited K^+- and nicotine-induced catecholamine secretion from cultured rat adrenomedullary cells (Jorgensen *et al.*, 2002), most available evidence indicates a potent catecholamine secretagogue action of this peptide. In fact, PACAP (from 10^{-10} to 10^{-7} *M*) increased basal NE and E

release from cultured human (Mazzocchi *et al.*, 2002b; Payet *et al.*, 2003), bovine (Babinski *et al.*, 1996; Choi *et al.*, 1999; Isobe *et al.*, 1993, 1996; Morita *et al.*, 2002; O'Farrell and Marley, 1997; Perrin *et al.*, 1995; Tanaka *et al.*, 1996) and rat adrenomedullary (Watanabe *et al.*, 1992), and PC12 cells (Taupenot *et al.*, 1998, 1999), as well as from dispersed rat chromaffin cells (Przywara *et al.*, 1996) and rat adrenomedullary slices (Mazzocchi *et al.*, 2002a). PACAP was also shown to enhance nicotine- and muscarine-induced catecholamine release from dispersed guinea pig adrenomedullary cells (Inoue *et al.*, 2000). This observation, coupled with the demonstration that catecholamine exocytosis induced by K^+ or nicotinic-R activation is immediate, whereas that elicited by PACAP has a latency period of 7 s (Przywara *et al.*, 1996), confirms that PACAP does not act via cholinergic Rs (see above). Despite some studies suggested that the catecholamine secretagogue action of PACAP is exclusively mediated by PAC_1-Rs (Babinski *et al.*, 1996; Isobe *et al.*, 1993; Payet *et al.*, 2003), investigations carried out using selective PACAP/VIP R agonists and antagonists demonstrated that at least in humans and rats, all three R subtypes are involved (Mazzocchi *et al.*, 2002a,b). In fact, PAC_1-R and $VPAC_1$-R antagonists alone or together only partially blocked the catecholamine response to PACAP38, and the $VPAC_2$-R agonist elicited a sizable NE and E release.

Consistent evidence supports the contention that PACAP not only stimulates catecholamine release, but also enhances its biosynthesis by up-regulating the expression and activity of the enzymes involved in NE and E synthesis, namely TH, dopamine β-hydroxylase (DβH), and PNMT. PACAP38, via PAC_1-Rs, enhanced TH and DβH expression and activity in cultured bovine (Choi *et al.*, 1999; Houchi *et al.*, 1994; Isobe *et al.*, 1996; Rius *et al.*, 1994; Tönshoff *et al.*, 1997), and TH mRNA in cultured rat adrenomedullary cells (Hong *et al.*, 1998). The up-regulation of TH is also in keeping with the reported PACAP-induced rise in dopamine release from rat PC12 cells (Aoyagi and Takahashi, 2001). PNMT mRNA was found to be either increased due to the decrease in its degradation rate (Tönshoff *et al.*, 1997) or unchanged with decreased PNMT activity, suggesting that PACAP enhances NE over E synthesis (Choi *et al.*, 1999). Of interest, there is proof that PACAP mRNA expression directly correlates with TH and PNMT mRNAs and E content in intraadrenal human pheochromocytomas (Isobe *et al.*, 2003), but not neuroblastomas (Isobe *et al.*, 2004). These observations suggest that an autocrine–paracrine mechanism is operative in pheochromocytomas, by which endogenous PACAP enhances catecholamine biosynthesis.

In addition to stimulating catecholamine secretion, PACAP, via PAC_1-Rs, has been reported to raise Leu-enkephalin (ENK) (Babinski *et al.*, 1996), Met-ENK (Hahm *et al.*, 1998), and secretoneurin secretion (Turquier *et al.*, 2001), brain natriuretic peptide (BNP) and ENK peptide biosynthesis

(Babinski *et al.*, 1996; Hahm *et al.*, 1998; Wilson, 1987) and secretogranin-II mRNA in cultured bovine adrenomedullary cells (Turquier *et al.*, 2001), as well as chromogranin expression in rat PC12 cells (Taupenot *et al.*, 1998).

B. Catecholamine Secretion in Lower Vertebrates

VIP and PACAP were found to increase E, but not NE, secretion from chromaffin tissue of teleost interrenals, probably via the PAC_1-R (Montpetit and Perry, 2000; Montpetit *et al.*, 2003). The ip injection of VIP acutely raised catecholamine blood concentration in lizards, and its prolonged administration increased the number of E (PNMT-positive) cells over that of NE (PNMT-negative) cells, thereby shifting secretion from NE to E (De Falco *et al.*, 2003).

C. Mechanism of Action

In Section III it was indicated that PAC_1-Rs, $VPAC_1$-Rs, and $VPAC_2$-Rs are expressed in the adrenal medulla: hence, on the basis of their affinity with their endogenous ligands (see Section II.B) it is conceivable that VIP acts via $VPAC_1$-Rs and $VPAC_2$-Rs, and PACAP via all PACAP/VIP R subtypes. Although VIP and PACAP obviously share common mechanisms of action, for convenience the two ligands will be surveyed separately.

1. VIP

VIP was found to enhance catecholamine release by activating the AC/PKA cascade in bovine and rat adrenomedullary cells. In fact, VIP raised cAMP production with an ensuing increase in TH phosphorylation (Anderova *et al.*, 1998; Malhotra *et al.*, 1989; Olasmaa *et al.*, 1992; Waymire *et al.*, 1991; Wilson, 1988). Findings also indicate that VIP stimulates the PLC/PKC cascade in bovine and rat adrenal medulla (Houchi *et al.*, 1987; Malhotra *et al.*, 1988, 1989). As mentioned in Section V.A, VIP did not affect basal catecholamine secretion from bovine adrenomedullary cells, but increased it when cultured cells were pretreated with PTX: the hypothesis has been advanced that a PTX-sensitive G protein exerts a tonic inhibition of catecholamine release by preventing VIP-induced PLC activation (Wilson, 1992). Although some investigators affirmed that in rats $[Ca^{2+}]_i$ increase was not coupled with VIP-elicited catecholamine secretion (Malhotra and Wakade, 1987; Malhotra *et al.*, 1988), other evidence indicated that it underlies the long-lasting catecholamine secretagogue effect of VIP (Anderova *et al.*, 1998). In contrast to PACAP (see below), VIP did not exert its

catecholamine secretagogue action through mechanisms involving an increase in Ca^{2+} influx, because neither Ca^{2+} channel blockade (Gaspo *et al.*, 1997) nor removal of extracellular Ca^{2+} (Malhotra and Wakade, 1987; Misbahuddin *et al.*, 1988) affected it.

2. PACAP

Evidence indicates that PACAP enhances catecholamine release via PAC_1-Rs coupled to the AC/PKA pathway. This has been demonstrated in cultured human fetal (Yon *et al.*, 1998), pig (Isobe *et al.*, 1993, 1994), bovine (Houchi *et al.*, 1995; Perrin *et al.*, 1995), and rat adrenomedullary cells (Chowdhury *et al.*, 1994; Guo and Wakade, 1994; Przywara *et al.*, 1996; Watanabe *et al.*, 1992), dispersed guinea pig chromaffin cells (Inoue *et al.*, 2000), and rat adrenal medulla slices (Mazzocchi *et al.*, 2002a). Findings also showed that the catecholamine secretagogue action of PACAP involves the activation of the PLC/PKC cascade in pig (Isobe *et al.*, 1993, 1994), bovine (Houchi *et al.*, 1995), and rat adrenomedullary cells (Chowdhury *et al.*, 1994; Guo and Wakade, 1994; Mazzocchi *et al.*, 2002a). Mazzocchi *et al.* (2002a) provided convincing proof that in rats PACAP38 stimulates catecholamine secretion through PAC_1-Rs, $VPAC_1$-Rs, and $VPAC_2$-Rs coupled to the AC, AC and PLC, and PLC cascades, respectively. In fact, (1) PAC_1-R and $VPAC_1$-R antagonists suppressed the cAMP response, the $VPAC_1$-R antagonist decreased the IP_3 response, and a $VPAC_2$-R agonist raised IP_3, but not cAMP production; and (2) the inhibitors of the AC/PKA and PLC/PKC cascades decreased the catecholamine response to PACAP38, and when added together abrogated it, and a PLC inhibitor annulled the catecholamine response to a $VPAC_2$-R agonist.

PACAP was found to elicit an increase in $[Ca^{2+}]_i$ in adrenomedullary cells of humans (Chamoux *et al.*, 1998; Payet *et al.*, 2003), cows (Morita *et al.*, 2002; Perrin *et al.*, 1995; Tanaka *et al.*, 1996, 1998), rats (Chowdhury *et al.*, 1994; Guo and Wakade, 1994; Przywara *et al.*, 1996; Watanabe *et al.*, 1992), and frogs (Yon *et al.*, 1994a), as well as in rat PC12 cells (Osipenko *et al.*, 2000; Taupenot *et al.*, 1999). In mammals, the $[Ca^{2+}]_i$ response to PACAP was biphasic, showing an initial transient phase and a sustained phase. The initial phase was found to depend on Ca^{2+} release from intracellular stores (Morita *et al.*, 2002; Osipenko *et al.*, 2000; Payet *et al.*, 2003; Watanabe *et al.*, 1992). However, it was not influenced by either PLC inhibitors or IP_3-R blockers, but was suppressed by ryanodine, indicating that it ensues from Ca^{2+} mobilization from IP_3-insensitive ryanodine/caffeine-sensitive Ca^{2+} stores (Payet *et al.*, 2003; Tanaka *et al.*, 1996, 1998). Conversely, the sustained phase was dependent on Ca^{2+} influx, which may occur through either the indirect activation of Ca^{2+} channels by the increase in $[Ca^{2+}]_i$ (store-operated Ca^{2+} channels) or their direct activation (Payet

et al., 2003). In keeping with this last contention, abundant evidence indicates the main involvement of dihydropyridine-sensitive L-type Ca^{2+} channels in the catecholamine response to PACAP (Fukushima *et al.*, 2001a,b; Isobe *et al.*, 1993; O'Farrell and Marley, 1997; Osipenko *et al.*, 2000; Tanaka *et al.*, 1996; Taupenot *et al.*, 1998). It was reported that the increase in $[Ca^{2+}]_i$ activates voltage-independent Na^+ channels, which, by eliciting Na^+ influx and membrane depolarization, may in turn activate L-type Ca^{2+} channels (Isobe *et al.*, 1993; O'Farrell and Marley, 1997; Tanaka *et al.*, 1996): in fact, Na^+ channel blockers were found to blunt the PACAP-induced increase in both $[Ca^{2+}]_i$ and catecholamine secretion. However, there is evidence that PACAP is able to evoke depolarizing cation currents in rat PC12 cells (Aoyagi and Takahashi, 2001; Osipenko *et al.*, 2000). Apamin was shown to potentiate the catecholamine response to PACAP without affecting basal secretion, and the potentiating effect disappeared in the presence of the L-type Ca^{2+} channel blocker nifedipine (Fukushima *et al.*, 2002). Because apamin inhibits small conductance K^+ channels (SKca), it was suggested that an intrinsic counterregulatory mechanism is operative in adrenomedullary cells, by which PACAP-induced activation of L-type Ca^{2+} channels and the increase in $[Ca^{2+}]_i$ open SKca, which, by eliciting K^+ efflux, may in turn inhibit L-type Ca^{2+} channels. Of interest, the PACAP-induced increase in Ca^{2+} influx may depend on the activation not only of the L-type, but also of the N-type and Q-type Ca^{2+} channels, inasmuch as single or combined antagonists of these channels (e.g., ω-conotoxin) decreased the catecholamine response to PACAP (O'Farrell and Marley, 1997). Before concluding, we wish to recall that findings indicate that in rat PC12 cells the initial phase of PACAP-induced $[Ca^{2+}]_i$ increase depends on the activation of L-type Ca^{2+} channels, and the sustained rise on the IP_3-sensitive Ca^{2+} release from intracellular stores, which in turn through store-operated Ca^{2+} channels increases Ca^{2+} influx (Taupenot *et al.*, 1999).

The PACAP-induced up-regulation of TH and DβH expression and activity has been reported to occur via the activation of the AC/PKA cascade (Choi *et al.*, 1999; Marley *et al.*, 1996; Rius *et al.*, 1994) or of both the AC/PKA and PLC/PKC pathways (Isobe *et al.*, 1993, 1994, 1996). PKA was found to increase and PKC to decrease PNMT expression in bovine chromaffin cells (Choi *et al.*, 1999). AC/PKA signaling has been shown to mediate PACAP-induced chromogranin expression in rat PC12 cells (Taupenot *et al.*, 1998), and both PKA and PKC have been reported to up-regulate bovine neuropeptide (Babinski *et al.*, 1996), secretogranin-II (Turquier *et al.*, 2001), and Met-ENK biosynthesis (Hahm *et al.*, 1998). Enhanced Ca^{2+} influx appeared to underlie the stimulating effect of PACAP on secretoneurin (Turquier *et al.*, 2001) and Met-ENK secretion (Hahm *et al.*, 1998).

Collectively, available investigations provide consistent evidence that the endogenous ligands of PACAP/VIP Rs, either locally synthesized or released

by splanchnic nerves, stimulate the synthesis and release of catecholamine from adrenomedullary cells. All subtypes of Rs seem to mediate this effect, PAC_1-Rs being coupled to AC, $VPAC_1$-Rs to AC and PLC, and perhaps $VPAC_2$-Rs to only PLC. The increase in the $[Ca^{2+}]_i$, ensuing from the stimulation of either IP_3- or ryanodine/caffeine-sensitive Ca^{2+} release from intracellular stores or Ca^{2+} influx mainly by activation of L-type Ca^{2+} channels, also seems to play a pivotal role in the catecholamine secretagogue action of VIP and PACAP.

VI. Effects of Endogenous Ligands of PACAP/VIP Receptors on Adrenal Growth

A. Adrenal Cortex

The *in vivo* chronic treatment with VIP apparently did not affect the number of ZG cells in the rat adrenals (Mazzocchi *et al.*, 1987; Rebuffat *et al.*, 1994) or cause a moderate hyperplasia (Malendowicz and Nussdorfer, 1993). In keeping with this last observation, VIP (10^{-6} *M*) was found to increase cell proliferation in rat capsule ZG maintained in organotypic cultures, via a mechanism not involving mitogen-activated protein kinase (MAPK) p42/p44 cascade (Whitworth *et al.*, 2002). Different findings were obtained in adrenocortical cell lines: in fact, at steroidogenic concentrations, VIP inhibited proliferation of the mouse Y-1 tumor cell line (Kowal *et al.*, 1977) and did not affect that of human H-295 cells (Haidan *et al.*, 1998).

The prolonged (7-day) infusion with VIP increased the volume of ZG cells, along with that of the organelles involved in steroid synthesis (mitochondria and smooth endoplasmic reticulum) (Nussdorfer, 1986). The volume of the lipid droplet compartment, which stores the steroid hormone precursor cholesterol, was decreased, and the aldosterone secretory capacity of ZG cells was enhanced. Opposing findings were obtained by treating the rats with a VIP-A. ZF/R cells were not apparently affected (Mazzocchi *et al.*, 1987; Rebuffat *et al.*, 1994).

As far as we are aware, no studies are available on the possible growth effect of PACAP on the adrenal cortex.

B. Adrenal Medulla

Although PACAP has been reported to enhance the basal mitotic activity of cultured rat adrenomedullary cells (Tischler, 1995), it inhibited proliferation of rat PC12 cells (Vaudry *et al.*, 2002). PACAP also blunted the mitogenic

effect of NGF (Tischler, 1995) and lowered DNA synthesis of cultures exposed to insulin growth factor-II and fibroblast growth factor-2 (Frodin *et al.*, 1995). However, in this last model, PACAP increased the number of cells, probably by enhancing their survival. Because VIP was ineffective, the involvement of PAC_1-Rs has been suggested (Frodin *et al.*, 1995). Of interest, VIP has been shown to down-regulate Bcl-2 and to up-regulate Bax expression in chromaffin tissue of lizards, suggesting its proapoptotic effect (De Falco *et al.*, 2001). It remains to be determined whether these findings indicate an antiapoptotic effect of PAC_1-Rs and a proapoptotic effect of $VPAC_1$-Rs and/or $VPAC_2$-Rs.

There is general agreement that PACAP exerts a promoting effect on neuronal differentiation (neurite outgrowth) of medullary chromaffin cells, which appears to be mediated by PAC_1-Rs because of VIP ineffectiveness. This has been demonstrated in cultured rat adrenomedullary (Frodin *et al.*, 1995; Wolf and Krieglstein, 1995) and PC12 cells (Barrie *et al.*, 1997; Onoue *et al.*, 2001; Sakai *et al.*, 2001, 2004; Vaudry *et al.*, 2002), and the bulk of evidence indicates the involvement of the MAPK p42/p44 pathway. Hence, PACAP, via PAC_1-Rs, seems to inhibit growth factor-induced proliferation and to favor neuronal differentiation of adrenomedullary cells. In keeping with this, microarray analysis showed that PACAP up-regulates the expression of 75 genes and down-regulates that of 70 genes in rat PC12 cells, among which are those involved in neuritogenesis and cell proliferation, respectively (Grumolato *et al.*, 2003).

VII. Concluding Remarks

The preceding sections have shown that numerous investigations strongly suggest that VIP and PACAP play a potentially important role in the functional regulation of the adrenal gland. These peptides are contained in the adrenal medulla and, acting in an autocrine–paracrine manner, modulate adrenal functions through PACAP/VIP Rs located in both adrenocortical and adrenomedullary cells. In fact, the minimal effective concentrations of VIP and PACAP needed to elicit sizable adrenal responses are in the nanomolar order, whereas their levels in the systemic blood are at least three order of magnitude less (Arimura and Shioda, 1995; Fahrenkrug, 1989). In contrast, it can be calculated that the adrenal content of VIP and PACAP, under basal conditions and upon their 30% release, may give rise to local concentrations of about 5% 10^{-8} *M* and 2.5% 10^{-8} *M*, respectively (Nussdorfer, 1996).

However, despite extensive experimental work, the relevance of the role played by VIP and PACAP in the fine-tuning of adrenal functions under

physiological and paraphysiological conditions remains to be established. In fact, only a few experiments have been carried out aimed at demonstrating that the prolonged suppression of the endogenous VIP and PACAP systems may induce marked alterations in adrenal function. *In vivo* prolonged administration of a VIP-A was found to lower basal plasma aldosterone concentrations (see Section IV.A.1) and to decrease the growth and steroidogenic capacity of rat ZG (see Section VI.A), thereby suggesting that endogenous VIP is involved in the maintenance of normal mineralocorticoid secretion. Mice with targeted deletion of the PACAP gene, although displaying normal glucocorticoid and catecholamine blood levels (Gray *et al.*, 2001), exhibit impaired catecholamine response to insulin-induced hypoglycemic stress (see Section V.A.2), making it likely that PACAP may function as an "emergency response" cotransmitter in the adrenal medulla (Hamelink *et al.*, 2003). Obviously, it cannot be ruled out that endogenous VIP and PACAP systems may play a role in adrenocortical functional control under conditions up-regulating their synthesis in the adrenal gland. Based on this possibility, findings indicate that prolonged Na^+ depletion, a condition enhancing aldosterone secretion, is able to up-regulate VIP and its R expression in and to enhance aldosterone response to VIP of rat ZG (see Section IV.A.1).

Other topics surely merit further investigative effort. VIP has been reported to induce a potent stimulation of adrenal androgen hormone release (see Section IV.B.1). The regulation of adrenal androgen secretion is still controversial, and, in addition to ACTH, the existence of a specific cortical-androgen-stimulating hormone (CASH) has been frequently suggested (Mellon *et al.*, 1991; Parker and Odell, 1980; Penhoat *et al.,* 1991). Hence, the possibility should be explored that VIP, and perhaps PACAP, may be CASHs.

Compelling evidence indicates that VIP and PACAP and their Rs are highly expressed in human pheochromocytomas and rat PC12 pheochromocytoma cells. The secretory response to VIP and PACAP of pheochromocytoma cells is higher than that of normal adrenomedullary cells, and findings are available that PACAP expression directly correlates with that of TH and PNMT, as well as with E content (see Section V.A). Taken together, these observations suggest that endogenous VIP and PACAP may enhance catecholamine biosynthesis and secretion in pheochromocytomas through an autocrine–paracrine mechanism. However, these peptides are unlikely to be involved in the pathogenesis of pheochromocytomas, inasmuch as recent studies showed that they exert an inhibitory effect on the proliferative activity and a promoting action on neuronal differentiation of rat PC12 cells (see Section VI.B). VIP and PACAP enhance the secretion and growth of the ZG (see Sections IV.A and VI.A): hence, their elevated expression in pheochromocytomas could suggest that they are involved in the pathophysiological

bases of some rare cases of Conn's adenomas or idiopathic primary aldosteronism associated with secreting pheochromocytomas (Gordon *et al.*, 1994; Inoue *et al.*, 1986; Tan *et al.*, 1996; Wajiki *et al.*, 1985).

The adrenal cortex and medulla are provided with abundant VIPergic and PACAPergic nerve fibers that upon stimulation locally release VIP and PACAP (see Section III.A). In light of this, another formidable problem remains to be addressed: how does the central nervous system selectively control VIPergic and PACAPergic fiber outflow to the adrenal gland, thereby modulating its secretory activity?

The answer to these and many other basic questions, along with the development of new, potent, and highly selective agonists and antagonists of PACAP/VIP Rs, will not only increase our knowledge of the adrenal cytophysiology, but also, and more importantly, could open novel perspectives for the treatment of many diseases coupled with dysregulation of the adrenal gland.

Acknowledgments

We wish to thank Miss Alberta Coi for her secretarial support and invaluable help in the provision of bibliographic items.

REFERENCES

Aguilera, G., Millan, M. A., Hauger, R. L., and Catt, K. J. (1987). Corticotropin-releasing factor receptors: Distribution and regulation in brain, pituitary, and peripheral tissues. *Ann. N. Y. Acad. Sci.* **512,** 48–66.

Ahmed, C. E., Dees, W. L., and Ojeda, S. R. (1986). The immature rat ovary is innervated by vasoactive intestinal peptide (VIP)-containing fibers and responds to VIP with steroid secretion. *Endocrinology* **118,** 1682–1689.

Albertin, G., Malendowicz, L. K., Macchi, C., Markowska, A., and Nussdorfer, G. G. (2000). Cerebellin stimulates the secretory activity of the rat adrenal gland: *In vitro* and *in vivo* studies. *Neuropeptides* **34,** 7–11.

Alexander, L. D., and Sander, L. D. (1994). Vasoactive intestinal peptide stimulates ACTH and corticosterone release after injection into the PVN. *Regul. Pept.* **51,** 221–227.

Alexander, L. D., and Sander, L. D. (1995a). Involvement of vasopressin and corticotropin-releasing hormone in VIP- and PHI-induced secretion of ACTH and corticosterone. *Neuropeptides* **28,** 167–173.

Alexander, L. D., and Sander, L. D. (1995b). VIP antagonist demonstrates differences in VIP- and PHI-mediated stimulation and inhibition of ACTH and corticosterone secretion in rats. *Regul. Pept.* **59,** 321–333.

Alexander, L. D., Sander, L. D., Hooper, T., and Washington, V. (1994). Peptide histidine isoleucine-induced elevations in ACTH and corticosterone in the rat. *Peptides* **15,** 1021–1025.

Alexandre, D., Vaudry, H., Grumolato, L., Turquier, V., Fournier, A., Jégou, S., and Anouar, J. (2002). Novel splice variants of type I pituitary adenylate cyclase-activating polypeptide

receptor in frog exhibit altered adenylate cyclase stimulation and differential relative abundance. *Endocrinology* **143,** 2680–2692.

Ambrosi, B., Bochicchio, D., Sartorio, A., Morabito, F., and Faglia, G. (1987). Vasoactive intestinal polypeptide enhances ACTH levels in some patients with adrenocorticotropin-secreting pituitary adenoma. *Acta Endocrinol. (Copenhagen)* **116,** 216–220.

Anderova, M., Duchênne, A. D., Barbara, J. G., and Takeda, K. (1998). Vasoactive intestinal peptide potentiates and directly stimulates catecholamine secretion from rat adrenal chromaffin cells. *Brain Res.* **809,** 97–106.

Andreis, P. G., Neri, G., and Nussdorfer, G. G. (1991a). Corticotropin-releasing hormone (CRH) directly stimulates corticosterone secretion by the rat adrenal gland. *Endocrinology* **128,** 1198–1200.

Andreis, P. G., Neri, G., Belloni, A. S., Mazzocchi, G., and Nussdorfer, G. G. (1991b). IL-1β enhances corticosterone secretion by acting directly on the rat adrenal gland. *Endocrinology* **129,** 53–57.

Andreis, P. G., Neri, G., Mazzocchi, G., Musajo, F. G., and Nussdorfer, G. G. (1992). Direct secretagogue effect of corticotropin-releasing factor on the rat adrenal cortex: The involvement of the zona medullaris. *Endocrinology* **131,** 69–72.

Andreis, P. G., Malendowicz, L. K., Belloni, A. S., and Nussdorfer, G. G. (1995). Effects of pituitary adenylate cyclase-activating polypeptide (PACAP) on the rat adrenal secretory activity: Preliminary *in vitro* studies. *Life Sci.* **56,** 135–142.

Andreis, P. G., Neri, G., Prayer-Galetti, T., Rossi, G. P., Gottardo, G., Malendowicz, L. K., and Nussdorfer, G. G. (1997). Effects of adrenomedullin on the human adrenal gland: An *in vitro* study. *J. Clin. Endocrinol. Metab.* **82,** 1167–1170.

Aoyagi, K., and Takahashi, M. (2001). Pituitary adenylate cyclase-activating polypeptide enhances Ca^{2+}-dependent neurotransmitter release from PC12 cells and cultured cerebellar granule cells without affecting intracellular Ca^{2+} mobilization. *Biochem. Biophys. Res. Commun.* **286,** 646–651.

Apa, R., Lanzone, A., Mastrandea, M., Miceli, F., De Feo, D., Caruso, A., and Mancuso, S. (1997). Control of human luteal steroidogenesis: Role of growth hormone-releasing hormone, vasoactive intestinal peptide, and pituitary adenylate cyclase-activating peptide. *Fertil. Steril.* **68,** 1097–1102.

Arimura, A. (1998). Perspectives on pituitary adenylate cyclase-activating polypeptide (PACAP) in the neuroendocrine, endocrine, and nervous system. *Jpn. J. Physiol.* **48,** 301–331.

Arimura, A. (2003). PACAP: Discovery, gene, receptors. *In* "Pituitary Adenylate Cyclase-Activating Polypeptide" (H. Vaudry and A. Arimura, Eds.), pp. 1–24. Kluwer Academic Pub., Norwell, MA.

Arimura, A., and Shioda, S. (1995). Pituitary adenylate cyclase-activating polypeptide (PACAP) and its receptors: Neuroendocrine and endocrine interactions. *Front. Neuroendocrinol.* **16,** 53–58.

Arimura, A., Somogyvari-Vigh, A., Miyata, A., Mizuno, K., Coy, D. H., and Kitada, C. (1991). Tissue distribution of PACAP as determined by RIA: Highly abundant in the rat brain and testes. *Endocrinology* **129,** 2787–2789.

Babinski, K., Bodart, V., Roy, M., De Lean, A., and Ong, H. (1996). Pituitary adenylate cyclase-activating polypeptide (PACAP) evokes long-lasting secretion and *de novo* biosynthesis of bovine adrenal medullary neuropeptide. *Neuropeptides* **30,** 572–582.

Bagdy, G., Calogero, A. E., Szemeredi, K., Chrousos, G. P., and Gold, P. W. (1990). Effect of cortisol treatment on brain and adrenal corticotropin-releasing hormone (CRH) content and other parameters regulated by CRH. *Regul. Pept.* **31,** 83–92.

Barbara, J. G., and Takeda, K. (1995). Voltage-dependent currents and modulation of calcium channel expression in zona fasciculata cells from rat adrenal gland. *J. Physiol. (London)* **488,** 609–622.

Barrie, A. P., Clohessy, A. M., Buensuceso, C. S., Rogers, M. V., and Allen, J. M. (1997). Pituitary adenylyl cyclase-activating peptide stimulates extracellular signal-regulated kinase 1 or 2 (ERK 1/2) activity in a Ras-independent, mitogen-activated protein kinase/ERK kinase 1 or 2-dependent manner in PC12 cells. *J. Biol. Chem.* **272,** 19666–19671.

Berghorn, K. A., Li, C., Nathanielsz, P. W., and McDonald, T. J. (2000). VIP innervation: Sharp contrast in fetal sheep and baboon adrenal glands suggests differences in developmental regulation. *Brain Res.* **877,** 271–280.

Bernet, F., Bernard, J., Laborie, C., Montel, V., Maubert, E., and Dupouy, J. P. (1994). Neuropeptide Y (NPY)- and vasoactive intestinal peptide (VIP)-induced aldosterone secretion by rat capsule/glomerulosa zone could be mediated by catecholamines via β1 adrenergic receptors. *Neurosci. Lett.* **166,** 109–112.

Birnbaum, R. S., Alfonzo, M., and Kowal, J. (1980). Vasoactive intestinal peptide- and adrenocorticotropin-stimulated adenyl cyclase in cultured adrenal tumor cells: Evidence for a specific vasoactive intestinal peptide receptor. *Endocrinology* **106,** 1270–1275.

Bloom, S. R., Edwards, A. V., and Jones, C. T. (1987). Adrenal cortical responses to vasoactive intestinal peptide in conscious hypophysectomized calves. *J. Physiol. (London)* **391,** 441–450.

Bloom, S. R., Edwards, A. V., and Jones, C. T. (1988). The adrenal contribution to the neuroendocrine responses to splanchnic nerve stimulation in conscious calves. *J. Physiol. (London)* **397,** 513–526.

Bodart, V., Babinski, K., Ong, H., and De Lean, A. (1997). Comparative effect of pituitary adenylate cyclase-activating polypeptide on aldosterone secretion in normal bovine and human tumorous adrenal cells. *Endocrinology* **138,** 566–573.

Bodnar, M., Sarrieau, A., Deschepper, C. F., and Walker, C. D. (1997). Adrenal vasoactive intestinal peptide participates in neonatal corticosteroid production in the rat. *Am. J. Physiol.* **273,** R1163–R1172.

Bornstein, S. R., Ehrhart-Bornstein, M., Stromeyer, H. G., Adler, G., Scherbaum, W. A., and Holst, J. J. (1992). Vasoactive intestinal peptide (VIP) stimulates androstenedione release in isolated perfused pig adrenals. *Life Sci.* **52,** 135–140.

Bornstein, S. R., Haidan, A., and Ehrhart-Bornstein, M. (1996). Cellular communication in the neuro-adrenocortical axis: Role of vasoactive intestinal polypeptide (VIP). *Endocr. Res.* **22,** 819–829.

Bornstein, S. R., Ehrhart-Bornstein, M., and Scherbaum, W. A. (1997). Morphological and functional studies of the paracrine interaction between cortex and medulla in the adrenal gland. *Microsc. Res. Tech.* **36,** 520–533.

Brabet, P., Diriong, S., Journot, L., Bockaert, J., and Taviaux, S. (1996). Localization of the human pituitary adenylate cyclase-activating polypeptide receptor ($PACAP_1$-R) gene to 7p15-p14 by fluorescence *in situ* hybridization. *Genomics* **38,** 100–102.

Breault, L., Yon, L., Montero, M., Chouinard, L., Contesse, V., Delarue, C., Fournier, A., Lehoux, J. G., Vaudry, H., and Gallo-Payet, N. (2000). Occurrence and effect of PACAP in the human fetal adrenal gland. *Ann. N.Y. Acad. Sci.* **921,** 429–433.

Bryant, M., Bloom, S. R., Polak, J. M., Albuquerque, R. H., Modlin, I., and Pearse, A. G. (1976). Possible dual role for vasoactive intestinal peptide as gastro-intestinal hormone and neuro-transmitter substance. *Lancet* **1,** 991–993.

Cauvin, A., Van der Meers, A., Van der Meers-Piret, M. C., Robberecht, P., and Christophe, J. (1989). Variable distribution of three molecular forms of peptide histidine isoleucinamide in rat tissues: Identification of the large molecular form as peptide histidine valine(1–42). *Endocrinology* **125,** 2645–2655.

Chamoux, E., Breault, L., Le Houx, J. G., and Gallo-Payet, N. (1998). Comparative effects of ACTH, PACAP, and VIP on fetal human adrenal cells. *Endocr. Res.* **24,** 943–946.

Cheung, C. Y. (1988). Ontogeny of adrenal VIP content and release from adrenocortical cells in the ovine fetus. *Peptides* **9,** 107–111.

Cheung, C. Y., and Holzwarth, M. A. (1986). Fetal adrenal VIP distribution and effects on medullary catecholamine secretion. *Peptides* **7,** 413–418.

Chiodera, P., Volpi, R., Capretti, L., and Coiro, V. (1995). Effects of IV infused pituitary adenylate cyclase-activating polypeptide on arginine-vasopressin and oxytocin secretion in man. *Neuroreport* **11,** 1490–1492.

Choi, H. J., Park, S. Y., and Hwang, O. (1999). Differential involvement of PKA and PKC in regulation of catecholamine enzyme genes by PACAP. *Peptides* **20,** 817–822.

Chowdhury, P. S., Guo, X., Wakade, T. D., Przywara, D. A., and Wakade, A. R. (1994). Exocytosis from a single rat chromaffin cell by cholinergic and peptidergic neurotransmitters. *Neuroscience* **59,** 1–5.

Cobb, V. J., Williams, B. C., Mason, J. I., and Walker, S. W. (1997). Direct stimulation of cortisol secretion from the human NCI-H295 adrenocortical cell line by vasoactive intestinal polypeptide. *J. Hypertens.* **15,** 1735–1738.

Cryer, P. E. (1992). The adrenal medulla. *In* "The Adrenal Gland" (V. T. H. James, Ed.), 2nd ed., pp. 465–489. Raven Press, New York.

Csaba, Z. S., Csernus, V., and Gerendai, I. (1997). Local effect of PACAP and VIP on testicular function in immature and adult rat. *Peptides* **18,** 1561–1567.

Cunningham, L. A., and Holzwarth, M. A. (1988). Vasoactive intestinal peptide stimulates adrenal aldosterone and corticosterone secretion. *Endocrinology* **122,** 2090–2097.

Cunningham, L. A., and Holzwarth, M. A. (1989). Autoradiographic distribution of ^{125}I-VIP binding in the rat adrenal cortex. *Peptides* **10,** 1105–1108.

Dave, J. R., Eiden, L. E., and Eskay, R. L. (1985). Corticotropin-releasing factor binding to peripheral tissue and activation of the adenylate cyclase-adenosine 3′,5′-monophosphate system. *Endocrinology* **116,** 2152–2159.

Davoren, J. B., and Hsueh, A. J. W. (1985). Vasoactive intestinal peptide: A novel stimulator of steroidogenesis by cultured rat granulosa cells. *Biol. Reprod.* **33,** 37–52.

De Falco, M., Laforgia, V., Fedele, V., De Luca, L., Cottone, G., De Falco, G., and De Luca, A. (2001). Vasoactive intestinal peptide stimulation modulates the expression of Bcl-2 family members in the adrenal gland of the lizard *Podarcis sicula*. *Histochem. J.* **33,** 639–645.

De Falco, M., Laforgia, V., Valiante, S., Virgilio, F., Vazano, L., and De Luca, A. (2002). Different patterns of expression of five neuropeptides in the adrenal gland and kidney of two species of frog. *Histochem. J.* **34,** 21–26.

De Falco, M., Sciarrillo, R., Capaldo, A., Laforgia, V., Varano, L., Cottone, G., and De Luca, A. (2003). Shift from noradrenaline to adrenaline production in the adrenal gland of the lizard, *Podarcis sicula*, after stimulation with vasoactive intestinal peptide (VIP). *Gen. Comp. Endocrinol.* **131,** 325–337.

Delarue, C., Contesse, V., Langlet, S., Sicard, F., Perraudin, V., Lefebvre, H., Kodjo, M., Leboulenger, F., Yon, L., Gallo-Payet, N., and Vaudry, H. (2001). Role of neurotransmitters and neuropeptides in the regulation of the adrenal cortex. *Rev. Endocr. Metab. Disord.* **2,** 253–267.

Dun, N. J., Tang, H., Dun, S. L., Huang, R., Dun, E. C., and Wakade, A. R. (1996). Pituitary adenylate cyclase-activating polypeptide-immunoreactive sensory neurons innervate rat adrenal medulla. *Brain Res.* **716,** 11–21.

Edwards, A. V., and Jones, C. T. (1993a). Adrenal cortical and medullary responses to acetylcholine and vasoactive intestinal peptide in conscious calves. *J. Physiol. (London)* **468,** 515–527.

Edwards, A. V., and Jones, C. T. (1993b). Autonomic control of adrenal function. *J. Anat.* **183,** 291–307.

Edwards, A. V., and Jones, C. T. (1994). Adrenal responses to the peptide PACAP in conscious functionally hypophysectomized calves. *Am. J. Physiol.* **266,** E870–E876.

Ehrhart-Bornstein, M., Bornstein, S. R., Scherbaum, W. A., Pfeiffer, E. F., and Holst, J. J. (1991). Role of vasoactive intestinal peptide in a neuroendocrine regulation of the adrenal cortex. *Neuroendocrinology* **54,** 623–628.

El-Gehani, F., Tena-Sempere, M., and Huhtaniemi, I. (1998a). Vasoactive intestinal peptide is an important endocrine regulatory factor of fetal rat testicular steroidogenesis. *Endocrinology* **139,** 1474–1480.

El-Gehani, F., Tena-Sempere, M., and Huhtaniemi, I. (1998b). Vasoactive intestinal peptide stimulates testosterone production by cultured fetal rat testicular cells. *Mol. Cell. Endocrinol.* **140,** 175–178.

Enyedi, P., Szabo, B., and Spät, A. (1983). Failure of vasoactive intestinal peptide to stimulate aldosterone production. *Acta Physiol. Hung.* **61,** 77–79.

Fahrenkrug, G. (1989). Vasoactive intestinal peptide. *Handb. Physiol. Sect. 6: Gastrointest. Syst.* **2,** 691–702.

Fahrenkrug, J., Buhl, T., and Hannibal, J. (1995). PreproPACAP-derived peptides occur in VIP-producing tumors and co-exist with VIP. *Regul. Pept.* **22,** 89–98.

Fang, V. S., Juan, C. C., Hsu, Y. P., Won, J. G. S., and Ho, L. T. (2001). The stimulatory effect of vasoactive intestinal peptide on the cortisol production of guinea pig zona fasciculata cells: An extra-ACTH regulatory model of the adrenocortical functions. *Chinese J. Physiol.* **44,** 73–79.

Feuilloley, M., Geymonat, M., Yon, L., Delarue, C., Fasolo, A., and Vaudry, H. (1992). *In vitro* study of the effect of adenosine on frog adrenocortical cells. *Gen. Comp. Endocrinol.* **86,** 453–459.

Firoz-Ahmad, M., Appa-Rao, V., Prasad, A., Alim, A., and Nussdorfer, G. G. (2000). Vasoactive intestinal peptide (VIP) increases cortisol blood concentration in the palm squirrel (*Funanbulus pennanti*, Wrongton): Evidence of a direct effect of VIP on adrenal gland. *Biomed. Res.* **21,** 173–175.

Frodin, M., Hannibal, J., Wulff, B., Gammeltoft, S., and Fahrenkrug, J. (1995). Neuronal localization of pituitary adenylate cyclase-activating polypeptide 38 in the adrenal medulla and growth-inhibitory effect on chromaffin cells. *Neuroscience* **65,** 599–608.

Fukushima, Y., Hikichi, H., Mizukami, K., Nagayama, T., Yoshida, M., Suzuki-Kusaba, M., Hisa, H., Kimura, T., and Satoh, S. (2001a). Role of endogenous PACAP in catecholamine secretion from the rat adrenal gland. *Am. J. Physiol.* **281,** R1562–R1567.

Fukushima, Y., Nagayama, T., Kawashima, H., Hikichi, H., Yoshida, M., Suzuki-Kusaba, M., Hisa, H., Kimura, T., and Satoh, S. (2001b). Role of calcium channels and adenylate cyclase in the PACAP-induced adrenal catecholamine secretion. *Am. J. Physiol.* **281,** R495–R501.

Fukushima, Y., Nagayama, T., Hikici, H., Mizukami, K., Yoshida, M., Suzuki-Kusaba, M., Hisa, H., Kimura, T., and Satoh, S. (2002). Role of K^+ channels in the PACAP-induced catecholamine secretion from the rat adrenal gland. *Eur. J. Pharmacol.* **437,** 69–72.

Gaspo, R., Yamaguchi, N., and De Champlain, J. (1995). Correlation between neural release of VIP and adrenomedullary catecholamine secretion *in vivo*. *Am. J. Physiol.* **268,** R1449–R1455.

Gaspo, R., La Marche, L., De Champlain, J., and Jamaguchi, N. (1997). Canine adrenal catecholamine response to VIP is blocked by PACAP(6–27) *in vivo*. *Am. J. Physiol.* **272,** R1606–R1612.

Geng, G. J., Gaspo, R., Trabelsi, F., and Yamaguchi, N. (1997). Role of L-type Ca^{2+} channel in PACAP-induced adrenal catecholamine release *in vivo*. *Am. J. Physiol.* **273,** R1339–R1345.

George, F. W., and Ojeda, S. R. (1987). Vasoactive intestinal peptide enhances aromatase activity in the neonatal rat ovary before development of primary follicles or responsiveness to follicle-stimulating hormone. *Proc. Natl. Acad. Sci. USA* **84,** 5803–5807.

Ghatei, M. A., Takahashi, K., Suzuki, Y, Gardiner, J., Jones, P. M., and Bloom, S. R. (1993). Distribution and molecular characterization of pituitary adenylate cyclase-activating

polypeptide and its precursor encoding messenger RNA in human and rat tissues. *J. Endocrinol.* **136,** 159–166.

Ginda, W. J., Nussdorfer, G. G., and Malendowicz, L. K. (1999). Effects of bilateral splanchnic-nerve section and chemical sympathectomy on PACAP-38 content in the rat adrenals. *Horm. Metab. Res.* **31,** 367–369.

Glaz, E., Racz, K., Varga, I., Kiss, R., Sergev, O., Futo, L., Szecseny, A., and Schaff, Z. (1988). Atrial natriuretic peptide directly inhibits corticosteroid biosynthesis in human aldosterone-producing adenoma. *Acta Med. Hung.* **45,** 377–386.

Gobbetti, A., and Zerani, M. (2002). Pituitary adenylate cyclase-activating polypeptide induces testicular testosterone synthesis through PGE2 mediation in crested newt, *Triturus carnifex*. *J. Exp. Zool.* **293,** 73–80.

Gobbetti, A., Zerani, M., Miano, A., Bramucci, M., Murri, O., and Amici, D. (1997). Presence of pituitary adenylate cyclase-activating polypeptide 38-immuno-like material in the brain and ovary of the female crested newt, *Triturus carnifex*: Its involvement in the ovarian synthesis of prostaglandins and steroids. *J. Endocrinol.* **152,** 141–146.

Gonzalez, B. J., Basile, M., Vaudry, D., Fournier, A., and Vaudry, H. (1998). Pituitary adenylate cyclase-activating polypeptide. *Ann. Endocrinol. (Paris)* **59,** 364–405.

Gordon, R. D., Bachmann, A. W., Klem, A. S., Tunny, T. J., Stowasser, M., Storie, W. J., and Rutherford, J. G. (1994). An association of primary aldosteronism and adrenaline–secreting pheochromocytoma. *Clin. Exp. Pharmacol. Physiol.* **21,** 219–222.

Gotoh, E., Yamagami, T., Yamamoto, H., and Okamoto, H. (1988). Chromosomal assignment of human VIP/PHM-27 gene to 6q26—q27 region by spot blot hybridization and *in situ* hybridization. *Biochem. Int.* **17,** 555–562.

Gozes, I., and Tsafriri, A. (1986). Detection of vasoactive intestinal peptide-encoding messenger ribonucleic acid in the rat ovaries. *Endocrinology* **119,** 2606–2610.

Gräs, S., Ovesen, P., Andersen, A. N., Sørensen, S., Fahrenkrug, J., and Ottesen, B. (1994). Vasoactive intestinal polypeptide and peptide histidine methionine. Presence in human follicular fluid and effects on DNA synthesis and steroid secretion in cultured human granulosa/lutein cells. *Hum. Reprod.* **9,** 1053–1057.

Gräs, S., Hannibal, J., Georg, B., and Fahrenkrug, J. (1996). Transient periovulatory expression of pituitary adenylate cyclase-activating polypeptide in rat ovarian cells. *Endocrinology* **17,** 4779–4785.

Gräs, S., Hannibal, J., and Fahrenkrug, J. (1999). Pituitary adenylate cyclase-activating polypeptide is an auto/paracrine stimulator of acute progesterone accumulation and subsequent lutinization in cultured periovulatory granulosa/lutein cells. *Endocrinology* **140,** 2199–2205.

Gräs, S., Hedetoft, C., Henneberg-Pedersen, S., and Fahrenkrug, J. (2000). Pituitary adenylate cyclase-activating polypeptide stimulates acute progesterone production in rat granulosa/lutein cells via two receptor subtypes. *Biol. Reprod.* **63,** 206–212.

Gray, S. L., Cummings, K. J., Jirik, F. R., and Sherwood, N. M. (2001). Targeted disruption of the pituitary adenylate cyclase-activating polypeptide gene results in early postnatal death associated with dysfunction of lipid and carbohydrate metabolism. *Mol. Endocrinol.* **15,** 1739–1747.

Grumolato, L., Elkahloun, A. G., Ghzili, H., Alexandre, D., Coulouarn, C., Yon, L., Salier, J. P., Eiden, L. E., Fournier, A., Vaudry, H., and Anouar, Y. (2003). Microarray and suppression subtractive hybridization analyses of gene expression in pheochromocytoma cells reveal pleiotropic effects of pituitary adenylate cyclase-activating polypeptide on cell proliferation, survival, and adhesion. *Endocrinology* **144,** 2368–2379.

Guo, X., and Wakade, A. R. (1994). Differential secretion of catecholamines in response to peptidergic and cholinergic transmitters in rat adrenals. *J. Physiol. (London)* **475,** 539–545.

Hacker, G. W., Bishop, A. E., Terenghi, G., Varndell, I. M., Aghahowa, J., Pollard, K., Thurner, J., and Polak, J. M. (1988). Multiple peptide production and presence of general neuroendocrine markers detected in 12 cases of human pheochromocytoma and in mammalian adrenal glands. *Virchows Arch.* **412,** 399–411.

Hahm, S. H., Hsu, C. M., and Eiden, L. E. (1998). PACAP activates calcium influx-dependent and -independent pathways to couple Met-enkephalin secretion and biosynthesis in chromaffin cells. *J. Mol. Neurosci.* **11,** 43–56.

Haidan, A., Hilbers, U., Bornstein, S. R., and Ehrhart-Bornstein, M. (1998). Human adrenocortical NCI-H295 cells express VIP receptors. Steroidogenic effect of vasoactive intestinal peptide (VIP). *Peptides* **19,** 1511–1517.

Hakanson, R., Sundler, F., and Vodman, R. (1982). Distribution and topography of peripheral VIP nerve fibers: Functional implication. *In* "Vasoactive Intestinal Peptide" (S. I. Said, Ed.), pp. 121–144. Raven Press, New York.

Hamelink, C., Tjurmina, O., Damadzic, R., Young, W. S., Weibe, E., Lee, H. W., and Eiden, L. E. (2002). Pituitary adenylate cyclase-activating polypeptide is a sympathoadrenal neurotransmitter involved in the catecholamine regulation and glucohomeostasis. *Proc. Natl. Acad. Sci. USA* **99,** 461–466.

Hamelink, C., Weihe, E., and Eiden, L. E. (2003). PACAP: An "emergency response" co-transmitter in the adrenal medulla. *In* "Pituitary Adenylate Cyclase-Activating Polypeptide" (H. Vaudry and A. Arimura, Eds.), pp. 227–249. Kluwer Academic Publisher, Norwell, MA.

Harmar, A. J., Arimura, A., Gozes, I., Journot, L., Laburthe, M., Pisegna, J. R., Rawlings, S. R., Robberecht, P., Said, S. I., Szeedharan, S. P., Wank, S. A., and Waschek, J. A. (1998). International union of pharmacology. XVIII. Nomenclature of receptors for vasoactive intestinal peptide and pituitary adenylate cyclase-activating polypeptide. *Pharmacol. Rev.* **50,** 265–270.

Harmar, A. J., Sheward, W. J., Morrison, C. F., Waser, B., Gugger, M., and Reubi, J. C. (2004). Distribution of the $VPAC_2$ receptor in peripheral tissues of the mouse. *Endocrinology* **145,** 1203–1210.

Hashimoto, H., Ishihara, T., Shigemoto, R., Mori, K., and Nagata, S. (1993). Molecular cloning and tissue distribution of a receptor for pituitary adenylate cyclase-activating polypeptide. *Neuron* **11,** 333–342.

Hashimoto, K., Murakami, K., Hattori, T., Niimi, M., Fujimo, K., and Ota, Z. (1984). Corticotropin-releasing factor (CRF)-like immunoreactivity in the adrenal medulla. *Peptides* **5,** 707–712.

Hassoun, J., Monges, G., Giraud, P., Henry, J. F., Charpin, C., Payan, H., and Toga, M. (1984). Immunohistochemical study of pheochromocytomas. An investigation of methionine-enkefalin, vasoactive intestinal peptide, somatostatin, corticotropin, beta-endorphin, and calcitonin in 16 tumors. *Am. J. Pathol.* **114,** 56–63.

Heindel, J. J., Sneeden, J., Powell, C. J., Davis, B., and Culler, M. D. (1996). A novel hypothalamic peptide, pituitary adenylate cyclase-activating peptide, regulates the function of rat granulosa cells *in vitro*. *Biol. Reprod.* **54,** 523–530.

Heym, C. (1997). Immunocytochemical correlates of an extrapituitary adrenocortical regulation in man. *Histol. Histopathol.* **12,** 567–581.

Hinson, J. P., and Kapas, S. (1995). Effects of sodium depletion on the response of rat adrenal zona glomerulosa cells to stimulation by neuropeptides: Actions of vasoactive intestinal peptide, enkephalin, substance P, neuropeptide Y, and corticotropin-releasing hormone. *J. Endocrinol.* **146,** 209–214.

Hinson, J. P., and Kapas, S. (1996). Effect of splanchnic nerve section and compensatory adrenal hypertrophy on rat adrenal neuropeptide content. *Regul. Pept.* **61,** 105–109.

Hinson, J. P., Kapas, S., Orford, C. D., and Vinson, G. P. (1992). Vasoactive intestinal peptide stimulation of aldosterone secretion by rat adrenal cortex may be mediated by the local release of catecholamines. *J. Endocrinol.* **133,** 253–258.

Hinson, J. P., Cameron, L. A., Purbrick, A., and Kapas, S. (1994a). The role of neuropeptides in the regulation of adrenal vascular tone: Effects of vasoactive intestinal polypeptide, substance P, neuropeptide Y, neurotensin, Met-enkephalin, and Leu-enkephalin on perfusion medium flow rate in the intact perfused rat adrenal. *Regul. Pept.* **51,** 55–61.

Hinson, J. P., Purbrick, A., Cameron, L. A., and Kapas, S. (1994b). The role of neuropeptides in the regulation of adrenal zona fasciculata/reticularis function: Effects of vasoactive intestinal polypeptide, substance P, neuropeptide Y, Met- and Leu-enkephalin, and neurotensin on corticosterone secretion in the intact perfused rat adrenal gland *in situ*. *Neuropeptides* **26,** 391–397.

Hinson, J. P., Ho, M. M., Vinson, G. P., and Kapas, S. (1996). Vasoactive intestinal peptide is a local regulator of adrenocortical function. *Endocr. Res.* **22,** 831–838.

Hinson, J. P., Puddefoot, J. R., and Kapas, S. (1999). Actions of vasoactive intestinal peptide on the rat adrenal zona glomerulosa. *J. Endocrinol.* **161,** 51–57.

Hinson, J. P., Renshaw, D., Carroll, M., and Kapas, S. (2001). Regulation of rat adrenal vasoactive intestinal peptide content: Effects of adrenocorticotropic hormone treatment and changes in dietary sodium intake. *J. Neuroendocrinol.* **13,** 769–773.

Hokfelt, T., Lundberg, J. M., Schultzberg, J. M., and Fahrenkrug, J. (1981). Immunohistochemical evidence for a local VIP-ergic neuron system in the adrenal gland of the rat. *Acta Physiol. Scand.* **113,** 575–576.

Holgert, H., Holmberg, K., Hannibal, J., Fahrenkrug, J., Brimijoin, J., Hartman, B. K., and Hokfelt, T. (1996). PACAP in the adrenal gland: Relationship with choline acetyltransferase, enkephalin, and chromaffin cells and effects of immunologic sympathectomy. *Neuroreport* **20,** 297–301.

Holzwarth, M. A. (1984). The distribution of vasoactive intestinal peptide in the rat adrenal cortex and medulla. *J. Auton. Nerv. Syst.* **11,** 269–283.

Hong, M., Yon, L., Fournier, A., Vaudry, H., and Pelletier, G. (1998). Effect of pituitary adenylate cyclase-activating polypeptide (PACAP) on tyrosine hydroxylase gene expression in the rat adrenal medulla. *Ann. N.Y. Acad. Sci.* **865,** 478–481.

Hosoya, M., Kimura, C., Ogi, K., Ohkubo, S., Miyamoto, Y., Shimizu, M., Onda, H., Oshimura, M., Arimura, A., and Fujino, M. (1992). Structure of the human pituitary adenylate cyclase–activating polypeptide (PACAP) gene. *Biochim. Biophys. Acta* **1129,** 199–206.

Houchi, H., Oka, M., Misbahuddin, M., Morita, K., and Nakanishi, A. (1987). Stimulation by vasoactive intestinal polypeptide of catecholamine synthesis in isolated bovine adrenal chromaffin cells: Possible involvement of protein kinase C. *Biochem. Pharmacol.* **36,** 1551–1554.

Houchi, H., Hamano, S., Masuda, Y., Ishimura, Y., Azuma, M., Ohuchi, T., and Oka, M. (1994). Stimulatory effect of pituitary adenylate cyclase-activating polypeptide on catecholamine synthesis in cultured bovine adrenal chromaffin cells: Involvement of tyrosine hydroxylase phosphorylation caused by Ca^{2+} influx and cAMP. *Jpn. J. Pharmacol.* **66,** 323–330.

Houchi, H., Okuno, M., Kitamura, K., Minakuchi, K., Ishimura, Y., Ohuchi, T., and Oka, M. (1995). Calcium efflux from cultured bovine adrenal chromaffin cells induced by pituitary adenylate cyclase-activating polypeptide (PACAP): Possible involvement of an Na^{+}/Ca^{2+} exchange mechanism. *Life Sci.* **56,** 1825–1834.

Huffman, L. J., Connors, J. M., and Hedge, G. A. (1988). VIP and its homologues increase vascular conductance in certain endocrine and exocrine glands. *Am. J. Physiol.* **254,** E435–E442.

Hurley, J. D., Gardiner, J. V., Jones, P. M., and Bloom, S. R. (1995). Cloning and molecular characterization of complementary deoxyribonucleic acid corresponding to a novel form of pituitary adenylate cyclase-activating polypeptide messenger ribonucleic acid in the rat testis. *Endocrinology* **136,** 550–557.

Inoue, J., Oishi, S., Naomi, S., Umeda, T., and Sato, T. (1986). Pheochromocytoma associated with adrenocortical adenoma: Case report and literature review. *Endocrinol. Jpn.* **33,** 67–74.

Inoue, M., Fujishiro, N., Ogawa, K., Muroi, M., Sakamoto, Y., Imanaga, I., and Shioda, S. (2000). Pituitary adenylate cyclase-activating polypeptide as a neuromodulator in guinea pig adrenal medulla. *J. Physiol. (London)* **528,** 473–487.

Isobe, K., Nakai, T., and Takuwa, Y. (1993). Ca^{2+}-dependent stimulatory effect of pituitary adenylate cyclase-activating polypeptide on catecholamine secretion from cultured porcine adrenal medullary chromaffin cells. *Endocrinology* **132,** 1757–1765.

Isobe, K., Nomura, F., Takekoshi, K., and Nakai, T. (1994). Pertussis toxin pre-treatment enhances catecholamine secretion induced by pituitary adenylate cyclase-activating polypeptide in cultured porcine adrenal medullary chromaffin cells: A possible role of the inositol lipid cascade. *Neuropeptides* **27,** 269–275.

Isobe, K., Yukimasa, N., Nakai, T., and Takuwa, Y. (1996). Pituitary adenylate cyclase-activating polypeptide induces gene expression of the catecholamine synthesizing enzymes, tyrosine hydroxylase, and dopamine beta-hydroxylase, through 3′,5′-cyclic adenosine monophosphate- and protein kinase C-dependent mechanisms in cultured porcine adrenal medullary chromaffin cells. *Neuropeptides* **30,** 167–175.

Isobe, K., Tatsuno, I., Yashiro, T., Nanmoku, T., Takekoshi, K., Kawakami, Y., and Nakai, T. (2003). Expression of mRNA for PACAP and its receptors in intra- and extra-adrenal human pheochromocytomas and their relationship to catecholamine synthesis. *Regul. Pept.* **110,** 213–217.

Isobe, K., Kaneko, M., Kaneko, S., Nissato, S., Nanmoku, T., Takekoshi, K., Okuda, Y., and Kawakami, Y. (2004). Expression of mRNAs for PACAP and its receptor in human neuroblastomas and their relationship to catecholamine synthesis. *Regul. Pept.* **123,** 29–32.

Itoh, S., and Hirota, R. (1983). Inhibitory effect of cholecystokinin octapeptide on vasoactive intestinal peptide-induced stimulation of adrenocortical secretion. *Jpn. J. Physiol.* **33,** 301–304.

Itoh, S., Hirota, R., and Katsuura, G. (1982). Effects of cholecystokinin octapeptide and vasoactive intestinal polypeptide on adrenocortical secretion in the rat. *Jpn. J. Physiol.* **32,** 553–560.

Johnson, A. L., and Tilly, J. L. (1988). Effects of vasoactive intestinal peptide on steroid secretion and plasminogen activator activity in granulosa cells of the hen. *Biol. Reprod.* **38,** 296–303.

Jorgensen, M. S., Liu, J., Adams, J. M., Titlow, W. B., and Jackson, B. A. (2002). Inhibition of voltage-gated Ca^{2+} current by PACAP in rat adrenal chromaffin cells. *Regul. Pept.* **103,** 59–65.

Kasson, B. G., Lim, P., and Hsueh, A. J. W. (1986). Vasoactive intestinal peptide stimulates androgen biosynthesis by cultured neonatal testicular cells. *Mol. Cell. Endocrinol.* **48,** 21–29.

Kawai, K., Yokota, C., Ohashi, S., Isobe, K., Suzuki, S., Nakai, T., and Yamashita, K. (1994). Pituitary adenylate cyclase-activating polypeptide: Effects on pancreatic-adrenal hormone secretion and glucose-lipid metabolism in normal conscious dogs. *Metabolism* **43,** 739–744.

Ko, C., and Park-Sarge, O. K. (2000). Progesterone receptor activation mediates LH-induced type-I pituitary adenylate cyclase-activating polypeptide receptor (PAC_1) gene expression in rat granulosa cells. *Biochem. Biophys. Res. Commun.* **277,** 270–279.

Koh, P. O., Kwang, S. D., Kang, S. S., Cho, G. J., Chun, S. Y., Kwon, H. B., and Choi, W. S. (2000). Expression of pituitary adenylate cyclase-activating polypeptide (PACAP) and PACAP type IA receptor mRNAs in granulosa cells of preovulatory follicles of the rat ovary. *Mol. Reprod. Dev.* **55,** 379–386.

Kondo, H. (1985). Immunohistochemical analysis of the localization of neuropeptides in the adrenal gland. *Arch. Histol. Jpn.* **48,** 453–481.

Kondo, H., Kuramoto, H., and Fujita, T. (1986). An immuno-electron-microscopic study of the localization of VIP-like immunoreactivity in the adrenal gland of the rat. *Cell Tissue Res.* **245,** 531–538.

Kong, J. K., Thureson-Klein, A., and Klein, R. L. (1989). Differential distribution of neuropeptides and serotonin in pig adrenal glands. *Neuroscience* **28,** 765–775.

Kotani, E., Usuki, S., and Kubo, T. (1997a). Detection of pituitary adenylate cyclase-activating polypeptide messenger ribonucleic acid (PACAP mRNA) and PACAP receptor mRNA in the rat ovary. *Biomed. Res.* **18,** 199–204.

Kotani, E., Usuki, S., and Kubo, T. (1997b). Effect of pituitary adenylate cyclase-activating polypeptide (PACAP) on production of progesterone in cultured luteal cells from rat ovary. *Biomed. Res.* **18,** 335–341.

Kotani, E., Usuki, S., and Kubo, T. (1997c). Rat corpus luteum expresses both PACAP and PACAP type IA receptor mRNAs. *Peptides* **18,** 1453–1455.

Kotani, E., Usuki, S., and Kubo, K. (1998). Effect of pituitary adenylate cyclase-activating polypeptide (PACAP) on progestin biosynthesis in cultured granulosa cells from the rat ovary and expression of mRNA encoding PACAP type IA receptor. *J. Reprod. Fertil.* **112,** 107–114.

Kowal, J., Horst, I., Pensky, J., and Alfonzo, M. A. (1977). A comparison of the effects of ACTH, VIP, and cholera toxin on adrenal cAMP and steroid synthesis. *Ann. N.Y. Acad. Sci.* **297,** 314–328.

Lamouche, S., and Yamaguchi, N. (2001). Role of PAC_1 receptor in adrenal catecholamine secretion induced by PACAP and VIP *in vivo*. *Am. J. Physiol.* **280,** R510–R518.

Lamouche, S., and Yamaguchi, N. (2003). PACAP release from the canine adrenal gland *in vivo*: Its functional role in severe hypotension. *Am. J. Physiol.* **284,** R588–R597.

Lamouche, S., Martineau, D., and Yamaguchi, N. (1999). Modulation of adrenal catecholamine release by PACAP *in vivo*. *Am. J. Physiol.* **276,** R162–R170.

Larcher, A., Delarue, C., Idres, S., and Vaudry, H. (1992). Interactions between vasotocin and other corticotropic factors on the frog adrenal gland. *J. Steroid Biochem. Mol. Biol.* **41,** 795–798.

Leboulenger, F., Leroux, P., Delarue, C., Tonon, M. C., Charnay, Y., Dubois, P. M., Coy, H. D., and Vaudry, H. (1983a). Colocalization of vasoactive intestinal peptide (VIP) and enkephalin in chromaffin cells of the adrenal gland of amphibian. Stimulation of corticosteroid production by VIP. *Life Sci.* **32,** 375–383.

Leboulenger, F., Leroux, P., Tonon, M. C., Coy, H. D., Vaudry, H., and Pelletier, G. (1983b). Coexistence of vasoactive intestinal peptide and enkephalins in the adrenal chromaffin granules of the frog. *Neurosci. Lett.* **37,** 221–225.

Leboulenger, F., Perroteau, I., Netchitailo, P., Lihrmann, I., Leroux, P., Delarue, C., Coy, H. D., and Vaudry, H. (1984). Action of vasoactive intestinal peptide (VIP) on amphibian adrenocortical function *in vitro*. *Peptides* **4,** 299–303.

Leboulenger, F., Benyamina, M., Delarue, C., Netchitailo, P., Saint-Pierre, S., and Vaudry, H. (1988). Neuronal and paracrine regulation of adrenal steroidogenesis: Interactions between acetylcholine, serotonin, and vasoactive intestinal polypeptide (VIP) on corticosteroid production by frog interrenal tissue. *Brain Res.* **453,** 103–109.

Lee, H. W., Hahm, S. H., Hsu, C. M., and Eiden, L. E. (1999a). Pituitary adenylate cyclase-activating polypeptide regulation of vasoactive intestinal polypeptide transcription requires Ca^{2+} influx and activation of the serine/threonin phosphatase calcineurin. *J. Neurochem.* **73,** 1769–1772.

Lee, L., Park, H. J., Choi, H. S., Kwon, H. B., Arimura, A., Lee, B. J., Choi, W. S., and Chun, S. Y. (1999b). Gonadotropin stimulation of pituitary adenylate cyclase-activating polypeptide (PACAP) messenger ribonucleic acid in the rat ovary and the role of PACAP as follicle survival factor. *Endocrinology* **140,** 818–826.

Lesouhaitier, O., Esneu, M., Kodjo, M. K., Hamel, C., Contesse, V., Yon, L., Remy-Jouet, I., Fasolo, A., Fournier, A., Vandesande, F., Pelletier, G., Conlon, J. M., Roubos, E. W., Feuilloley, M., Delarue, C., Leboulenger, F., and Vaudry, H. (1995). Neuroendocrine communication in the frog adrenal gland. *Zool. Sci.* **12,** 255–264.

Li, Q., Johansson, H., and Grimelius, L. (1999). Innervation of human adrenal gland and adrenal cortical lesions. *Virchows Arch.* **435,** 580–589.

Li, Z. G., Queen, G., and La Bella, F. S. (1990). Adrenocorticotropin, vasoactive intestinal polypeptide, growth hormone-releasing factor, and dynorphin compete for common receptors in brain and adrenal. *Endocrinology* **126,** 1327–1333.

Lightly, E. R. T., Walker, S. W., Bird, I. M., and Williams, B. C. (1990). Subclassification of β-adrenoceptors responsible for steroidogenesis in primary cultures of bovine adrenocortical zona fasciculata/reticularis cells. *Br. J. Pharmacol.* **99,** 709–712.

Linnoila, R. I., De Augustine, R. P., Hervonen, A., and Miller, R. J. (1980). Distribution of (Met^5)- and (Leu^5)-enkephalin, vasoactive intestinal polypeptide- and substance P-like immunoreactivities in human adrenal glands. *Neuroscience* **5,** 2247–2259.

MacArthur, L., and Eiden, L. E. (1996). Neuropeptide genes: Targets of activity-dependent signal transduction. *Peptides* **17,** 721–728.

Mackay, M., Fantes, J., Scherer, S., Boyle, S., West, K., Tsui, L. C., Belloni, E., Lutz, E., Van Heiningen, V., and Harman, A. J. (1996). Chromosomal localization in mouse and human of the vasoactive intestinal peptide receptor type 2 gene: A possible contributor to the holoprosencephaly 3 phenotype. *Genomics* **37,** 345–353.

Magistretti, P. J., Hof, P. R., Martin, J. L., Dietl, M., and Palacios, J. M. (1988). High and low affinity binding sites for vasoactive intestinal peptide (VIP) in the rat kidney revealed by light microscopic autoradiography. *Regul. Pept.* **23,** 145–152.

Malendowicz, L. K., and Nussdorfer, G. G. (1993). Unusual effect of prolonged vasoactive intestinal peptide (VIP) administration on the adrenal growth and corticosterone secretion in the rat. *Neuropeptides* **25,** 145–150.

Malendowicz, L. K., Andreis, P. G., Markowska, A., Nowak, M., Warchol, J. B., Neri, G., and Nussdorfer, G. G. (1994). Effects of neuromedin U-8 on the secretory activity of the rat adrenal cortex: Evidence for an indirect action requiring the presence of the zona medullaris. *Res. Exp. Med.* **194,** 69–79.

Malhotra, R. K., and Wakade, A. R. (1987). Vasoactive intestinal polypeptide stimulates the secretion of catecholamines from the rat adrenal gland. *J. Physiol. (London)* **388,** 285–294.

Malhotra, R. K., Wakade, T. D., and Wakade, A. R. (1988). Vasoactive intestinal polypeptide and muscarine mobilize intracellular Ca^{2+} through breakdown of phosphoinositides to induce catecholamine secretion: Role of IP3 in exocytosis. *J. Biol. Chem.* **263,** 2123–2126.

Malhotra, R. K., Wakade, T. D., and Wakade, A. R. (1989). Cross-communication between acetylcholine and VIP in controlling catecholamine secretion by affecting cAMP, inositol triphosphate, protein kinase C, and calcium in rat adrenal medulla. *J. Neurosci.* **9,** 4150–4157.

Marley, P. D., Cheung, C. Y., Thomson, K. A., and Murphy, R. (1996). Activation of tyrosine hydroxylase by pituitary adenylate cyclase-activating polypeptide (PACAP-27) in bovine adrenal chromaffin cells. *J. Auton. Nerv. System* **60,** 141–146.

Maubert, E., Tramu, G., Croix, D., Beauvillan, C. J., and Dupouy, J. P. (1990). Co-localization of vasoactive intestinal polypeptide in the nerve fibers of the rat adrenal gland. *Neurosci. Lett.* **113,** 121–126.

Mazzocchi, G., Robba, C., Malendowicz, L. K., and Nussdorfer, G. G. (1987). Stimulatory effect of vasoactive intestinal peptide (VIP) on the growth and steroidogenic capacity of rat adrenal zona glomerulosa. *Biomed. Res.* **8,** 19–23.

Mazzocchi, G., Malendowicz, L. K., Meneghelli, V., Gottardo, G., and Nussdorfer, G. G. (1993a). Vasoactive intestinal polypeptide (VIP) stimulates hormonal secretion of the rat adrenal cortex *in vitro*: Evidence that adrenal chromaffin cells are involved in the mediation of

the mineralocorticoid but not glucocorticoid secretagogue action of VIP. *Biomed. Res.* **14,** 435–440.

Mazzocchi, G., Musajo, F. G., Malendowicz, L. K., Andreis, P. G., and Nussdorfer, G. G. (1993b). IL-1β stimulates corticotropin-releasing hormone (CRH) and adrenocorticotropin (ACTH) release by rat adrenal gland *in vitro*. *Mol. Cell. Neurosci.* **4,** 267–270.

Mazzocchi, G., Malendowicz, L. K., Andreis, P. G., Meneghelli, V., Markowska, A., Belloni, A. S., and Nussdorfer, G. G. (1994a). Neuropeptide K enhances glucocorticoid release by acting directly on the rat adrenal gland: The possible involvement of zona medullaris. *Brain Res.* **661,** 91–96.

Mazzocchi, G., Malendowicz, L. K., Markowska, A., and Nussdorfer, G. G. (1994b). Effect of hypophysectomy on corticotrophin-releasing hormone and adrenocorticotropin immunoreactivities in the rat adrenal gland. *Mol. Cell. Neurosci.* **5,** 345–349.

Mazzocchi, G., Malendowicz, L. K., and Nussdorfer, G. G. (1994c). Stimulatory effect of vasoactive intestinal peptide (VIP) on the secretory activity of dispersed rat adrenocortical cells: Evidence for the interaction of VIP with ACTH receptors. *J. Steroid Biochem. Mol. Biol.* **48,** 507–510.

Mazzocchi, G., Malendowicz, L. K., Belloni, A. S., and Nussdorfer, G. G. (1995a). Adrenal medulla is involved in the aldosterone secretagogue effect of substance P. *Peptides* **16,** 351–355.

Mazzocchi, G., Malendowicz, L. K., Meneghelli, V., Gottardo, G., and Nussdorfer, G. G. (1995b). *In vitro* and *in vivo* studies of the effects of arginine-vasopressin on the secretion and growth of rat adrenal cortex. *Histol. Histopathol.* **10,** 359–370.

Mazzocchi, G., Malendowicz, L. K., Macchi, C., Gottardo, G., and Nussdorfer, G. G. (1996a). Further investigations on the effects of neuropeptide-Y (NPY) on the secretion and growth of rat adrenal zona glomerulosa. *Neuropeptides* **30,** 19–27.

Mazzocchi, G., Musajo, F. G., Neri, G., Gottardo, G., and Nussdorfer, G. G. (1996b). Adrenomedullin stimulates steroid secretion by the isolated perfused rat adrenal gland *in situ*: Comparison with calcitonin gene-related peptide effects. *Peptides* **17,** 853–857.

Mazzocchi, G., Gottardo, G., and Nussdorfer, G. G. (1997a). Pituitary adenylate cyclase-activating polypeptide enhances steroid production by interrenal glands in fowls: Evidence for an indirect mechanism of action. *Horm. Metab. Res.* **29,** 86–87.

Mazzocchi, G., Gottardo, G., and Nussdorfer, G. G. (1997b). Catecholamines stimulate steroid secretion of dispersed fowl interrenal cells, acting through the β-receptor subtype. *Horm. Metab. Res.* **29,** 168–170.

Mazzocchi, G., Malendowicz, L. K., Rebuffat, P., Gottardo, G., and Nussdorfer, G. G. (1997c). Neurotensin stimulates CRH and ACTH release by rat adrenal medulla *in vitro*. *Neuropeptides* **31,** 8–11.

Mazzocchi, G., Malendowicz, L. K., Rebuffat, P., Tortorella, C., and Nussdorfer, G. G. (1997d). Arginine-vasopressin stimulates CRH and ACTH release by rat adrenal medulla, acting via the V1 receptor subtype and a protein kinase C-dependent pathway. *Peptides* **18,** 191–195.

Mazzocchi, G., Gottardo, G., and Nussdorfer, G. G. (1998a). Paracrine control of steroid hormone secretion by chromaffin cells in the adrenal gland of lower vertebrates. *Histol. Histopathol.* **13,** 209–220.

Mazzocchi, G., Malendowicz, L. K., Musajo, F. G., Gottardo, G., Markowska, A., and Nussdorfer, G. G. (1998b). The role of endothelins in the regulation of vascular tone in the *in situ* perfused rat adrenals. *Am. J. Physiol.* **274,** E1–E5.

Mazzocchi, G., Rebuffat, P., Gottardo, G., and Nussdorfer, G. G. (1998c). Vasoactive intestinal peptide stimulates rat adrenal glucocorticoid secretion, through an ACTH receptor-dependent activation of the adenylate cyclase signaling pathway. *Horm. Metab. Res.* **30,** 241–243.

Mazzocchi, G., Andreis, P. G., De Caro, R., Aragona, F., Gottardo, L., and Nussdorfer, G. G. (1999). Cerebellin enhances *in vitro* secretory activity of human adrenal gland. *J. Clin. Endocrinol. Metab.* **84,** 632–635.

Mazzocchi, G., Malendowicz, L. K., Neri, G., Andreis, P. G., Ziolkowska, A., Gottardo, L., Nowack, K. W., and Nussdorfer, G. G. (2002a). Pituitary adenylate cyclase-activating polypeptide and PACAP receptor expression and function in the rat adrenal gland. *Int. J. Mol. Med.* **9,** 233–243.

Mazzocchi, G., Malendowicz, L. K., Rebuffat, P., Gottardo, L., and Nussdorfer, G. G. (2002b). Expression and function of VIP, PACAP and their receptors in the human adrenal gland. *J. Clin. Endocrinol. Metab.* **87,** 2575–2580.

Mellon, S. H., Shively, J. E., and Miller, W. L. (1991). Human proopiomelanocortin(79–96), a proposed androgen stimulatory hormone, does not affect steroidogenesis in cultured human fetal adrenal cells. *J. Clin. Endocrinol. Metab.* **72,** 19–22.

Misbahuddin, M., Oka, M., Nakanishi, A., and Morita, K. (1988). Stimulatory effect of vasoactive intestinal polypeptide on catecholamine secretion from isolated guinea pig adrenal chromaffin cells. *Neurosci. Lett.* **92,** 202–206.

Miyata, A., Arimura, A., Dahl, D. H., Minamino, N., Uehara, A., Jiang, L., Culler, M. D., and Coy, D. H. (1989). Isolation of a novel 38-residue hypothalamic peptide that stimulates adenylate cyclase in pituitary cells. *Biochem. Biophys. Res. Commun.* **164,** 567–574.

Miyata, A., Dahl, D. H., Jiang, L., Kitada, C., Kubo, K., Fujino, M., Minamino, N., and Arimura, A. (1990). Isolation of a neuropeptide corresponding to the N-terminal 27 residues of the pituitary adenylate cyclase-activating polypeptide with 38 residues (PACAP38). *Biochem. Biophys. Res. Commun.* **170,** 643–648.

Moller, K., and Sundler, F. (1996). Expression of pituitary adenylate cyclase-activating peptide (PACAP) and PACAP type I receptors in the rat adrenal medulla. *Regul. Pept.* **63,** 129–139.

Montpetit, C. J., and Perry, S. F. (2000). Vasoactive intestinal polypeptide- and pituitary adenylate cyclase-activating polypeptide-mediated control of catecholamine release from chromaffin tissue in the rainbow trout, *Oncorhynchus mykiss*. *J. Endocrinol.* **166,** 705–714.

Montpetit, C. J., Shahsavarani, A., and Perry, S. F. (2003). Localisation of VIP-binding sites exhibiting properties of VPAC receptors in chromaffin cells of rainbow trout (*Oncorhynchus mykiss*). *J. Exp. Biol.* **206,** 1917–1927.

Moreno, A. M., Castilla-Guerra, L., Martinez-Torres, M. C., Torres-Olivera, F., Fernandez, E., and Galera-Davidson, H. (1999). Expression of neuropeptides and other neuroendocrine markers in human phaeochromocytomas. *Neuropeptides* **33,** 159–163.

Morera, A. M., Cathiard, A. M., Laburthe, M., and Saez, J. M. (1979). Interaction of vasoactive intestinal peptide (VIP) with a mouse adrenal cell line (Y-1): Specific binding and biologic effects. *Biochem. Biophys. Res. Commun.* **90,** 78–85.

Morita, K., Sakakibara, A., Kitayama, S., Kumagai, K., Tanne, K., and Dohi, T. (2002). Pituitary adenylate cyclase-activating polypeptide induces a sustained increase in intracellular free Ca^{2+} concentration and catecholamine release by activating Ca^{2+} influx via receptor-stimulated Ca^{2+} entry, independent of store-operated Ca^{2+} channels, and voltage-dependent Ca^{2+} channels in bovine adrenal medullary chromaffin cells. *J. Pharmacol. Exp. Ther.* **302,** 972–982.

Murakami, Y., Nishiki, M., Yamauchi, K., Koshimura, N., Yanaihara, N., and Kato, Y. (1996). Effects of pituitary adenylate cyclase-activating polypeptide on prolactin, growth hormone, and cortisol secretion in normal male subjects. *Biomed. Res.* **17,** 161–164.

Murase, T., Kondo, K., Otake, K., and Oiso, Y. (1993). Pituitary adenylate cyclase-activating polypeptide stimulates arginine vasopressin release in conscious rats. *Neuroendocrinology* **57,** 1092–1096.

Muroi, M., Arimura, A., and Shioda, S. (1999). PACAP receptor expression in the rat adrenal medulla by *in situ* hybridization and immunocytochemistry. *Regul. Pept.* **83,** 54(Abst. 66).

Neri, G., Andreis, P. G., Prayer-Galetti, T., Rossi, G. P., Malendowicz, L. K., and Nussdorfer, G. G. (1996). Pituitary adenylate cyclase-activating peptide enhances aldosterone secretion of human adrenal gland: Evidence for an indirect mechanism, probably involving the local release of catecholamines. *J. Clin. Endocrinol. Metab.* **81,** 169–173.

Netchitailo, P., Perroteau, I., Feuilloley, M., Pelletier, G., and Vaudry, H. (1985). *In vitro* effect of cytochalasin B on adrenal steroidogenesis in frog. *Mol. Cell. Endocrinol.* **43,** 205–213.

Nicol, M. R., Cobb, V.J, Williams, B. C., Morley, S. D., Walker, S. W., and Mason, J. I. (2004). Vasoactive intestinal peptide (VIP) stimulates cortisol secretion from the H295 human adrenocortical tumour cell line via $VPAC_1$ receptors. *J. Mol. Endocrinol.* **32,** 869–877.

Nilsson, S. F. (1994). PACAP-27 and PACAP-38: Vascular effects in the eye and some other tissues in the rabbit. *Eur. J. Pharmacol.* **21,** 17–25.

Nogi, H., Hashimoto, H., Fujita, T., Hagihara, N., Matsuda, T., and Baba, A. (1997). Pituitary adenylate cyclase-activating polypeptide (PACAP) receptor mRNA in the rat adrenal gland: Localization by *in situ* hybridization and identification of splice variants. *Jpn. J. Pharmacol.* **75,** 203–208.

Nowak, K. W., Neri, G., Nussdorfer, G. G., and Malendowicz, L. K. (1999). Comparison of the effects of VIP and PACAP on steroid secretion of dispersed rat adrenocortical cells. *Biomed. Res.* **20,** 127–132.

Nowak, M., Markowska, A., Nussdorfer, G. G., Tortorella, C., and Malendowicz, L. K. (1994). Evidence that endogenous vasoactive intestinal peptide (VIP) is involved in the regulation of rat pituitary-adrenocortical function: *In vivo* studies with a VIP antagonist. *Neuropeptides* **27,** 297–303.

Nussdorfer, G. G. (1986). Cytophysiology of the adrenal cortex. *Int. Rev. Cytol.* **98,** 1–405.

Nussdorfer, G. G. (1996). Paracrine control of adrenal cortical function by medullary chromaffin cells. *Pharmacol. Rev.* **48,** 495–530.

Nussdorfer, G. G. (2001). Proadrenomedullin-derived peptides in the paracrine control of the hypothalamo-pituitary-adrenal axis. *Int. Rev. Cytol.* **206,** 249–284.

Nussdorfer, G. G. (2003). Function of PACAP in the adrenal cortex. *In* "Pituitary Adenylate Cyclase-Activating Polypeptide" (H. Vaudry and A. Arimura, Eds.), pp. 207–225. Kluwer Academic Publisher, Norwell, MA.

Nussdorfer, G. G., and Malendowicz, L. K. (1998a). Role of tachykinins in the regulation of the hypothalamo-pituitary-adrenal axis. *Peptides* **19,** 949–968.

Nussdorfer, G. G., and Malendowicz, L. K. (1998b). Role of VIP, PACAP and related peptides in the regulation of the hypothalamo-pituitary-adrenal axis. *Peptides* **19,** 1443–1467.

Nussdorfer, G. G., and Mazzocchi, G. (1987). Vasoactive intestinal peptide (VIP) stimulates aldosterone secretion by rat adrenal gland *in vivo*. *J. Steroid Biochem.* **26,** 203–205.

Nussdorfer, G. G., and Mazzocchi, G. (1998). Immune-endocrine interactions in the mammalian adrenal gland: Facts and hypotheses. *Int. Rev. Cytol.* **183,** 143–184.

Nussdorfer, G. G., Rossi, G. P., and Belloni, A. S. (1997a). The role of endothelins in the paracrine control of the secretion and growth of the adrenal cortex. *Int. Rev. Cytol.* **171,** 267–308.

Nussdorfer, G. G., Rossi, G. P., and Mazzocchi, G. (1997b). Role of the adrenomedullin and related peptides in the regulation of the hypothalamo-pituitary-adrenal axis. *Peptides* **18,** 1079–1089.

Nussdorfer, G. G., Rossi, G. P., Malendowicz, L. K., and Mazzocchi, G. (1999). Autocrine-paracrine endothelin system in the physiology and pathology of steroid-secreting tissues. *Pharmacol. Rev.* **51,** 403–438.

Nussdorfer, G. G., Bahçelioglu, M., Neri, G., and Malendowicz, L. K. (2000). Secretin, glucagon, gastrin inhibitory polypeptide, parathyroid hormone, and related peptides in the regulation of the hypothalamo-pituitary-adrenal axis. *Peptides* **21,** 309–324.

O'Farrell, M., and Marley, P. D. (1997). Multiple calcium channels are required for pituitary adenylate cyclase-activating polypeptide-induced catecholamine secretion from bovine cultured adrenal chromaffin cells. *Naunyn-Schmiedeberg's Arch. Pharmacol.* **56,** 536–542.

Ojeda, S. R., Hernan, L., and Ahmed, C. E. (1989). Potential relevance of vasoactive intestinal peptide to ovarian physiology. *Semin. Reprod. Endocrinol.* **7,** 52–60.

Olasmaa, M., Guidotti, A., and Costa, E. (1992). Vasoactive intestinal polypeptide facilitates tyrosine hydroxylase induction by cholinergic agonists in bovine adrenal chromaffin cells. *Mol. Pharmacol.* **41,** 456–464.

Onoue, S., Waki, Y., Nagano, Y., Satoh, S., and Kashimoto, K. (2001). The neuromodulatory effects of VIP/PACAP on PC12 cells are associated with their N-terminal structures. *Peptides* **22,** 867–872.

Onoue, S., Endo, K., Yajima, T., and Kashimoto, K. (2002). Pituitary adenylate cyclase-activating polypeptide regulates the basal production of nitric oxide in PC12 cells. *Life Sci.* **71,** 205–214.

Oomori, Y., Okuno, S., Fujisawa, H., Iuchi, H., Ishikawa, K., Satoh, Y., and Ono, K. (1994). Ganglion cells immunoreactive for catecholamine-synthesizing enzymes, neuropeptide Y, and vasoactive intestinal polypeptide in the rat adrenal gland. *Cell Tissue Res.* **275,** 201–213.

Osipenko, O. N., Barrie, A. P., Allen, J. M., and Gurney, A. M. (2000). Pituitary adenylate cyclase-activating polypeptide activates multiple intracellular signaling pathways to regulate ion channels in PC12 cells. *J. Biol. Chem.* **275,** 16626–16631.

Ottesen, B., and Fahrenkrug, J. (1995). Vasoactive intestinal polypeptide and other preprovasoactive intestinal polypeptide-derived peptides in the female and male genital tract: Localization, biosynthesis, and functional and clinical significance. *Am. J. Obstet. Gynecol.* **172,** 1615–1631.

Ottesen, B., Pedersen, B., Nielsen, J., Dalgaard, D., and Fahrenkrug, J. (1986). Effect of vasoactive intestinal polypeptide (VIP) on steroidogenesis in women. *Regul. Pept.* **16,** 299–304.

Parker, L. N., and Odell, W. D. (1980). Control of androgen secretion. *Endocr. Rev.* **1,** 392–410.

Payet, M. D., Bilodeau, L., Breault, L., Fournier, A., Yon, L., Vaudry, H., and Gallo-Payet, N. (2003). PAC_1 receptor activation by PACAP-38 mediates Ca^{2+} release from a cAMP-dependent pool in human fetal adrenal gland chromaffin cells. *J. Biol. Chem.* **278,** 1663–1670.

Penhoat, A., Sanchez, P., Jaillard, C., Langlois, D., Bégeot, M., and Saez, J. M. (1991). Human proopiomelanocortin(79–96), a proposed androgen-stimulating hormone, does not affect steroidogenesis in cultured human adult adrenal cells. *J. Clin. Endocrinol. Metab.* **72,** 23–26.

Perrin, D., Germeshausen, A., Soling, H. D., Wuttke, W., and Jarry, H. (1995). Enhanced cAMP production mediates the stimulatory action of pituitary adenylate cyclase-activating polypeptide (PACAP) on *in vitro* catecholamine secretion from bovine adrenal chromaffin cells. *Exp. Clin. Endocrinol. Diabetes* **103,** 81–87.

Przywara, D. A., Guo, X., Angelilli, M. L., Wakade, T. D., and Wakade, A. R. (1996). A non-cholinergic transmitter, pituitary adenylate cyclase-activating polypeptide, utilizes a novel mechanism to evoke catecholamine secretion in rat adrenal chromaffin cells. *J. Biol. Chem.* **271,** 10545–10550.

Quarles Van Ufford-Mannesse, P., Castro-Cabezas, M., Vroom, T. M., van Gils, A. P. G., Lips, C. J. M., and Niermeijer, P. (1999). A patient with neurofibromatosis type I and watery diarrhoea syndrome due to a VIP-producing adrenal pheochromocytoma. *J. Int. Med.* **246,** 231–234.

Rebuffat, P., Nowak, K. W., Tortorella, C., Musajo, F. G., Gottardo, G., Mazzocchi, G., and Nussdorfer, G. G. (1994). Evidence that endogenous vasoactive intestinal peptide (VIP) plays a role in the maintenance of the growth and steroidogenic capacity of rat adrenal zona glomerulosa. *J. Steroid Biochem. Mol. Biol.* **51,** 81–88.

Rebuffat, P., Mazzocchi, G., Macchi, C., Malendowicz, L. K., Gottardo, G., and Nussdorfer, G. G. (1999). Mechanisms and receptor subtypes involved in the stimulatory action of endothelin-1 on rat adrenal zona glomerulosa. *Int. J. Mol. Med* **3,** 307–310.

Rebuffat, P., Macchi, C., Malendowicz, L. K., and Nussdorfer, G. G. (2000). Comparison of the signaling mechanisms involved in the ETB receptor-mediated secretagogue action of endothelin-1 on dispersed zona glomerulosa of the rat adrenal gland. *Int. J. Mol. Med.* **5,** 43–47.

Reid, S. G., Fritsche, R., and Jönsson, A. C. (1995). Immunohistochemical localization of bioactive peptides and amines associated with the chromaffin tissue of five species of fish. *Cell Tissue Res.* **280,** 499–512.

Renshaw, D., Thomson, L. M., Carrol, M., Kapas, S., and Hinson, J. P. (2000). Actions of neuropeptide Y on the rat adrenal cortex. *Endocrinology* **141,** 169–173.

Rius, R. A., Guidotti, A., and Costa, E. (1994). Pituitary adenylate cyclase-activating polypeptide (PACAP) potently enhances tyrosine hydroxylase (TH) expression in adrenal chromaffin cells. *Life Sci.* **54,** 1735–1743.

Robberecht, P., Vertongen, P., Langer, I., and Perret, J. (2003). Development of selective ligands for PAC_1, $VPAC_1$ and $VPAC_2$ receptors. *In* "Pituitary Adenylate Cyclase-Activating Polypeptide" (H. Vaudry and A. Arimura, Eds.), pp. 49–67. Kluwer Academic Publisher, Norwell, MA.

Romanelli, F., Fillo, S., Isidori, A., and Conte, D. (1997). Pituitary adenylate cyclase-activating polypeptide regulates rat Leydig cell function *in vitro*. *Neuropeptides* **31,** 311–317.

Rossato, M., Nogara, A., Gottardello, F., Bordon, P., and Foresta, C. (1997). Pituitary adenylate cyclase-activating polypeptide stimulates rat Leydig cells steroidogenesis through a novel transduction pathway. *Endocrinology* **138,** 3228–3235.

Said, S. I. (1976). Evidence for secretion of vasoactive intestinal peptide by tumors of pancreas, adrenal medulla, thyroid, and lung: Support for the unifying APUD concept. *Clin. Endocrinol.* **5,** 201S–204S.

Said, S. I., and Mutt, V. (1970). Polypeptide with broad biologic activity: Isolation from small intestine. *Nature* **225,** 863–864.

Sakai, Y., Hashimoto, H., Shintani, N., Tomimoto, S., Tanaka, K., Ichibori, A., Hirose, M., and Baba, A. (2001). Involvement of p38 MAP kinase pathway in the synergistic activation of PACAP mRNA expression by NGF and PACAP in PC12h cells. *Biochem. Biophys. Res. Commun.* **285,** 656–661.

Sakai, Y., Hashimoto, H., Shintani, N., Katoh, H., Negishi, M., Kawaguchi, C., Kasai, A., and Baba, A. (2004). PACAP activates Rac1 and synergizes with NGF to activate ERK1/2, thereby inducing neurite outgrowth in PC12 cells. *Mol. Brain Res.* **123,** 18–26.

Sasaki, A., Sato, S., Go, M., Murakami, O., Hanew, K., and Yoshinaga, K. (1987). Potentiation of histidine methionine (PHM) on corticotropin-releasing hormone (CRH)-induced ACTH secretion in humans. *J. Clin. Endocrinol. Metab.* **65,** 1305–1307.

Sasaki, A., Yumita, S., Kimura, S., Miura, Y., and Yoshinaga, K. (1990). Immunoreactive corticotropin-releasing hormone, growth hormone-releasing hormone, somatostatin, and peptide histidine methionine are present in adrenal pheochromocytomas but not in extra-adrenal pheochromocytomas. *J. Clin. Endocrinol. Metab.* **70,** 996–999.

Scaldaferri, L., Arora, K., Lee, S. H., Catt, K. J., and Moretti, C. (1996). Expression of PACAP and its type-I receptor isoforms in the rat ovary. *Mol. Cell. Endocrinol.* **117,** 227–232.

Schmidt, G., Jørgensen, J., Kannisto, P., Liedberg, F., Ottesen, B., and Owman, C. (1990). Vasoactive intestinal peptide in the PMSG-primed immature rat ovary and its effect on ovulation in the isolated rat ovary perfused *in vitro*. *J. Reprod. Fertil.* **90,** 465–472.

Sherwood, N. M., Kruechl, S. L., and McRory, J. E. (2000). The origin and function of the pituitary adenylate cyclase-activating polypeptide (PACAP)/glucagon superfamily. *Endocr. Rev.* **21,** 619–670.

Shioda, S., Legradi, G., Leung, W., Nakajo, S., Nakaya, K., and Arimura, A. (1994). Localization of pituitary adenylate cyclase-activating polypeptide and its messenger ribonucleic acid in the rat testis by light and electron microscopic immunocytochemistry and *in situ* hybridization. *Endocrinology* **135,** 818–825.

Shioda, S., Shimoda, Y., Hori, T., Mizushima, H., Ajiri, T., Funahashi, H., Ohtaki, K., and Ryushi, T. (2000). Localization of the pituitary adenylate cyclase-activating polypeptide receptor and its mRNA in the rat adrenal medulla. *Neurosci. Lett.* **295,** 81–84.

Shioda, S., Zhou, C. J. I., Ohtaki, H., and Yada, T. (2003). PACAP receptor signaling. *In* "Pituitary Adenylate Cyclase-Activating Polypeptide" (H. Vaudry and A. Arimura, Eds.), pp. 95–124. Kluwer Academic Publisher, Norwell, MA.

Shiotani, Y., Kimura, S., Ohshige, Y., Yanaihara, C., and Yanaihara, N. (1995). Immunohistochemical localization of pituitary adenylate cyclase-activating polypeptide (PACAP) in the adrenal medulla of the rat. *Peptides* **16,** 1045–1050.

Shivers, B. D., Gorcs, T. J., Gottshall, P. E., and Arimura, A. (1991). Two high-affinity binding sites for pituitary adenylate cyclase-activating polypeptide have different tissue distributions. *Endocrinology* **128,** 3055–3065.

Spengler, D., Waeber, C., Pantaloni, C., Holsboer, F., Bockaert, J., Seeburg, P. H., and Journot, I. (1993). Differential signal transduction by five splice variants of the PACAP receptor. *Nature* **365,** 170–175.

Spicer, L. J., Langhout, D. J., Alpizar, E., Williams, S. K., Campbell, R. M., Mowles, T. F., and Enright, W. J. (1992). Effects of growth hormone-releasing factor and vasoactive intestinal peptide on proliferation and steroidogenesis of bovine granulosa cells. *Mol. Cell. Endocrinol.* **83,** 73–78.

Spinazzi, R., Andreis, P. G., and Nussdorfer, G. G. (2005). Neuropeptide-Y and Y-receptors in the autocrine-paracrine regulation of adrenal gland under physiological and pathophysiological conditions. *Int. J. Mol. Med.* **15,** 3–13.

Sreedharan, S. P., Huang, J. X., Cheung, M. C., and Goetzl, E. J. (1995). Structure, expression, and chromosomal localization of the type I human vasoactive intestinal peptide receptor gene. *Proc. Natl. Acad. Sci. USA* **92,** 2939–2943.

Tabarin, A., Chen, D., Hakkanson, R., and Sundler, F. (1994). Pituitary adenylate cyclase-activating polypeptide in the adrenal gland of mammals: Distribution, characterization, and responses to drugs. *Neuroendocrinology* **59,** 113–119.

Takahashi, K., Totsune, K., Murakami, O., Sone, M., Itoi, K., Miura, Y., and Mouri, T. (1993). Pituitary adenylate cyclase-activating polypeptide (PACAP)-like immunoreactivity in pheochromocytomas. *Peptides* **14,** 365–369.

Tan, G. H., Carney, J. A., Grant, C. S., and Young, W. F., Jr. (1996). Coexistence of bilateral pheochromocytoma and idiopathic hyperaldosteronism. *Clin. Endocrinol.* **44,** 603–609.

Tanaka, K., Shibuya, I., Nagatomo, T., Yamashita, H., and Kanno, T. (1996). Pituitary adenylate cyclase-activating polypeptide causes rapid Ca^{2+} release from intracellular stores and long lasting Ca^{2+} influx mediated by Na^{+} influx-dependent membrane depolarization in bovine adrenal chromaffin cells. *Endocrinology* **137,** 956–966.

Tanaka, K., Shibuya, I., Uezono, Y., Ueta, Y., Toyohita, Y., Yanagihara, N., Izumi, F., Kanno, T., and Yamashita, H. (1998). Pituitary adenylate cyclase-activating polypeptide causes Ca^{2+} release from ryanodine/caffeine stores through a novel pathway independent of inositol trisphosphates and cyclic AMP in bovine adrenal medullary cells. *J. Neurochem.* **70,** 1652–1661.

Taupenot, L., Mahata, S. K., Wu, H., and O'Connor, D. T. (1998). Peptidergic activation of transcription and secretion in chromaffin cells. *Cis* and *trans* signaling determinants of pituitary adenylate cyclase-activating polypeptide (PACAP). *J. Clin. Invest.* **101,** 863–876.

Taupenot, L., Mahata, M., Mahata, S. K., and O'Connor, D. T. (1999). Time-dependent effects of the neuropeptide PACAP on catecholamine secretion. Stimulation and desensitization. *Hypertension* **34,** 1152–1162.

Tischler, A. S., Riseberg, J. C., and Gray, R. (1995). Mitogenic and antimitogenic effects of pituitary adenylate cyclase-activating polypeptide (PACAP) in adult rat chromaffin cell cultures. *Neurosci. Lett.* **189,** 135–138.

Tönshoff, C., Hemmick, L., and Evinger, M. J. (1997). Pituitary adenylate cyclase-activating polypeptide (PACAP) regulates expression of catecholamine biosynthetic enzyme genes in bovine adrenal chromaffin cells. *J. Mol. Neurosci.* **9,** 127–140.

Törnell, J., Carlsson, B., and Hillensjö, T. (1988). Vasoactive intestinal peptide stimulates oocyte maturation, steroidogenesis, and cyclic adenosine 3′-5′-monophosphate production in isolated preovulatory rat follicles. *Biol. Reprod.* **39,** 213–220.

Tornøe, K., Hannibal, J., Børglum-Jensen, T., Georg, B., Fledelius-Rickelt, L., Bolding-Andreansen, M., Fahrenkrug, J., and Holst, J. J. (2000). PACAP-(1–38) as neurotransmitter in the porcine adrenal glands. *Am. J. Physiol.* **279,** E1413–E1425.

Toth, I. E., and Hinson, J. P. (1995). Neuropeptides in the adrenal glands: Distribution, localization of receptors, and effects on steroid hormone biosynthesis. *Endocr. Res.* **21,** 39–51.

Trzeciak, W. H., Ahmed, C. E., Simpson, E. R., and Ojeda, S. R. (1986). Vasoactive intestinal peptide induces the synthesis of the cholesterol side-chain cleavage enzyme complex in cultured rat ovarian granulosa cells. *Proc. Natl. Acad. Sci. USA* **83,** 7490–7494.

Trzeciak, W. H., Waterman, M. R., Simpson, E. R., and Ojeda, S. R. (1987). Vasoactive intestinal peptide regulates cholesterol side-chain cleavage cytochrome P-450 (P-450scc) gene expression in granulosa cells from immature rat ovaries. *Mol. Endocrinol.* **1,** 500–504.

Tsuchiya, T., Suzuki, Y., Suzuki, H., Ohtake, R., and Shimoda, S. I. (1990). Changes in adrenal neuropeptides content [peptide 7B2, neuropeptide Y (NPY), and vasoactive intestinal polypeptide(VIP)] induced by pharmacological and hormonal manipulations. *J. Endocrinol. Invest.* **13,** 381–389.

Tsukada, T., Horovitch, S. J., Montminy, M. R., Mandel, G., and Goodman, R. H. (1985). Structure of the human vasoactive intestinal polypeptide gene. *DNA Cell Biol.* **4,** 293–300.

Tsukada, T., Fukushima, M., Takebe, H., and Nakai, Y. (1995). Vasoactive intestinal peptide gene expression in the rat pheochromocytoma cell line PC12. *Mol. Cell. Endocrinol.* **107,** 231–239.

Turquier, V., Yon, L., Grumolato, L., Alexandre, D., Fournier, A., Vaudry, H., and Anouar, Y. (2001). Pituitary adenylate cyclase-activating polypeptide stimulates secretoneurin release and secretogranin II gene transcription in bovine adrenochromaffin cells through multiple signaling pathways and increased binding of pre-existing activator protein-1-like transcription factors. *Mol. Pharmacol.* **60,** 42–52.

Van Rampelbergh, J., Gourlet, P., De Neef, P., Robberecht, P., and Waelbroeck, M. (1996). Properties of the pituitary adenylate cyclase-activating polypeptide I and II receptors, vasoactive intestinal peptide-1, and chimeric amino-terminal pituitary adenylate cyclase-activating polypeptide/vasoactive intestinal peptide-1 receptors: Evidence for multiple receptor states. *Mol. Pharmacol.* **50,** 1596–1604.

Vaudry, D., Gonzalez, B. J., Basille, M., Yon, L., Fournier, A., and Vaudry, H. (2000). Pituitary adenylate cyclase-activating polypeptide and its receptors: From structure to functions. *Pharmacol. Rev.* **52,** 269–324.

Vaudry, D., Chen, Y., Ravni, A., Hamelink, C., Elkahloun, A. G., and Eiden, L. E. (2002). Analysis of the PC12 cell transcriptome after differentiation with pituitary adenylate cyclase-activating polypeptide (PACAP). *J. Neurochem.* **83,** 1272–1284.

Viale, G., Dell'Orto, P., Moro, E., Cozzaglio, L., and Coggi, G. (1985). Vasoactive intestinal polypeptide-, somatostatin-, and calcitonin-producing adrenal pheochromocytoma associated

with the watery diarrhea (WDHH) syndrome: First case report with immunohistochemical findings. *Cancer* **55,** 1099–1106.

Vinson, G. P., and Hinson, J. P. (1992). Blood flow and hormone secretion in the adrenal gland. *In* "The Adrenal Gland" (V. H. T. James, Ed.), pp. 71–86. Raven Press, New York.

Vinson, G. P., Hinson, J. P., and Toth, I. E. (1994). The neuroendocrinology of the adrenal cortex. *J. Neuroendocrinol.* **6,** 235–246.

Vrezas, I., Willenberg, H. G., Mansmann, G., Hiroi, N., Fritzen, R., and Bornstein, S. R. (2003). Ectopic adrenocorticotropin (ACTH) and corticotropin-releasing hormone (CRH) production in the adrenal gland: Basic and clinical aspects. *Microsc. Res. Tech.* **61,** 308–314.

Wajiki, M., Ogawa, A., Fukui, J., Komiya, I., Yamada, T., and Maruyama, Y. (1985). Coexistence of aldosteronoma and pheochromocytoma in adrenal gland. *J. Surg. Oncol.* **28,** 75–78.

Wakade, A. R. (1998). Multiple transmitter control of catecholamine secretion in rat adrenal medulla. *Adv. Pharmacol.* **45,** 595–598.

Wakade, T. D., Blank, M. A., Malhotra, R. K., Pourcho, R., and Wakade, A. R. (1991). The peptide VIP is a neurotransmitter in rat adrenal medulla: Physiological role in controlling catecholamine secretion. *J. Physiol. (London)* **444,** 349–362.

Watanabe, H., and Tamura, T. (1994). Stimulation by peptide histidine methionine (PHM) of adrenocorticotropin secretion in patients with Cushing's disease: A comparison with the effect of vasoactive intestinal peptide (VIP) and a study on the effect of combined administration of corticotropin-releasing hormone with PHM or VIP. *J. Clin. Endocrinol. Metab.* **78,** 1372–1377.

Watanabe, T., Masuo, Y., Matsumoto, H., Suzuki, N., Ohtaki, T., Matsuda, Y., Kitada, C., Tsuda, M., and Fujino, M. (1992). Pituitary adenylate cyclase-activating polypeptide provokes cultured rat chromaffin cells to secrete adrenaline. *Biochem. Biophys. Res. Commun.* **182,** 403–411.

Watanabe, T., Shimamoto, N., Takahashi, A., and Fujino, M. (1995). PACAP stimulates catecholamine release from adrenal medulla: A novel noncholinergic secretagogue. *Am. J. Physiol.* **269,** E903–E909.

Waymire, J. C., Craviso, G. L., Lichteig, K., Johnston, J. P., Baldwin, C., and Zigmond, R. E. (1991). Vasoactive intestinal peptide stimulates catecholamine biosynthesis in isolated adrenal chromaffin cells: Evidence for a cyclic AMP-dependent phosphorylation and activation of tyrosine hydroxylase. *J. Neurochem.* **57,** 1313–1324.

Whitworth, E. J., Hinson, J. P., and Vinson, G. P. (2002). Neuropeptides and adrenocortical proliferation *in vitro*. *Endocr. Res.* **28,** 677–681.

Wilson, S. P. (1987). Vasoactive intestinal peptide and substance P increase levels of enkephalin-containing peptides in adrenal chromaffin cells. *Life Sci.* **40,** 623–628.

Wilson, S. P. (1988). Vasoactive intestinal peptide elevates cyclic AMP levels and potentiates secretion in bovine adrenal chromaffin cells. *Neuropeptides* **11,** 17–21.

Wilson, S. P. (1992). Vasoactive intestinal peptide is a secretagogue in bovine chromaffin cells pretreated with pertussis toxin. *Neuropeptides* **23,** 187–192.

Wolf, N., and Krieglstein, K. (1995). Phenotypic development of neonatal rat chromaffin cells in response to adrenal growth factors and glucocorticoids: Focus on pituitary adenylate cyclase-activating polypeptide. *Neurosci. Lett.* **200,** 207–210.

Yamaguchi, N. (1993). *In vivo* evidence for adrenal catecholamine release mediated by non–nicotinic mechanism: Local medullary effect of VIP. *Am. J. Physiol.* **265,** R766–R771.

Yanaihara, H., Vigh, S., Kozicz, T., Somogyvári-Vigh, A., and Arimura, A. (1998). Immunohistochemical demonstration of the intracellular localization of pituitary adenylate cyclase-activating polypeptide-like immunoreactivity in the rat testis using the stamp preparation. *Regul. Pept.* **78,** 83–88.

Yiangou, Y., Di Marzo, V., Spokes, R. A., Panico, M., Morris, H. R., and Bloom, S. R. (1987). Isolation, characterization, and pharmacological actions of peptide histidine valine-42, a novel prepro-vasoactive intestinal peptide-derived peptide. *J. Biol. Chem.* **262,** 14010–14013.

Yon, L., Feuilloley, M., Chartrel, N., Arimura, A., Fournier, A., and Vaudry, H. (1993a). Localization, characterization, and activity of pituitary adenylate cyclase-activating polypeptide in the frog adrenal gland. *J. Endocrinol.* **139,** 183–194.

Yon, L., Jeandel, L., Chartrel, N., Feuilloley, M., Conlon, J. M., Arimura, A., Fournier, A., and Vaudry, H. (1993b). Neuroanatomical and physiological evidence for the involvement of pituitary adenylate cyclase-activating polypeptide (PACAP) in the regulation of the distal lobe of the frog pituitary. *J. Neuroendocrinol.* **5,** 289–296.

Yon, L., Chartrel, N., Feuilloley, M., De Marchis, S., Fournier, A., De Rijk, E., Pelletier, G., Roubos, E., and Vaudry, H. (1994a). Pituitary adenylate cyclase-activating polypeptide stimulates both adrenocortical cells and chromaffin cells in the frog adrenal gland. *Endocrinology* **135,** 2749–2758.

Yon, L., Chartrel, N., Feuilloley, M., Jeandel, L., Gracia-Navarro, F., Fournier, A., Arimura, A., Colon, J. M., and Vaudry, H. (1994b). Distribution and neuroendocrine actions of pituitary adenylate cyclase-activating polypeptide (PACAP) in amphibians. *In* ''Vasoactive Intestinal Peptide, Pituitary Adenylate Cyclase-Activating Polypeptide, and Related Regulatory Peptides'' (G. Rossellini, Ed.), pp. 342–354. World Scientific Press, Singapore.

Yon, L., Chartrel, N., Montero, M., Bellancourt, G., Feuilloley, M., Roubos, E., Arimura, A., Conlon, J. M., Fournier, A., and Vaudry, H. (1996). Pituitary adenylate cyclase-activating polypeptide regulates both adrenocortical and chromaffin cell activity in the frog adrenal gland. *Ann. N.Y. Acad. Sci.* **805,** 697–701.

Yon, L., Breault, L., Contesse, V., Bellancourt, G., Delarue, C., Fournier, A., Lehoux, J. G., Vaudry, H., and Gallo-Payet, N. (1998). Localization, characterization, and second messenger coupling of pituitary adenylate cyclase-activating polypeptide receptors in the fetal human adrenal gland during the second trimester of gestation. *J. Clin. Endocrinol. Metab.* **83,** 1299–1305.

Yoshikawa, M., Saito, H., Sano, T., Ohuchi, T., Ishimura, Y., Morita, K., Saito, S., and Oka, M. (1990). Localization and release of immunoreactive vasoactive intestinal polypeptide in bovine adrenal medulla. *Neurosci. Lett.* **111,** 75–79.

Zhong, Y., and Kasson, B. G. (1994). Pituitary adenylate cyclase-activating polypeptide stimulates steroidogenesis and adenosine 3′,5′-monophosphate accumulation in cultured rat granulosa cells. *Endocrinology* **135,** 207–213.

This page intentionally left blank

Ultrastructural Dynamics of Human Reproduction, from Ovulation to Fertilization and Early Embryo Development[1]

Giuseppe Familiari,* Rosemarie Heyn,* Michela Relucenti,*
Stefania A. Nottola,* and A. Henry Sathananthan†
*Laboratory of Electron Microscopy, Pietro M. Motta
Department of Anatomy, University of Rome, "La Sapienza," 00161 Rome, Italy
†Monash Institute of Reproduction and Development
Monash University, Melbourne, Australia 3168

This study describes the updated, fine structure of human gametes, the human fertilization process, and human embryos, mainly derived from assisted reproductive technology (ART). As clearly shown, the ultrastructure of human reproduction is a peculiar multistep process, which differs in part from that of other mammalian models, having some unique features. Particular attention has been devoted to the (1) sperm ultrastructure, likely "Tygerberg (Kruger) strict morphology criteria"; (2) mature oocyte, in which the MII spindle is barrel shaped, anastral, and lacking centrioles; (3) three-dimensional microarchitecture of the zona pellucida with its unique supramolecular filamentous organization; (4) sperm–egg interactions with the peculiarity of the sperm centrosome that activates the egg and organizes the sperm aster and mitotic spindles of the embryo; and (5) presence of viable cumulus cells whose metabolic activity is closely related to egg and embryo behavior in *in vitro* as well as *in vivo* conditions, in a sort of extraovarian "microfollicular unit." Even if the ultrastructural morphodynamic features of human fertilization are well understood, our knowledge about *in vivo* fertilization is still very limited and the complex sequence of *in vivo* biological steps involved in human reproduction is only partially reproduced in current ART procedures.

[1]Dedicated to the Late Professor Pietro M. Motta, Rome (1942–2002).

International Review of Cytology, Vol. 249

0074-7696/06 $35.00
DOI: 10.1016/S0074-7696(06)49002-1

KEY WORDS: Electron microscopy, Sperm, Oocyte, Fertilization, Cumulus cells, Zona pellucida.

I. Introduction

Edwards and Brody (1995) stated that the study of *in vitro* fertilization and early human embryology has left the world with an abiding appreciation of basic reproductive processes that can be understood in an orderly, predictable, and finite manner. Moreover, technology in assisted human reproduction is rapidly advancing, starting in 1978 with the birth of Louise Brown, followed by the first births using frozen embryos in the 1980s and the microinjection of spermatozoa (intracytoplasmic sperm injection, ICSI) for the treatment of male infertility at the beginning of the 1990s. In some instances, new technologies were also adopted for clinical application before adequate research proved their efficiency or safety.

In recent years, debate has arisen among politicians, philosophers, and biomedical professionals who indicated that a strict law on human conception and its correlates was inevitable, as in the case of Italy, until a controversial law was recently passed (Clarke, 2003). Consequent to political and ethical reasons, basic research on human gametes and embryos is often limited, so that most of our information on gametes, fertilization, and early embryos has come from studies on mammals, whereas less information is available from humans (Familiari *et al.*, 1991; Grudzinskas and Yovich, 1995a,b; Hoodbhoy and Dean, 2004; Jungnickel *et al.*, 2003; Olds-Clarke, 2003; Primakoff and Myles, 2002; Talbot *et al.*, 2003; Trounson and Gosden, 2003; Van Blerkom and Motta, 1989; Yanagimachi, 1994).

Although the importance of cell culture technology evolved in clinical practice, we believe that it is equally important that knowledge of the ''basic biology'' of human gametes and embryos is a prerequisite. In our opinion, the concept of ''basic biology'' encompasses genetics as well as proteomics and cellular function integrated with the cell ultrastructure. Since the first three-dimensional (3-D) ultrastructural pictures of human gametes were obtained by our group, founded and directed by the late Professor Pietro M. Motta (Familiari *et al.*, 1987) and the Monash group (Sathananthan *et al.*, 1986a, 1993), knowledge about the cellular biology of human gametes and fertilization rapidly increased, as morphological techniques became more sophisticated, allowing a very accurate ultrastructural appreciation of human gametes and their interactions. Therefore, the aim of the present article is to describe the updated, fine structure of human gametes, the human fertilization process, and human embryos, derived from

assisted reproductive technology (ART). This will help to more clearly define the ultrastructural map of the morphodynamics and functional events implicated in human embryology. Results were mainly obtained using transmission electron microscopy (TEM), high-resolution scanning electron microscopy (SEM), and confocal microscopy (CFM) correlated with cytochemical and immunochemical techniques.

II. Sperm Structure and Function

The World Health Organization released a manual in 1999 that recommends that an ideal, mature spermatozoon have an oval–shaped and regular head with a pale anterior region, the acrosome, constituting 40–70% of the head area, and a darker posterior region. The length-to-width ratio of the head should be 1.50–1.75. The tail should be single and straight (not coiled, nicked, or bent over itself) and attached symmetrically in a fossa located in the broad base of the head. The first part of the tail is the midpiece and should be somewhat thicker. Finally, a normal cytoplasmic droplet appears at the base of the head, has a smooth and regular profile, and is less than one-third of a normal sperm head (ESHRE, 2002) (Fig. 1).

Mammalian spermatozoa are characterized by their specialized and unique cytoskeleton, in particular, the presence of outer dense fibers and a fibrous sheath, perinuclear theca, mitochondrial capsule, and acrosome (Catalano *et al.*, 2001). Regarding humans, inter– and individual variations concerning number, concentration, motility, and viability of spermatozoa are commonly reported in fresh ejaculated semen (Buffone *et al.*, 2004). In addition, morphologically abnormal spermatozoa are observed in the semen of men with proven fertility. In fact, no two sperm look alike in fine structure and it is often hard to define a normal spermatozoon that might fertilize an egg.

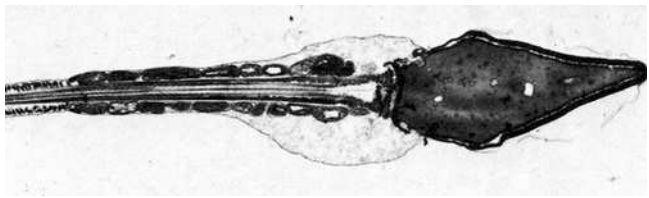

FIG. 1 Normal motile sperm. Note swelling of the plasma membrane. (TEM, 13000X.) (From Sathananthan, 1996.)

The more recent procedures in the field of ART have become less dependent on sperm quality (Muratori *et al.*, 2000). In fact, ICSI requires only one single spermatozoon of good or fair quality to achieve fertilization. Microscopic evaluation is fundamental in determining if one spermatozoon possesses characteristics of viability. TEM of ejaculate is a useful tool to elucidate fine structure and inheritable genetic disorders in patients selected for ICSI (Carbone *et al.*, 1998). With light microscopy (LM), the human spermatozoon shows two major subcellular regions: a head and flagellum (Toshimori, 2003). With TEM, it is possible to determine that the flagellum has several parts: a connecting piece (or neck) in contact with the head, a centrosome, a middle piece (midpiece), and a tail with an axoneme (de Kretser and Kerr, 1994; ESHRE, 2002; Fawcett, 1975; Holstein and Roosen-Runge, 1981; Sathananthan, 1996).

Besides electron microscopy, several other techniques, coupled with computerized analysis, have been used in the morphological evaluation of normal and pathological sperm (Celik-Ozenci *et al.*, 2003; Ramos *et al.*, 2002; Sathananthan, 1996). In recent years atomic force microscopy (AFM) has been used as a useful tool in the study of sperm topography. It provides detailed structural information and 3-D images, especially regarding basic research on fertilization and modifications of the normal and pathological cell surface, as well as useful information for ART laboratories (Baccetti *et al.*, 2002; Carbone *et al.*, 1998; Joshi *et al.*, 2000, 2001).

Electron microscopy represents a valuable tool in the understanding of sperm morphological alterations, the most frequent of which are acrosomal, centrosomal, and axonemal defects (Baccetti *et al.*, 2002). The morphologic abnormalities can involve any region of the sperm cell (ESHRE, 2002) and are related to both incomplete maturation, such as the presence of persistent cytoplasmic residues or overabundant cytoplasm (ESHRE, 2002; Gergely *et al.*, 1999), aging (the presence of straight and unusually thin sperm), or malformations resulting from traumas, infections, drug administration, or the mutagenic effects of radiation. Severe malformations in the morphology and function of spermatozoa can also result from genetic or endocrine disorders (Turner, 2003). Chromatin disorganization, mitochondria altered assembly, and plasma membrane disruptions are all important and frequently found defects revealed by TEM semen analysis in ART procedures (Baccetti *et al.*, 2002). Today a correct and complete evaluation of male semen quality for men who attempt ART has to be based, mainly or exclusively, on ultrastructural and molecular properties. The submicroscopic evaluation of sperm features allows a precise grouping of infertile subjects into strictly delimited categories of pathologies (Baccetti *et al.*, 2002).

Controversial results are also found on the effect of follicle-stimulating hormone (FSH) on sperm quality and pregnancy rate. Baccetti *et al.* (2004) demonstrated a positive role of FSH therapy in infertile males before ICSI,

which was correlated with an increased pregnancy rate in treated couples. They showed a significant improvement in sperm quality, which could positively influence the quality and early stages of embryo development, thereby increasing the probability of embryo implantation (Baccetti *et al.*, 2004). A human spermatozoon has a volume of 28 μm^3 and a surface area of 120 μm^2 (Gilmore *et al.*, 1997). If measured by TEM and AFM it is about 60 μm long (Joshi *et al.*, 2000; Sathananthan, 1996). The midpiece is about 5–8 μm long and 1 μm in diameter; the tail is divided in a principal piece, 45 μm long, and terminates in an end piece, 5 μm in length (ESHRE, 2002; Sathananthan, 1996).

A. Head

The head of a spermatozoon has a smooth and oval configuration from the front, while it appears pyriform in profile. In the head, two major structures are localized: the acrosome and nucleus, surrounded by the plasma membrane. The nucleus is partially capped in its anterior part by the acrosome (Fawcett, 1975; Sathananthan, 1996). The head is 4.5–5.16 μm long, about 2.5–4.12 μm wide and 846 nm in height (ESHRE, 2002; Joshi *et al.*, 2000; Sathananthan, 1996) (Figs. 2 and 3).

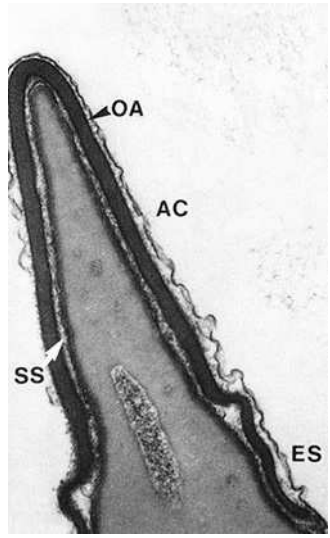

FIG. 2 Sperm head with intact surface membranes. The outer plasma membrane, acrosome, and subacrosomal space are clearly visible. AC, acrosome cap; ES, equatorial segment; OA, outer acrosome membrane; SS, subacrosomal space. (TEM, 27000X.) (From Chen and Sathananthan, 1986.)

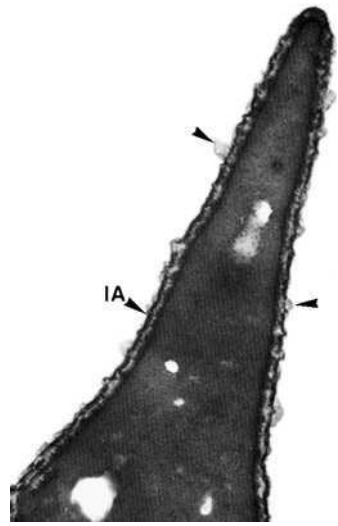

FIG. 3 Acrosome-reacted sperm. The outer membranes and acrosome matrix have disappeared, exposing the inner acrosome membrane. The subacrosomal space surrounds the nuclear envelope and the compact chromatin. Note polyp-like extrusions of the subacrosomal space (arrows). IA, inner acrosome membrane. (TEM, 27000X.) (From Chen and Sathananthan, 1986.)

1. Acrosome

The acrosome is located between the plasma membrane and the nucleus. In particular, it corresponds to a modified lysosome, which surrounds the anterior part of the nucleus (Figs. 2 and 3). The acrosomal matrix contains hydrolytic enzymes, mainly hyaluronidase, and a protease called acrosin. These molecules help the sperm to digest a pathway through both the cumulus matrix and the zona pellucida, the outer egg vestments. The post-acrosomal segment is placed below the acrosome of the head, and corresponds to the region where sperm–egg membrane fusion usually occurs (Millette, 1999; Sathananthan *et al.*, 1986a,b, 1993). The acrosome cap is attached to a narrower equatorial region, about 1.6 μm in length (Joshi *et al.*, 2001). Acrosomal characteristics are also considered in procedures of ART (Baccetti *et al.*, 2002).

2. Nucleus and Associated Structures

Alterations in the nuclear shape and in the chromatin status (index of apoptosis) are aberrations that are extremely frequent in spermatozoa of infertile men, and that are implicated in ART failures (Baccetti *et al.*, 2002).

3. Perinuclear Theca (PT)

The PT is a rigid layer of cytoplasm that surrounds the sperm nucleus (Lecuyer *et al.*, 2000; Longo *et al.*, 1987; Sutovsky and Schatten, 2000). This structure is made up of proteins with cytoskeletal features, not completely defined (Mujica *et al.*, 2003). The PT has two regional domains, the subacrosomal and the postacrosomal segments. Calicin (Lecuyer *et al.*, 2000), calmodulin, and AJ-p90 antigen (Jassim *et al.*, 1993; Kann *et al.*, 1991) were found in human sperm. The exact function of this structure in humans is not well understood.

4. The Nuclear Envelope

The sperm nuclear envelope has a characteristic distribution of nuclear pores. They are present on the most posterior part of the nucleus in the residual cytoplasm, and are absent from the surface covering of the condensed chromatin. The nuclear envelope at the base of the head is continuous with the basal plate. The posterior ring is a circular area of fusion between the nuclear envelope and plasma membrane, and corresponds to the posterior edge of the acrosome. The redundant nuclear envelope forms some folds caudally to the posterior ring (Fawcett, 1975) (Fig. 4).

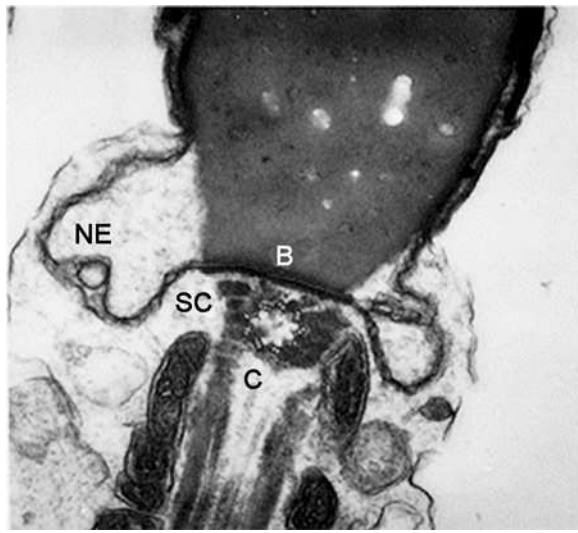

FIG. 4 Sperm neck region showing the proximal centriole. B, basal plate; NE, nuclear envelope; C, centriole; SC, segmented columns. (TEM, 16000X.) (From Chen and Sathananthan, 1986.)

5. Chromatin Pattern

In most mammals the sperm nucleus has a quite homogeneous electronic density; in humans it shows a variable condensed chromatin. The nucleus contains highly condensed DNA and has translucent vacuoles. Whether this chromatin pattern could be due to apoptosis is still a matter of debate. DNA fragmentation in ejaculated sperm should be considered as a marker of poor functional activity rather than an index of apoptosis (Lachaud *et al.*, 2004; Muratori *et al.*, 2000). DNA–fragmented sperm are not cells that are committed to death, but rather retain several abnormalities that are compatible with a lower degree of maturation. In fact, DNA–fragmented sperm are less motile, more immature, and even less susceptible to hypoosmotic swelling, which indicates a lower functional integrity of the sperm membrane (Muratori *et al.*, 2000). Gandini *et al.* (2000), in turn, indicate that sperm apoptotic DNA fragmentation is usually revealed in the seminal fluid. These studies demonstrated that the percentage of apoptosis in normozoospermic subjects is significantly lower than in patients with oligoasthenoteratozoospermia (OAT), Hodgkin's disease, or testicular cancer, confirming that DNA fragmentation is one of the characteristics of spermatogenetic failure, and depends on the pathophysiological condition of the subject and on a deregulation of spermatogenesis control systems (Gandini *et al.*, 2000). Therefore, the importance of an accurate characterization of DNA integrity is fundamental in ICSI procedures, because the injection-induced mechanical bypass of the natural selective barriers of the oocyte with an abnormal sperm may account for fertilization failures or for inherited transmitted damage to the newborn (Muratori *et al.*, 2000). Selection of sperm for ICSI is subjectively based on gross morphological assessment under the inverted microscope. Obviously the physiology and genetic make-up of the sperm is as important as its morphology.

The posterior surface of the nucleus lines the implantation fossa, the site of attachment of the flagellum. This region of the nuclear envelope is covered on its outer surface by a thick layer of very dense material, the basal plate, which lines the fossa and provides attachment for a large number of fine filaments, which extend into it from the articular surface of the connecting piece (Fawcett, 1975) (Fig. 4).

B. Flagellum

The flagellum represents the propulsive force of the sperm, allowing it to reach the ovum and penetrate and fertilize it. Although ART techniques such as ICSI minimize the requirement of sperm motility, a precise identification of ultrastructural defects of the flagellum is necessary to avoid the transmission of genetic defects to future generations. Knowledge of the fine structural

flagellar characteristics may also result in the realization of an effective safe male contraceptive (Turner, 2003). TEM and SEM show that it has distinct sections: a connecting piece or neck, an axially attached middle piece, and a tail divided into a principal piece and an end piece (Fawcett, 1975; Sathananthan, 1996).

1. Connecting Piece (Neck)

The connecting piece links the head to the flagellum. The concavity of the basal plate, lining the implantation fossa of the nucleus, holds the capitolium, a convex articular region. Fine filaments lie in the space between the capitolium and the basal plate, aiding head–flagellum attachment. Nine segmented columns extend backward from the capitolium and overlap their caudal end with the anterior tip of the dense fibers (Fawcett, 1975) (Figs. 1 and 4).

Just beneath the capitolium there is a vault or "blackbox" occupied by a transverse or obliquely oriented proximal centriole. The sperm proximal centriole has the typical "9 + 2" organization of microtubules. The sperm distal centriole is vestigial or mostly disorganized in the mature spermatozoon in that the axoneme of the sperm flagellum originates during spermiogenesis; in fact, round and elongating spermatids possess both proximal and distal centrioles (Manandhar *et al.*, 2000; Sathananthan *et al.*, 2001). Remnants of the distal centriole may be found in mature sperm adhering to the inner aspect of some of the nine segmented columns (Sathananthan *et al.*, 2001). The use of a sperm with impaired motility for ART techniques often results in poor embryo outcome due to centrosomal dysfunction. In fact, if one centriole is nonfunctional it is probable that the other one is also nonfunctional, since they arise from the same mother centriole during centriolar genesis. The dominant, proximal centriole is inherited by the human embryo and organizes the sperm aster at fertilization and the first mitotic spindle during embryogenesis (Sathananthan, 1998a,b,c; Sathananthan *et al.*, 1996, 1997, 2001; Schatten, 1994).

2. Middle Piece

The midpiece contains the corresponding tract of the axoneme, the outer dense fibers, all enveloped by the mitochondrial sheath, a spiral of mitochondria, that provides ATP for motility (Figs. 1 and 5).

3. Axoneme

The axoneme has nine doublets of microtubules, which surround a central doublet. The central pair of microtubules of the axoneme extends proximally through the interior of the connecting piece as far anteriorly as the proximal

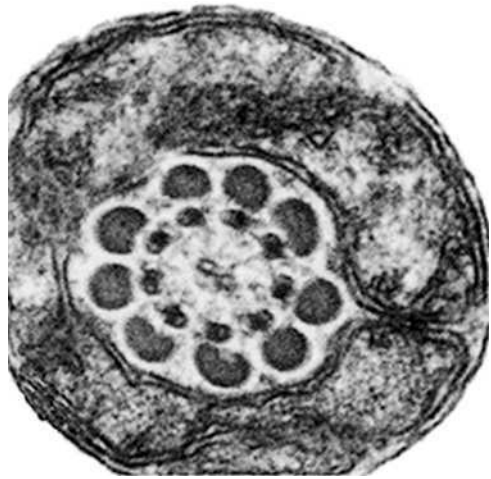

FIG. 5 Normal midpiece showing axoneme (with a typical "9 + 2" arrangement of microtubules), dense fibers, mitochondrial sheath, and plasma membrane. (TEM, 22000X.) (From Sathananthan, 1996.)

centriole. The outer doublets consist of two subunits, A and B. Subunit A is a complete microtubule about 26 nm in diameter, made up of 13 straight protofilaments 3.5 nm in diameter, each composed of 80 Å dimers of tubulin. Subunit B is C-shaped in section, attaches to the wall of subunit A, and is composed of similar dimeric units of tubulin in about 10 protofilaments. Two diverging arms project from subunit A toward the next doublet in the row. The arms are formed of dynein, a protein with ATPase activity. Two slender nexin links connect subunit A to the adjacent doublets; a radial spoke joins subunit A to a helical sheath that wraps the central pair of microtubules. Thirteen protofilaments are arranged in the central microtubules, which are joined to one another along their length by regularly spaced bridges. They are finally enclosed with a sheath of helically wound 60-Å filaments (Fawcett, 1975) (Figs. 1, 5, and 6).

4. Outer Dense Fibers (ODF)

Nine dense fibers surround the peripheral doublets of microtubular axonemes, so in cross–section a "9 + 9 + 2" pattern can be observed. Each fiber is fixed anteriorly to one of the segmented columns of the connecting piece. The fibers run longitudinally down the doublets of the axoneme. The cross-sectional area and shape of the dense fibers differ from each other. Abundant disulfide cross-linking stabilizes the fibers. Up to now ODF are

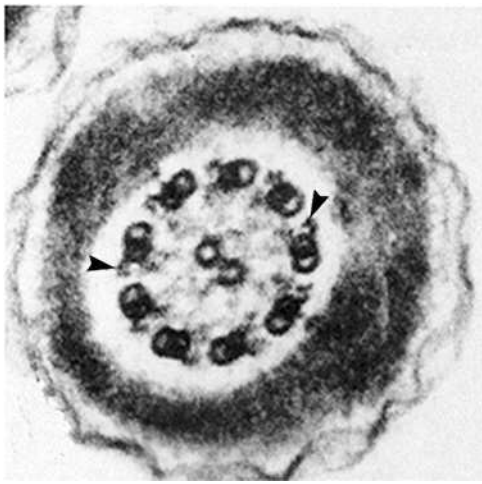

FIG. 6 Normal tail with axoneme, fibrous sheath, and plasma membrane. Note dynein arms (arrows) and radial spokes in the axoneme. (TEM, 35000X.) (From Sathananthan, 1996.)

thought to be incapable of active motility, and sperm tail elastic recall is thought to be probably due to the passive elastic properties of these fibers (Millette, 1999). The human outer dense fibers consist of about 10 major and at least 15 minor proteins (Fawcett, 1975; Petersen *et al.*, 1999; Turner, 2003) (Figs. 1 and 5).

5. Mitochondrial Sheath

This consists of approximately 50–75 mitochondria, arranged in 11–15 turns, which helically wrap the ODF of the axoneme (Hirata *et al.*, 2002; Vorup-Jensen *et al.*, 1999). Mitochondria are arranged end to end, displaying a crescent shape (Figs. 1 and 5). These organelles become mechanically stable and resistant to the hypoosmotic environment because of the mitochondria capsule, a characteristic structure formed by disulfide bonds between the cysteine and proline-rich proteins. One of the proteins making up the mitochondria capsule is the phospholipid hydroperoxide glutathione peroxidase (PHGPx), which has an antioxidative function during spermatogenesis, while in the mature sperm the protein loses its enzymatic activity and is used as a structural protein forming the mitochondrial capsule (Hirata *et al.*, 2002). A lower expression level of mitochondrial PHGPx is reported in certain cases of male infertility (Hirata *et al.*, 2002). As the mitochondrial sheath ends, the annulus appears, a thick ring of granular dense material, which strictly adheres to the plasma membrane (Fig. 1). This structure probably prevents

the mitochondria from falling down in the tail during sperm movements (Fawcett, 1993).

Longitudinal profiles of the middle piece, observed by AFM (Joshi *et al.*, 2000), show a ripple-like structure; its transverse profile reveals a rapid symmetrical plateau of 1860.84 nm with a well-marked canal at the top. The longitudinal profile shows each mitochondrion that surrounds the axoneme in the middle piece. These mitochondria are 214.61 nm in length.

By means of X-ray microscopy, Vorup-Jensen *et al.* (1999) demonstrated two morphologically distinct mitochondrial shapes: compact and tightly wrapped organelles around the axoneme, and transformed mitochondria that showed circular areas, loosely wrapped around the axoneme or distended.

6. Tail

Two parts of the tail are recognized: the principal piece and end piece.

a. Principal Piece The following structures can be found, starting from the most internal one: axoneme, outer dense fibers, and fibrous sheath. As the axoneme and ODF have the same characteristics found in the middle piece (Fawcett, 1993), this section will refer only to the fibrous sheath (Figs. 1 and 6).

The fibrous sheath is a tapering cylinder that begins immediately behind the annulus (caudal limit of the middle piece) and encases both the ODF and axoneme (Catalano *et al.*, 2001). It is made up of two longitudinal columns, which run down the entire fibrous sheath length, and of a series of ribs parallel to each other and perpendicularly oriented with respect to the longitudinal columns. Occasionally branches and anastomoses within neighboring ribs can be observed. The ODF 3 and 8 end at the caudal limit of the middle piece, so the longitudinal columns become contiguous with 3 and 8 microtubule doublets with which they connect. This tie splits the residual ODF in a "4 + 3" arrangement. This asymmetric distribution is responsible for the tail wave movements. The longitudinal columns become smaller and the ribs more slender as the principal piece tapers along its length. The fibrous sheath ends abruptly, fixing the boundary of the principal piece (Catalano *et al.*, 2001; Eddy *et al.*, 2003). The isolation and characterization of the human fibrous sheath proteins, described for the first time by Jassim *et al.* (1992), have also been confirmed by Kim *et al.* (1997). They found that sodium dodecyl sulfate polyacrylamide gel electrophoresis (SDS–PAGE) reveals 14 protein bands; the most intensely stained were those of 84, 72, 66.2, 57, 32, and 28.5 kDa.

b. End Piece The final piece of the spermatozoon, the end piece, is made up of only the axoneme and plasma membrane, because the fibrous sheath and

the outer dense fibers end at the caudal tip of the principal piece (Fawcett, 1975; Sathananthan, 1996).

C. Plasma Membrane

Infertility in men is frequently due to loss of integrity in the sperm plasma membrane (Batova *et al.*, 1998; Wassarman, 1990b). The sperm plasma membrane is a highly polarized and strictly regionally organized structure. It undergoes dynamic changes and reorganization during capacitation and fertilization processes. The complex architecture of the plasma membrane allows the sperm to achieve the various membrane fusion processes required for fertilization (Flesh and Gadella, 2000; Millette, 1999; Rajeev and Reddy, 2004). On the head there is a thick glycoprotein layer, which contains surface antigens (Motta and Van Blerkom, 1984).

1. Membrane Lipids

The sperm cell lacks the set of organelles that permits lipid synthesis and breakdown. The lipid composition of the human sperm plasma membrane is as follows: phospholipids about 70% (50% phosphocholine glycerides; 30% phosphoethanolamine glycerides; 12.5% sphingomyelins; 3% phosphatidylserine; 2.5% cardiolipin; and about 2% phosphatidylinositol, according to Mann and Lutwak-Mann, 1981), neutral lipids about 25% (cholesterol in humans is 40% of total lipids), and glycolipids about 5% (in humans 98% of glycolipids are seminolipids) (Gadella *et al.*, 1992).

2. Membrane Proteins

It is necessary to point out that sperm cells, after spermatogenesis, are unable to synthesize proteins, because they do not have ribosomes or rough endoplasmic reticulum. Proteins that have been characterized belong either to the fertilin superfamily, involved in sperm–egg interactions, or are protein tyrosine kinases that mediate the acrosomic reaction; Ca^{2+} channel proteins are also present. Rajeev and Reddy (2004) provided a sperm plasma membrane protein profile using different chromatographic techniques. They found 16–18 major and 12–15 minor protein bands.

III. Human Mature Egg

Although the literature on mice oocyte morphology is very extensive, studies focusing on the human oocyte are relatively scarce (El shafie *et al.*, 2000; Grudzinskas and Yovich, 1995b; Hoodbhoy and Dean, 2004; Jungnickel

et al., 2003; Olds-Clarke, 2003; Primakoff and Myles, 2002; Talbot *et al.*, 2003; Trounson and Gosden, 2003; Yanagimachi, 1994). Therefore, it is relevant to describe accurately the microarchitecture and ultrastructure of the human mature egg (HME), especially for the clinically derived implications when considering ART.

A. Gross Morphology

The HME exits from the ovary surrounded by cumulus cells in the so-called cumulus–oocyte complex (COC) (Fig. 7). In this section we will refer to the HME, without considering the cumulus cells. Strictly, the HME is a structure consisting of two cells, the smaller called the first polar body and the larger called the oocyte, enclosed in an extracellular glycoproteic matrix, the zona pellucida (ZP) (Figs. 7–9). The ZP is 17 μm thick and 1.89 10^6 μm^3 in volume (Goyanes *et al.*, 1990). Oocyte and ZP are separated by a thin perivitelline space in which the second polar body is enclosed.

1. Oocyte

A human oocyte of a Graafian follicle has a diameter of 116.9–130 μm, a surface area of 4.5 10^4 μm^2, and a volume of 1.43 10^6 mm^3 (Goyanes *et al.*, 1990; Picton *et al.*, 2001), representing one of the largest mammalian cells (Figs. 7–9). At the end of the growth period and prior to meiotic maturation,

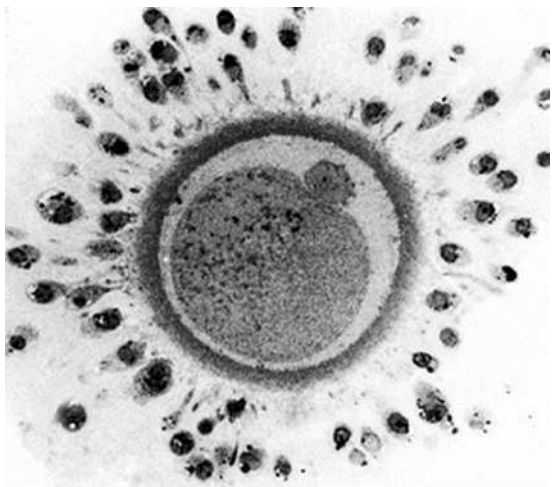

FIG. 7 Mature oocyte with polar body and expanding cumulus cells. (Light microscopy, 100X.) (From Sathananthan, 1985.)

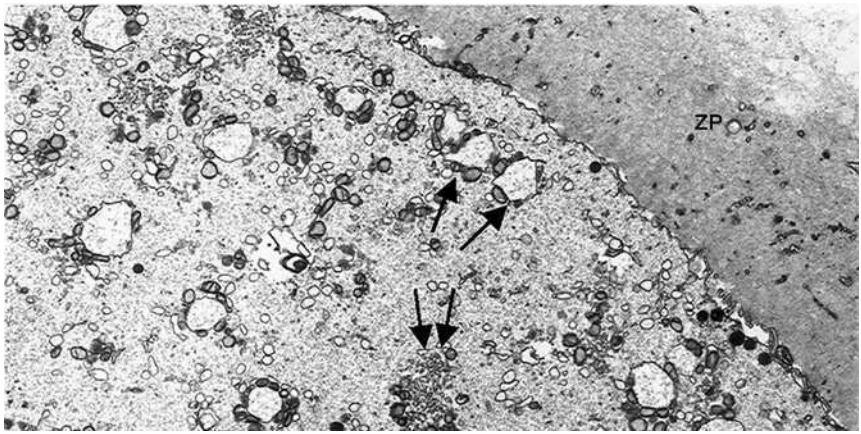

FIG. 8 Mature oocyte. Note the presence of numerous mitochondria–vesicle complexes (arrows) and mitochondria smooth endoplasmic reticulum aggregates (double arrows) in the ooplasm. ZP, zona pellucida. (TEM, 3800X.) (From Motta *et al.*, 1995d.)

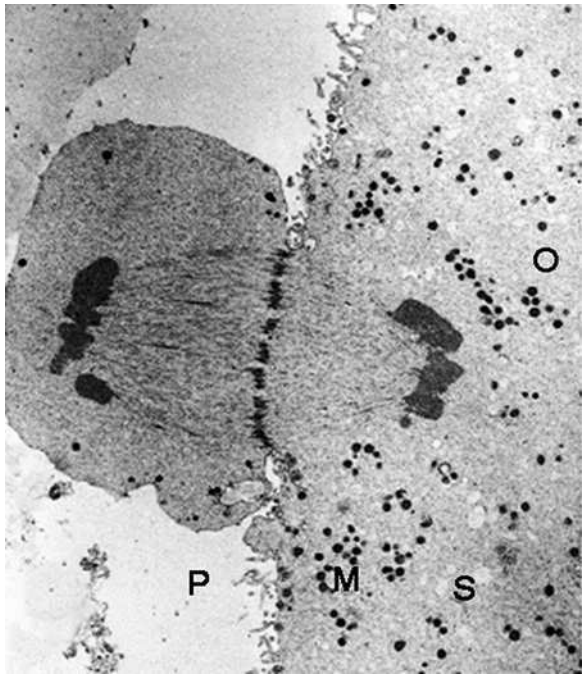

FIG. 9 Telophase II of second maturation showing the abstriction of the second polar body at the level of the interbody. The spindle is barrel–shaped with chromosomes at either pole and nuclei forming within the ooplasm and in the second polar body. The interbody has now contracted. (TEM, 7000X.) (From Sathananthan, 1985.)

the oocyte nucleus is large, pale, and relatively transcriptionally inactive, the so-called germinal vesicle (GV) nucleus (Gonzales-Santander and Clavero Nuez, 1973).

During and after ovulation, oocyte maturation takes place in several stages, including the breakdown of the nuclear membrane germinal vesicle, the first meiotic division including extrusion of the first polar body, the formation of the second meiotic spindle, and the arrest of meiosis at the second meiotic metaphase (Sathananthan, 1985; Veeck, 1999). Therefore, the so-called "mature" oocyte is dormant in the metaphase of the second meiotic division (MII), which is why a birefringent spindle can be imaged inside the ooplasm by means of a Polscope (Wang *et al.*, 2001). A healthy mature HME has a clear cytoplasm with uniform texture and homogeneous fine granularity, a round or ovoid first polar body with smooth surface, and a normal–sized perivitelline space (Mikkelsen and Lindenberg, 2001). The HME morphology includes variations such as shape, color, granularity, and homogeneity of the ooplasm, size of the perivitelline space, vacuolizations, inclusions, and abnormalities of the first polar body or of the zona pellucida (Balaban *et al.*, 1998; De Sutter *et al.*, 1996; Ebner *et al.*, 2000; Serhal *et al.*, 1997; Xia, 1997). However, many HMEs exhibit a number of variations and the so-called ideal HME has been found to represent about one-third to one-half of all oocytes retrieved in an ICSI program (Balaban *et al.*, 1998; de Sutter *et al.*, 1996; Ebner *et al.*, 2000; Kahraman *et al.*, 2000; Xia, 1997). Differences in ooplasmic texture and density have been described when handling the HME for ICSI procedures (Ebner *et al.*, 2003c).

2. First Polar Body

Extrusion of the first polar body and formation of the MII oocyte occur 32 h after ovarian stimulation, 6–8 h before ovulation (Miyara *et al.*, 2003) (Fig. 9).

It has been suggested that optimal nuclear maturation in the HME may be evidenced by an intact first polar body (Ebner *et al.*, 2000; Mikkelsen and Lindenberg, 2001; Xia, 1997). ICSI of the HME with an intact well-shaped first polar body yields higher fertilization rates and higher quality embryos (Ebner *et al.*, 2000). From these data it could be hypothesized that the morphology of the first polar body provides an acceptable prognostic value with regard to fertilization rate and embryo quality (Ebner *et al.*, 2000, 2002). However, these conclusions have not been confirmed in other studies published more recently (De Santis *et al.*, 2005). The position of the first polar body is an unreliable predictor of the exact MII spindle location in human oocytes (Cooke *et al.*, 2003). These data confirm the findings reported by Hardarson *et al.* (2000) who showed that the majority of MII oocyte spindles are in the same hemisphere as the first polar body. This spatial difference is

more likely due to movement of the first polar body than to the spindle. Speculation that the shift of the polar body may be caused by the egg denuding process is incorrect (Hardarson *et al.*, 2000), as displacement has been seen in both *in vivo* and *in vitro* matured eggs denuded from cumulus cells prior to polar body extrusion.

B. Ultrastructure

1. Oolemma

The oocyte plasma membrane extends over many surface microvilli, which have a core of actin filaments (Sathananthan *et al.*, 1993).

a. The Metaphase II Spindle The MII spindle is barrel–shaped, anastral, and is composed of numerous microtubules. It normally shows slightly pointed poles formed by organized microtubules traversing from one pole to another (Sathananthan *et al.*, 1993). The spindle is located at the periphery of the oocyte, both in GV and MII oocytes, and is oriented perpendicularly to the plasma membrane (Boiso *et al.*, 2002). There are no centrioles; human oocytes have a reduced, nonfunctional centrosome and the spindle MT terminate abruptly or in ill-defined specks of granular material (Sathananthan, 2003a,b; Sathananthan *et al.*, 1993). Chromosomes, in turn, are arranged on the equatorial plate of the meiotic spindle in a cortical region of the ooplasm devoid of organelles (Boiso *et al.*, 2002; Motta *et al.*, 2003) (Fig. 9).

The presence of an organized spindle ensures the fidelity of chromosome segregation, and is thus an essential feature of the healthy MII oocytes (Miyara *et al.*, 2003). Disruption of the meiotic spindle results in rearrangement or scatter of chromosomes throughout the cytoplasm and may contribute to aneuploidy after fertilization (Wang *et al.*, 2001).

Szollosi *et al.* (1986) reported that the maternal spindle is attached to the cell periphery, whereas Payne *et al.* (1997) stated that in time-lapse recordings they noticed the metaphase plate remained stationary while the ooplasm moved. Recent data on Polscope observations (Rienzi *et al.*, 2005a) showed that the MII spindle can be visualized in 90% of analyzed oocytes. This suggests that the presence of the spindle cannot be considered an indicator of oocyte quality, while the absence of the spindle can be assumed to be an indicator of the poor quality of the oocyte (De Santis *et al.*, 2005).

b. Smooth Endoplasmic Reticulum (SER) and Voluminous Cytoplasmic Aggregates Mitochondria are characteristically associated with SER membranes, forming numerous and voluminous structures scattered in the cortical areas of the ooplasm. In particular, these structures are composed

of tubular membranes of SER anastomosed with each other and closely intermingling with mitochondria (M-SER aggregates) and large vesicles filled with flocculent slightly electron-dense material surrounded by a rim of mitochondria (M-V complexes) (Figs. 8 and 10). The formation of these aggregates starts from the fusion of SER membranes and tubules that are subsequently surrounded by mitochondria. The M-SER aggregates probably represent a precursor of the M-V complex (Motta *et al.*, 1988, 2000, 2003). These aggregates increase in content during the preovulatory maturation period, and are sensitive to gonadotrophin stimulation. In fact, such large hypertrophic aggregates are not common in either oocytes recovered after buserelin down-regulation, in natural cycle oocytes, or in oocytes matured *in vitro* (Sathananthan, 2003a,b).

This association between mitochondria and membranes of SER likely represents a single functional apparatus that we hypothesize to be involved in Ca^{2+} balance and storage. In fact, the human oocyte expresses calcium sequestration and release proteins, on the surface of SER membranes, in highly organized and developmentally regulated patterns. In addition to

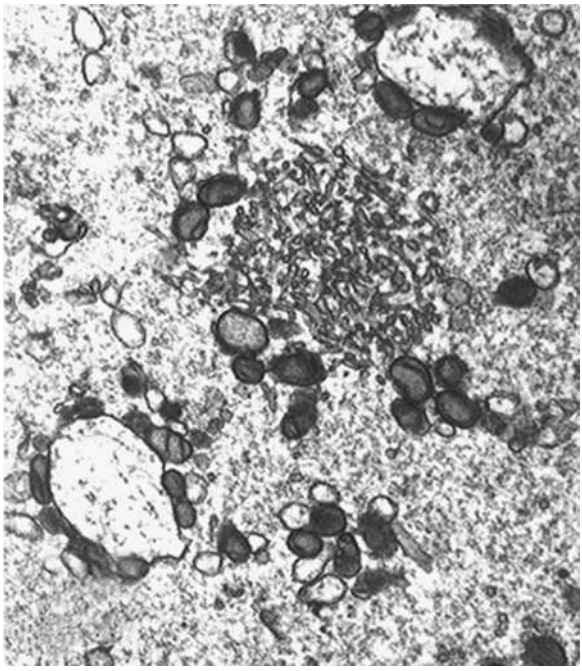

FIG. 10 Mature oocyte. Numerous rounded mitochondria are seen forming aggregates with smooth endoplasmic reticulum and complexes with long vesicles. (TEM, 12500X.)

different ER shapes, mitochondria may also act as a source for intracellular calcium (Balakier *et al.*, 2002). The developmental alteration of the calcium sequestration and release protein distribution may reflect the dynamic rearrangement of the M-SER M-V structures.

The aggregates could also be involved in lipid or steroid synthesis, since they are occasionally associated with dense lipid inclusions, which are quite rare in oocytes (Sathananthan, 2003a,b).

The smooth endoplasmic reticulum is organized either as isolated vesicles or aggregates of tubular elements (Sathananthan *et al.*, 1993). Conventional SER membranes are rare (Motta *et al.*, 2003).

c. Cortical Granules These structures were first identified using electron microscopy and originate from the Golgi body (Gulyas, 1976; Manna *et al.*, 2001; Sathananthan *et al.*, 1993). Cortical granules are small secretory granules (0.2–0.6 μm in diameter) that increase in number during oocyte growth and migrate toward the cortex, assuming a position 0.4–0.6 μm beneath the plasma membrane (Ducibella *et al.*, 1994) (Figs. 8 and 11). A strong correlation between cortical granule translocation and quality of the metaphasic plate has been observed; microtubules are probably involved in

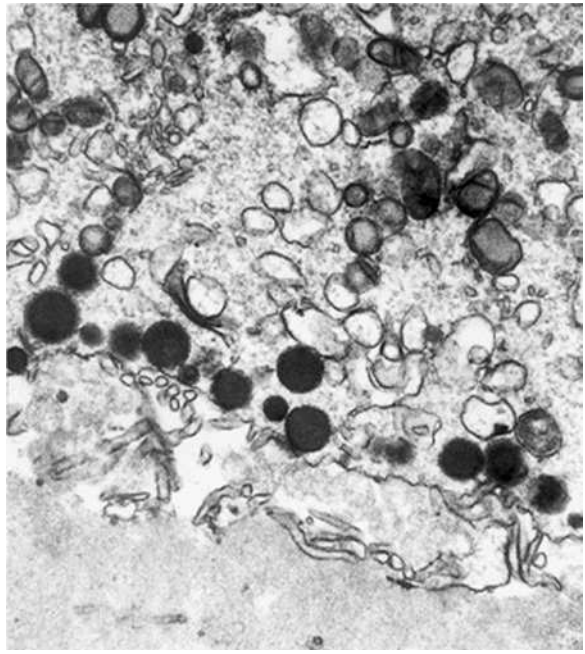

FIG. 11 Mature oocyte. Cortical granules are just beneath the oolemma. (TEM, 12500X.)

the correct translocation of the cortical granules (Abbott *et al.*, 2001). Alternatively, an important role could be played by the Ca^{2+}-dependent signaling component necessary for cortical granule translocation and extrusion (Abbot *et al.*, 2001).

Mammalian cortical granules contain glycosaminoglycans, proteases, acid phosphatases, and peroxidases (Hoodbhoy and Talbot, 1994; Moller and Wassarman, 1989).

Several studies suggest that the wheat germ agglutinin (WGA) and *Lens culinaris* agglutinin (LCA) lectins specifically recognize cortical granules in different human oocytes (Ghetler *et al.*, 1998; Sengoku *et al.*, 1999). Recently, Jiménez-Movilla *et al.* (2004) demonstrated by means of lectin-gold cytochemistry the presence of the following carbohydrate residues in the granules: GlcNAc (WGA), Fuc (AAA), Galβ1, 4GlcNAc (DSA), GalNAc (MPA and AIA), Neu5cα2, 3Galβ1, 4GlcNAc (MAA), Neu5Acα2,3Galβ1, 3GalNAc (after neuraminidase treatment followed by PNA binding), and biantennary and/or triantennary bisecting type N-glycans (E-PHA). They showed that the intensity of lectin binding to the cortical granules was not uniform, suggesting that a different population of cortical granules exists in the human oocyte. Cytochemical analysis of human cortical granules suggests similarities in glycosylation to ZP glycoproteins, but not to cortical granules from other mammalian species (Jiménez-Movilla *et al.*, 2004).

d. Other Cell Organelles The mature oocyte has few ribosomes and no rough endoplasmic reticulum. Golgi membranes are quite rare (Sathananthan *et al.*, 1993). These microstructural aspects reflect the inactive nature of the oocytes with respect to protein synthesis and secretion (Sathananthan, 2003a,b). Hence, Golgi activity seems to be arrested at MII after cortical granule synthesis has been completed in maturing oocytes.

Mitochondria are rounded with dense matrices and few arch-like or transverse cristae (Motta *et al.*, 2000, 2003; Sathananthan, 2003a,b). They are abundant and distributed throughout the ooplasm. Some mitochondria may present clear vacuoles within their matrices and a few are extremely large (Sathananthan, 2003a,b). Primary lysosomes are sparse in the mature oocyte but increase in number in aging oocytes. Secondary and tertiary lysosomes are commonly found in immature oocytes with signs of atresia. Occasionally, lysosomes may be associated with dense phagosomes or located in multivesicular bodies. These also increase with aging in culture (Sathananthan, 2003a,b). Small profiles of annulate lamellae may be found in mature oocytes, consisting of a few stacks of double membranes resembling the nuclear envelope (Sathananthan *et al.*, 1993).

e. Multiparameter Analysis of HME Clear criteria for evaluating oocyte morphology are very important for the performance of ICSI (Xia, 1997).

Human oocyte grading is based on three factors: first polar body morphology, size of the perivitelline space, and cytoplasmic inclusions, and is significantly related to fertilization rate and embryo quality after ICSI (Xia, 1997).

The quality of oocytes is characterized by interrelated factors, generally classified as nuclear and cytoplasmic "competence" (Miyara *et al.*, 2003). It is important that the evaluation of oocyte maturation in humans should include an adequate assessment of developmental competence, i.e., the ability of the oocyte to develop after fertilization (Trounson *et al.*, 2001).

i. Nuclear Competence Nuclear competence characterizes the quality of oocyte chromatin and spindle, which is essentially governed by metaphase-promoting factor (MPF) activity (Miyara *et al.*, 2003). Nuclear maturation involves resumption of meiosis by the germinal vesicle oocyte and its progression to MII after emission of the first polar body (Cekleniak *et al.*, 2001).

ii. Cytoplasmic Competence Whereas resumption of meiosis can be assessed easily after extrusion of the first polar body, cytoplasmic maturation involves several physiological processes that prepare the egg for activation, fertilization, and preimplantation development and may not be well assessed using light microscopy (Eppig, 1996). Cytoplasmic maturation encompasses complex tightly orchestrated biochemical molecular and cellular changes within the ooplasm to ensure both formation of a bipolar spindle and chromosome alignment and to support normal fertilization and subsequent development (Cekleniak *et al.*, 2001). During its final maturation the oocyte acquires a complex cytoplasmic organization consisting of neogenesis, modification, and redistribution of organelles in specific ooplasmic areas (Motta *et al.*, 2003).

Cytoplasmic maturation can be considered as the sum of the processes by which the mammalian oocyte changes from a developmentally incompetent cell, arrested at metaphase II, to one with the capacity to support fertilization and early embryonic development. Another criteria of cytoplasmic maturation is its ability to decondense the sperm chromatin following sperm penetration and to transform it into the male pronucleus (Navara *et al.*, 1995). The sperm decondensation factor is synthesized during oocyte maturation (Moor and Gandolfi, 1987) and prepares the egg to respond to spermatozoa with Ca^{2+} transients (Cheung *et al.*, 2000).

2. Microstructural Pathology of the Oocyte

Preovulatory (MII) oocytes may normally show some morphological abnormalities. According to Ebner *et al.* (2001, 2003b), these can be divided into cytoplasmic and extracytoplasmic. Deficient cytoplasmic maturity is associated with granularity or discoloration of the cytoplasm, SER aggregation,

vacuolization, and inclusions such as refractive bodies, all visible at the light microscopy level.

Vacuolization is probably the most apparent and dynamic cytoplasmic dysmorphism in human oocytes. Vacuoles vary in size as well as in number and they are membrane-bound cytoplasmic inclusions filled with fluid that is almost identical to the perivitelline fluid (Van Blerkom, 1990). Recently, Ebner *et al.* (2005) identified three types of vacuoles: those already present at oocyte collection, which develop during maturation, those artificially created by ICSI, and those accompanied by developmental arrest. The later the vacuoles arose, the more detrimental is their effect on blastocyst formation (Ebner *et al.*, 2005).

Extracytoplasmic abnormalities, in turn, include irregularities in oocyte shape, perivitelline space enlargement with the eventual presence of debris, first polar body fragmentation, and structural modifications of the oolemma and ZP. Suboptimal cytoplasmic texture may compromise the microtubule-organized concentration of mitochondria to perinuclear regions and thus impair cell cycle regulation severely (Ebner *et al.*, 2001, 2003b). The presence of pronucleus-sized vacuoles in MII oocytes during ICSI is associated, at the ultrastructural level, with tubular-type smooth ER clusters, related to high levels of estradiol and less chance of a successful pregnancy (Otsuki *et al.*, 2004).

Ultrastructural abnormalities in MII oocytes have been extensively studied by Sathananthan's group (Sathananthan, 1990, 1991, 1994a,b, 2003a,b; Sathananthan *et al.*, 1993). Oocytes at this stage may show dense ooplasms with progressive vacuolization caused by swelling of vesicular SER. Oocytes retrieved from older women also show aberrations of the MII spindle, which could lead to aneuploidy. A prolonged culture of the human oocyte seems to be the agent that most affects the microstructure of the cytoskeleton, MII spindle, SER, and mitochondria, throughout a process of "aging" of the oocyte, often culminating in cell death. In fact, mature oocytes aging in culture (48–72 h) frequently show (Sathananthan, 2003a,b) (1) centripetal dislocation of the spindles together with an attenuation at the poles and disorganization or loss of the MII spindle; (2) centripetal migration of cortical granules and formation of large clusters of cortical granules beneath the surface as a consequence of disorganization of the cortical cytoskeleton; (3) the appearance of lipofuscin bodies and occasional ingestion of ZP material; (4) a progressive swelling of vesicular SER culminating in the formation of clear vacuoles in the cytoplasm; and (5) clouding or aggregation of mitochondria and a progressive increase in their stromal density, culminating in the formation of dense bodies in their matrices, which has an adverse effect on respiration, so that the viability of the oocyte is progressively diminished.

3. Egg Vestments

The egg vestments are the ZP and the matrix within perivitelline space (PVS) (nearest to the oocyte), surrounded by the cumulus oophorus.

a. Zona Pellucida and Perivitelline Space The ZP is a translucid, relatively thick extracellular matrix surrounding the oocyte, ovulated eggs, and preimplantation embryos. It is secreted by the oocyte during follicular development in the ovary (Garside *et al.*, 1997). Several functions are accomplished by this matrix: it supports communication between oocytes and follicular cells during oogenesis, protects oocytes and embryos during development, and modulates gamete interaction (Høst *et al.*, 2002; Wassarman, 1999) (Fig. 8).

Zona layers are laid down in a temporal sequence, with the inner layer laid down last (Qi *et al.*, 2002). The molecular composition of the human ZP has been previously determined (Moos *et al.*, 1995; Sacco *et al.*, 1981; Shabanowitz and O'Rand, 1988). This matrix is a lattice made up of three glycoproteins named ZP1 (80–120 kDa), ZP2 (64–78 kDa), and ZP3 (57–73 kDa) that do not coincide exactly with those described for the mouse (Rankin and Dean, 2000). Each class of glycoprotein is posttranslationally modified and contains a number of different charge isomers providing a high degree of heterogeneity within the zona matrix. In humans, ZP3 was identified as the spermatozoa-binding protein and inducer of the acrosome reaction (Brewis *et al.*, 1996). However, recent genetic data in mice are more consistent with the 3-D structure of the ZP, rather than a single protein (or carbohydrate), determining sperm binding (Hoodbhoy and Dean, 2004). Genes codifying for ZP proteins from a variety of mammalian species are referred to as ZPA, ZPB, and ZPC (Harris *et al.*, 1994). However, four ZP genes are expressed in human oocytes (ZP1, ZP2, ZP3, and ZPB), and preliminary data obtained by Lefievre *et al.* (2004) show that the four corresponding ZP proteins are present in the human ZP, as a fundamental difference from the mouse model. A recent study reveals variable glycosylation of the human ZP throughout its thickness, with pronounced differences between the most external and internal regions of this matrix. This heterogeneous carbohydrate composition could be responsible for the different sperm–binding ability detected between the outer and inner regions of the ZP (Jiménez-Movilla *et al.*, 2004). In addition, human ZP glycoproteins express some carbohydrate sequences not previously detected in other species (Jiménez-Movilla *et al.*, 2004).

The thickness of the ZP of the MII oocyte in humans is about 15–18 μm, twice as thick as that of the mouse (Blake *et al.*, 2001; Goyanes *et al.*, 1990; Rankin and Dean, 2000), and is inversely correlated with estrogen levels

(Høst *et al.*, 2002). The molecules contributing to the inner portion of the zona are more densely packed than those of the outer portion. This may be due to the stretching of the external portion of the coat necessary to accommodate oocyte enlargement, a >300-fold increase in cell volume (Wassarman, 1990a). The fine structure of the human zona is reviewed by means of various ultrastructural techniques.

The PVS is a space between the oolemma and ZP containing a well-developed hyaluronan-rich extracellular matrix (Talbot and Dandekar, 2003). This space is relatively small around immature oocytes, whereas after extrusion of the first polar body it becomes asymmetrical and enlarged around the first polar body, and it retains this appearance until fertilization (Figs. 7–9). When observed by electron microscopy in the presence of ruthenium red (RR), this matrix appears to consist of electron-dense granules and filaments, and both filaments and granules appear to attach to the oolemma (Dandekar *et al.*, 1992). It is not known if the granular filamentous matrix in the PVS of unfertilized oocytes plays any role in oogenesis or fertilization; however, Talbot and Dandekar (2003) hypothesize a role during fertilization in that hyaluronan, which can inhibit membrane fusion, must be negotiated by the fertilizing sperm.

b. ZP in Immature, Mature, and Atretic Oocytes and Its Properties in Sperm Binding The 3-D zona structure resembles a delicate "meshwork" of thin interconnected filaments that varies in texture wideness according to the maturation stage of the oocyte (Familiari *et al.*, 1992a,b, 2001, 2006) (Figs. 12–15).

In human *in vitro* fertilization (IVF) experiments, capacitated spermatozoa penetrate oocytes in metaphase II but not oocytes at metaphase I (Tesarik *et al.*, 1988a). This observation has suggested that the ZP of human oocytes approaching meiotic maturity undergoes maturational changes, becoming more susceptible to sperm penetration. Marked differences in the ZP ultrastructure of metaphase I and metaphase II oocytes fixed immediately upon recovery have been noted. The ZP of metaphase I oocytes showed a compact and homogeneous aspect, while the ZP of metaphase II oocytes appeared as a highly porous structure.

Studies carried out by our group (Familiari *et al.*, 1988, 1989) agreed with the above observations. In fact, we have investigated by conventional SEM the ZP structure and the early interactions between the human oocyte and spermatozoa. Two basically different ZP patterns were observed: the first is a multilayered large mesh network resembling a spongy structure (Fig. 12), and the second shows a compact and smooth surface. The latter was commonly seen in cultured oocytes belonging to immature and atretic groups. These results have suggested that the spongy appearance of the ZP was

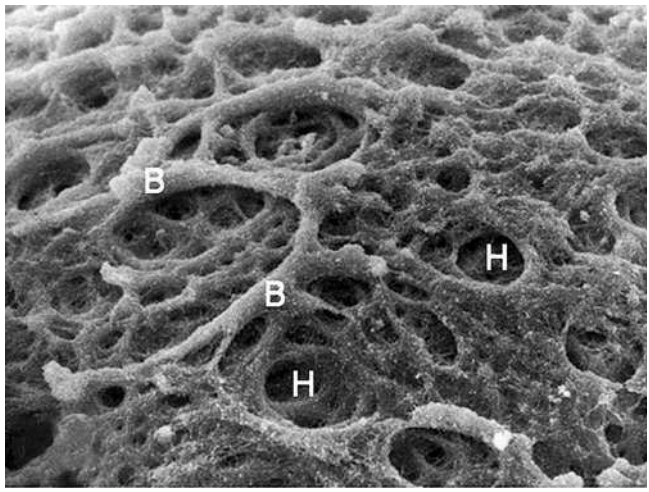

FIG. 12 Mature oocyte. Outer surface of the spongy zona pellucida. The spongy appearance is due to the presence of branches (B) surrounding holes (H). (High-resolution SEM, 1500X.)

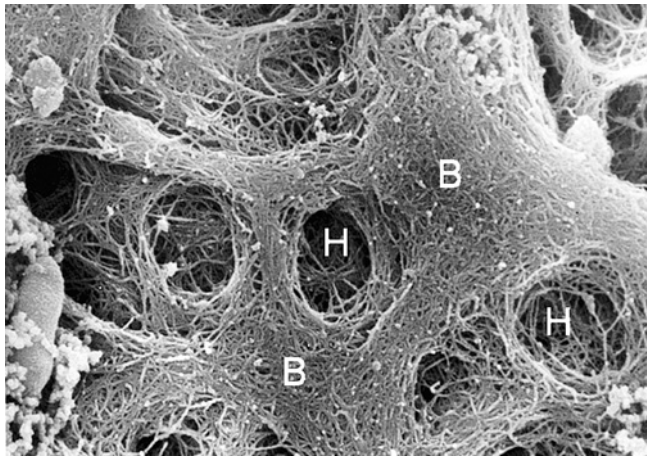

FIG. 13 Mature oocyte. Outer surface of the spongy zona pellucida. Note the tight meshed arrangement of filaments in correspondence to branches (B), and a large meshed network of filaments within the holes (H). (SEM with Sap-RR-Os-Tc method, 9000X.) (From Familiari *et al.*, 1992b.)

mainly related to oocyte development and maturity. However, greater numbers of penetrating spermatozoa were noted on oocytes showing the mesh-like ZP, whereas few if any sperm appeared flattened against the ZP surface

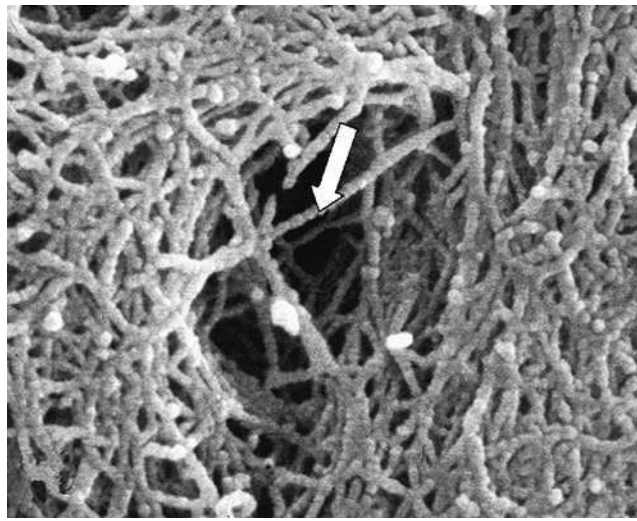

FIG. 14 Mature oocyte. Outer surface of the zona pellucida at high magnification. A different pattern of filament aggregation can be seen (arrow). Note that filaments have a "bead-on-a-string" structure. (SEM with Sap-RR-Os-Tc method, 75000X.) (From Familiari *et al.*, 1992b.)

of oocytes showing the more compact, smoother ZP. The inner surface of the ZP, as seen by conventional SEM, showed a compact structure in all cases (G. Familiari, unpublished observations).

In light of these results, we have hypothesized that the condensation of the outer aspect of the ZP caused a disorientation of sperm-binding sites, which would result in reduced sperm binding and penetration capacity, thus leading to impairment of *in vitro* oocyte fertilizability.

A detailed description of the filaments within the multilayered mesh network was obtained by high-resolution SEM and the saponin–ruthenium red–osmium tetroxide–thiocarbohydrazide (Sap-RR-Os-TC) method (Familiari *et al.*, 1992a). This method allowed straight or curved filaments, 0.1–0.4 μm in length and 10–14 nm in thickness, to be observed by TEM and 22–28 nm thick as seen by SEM. This difference in thickness is due to the chemical coating considered for SEM sample preparation. The filament arrangement was remarkably different between the inner and outer surfaces of the ZP and among the various maturation stages of the oocyte studied. The outer surface of the mature oocyte consisted of filaments arranged in a multilayered network that appears compact in the zones delimiting the meshes of the network, whereas it appears loose in the mesh holes. The latter seemed empty when observed with conventional SEM. They were, in turn, made up of a loose filament arrangement when observed with the Sap-RR-Os-TC

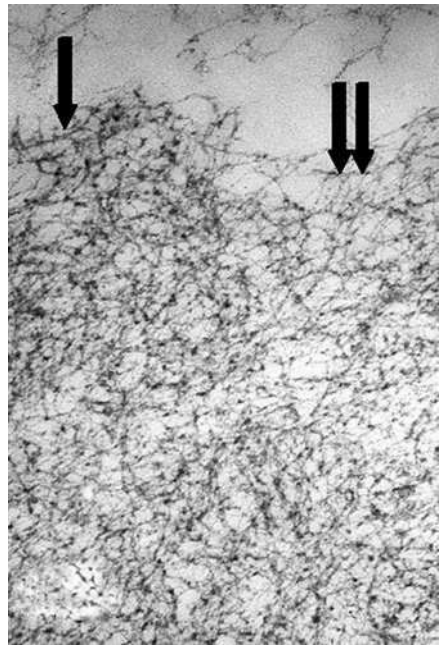

FIG. 15 Mature oocyte. High-power view of the outer portion of the zona pellucida. A regular alternating pattern of zones with filaments arranged in tight (single arrow) or loose (double arrow) meshed networks was present. (TEM with Sap-RR-Os method, 27700X.) (From Familiari *et al.*, 1992b.)

method (Figs. 13–15). Immature and atretic oocytes displayed almost exclusively a tight meshed network of filaments. The inner surface of the ZP belonging to unfertilized oocytes at any stage was arranged in repetitive structures characterized by numerous short and straight filaments that anastomosed with each other, sometimes forming small, rounded structures at the intersections (Familiari *et al.*, 1992b, 2001, 2006). Windt *et al.* (2001) have done an ultrastructural evaluation of recurrent and *in vitro* maturation-resistant metaphase I arrested oocytes and they have considered the "narrow and fibrous" appearance of the ZP as characteristic of the immature stage.

The influence of elevated pH levels on the structural and functional characteristics of human ZP has been investigated by Henkel *et al.* (1995). Fresh and salt-stored immature oocytes were randomly incubated in either synthetic human tubal fluid medium (untreated zonae) or in a chemically defined medium (treated zonae). Sperm binding experiments using hemizona assay conditions exhibited a 10-fold increased binding of sperm to treated

compared to untreated oocytes. Recordings during incubation showed higher pH levels in treated versus untreated ZP. The surface of treated ZP showed a spongy appearance, whereas that of untreated ZP appeared compact and smooth. Moreover, treated ZP was related to a marked increase of sperm binding, suggesting that altered ZP surfaces enhance sperm binding. The ZP of both fresh and salt-stored oocytes showed fine granular matrices of light to medium electron density. The ZP of oocytes incubated in standard medium showed a compact, granular, and medium electron-dense shape with smooth and homogeneous surfaces, whereas treated ZP showed numerous openings on their surfaces and a marked spongy appearance. In addition, acidic ZP solvents may have significantly improved sperm binding to immature ZP in sperm–oocyte coincubation if compared to control samples supplemented with basic ZP solvents, which have exhibited sperm binding ranges corresponding to those reported for prophase and metaphase I oocytes (Henkel *et al.*, 1995). The marked spongy appearance of the surface belonging to treated ZP was likely due to the effect of the particular culture medium on the fine structure of the ZP matrix, thus causing a manifold increased surface. These structural changes were possibly due to the slightly increased pH levels in the medium.

On the basis of these data, we propose that oocyte maturation in humans is accompanied by 3-D modifications in the arrangement of ZP filaments, which may be relevant in the processes of binding, penetration, and selection of spermatozoa (Familiari *et al.,* 1992a, 2001, 2006).

In contrast to our results, Magerkurth *et al.* (1999) reported that oocytes had an extremely heterogeneous morphology of the ZP surface, within and among patients. Furthermore, Magerkurth *et al.* (1999) described four different types of ZP morphology considering four categories of oocytes (mature, immature, fertilized, and unfertilized), from a porous, net-like structure to a nearly smooth and compact surface. They found no correlation between ZP type and oocyte maturity or fertilizability and, therefore, they suggested that the heterogeneous morphology of the ZP does not play an important role in sperm–oocyte interaction. Nevertheless, recent observations of our group on the microanatomy of the ZP surface in inseminated but unfertilized mature human oocytes derived from ART (Familiari *et al.*, 2001, 2005) have supported our previous results (Familiari *et al.*, 1988, 1992a,b). Following a comparative analysis of traditional SEM techniques (gold coating and conductive staining methods) and the Sap-RR-Os-TC method, the main aspect of the ZP by traditional SEM consisted mostly (78.5%) of a porous, net-like structure. After the Sap-RR-Os-TC method, most oocytes (86.1%) showed the ZP consisting of alternating tight and large meshed networks (Familiari *et al.*, 2001, 2006). Therefore, the well-standardized procedures, the stabilizing action of the conductive staining on the ZP material, and the results obtained with the Sap-RR-Os-TC method strongly

emphasize that ZP changes occurring in oocytes of various groups are not artifacts but genuine features, very likely related to their actual maturation status.

Further, molecular support for our ultrastructural data arises from the last *supramolecular model* as the basis for egg–sperm recognition (Hoodbhoy and Dean, 2004; Rankin *et al.*, 2003). Rankin *et al.* (2003) proposed a model in which the ZP is composed, at least, of ZP2 and ZP3, forming a 3-D matrix around ovulated eggs to which sperm will bind. Following fertilization and cortical granule exocytosis, the cleavage of ZP2 modifies the 3-D structure of the ZP matrix without loss of zona components, so that sperm can no longer bind (Baranska *et al.*, 1975; Familiari *et al.*, 1992b, 2001, 2006; Funahashi *et al.*, 2001; Jackowski and Dumont, 1979). On the basis of the above evidence, it is rather logical to hypothesize that the 3-D network of ZP filaments is not ''randomly'' arranged but structured to accomplish fertilization of the mature oocyte.

c. Cumulus Oophorus and the Cumulus Matrix

i. Cumulus Oophorus Cells: Their Function in the Postovulatory Period on Oocyte Maturation The human mature oocyte, at ovulation, is covered by a large cumulus cells mass, called the ''cumulus oophorus,'' even during IVF procedures. The cumulus mass is composed of about 20,000 irregularly rounded cumulus cells (Figs. 7 and 16) joined by means of linear and annular gap junctions (Motta *et al.*, 1988, 1991, 1995a; Nottola *et al.*, 1998, 2001). Although the rate of ovum denudation increases with time, human cumulus

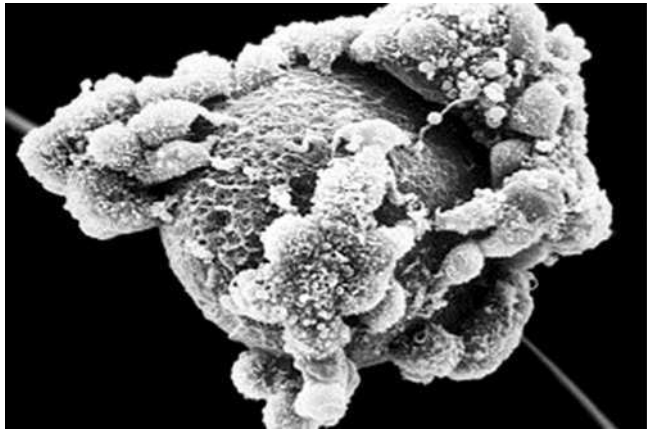

FIG. 16 Mature unfertilized oocyte (IVF). Rounded or oval cumulus corona cells are seen directly in contact with the outer aspect of the zona pellucida. (SEM, 1350X.)

cells continue to surround the egg and its ZP before fertilization within the tube, during fertilization, as well as 72 h after fertilization around the segmented embryo (Motta *et al.*, 1995a; Ortiz *et al.*, 1982). Once released from the follicle at ovulation, the cumulus mass surrounding the oocyte undergoes characteristic structural changes, likely resembling a true luteinization in IVF protocols as well as in *in vivo* human reproduction (Motta *et al.*, 1994b, 1995a,b; Nottola *et al.*, 1989, 1991) (Figs. 17–19). These changes also occur in parallel within the ovary in the granular cells of the post-ovulatory follicle (Gulyas, 1984; Rotmensch *et al.*, 1986). The cumulus mass, after a luteinizing hormone (LH) surge, synthesizes and deposits a mucoelastic extracellular matrix, leading to expansion and detachment from the wall of the follicle (Dandekar *et al.*, 1992; Familiari *et al.*, 2000; Salustri *et al.*, 1999).

The close functional relationships between oocyte and cumulus cells do not end at ovulation, but are modified, acquiring different morpho-functional characteristics, and are important for oocyte maturation and embryo viability, as shown in IVF procedures. The cumulus cells play an important role in the induction of meiotic resumption and as a support for cytoplasmic maturation in mammals (Tanghe *et al.*, 2002). Moreover, the cytoplasmic maturation of human oocytes is also improved, maintaining cumulus cells during culture in IVF protocols (Goud *et al.*, 1998).

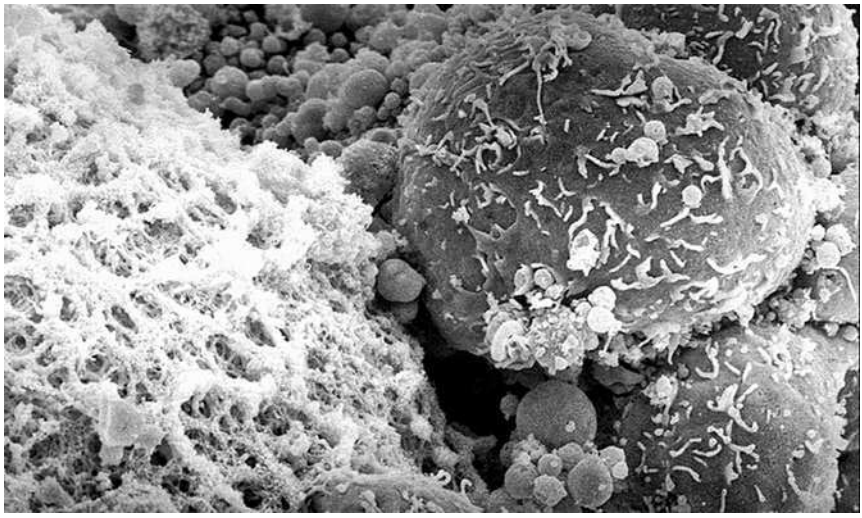

FIG. 17 Mature unfertilized oocyte (IVF). Cumulus cells irregularly rounded have blebs and microvilli on the surface. (SEM, 3100X.)

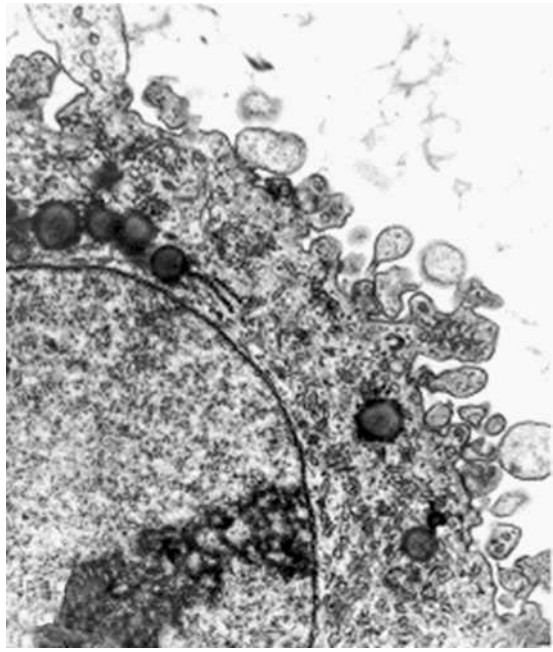

FIG. 18 Mature unfertilized oocyte (IVF). Cumulus cell. Lipid droplets and numerous organelles are seen. The nucleus contains dispersed chromatin and reticular nucleolus. The cell membrane shows blebs and microvilli. (TEM, 3800X.)

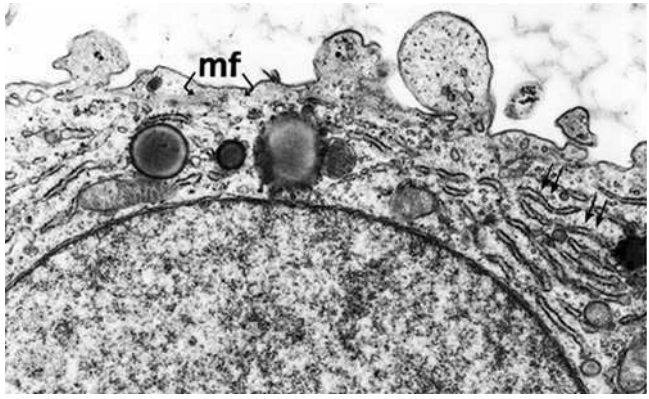

FIG. 19 Mature unfertilized oocyte (IVF). Cumulus cell. Parallel stacks of cisternae of rough endoplasmic reticulum (double arrows) and lipid droplets are seen in the cytoplasm. Bundles of filaments (mf) are present in the subplasmalemmal area. (TEM, 21000X.) (From Nottola *et al.*, 1991.)

Other studies showed that a simple coculture system using autologous cumulus cells can result in significantly improved human embryo morphology, implantation rates, and clinical pregnancy rates during *in vitro* fertilization (Carrell *et al.*, 1999); in addition, other observations demonstrated that cumulus-removed oocytes in prophase or metaphase I of meiosis, compared to cumulus-removed oocytes at metaphase II, resulted in lower fertilization rates, in a lower incidence of blastocyst stage development, and in a lower percentage of top-scoring blastocysts (Huang *et al.*, 2002).

Cumulus cells exert some of their effects on the human oocyte via gap junctions (Motta *et al.*, 1994a), via paracrine signals, which may explain the beneficial effect of coculture of granulosa cells (Dandekar *et al.*, 1991) or by an apocrine mechanism for the storage and release of growth factors and proteins (Antczak *et al.*, 1997). Some of these proteins (leptin and STAT3) are expressed and selectively distributed in mature oocytes and developing embryos, which is suggestive of their role during embryogenesis (Antczak and Van Blerkom, 1997). Furthermore, CD44, a transmembrane glycoprotein expressed in human cumulus cells, play an important role in oocyte maturation (Ohta *et al.*, 1999). As shown in porcine oocytes, the hyaluronan–CD44 interaction during cumulus expansion regulates the disruption of gap junctions in cumulus–oocyte complexes and concurrently controls the occurrence of meiotic resumption (Yokoo and Sato, 2004).

ii. Cumulus Oophorus Cell Ultrastructure The cumulus cells we studied belong to human oviductal oocytes obtained during physiological cycles (Motta *et al.*, 1995a), and from human preovulatory oocytes, obtained after ovarian superstimulation, and unfertilized after *in vitro* insemination during ART procedures (Motta *et al.*, 1995b, 1999; Nottola *et al.*, 1989, 1991). By TEM and SEM, cumulus cells are irregularly rounded and are provided with cytoplasmic expansions, mainly blebs of various sizes and density, and a few short microvilli (Figs. 17 and 18). Although in some cases joined by small gap junctions, cumulus cells appear by TEM to be separated by large intercellular spaces, considered a morphological sign of the expansion of the cumulus mass that usually accompanies the final process of the oocyte (Larsen *et al.*, 1991). The nuclei of the cumulus cells contain dispersed chromatin and one to three nucleoli at maturation.

Our observations revealed that the cumulus cells surrounding the oocytes contain primarily mitochondria with lamellar to tubular cristae, abundant membranes of SER, and numerous lipid droplets, often surrounded by a few concentric membranes of SER and/or in close contact with microtubules and microfilaments. Spherical membrane-bound structures (0.1–0.4 μm in size) of moderate electron density, likely corresponding to microperoxisomes, are also present in the cytoplasm, together with Golgi membranes, RER cisternae, and polyribosomes (Motta *et al.*, 1994b, 1995a,b, 1999; Nottola *et al.*, 1989, 1991) (Figs. 18 and 19). This organular pattern is

normally characteristic of metabolically active luteal cells involved in steroid synthesis (Gulyas, 1984). Furthermore, the occurrence in the cytoplasm of these cells of an extensive cytoskeletal network, capable of entrapping and/or moving organelles together (Carnegie *et al.*, 1987), as well as the presence of microperoxisomes, strengthen the hypothesis that cumulus cells have full steroidogenic ability. Ultrastructural signs of steroidogenesis are present in the cumulus cells belonging to both oviductal and *in vitro* inseminated oocytes, in particular during and shortly after fertilization (Motta *et al.*, 1994b, 1995a,b; Nottola *et al.*, 1989, 1991).

iii. Role of the Cumulus Oophorus in the Production of Hormones and Other Molecules Our ultrastructural findings corroborate other biochemical data on the presence of small amounts of estrogens and progesterone in the culture medium conditioned from oocyte–cumulus complexes (Shutt and Lopata, 1981). In this regard, aromatase activity was demonstrated in human cumulus cells surrounding both inseminated and noninseminated oocytes in an ART program (Motta *et al.*, 1995c). Aromatase is not uniformly distributed in cumulus cell populations and results are more intense around oocytes subjected to insemination, whereas around noninseminated oocytes, only the outer layer of the cumulus cells appears positive. These results further suggest the presence of steroidogenic activity (Motta *et al.*, 1995c).

Human cumulus cells also secrete vascular endothelial growth factor (VEGF) (Abbas *et al.*, 2003), and cytokines such as interleukin (IL)-1α, IL-6, and tumor necrosis factor (TNF)-α (Tarlatzis and Bili, 1997). Interesting observations of Goud *et al.* (1998) showed that supplementation of the maturation medium with epidermal growth factor (EGF) or maintenance of the cumulus cells during culture improves the nuclear and cytoplasmic maturation of human oocytes *in vitro*.

Recent studies showed the presence of both macrophages and $CD4^+$ T cells in cumuli surrounding human oocytes obtained from ART protocols (Piccinni *et al.*, 2001). It was shown that $CD4^+$ T cell clones, generated from T cells of these cumuli, have a greater potential to produce IL-4 and leukemia inhibitory factor (LIF) than $CD4^+$ T cell clones generated from peripheral blood or ovary specimens from the same women; in addition, IL-4 and LIF were found to be constitutively expressed *in vivo* by CC cells (Piccinni *et al.*, 2001). Therefore, T cells present in the cumulus produce cytokines that, interacting with cumulus progesterone production, may provide a microenvironment suitable for preimplantation development of the human embryo (Piccinni *et al.*, 2001), although there seems to be no association between follicular fluid IL-1β concentrations and pregnancy outcome of ART cycles (Hofmann *et al.*, 2004).

Immunocytochemical data presented in our observations demonstrated that human cumulus cells are able to produce adhesive proteins such as fibronectin and tenascin-c in the postovulatory period (Familiari *et al.*,

1996; Motta *et al.*, 1999; Relucenti *et al.*, 2005). In particular, the immunohistochemical data demonstrated that their production is not homogeneous in the cumulus cells population. In fact, fibronectin immunoreactivity was shown mostly by inner cumulus cells and especially in corona radiata cells, whereas tenascin-c was produced by some specialized cells scattered in the entire cumulus mass (Familiari *et al.*, 1996; Motta *et al.*, 1999; Relucenti *et al.*, 2005) (Fig. 20).

A possible role for fibronectin and tenascin-C may be postulated in the final maturation of the ovum, in the tubal pick-up, and in the complex dialogue with the tubal epithelium.

Studies by our group (Motta *et al.*, 1994b, 1995a–d; Nottola *et al.*, 1991) revealed that steroid secretion of the cumulus cells may ensure an adequate microenvironment in which normal fertilization and early embryo development occur. Therefore, the secretion of fibronectin and tenascin-C by groups of CC cells may emphasize this role, possibly helping to modulate the "complex biochemical dialogue" between the ovum (and, later, the embryo) and the oviduct, thus creating a favorable egg–tubal milieu (Familiari *et al.*, 1996).

Recently, Honda *et al.* (2004), analyzing human mature MII oocytes from ICSI trials, showed that the follicular fluid concentration of fibronectin

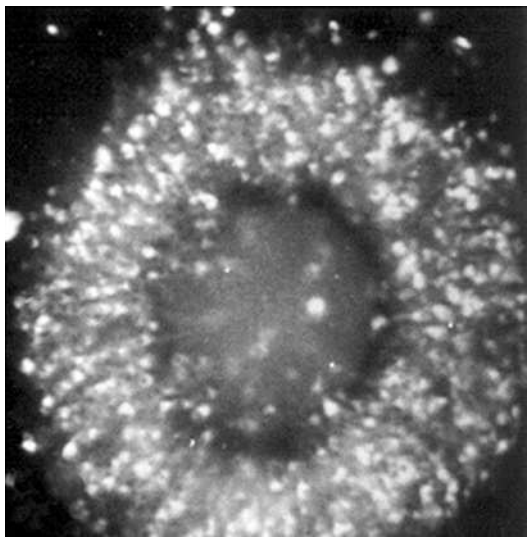

FIG. 20 Mature oocyte without culture. Antibody against tenascin-C. Numerous positive cells are scattered in the entire cumulus corona mass. (Confocal laser microscopy, 170X.) (From Familiari *et al.*, 1996.)

correlated with the morphology of oocyte cytoplasm. These findings strongly support our previous data on fibronectin–cumulus cell production, and evidence their physiological significance in granulosa cell luteinization and oocyte quality. All reported observations demonstrate that the cumulus oophorus is a highly morphodynamic and complex structure, which, both *in vitro* and *in vivo*, is composed of different specialized subpopulations and secretes several substances, such as estrogens, progesterone, adhesive proteins, and cytokines, providing a suitable chemical microenvironment that is essential during its journey from ovulation to implantation.

iv. Role of the Cumulus Oophorus in the Production of Extracellular Matrix Cumulus cells synthesize an extensive extracellular matrix induced by ovulatory stimulus under the control of oocyte-derived factors, leading to the characteristic preovulatory expansion of the cumulus–oocyte complex (Salustri *et al.*, 1994, 1999; Zhuo and Kimata, 2001). The cumulus matrix is mainly composed of hyaluronan, proteoglycans, and proteins, as well as extrafollicularly originated serum-derived hyaluronan-associated proteins, that are covalently bound to hyaluronan (Salustri *et al.*, 1994, 1999; Zhuo and Kimata, 2001). The cumulus matrix also contains other glycosaminoglycans such as heparan sulfate and chondroitin sulfate (Drahorad *et al.*, 1991) and other proteins including inter-α-trypsin inhibitor, which is present throughout the matrix, covalently linked to chains of hyaluronan during cumulus expansion in mammals, thereby stabilizing the cumulus matrix and retaining it in the complex (Chen *et al.*, 1996). Adhesive molecules such as fibronectin and tenascin-C are also present in the extracellular matrix at ovulation (Familiari *et al.*, 1996, 2000) (Fig. 20). Tenascin-C largely colocalizes with fibronectin in the extracellular matrix (Riou *et al.*, 1988), and glycosaminoglycans modulate fibronectin matrix assembly and are essential for matrix incorporation of tenascin-C (Chung and Erickson, 1997). In the cumulus extracellular compartment further studies need to ascertain the colocalization of these adhesive proteins within the hyaluronan matrix.

Recent findings showed that pentraxin3 (PTX3) is also involved in cumulus matrix stability (Varani *et al.*, 2002), and that is expressed in the human cumulus oophorus as well (Salustri *et al.*, 2004). In particular, Salustri *et al.* (2004) show that PTX3 does not interact directly with hyaluronan, but it binds the cumulus matrix hyaluronan tumor necrosis factor α-induced protein 6 (TGS6), and thereby may form multimolecular complexes that can cross-link hyaluronan chains, stabilizing the matrix, and playing a crucial role in cumulus expansion.

From an ultrastructural point of view, the extracellular matrix present around the human oocyte and the cumulus was examined by TEM following fixation in the presence of RR (Dandekar and Talbot, 1992; Dandekar *et al.*, 1992), with Sap-RR-Os-TC using both high-resolution SEM and TEM (Familiari *et al.*, 1992a, 2000).

Studies using TEM on human mature oocytes, obtained from ART protocols, showed an extracellular matrix composed of thin filaments and granules at the interconnections of the filaments, which were interpreted as hyaluronic acid chains and bound proteoglycans, respectively (Dandekar *et al.*, 1992; Familiari *et al.*, 2000). In particular, studies of Dandekar *et al.* (1992), following enzymatic digestions, removed granules with affinity-purified trypsin and filaments with *Streptomyces* hyaluronidase, demonstrating that at the ultrastructural level, filaments corresponded to hyaluronan filaments, whereas granules corresponded to protein molecules.

The cumulus oophorus extracellular matrix is present between cumulus and corona radiata cells, on the surface of the ZP and in the PVS (Dandekar and Talbot, 1992; Dandekar *et al.*, 1992; Familiari *et al.*, 2000). Using high-resolution SEM, a 3-D structure of the extracellular matrix shows that the matrix is composed of an array of thin filaments (20–30 nm in thickness) anastomosed to form a very fine and regular network covering the ZP and cumulus cells. Microgranules were present at the filament cross-connection points. Furthermore, this matrix still covered the surface areas of the ZP lacking "corona radiata" cells, when human oocytes were denuded of corona cells and still maintained for 4 days in culture (Familiari *et al.*, 2000). These observations suggest that extracellular matrix filaments were linked to ZP filaments in a covalent fashion.

v. Presumptive Roles of Extracellular Matrix (ECM) in the Postovulatory Period The functional role of the ECM in the extrusion of the oocyte at ovulation, its capture by the ciliated epithelial cells of the tubal infundibulum, and its transport to the fertilization site is well understood in mammals (Talbot *et al.*, 2003; Tanghe *et al.*, 2002; Van Soom *et al.*, 2002; Yanagimachi, 1994). In fact, removal of the cumulus cells and hyaluronan matrix by means of hyaluronidase prevented oocyte pick-up in hamsters (Mahi-Brown and Yanagimachi, 1983). On the other hand, the cumulus matrix is responsible for adhesion between the hamster cumulus–oocyte complexes and the cilia of the oviduct, although the exact biochemical nature of this adhesion remains to be elucidated (Lam *et al.*, 2000). Therefore, cumulus cells and their matrix are probably not always important for oocyte pick-up or transport toward the oviductal ampulla, since in some mammalian species they are not important in this phase (Moore and Bedford, 1978).

No direct evidence has been found in this field for human *in vivo* reproduction. Moreover, the presence of the matrix around human oocytes after a long time in *in vitro* culture (Familiari *et al.*, 2000), the production of adhesive proteins in *in vitro* culture (Familiari *et al.*, 1996), and the presence of rather metabolically active cumulus cells around human embryos *in vivo* (Motta *et al.*, 1995a) strongly suggest a positive role for the cumulus cells and their matrix during the postovulatory period in oocyte pick-up and tubal transport.

IV. Gamete Interaction and Fertilization

Gamete interaction is an essential event leading to fertilization in mammals. It includes the series of biochemical processes and morphological changes by which gametes (sperm and mature oocytes) recognize each other and fuse together to finally trigger embryo cleavage. The process of fertilization is primarily mediated by gamete surface proteins, acting in a sequential pattern, to orchestrate the close approach and ultimate fusion of the two cells (Inoue *et al.*, 2005; Primakoff and Myles, 2002; Schultz and Williams, 2005). Among these events, sperm penetration of the egg coats, binding and fusion with the oolemma, activation of the oocyte, and decondensation of the sperm head are included.

A. Sperm Penetration of the Egg Coats

Before reaching the final goal of fertilization the capacitated sperm have to penetrate the egg vestments, cumulus oophorus, and ZP. The fertilizing human sperm penetrates the cumulus oophorus and corona radiata (Fig. 21) with the acrosome intact and binds to the surface of the ZP by the plasma membrane overlying the acrosome. The binding reaction stimulates the acrosome reaction, which occurs on the surface of the ZP and continues

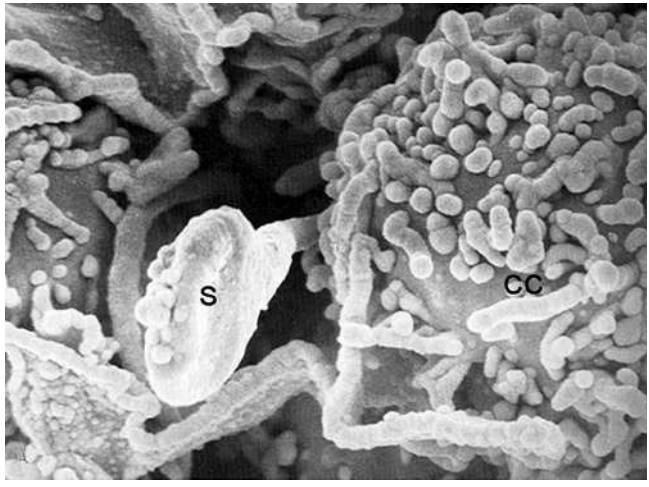

FIG. 21 Fertilized polypronuclear ovum. Human cumulus-corona cells. A spermatozoon (S) is seen in close contact with the cumulus-corona cells (CC). (SEM, 11500X.) (From Nottola *et al.*, 1991.)

during the early stages of sperm–ZP penetration, but is complete by the time the sperm reaches the inner third of the ZP (Baker *et al.*, 2000; Sathananthan *et al.*, 1993).

Several interconnected events are needed to achieve fertilization: successful sperm capacitation, the passage through the cumulus oophorus, the binding to the ZP, the acrosome reaction, the penetration of the ZP, the binding and fusion with the oolemma, and decondensation of the sperm head to form the male pronucleus.

1. Cumulus Oophorus Modulates Sperm Penetration

The cumulus oophorus has several favorable effects on the overall fertilization process. It creates a microenvironment that facilitates sperm capacitation, acrosome reaction, and penetration. It prevents changes in the oocyte, which are unfavorable for subsequent fertilization, such as premature cortical exocytosis and subsequent zona hardening (Tanghe *et al.*, 2002; Van Soom *et al.*, 2002).

The cumulus oophorus is able to entrap and guide the sperm toward the oocyte, and, at least *in vivo*, probably decreases polyspermy (Van Soom *et al.*, 2002) and stimulates human sperm velocity (Fetterolf *et al.*, 1994). It increases the number of fertilizing sperm around the oocyte by means of a sort of chemotaxis involving molecular signals. Cumulus cells closest to the oocyte secrete an attractant for spermatozoa, creating a gradient within the cumulus oophorus (Eisenbach, 1999, 2004). Recent studies suggest that human sperm chemoattractants are secreted not only prior to ovulation within the follicle, as earlier studies have demonstrated (Eisenbach, 1999, 2004), but also after oocyte maturation outside the follicle, and that there are two chemoattractant origins: the mature oocyte and the surrounding cumulus cells *in vitro* (Sun *et al.*, 2005). As suggested by Sun *et al.* (2005), a reasonable sequence of events indicates that the capacitated mammalian sperm, released from the sperm reservoir at the isthmus, are first guided by thermotaxis from the cooler sperm storage site toward the warmer fertilization site in the ampulla (Bahat *et al.*, 2003). Passive contractions of the oviduct may assist the sperm to reach the fertilization site. There, the sperm sense the chemoattractant secreted by cumulus cells and reach the cumulus by chemotaxis. Once within the cumulus matrix, the sperm sense the more potent chemoattractant, secreted from the oocyte, and navigate to the oocyte by chemotaxis (Sun *et al.*, 2005).

The cumulus oophorus selects morphological normal spermatozoa during IVF (Carrell *et al.*, 1993). Moreover, cumulus corona cells and leukocytes can phagocytose supernumerary and/or abnormal sperm in the *in vivo* fertilization process (Motta *et al.*, 1995b; Nottola *et al.*, 1998; Sathananthan *et al.*, 1993) (Fig. 22).

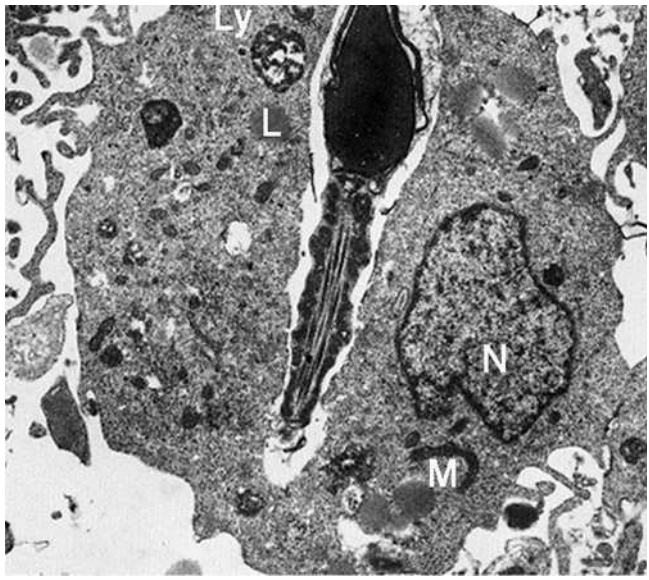

FIG. 22 Phagocytosis of a sperm by cumulus cells. The micrograph shows a corona cell that has completely phagocytosed an acrosome-intact sperm attached to its midpiece. The corona cell shows a nucleus (N), mitochondria (M), lipid globules (L), and lysosomes (Ly) and sometimes extends long filiform processes during sperm phagocytosis. (TEM, 15400X.) (From Sathananthan *et al.*, 1993.)

As already stated, it is known that human cumulus cells secrete proteins (Sullivan *et al.*, 1990; Tesarik *et al.*, 1988b), among which are adhesive proteins such as fibronectin and tenascin-C (Familiari *et al.*, 1996, 2000; Relucenti *et al.*, 2005), as well as steroids *in vitro* (Motta *et al.*, 1995c; Tarlatzis and Bili, 1997). It has been suggested that progesterone is a possible inducer of acrosome reaction in humans (Bronson *et al.*, 1999). Progesterone interacts with specific sperm binding sites located on the sperm plasma membrane and induces a dramatic increase in cytosolic Ca^{2+}, which leads to membrane fusion.

Controversial results are found in the literature about a possible role for fibronectin on sperm function. In fact, the addition of fibronectin, among other carbohydrates and glycoproteins, in bovine fertilization *in vitro* results in a potent inhibition of oocyte penetration, producing a significant reduction in total and progressive sperm motility (Tanghe *et al.*, 2004). However, fibronectin, a component of the cumulus extracellular matrix, was found to stimulate acrosomal exocytosis in boar sperm (Mattioli *et al.*, 1998). These differences may be explained by the different experimental protocols used in these studies. Further observations need to clarify the possible role of

fibronectin in human IVF, on the progression of human spermatozoa toward the cumulus envelope.

Sperm capacitation and/or penetration are probably oxygen tension and/or reactive oxygen species (ROS) dependent. Oxygen tension is also involved in the production of ROS. Low ROS levels can promote a redox-regulated cAMP-mediated pathway that plays a central role in the induction of sperm capacitation. Excessive amounts of ROS cause a loss of sperm function associated with peroxidative damage to the sperm plasma membrane (Baker and Aitken, 2004). When sperm are fertilizing cumulus-denuded oocytes, they are continuously exposed to the influence of atmospheric oxygen tension; lower oxygen tension inside the cumulus oophorus could minimize the possible dangerous influence of ROS. Whether cumulus cells are able to modulate oxygen tension and/or ROS is currently under investigation.

The cumulus oophorus can promote oocyte fertilizability by preventing changes in the oocyte, such as precocious zona hardening, which are unfavorable for normal fertilization. Cumulus cells reduce the inhibitory effect that the follicular fluid exerts on sperm–zona binding *in vitro* (Hong *et al.*, 2003). Cumulus oophorus cells' apoptosis is correlated with the maturation stage of the enclosed oocyte. Høst *et al.* (2002) found that a higher proportion of apoptosis-activated cumulus cells is present in metaphase I oocyte–cumulus complexes and germinal vesicle stage oocyte–cumulus complexes. Another important finding was that the degree of apoptosis of cumulus cells that surround a metaphase II oocyte influences the fertilization rate of the oocyte after ICSI (Høst *et al.*, 2002).

2. Sperm Penetration of Cumulus Oophorus Extracellular Matrix

To fertilize the oocyte, the capacitated sperm need to pass through the extracellular matrix of the cumulus oophorus. As already stated, an important part of the expanded cumulus matrix is composed of glycosaminoglycans, such as hyaluronic acid, heparan sulfate, and chondroitin sulfate (Drahorad *et al.*, 1991). Hyaluronic acid has also been proposed to bind to sperm plasma membrane protein PH-20, resulting in spermatozoa with higher basal calcium levels. As a consequence, these spermatozoa are more responsive to induction of acrosome reaction after binding to the ZP (Sabeur *et al.*, 1998). Hyaluronic acid might, therefore, be a candidate molecule to improve capacitation of spermatozoa (Sabeur *et al.*, 1998). The sperm protein PH-20, which is present on the plasma membrane of human sperm (Lin *et al.*, 1994), disrupts the hyaluronan macromolecular structure of the matrix with its hyaluronidase activity. Reasonably, hyperactivated spermatozoa should penetrate the viscous cumulus matrix more easily than nonhyperactivated spermatozoa (Tesarik *et al.*, 1990). The human cumulus matrix also

exerts a beneficial effect on sperm motility, probably by acting preferentially on hyperactivated spermatozoa (Tesarik *et al.*, 1990).

Studies by Salustri *et al.* (2004) demonstrated that oocytes ovulated by PTX3-null female mice were not fertilized *in vivo*, but could be fertilized *in vitro*. These results are consistent with the crucial role assigned to normal cumulus expansion for sperm recruitment *in vivo*, a role possibly connected with the presence of a very low number of spermatozoa of the site of *in vivo* fertilization, and with the necessity for sperm to be guided to the oocyte (Eisenbach, 1999). Since PTX3 is also expressed in human cumulus extracellular matrix, it is likely to have the same role in human fertilization, in which the absence of PTX3 might perturb interactions of the sperm with the matrix during the *in vivo* fertilization process (Salustri *et al.*, 2004). Future ultrastructural studies need to show the 3-D relationships between sperm and the cumulus matrix.

3. Sperm Penetration of the ZP

Mouse and human spermatozoa exhibit order-specific binding to the ZP. These two mammals have adopted a biological strategy in which the supramolecular structure of the ZP varies to enhance the binding of their cognate spermatozoa, which are so different from a morphological point of view (Rankin and Dean, 2000). SEM studies show no differences in the fine structure of the ZP between mature unfertilized eggs and fertilized human pronuclear stage oocytes. In unfertilized oocytes, the ZP appears porous, with a large number of ring-shaped structures, randomly superimposed in several layers. The superficial pores have a mean diameter of 4 μm, with the diameter decreasing in more inner lying pores (Familiari *et al.*, 1988, 1989, 1991).

Pelletier *et al.* (2004) have quantitatively characterized zona layers in living immature and mature oocytes. Their study demonstrates not only that the overall zona thickness varies but that the thickness and molecular organization of subzonal layers (named 1, 2, and 3, starting from the innermost) vary as well. Fertilization rates strongly depend on the ability of sperm to bind to the ZP. The zona binding is powerfully influenced by sperm morphology, in particular, the normal shape of the acrosome (Liu and Baker, 1992). Results presented by Liu and Baker (2000) showed that defective sperm–zona interaction is the major cause for low fertilization rates with standard IVF. However, sperm with abnormal acrosomes can accomplish the acrosome reaction (Sathananthan, 1996).

The ZP has multiple functions during fertilization (Rankin and Dean, 2000). It acts as a powerful selection for sperm with normal morphology (Liu and Baker, 1992). The existence of the ZP implies a dual role. First, it mediates initial sperm–egg recognition, an essential first step in fertilization,

and represents a major barrier for fertilization in that it blocks polyspermy (Rankin and Dean, 2000); second, it processes spermatozoa so that it also has a positive role in facilitating fertilization (Stanger *et al.*, 2001). In fact, the ZP allows sperm penetration and subsequent fusion with the egg oolemma. It triggers the acrosome reaction so that only acrosome–intact spermatozoa bind to the ZP (Rankin and Dean, 2000; Stanger *et al.*, 2001).

The acrosome area of the sperm head acts as a selected morphometric parameter and a specific size (about 5 μm^2) is selected for sperm to be bound to the zona. Anterior symmetry of the sperm and width of the midpiece region at the junction with the head are other parameters selected by zona binding (Garrett *et al.*, 1997). A quantification of the relationship between sperm morphometry and zona binding ability will result in better discrimination of fertile and subfertile men based on sperm morphology.

The physiological fertilization process involves binding of acrosome–intact sperm to the surface of the ZP and the binding process stimulates the acrosome reaction to occur on the surface of the zona (Baker *et al.*, 2000; Rankin and Dean, 2000). These findings are corroborated by electron microscopy studies on human fertilization, in which it is clearly shown that sperm within the inner third of the zona are all completely acrosome reacted, and that during sperm penetration the zona material shows clear areas around sperm heads presumably representing digested pathways by acrosomal enzymes (Chen and Sathananthan, 1986; Sathananthan, 1996; Sathananthan *et al.*, 1982, 1993).

At SEM and TEM analysis, most commonly, a flat, tangential attachment of the sperm head to the surface of the ZP appears, which is then followed by intrusion into the zona in precisely this horizontal position. However, vertical binding with penetration by the tip of the head also occurs. In oocytes in which large, cluster-like numbers of bound spermatozoa are visible, vertical binding and penetration are in the usual positions (Familiari *et al.*, 1988, 1989; Sathananthan *et al.*, 1982, 1993; Schwartz, 2003) (Figs. 23–25).

4. Sperm–Oocyte Interactions

The sperm crosses the perivitelline space and binds to the oolemma. In some mammals, the plasma membrane of the equatorial segment of the sperm fuses with the microvillous processes of the oocyte. The sperm is then engulfed by the oocyte, which triggers the cortical granule reaction that promotes changes in the inner third of the ZP and in the oolemma. These structural changes further inhibit sperm binding to the matrix and penetration to the ooplasm (a process referred to as zona hardening), avoiding polyspermy in mammals (Primakoff and Myles, 2002; Rankin and Dean, 2000; Talbot *et al.*, 2003; Yanagimachi, 1994). The sequence of events in sperm-oocyte interactions was studied in detail in human gametes from ART

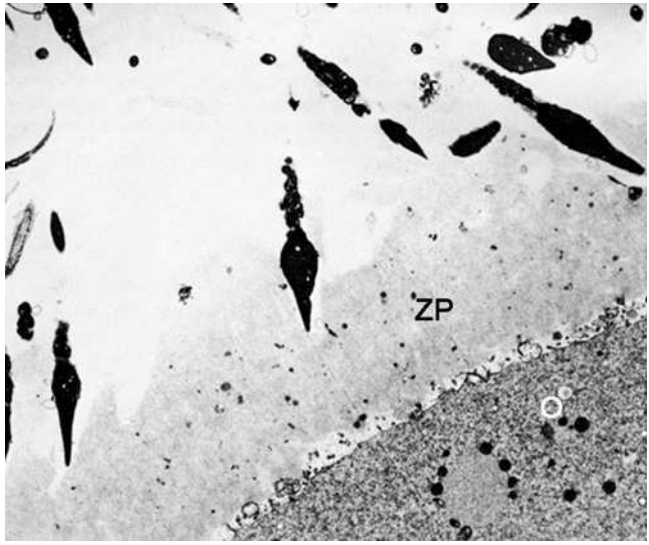

FIG. 23 Numerous sperm in the outer region of the zona pellucida (ZP) of a polyspermic ovum (O). All the sperm have reacted acrosomes and they are penetrating the zona from all directions. Clear areas around the sperm presumably represent digested pathways by acrosomal enzymes. (TEM, 7500X.) (From Sathananthan *et al.*, 1982.)

protocols by TEM (Sathananthan, 1996; Sathananthan *et al.*, 1993). The principal steps are described.

a. Sperm–Oocyte Membrane Fusion The plasma membrane of the mid-segment of the sperm head (postacrosomal region and equatorial vestige) fuses with the oolemma (Fig. 26). This involves the spontaneous fusion of two cells, the spermatozoon and the egg. The molecular basis of adhesion and fusion is an active area of research, but many questions remain unresolved. Some studies proposed that in sperm–oolemma binding, fibronectin and vitronectin were expressed on the surface of capacitated sperm or released during the acrosome reaction, and therefore they act as ligands for integrins on the oolemma, playing a role in sperm–oolemma adhesion (Fusi *et al.*, 1996; Hoshi *et al.*, 1994). The fusogenic zone undergoes molecular changes demonstrable by freeze-fracture TEM. Integrins (α and β) on the oolemma and fertilin (α and β), specific sperm receptors in the fusion domain of sperm or cyritestin, have been implicated in sperm–oocyte binding and fusion in mammals (Stein *et al.*, 2004; Sutovsky and Schatten, 2000). CD9, a tetraspanin superfamily protein on the egg membrane, regulates the interaction of fertilin with integrin (Le Naour *et al.*, 2000; Miyado *et al.*, 2000).

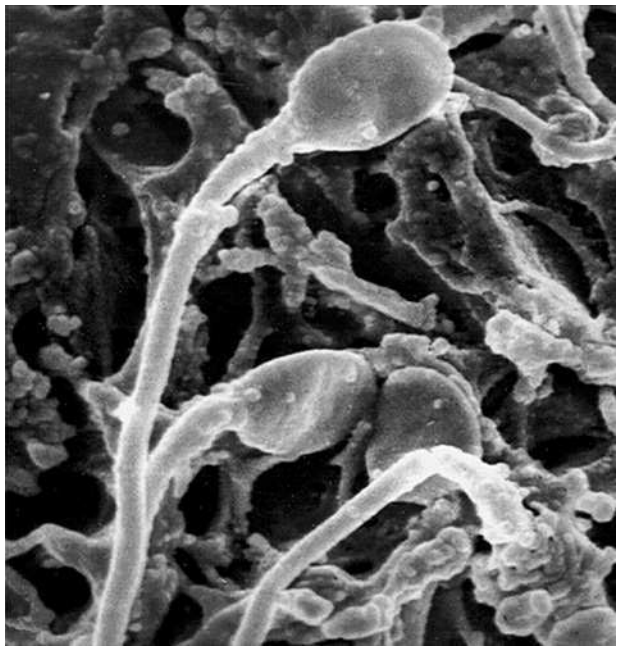

FIG. 24 Human zona pellucida, mature oocyte. The spermatozoa are seen tangentially attached on the spongy zona pellucida or actively penetrating the zona through its fenestrations. (SEM, 7000X.) (From Familiari *et al.*, 1988.)

Unfortunately, in mammalian sperm–egg fusion no clear evidence suggests the participation of egg integrins; in addition, the role of ADAM family proteins on the sperm surface is controversial (Primakoff and Myles, 2002; Talbot *et al.*, 2003). Novel strategies such as gene knockout experiments or the study of oocyte proteomics will better explain this complex relationship (Coonrod *et al.*, 2004). In fact, very recently, Inoue *et al.* (2005), using a knockout approach and gene cloning, identified a mouse sperm fusion-related antigen, and showed that the antigen is a novel immunoglobulin superfamily protein. They named this protein Izumo, and demonstrated that Izumo protein is essential for sperm–egg fusion.

Furthermore, they showed that human sperm also contain Izumo, and addition of the antibody against human Izumo left the sperm unable to fuse with zona-free hamster eggs (Inoue *et al.*, 2005). As summarized by Schultz and Williams (2005), molecules on the sperm surface, such as fertilin and cyritestin, may be involved in sperm–egg binding, whereas Izumo protein is essential for membrane fusion; on the egg, CD9 is required for fusion and might collaborate with other proteins such as integrins or glycosylphosphatidylinositol (GPI)-anchored proteins (Schultz and Williams, 2005). Once

FIG. 25 Fertilized egg. An acrosome–reacted sperm deep in the zona pellucida. The sperm has described a clear pathway and is about to enter the perivitelline space. The zona substance is denser and more compact in this region since the egg has been fertilized. (TEM, 35700X.) (From Chen and Sathananthan, 1986.)

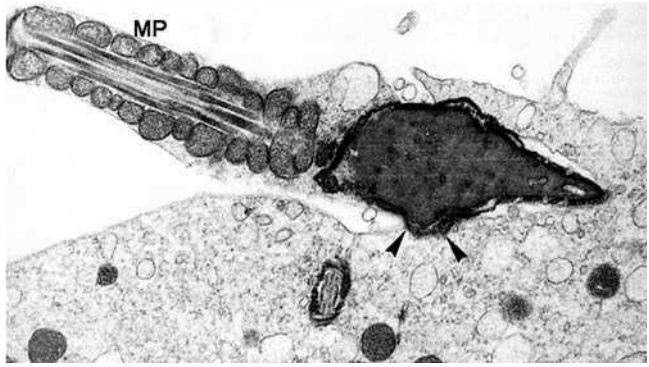

FIG. 26 Sperm–egg fusion. Initial sperm–egg interaction. The sperm is penetrating tangentially and its head has been engulfed by a phagocytic process of the egg cortex; sperm–egg membrane fusion has occurred in the mid segment of the sperm head (arrows). The spermatozoon is still attached to its midpiece (MP) and tail. (TEM, 27300X.) (From Sathananthan *et al.*, 1993.)

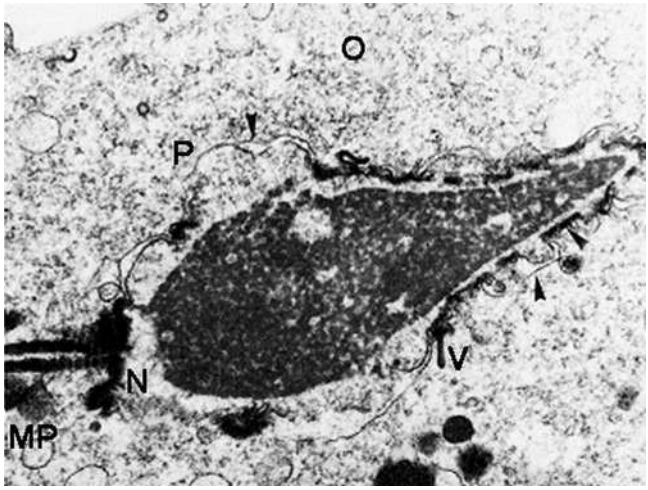

FIG. 27 Sperm incorporation during polyspermic fertilization. A recently incorporated sperm beginning chromatin decondensation. The sperm nuclear envelope has inflated at several points, breaking the inner acrosomal membrane (arrow). The remnants of the equatorial vestige are still evident. O, ooplasm; I, inner acrosomal membrane; P, postacrosomal segment; MP, midpiece; V, vestige; N, neck. (TEM, 35700X.) (From Sathananthan *et al.*, 1993.)

fusion occurs, the sperm nucleus expands to form a male pronucleus within the ooplasm while the sperm midpiece is still attached to the basal plate. The compact DNA in the nucleus of the sperm head expands while its nuclear envelope inflates and dismantles. A new pronuclear envelope is formed by vesicular SER contributed by the ooplasm and original segments of the sperm nuclear envelope. The proximal centriole, mitochondria of the midpiece, and remnants of the tail axoneme persist after fertilization up to the time of syngamy, which occurs approximately 20 h after fusion or even longer (Sathananthan, 1990, 1996; Sathananthan and Chen, 1986; Sathananthan *et al.*, 1986a,b) (Figs. 27–29).

The presence of paternally derived centrioles in fertilized human oocytes at fertilization is a very valuable contribution of sperm to the process of embryonic development (Sathananthan *et al.*, 1991, 1996). In fact, human oogonia present a pair of well-defined centrioles, which are involved in cell division. These are lost during oogenesis, and the mature oocyte is devoid of centrioles, as in most mammals. Neither does the human oocyte have granular centrosomal material at meiotic spindle poles, present in mouse oocytes, which have a dominant maternal centrosome.

Thus, the oocyte centrosome is greatly reduced or inactivated in humans. The functionality of the centrosome is, however, restored after fertilization in the zygote with some maternal input of γ-tubulin around the sperm centriole,

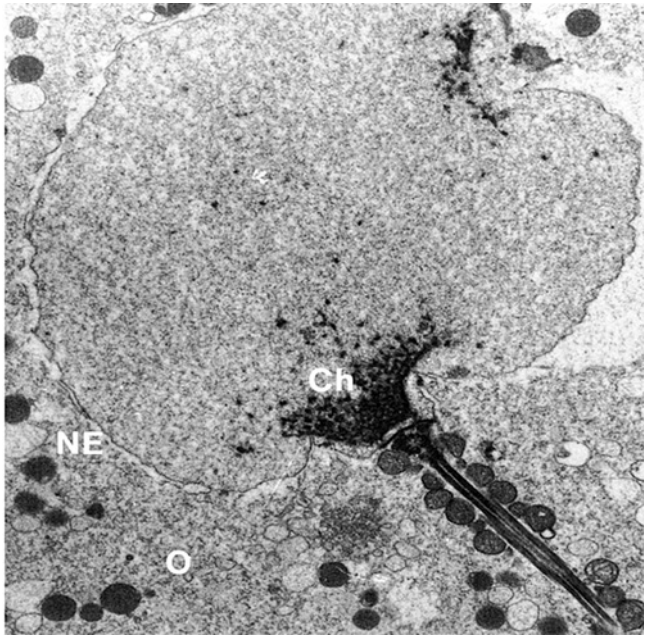

FIG. 28 Later stages of sperm incorporation after polyspermic fertilization. Normal sperm incorporation. The chromatin has decondensed and the nuclear envelope has inflated. The spermatozoon is still attached to the neck and midpiece, which shows sperm mitochondria. Sperm chromatin (Ch) is still decondensing in the posterior region close to the basal plate. (TEM, 15400X.) (From Sathananthan *et al.*, 1986b.)

which duplicates at the pronuclear stage, forms a sperm aster, and proceeds to form the first mitotic spindle (Sathananthan, 1997a,b, 1998a–c; Sathananthan *et al.*, 1996, 2001; Schatten, 1994; Sutovsky and Schatten, 2000).

Sperm centrosomal dysfunction could lead to aberrant embryonic development based on centriolar defects in sperm with impaired motility (Sathananthan *et al.*, 1999a,b, 2001). These morphological observations may have great relevance during IVF or ICSI procedures. Moreover, aberrant embryonic cleavage is quite common in IVF, as well as ICSI, and only 10–15% of all embryos transferred implant in the uterus. Ultrastructural data (Sathananthan, 2000; Sathananthan *et al.*, 1989, 1996, 1999a,b, 2001) agree with clinical evidence that immotile sperm compromises embryo development, which results in very low or no pregnancy rates after ICSI (Vandervorst *et al.*, 1997).

b. Extrusion of the Second Polar Body Simultaneously with sperm–egg fusion the second polar body is extruded into the perivitelline space and the fertilized ovum completes the second meiotic maturation division. The

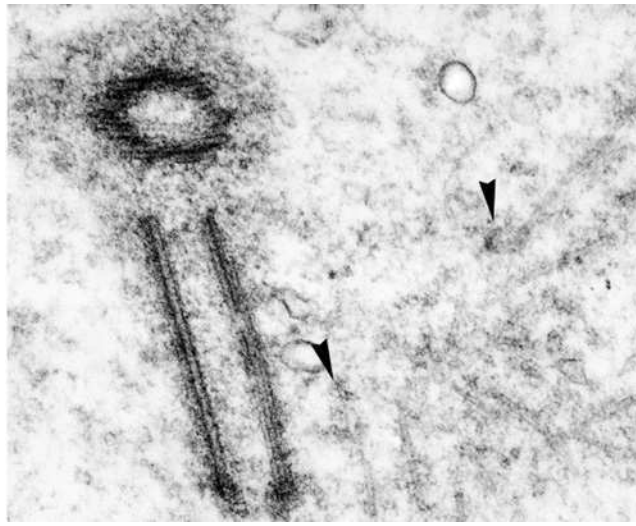

FIG. 29 Sperm aster in a human embryo. A sperm aster at one spindle pole at prometaphase of mitosis in a fertilized ovum at syngamy. It shows duplicated centrioles with dense pericentriolar material, which is unevenly distributed over the daughter centriole, cut in longitudinal section. The astral microtubules terminate in dense specks of pericentriolar material (arrows). (TEM, 50000X.) (From Sathananthan *et al*.,1996.)

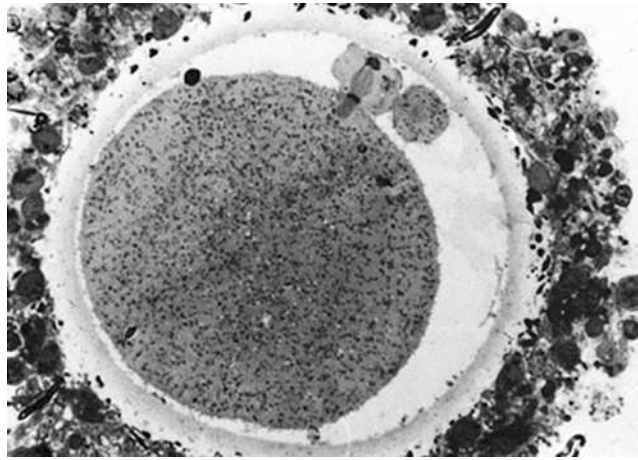

FIG. 30 Fertilized egg. Extrusion of the second polar body. Note several dark sperm in the outer zona. (Light microscopy, 150X.) (From Lopata *et al.*, 1980.)

anaphase II spindle (Fig. 30) is barrel–shaped and anastral with chromosomes at either pole and a dense interbody at the equator of the spindle. Excess maternal chromosomes are extruded into the second polar body while the chromosomes retained in the ooplasm form a female pronucleus. The nuclear envelope is elaborated in much the same way as seen with the male pronucleus organized by flattened vesicles of smooth endoplasmic reticulum. A nucleus like the female pronucleus is formed in the second polar body in a similar way. The second polar body is usually extruded alongside the first polar body, and the fertilized egg thus has two polar bodies (Lopata *et al.*, 1980; Sathananthan, 1985).

c. Cortical Reaction As soon as the sperm fuses with the egg, the cortical granules beneath the oolemma release their contents into the PVS by exocytosis in response to inositol triphosphate-induced calcium rise, generated by fertilization or parthenogenetic activation (Schultz and Kopf, 1995; Sun, 2003). This reaction is believed to take place in a few seconds all around the egg, usually beginning at the point of sperm fusion. Once the granular contents of the cortical granules are released into the PVS they disperse and interact with the ZP, producing the zona reaction resulting in a block of polyspermy (Sathananthan and Trounson, 1982a,b; Sathananthan *et al.*, 1993) (Figs. 31–33). However, their direct role in this process is still not fully known, due to limited data on cortical granule composition and its effect on the ZP (Hoodbhoy and Talbot, 1994; Sun, 2003; Yanagimachi, 1994).

d. Zona Reaction The zona reaction involves the interaction of cortical granule contents with the glycoproteins of the ZP, establishing a primary block to polyspermy at the level of the ZP. The reaction is described as a chemical hardening process that prevents supernumerary sperm from entering the perivitelline spaces after fertilization. This process is characterized by morphological changes that begin in the inner ZP and then are seen in the mid-ZP portion. At an ultrastructural level, in humans, these changes are described as the presence of "blobs or striae of dense material" (Sathananthan, 1984; Sathananthan and Trounson, 1982a,b; Sathananthan *et al.*, 1982) (Fig. 33).

Including RR during fixation, Dandekar and Talbot (1992) demonstrated the existence of cortical granule exudates in the PVS of fertilized human eggs. In particular, not all cortical granule components diffuse into the ZP, but much of the cortical granule exudates dehisces and is trapped in the perivitelline space forming a new coat around the fertilized oocyte. This material, called a "cortical granule envelope," is observed in all developmental stages, up to and including the blastocyst. At the TEM level, this envelope is composed of electron-dense granules, distinct in size and texture from those found around unfertilized oocytes (Dandekar *et al.*, 1992). Talbot

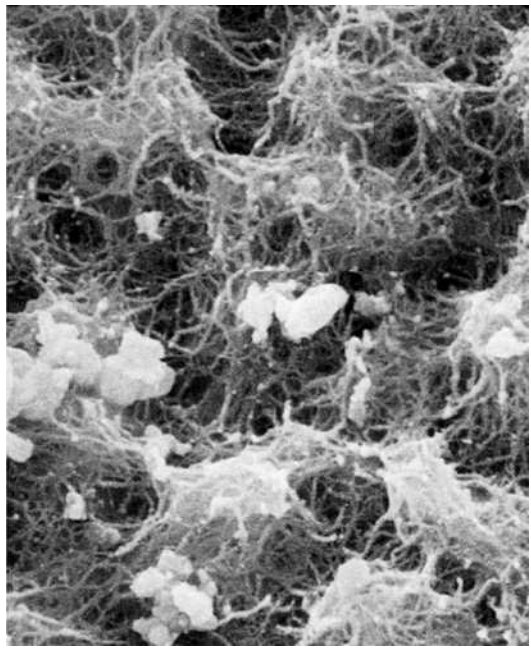

FIG. 31 Fertilized polypronuclear ovum. Human zona pellucida. The inner surface of the zona pellucida shows bulging areas of condensed, closely packed filaments. (High-resolution SEM with Sap-RR-Os-Tc method, 25000X.) (From Familiari *et al.*, 1992b.)

and Dandekar (2003) suggested that it plays a role in blocking polyspermy in mammals as well as in humans.

As reported (Talbot and Dandekar, 2003), the idea that the cortical granule envelope functions in blocking polyspermy in humans is further supported by the observation that human oocytes undergoing IVF procedures are often polyspermic and that such oocytes often show a large number of undispersed cortical granules in their PVS (Dandekar *et al.*, 1992; Sathananthan and Trounson, 1982a,b). Therefore, these are granules that have undergone exocytosis but whose contents have not dispersed to form a cortical granule envelope, further leading to failure to block polyspermy in humans (Talbot and Dandekar, 2003).

Other data related to human polyspermy and its possible relationship with the formation of the ''cortical granule envelope'' arose from human oocytes undergoing subzonal insemination (Tesarik and Mendoza, 1994). Very few acrosome-reacted sperm were able to fuse with the oolemma when they were injected into the perivitelline space of aged human oocytes. This fact could be due to a polyspermy-preventing mechanism at the oolemma, probably

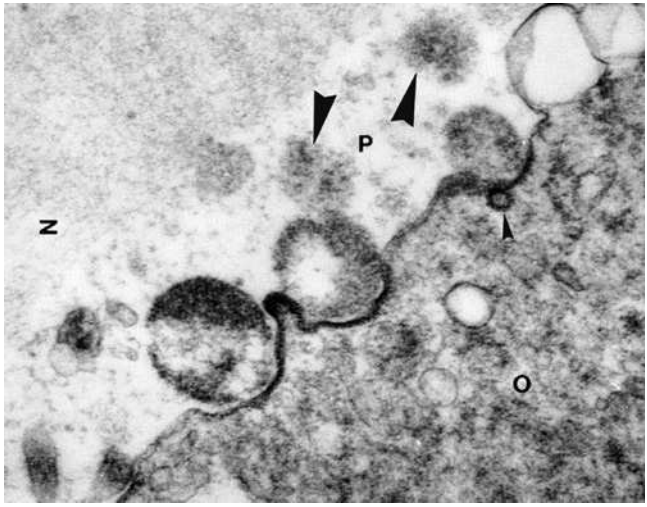

FIG. 32 Cortical reaction. The released contents of cortical granules remain for some time within the perivitelline space where they can interact with the inner face of the zona pellucida (thick arrows). The cortical granules are shown discharging their contents and a pynocytotic caveolus is evident at the base of one cortical granule (small arrow). The oolemma at the site of release is denser in appearance. O, ooplasm; Z, zona pellucida; P, perivitelline space. (TEM, 70000X.) (From Sathananthan and Trounson, 1982b.)

related to a partial cortical reaction occurring in aged oocytes, even if the status of the cortical granule in this particular situation was not known. In addition, this fact may be partially explained by the observation that sperm can readily penetrate human oocytes if the ZP and consequently the "cortical granule envelope" are removed (Soupart and Strong, 1975; Tesarik, 1989).

When observed at both high-resolution SEM and TEM using Sap-RR-Os-TC (Familiari *et al.*, 1992a), the inner surface of the human ZP in fertilized ova and embryos displayed numerous areas where filaments fuse together (Familiari *et al.*, 1992b) (Fig. 31). However, the outer ZP presented the same pattern as observed in human mature oocytes, suggesting that the cortical reaction gives rise to modifications in the inner layer of the ZP consisting of regularly disposed areas of very closely packed filaments (Familiari *et al.*, 1992b). These ultrastructural 3-D data are not in contrast to the observations of Dandekar and Talbot (1992), and probably this filament condensation, together with the formation of the "cortical nuclear envelope," could be related to the process of "zona reaction," which plays a role in the mechanisms related to the block of polyspermy.

Other morphological 3-D observations obtained by Nikas *et al.* (1994), using traditional SEM, showed that in fertilized oocytes with three pronuclei

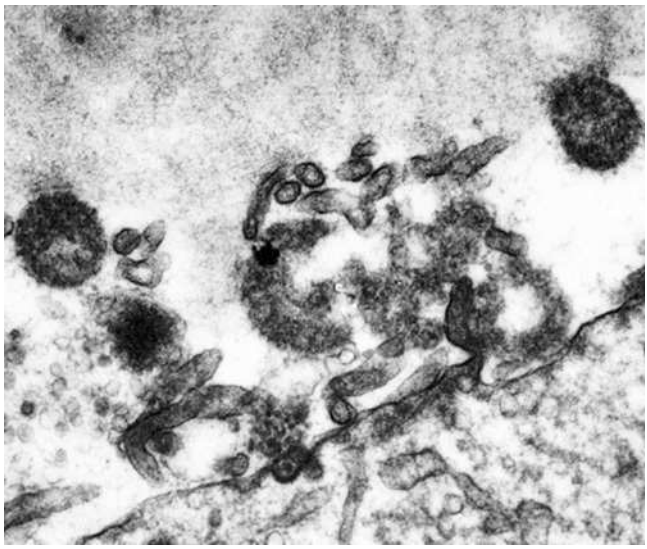

FIG. 33 Zona reaction. The interaction of released contents of cortical granules, which have decondensed and appear to gradually diffuse into the substance of the zona, with the inner face of the zona pellucida. (TEM, 70000X.) (From Sathananthan, 1984.)

the ZP is compact and the pores are obliterated by an amorphous material emerging from the inner zona. It was postulated that the substances released by the oocyte rapidly diffuse through the inner pores of the ZP, exerting a lytic action on ZP structures and causing them to melt and obstruct the pores, thus becoming a barrier for further sperm penetration.

These observations are in contrast to our studies on human ZP following fertilization and during cleavage. Although having observed polypronuclear ova, in which a disturbance owing to a cortical reaction may occur, they clearly demonstrated that the ultrastructural surface aspects of the ZP do not change after fertilization or during cleavage (Familiari *et al.*, 1989, 1992b, 2001; Motta *et al.*, 1988). The discrepancy is probably due to the different preparatory techniques employed. In particular, in our observations, performed with both high-resolution SEM and TEM, we showed changes in the stereo-configuration of ZP filaments, whereas in the observations of Nikas *et al.* (1994) only structures with traditional SEM were described, as the superficial pores that exclusively result from filament stereo-configuration collapse during traditional SEM technical procedures (Familiari *et al.*, 1992b, 2001, 2006).

Further interesting results have been obtained by Funahashi *et al.* (2001) in pig oocytes about zona reaction, using TEM and an RR-saponin technique (Familiari *et al.*, 1992a). They showed that the fine structure of the ZP and

the ZP reaction at sperm penetration differs between pig oocytes fertilized *in vivo* and *in vitro*, and that the outer and inner pig ZP have different network organizations, probably due to an insufficient final maturation of the ZP during *in vitro* maturation, lacking oviductal glycoproteins (Funahashi *et al.*, 2001). In particular, the outer area of ZP always formed a concentrically arranged fibrillar network, whereas the inner area showed a much more compact, trabecule-like mesh. However, both areas, but particularly the outer network, were much more compacted after the zona reaction. Clear differences in the degree of fibrillar aggregation of the inner zona were also observed in *in vitro* and *in vivo* zygotes, being much higher in the latter (Funahashi *et al.*, 2001). Therefore, it is also possible to propose that a zona reaction is a result of an ultrastructural modification, including ZP variations as well as cortical granule envelope formation, but it is possible to suppose that a zona reaction, detected mainly from *in vitro* studies, may be different in an *in vivo* situation.

With the Polscope, an orientation-independent polarized light microscope, the ZP of the normally fertilized human oocytes exhibits a trilaminar structure. However, abnormal zona in polyspermic oocytes exhibited minute discontinuities in the inner zona layer (Wang *et al.*, 2003). These easy and noninvasive observations provide a method to diagnose abnormality in the block of polyspermy in the inner layer of the ZP as ultrastructurally shown in our previous studies (Familiari *et al.*, 1992a,b). Presumably, a defective ZP did not establish a functional zona block. Several studies have demonstrated that the thickness and integrity of the ZP are related to a patient's level of estradiol during stimulation (Bertrand *et al.*, 1996). However, how stimulation induces ZP abnormality in humans is still unclear (Wang *et al.*, 2003).

It is necessary to further study this phenomenon in humans. Perhaps from animal models it can be hypothesized that monospermic fertilization takes place only when fully mature oocytes with normal ZP are inseminated with optimal sperm concentrations and in optimized conditions. Incomplete oocyte cytoplasmic maturation, abnormal ZP, a high concentration of sperm, inappropriate supplementations and insemination medium, and other odd factors during fertilization are all related to polyspermic fertilization (Wang *et al.*, 2003).

Other studies have also shown that there is a secondary block to polyspermy after sperm subzonal insemination (SUZI) at the level of the oolemma after cortical granule membranes are incorporated into the oolemma. It must be realized that much of the sperm plasma membrane is also incorporated into the oolemma and the resulting membrane is a mosaic of membranes after sperm–egg fusion (Sathananthan *et al.*, 1993).

In addition, evidence for a membrane block in human eggs also comes from IVF experiments of ZP-free human eggs (Sengoku *et al.*, 1995). These

observations demonstrated that human eggs are resistant to penetration by additional sperm, indicating that the changes in the egg membrane upon fertilization might be able to reduce receptivity to sperm (Sengoku *et al.*, 1995). Concerning the mechanism of membrane block to polyspermy, egg actin and calcium signaling are involved in the establishment of such a membrane block to polyspermy (McAvey *et al.*, 2002).

No direct evidence exists to explain this mechanism in human oocytes; moreover, other studies showed that polyspermy is higher in human eggs inseminated by partial zona dissection at later times after egg retrieval, suggesting that aged human eggs may be less able to establish a membrane block of polyspermy (Malter *et al.*, 1989). In addition, the explanation may be obtained from mammalian models that confirmed the ability of the membrane block to prevent polyspermy and a failure of this mechanism related to membrane and cortical abnormalities in postovulatory mouse aged eggs (Wortzman and Evans, 2005). It was shown that mouse aged eggs are less able to establish a membrane block to prevent polyspermy, and that aged eggs develop cytoskeletal abnormalities that may affect membrane and cortical function, such as the ability of the egg membrane to support sperm–egg fusion (Wortzman and Evans, 2005).

e. Pronuclear Association Once the male and female pronuclei are formed, they migrate to the center of the egg where they become closely associated with one another but do not fuse. This process is thought to be mediated by microtubules originating from a sperm aster. After pronuclear association the envelope breaks down and the maternal and paternal chromosomes come together during the process of syngamy, which is regarded as the culmination of fertilization. A pronuclear association takes place usually 12–16 h after fertilization and syngamy about 20 h after *in vitro* fertilization (Sathananthan *et al.*, 1993) (Figs. 34 and 35).

B. Molecular Implications: Oocyte Activation

Sperm–oocyte membrane fusion initiates a cascade of events that transforms the egg into an embryo. These involve complex morphological, physiological, and molecular processes in the egg, primarily induced by the fertilizing sperm cell (Sathananthan *et al.*, 2004). Some of the molecular interactions have been documented in the past decade in mammals and may be applicable to humans with caution (Battaglia, 1998; Flaherty *et al.*, 1998; Sutovsky and Schatten, 2000; Williams, 2002).

Gamete membrane fusion followed by sperm incorporation opens a gateway for the transduction of specific signals induced by the sperm cell, which

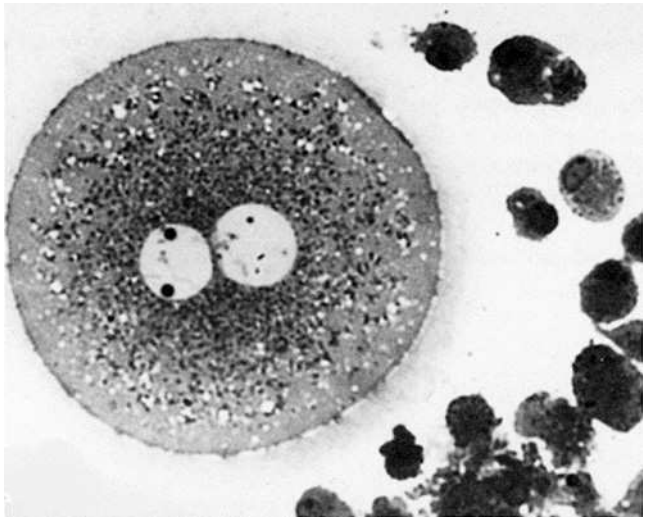

FIG. 34 Normal two pronuclear ovum with male and female pronuclei, closely associated in the central ooplasm. Nucleoli are visible in the pronuclei and the cytoplasm is vacuolated. Note the characteristic concentration of organelles around the pronuclei. (Light microscopy, 400X.) (From Sathananthan *et al.*, 1993.)

occurs in a few seconds, minutes, or several hours. These trigger the cascade of morphological and physiological events outlined above. One of the immediate changes in the human oocyte soon after sperm–egg fusion, demonstrated by confocal laser scanning microscopy, is the release of calcium (Ca^{2+} oscillations) within the oocyte, which occurs repetitively in waves and is transient in nature (Sousa *et al.*, 1996; Tesarik *et al.*, 1995). These oscillations originate from the point of sperm–egg membrane fusion and spread throughout the periphery of the oocyte first before spreading into the central ooplasm (periphery to center propagation). The central oscillations are sustained after the peripherals disappear. Ca^{2+} is apparently released from internal stores (presumably SER) within the oocyte. It is mediated by the production of inositol 1,4,5-triphosphate (IP_3), which sensitizes the SER to release Ca^{2+} (Battaglia, 1998; Flaherty *et al.*, 1998; Sutovsky and Schatten, 2000; Williams, 2002). We have demonstrated two types of SER in the oocyte, peripheral aggregates of tubular SER and vesicular elements of SER spread throughout the ooplasm (Sathananthan *et al.*, 1986a,b, 1993), which could well be involved in these waves of Ca^{2+} release. This is possibly the principal function of SER in oocytes. The oscillations occur about 20 min after insemination or are delayed (4 h or more) after ICSI, possibly due to the mode of sperm incorporation after acrosome deletion in the ooplasm.

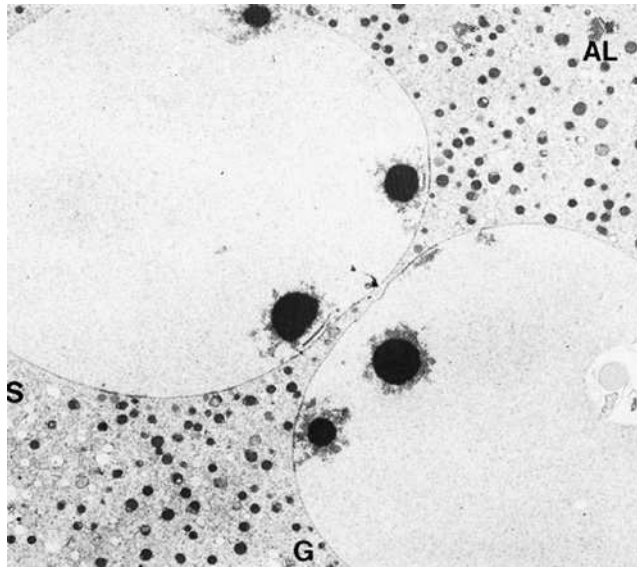

FIG. 35 Normally fertilized two pronuclear ovum. Close association between male and female pronuclei is evident in the center of the oocyte. One pronucleus is slightly larger than the other and both contain highly electron-dense, compact nucleoli associated with chromatin. Note the conglomeration of cellular organelles, particularly mitochondria, around the pronuclei. S, vesicular SER; G, Golgi complex; AL, annulate lamellae. (TEM, 5900X.) (From Sathananthan *et al.*, 1993.)

Two main theories have been postulated to explain activation of the oocyte at the molecular level (Battaglia, 1998; Flaherty *et al.*, 1998; Sutovsky and Schatten, 2000; Williams, 2002): a receptor-mediated theory and a cytosolic soluble sperm factor theory.

The receptor-mediated theory postulates a receptor–ligand interaction between the sperm and oocyte plasma membranes that triggers a signaling cascade that culminates in activation. This could be more applicable to IVF where the fusogenic midsegment of the sperm fuses with the oolemma, followed by total incorporation of the sperm plasma membrane into the egg membrane.

The cytosolic soluble sperm factor theory postulates the release of a sperm-soluble factor into the ooplasm, which initiates Ca^{2+} release. This factor, called "oscillin," could originate from either the fusogenic midsegment in humans, since it has been localized in the equatorial region of the sperm acrosome in mammals (Parrington *et al.*, 1996), or from the perinuclear theca (Sutovsky and Schatten, 2000).

The cytosolic theory seems to be more acceptable, since it can also explain activation after ICSI (Flaherty *et al.*, 1998), where no sperm–egg membrane

fusion occurs. After both IVF and ICSI, the sperm-induced, secondary Ca^{2+} signaling cascade has been documented (Battaglia, 1998; Flaherty *et al.*, 1998; Parrington *et al.*, 1996; Sousa *et al.*, 1996; Sutovsky and Schatten, 2000; Tesarik *et al.*, 1995; Williams, 2002), which in turn is thought to trigger the early events of fertilization.

The events that occur simultaneously with sperm incorporation are sperm aster formation (activation of the sperm centrosome), the cortical reaction preventing polyspermy, completion of egg maturation, sperm DNA decondensation, and pronuclear assembly (Battaglia, 1998; Sathananthan, 1996, 1998a,b, 2000; Sathananthan *et al.*, 1993). The secondary Ca^{2+} release induced by sperm oscillin or other sperm factor could be implicated in all of these processes. However, we must now ask whether the sperm centrosome, per se, is also involved in the initiation of oocyte activation, since it clearly initiates mitosis in the human embryo. If all other events of activation occur and cleavage of the fertilized egg does not occur, development has failed. It is time to consider all the morphological, physiological, biochemical, and molecular processes involved in human fertilization to understand the complexities of sperm–egg interaction.

V. The Embryo

A. Ultrastructure of the Preimplantation Embryo

High pregnancy rates have been obtained using cultured blastocysts for embryo transfer within ART (Makabe *et al.*, 2001; Sathananthan *et al.*, 2003a). However, only 30–50% of embryos cleave regularly to the blastocyst stage *in vitro*, mostly due to elevated apoptotic phenomena, chromosomal abnormalities, genetic defects, immunological rejection, and uterine factors (Levy *et al.*, 2001).

There are several morphological changes during the development of pronuclear zygotes, most of which can be assessed by means of noninvasive microscopic observations (Tesarik and Greco, 1999; Tesarik *et al.*, 2000). Among these morphological changes, there is an early phase of nucleologenesis that consists of the assembly, growth, and fusion of nucleolar precursor bodies (Tesarik and Greco, 1999). Zygotes with good pronuclear morphology and equatorial nucleolar alignment on day 1 (one-cell stage) have a greater chance of developing to blastocysts (Menezes *et al.*, 2003; Scott *et al.*, 2000; Tesarik and Greco, 1999; Van Blerkom *et al.*, 2000). More important in nucleolar alignment is the chromatin associated with these nucleoli that will eventually condense into the maternal and paternal chromosomes in syngamy (A. H. Sathananthan, personal communication). The speed of

pronuclear development normally varies even in zygotes with excellent developmental potential; furthermore, rather than absolute speed, synchrony of pronuclear development appears to be more relevant (Tesarik and Greco, 1999). In general, IVF embryos develop to blastocysts faster than ICSI embryos (Menezes *et al.*, 2003). The application of parameters regarding pronuclear morphology and orientation in the decision about the number and grade of embryos to be transferred will optimize embryo selection for transfer and will improve pregnancy rates, while diminishing the risk of a pregnancy involving multiple embryos (Gianaroli *et al.*, 2003; Kattera and Chen, 2004; Tesarik *et al.*, 2000).

Scott *et al.* (2000) reported that the rapid coalescence of nucleoli, resulting in two or three very large nucleoli per nucleus by 16–18 h postinsemination, is associated with early embryo compaction, little possibility of forming a blastocyst, and implantation failure. Zygotes with unpolarized pronuclei or scattered localization of nucleolar precursor bodies in pronuclei show significantly slower cleavage rates than zygotes having at least one pronucleus polarized (Salumets *et al.*, 2001). This could be applied to the chromatin as well.

Embryos to be selected for transfer should show a perinuclear halo on day 2 of development (Ebner *et al.*, 2003a; Salumets *et al.*, 2001). The presence of a cytoplasmic halo in zygotes relates to microtubule-mediated withdrawal of mitochondria and other cytoplasmic components to the perinuclear region and has a positive prognostic value on blastocyst quality and competence (Ebner *et al.*, 2003a; Salumets *et al.*, 2001; Van Blerkom *et al.*, 2000). Pronuclear oocytes with high competence features show differences in the distribution of mitochondria that correlate with microtubular organization arranged from the vicinity of the pronuclear membranes (Van Blerkom *et al.*, 2000).

The early cleavage stage classically considers a zygote formed by two cells on days 1–2, four cells on day 2, or six to eight cells on day 3 of *in vitro* culture (El-Toukhy *et al.*, 2003; Sathananthan *et al.*, 2003a) (Fig. 36). Embryos that divide more quickly following insemination have been shown to produce higher pregnancy rates than those that divide later (Wharf, 2003). When seen by SEM a two-cell stage embryo shows a second polar body that is covered with numerous microvilli; its cytoplasm, if freeze-fractured, reveals small and round mitochondria with few small peripheral cristae and membranes of the smooth endoplasmic reticulum (Makabe *et al.*, 2001). By TEM, in turn, at this stage, numerous mitochondria surrounding the nucleus, fragments of annulate lamellae in the nucleoplasm, and electron-dense nucleolar precursor bodies were present. Small cell fragments in the PVS as well as vacuolized blastomeres have also been reported in normal blastomeres. Although wide spatial contacts occur between blastomeres, neither communication nor mechanical adhesive junctions have been observed in early cleaving embryos (Motta *et al.*, 1988, 1995b, 2000; Nottola *et al.*, 2001). Primitive cell junctions

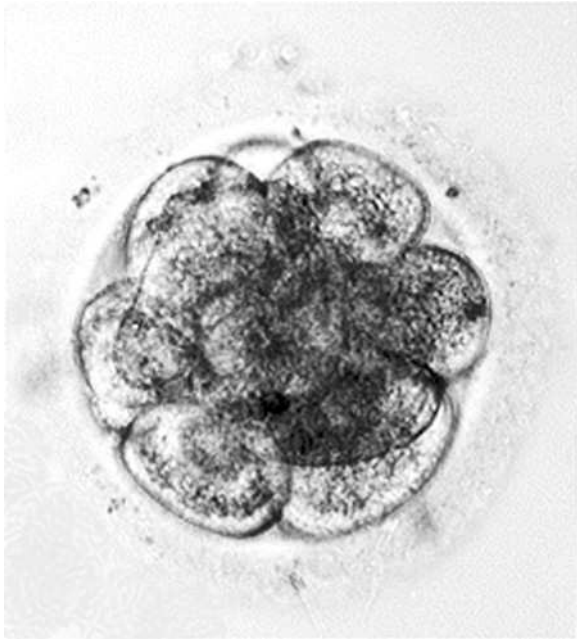

FIG. 36 Morula. (Light microscopy, 120X.)

resembling desmosomes were, however, seen in early embryos (Sathananthan *et al.*, 1993). During the formation of two-cell embryos the highest density of microtubules is found in the apical cytoplasm in contrast to undetectable microtubules in the basal regions where segregation of cytoplasm into daughter blastomeres takes place (Van Blerkom *et al.*, 2000).

Four-cell stage embryos show round or oval mitochondria with a less dense matrix and numerous transverse cristae, mitochondria–vesicle complexes in the subplasmalemmal area, Golgi complexes, and a central cleavage cavity (Motta *et al.*, 1988, 1995b, 2000; Nottola *et al.*, 2001). Mitochondria–vesicle complexes tend to decrease in number and size as cleavage advances from the two-cell to four-cell stage (Motta *et al.*, 1988, 1995b, 2000; Nottola *et al.*, 2001) (Figs. 37 and 38). The freeze-fractured surface of the blastomeres at this stage shows by SEM small vacuoles and round mitochondria (Makabe *et al.*, 2001). Large tubular smooth endoplasmic reticulum aggregates can be found by TEM in four-, five-, and six-cell stage embryos after ICSI, sometimes associated with mitochondria (Makabe *et al.*, 2001; Sathananthan *et al.*, 1997).

At day 4, most embryos are at the morula stage and compaction is completed. At day 5, a series of phenomena occurs: cavitation is initiated

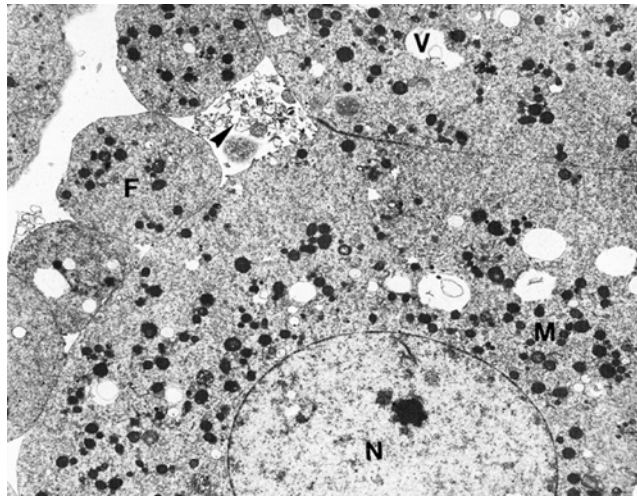

FIG. 37 Partially fragmented four-cell embryo. Two blastomeres of a four-cell embryo are associated with a few enucleated cytoplasmic fragments, which are usually found in the perivitelline space. Such fragments can also occur in the cleavage cavity surrounded by blastomeres. Each fragment has no nucleus but has mitochondria and other cytoplasmic components. Cellular debris may also be associated with these fragments (arrows). V, vacuoles; N, nucleus; M, mitochondria; F, cytoplasmic fragments. (TEM, 5080X.) (From Sathananthan *et al.*, 1993.)

(grades 1–3) with the appearance of a few pockets of blastocoelic fluid that gradually coalesce; subsequently the embryo fully expands (grade 4) and increases in size due to further accumulation of fluid, whereas the inner cell mass becomes an evident morphological feature, forming the blastocyst (Fig. 39).

According to Sathananthan *et al.* (2003a), blastocysts may be classified according to their age, growth, morphology, and activity (cavitation; capacity to expand and hatch out spontaneously) into the following categories:

1. Early blastocyst at day 5: morula cavitation and formation of the blastocoele.
2. Mid-blastocyst between days 5 and 6: increase in cell number, inner cell mass (future embryo) and trophoblast (future placenta), and the blastocele becomes clearly demarcated.
3. Expanded blastocyst at day 6: large blastocele with a thin ZP.
4. Hatching blastocyst between days 6 and 7: the embryo emerges (breached ZP) and shows signs of cellular extrusion outside of the external surface of the ZP.
5. Hatched blastocyst at day 7: blastocysts collapse and reexpand, causing the trophoblast to expand or contract (Menezes *et al.*, 2003).

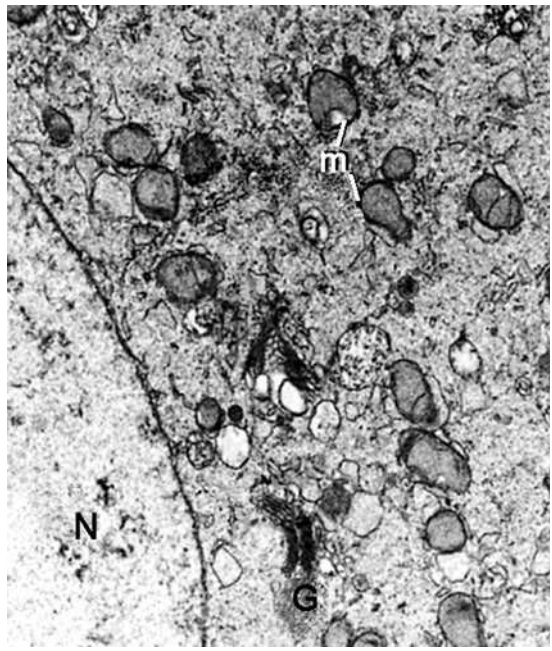

FIG. 38 Four-cell embryo. Note the presence of round mitochondria (m) in a blastomere cytoplasm. A Golgi complex (G) is also seen. N, nucleus. (TEM, 6500X.) (From Motta *et al.*, 1988.)

It is essential to have a healthy, robust, and active blastocyst deriving from a normal cleavage stage embryo. The early embryo's viability can be evaluated by means of morphological parameters, throughout the organization and size of the blastocoele and inner cell mass, and timing of blastocyst development. Normal blastocysts (Fig. 40) show elongated squamous trophoblast cells among which junctional complexes with desmosomes forming a terminal web, tight and gap junctions, as well as interlocking microvilli are observed (Sathananthan *et al.*, 2003a,b). The nucleolus may have a reticular shape. For cells comprising the inner cell mass, their cytoplasm is filled with tubular mitochondria, rough endoplasmic reticulum, Golgi complexes, gap junctions, and bundles of intermediate filaments (Sathananthan *et al.*, 2003a,b). Some of these inner cells (Makabe *et al.*, 2001) as well as trophectoderm cells (Levy *et al.*, 2001) undergo apoptosis. Furthermore, as seen by means of both TUNEL analysis and annexin-V assay, the incidence of cell death seems to correlate with cell number and embryo quality (Levy *et al.*, 2001).

Makabe *et al.* (2001) have elegantly illustrated the 3-D inner structure of blastocysts at day 5 of culture using high-resolution SEM, the

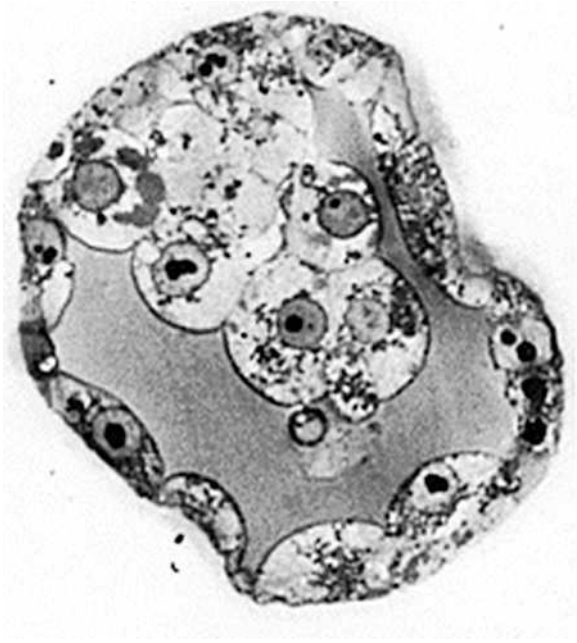

FIG. 39 Cavitating early blastocyst showing inner cell mass, trophoblast, and blastocoele. (Light microscopy, 400X.) (From Sathanathan *et al.*, 1990.)

osmium–dimethyl sulfoxide–osmium (ODO) method, and stereo pairs. On day 6 the inner cell mass shows the formation of a primitive endoderm with characteristic phagocytic vacuoles. In addition, an invasive syncytiotrophoblast appears at the embryonic pole at the onset of hatching. Hatching mostly occurs at a point opposite to the inner cell mass and is likely a mechanical and chemical process in which zona-breaker cells interact with the ZP by means of some secretory activity (Menezes *et al.*, 2003; Sathananthan *et al.*, 2003a,b).

Syncytiotrophoblast cells are characterized by their multiple nuclei, surface microvilli, bundles of tonofilaments, and SER. Dividing cells in mitosis have centrosomes with double centrioles at spindle poles and pericentriolar material; typical centrioles are found in all embryonic cells derived from sperm centrosome (Menezes *et al.*, 2003; Sathananthan *et al.*, 2003a,b). When seen by TEM, a low percentage of the cells appears to be dividing at any given stage whereas some degenerating cells may also be observed in association with phagocytic cells. Specialized trophoblastic transparent bubble-like cells, the ''plump zona-breakers,'' emerge from a particular place in the ZP and show a direct spatial relationship with hatching points. These

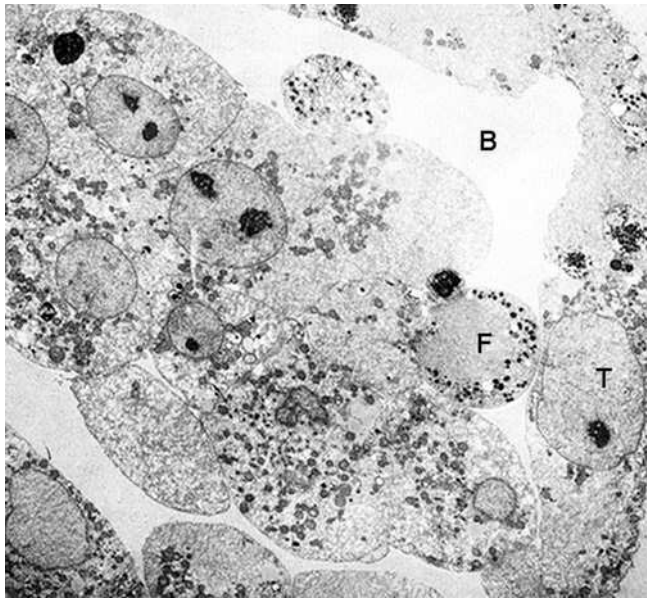

FIG. 40 Early human blastocyst at low magnification. The early blastocyst has an outer trophoblast and a fairly large inner cell mass, since it is cavitating. The trophoblast cells form an outer epithelium while the inner cell mass cells are in close contact with one another. All cells have reticulate nucleoli in their nuclei. Two cells fragments derived from an early cleavage stage are seen in the cavity of the blastocoele. B, blastocoele; F, fragments; T, trophoblast. (TEM, 2000X.) (From Sathananthan *et al.*, 1990.)

cells show surface microvilli and stretch around the ZP, likely aiding in opening it to allow the emergence of the embryo (Fong *et al.*, 2001; Menezes *et al.*, 2003; Sathananthan *et al.*, 2003a,b).

B. Ultrastructural Pathology of the Preimplantation Embryo

Deviations from a presumed normal zygote morphology include size irregularity of individual blastomeres, vacuolization, unequal pronuclear size, dense cytoplasmic granulation, and the presence of many small, scattered nucleoli (Ebner *et al.*, 2003a; Scott *et al.*, 2000; Tesarik and Greco, 1999). Abnormal patterns of pronuclear morphology are not necessarily linked to embryo demise but rather signal irregularities of zygote development that are not always irreversible (Tesarik and Greco, 1999). Either slow (<5 cells on day 3) or fast cleavage has a significant negative association with normal blastocyst formation (Alikani *et al.*, 2000; Scott *et al.*, 2000). The presence of

multinucleated, usually binucleated cells on day 2 and/or 3, in the inner cell mass, trophoblast, and endoderm, is associated with the ability of the embryo to compact, cavitate, and form a blastocyst, as well as with chromosomal abnormalities (Sathananthan *et al.*, 2003a,b). The frequency of multinuclearity is higher among three-cell embryos at day 2 than among two- and four-cell embryos and may reflect a major delay in arrested division of one of the two blastomeres composing a two-cell stage embryo (Hnida *et al.*, 2004). Multinucleated blastomeres are usually significantly larger than non-multinucleated sibling ones at the two-, three-, and four-cell stage (Hnida *et al.*, 2004). An inability to grow, expand, and hatch and the presence of degenerating cells in the blastocyst represent other relevant morphological parameters (Alikani *et al.*, 2000; Fong *et al.*, 2001; Menezes *et al.*, 2003; Sathananthan *et al.*, 2003a,b). The appearance of nuclear membranes prior to cell cleavage may indicate an abnormal cell cleavage (Hnida *et al.*, 2004).

Critical steps in blastocyst culture are expansion and hatching on days 5–7. Zona hardening represents the main cause of hatching failure (Sathananthan *et al.*, 2003b). Abnormal blastocysts may show several morphological features: small or excessive cell number, small size, disorganization (loss of cell-to-cell contacts), or absence of the inner cell mass. These features are associated with inactive zona-breakers or degenerating cells at points of hatching (Sathananthan *et al.*, 2003b). In addition, early detachment of the blastocysts from the enclosed zonae and the presence of fragments in the PVS either between the zona and the trophoblast or within the blastocoele should also be considered as being negatively correlated with the normal development of the blastocyst (Sathananthan *et al.*, 2003b). According to Van Blerkom *et al.* (2001), fragmented embryos at the pronuclear and early cleavage stages when seen by TEM show spherical elements arranged in columns that usually contain no organelles in the cytoplasm. Cytoplasmic continuity between the fragments and the underlying blastomere(s) may suggest a means by which resorption could occur. A discontinuous plasma membrane encloses all the lysed fragments (Van Blerkom *et al.*, 2001). High fragmentation (>15% according to Alikani *et al.*, 2000; >25% according to Hardy *et al.*, 2003) of early embryos could interfere with blastocyst hatching and subsequent implantation. The mean blastomere volume decreases significantly with increasing degree of fragmentation (Hnida *et al.*, 2004).

Moreover, blastomere size can be evaluated by computer-assisted multilevel analysis and may represent a biomarker for embryo quality in regard to both embryonic fragmentation and multinuclearity (Hnida *et al.*, 2004, 2005). The patterns of fragmentation may not be characteristic of apoptosis or indicative of programmed cell death but rather may relate to an oncosis-like process, even if culture does not occur under severe oxygen deprivation (Van Blerkom *et al.*, 2001). Certain common forms of spontaneous fragmentation affecting early human embryos are not lethal, and clusters of apparent

fragments are often transient structures, which disappear by resorption or lysis (Van Blerkom *et al.*, 2001). Another hypothesis attributes embryo fragmentation to the activation of programmed cell death pathways, especially in instances in which fragmentation is accompanied by cleavage arrest or the complete destruction of all blastomeres (Jurisicova *et al.*, 1996; Yang *et al.*, 1998).

It is important to point out that apoptosis may be a normal feature in human preimplantation development *in vivo* with an active role in removing genetically abnormal or mutated cells (Levy *et al.*, 2001). There are several time points when *in vitro*–produced embryos are particularly susceptible to cellular fragmentation, arrest, and apoptosis (Jurisicova and Acton, 2004). In particular, Jurisicova and Acton (2004) proposed that the morphological hallmark of arrested embryos *in vitro*, the partial shrinking of blastomeres and formation of cytoplasmic vesicles, may be the result of an attempt by the cells to save themselves by catabolizing their own cytoplasm. Thus, if the embryo possesses a battery of transcripts that would strongly promote survival but finds itself in inadequate culture conditions, it may trigger an autophagic mode of death. However, an embryo originating from an oocyte with imbalanced cell death machinery or a zygote that fails to execute basic embryonic decisions would opt for the rapid apoptotic mode of death, accompanied by cellular fragmentation (Jurisicova and Acton, 2004). Further studies are needed to provide an accurate map of human preimplantation embryo development.

C. Embryonic Coats

The early embryo is covered by the ZP, which is a special extracellular matrix, and by the cells composing the cumulus oophorus.

1. Zona Pellucida

The ZP has important functions during preimplantation development until the blastocyst stage, at which time the embryo escapes from the zona and implants in the endometrium (Rankin and Dean, 2000). The presence of the ZP around the early embryo creates a sort of embryo encapsulation that likely aids in creating a suitable microenvironment, allowing autocrine stimulation of blastomeres by embryo-derived substances. It also ensures maximum contact between blastomeres prior to compaction, affords protection for the early embryo during its transit down the oviduct and from the maternal immune system, and inhibits ectopic tubal implantation (Denker, 2000; Herrler and Beier, 2000; Rankin and Dean, 2000; Stanger *et al.*, 2001). In addition, the ZP protects the embryo from pathogenic agents and also

modulates embryo–maternal early signaling (Denker, 2000; Herrler and Beier, 2000).

Garside *et al.* (1997) have used the inverted microscope to measure the average ZP thickness of *in vitro* cultured embryos. They concluded that this parameter decreases during *in vitro* culture (17.7 ± 0.14 μm on day 1, 16.3 ± 0.14 μm on day 2, and 14.9 ± 0.14 μm on day 3) and that these changes are more evident in good quality embryos. Pelletier *et al.* (2004), in turn, have quantitatively characterized the ultrastructural arrangement of three different layers of ZP in living cleavage-stage (day 3) embryos by means of the Polscope. All the three layers (1, 2, and 3) constituting the ZP are thinner in embryos (15.2 ± 2.9 μm) than in eggs. However, layers 1 and 2 contribute proportionally less with respect to layer 3 (the outer one) to the overall thinning process, thus indicating a possible stretching of the zona as the embryo increases in diameter (Pelletier *et al.*, 2004). The ZP thickness of transferred embryos significantly correlates with the number of blastomeres, embryo grade, and fragmentation. Therefore, it may have a clinical diagnostic value representing a potentially reliable parameter for embryo selection (Gabrielsen *et al.*, 2000; Garside *et al.*, 1997).

Using high-resolution SEM we showed that the ZP in human polypronuclear embryos (two–four blastomeres) displayed a spongy, fenestrated outer surface and a smooth inner surface comparable to that seen in mature oocytes (Familiari *et al.*, 1989, 1992b) (Fig. 41). Therefore, in ZP covering polypronuclear embryos, amorphous material emerging from the inner zona and melting the pores was observed, even if Nikas *et al.* (1994) showed it

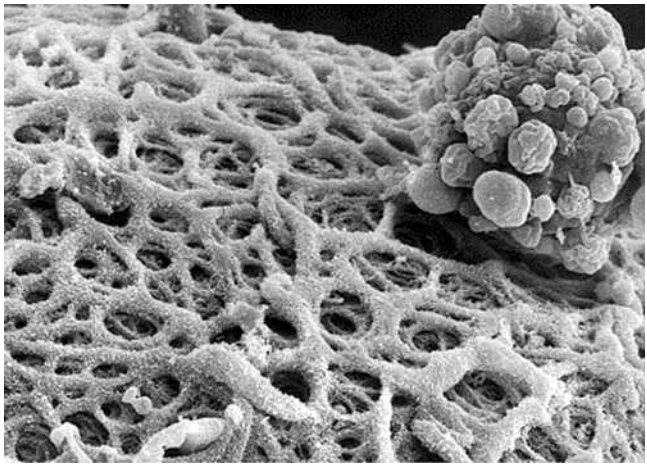

FIG. 41 Two-cell polypronuclear embryo with cumulus corona cells. The zona pellucida shows a spongy surface. (High-resolution SEM, 1500X.) (From Familiari *et al.*, 2006.)

in the ZP of fertilized ova at the pronuclear stage. Probably different oocyte timing or different preparatory techniques may account for this microstructural difference.

When the human polypronuclear embryo (two–four blastomeres) ZP was studied in specimens treated with saponin, RR, and thiocarbohydrazide (Familiari *et al.*, 1992a) with the aid of both SEM and TEM, a peculiar architecture was evidenced. The ZP outer part and surface were characterized by filaments arranged in a regular pattern of alternating tight meshed and large meshed networks. The large meshed network had the same distribution of fenestrations as was seen on the spongy outer ZP of samples observed with classical SEM (Familiari *et al.*, 1992b). However, the inner part and surface of the ZP were characterized by the presence of bulging areas of condensed and closely-packed filaments, as observed in fertilized ova at the pronuclear stage (Familiari *et al.*, 1992b). Therefore, these ultrastructural data, obtained through a more sophisticated technique (Familiari *et al.*, 1992b), showed that the embryo ZP is composed of filaments arranged in a complex fashion, similar to mature oocytes in the external part of the ZP, and typically reorganized in the inner part as a consequence of cortical reaction.

Furthermore, SEM data on the ZP belonging to human blastocysts obtained throughout ART protocols by Nottola *et al.* (2005) showed that the ZP ultrastructure in healthy blastocysts was characterized by numerous large fenestrations, formed by networked filaments, rather similar to that of healthy mature oocytes and early embryos, whereas degenerated, dark, and irregular blastocysts show a more compact ZP, comparable to that of immature/atretic oocytes (Familiari *et al.*, 1988, 1989, 1992b) (Fig. 42). Although some controversy exists (Rankin and Dean, 2000), the ZP is not an essential component of human embryogenesis or pregnancy. In fact, its absence does not inhibit embryo development in that the cumulus corona cells provide enough support to maintain blastomere interaction, embryo viability, and pregnancy (Stanger *et al.*, 2001).

Finally, the ZP is increasingly stretched until it is almost invisible (Alikani *et al.*, 2000; Menezes *et al.*, 2003). Nonetheless, the characteristic hatching process observed *in vitro* that includes expansion of the blastocele and distension and thinning of the ZP before rupture may even correspond to artifacts (Blake *et al.*, 2001). Normally, the blastocyst hatches *in vivo* on day 6 or 7 after fertilization, at which time it implants in the endometrium (Fong *et al.*, 2001; Sathananthan *et al.*, 2003b). Several methods have been proposed regarding assisted hatching. Some of them consider mechanical assisted hatching (partial zona dissection); others use chemical drilling techniques such as acid Tyrode assisted hatching or pronase thinning of the ZP. Assisted hatching may be of benefit in cases in which the embryo shows a thick ZP (Balaban *et al.*, 2002). Blake *et al.* (2001), based on the success of laser ZP thinning, considered this an alternative approach to assisted

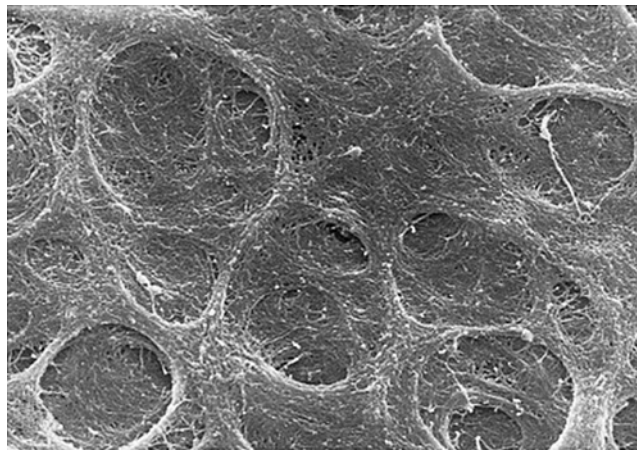

FIG. 42 Clear ICSI full blastocyst. The zona pellucida outer surface is characterized by a spongy texture with expanded flattened fenestrations. (SEM, 13000X.) (From Nottola *et al.*, 2005.)

hatching; they also illustrated by SEM the hatching site within the laser thinned region. This latter technique is technically the easiest procedure (Balaban *et al.*, 2002); it does not consider breaching the zona and avoids the potential risk of blastomere loss or embryonic infection (Blake *et al.*, 2001).

2. Cumulus Oophorus and Extracellular Matrix

Human pronuclear eggs and embryos, recovered from the tubal fluid after 70–80 h of the LH peak, with a developmental age ranging between 35 and 50 h, were still surrounded by clusters of cumulus cells (Motta *et al.*, 1995a) (Fig. 43). In this developmental stage, an enhancement of the steroidosynthetic characteristics occurred in the outer layers of the cumulus mass, excluding corona cells, which still appeared capable of synthesizing peptides. In fact, the cytoplasm of most CC cells possessed abundant organelles typical of steroidogenesis, such as mitochondria with tubular or villiform cristae, a well-developed SER, and electron–dense lipid droplets often surrounded by SER or in close contact with microtubules and microfilaments (Motta *et al.*, 1995a) (Fig. 44).

Similar results were obtained in bovine embryos, in which surrounding cumulus cells were in an actively transforming state and showed an ultrastructural pattern of luteinization and viability (Familiari *et al.*, 1998). The cumulus cells that surround the early embryo following ART procedures (a three-pronuclear zygote up to embryos of three to eight cells) also have cytoplasm with similar ultrastructural features if compared to cumulus cells

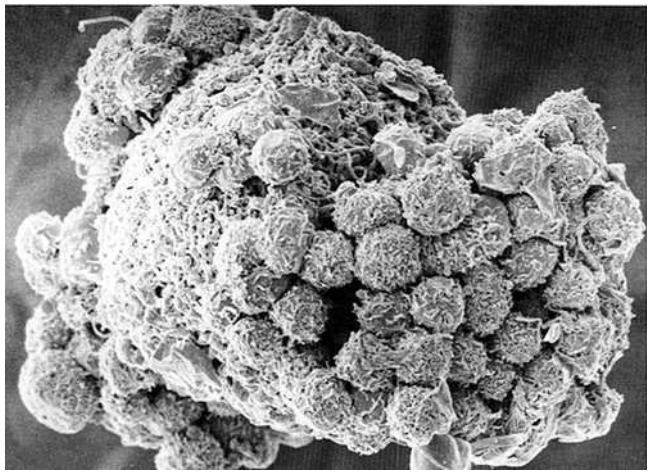

FIG. 43 Cumulus cells surrounding a human four-cell embryo (IVF). The cell surface is mainly covered by microvilli of various length and density. (SEM, 1500X.) (From Nottola *et al.*, 1991.)

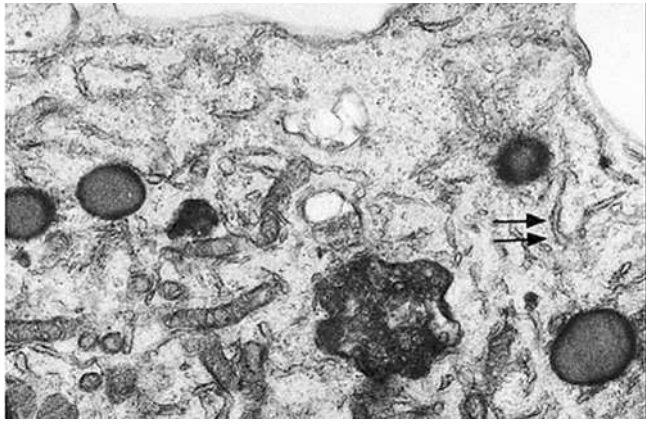

FIG. 44 Polypronuclear embryo (IVF). Some rough endoplasmic reticulum membranes (double arrows) are dispersed in the cumulus corona cell cytoplasm. Lipid droplets and bacilliform mitochondria are also seen. (TEM, 19000X.) (From Nottola *et al.*, 1991.)

surrounding the fertilized oocyte. However, lipid droplets appear numerous and denser; mitochondria show pleomorphism, most of them oval-shaped and with lamellar to tubular cristae; and the smooth endoplasmic reticulum is abundant. The surface of cumulus cells shows microvilli and blebs (Motta *et al.*, 1991, 1994b; Nottola *et al.*, 1991).

All the above morphological features support the hypothesis that embryonic cumulus cells luteinize like parietal granulosa cells, generating a steroid hormonal microenvironment in the oviduct, which may affect zygote segmentation. In addition, aromatase activity, which is the enzyme involved in the synthesis of estrogens throughout the transformation of testosterone in 17β-estradiol, was detected in an intense fashion in cumulus cells surrounding embryos, more than observed in cumulus cells surrounding unfertilized oocytes (Motta *et al.*, 1995c).

In addition, the presence of aromatase strongly suggests steroidogenic activity, and that a small amount of estrogen may be useful for the embryo, positively modulating the microenvironment in which it develops.

In *in vivo* conditions, CC cells showing spermiophagic activity, as well as activated macrophages, leukocytes, and red blood cells, were also found in the cumulus mass. The macrophages may play a local role both by phagocytic activity and by modulating the steroid secretion of the neighboring cumulus cells, which occurs in the ovarian follicle and in the corpus luteum (Motta *et al.*, 1995a).

In conclusion, the cumulus cells enclosing the cleavage-stage embryo represent a highly dynamic structure; cumulus corona cells may be used as a de facto zona enclosure (Stanger *et al.*, 2001) that appears to be beneficial for healthy embryogenesis (Familiari *et al.*, 1998; Motta *et al.*, 1995a,b, 1998; Nottola *et al.*, 1998, 2001), implantation, and pregnancy (Stanger *et al.*, 2001), provided by diverse cell populations in addition to oviductal cells. A complex, well-regulated, autocrine and paracrine, species-specific crosstalk of growth factors and extracellular matrix components between the embryo and the different cell types involved, during tubal sojourn, favors right embryo development in terms of time and location (Einspanier *et al.*, 1997; Hardy and Spanos, 2002).

As stated by Hunter *et al.* (2005), cumulus cell suspension represents a potential route of amplification of early pregnancy signals from the embryo to influence the pattern of ovarian steroid secretion and perhaps that of folliculogenesis. Considering the relatively low concentration of hormones generated by cumulus cell suspension, a vascular countercurrent transfer of information from the fallopian tube to the ipsilateral ovary was postulated (Hunter *et al.*, 2005).

The human embryo produces cytokines and growth factors such as interleukins, prostaglandins, VEGF, and receptors for endometrial signals such as the LIF receptor, colony-stimulating factor receptor, insulin-like growth factors, and heparin-binding epidermal growth factor receptor (Hoozemans *et al.*, 2004). The time-sequent embryo–endometrial dialogue involves cycle-dependent expression of molecules during a particular temporal and spatial expression of factors that allows the embryo to implant via signaling, appositioning, attachment, and invasion, in a specific time frame. In humans, preimplantation development from zygote to blastocyst occurs from day 1 to

5 after ovulation. As the embryo reaches the blastocyst stage on day 5, within 48 h of reaching the uterus, the blastocyst begins to hatch from the ZP and then implants. Integrin molecules, L-selectin ligands, mucin-1, heparin-binding epidermal growth factor, and pinopodes are involved in appositioning and attachment (Hoozemans *et al.*, 2004; Nikas and Makrigiannakis, 2003). A pregnancy rate of approximately 15% per cycle renders the process of human reproduction inefficient, and the process of human embryo implantation is far from being fully understood. Future research should focus on further evaluation of this process.

VI. Concluding Remarks and Future Directions

Knowledge of sperm, oocyte, and embryo morphology is very useful for the clinician and the biologist cooperating in ART technology, since it is related to ART outcome. Interesting observations obtained by performing preimplantation genetic diagnosis for aneuploidy screening confirmed the relationship between best embryo morphological quality and implantation potential, even if embryo selection on the basis of morphology is not always conclusive (Staessen *et al.*, 2004). Furthermore, it is well known that good zygote and embryo ''quality'' may be defined by simple morphological criteria at the inverted microscope, having a fair chance of selecting a chromosomally normal embryo concurrent with morphological selection (De Placido *et al.*, 2002; Gianaroli *et al.*, 2003; Lundin, 2004; Rienzi *et al.*, 2005b). Other recent data on oocyte quality and ICSI outcome showed that ICSI outcome is strictly related to a better quality of oocyte cohort selected during superovulation (Wang *et al.*, 2004).

The morphology of the human sperm in assisted reproduction is another clinically important parameter. In fact, evaluation of sperm morphology by light microscopy, according to ''Tygerberg (Kruger) strict sperm morphology criteria,'' may be helpful in assisting the scientist working in IVF laboratories dealing with infertility problems (Kruger and Franken, 2004). Moreover, in spite of developments in ART, fertilization failures are still a reality. An explanation for such situations is often lacking, and implementation of ultrastructural analysis can assist in determining the cause of fertilization failure. In this field, as treated in this study, the ultrastructural observation of sperm is very useful in patients whose sperm show severe abnormal motility and morphology in routine semen analysis; in these cases, generally electron microscopic findings correlate with success or failure of IVF and can screen for potentially inheritable genetic disorders.

Similarly, knowledge of the ultrastructure of the human mature oocyte and preimplantation embryo, observed *in vivo* as well as during ART procedures,

may be useful in the diagnosis of fertilization failure, especially regarding sperm–oocyte interaction (including sperm penetration of the cumulus oophorus, sperm–zona binding, sperm–zona penetration, sperm–oocyte interactions, and zona reaction), oocyte activation, the preimplantation embryo, and embryonic coats. In fact, as reviewed by Mahutte and Arici (2003), good knowledge of microstructural events in normal fertilization is a prerequisite for tests that may be useful in assessing the likelihood of successful fertilization in both IVF and ICSI procedures. These tests also include assessment of sperm–ZP binding, assessment of ZP penetration and acrosome reaction, semen characteristics on the day of oocyte retrieval, fertilization performance in previous *in vitro* fertilization cycles, and the sperm creatine kinase and the heat shock protein H2 ratio (Mahutte and Arici, 2003). In the future, oocyte biopsy can be used in the parent oocytes to judge age-related changes (Goud *et al*., 2005).

From a biological point of view, results presented in this study clearly show that the ultrastructure of human reproduction is a peculiar multistep process that differs from that of other mammalian models. In fact, even if the general organization of human fertilization conforms to that of most mammals, it has some unique features. As discussed in this study, the mature oocyte has basic cellular organelles, but the MII spindle is barrel–shaped, anastral, and lacks centrioles. Osmiophilic centrosomes are not demonstrable in human eggs, since the maternal centrosome is not functional. The sperm centrosome activates the egg and organizes the sperm aster and mitotic spindles of the embryo after fertilization.

The human ZP is composed of thin filaments, arranged in a complex pattern, containing ZP glycoproteins. Mechanisms of binding and penetration of the sperm in the glycoprotein filaments of ZP are well known, even if humans possess four glycoprotein-assembling filaments and not three as in other mammalian species. As stated by Conner *et al.* (2005), the increased complexity of the ZP in humans and other species across the evolutionary tree now demands that we reconsider our reliance on the mouse model for understanding early fertilization events.

Human oocyte and embryo behavior seems closely related to morphodynamic metabolic activities of neighboring somatic cells, since, as discussed in this study, the viability of cumulus cells surrounding the oocyte as well as the embryo, both *in vitro* and *in vivo*, is demonstrated. Therefore, the metabolic activity of somatic cells is not restricted to persistence in the ovarian follicle but continues inside the extraovarian "microfollicular unit" (oocyte and companion cumulus cells) at the time of ovulation or at follicular aspiration for ART procedures.

Clinically, high rates of blastocyst formation have been reported with the use of cocultures, and this has been proposed as a salvage treatment option for couples with repeated implantation failures (Urman and Balaban, 2005).

Similar results were obtained by the use of complex sequential media, even if well-designed randomized studies that compare cocultures with simple or sequential media do not exist (Urman and Balaban, 2005). Whether cocultures are really beneficial in patients with repeated implantation failures should be investigated in future randomized trials.

Some aspects of human sperm and oocyte pathology have been discussed in this study; specific pathological conditions of cumulus cells, such as overripeness and hyperluteinization or defective secretion of proteins or steroids, should be investigated further to attain more precise information regarding infertility and its treatment. Our knowledge about human *in vivo* fertilization is still very limited and the complex sequence of *in vivo* biological steps involved in human reproduction is only partially reproduced in current ART procedures.

As stated by our late Professor Pietro Motta (Motta *et al.*, 1995d): "Certainly, in the near future, all open questions will be approached and presumably resolved by new technologies and left behind by generations of valid researchers. They nevertheless must be aware that their studies challenge not only the life mystery itself, but in particular the destiny of the human being." Even if stated 10 years ago, these words are still accurate today.

Acknowledgments

Thanks are due to Ezio Battaglione, Gianfranco Franchitto, and Antonio Familiari for their skillful technical assistance. Funds were provided by Italian MIUR (PRIN-COFIN and University of Rome "La Sapienza" Grants 2002–2004).

REFERENCES

Abbas, M. M., Evans, J. J., Sin, I. L., Gooneratne, A., Hill, A., and Benny, P. S. (2003). Vascular endothelial growth factor and leptin: Regulation in human cumulus cells and in follicles. *Acta Obstet. Gynecol. Scand.* **82,** 997–1003.

Abbott, A. L., Fissore, R. A., and Ducibella, T. (2001). Identification of a translocation deficiency in cortical granule secretion in preovulatory mouse oocytes. *Biol. Reprod.* **65,** 1640–1647.

Alikani, M., Calderon, G., Tomkin, G., Garrisi, J., Kokot, M., and Cohen, J. (2000). Cleavage anomalies in early human embryos and survival after prolonged culture *in vitro*. *Hum. Reprod.* **15,** 2634–2643.

Antczak, M., and Van Blerkom, J. (1997). Oocyte influences on early development: The regulatory proteins leptin and STAT3 are polarized I mouse and human oocytes and differentially distributed within the cells of the preimplantation embryo. *Mol. Hum. Reprod.* **3,** 1067–1086.

Antczak, M., Van Blerkom, J., and Clark, A. (1997). A novel mechanism of vascular endothelial growth factor, leptin and transforming growth factor-β2 sequestration in a subpopulation of human ovarian follicle cells. *Hum. Reprod.* **12,** 2226–2234.

Baccetti, B., Capitani, S., Collodel, G., Strehler, E., and Piomboni, P. (2002). Recent advances in human sperm pathology. *Contraception* **65,** 283–287.

Baccetti, B., Piomboni, P., Bruni, E., Capitani, S., Gambera, L., Moretti, E., Sterzik, K., and Strehler, E. (2004). Effect of follicle-stimulating hormone on sperm quality and pregnancy rate. *Asian J. Androl.* **6,** 133–137.

Bahat, A., Tur-Kaspa, I., Gakamsky, A., Giojalas, L. C., Breitbart, H., and Eisembach, M. (2003). Thermotaxis of mammalian sperm cells: A potential navigation mechanism in the female genital tract. *Nat. Med.* **9,** 149–150.

Baker, H. W. G., Liu, D. Y., Garrett, C., and Martic, M. (2000). The human acrosome reaction. *Asian J. Androl.* **2,** 172–178.

Baker, M. A., and Aikten, R. J. (2004). The importance of redox regulated pathways in sperm cell biology. *Mol. Cell. Endocrinol.* **216,** 47–54.

Balaban, B., Urman, B., Sertac, A., Alatas, C., Aksoi, S., and Mercan, R. (1998). Oocyte morphology does not affect fertilization rate, embryo quality and implantation rate after cytoplasmic sperm injection. *Hum. Reprod.* **13,** 3431–3433.

Balaban, B., Urman, B., Alatas, C., Mercan, R., Mumcu, A., and Isiklar, A. (2002). A comparison of four different techniques of assisted hatching. *Hum. Reprod.* **17,** 1239–1243.

Balakier, H., Dziak, E., Sojecki, A., Librach, C., Michalak, M., and Opas, M. (2002). Calcium-binding proteins and calcium-release channels in human maturing oocytes, pronuclear zygotes and early preimplantation embryo. *Hum. Reprod.* **17,** 2938–2947.

Baranska, W., Konwinski, M., and Kujama, M. (1975). Fine structure of the zona pellucida of unfertilized egg cells and embryos. *J. Exp. Zool.* **192**(2), 193–202.

Batova, I. N., Ivanova, M. D., Mollova, M. V., and Kyurkchiev, S. D. (1998). Human sperm surface glycoprotein involved in sperm-zona pellucida interaction. *Int. J. Androl.* **21,** 141–153.

Battaglia, D. E. (1998). Questions about oocyte activation: Answers from ICSI? *In* "Treatment of Infertility: The New Frontiers" (M. Filicore and C. Flamigni, Eds.), pp. 249–256. Communications Media for Education, Princeton, NJ.

Bertrand, E., Bergh, M. V., and Enghert, Y. (1996). Clinical parameters influencing human zona pellucida thickness. *Fertil. Steril.* **66,** 408–411.

Blake, D. A., Forsberg, A. S., Johansson, B. R., and Wikland, M. (2001). Laser zona pellucida thinning—an alternative approach to assisted hatching. *Hum. Reprod.* **16,** 1959–1964.

Boiso, I., Martí, M., Santaló, J., Ponsá, M., Barri, P. N., and Veiga, A. (2002). A confocal microscopy analysis of the spindle and chromosome configurations of human oocytes cryopreserved at the germinal vesicle and metaphase II stage. *Hum. Reprod.* **17,** 1885–1891.

Brewis, I. A., Clayton, R., Barratt, C. L., Hornby, D. P., and Moore, H. D. (1996). Recombinant human zona pellucida glycoprotein 3 induces calcium influx and acrosome reaction in human spermatozoa. *Mol. Hum. Reprod.* **2,** 583–589.

Bronson, R. A., Peresleni, T., and Golightly, M. (1999). Progesterone promotes the acrosome reaction in capacitated human spermatozoa as judged by flow cytometry and CD46 staining. *Mol. Hum. Reprod.* **5,** 507–512.

Buffone, M. G., Doncel, G. F., Marin Briggiler, C. I., Vazquez-Levin, M. H., and Calamera, J. C. (2004). Human sperm subpopulations: Relationship between functional quality and protein tyrosine phosphorylation. *Hum. Reprod.* **19,** 139–146.

Carbone, D. J., Jr., McMahon, J. T., Levin, H. S., Thomas, A. J., Jr., and Agarwal, A. (1998). Role of electron microscopy of sperm in the evaluation of male infertility during the era of assisted reproduction. *Urology* **52,** 301–305.

Carnegie, J. A., Dardick, I., and Tsang, B. K. (1987). Microtubules and the gonadotropic regulation of granulosa cell steroidogenesis. *Endocrinology* **120,** 819–828.

Carrell, D. T., Middleton, R. G., Peterson, C. M., Jones, K. P., and Urry, R. L. (1993). Role of the cumulus in the selection of morphologically normal sperm and induction of the acrosome reaction during human *in vitro* fertilization. *Arch. Androl.* **31,** 133–137.

Carrell, D. T., Peterson, C. M., Jones, K. P., Hatasaka, H. H., Udoff, L. C., Cornwell, C. E., Thorp, C., Kuneck, P., Erickson, L., and Campbell, B. (1999). A simplified coculture system using homologous, attached cumulus tissue results in improved human embryo morphology and pregnancy rates during *in vitro* fertilization. *J. Assist. Reprod. Genet.* **16,** 344–349.

Catalano, R., Hillhouse, E. W., and Vlad, M. (2001). Developmental expression and characterization of FS39, a testis complementary DNA encoding an intermediate filament-related protein of the sperm fibrous sheath. *Biol. Reprod.* **65,** 277–287.

Cekleniak, N. A., Combelles, C. M. H., Ganz, D. A., Fung, J., Albertini, D. F., and Racowsky, C. (2001). A novel system for *in vitro* maturation of human oocytes. *Fertil. Steril.* **75,** 1185–1193.

Celik-Ozenci, C., Catalanotti, J., Jakab, A., Aksu, C., Ward, D., Bray-Ward, P., Demir, R., and Huszar, G. (2003). Human sperm maintain their shape following decondensation and denaturation for fluorescent in situ hybridisation: Shape analysis and objective morphometry. *Biol. Reprod.* **69,** 1347–1355.

Chen, C., and Sathananthan, A. H. (1986). Early penetration of human sperm through the vestments of human eggs *in vitro*. *Arch. Androl.* **16,** 183–197.

Chen, L., Zhang, H., Powers, R. W., Russel, P. T., and Larsen, W. J. (1996). Covalent linkage between proteins of the inter-α-inhibitor family and hyaluronic acid is mediated by a factor produced by granulosa cells. *J. Biol. Chem.* **271,** 19409–19414.

Cheung, A., Swann, K., and Carroll, J. (2000). The ability to generate normal Ca^{2+} transients in response to spermatozoa develops during the final stages of oocyte growth and maturation. *Hum. Reprod.* **15,** 1389–1395.

Chung, C. Y., and Erickson, H. P. (1997). Glycosaminoglycans modulate fibronectin matrix assembly and are essential for matrix incorporation of tenascin-c. *J. Cell Sci.* **110,** 1413–1419.

Clarke, H. (2003). Italy approves controversial legislation on fertility treatment. *Lancet* **362,** 2076.

Conner, S. J., Lefievre, L., Hugbes, D. C., and Barrat, C. L. R. (2005). Cracking the egg: Increased complexity in the zona pellucida. *Hum. Reprod.* **20,** 1148–1152.

Cooke, S., Tyler, J. P. P., and Driscoll, G. L. (2003). Meiotic spindle location and identification and its effect on embryonic cleavage plane and early development. *Hum. Reprod.* **18,** 2397–2405.

Coonrod, S. A., Calvert, M. E., Reddi, P. P., Kasper, E. N., Digilio, L. C., and Herr, J. C. (2004). Oocyte proteomics: Localisation of mouse zona pellucida protein 3 to the plasma membrane of ovulated mouse eggs. *Reprod. Fertil. Dev.* **16,** 69–78.

Dandekar, P., and Talbot, P. (1992). Perivitelline space of mammalian oocytes: Extracellular matrix of unfertilized oocytes and formation of a cortical granule envelope following fertilization. *Mol. Reprod. Dev.* **31,** 135–143.

Dandekar, P., Martin, M., and Glass, R. (1991). Maturation of immature oocytes by coculture with granulosa cells. *Fertil. Steril.* **55,** 95–99.

Dandekar, P., Aggeler, J., and Talbot, P. (1992). Structure, distribution and composition of the extracellular matrix of human oocytes and cumulus masses. *Hum. Reprod.* **7,** 391–398.

De Kretser, D. M., and Kerr, J. B. (1994). The cytology of the testis. *In* "The Physiology of Reproduction" (2nd ed.), (E. Knobil and J. Neill, Eds.), p. 1177. Raven Press, New York.

Denker, H. W. (2000). Structural dynamics and function of early embryonic coats. *Cells Tissues Organs* **166,** 180–207.

De Placido, G., Wilding, M., Strina, I., Alviggi, E., Alviggi, C., Mollo, A., Varicchio, M. T., Tolino, A., Schiattarella, C., and Dale, B. (2002). High outcome predictability after IVF using a combined score for zygote and embryo morphology and growth rate. *Hum. Reprod.* **17,** 2402–2409.

De Santis, L., Cino, I., Rabellotti, E., Calzi, F., Persico, P., Borini, A., and Coticchio, G. (2005). Polar body morphology and spindle imaging as predictors of oocyte quality. *Reprod. BioMed. Online* **11,** 36–42.

De Sutter, P., Dozortsev, D., Quian, C., and Dhont, M. (1996). Oocyte morphology does not correlate with fertilization rate and embryo quality after intracytoplasmic sperm injection. *Hum. Reprod.* **11,** 595–597.

Drahorad, J., Tesarik, J., Cechova, D., and Vilim, V. (1991). Proteins and glycosaminoglycans in the intercellular matrix of the human cumulus-oophorus and their effect on conversion of proacrosin to acrosin. *J. Reprod. Fertil.* **93,** 253–262.

Ducibella, T., Duffy, P., and Buetow, J. (1994). Quantification and localization of cortical granules during oogenesis in the mouse. *Biol. Reprod.* **50,** 467–473.

Ebner, T., Yaman, C., Moser, M., Sommergruber, M., Feichtinger, O., and Tews, G. (2000). Prognostic value of the first polar body morphology on fertilization rate and embryo quality in intracytoplasmic sperm injection. *Hum. Reprod.* **15,** 427–430.

Ebner, T., Yaman, C., Moser, M., Sommergruber, M., Jesacher, K., and Tews, G. (2001). A prospective study on oocyte survival rate after ICSI: Influence of injection technique and morphological features. *J. Assist. Reprod. Genet.* **18,** 601–606.

Ebner, T., Moser, M., Sommergruber, M., Yaman, C., Pfleger, U., and Twes, G. (2002). First polar body morphology and blastocyst formation rate in ICSI patients. *Hum. Reprod.* **17,** 2415–2418.

Ebner, T., Moser, M., Sommergruber, M., Gaiswinkler, U., Wiesinger, R., Puchner, M., and Tews, G. (2003a). Presence, but not type or degree of extension, of a cytoplasmic halo has a significant influence on preimplantation development and implantation behaviour. *Hum. Reprod.* **18,** 2406–2412.

Ebner, T., Moser, M., Sommergruber, M., and Tews, G. (2003b). Selection based on morphological assessment of oocytes and embryos at different stages of preimplantation development: A review. *Hum. Reprod. Update* **9,** 251–262.

Ebner, T., Moser, M., Sommergruber, M., Puchner, M., Wiesinger, R., and Tews, G. (2003c). Developmental competence of oocytes showing increased cytoplasmic viscosity. *Hum. Reprod.* **18,** 1294–1298.

Ebner, T., Moser, M., Sommergruber, M., Gaiswinkler, U., Shebl, O., Jesaker, K., and Tews, G. (2005). Occurrence and developmental consequences of vacuoles throughout preimplantation development. *Fertil. Steril.* **83,** 1635–1640.

Eddy, E. M., Kiotaka, T., and O'Brien, D. (2003). Fibrous sheath of mammalian spermatozoa. *Microsc. Res. Tech.* **61,** 103–115.

Edwards, R. G., and Brody, S. A. (1995). "Principle and Practice of Assisted Human Reproduction." W.B. Saunders Company, Philadelphia.

Einspanier, R., Lauer, B., Gabler, C., Kamhuber, M., and Schams, D. (1997). Egg-cumulus-oviduct interactions and fertilization. *Adv. Exp. Med. Biol.* **424,** 279–289.

Eisenbach, M. (1999). Sperm chemotaxis. *Rev. Reprod.* **4,** 56–66.

Eisenbach, M. (2004). "Chemotaxis." Imperial College Press, London.

El Shafie, M., Sousa, M., Windt, M. L. and Kruger, T. F. (Eds.) (2000). "An Atlas of the Ultrastructure of Human Oocytes. A Guide for Assisted Reproduction." Parthenon Publishing Group, New York.

El-Toukhy, T., Khalaf, Y., Al Darazi, K., Andritsos, V., Taylor, A., and Braude, P. (2003). Effect of blastomere loss on the outcome of frozen embryo replacement cycles. *Fertil. Steril.* **79,** 1106–1111.

Eppig, J. J. (1996). The ovary: Oogenesis. *In* "Scientific Essentials in Reproductive Medicine" (S. G. Hiller, H. C. Kitchener and J. P. Neilson, Eds.), pp. 147–159. W.B. Saunders Company, London.

ESHRE Monographs. (2002). Sperm morphology. "Manual on Basic Semen Analysis 2002," pp. 13–17. Oxford University Press, Oxford, UK.

Familiari, G., Nottola, S. A., Petrillo, S., Micara, G., Aragona, C., and Motta, P. M. (1987). The application of electron microscopy in the evaluation of *in vitro* unfertilized human oocytes. *In* "Morphological Basis of Human Reproductive Function" (G. Spera and D. De Kretser, Eds.), pp. 99–104. Plenum Press, New York.

Familiari, G., Nottola, S. A., Micara, G., Aragona, C., and Motta, P. M. (1988). Is the sperm-binding capability of the zona pellucida linked to its surface structure? A scanning electron microscopic study of human *in vitro* fertilization. *J.* In Vitro *Fertil. Embryo Transf.* **5,** 134–143.

Familiari, G., Nottola, S. A., Micara, G., Aragona, C., and Motta, P. M. (1989). Human *in vitro* fertilization: The fine three-dimensional architecture of the zona pellucida. *Prog. Clin. Biol. Res.* **296,** 335–344.

Familiari, G., Makabe, S. and Motta, P. M. (Eds.) (1991). "Ultrastructure of the Ovary: Physiology and Pathology." Kluwer Academic Publishers, Boston.

Familiari, G., Nottola, S. A., Macchiarelli, G., Familiari, A., and Motta, P. M. (1992a). A technique for exposure of the glycoproteic matrix (zona pellucida and mucus) for scanning electron microscopy. *Micros. Res. Tech.* **23,** 225–229.

Familiari, G., Nottola, S. A., Macchiarelli, G., Micara, G., Aragona, C., and Motta, P. M. (1992b). Human zona pellucida during *in vitro* fertilization: An ultrastructural study using saponin, ruthenium red, and osmium-thiocarbohydrazide. *Mol. Reprod. Dev.* **32,** 51–61.

Familiari, G., Verlengia, C., Nottola, S. A., Renda, T., Micara, G., Aragona, C., Zardi, L., and Motta, P. M. (1996). Heterogeneous distribution of fibronectin, tenascin-C, and laminin immunoreactive material in the cumulus-corona cells surrounding mature human oocytes from IVF-ET protocols—evidence that they are composed of different subpopulations: An immunohistochemical study using scanning confocal laser and fluorescence microscopy. *Mol. Reprod. Dev.* **43,** 392–402.

Familiari, G., Verlengia, C., Nottola, S. A., Tripodi, A., Hyttel, R., Macchiarelli, G., and Motta, P. M. (1998). Ultrastructural features of bovine cumulus-corona cells surrounding oocytes, zygotes and early embryos. *Reprod. Fertil. Dev.* **10,** 315–326.

Familiari, G., Verlengia, C., Nottola, S. A., Micara, G., Aragona, C., and Motta, P. M. (2000). Fibronectin in the extracellular cumulus matrix of human mature oocytes. Ultrastructural and immunochemical observations. *Hum. Reprod.* **15,** 160–161.

Familiari, G., Relucenti, M., Ermini, M., Verlengia, C., Nottola, S. A., and Motta, P. M. (2001). The human zona pellucida and scanning electron microscopy. Reality or artifacts? *Ital. J. Anat. Embryol.* **106**(2 Suppl. 2), 33–41.

Familiari, G., Relucenti, M., Heyn, R., Micara, G., and Correr, S. (2006). Three dimensional structure of the zona pellucida at ovulation. *Micros. Res. Tech.* (In press).

Fawcett, D. W. (1975). The mammalian spermatozoon. *Dev. Biol.* **44,** 394–436.

Fawcett, D. W. (1993). "Bloom and Fawcett. A Textbook of Histology." Chapman and Hall, New York.

Fetterolf, P. M., Jurisicova, A., Tyson, J. E., and Casper, R. F. (1994). Conditioned medium from human cumulus oophorus cells stimulates human sperm velocity. *Biol. Reprod.* **51,** 184–192.

Flaherty, S. P., Payne, D., and Mathews, C. D. (1998). "Fertilization Failures after ICSI. Treatment of Infertility: The New Frontiers," pp. 269–282. Communications Media for Education, Princeton, NJ.

Flesh, F. M., and Gadella, B. M. (2000). Dynamics of the mammalian sperm plasma membrane in the process of fertilization. *Biochim. Biophys. Acta* **1469,** 197–235.

Fong, C. Y., Bongso, A., Sathananthan, H., Ho, J., and Ng, S. C. (2001). Ultrastructural observations of enzymatically treated human blastocysts: Zona-free blastocyst transfer and rescue of blastocysts with hatching difficulties. *Hum. Reprod.* **16,** 540–546.

Funahashi, H., Ekwall, H., Kikuki, K., and Rodriguez-Martinez, H. (2001). Transmission electron microscopy studies of the zona reaction in pig oocytes fertilized *in vivo* and *in vitro*. *Reproduction* **122,** 443–452.

Fusi, F. M., Bernocchi, N., Ferrari, A., and Bronson, R. A. (1996). Is vitronectin the velcro that binds the gametes together? *Mol. Hum. Reprod.* **2,** 859–866.

Gabrielsen, A., Bhatnager, P. R., Petersen, K., and Lindenberg, S. (2000). Influence of zona pellucida thickness of human embryos on clinical pregnancy outcome following *in vitro* fertilization treatment. *J. Assist. Reprod. Genet.* **17,** 323–328.

Gadella, B. M., Colenbrander, B., van Golde, L. M., and Lopes-Cardozo, M. (1992). Characterization of three arylsulfatases in semen: Seminolipid sulfohydrolase activity is present in seminal plasma. *Biochim. Biophys. Acta* **1128,** 155–162.

Gandini, L., Lombardo, F., Paoli, D., Caponecchia, L., Familiari, G., Verlengia, C., Dondero, F., and Lenzi, A. (2000). Study of apoptotic DNA fragmentation in human spermatozoa. *Hum. Reprod.* **15,** 830–839.

Garrett, C., Liu, D. Y., and Baker, H. W. G. (1997). Selectivity of the human sperm-zona pellucida binding process to sperm head morphometry. *Fertil. Steril.* **67,** 362–371.

Garside, W. T., Loret de Mola, J. R., Bucci, J. A., Tureck, R. W., and Heyner, S. (1997). Sequential analysis of zona thickness during *in vitro* culture of human zygotes: Correlation with embryo quality, age, and implantation. *Mol. Reprod. Dev.* **47,** 99–104.

Gergely, A., Kovanci, E., Senturk, L., Cosmi, E., Vigue, L., and Huszar, G. (1999). Morphometric assessment of matured and diminished maturity human spermatozoa: Sperm regions that reflect differences in maturity. *Hum. Reprod.* **14,** 2007–2014.

Ghetler, Y., Raz, T., Ben Nun, I., and Shalgi, R. (1998). Cortical granules reaction after intracytoplasmic sperm injection. *Mol. Hum. Reprod.* **4,** 289–294.

Gianaroli, L., Magli, M. C., Ferraretti, A. P., Fortini, D., and Grieco, N. (2003). Pronuclear morphology and chromosomal abnormalities as scoring criteria for embryo selection. *Fertil. Steril.* **80,** 341–349.

Gilmore, J. A., Liu, J., Gao, D. Y., and Critser, J. K. (1997). Determination of optimal cryoprotectants and procedures for their addition and removal from human spermatozoa. *Hum. Reprod.* **12,** 12–18.

Gonzales-Santander, R., and Clavero Nuez, J. A. (1973). The fine structure of the human oocyte. *Acta Anat.* **84,** 106–117.

Goud, A. P., Goud, P. T., Diamond, M. P., Oostveldt, P., and Hughes, M. R. (2005). Microtubule turnover in ooplasm biopsy reflects ageing phenomena in the parent oocyte. *Reprod. BioMed. Online* **11,** 43–52.

Goud, P. T., Goud, A. P., Qian, C., Laverge, H., Van der Elst, J., De Sutter, P., and Dhont, M. (1998). *In-vitro* maturation of human germinal vesicle stage oocytes: Role of cumulus cells and epidermal growth factor in the culture medium. *Hum. Reprod.* **13,** 1638–1644.

Goyanes, V. J., Ron-Corzo, A., Costas, E., and Maniero, E. (1990). Morphometric categorization of the human oocyte and early conceptus. *Hum. Reprod.* **5,** 613–618.

Grudzinskas, J. G., and Yovich, J. L. (1995a). "Gametes – The Spermatozoon." Cambridge University Press, New York.

Grudzinskas, J. G., and Yovich, J. L. (1995b). "Gametes – The Oocyte." Cambridge University Press, New York.

Gulyas, B. J. (1976). Ultrastructural observations on rabbit, hamster and mouse eggs following electrical stimulation *in vitro*. *Am. J. Anat.* **147,** 203–218.

Gulyas, B. J. (1984). Fine structure of the luteal tissue. *In* "Ultrastructure of Endocrine Cells and Tissues" (P. M. Motta, Ed.), pp. 238–254. Martinus Nijhoff Publishers, The Hague, Netherlands.

Hardarson, T., Lundin, K., and Hamberger, L. (2000). The position of the metaphase II spindle cannot be predicted by the location of the first polar body in the human oocyte. *Hum. Reprod.* **15,** 1372–1376.

Hardy, K., and Spanos, S. (2002). Growth factor expression and function in the human and mouse preimplantation embryo. *J. Endocrinol.* **172,** 221–236.

Hardy, K., Stark, J., and Winston, R. M. L. (2003). Maintenance of the inner cell mass in human blastocysts from fragmented embryos. *Biol. Reprod.* **68,** 1165–1169.

Harris, J. D., Hibler, D. W., Fontenot, G. K., Hsu, K. T., Yurewicz, E. C., and Sacco, A. G. (1994). Cloning and characterisation of zona pellucida genes and cDNAs from a variety of mammalian species: The ZPA, ZPB and ZPC gene families. *DNA Seq.* **4,** 361–393.

Henkel, R., Cooper, S., Kaskar, K., Schill, W. B., Habenicht, U. F., and Franken, D. R. (1995). Influence of elevated pH levels on structural and functional characteristics of the human zona pellucida: Functional morphological aspects. *J. Assist. Reprod. Genet.* **12,** 644–649.

Herrler, A., and Beier, H. M. (2000). Early embryonic coats: Morphology, function, practical applications. An overview. *Cells Tissues Organs* **166,** 233–246.

Hirata, S., Kazuhiko, H., Shoda, T., and Mabuchi, T. (2002). Spermatozoon and mitochondrial DNA. *Reprod. Med. Biol.* **1,** 41–47.

Hnida, C., Engenheiro, E., and Ziebe, S. (2004). Computer-controlled, multilevel, morphometric analysis of blastomere size as biomarker of fragmentation and multinuclearity in human embryos. *Hum. Reprod.* **19,** 288–293.

Hnida, C., Agerholm, I., and Ziebe, S. (2005). Traditional detection versus computer-controlled multilevel analysis of nuclear structures from donated human embryos. *Hum. Reprod.* **20,** 665–671.

Hofmann, T., Zollner, U., Zollner, K. P., and Dietl, J. (2004). Relationship between fertilization results, pronuclear, embryo and blastocyst morphology and IVF/ICSI outcome and intrafollicular concentration of IL 1β. *Hum. Reprod.* **19**(Suppl. 1), i144–i145.

Holstein, A. F., and Roosen-Runge, E. C. (1981). "Atlas of Human Spermatogenesis." Grosse Verlag, Berlin.

Honda, T., Fujivara, H., Yoshioka, S., Yamada, S., Nakayama, T., Egawa, M., Nishioka, Y., Takahashi, A., and Fujii, S. (2004). Laminin and fibronectin concentrations of the follicular fluid correlate with granulose cell luteinization and oocyte quality. *Reprod. Med. Biol.* **3,** 43–49.

Hong, S. J., Tse, J. Y., Ho, P. C., and Yeung, W. S. (2003). Cumulus cells reduce the spermatozoa-zona binding inhibitory activity of human follicular fluid. *Fertil. Steril.* **79** (Suppl. 1), 802–807.

Hoodbhoy, T., and Dean, J. (2004). Insights into the molecular basis of sperm-egg recognition in mammals. *Reproduction* **127,** 417–422.

Hoodbhoy, T., and Talbot, P. (1994). Mammalian cortical granules: Contents, fate and function. *Mol. Reprod. Dev.* **39,** 439–448.

Hoozemans, D. A., Schats, R., Lambalk, C. B., Homburg, R., and Hompes, P. G. A. (2004). Human embryo implantation: Current knowledge and clinical implications in assisted reproductive technology. *Reprod. BioMed. Online* **9,** 692–715.

Hoshi, K., Sasaki, H., Yanagida, K., Sato, A., and Tsuiki, A. (1994). Localization of fibronectin on the surface of human spermatozoa and relation to the sperm-egg interaction. *Fertil. Steril.* **61,** 542–547.

Høst, E., Gabrielsen, A., Lindenberg, S., and Smidt-Jensen, S. (2002). Apoptosis in human cumulus cells in relation to zona pellucida thickness variation, maturation stage, and cleavage of the corresponding oocyte after intracytoplasmic sperm injection. *Fertil. Steril.* **77,** 511–515.

Huang, F. J., Huang, H. W. M., Lan, K. C., Kung, F. T., Lin, Y. C., Chang, H. W., and Chang, S. Y. (2002). The maturity of human cumulus free oocytes is positively related to blastocyst development and viability. *J. Assist. Reprod. Genet.* **19,** 555–560.

Hunter, R. H. F., Einer-Jensen, N., and Greve, T. (2005). Somatic cell amplification of early pregnancy factors in the Fallopian tube. *Ital. J. Anat. Embryol.* **110**(2 Suppl. 1), 195–203.

Inoue, N., Ikawa, M., Isotani, A., and Okabe, M. (2005). The immunoglobulin superfamily protein Izumo is required for sperm to fuse with eggs. *Nature* **434,** 234–238.

Jackowski, S., and Dumont, J. (1979). Surface alterations of the mouse zona pellucida and ovum following *in vitro* Fertilization: Correlation with cell cycle. *Biol. Reprod.* **20**(2), 150–161.

Jassim, A., Gillott, D. J., Al-zuhdi, Y., Gray, A., Foxton, R., and Bottazzo, G. F. (1992). Isolation and biochemical characterization of the human sperm tail fibrous sheath. *Hum. Reprod.* **7,** 86–94.

Jassim, A., Foxon, R., Purkis, P., Gray, A., and Al-Zuhdi, Y. (1993). Aj-p90 antigen: A novel protein of the perinuclear theca in human sperm subacrosome. *J. Reprod. Immunol.* **23,** 169–188.

Jiménez-Movilla, M., Aviles, M., Gomez-Torres, M. J., Fernandez-Colom, P. J., Castells, M. T., deJuan, J., Romeu, A., and Ballesta, J. (2004). Carbohydrate analysis of the zona pellucida and cortical granules of human oocytes by means of ultrastructural cytochemistry. *Hum. Reprod.* **19,** 1842–1855.

Joshi, N. V., Medina, H., Colasante, C., and Osuna, A. (2000). Ultrastructural investigation of human sperm using atomic force microscopy. *Arch. Androl.* **44,** 51–57.

Joshi, N., Medina, H., Crúz, I., and Osuna, J. (2001). Determination of the ultrastructural pathology of human sperm by atomic force microscopy. *Fertil. Steril.* **75,** 961–965.

Jungnickel, M. K., Sutton, K. A., and Florman, H. M. (2003). In the beginnings: Lessons from fertilization in mice and worms. *Cell* **114,** 401–404.

Jurisicova, A., and Acton, M. (2004). Deadly decisions: The role of genes regulating programmed cell death in human preimplantation embryo development. *Reproduction* **128,** 281–291.

Jurisicova, A., Varnuza, S., and Casper, R. F. (1996). Programmed cell death and human embryo fragmentation. *Mol. Hum. Reprod.* **2,** 93–98.

Kahraman, S., Yakm, K., Donmez, E., Samh, H., Bahce, M., Cengiz, G., Sertyel, S., Samh, M., and Imirzahoglu, N. (2000). Relationship between granular cytoplasm of oocytes and pregnancy outcome following intracytoplasmic sperm injection. *Hum. Reprod.* **15,** 2390–2393.

Kann, M. L., Feinberg, J., Rainteau, D., Dadoune, J. P., Weinman, S., and Fouquet, J. P. (1991). Localization of calmodulin in perinuclear structures of spermatids and spermatozoa: A comparison of six mammalian species. *Anat. Rec.* **230,** 481–488.

Kattera, S., and Chen, C. (2004). Developmental potential of human pronuclear zygotes in relation to their pronuclear orientation. *Hum. Reprod.* **19,** 294–299.

Kim, Y. H., de Kretser, D. M., Temple-Smith, P. D., Hearn, M. T. W., and McFarlane, J. R. (1997). Isolation and characterization of human and rabbit sperm tail fibrous sheath. *Mol. Hum. Reprod.* **3,** 307–313.

Kruger, T. F. and Franken, D. R. (Eds.) (2004). ''Atlas of Human Sperm Morphology Evaluation.'' Taylor and Francis, London.

Lachaud, C., Tesarik, J., Canadas, M. L., and Mendoza, C. (2004). Apoptosis and necrosis in human ejaculated spermatozoa. *Hum. Reprod.* **19,** 607–610.

Lam, X., Gieseke, C., Knoll, M., and Talbot, P. (2000). Assay and importance of adhesive interaction between hamster (Mesocricetus auratus) oocyte-cumulus complexes and the oviductal epithelium. *Biol. Reprod.* **62,** 579–588.

Larsen, W. J., Wert, S. E., Chen, L., Russell, P., and Hendrix, E. M. (1991). Expansion of the cumulus-oocyte complex during the preovulatory period: Possible roles in oocyte maturation,

ovulation and fertilization. *In* "Ultrastructure of the Ovary" (G. Familiari, S. Makabe and P. M. Motta, Eds.), pp. 45–61. Kluwer Academic Publishers, Boston, MA.

Lecuyer, C., Dacheux, J. L., Hermand, E., Mazeman, E., Rousseaux, J., and Rousseaux-Prevost, R. (2000). Actin-binding properties and colocalization with actin during spermiogenesis of mammalian sperm calicin. *Biol. Reprod.* **63,** 1801–1810.

Lefievre, L., Conner, S. J., Salpekar, A., Olufowobi, O., Ashton, P., Pavlovic, B., Lenton, W., Afnan, M., Brewis, I. A., Monk, M., Hughes, D. C., and Barrat, C. L. R. (2004). Four zona pellucida glycoproteins are expressed in the human. *Hum. Reprod.* **19,** 1580–1586.

Le Naour, F., Rubinstein, E., Jasmin, C., Prenant, M., and Boucheix, C. (2000). Severely reduced female fertility in CD9-deficient mice. *Science* **287,** 319–321.

Levy, R. R., Cordonier, H., Czyba, J. C., and Guerin, J. F. (2001). Apoptosis in preimplantation mammalian embryo and genetics. *Ital. J. Anat. Embryol.* **106**(2 Suppl. 2), 101–108.

Lin, Y., Mahan, K., Lathrop, W. F., Myles, D. G., and Primakoff, P. (1994). A hyaluronidase activity of the sperm plasma membrane protein PH-20 enables sperm to penetrate the cumulus cells layer surrounding the egg. *J. Cell Biol.* **125,** 1157–1163.

Liu, D. Y., and Baker, H. W. G. (1992). Morphology of spermatozoa bound to the zona pellucida of human oocytes that failed to fertilize *in vitro*. *J. Reprod. Fertil.* **94,** 71–84.

Liu, D. Y., and Baker, H. W. G. (2000). Defective sperm-zona pellucida interaction: A major cause of failure of fertilization in clinical *in-vitro* fertilization. *Hum. Reprod.* **15,** 702–708.

Longo, F. J., Krohne, G., and Franke, W. W. (1987). Basic proteins of the perinuclear theca of mammalian spermatozoa and spermatids: A novel class of cytoskeletal elements. *J. Cell Biol.* **105,** 1105–1120.

Lopata, A., Sathananthan, A. H., McBrain, J. C., Johnston, W. I. H., and Spiers, A. L. (1980). The ultrastructure of the preovulatory human egg fertilized *in vitro*. *Fertil. Steril.* **33,** 12–20.

Lundin, K. (2004). What is a good embryo morphological criteria. *Hum. Reprod.* **19**(Suppl. 1), 68.

Magerkurth, C., Topfer-Petersen, E., Schwartz, P., and Michelmann, H. W. (1999). Scanning electron microscopy analysis of the human zona pellucida: Influence of maturity and fertilization on morphology and sperm binding pattern. *Hum. Reprod.* **14,** 1057–1066.

Mahi-Brown, L. A., and Yanagimachi, R. (1983). Parameters influencing ovum pickup by the oviductal fimbria in the golden hamster. *Gamete Res.* **8,** 1–10.

Mahutte, N., and Arici, A. (2003). Failed fertilization: It is predictable? *Curr. Op. Obstet. Gynecol.* **15,** 211–218.

Makabe, S., Naguro, T., Nottola, S. A., and Motta, P. M. (2001). Ultrastructural dynamic features of *in vitro* fertilization in humans. *Ital. J. Anat. Embryol.* **106**(2 Suppl. 2), 11–20.

Malter, H., Talansky, B., Gordon, J., and Cohen, J. (1989). Monospermy and polyspermy after partial dissection of reinseminated human oocytes. *Gamete Res.* **23,** 377–386.

Manandhar, G., Simerly, C., and Schatten, G. (2000). Highly degenerated distal centrioles in rhesus and human spermatozoa. *Hum. Reprod.* **15,** 256–263.

Mann, T., and Lutwak-Mann, C. (1981). "Male Reproductive Function and Semen." Springer-Verlag, Berlin.

Manna, C., Rienzi, L., Greco, E., Sbracia, M., Rahman, A., Poverini, R., Siracusa, G., and De Felici, M. (2001). Zona pellucida solubility and cortical granule complements in human oocytes following assisted reproductive techniques. *Zygote* **9,** 201–210.

Mattioli, M., Lucidi, P., and Barboni, B. (1998). Expanded cumuli induce acrosome reaction in boar sperm. *Mol. Reprod. Dev.* **51,** 445–453.

McAvey, B. A., Wortzman, G. B., Williams, C. J., and Evans, J. P. (2002). Involvement of calcium signalling and the actin cytoskeleton in the membrane block to polyspermy in mouse oocytes. *Biol. Reprod.* **76,** 1342–1352.

Menezes, J., Gunasheela, S., and Sathananthan, H. (2003). Video observations on human blastocyst hatching. *Reprod. BioMed. Online* **7,** 217–218.

Mikkelsen, A. L., and Lindenberg, S. (2001). Morphology of *in-vitro* matured oocytes: Impact on fertility potential and embryo quality. *Hum. Reprod.* **16,** 1714–1718.

Millette, C. (1999). Spermatozoa. *In* "Encyclopedia of Reproduction" (E. Knobil and J. Neill, Eds.), Vol. 4, pp. 586–596. Academic Press, San Diego, CA.

Miyado, K., Yamada, G., Yamada, S., Hasuwa, H., Nakamura, Y., Ryu, F., Suzuki, K., Kosai, K., Inoue, K., Ogura, A., Okabe, M., and Mekada, E. (2000). Requirement of CD9 on the egg plasma membrane for fertilization. *Science* **287,** 321–324.

Miyara, F., Aubriot, F. X., Glissant, A., Nathan, C., Douard, S., Stanovici, A., Herve, F., Dumont-Hassan, M., Lemeur, A., Cohen-Bacrie, P., and Debey, P. (2003). Multiparameter analysis of human oocytes at metaphase II stage after IVF failure in non–male infertility. *Hum. Reprod.* **18,** 1494–1503.

Moller, C. C., and Wassarman, P. M. (1989). Characterization of a proteinase that cleaves zona pellucida glycoprotein ZP2 following activation of mouse eggs. *Dev. Biol.* **132,** 103–112.

Moor, R. M., and Gandolfi, F. (1987). Molecular and cellular changes associated with maturation and early development of sheep eggs. *J. Reprod. Fertil.* **34**(Suppl.), 55–69.

Moore, H. D. M., and Bedford, J. M. (1978). An *in vivo* analysis of factors influencing the fertilization of hamster eggs. *Biol. Reprod.* **19,** 879–885.

Moos, J., Faundes, D., Kopf, G. S., and Schultz, R. M. (1995). Composition of the human zona pellucida and modifications following fertilization. *Hum. Reprod.* **10,** 2467–2471.

Motta, P. M. and Van Blerkom, J. (Eds.) (1984). "Ultrastructure of Reproduction: Gametogenesis, Fertilization, and Embryogenesis." Martinus Nijhoff Publishers, Kluwer Academic Publishers Group, Boston, MA.

Motta, P. M., Nottola, S. A., Micara, G., and Familiari, G. (1988). Ultrastructure of human unfertilized oocytes and polyspermic embryos in an IVF-ET program. *Ann. N.Y. Acad. Sci.* **541,** 367–383.

Motta, P. M., Familiari, G., Nottola, S. A., Micara, G., and Aragona, C. (1991). Microstructural events of human egg investments during *in vitro* fertilization. Ultrastructure of the zona pellucida and cumulus oophorus. *Bull. Assoc. Anat. (Nancy)* **75,** 89–91.

Motta, P. M., Makabe, S., Naguro, T., and Correr, S. (1994a). Oocyte-follicular cells association during development of human ovarian follicle. A study by high resolution scanning and transmission electron microscopy. *Arch. Histol. Cytol.* **57,** 369–394.

Motta, P. M., Pereda, J., Nottola, S. A., and Familiari, G. (1994b). Ultrastructural changes of human cumulus oophorus during fertilization and zygote segmentation. *In* "Serono Symposia Frontiers in Endocrinology" (T. Mori, T. Tominaga, T. Aono and M. Hiroi, Eds.), Vol. IV, pp. 89–95. Raven Press Books Ltd, New York.

Motta, P. M., Nottola, S. A., Pereda, J., Croxatto, H. B., and Familiari, G. (1995a). Ultrastructure of human cumulus oophorus: A transmission electron microscopic study on oviductal oocytes and fertilized eggs. *Hum. Reprod.* **10,** 2361–2367.

Motta, P. M., Nottola, S. A., Familiari, G., and Macchiarelli, G. (1995b). Ultrastructure of human fertilization. *In* "Immunocontraception" (O. Nillsson and R. Mattsson, Eds.), pp. 161–181. Serono Symposia, Frontiers in Endocrinology, Raven Press Books Ltd, New York.

Motta, P. M., Nottola, S. A., Familiari, G., Macchiarelli, G., Correr, S., Micara, G., Aragona, C., Hirabayashi, T., and Fujita, H. (1995c). Immunocytochemical localization of aromatase activity in the human cumulus oophorus. *Eur. J. Histochem.* **39,** 71–72.

Motta, P. M., Nottola, S. A., Familiari, G., Vizza, E., and Correr, S. (1995d). Ultrastructure of human reproduction from folliculogenesis to early embryo development. A review. *Ital. J. Anat. Embryol.* **100,** 9–52.

Motta, P. M., Makabe, S., Nottola, S. A., Macchiarelli, G., Familiari, G., and Correr, S. (1998). Morphodynamic events of human oocytes during folliculogenesis and in the extraovarian microfollicular unit. *Assisted. Reprod. Rev.* **8,** 205–216.

Motta, P. M., Nottola, S. A., Familiari, G., Macchiarelli, G., Correr, S., and Makabe, S. (1999). Structure and function of the human oocyte cumulus-corona cell complex before and after ovulation. *Protoplasma* **206,** 270–277.

Motta, P. M., Nottola, S. A., Makabe, S., and Heyn, R. (2000). Mitochondrial morphology in human fetal and adult female germ cell. *Hum. Reprod.* **15**(Suppl. 2), 129–147.

Motta, P. M., Nottola, S. A., Familiari, G., Makabe, S., Stallone, T., and Macchiarelli, G. (2003). Morphodynamics of the follicular-luteal complex during early ovarian development and reproductive life. *Int. Rev. Cytol.* **223,** 177–288.

Mujica, A., Navarro-Garcia, F., Hernandez-Gonzalez, E. O., and Juarez-Mosqueda, M. D. L. (2003). Perinuclear theca during spermatozoa maturation leading to fertilization. *Micros. Res. Tech.* **61,** 76–87.

Muratori, M., Piomboni, P., Baldi, E., Filimberti, E., Pecchioli, P., Moretti, E., Gambera, L., Baccetti, B., Biagiotti, R., Forti, G., and Maggi, M. (2000). Functional and ultrastructural features of DNA-fragmented human sperm. *J. Androl.* **21,** 903–912.

Navara, C. S., Simerly, C., Zoran, S., and Schatten, G. (1995). The sperm centrosome during fertilization in mammals: Implications for fertility and reproduction. *Reprod. Fertil. Dev.* **7,** 747–754.

Nikas, G., and Makrigiannakis, A. (2003). Endometrial pinopodes and uterine receptivity. *Ann. N.Y. Acad. Sci.* **997,** 120–123.

Nikas, G., Paraschos, T., Psychoyos, A., and Handyside, A. H. (1994). The zona reaction in human oocytes as seen with scanning electron microscopy. *Hum. Reprod.* **9,** 2135–2138.

Nottola, S. A., Familiari, G., Micara, C., Aragona, C., and Motta, P. M. (1989). The role of cumulus-corona cells surrounding *in vitro* human oocytes and polypronuclear ova: An ultrastructural study. *Prog. Clin. Biol. Res.* **296,** 345–354.

Nottola, S. A., Familiari, G., Micara, G., Aragona, C., and Motta, P. M. (1991). The ultrastructure of human cumulus-corona cells at the time of fertilization and early embryogenesis. A scanning and transmission electron microscopic study in an *in vitro* fertilization program. *Arch. Histol. Cytol.* **54,** 145–161.

Nottola, S. A., Macchiarelli, G., Familiari, G., Stallone, T., Sathananthan, A. H., and Motta, P. M. (1998). Egg-sperm interactions in humans: Ultrastructural aspects. *Ital. J. Anat. Embryol.* **103**(4 Suppl. 1), 85–101.

Nottola, S. A., Makabe, S., Stallone, T., Familiari, G., Macchiarelli, G., and Motta, P. M. (2001). *In vitro* fertilized human eggs. An electron microscopic study. *Ital. J. Anat. Embryol.* **106**(2 Suppl. 2), 75–83.

Nottola, S. A., Makabe, S., Stallone, T., Familiari, G., Correr, S., and Macchiarelli, G. (2005). Surface morphology of the zona pellucida surrounding human blastocyst obtained after *in vitro* fertilization. *Arch. Histol. Cytol.* **68,** 133–141.

Ohta, N., Saito, H., Kuzumaki, T., Takahashi, T., Ito, M. M., Saito, T., Nakahara, K., and Hiroi, M. (1999). Expression of CD44 in human cumulus and mural granulosa cells of individual patients in *in-vitro* fertilization programmes. *Mol. Hum. Reprod.* **5,** 22–28.

Olds-Clarke, P. (2003). Unresolved issues in mammalian fertilization. *Int. Rev. Cytol.* **232,** 129–184.

Ortiz, M. E., Salvatierra, A. M., Lopez, J., Fernandez, E., and Croxatto, H. B. (1982). Postovulatory aging of human ova: I. Light microscopic observations. *Gamete Res.* **6,** 11–17.

Otsuki, J., Okada, A., Morimoto, K., Nagai, Y., and Kubo, H. (2004). The relationship between pregnancy outcome and smooth endoplasmic reticulum clusters in MII human oocytes. *Hum. Reprod.* **19,** 1591–1597.

Parrington, J., Swann, K., Shevchenko, V. I., Sesay, A. K., and Lai, F. A. (1996). Calcium oscillations in mammalian eggs triggered by a soluble sperm protein. *Nature* **379,** 364–368.

Payne, D., Flaherty, S. P., Barry, M. F., and Matthews, C. D. (1997). Preliminary observation on polar body extrusion and pronuclear formation in human oocytes using time-lapse video cinematography. *Hum. Reprod.* **12,** 532–541.

Pelletier, C., Keefe, D. L., and Trimarchi, J. R. (2004). Noninvasive polarized light microscopy quantitatively distinguishes the multilaminar structure of the zona pellucida of living human eggs and embryos. *Fertil. Steril.* **81**(Suppl. 1), 850–856.

Petersen, C., Fuzesi, L., and Hoyer-Fender, S. (1999). Outer dense fibre proteins from human sperm tail: Molecular cloning and expression analyses of two cDNA transcripts encoding proteins of ~70kDa. *Mol. Hum. Reprod.* **5,** 627–635.

Piccinni, M. P., Scaletti, C., Mavilia, C., Lazzeri, E., Romagnani, P., Natali, I., Pellegrini, S., Livi, C., Romagnani, S., and Maggi, E. (2001). Production of IL-4 and leukemia inhibitory factor by T cells of the cumulus oophorus: A favorable microenvironment for pre-implantation embryo development. *Eur. J. Immunol.* **31,** 2431–2437.

Picton, H. M., Gosden, R. G., and Leibo, S. P. (2001). Cryopreservation of oocytes and ovarian tissue. *In* "Current Practices and Controversies in Assisted Reproduction." Chapter 3: Recent Medical Developments and Unresolved Issues in ART, Gamete Source Manipulation and Disposition, pp. 143–151. WHO, Geneva. http://www.int/reproductive-health/infertility/report_context.htm.

Primakoff, P., and Myles, D. G. (2002). Penetration, adhesion, and fusion in mammalian sperm-egg interaction. *Science* **296,** 2183–2185.

Qi, H., Williams, Z., and Wassarman, P. M. (2002). Secretion and assembly of zona pellucida glycoproteins by growing mouse oocytes microinjected with epitope-tagged cDNAs for mZP2 and mZP3. *Mol. Biol. Cell* **13,** 530–541.

Rajeev, S. K., and Reddy, K. V. R. (2004). Sperm membrane protein profiles of fertile and infertile men: Identification and characterization of fertility-associated sperm antigen. *Hum. Reprod.* **19,** 234–242.

Ramos, L., Hendriks, J. C. M., Peelen, P., Braat, D. D. M., and Wetzels, A. M. M. (2002). Use of computerized karyometric image analysis for evaluation of human spermatozoa. *J. Androl.* **23,** 882–888.

Rankin, T. L., and Dean, J. (2000). The zona pellucida: Using molecular genetics to study the mammalian egg coat. *Rev. Reprod.* **5,** 114–121.

Rankin, T. L., Coleman, J. S., Epifano, O., Hoodbhoy, T., Turner, S. G., Castle, P. E., Lee, E., Gore-Langton, R., and Dean, J. (2003). Fertility and taxon-specific sperm binding persist after replacement of mouse sperm receptors with human homologs. *Dev. Cell* **5,** 33–43.

Relucenti, M., Heyn, R., Correr, S., and Familiari, G. (2005). Cumulus oophorus extracellular matrix in the human oocyte: A role for adhesive proteins. *Ital. J. Anat. Embryol.* **110** (2 Suppl. 1), 219–224.

Rienzi, L., Ubaldi, F., Iacobelli, M., Minasi, M. G., Romano, S., and Greco, E. (2005a). Meiotic spindle visualization in the living human oocytes. *Reprod. BioMed. Online* **10,** 192–198.

Rienzi, L., Ubaldi, F., Iacobelli, M., Romano, S., Minasi, M. G., Ferrero, S., Sapienza, F., Baroni, E., and Greco, E. (2005b). Significance of morphological attributes of the early embryo. *Reprod. BioMed. Online* **10,** 669–681.

Riou, J. F., Shi, D. L., Chiquet, M., and Boucaut, J. C. (1988). Expression of tenascin in response to neural induction in amphibian embryos. *Development* **104,** 511–524.

Rotmensch, S., Dor, J., Furman, A., Rudak, E., Mashiach, S., and Amsterdam, A. (1986). Ultrastructural characterization of human granulosa cells in stimulated cycles: Correlation with oocyte fertilizability. *Fertil. Steril.* **45,** 671–679.

Sabeur, K., Cherr, G. N., Yudin, A. I., and Overstreet, J. W. (1998). Hyaluronic acid enhances induction of the acrosome reaction of human sperm through interaction with the PH-20 protein. *Zygote* **6,** 103–111.

Sacco, A. G., Yurewicz, E. C., Subraminian, M. G., and DeMayo, F. J. (1981). Zona pellucida composition: Species cross reactivity and contraceptive potential of antiserum to a purified pig zona antigen (PPZA). *Biol. Reprod.* **25,** 997–1008.

Salumets, A., Hydén-Granskog, C., Suikkari, A. M., Tiitinen, A., and Tuuri, T. (2001). The predictive value of pronuclear morphology of zygotes in the assessment of human embryo quality. *Hum. Reprod.* **16,** 2177–2181.

Salustri, A., Yanagishita, M., Camaioni, A., Tirone, E., and Hascall, V. C. (1994). Proteoglycan and hyaluronic acid synthesis by granulosa cells: Regulation by an oocyte factor and gonadotropins. *In* "Ovarian Cell Interactions, Genes to Physiology" (A. J. W. Hsueh and D. W. Schomberg, Eds.), pp. 38–48. Springer-Verlag, New York.

Salustri, A., Camaioni, A., Di Giacomo, M., Fulop, C., and Hascall, V. C. (1999). Hyaluronan and proteoglycans in ovarian follicles. *Hum. Reprod. Update* **5,** 293–301.

Salustri, A., Garlanda, C., Hirsch, E., De Acetis, M., Taccagno, A., Bottazzi, B., Doni, A., Bastone, A., Mantovani, G., Beck Peccoz, P., Salvatori, G., Mahoney, D. J., Day, M. A., Siracusa, G., Romani., L., and Mantovani, A. (2004). PTX3 plays a key role in the organization of the cumulus oophorus extracellular matrix and in *in vivo* fertilization. *Development* **131,** 1577–1586.

Sathananthan, A. H. (1984). Ultrastructural morphology of fertilization and early cleavage in the human. *In* "*In vitro* Fertilization and Embryo Transfer" (A. Trounson and C. Wood, Eds.), pp. 131–158. Churchill Livingstone, London.

Sathananthan, A. H. (1985). Maturation of the human oocyte *in vitro*: Nuclear events during meiosis (an ultrastructural study). *Gamete Res.* **12,** 237–254.

Sathananthan, A. H. (1990). Abnormal nuclear configurations encountered in human IVF. Possible genetic implications. *Assist. Reprod. Technol. Androl.* **1,** 115–133.

Sathananthan, A. H. (1991). The pathology of *in vitro* fertilization. *In* "Diagnostic Ultrastructure of Neoplastic Diseases" (J. M. Papadimitriou, D. W. Henderson and D. Spagnola, Eds.), pp. 435–450. Churchill Livingstone, Edinburgh.

Sathananthan, A. H. (1994a). Functional competence of abnormal spermatozoa. *In* "Bailliere's Clinical Obstetrics and Gynaecology. Micromanipulation Techniques" (S. Fishel, Ed.), Vol. 8, pp. 141–156. Bailliere Tindall, London.

Sathananthan, A. H. (1994b). Ultrastructural changes during meiotic maturation in mammalian oocytes: Unique aspects of the human oocyte. *Micros. Res. Tech.* **27,** 145–164.

Sathananthan, A. H. (1996). "Visual Atlas of Human Sperm Structure & Function for Assisted Reproductive Technology," p. 279. La Trobe and Monash University, National University, Singapore.

Sathananthan, A. H. (1997a). Ultrastructure of the human egg. *Hum. Cell* **10,** 21–38.

Sathananthan, A. H. (1997b). Mitosis in the human embryo: The vital role of the sperm centrosome (centriole). *Histol. Histopathol.* **12,** 827–856.

Sathananthan, A. H. (1998a). Paternal centrosomal dynamics in early human development and infertility. *J. Assist. Reprod. Genet.* **15,** 129–139.

Sathananthan, A. H. (1998b). Human gametes and fertilization. *In* "Modern Reproduction Medical View" (S. Suzuki, Ed.), pp. 12–21. Medical View: Tokyo.

Sathananthan, A. H. (1998c). Sperm centrioles and their role in mammalian development. *In* "Treatment of Infertility: The New Frontiers" (M. Filicore and C. Flamigni, Eds.), pp. 229–241. Communications Media for Education, Princeton, NJ.

Sathananthan, A. H. (2000). Ultrastructure of human gametes, fertilization and embryo development. *In* "Handbook of *in vitro* Fertilization," (A. O. Trounson and D. K. Gardner, Eds.), 2nd ed., pp. 431–464. CRC Press, Boca Raton, FL.

Sathananthan, A. H. (2003a). Human Fertilization CD-ROM. Tokyo.

Sathananthan, A. H. (2003b). Morphology and pathology of the human oocyte. *In* "Biology and Pathology of the Oocyte, Role in Fertility and Reproductive Medicine" (A. O. Trounson and R. G. Gosden, Eds.), pp. 185–208. Cambridge University Press, New York.

Sathananthan, A. H., and Chen, C. (1986). Sperm-oocyte membrane fusion in the human during monospermic fertilisation. *Gamete Res.* **15,** 177–186.

Sathananthan, A. H., and Trounson, A. O. (1982a). Ultrastructural observations on cortical granules in human follicular oocytes cultured *in vitro*. *Gamete Res.* **5,** 191–198.

Sathananthan, A. H., and Trounson, A. O. (1982b). Ultrastructure of cortical granule release and zona interaction in monospermic and polyspermic human ova fertilized *in vitro*. *Gamete Res.* **6,** 225–234.

Sathananthan, A. H., and Trounson, A. O. (2000). Ultrastructure of ICSI. *In* "Handbook of *in vitro* Fertilization," (A. O. Trounson and D. K. Gardner, Eds.), 2nd ed., pp. 465–482. CRC Press, Boca Raton, FL.

Sathananthan, A. H., Trounson, A. O., Wood, C., and Leeton, J. F. (1982). Ultrastructural observations on the penetration of human sperm into the zona pellucida of the human egg *in vitro*. *J. Androl.* **3,** 356–364.

Sathananthan, A. H., Trounson, A. O., and Wood, C. (1986a). "Atlas of Fine Structure of Human Sperm Penetration, Eggs and Embryos Cultured *in vitro*," p. 279. Praeger Scientific, Philadelphia, PA.

Sathananthan, A. H., Ng, S. C., Edirisinghe, R., Ratnam, S. S., and Wong, P. C. (1986b). Sperm oocyte interaction in the human during polyspermic fertilization *in vitro*. *Gamete Res.* **15,** 317–326.

Sathananthan, A. H., Ng, S. C., Trounson, A. O., Bongso, A., Laws-King, A., and Ratnam, S. S. (1989). Human micro-insemination by injection of single or multiple sperm: Ultrastructure. *Hum. Reprod.* **4,** 574–583.

Sathananthan, A. H., Bongso, A., Ng, S. C., Ho, J., Mok, H., and Ratnam, S. S. (1990). Ultrastructure of preimplementation human embryos co-cultured with human ampullary cells. *Human Reprod.* **5,** 309–318.

Sathananthan, A. H., Kola, I., Osborne, J., Trounson, A. O., Ng, S. C., Bongso, A., and Ratnam, S. S. (1991). Centrioles in the beginning of human development. *Proc. Natl. Acad. Sci. USA* **88,** 4806–4810.

Sathananthan, A. H., Ng, S. C., Bongso, A., Trounson, A. O., and Ratnam, S. S. (1993). "Visual Atlas of Early Human Development for Assisted Reproductive Technology." Serono. National University of Singapore, Singapore.

Sathananthan, A. H., Ratnam, S. S., Ng, S. C., Tarin, J. J., Gianaroli, L., and Trounson, A. O. (1996). The sperm centriole: Its inheritance, replication and perpetuation in early human embryos. *Hum. Reprod.* **11,** 345–356.

Sathananthan, A. H., Szell, A., Ng, S. C., Kausche, A., Lacham-Kaplan, O., and Trounson, A. O. (1997). Is the acrosome a prerequisite for sperm incorporation after intra-cytoplasmic sperm injection (ICSI)? *Reprod. Fertil. Dev.* **9,** 703–709.

Sathananthan, A. H., Ratnam, S. S., Trounson, A. O., and Edwards, R. G. (1999a). Early human development (CD-ROM). *Hum. Reprod. Update* **5,** 89.

Sathananthan, A. H., Tarin, J. J., Gianaroli, L., Ng, S. C., Dharmawardena, V., Magli, M. C., Fernando, R., and Trounson, A. O. (1999b). Development of the human dispermic embryo. *Hum. Reprod. Update* **5,** 553–560.

Sathananthan, A. H., Ratnasooriya, W. D., de Silva, P. K. R. A., and Menezes, J. (2001). Characterization of human gamete centrosomes for assisted reproduction. *Ital. J. Anat. Embryol.* **106,** 61–73.

Sathananthan, A.H, Gunasheela, S., and Menezes, J. (2003a). Critical evaluation of human blastocysts for assisted reproduction techniques and embryonic stem cell biotechnology. *Reprod. BioMed. Online* **7,** 219–227.

Sathananthan, A. H., Menezes, J., and Gunasheela, S. (2003b). Mechanics of human blastocyst hatching *in vitro*. *Reprod. BioMed. Online* **7,** 228–234.

Sathananthan, A. H., Ratnasooriya, W. D., Gunasheela, S., and Trounson, A. O. (2004). The human sperm: Its contribution to fertlization and embryogenesis. *In* "The Infertility Manual," (K. A. Rao, P. R. Brinsden and A.H Sathananthan, Eds.), 2nd ed., pp. 132–144. Jaypee Brothers, Delhi.

Schatten, G. (1994). The centrosome and its mode of inheritance: The reduction of the centrosome during gametogenesis and its restoration during fertilization. *Dev. Biol.* **165,** 299–335.

Schultz, R., and Williams, C. (2005). Sperm–egg fusion unscrambled. *Nature* **434,** 152–153.

Schultz, R. M., and Kopf, G. S. (1995). Molecular basis of mammalian egg activation. *Curr. Top. Dev. Biol.* **30,** 21–62.

Schwartz, P. (2003). Oocyte sperm interaction in the course of IVF: A scanning electron microscopy analysis. *Reprod. Biomed. Online* **7,** 205–210.

Scott, L., Alvero, R., Leondires, M., and Miller, B. (2000). The morphology of human pronuclear embryos is positively related to blastocyst development and implantation. *Hum. Reprod.* **15,** 2394–2403.

Sengoku, K., Tamate, K., Horikawa, M., Takaoka, Y., Ishikawa, M., and Dukelow, W. R. (1995). Plasma membrane block to polyspermy in human oocytes and preimplantation embryos. *J. Reprod. Fertil.* **105,** 85–90.

Sengoku, K., Tamate, K., Takaota, Y., Horikawa, M., Goishi, K., Okada, R., Tsuchiya, K., and Ishikawa, M. (1999). Requirement of sperm-oocyte plasma membrane fusion for establishment of the plasma membrane block to polyspermy in human pronuclear oocytes. *Mol. Reprod. Dev.* **5,** 183–188.

Serhal, P. F., Ranieri, D. M., Kinis, A., Marchant, S., Davies, M., and Khadum, I. M. (1997). Oocyte morphology predicts outcome of intracytoplasmic sperm injection. *Hum. Reprod.* **12,** 1267–1270.

Shabanowitz, R. B., and O'Rand, M. G. (1988). Characterization of the human zona pellucida from fertilized and unfertilized eggs. *J. Reprod. Fertil.* **82,** 151–161.

Shutt, D. A., and Lopata, A. (1981). The secretion of hormones during the culture of human preimplantation embryos with corona cells. *Fertil. Steril.* **35,** 413–416.

Soupart, P., and Strong, P. A. (1975). Ultrastructural observations on polyspermic penetration of zona pellucida-free human oocytes inseminated *in vitro*. *Fertil. Steril.* **26,** 523–537.

Sousa, M., Barros, A., and Tesarik, J. (1996). Developmental changes in calcium dynamics, protein kinase C distribution and endoplasmic organization in human preimplantation embryos. *Mol. Hum. Reprod.* **2,** 967–977.

Staessen, C., Michiels, A., Devroey, P., Liebaers, I., and Van Steirteghem, A. (2004). Is the morphologically best embryo the one that will implant? *Hum. Reprod.* **19** (Suppl. 1), 145–146.

Stanger, J. D., Stevenson, K., Lakmaker, A., and Woolcott, R. (2001). Pregnancy following fertilization of zona-free, coronal cell intact human ova. *Hum. Reprod.* **16,** 164–167.

Stein, K. K., Primakoff, P., and Myles, D. (2004). Sperm-egg fusion: Events at the plasma membrane. *J. Cell Sci.* **117,** 6269–6274.

Sullivan, R., Duchesne, C., Fahmy, N., Morin, N., and Dionne, P. (1990). Protein synthesis and acrosome reaction-inducing activity of human cumulus cells. *Hum. Reprod.* **5,** 830–834.

Sun, Q. Y. (2003). Cellular and molecular mechanisms leading to cortical reaction and polyspermy block in mammalian eggs. *Micros. Res. Tech.* **61,** 342–348.

Sun, T., Bahat, A., Gakamsky, A., Girsh, E., Katz, N., Giojalas, L. C., Tur-Kaspa, I., and Eisenbach, M. (2005). Human sperm chemotaxis: Both the oocyte and its surrounding cumulus cells secrete sperm chemoattractants. *Hum. Reprod.* **20,** 761–767.

Sutovsky, P., and Schatten, G. (2000). Paternal contributions to the mammalian zygote: Fertilization after sperm-egg fusion. *Int. Rev. Cytol.* **195,** 1–65.

Szollosi, D., Mandelbaum, J., Plachot, M., Salat-Baroux, J., and Cohen, J. (1986). Ultrastructure of human preovulatory oocyte. *J.* In Vitro *Fert. Embryo Transf.* **3,** 232–242.

Talbot, P., and Dandekar, P. (2003). Perivitelline space: Does it play a role in blocking polyspermy in mammals? *Microsc. Res. Tech.* **61,** 349–357.

Talbot, P., Shur, B. D., and Myles, D. G. (2003). Cell adhesion and fertilization: Steps in oocyte transport, sperm-zona pellucida interactions, and sperm-egg fusion. *Biol. Reprod.* **68,** 1–9.

Tanghe, S., Van Soom, A., Nauwynck, H., Coryn, M., and de Kruif, A. (2002). Minireview: Functions of the cumulus oophorus during oocyte maturation, ovulation, and fertilization. *Mol. Reprod. Dev.* **61,** 414–424.

Tanghe, S., Van Soom, A., Duchateau, L., Nauwynck, H., and De Kruif, A. (2004). Carbohydrates and glycoproteins involved in bovine fertilization *in vitro*. *Mol. Reprod. Dev.* **68,** 492–499.

Tarlatzis, B. C., and Bili, H. (1997). Steroid and cytokine production by human cumulus cells. *In* "Microscopy of Reproduction and Development: A Dynamic Approach" (P. M. Motta, Ed.), pp. 151–153. Antonio Delfino Editore, Rome.

Tesarik, J. (1989). The potential diagnostic use of human zona-free eggs prepared from oocytes that failed to fertilize *in vitro*. *Fertil. Steril.* **52,** 821–824.

Tesarik, J. (1990). Biology of human fertilization: The general and the special. *In* "From Ovulation to Implantation" (J. L. H. Evers and M. J. Heineman, Eds.), pp. 263–282. Elsevier, Amsterdam.

Tesarik, J., and Greco, E. (1999). The probability of abnormal preimplantation development can be predicted by a single static observation on pronuclear stage morphology. *Hum. Reprod.* **14,** 1318–1323.

Tesarik, J., and Mendoza, C. (1994). Most living acrosome reacted spermatozoa do not fuse with the oocyte when inserted into the perivitelline space. *Fertil. Steril.* **61,** 529–535.

Tesarik, J., Pilka, L., and Travnik, P. (1988a). Zona pellucida resistance to sperm penetration before the completion of human oocyte maturation. *J. Reprod. Fertil.* **83,** 487–495.

Tesarik, J., Pilka, L., Drahorad, J., Cechova, D., and Veselsky, L. (1988b). The role of cumulus cell-secreted proteins in the development of human sperm fertilizing ability: Implication in IVF. *Hum. Reprod.* **3,** 129–132.

Tesarik, J., Mendoza Oltras, C., and Testart, J. (1990). Effect of the human cumulus oophorus on movement characteristics of human capacitated spermatozoa. *J. Reprod. Fertil.* **88,** 665–675.

Tesarik, J., Sousa, M., and Mendoza, C. (1995). Sperm-Induced calcium oscillations of human oocytes show distinct features in oocyte center and periphery. *Mol. Reprod. Dev.* **41,** 257–263.

Tesarik, J., Junca, A. M., Hazout, A., Aubriot, F. X., Nathan, C., Cohen-Bacrie, P., and Dumont-Hassan, M. (2000). Embryos with high implantation potential after intracytoplasmic sperm injection can be recognized by a simple, non-invasive examination of pronuclear morphology. *Hum. Reprod.* **15,** 1396–1399.

Toshimori, K. (2003). Biology of spermatozoa maturation: An overview with an introduction to this issue. *Microsc. Res. Tech.* **61,** 1–6.

Trounson, A. O., and Gosden, R. G. (2003). "Biology and Pathology of the Oocyte, Role in Fertility and Reproductive Medicine." Cambridge University Press, New York.

Trounson, A. O., Anderiesz, C., and Jones, G. (2001). Maturation of human oocytes *in vitro* and their developmental competence. *Reproduction* **121,** 51–75.

Turner, R. (2003). Tales from the tail: What do we really know about sperm motility? *J. Androl.* **24,** 790–803.

Urman, B., and Balaban, B. (2005). Is there still a place for co-cultures in the era of sequential media? *Reprod. BioMed. Online* **10,** 492–496.

Van Blerkom, J. (1990). Occurrence and developmental consequences of aberrant cellular organization in meiotically mature human oocytes after exogenous ovarian hyperstimulation. *J. Electron Microsc. Tech.* **16,** 324–346.

Van Blerkom, J., and Motta, P. M. (1989). "Ultrastructure of Human Gametogenesis and Early Embryogenesis." Kluwer Academic Publishers, Boston, MA.

Van Blerkom, J., Davis, P., and Alexander, S. (2000). Differential mitochondrial distribution in human pronuclear embryos leads to disproportionate inheritance between blastomeres: Relationship to microtubular organization, ATP content and competence. *Hum. Reprod.* **15,** 2621–2633.

Van Blerkom, J., Davis, P., and Alexander, S. (2001). A microscopic and biochemical study of fragmentation phenotypes in stage-appropriate human embryos. *Hum. Reprod.* **16,** 719–729.

Vandervorst, M., Tournaye, H., Camus, M., Nagy, Z. P., Van Steirteghem, A., and Devroey, P. (1997). Patients with absolutely immotile spermatozoa and intracytoplasmic sperm injection. *Hum. Reprod.* **12,** 2429–2433.

Van Soom, A., Tanghe, S., De Pauw, I., Maes, D., and de Kruif, A. (2002). Function of the cumulus oophorus before and during mammalian fertilization. *Reprod. Domest. Anim.* **37,** 144–151.

Varani, S., Elvin, J. A., Yan, C., DeMayo, J., DeMayo, F. J., Horton, H. F., Byrne, M. C., and Matzuk, M. M. (2002). Knockout of pentraxin 3, a downstream target of growth differentiation factor-9, causes female subfertility. *Mol. Endocrinol.* **16,** 1154–1167.

Veeck, L. L. (1999). "An Atlas of Human Gametes and Conceptuses." Parthenon Publishing Group, Nashville, TN.

Vorup-Jensen, T., Hjort, T., Abraham-Peskir, J. V., Guttmann, P., Jensenius, J. C., Uggerhøj, E., and Medenwaldt, R. (1999). X-ray microscopy of human spermatozoa shows change of mitochondrial morphology after capacitation. *Hum. Reprod.* **14,** 880–884.

Wang, W. H., Meng, L., Hackett, R. J., Odenbourg, R., and Keefe, D. L. (2001). The spindle observation and its relationship with fertilization after intracytoplasmic sperm injection in living human oocytes. *Fertil. Steril.* **75,** 348–353.

Wang, W. H., Day, B. N., and Wu, G. M. (2003). How does polyspermy happen in mammalian oocytes? *Microsc. Res. Tech.* **61,** 335–341.

Wang, A., Takeuchi, T., Neri, Q. V., Baek, K., Rosenwaks, Z., and Palermo, G. D. (2004). Oocyte maturation rate predicts ICSI outcome. *Hum. Reprod.* **19**(Suppl. 1), i130–i131.

Wassarman, P. M. (1990a). Regulation of mammalian fertilization by zona pellucida glycoproteins. *J. Reprod. Fertil.* **42**(Suppl.), 79–87.

Wassarman, P. M. (1990b). Profile of a mammalian sperm receptor. *Development* **10,** 1–17.

Wassarman, P. M. (1999). Mammalian fertilization: Molecular aspects of gamete adhesion, exocytosis, and fusion. *Cell* **96,** 175–183.

Wharf, E. (2003). Early embryo development is an indicator of implantation potential. *Reprod. BioMed. Online* **8,** 212–218.

Williams, C. J. (2002). Signalling mechanisms of mammalian oocyte activation. *Hum. Reprod. Update* **8,** 313–321.

Windt, M. L., Coetzee, K., Kruger, T. F., Marino, H., Kitshoff, M. S., and Sousa, M. (2001). Ultrastructural evaluation of recurrent and *in-vitro* maturation resistant metaphase I arrested oocytes. *Hum. Reprod.* **16,** 2394–2398.

Wortzman, G. B., and Evans, J. P. (2005). Membrane and cortical abnormalities in post-ovulatory aged eggs: Analysis of fertilizability and establishment of the membrane block to polyspermy. *Mol. Hum. Reprod.* **11,** 1–9.

This page intentionally left blank

Chromosomal Variation in Mammalian Neuronal Cells: Known Facts and Attractive Hypotheses

Ivan Y. Iourov,* Svetlana G. Vorsanova,*† and Yuri B. Yurov*†
*National Research Center of Mental Health, Russian Academy of Sciences Moscow, Russia 119152
†Institute of Pediatrics and Pediatric Surgery, Roszdrav, Moscow, Russia 127412

Chromosomal mosaicism is still a genetic enigma. Although the mechanisms and consequences of this phenomenon have been studied for over 50 years, there are a number of gaps in our knowledge concerning causes, genetic mechanisms, and phenotypic manifestations of chromosomal mosaicism. Neuronal cell-specific chromosomal mosaicism is not an exception. Originally, neuronal cells of the mammalian brain were assumed to possess identical genomes. However, recent studies have shown chromosomal variations, manifested as chromosome abnormalities in cells of the developing and adult mammalian nervous system. Here, we review data obtained on the variation in chromosome complement in mammalian neuronal cells and hypothesize about the possible relevance of large-scale genomic (i.e., chromosomal) variations to brain development and functions as well as neurodevelopmental and neurodegenerative disorders. We propose to cover the term ''molecular neurocytogenetics to cover all studies the aim of which is to reveal chromosome variations and organization in the mammalian brain.

KEYWORDS: Mammalian brain, Aneuploidy, Chromosomal mosaicism, Brain development, Molecular cytogenetics, Polyploidy.

I. Introduction

Since the establishment of human chromosome numbers in 1956 (Tjio and Levan, 1956) and early reports on numerical chromosome abnormalities associated with human diseases (Ford *et al.*, 1959; Jacobs and Strong,

0074-7696/06 $35.00
DOI: 10.1016/S0074-7696(06)49003-3

1959; Jacobs *et al.*, 1959; Lejeune *et al.*, 1959), cytogenetic studies have become a part of human genetics. As a result a multitude of pathogenic and nonpathogenic conditions associated with regular as well as mosaic chromosomal abnormalities have been described. Chromosomal mosaicism—the presence of cell populations differing with respect to their chromosome complements in the same individual—is assumed to contribute to phenotypic variability and disease. Throughout the second half of the twentieth century, chromosomal mosaicism has been systematically described. However, our knowledge about causes and consequences of chromosomal mosaicism is surprisingly exiguous, especially for chromosomal mosaicism confined to a somatic tissue.

The mammalian brain is the control center that functions to store, compute, integrate, and transmit information acquired from the environment. The human brain is supposed to possess about one trillion neurons, each forming as many as several thousand connections with other neurons (Lodish *et al.*, 2000). The functions of neuronal cells connected to a neuron with abnormal chromosome complement should be affected. Therefore, the presence of neurons with chromosome abnormalities in the mammalian brain may be the cause for different pathogenic processes of the nervous system and contribute to neuronal diversity. The present review focuses on evidence for chromosome complement variations in the mammalian brain and the relevance to brain development, functions, and mechanisms underlying the etiology of neurodevelopmental and neurodegenerative disorders. To provide a better understanding of this subject, we present current knowledge about the causes and consequences of numerical chromosome abnormalities in humans and available molecular cytogenetic techniques for the identification of chromosomal mosaicism in the mammalian brain.

II. Numerical Chromosome Abnormalities: Origin and Consequences

A. Nondisjunctional Events

1. Meiotic Nondisjunction

Meiosis taking place only in the ovaries and testes is a process of generation of haploid gametes by a cell division process that consists of one round of DNA replication and two subsequent cell divisions. The first cell division, defined as meiosis I (MI), is characterized by chromosome conjugation and the segregation of homologous chromosomes. The second cell division, or

meiosis II (MII), is characterized by the segregation of the sister chromatids, and is similar to mitotic division. An error due to meiotic chromosome or sister chromatid malsegregation is usually defined as meiotic nondisjunction. Meiotic nondisjunction can occur during MI and MII. Generally, the result of meiotic nondisjunction is the regular form of aneuploidy (the presumable presence of trisomy or monosomy in all the cells of an organism).

The overall incidence of meiotic errors in humans is considered to be significantly increased versus other mammalian species (up to 15 times), occurring in 10–30% of fertilized human eggs. Moreover, aneuploidy due to meiotic errors is the most common cause of fetal death, stillbirth, and disorders associated with chromosome abnormalities in humans (Hassold and Hunt, 2001). Our knowledge about the origin and phenotypic manifestations of aneuploidy in humans is essentially acquired from studies of the most common aneuploidies in liveborns, e.g., trisomy of chromosome 21 (Down syndrome), trisomy of chromosome 18 (Edwards syndrome), monosomy of chromosome X (Turner syndrome), trisomy of chromosome X, and supernumerary chromosome X in a male karyotype (Klinefelter syndrome). It should be noted that regular forms of aneuploidy for the remaining chromosomes are usually associated with embryonic lethality or pregnancy loss in the first trimester. Summaries of data on the parental and meiotic origin of errors leading to the most frequent chromosomal abnormalities in human conceptuses (trisomy of chromosomes 16, 21, and 22) have indicated that meiotic nondisjunction is more likely to occur during maternal MI (Hassold and Hunt, 2001; Nicolaidis and Petersen, 1998). However, some exceptions of this rule seem to exist. Trisomy of chromosome 18 is more likely to be caused by maternal MII errors (Bugge *et al.*, 1998), and trisomy of chromosomes 7 and 8 is more frequently associated with mitotic nondisjunction (James and Jacobs, 1996; Zaragoza *et al.*, 1998). Studies of the origin of monosomy X in females with Turner syndrome have provided evidence that paternal chromosome X or Y is lost in 70–80% of cases (Jacobs *et al.*, 1997). Up to 50% of cases of 47,XXY (Klinefelter syndrome) may be attributed to paternal meiotic errors (Thomas *et al.*, 2000). It is noteworthy that meiotic nondisjunction is the best-studied biological process associated with chromosomal abnormalities in mammals. It allows meiotic nondisjunction to be considered as an adequate model for theoretical considerations concerning the occurrence and phenotypic manifestations of numerical chromosome abnormalities. In addition, the reduction to disomy of a trisomic conception occurring during the second or a subsequent cell division may lead to the production of mosaic trisomy in the fetus or mosaicism confined to the placenta (Robinson *et al.*, 1995; Wolstenholme, 1996). Therefore, it is reasonable to assume that this mechanism underlies the formation of tissue-specific mosaicism in a newborn with the possibility of trisomy confined to neuronal tissue.

2. Mitotic Nondisjunction

Mitosis, the final step of the cell cycle, is the process of somatic cell division by which the reproduction of cells is achieved. This mode of nuclear division makes available the production of daughter nuclei that are genetically identical to one another and to the original parent cell nucleus. Mitotic nondisjunction is characterized by the failure of sister chromatid distribution to opposite cell poles during the stage of mitosis known as anaphase. Errors in mitosis are usually attributed to the formation of tetraploid conceptions or chromosomal mosaicism in somatic tissues.

Aneuploidy due to mitotic nondisjunction is considered a consistent finding in all types of neoplasia. Therefore, it is not surprising that insight into our knowledge of mitotic nondisjunction is essentially provided by studies of tumorigenesis. The growing number of human cancer investigations suggests that the mitotic errors leading to numerical chromosome abnormalities are caused by sporadic mutations producing genome instability that can manifest as aneuploidy or polyploidy (Lengauer *et al.*, 1998; Rajagopalan and Lengauer, 2004). However, despite the increased interest in this phenomenon, we are still far from uncovering all the processes leading to mitotic errors. The increased rate of mosaic numerical chromosome abnormalities associated with mitotic nondisjunction (about 50%) is observed in preimplantation embryos and spontaneous abortions (Bielanska *et al.*, 2002; Munne *et al.*, 1994; Vorsanova *et al.*, 2005). Studies of the contribution of mitotic nondisjunction to the genesis of recognizable human malformation syndromes related to aneuploidy have indicated that from 3 to 18% of trisomy in liveborns is associated with mitotic errors (Antonarakis *et al.*, 1993; Hassold and Hunt, 2001; Nicolaidis and Petersen, 1998). Mosaic trisomy of chromosomes 7 and 8, as mentioned previously, is an exception, being extremely rare compared to other aneuploidy conditions (Nielsen and Wohert, 1991; Wolstenholme, 1996). Among cases of trisomy mosaicism in malformed liveborns associated with mitotic nondisjunction there are generally those characterized by the prevalence of an abnormal cell population. This suggests that only mosaic forms of aneuploidy with a large proportion of affected cells produce phenotypic manifestations associated with recognizable chromosome abnormality syndromes. This is further supported by a number of reports, mostly concerning trisomy 21, indicating that phenotypically normal individuals with minor phenotypic signs of the corresponding syndrome may have a significant cell population (up to 30%) with an abnormal chromosome complement (Clarke *et al.*, 1961; de A Moreira *et al.*, 2000). It should be noted that cases of low-level chromosomal mosaicism are barely detectable through a clinical examination as well as commonly used cytogenetic approaches. Nevertheless, even a small proportion of neuronal cells with abnormal chromosome complements can give rise

to pathogenic processes and produce phenotypic diversity. Chromosomal mosaicism caused by mitotic errors may be confined to specific tissue (Youssoufian and Pyeritz, 2002). If this tissue is brain, the presence of brain cells with an abnormal chromosome complement may be etiologically related to a number of neurodevelopmental alterations and neurodegenerative processes.

B. Autosomal Aneuploidy

Autosomal aneuploidy refers to cytogenetic abnormalities characterized by the presence or absence of the whole or part of an autosome (all chromosomes except X and Y) in karyotype. These can manifest either as a numerical abnormality (trisomy or monosomy) or the presence of additional supernumerary marker chromosomes derived from an autosome. The frequency of autosomal aneuploidy detected by routine cytogenetic techniques in human newborns is considered to be about 0.2% (Jacobs *et al*., 1992). The incidence increases to 4% among stillbirths and 21–30% among spontaneous abortions (Hassold and Hunt, 2001; Pflueger, 2005; Vorsanova *et al*., 2005; Warburton *et al*., 1991). This indicates that a major part of autosomal aneuploidy conditions is associated with early pregnancy loss. Apart from trisomy of chromosomes 13, 18, and 21, as well as additional supernumerary marker chromosomes, all remaining autosomal aneuploidy conditions are supposed to occur in liveborns as mosaic forms only. Mental impairment is a characteristic feature of all recognizable autosomal aneuploidy syndromes. It is frequently accompanied by morphological changes in the brain of affected children, supporting the contention that the presence of neuronal cells with a gained or lost autosome may be related not only to impaired functioning but to conspicuous morphological abnormalities.

Trisomy of chromosome 21 accounts for approximately 95% of cases of Down syndrome, considered the leading cause of mental retardation in humans, occurring in about 1 in 800 live births (Roizen and Patterson, 2003). The remainder is attributed to mosaic trisomy 21 and Robertsonian translocations (whole-arm rearrangements between the acrocentric chromosomes 13–15, 21, and 22) involving chromosome 21 (Antonarakis *et al*., 1993; Giraud and Mattei, 1975). The series of studies targeted to reveal the changes in the brain of trisomy 21-affected fetuses and liveborns has indicated the incidence of biochemical alterations within the fetal Down syndrome brain followed by apparent morphological abnormalities in the brain of newborns and older infants (Engidawork and Lubeck, 2003). A relatively small proportion of neuronal cells with an additional chromosome 21 does not produce such a distinct change of brain function as is produced in Down syndrome. However, low-level mosaicism for trisomy of chromosome 21 (less

than 1%) confined to the brain tissue may affect brain functioning, as each neuron is connected to several thousand other neurons. Trisomy of chromosome 18 is known as Edwards syndrome and is considered to be the second most frequent autosomal aneuploidy condition, occurring in at least 1:7000 newborns. The third most frequent autosomal aneuploidy syndrome is trisomy of chromosome 13 (Patau syndrome), having a frequency between 1:5000 and 1:29,000 liveborns (Forrester and Merz, 1999; Goldstein and Nielsen, 1988). These two syndromes are characterized by an exceedingly severe phenotype associated with multiple congenital malformations including mental deficiency. Affected children rarely survive beyond the first year of life. The remaining autosomal aneuploidy conditions are extremely rare in newborns (not more than 100–150 reported cases). The overall incidence of supernumerary marker chromosomes in human newborns is estimated as 0.043% with a minute contribution of sex chromosomes. This type of aneuploidy is characterized by extreme phenotypic variability, from a normal to a severely abnormal phenotype. Mosaic forms of supernumerary marker chromosomes are well described, and up to 54% of cases of additional marker chromosomes in a case–control study demonstrate mosaicism (Liehr *et al.*, 2004a). The generalization of our knowledge concerning autosomal aneuploidy provides evidence that either gain or loss of an autosome may affect brain development and function. Therefore, autosomal aneuploidy mosaicism confined to neuronal tissue should not be excluded when considering genetic abnormalities associated with neuropsychiatric diseases.

C. Numerical Abnormalities of the Sex Chromosomes

The fertilization of the X chromosome-bearing egg by a spermatozoa bearing either chromosome X or Y (sex chromosomes) underlies the determination of genetic mammalian sex (XX, female; XY, male). Numerical abnormalities of the sex chromosomes are considered to have less severe phenotypic manifestations in humans as compared to autosomal aneuploidy. This probably explains why the overall incidence of aneuploidy involving sex chromosomes is as high as 1 in 500 newborns. Monosomy of chromosome X is considered to be the cause of approximately 50% of cases diagnosed as Turner syndrome (1:2000–1:5000 female liveborns). The remainder represent cases of structural chromosome X abnormalities (up to 35%) as well as 45,X/46,XX or 45,X/46,XY mosaicism (about 17%) (Elsheikh *et al.*, 2002). In addition, monosomy of chromosome X is the single most frequent aneuploidy detected in spontaneous abortions. It accounts for 1–2% of all the clinically recognized pregnancies with less than 1% of affected fetuses surviving to term (Hook and Warburton, 1983). Typical symptoms of Turner syndrome are short stature

and ovarian failure with evidence for cognitive deficits in women with monosomy X (Elsheikh *et al*., 2002). Trisomy of chromosome X is assumed to be the most frequent sex chromosome aneuploidy in females occurring in 1:1000 newborn girls (Nielsen and Wohert, 1991). This chromosome abnormality seems to be characterized by increased phenotypic variability without any distinct recognizable malformation pattern. A large proportion of females with an additional X chromosome shows behavioral and cognitive disabilities. It should be noted that cases with two or three additional X chromosomes in the female karyotype with more severe congenital malformations and mental deficiency have occasionally been described. A supernumerary chromosome X in males is characteristic of a clinical entity known as Klinefelter syndrome (47,XXY), with a frequency of 0.1–0.2% in the general male population. The 47,XXY condition is commonly related to hypogonadism and male infertility with behavioral and cognitive abnormalities. About 20% of Klinefelter syndrome cases demonstrate 48,XXYY, 48,XXXY, 49,XXXXY, and 49,XXXYY karyotypes and 46,XY/47,XXY mosaicism, which is probably underestimated. The former conditions are usually associated with more severe phenotypic manifestations of Klinefelter syndrome, and the latter condition (mosaicism) is known to cause milder forms (Lanfranco *et al*., 2004). The second most common sex chromosome aneuploidy, 47,XYY, affects approximately 1 in 800–1000 males (Nielsen and Wohert, 1991). These individuals are characterized by insignificant phenotypic abnormalities unable to be diagnosed by a clinical examination. The main features of 47,XYY males are increased height, aggressive behavior, parochialism, and mild mental deficiency.

It should be noted that most comprehensive studies of chromosomal abnormalities in schizophrenia have indicated the occurrence of sex chromosome aneuploidy in cohorts of patients analyzed (Basset *et al*., 2000). Although the association between numerical sex chromosome abnormalities and schizophrenia remains uncertain, the possibility of a contribution of mosaic and probably regular forms of sex chromosome aneuploidy to the etiology of major psychiatric disorders has not been excluded.

A number of studies targeted to reveal morphological brain changes in individuals with 45,X, 47,XXX, 47,XXY, and 47,XXY karyotypes provide evidence for morphological brain abnormalities in these patients manifested as an enlarged temporal lobe (45,X), reduced size of the amygdala, and reduction of brain volumes (47,XXX and 47,XXY) (Patwardhan *et al*., 2002; Rae *et al*., 2004; Warwick *et al*., 1999). In conclusion, the possible relevance of numerical sex chromosome abnormalities to human cognitive disabilities and behavioral alterations should be noted. Therefore, the occurrence of sex chromosome aneuploidy in the human brain is expected to produce cognitive and behavioral abnormalities.

D. Polyploidy

Polyploidy is a numerical chromosome abnormality characterized by the presence of additional haploid sets of chromosomes. A commonly detected polyploidy in spontaneous abortions and liveborns is triploidy (three haploid chromosome sets) and tetraploidy (four haploid chromosome sets). In contrast to tetraploidy, triploidy is caused by errors in fertilization. Earlier hypotheses suggested that a number of mammalian somatic tissues are populated by polyploid cells. Adult neurons of mammals were assumed to be postmitotic cells characterized by a polyploid chromosome complement. Testing this hypothesis through histochemical techniques yielded controversial results (Bregnard *et al.*, 1975; Swartz and Bhatnagar, 1981). This is not surprising, as the techniques applied are not straightforward for chromosome complement identification. Later, reports on polyploidy in humans have shown that these conditions are usually associated with fetal lethality and are rarely observed in newborns (Schinzel, 2001). Therefore, all adult neurons of the mammalian brain are unlikely to be characterized by polyploid chromosome complements.

Mosaic forms of polyploidy are commonly found in spontaneous abortions (Vorsanova *et al.*, 2005). Mosaic triploidy with the majority of cells being diploid is associated with a recognizable dysmorphology syndrome in newborns known as diploid/triploid mosaicism (van de Laar *et al.*, 2002). Although the cumulative incidence of polyploidy/diploidy mosaicism in human liveborns is unknown, the dramatic changes associated with the presence of additional haploid chromosome sets in a cell should lead to apparent abnormal cellular processes. If polyploidy mosaicism is confined to the brain, neurodegenerative processes in affected individuals may be expected.

III. Chromosomal Mosaicism in Humans

A. Aneuploidy in Human Germline Cells

Cytogenetic analysis of mammalian gametes is considered the initial step in surveying the incidence of chromosome abnormality throughout ontogenesis. A major source of aneuploidy in humans is germline chromosomal mutations. Molecular cytogenetic studies of human sperm have demonstrated that 0.1–0.2% of spermatozoa are affected by chromosome-specific aneuploidy. The incidence of spermatozoa with hypo- or hyperhaploid chromosome complements is over 2% in terms of the entire genome (Fig. 1). It is noteworthy that the rate of aneuploidy in the mammalian sperm is highly

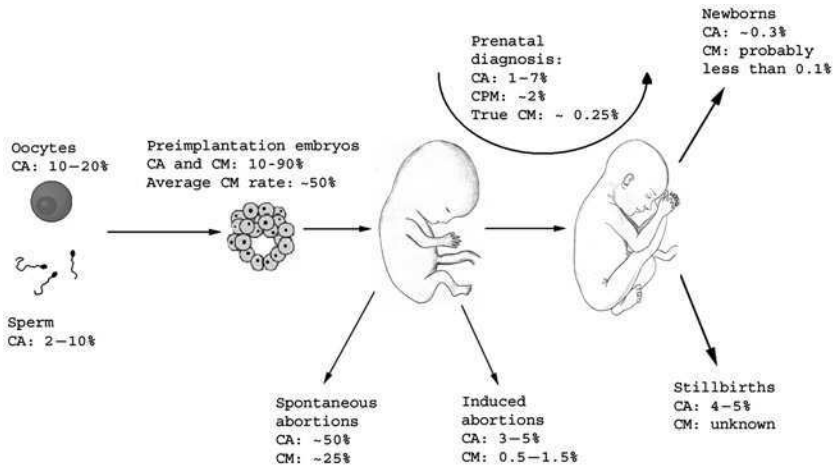

FIG. 1 Overview of the incidence of chromosomal abnormality and chromosomal mosaicism from gametes to newborns. CA, chromosomal abnormalities; CM, chromosomal mosaicism; CPM, confined placental mosaicism. For spontaneous abortions and prenatal diagnosis an average CM rate is shown; for newborns an average CA rate is given as well.

dependent on exogenous and endogenous effects (Griffin, 1996; Hassold and Hunt, 2001; Szczygiet and Kurpisz, 2001; Yurov *et al.*, 1996a). To date, aneuploidy has been evaluated in more than 10,000 human female gametes. The rate of chromosome abnormalities in human oocytes ranged from 10 to 20% with a strong correlation between maternal aging and an increased incidence of aneuploidy (Pellestor *et al.*, 2003; Rosenbusch, 2004). At first sight, neuronal cell-specific chromosomal mosaicism does not seem to be directly associated with germline chromosomal mutations; however, the latter is a basic process in the formation of chromosome abnormality, providing information on the occurrence and segregation of an abnormal chromosome complement throughout gestation followed by confinement to a somatic tissue.

B. Chromosomal Mosaicism Throughout Gestation

As the development of the human central nervous system (CNS) starts during the first few weeks of gestation, sporadic changes of chromosome complement within embryonic cell lines may lead to the formation of neuronal tissue-specific chromosomal mosaicism. Because of ethical and technical limitations, data on the occurrence of chromosomal mosaicism in human gestation are essentially obtained from studies of chromosome abnormalities

in preimplantation embryos, spontaneous abortions, and, much more rarely, induced abortions.

The introduction of *in vitro* fertilization (IVF) techniques allowed genetic analyses of early stage embryos. The main aim of cytogenetic analysis of preimplantation embryos is to provide a reliable diagnosis of chromosome abnormalities so as to attain successful prenatal development after IVF. Additionally, these studies are important in estimating the incidence of chromosomal mosaicism in early embryos. A current view of mosaicism in preimplantation embryos is that it largely depends on type of embryonic development (e.g., arrested, slow, or satisfactory), morphology, and developmental stage when subjected to analysis. The rate of chromosomal mosaicism in preimplantation embryos analyzed at different cleavage stages varies widely from 15 to 91% (Fig. 1). Mosaic chromosome abnormalities in preimplantation embryos include monosomy, trisomy, polyploidy, and haploidy (Bielanska *et al.*, 2002; Delhanty *et al.*, 1997; Munne and Cohen, 1998; Munne *et al.*, 1994). An additional consistent finding in mosaic preimplantation embryos is multiple chromosome imbalances referred to as "chaotic mosaicism," which are different in each cell analyzed (Delhanty *et al.*, 1997). As to detailed studies, diploid mosaic embryos are usually attributed to errors occurring at the second cell division or subsequent cell divisions. This indicates that mitotic nondisjunction is etiologically related to the formation of mosaicism in human embryos with correct pronuclear syngamy (Munne and Cohen, 1998; Munne *et al.*, 1994). Recent studies of mitotic errors associated with mosaicism in human preimplantation embryos have indicated that anaphase lagging is essential (Coonen *et al.*, 2004). It should be kept in mind that the presumed correspondence of IVF conditions to natural ones underlies all the theoretical issues of chromosomal mosaicism in preimplantation embryos. Notwithstanding, the latter seems to be a unique way to assess the rate of chromosomal mosaicism in humans at elemental stages of development. In the context of neuronal tissue-specific mosaicism, these analyses show evidence for error-prone patterns (in terms of number of chromosome abnormalities) of early human development before the onset of CNS formation.

To obtain indirect proof for neuronal cell-specific chromosomal mosaicism by surveying nondisjunctional events in gestation, causal mosaic chromosomal abnormalities in spontaneous abortions (the second human gestation period analyzed with respect to chromosomal mosaicism) should be assessed. Fetal deaths occurring between 6–8 and 20 weeks are generally defined as spontaneous abortions. Current estimates of cytogenetic abnormalities in human spontaneous abortions give 50% as an average detection rate. In most early studies the incidence of mosaicism in spontaneous abortions ranged from 2 to 5% among cytogenetically abnormal specimens (Hassold, 1982; Warburton *et al.*, 1978). A latter study indicated that the

frequency of chromosomal mosaicism in spontaneous abortions, representing both those confined to the placenta and generalized types, tended to be significantly higher than 10% (11 out of 54 specimens were mosaic) (Kalousek *et al.*, 1992). It is noteworthy that the majority of spontaneous abortions were ascertained through conventional cytogenetic analysis. However, these techniques appear to have low efficiency for detection of mosaicism because of culture procedure failure and moderate cell scoring potential. The former limitation suggested the use of molecular cytogenetic techniques as an initial screening approach for the identification of chromosome abnormalities in spontaneous abortions (Jobanputra *et al.*, 2002). The application of molecular cytogenetic techniques has shown that 48.3% of cytogenetically abnormal spontaneous abortions (89 abnormal out of 148 specimens) were characterized by chromosomal mosaicism with an abnormal clone content variation from 5 to 90% (Vorsanova *et al.*, 2005). Since the level of chromosomal mosaicism leading to pregnancy loss has not been established, it is difficult to delineate the rate of chromosomal mosaicism without causal effect in human pregnancy losses by comparing the incidence of chromosome abnormality in preimplantation embryos and spontaneous abortions. Further complications arise from the impossibility of assessing the level of mosaicism in all fetal tissues. Hence, the rate of chromosome abnormalities in unaborted pregnancies needs to be estimated. Studies of chromosomal abnormalities in induced abortions without medical indications are exceptionally rare. The rate of chromosome abnormalities in induced abortions was presumably estimated as less than 5% with the contribution of chromosomal mosaicism less than 1% (Kajii *et al.*, 1978; Tsuji and Nakano, 1978). An additional reliable report on the estimation of mosaic polyploidy in induced abortions (used as a control) gave a rate of less than 1.5% (Horiushi *et al.*, 1997). The assessment of current knowledge concerning mosaicism in spontaneous and induced abortions (Fig. 1) shows the presence of cell lines with abnormal chromosome complement, therefore supporting the assumption that chromosomal mosaicism may affect embryonic cells targeted to develop into neuronal tissue. However, it is noteworthy that detailed studies of chromosomal mosaicism in human spontaneous as well as induced abortions are few. Hopefully these types of studies will be the subject of future investigations.

Another possible source for estimating the rate of chromosomal mosaicism in human fetuses is prenatal diagnosis. This, however, is primarily designed to assess the opportunity of the fetus to be born without chromosomal aberrations. Therefore, cytogenetic studies in prenatal diagnosis are confined to the identification of chromosomal mosaicism in fetal tissues without any adverse effects in newborns because of chromosome abnormalities confined to the placenta. The recognized incidence of placental mosaicism revealed by chorionic villus sampling (mainly at 9–11 weeks of

gestation) is about 2% (Kalousek and Vekemans, 1996). Detailed prenatal investigations have demonstrated less than a 1% (38 of 4000 samples) incidence of chromosomal mosaicism in chorionic villi, with the majority of cases confined to placental mosaicism, apart from two cases that were neonate low-level mosaics (Stetten *et al.*, 2004). Cytogenetic studies of amniotic fluid are assumed to provide better information on the rate of true mosaicism in human fetuses. Large-scale population-based investigations (about 60,000 amniocenteses) have estimated the incidence of chromosomal mosaicism as 0–0.9% (Fig. 1) (Hsu and Perlis, 1984). This gives the impression that chromosomal mosaicism is rather uncommon in human conspectuses analyzed through cytogenetic prenatal diagnosis. However, the majority of studies of mosaicism in prenatal diagnosis were performed through conventional cytogenetic analysis and were limited in the number of cells (metaphase spreads) to score. Therefore, chromosomal mosaicism in fetal tissues may be significantly underestimated.

A pregnancy may end either as a stillbirth (in case of fetal death) or livebirth after week 20 of gestation. The rate of numerical chromosomal abnormalities in stillbirths is known to be about 5% (Fig. 1), being principally manifested as trisomy of chromosomes 13, 18, and 21 (Angell *et al.*, 1984). Unfortunately, there are few studies of chromosomal mosaicism in human stillbirths; hopefully, forthcoming investigations will fill this gap. The devastating effect of the majority of autosomal aneuploidy conditions probably explains the decrease by an order of magnitude in the incidence of chromosomal abnormalities in livebirths as compared to stillbirths. Current estimates determine the incidence of aneuploidy in newborns as approximately 0.3%, being essentially trisomy of chromosome 21 as well as 47,XXX, 47, XXY, and 47,XYY (Griffin, 1996; Hassold and Hunt, 2001). Although direct studies of chromosomal mosaicism in newborns have not been performed, clinical populations of newborns and children referred to pediatric institutions with congenital malformations and mental retardation show mosaic karyotypes in about 3.5% of cases (S. G. Vorsanova and Y. B. Yurov, unpublished observations).

The data on chromosomal mosaicism in human embryonic and fetal tissues as well as newborns (Fig. 1) support the suggestion that the rate of mosaicism is reduced throughout gestation (i.e., as the amount of cells increases through development the rate of mosaicism decreases). This is hardly explainable by selective pressure against chromosomally abnormal cells in cases of low-level mosaicism. In contrast, confinement of chromosome abnormalities to tissues not subjected to cytogenetic analysis appears to be a better explanation of the decrease. It should be noted that most studies of chromosomal mosaicism in human fetuses and newborns are performed by analyzing a limited number of tissues (chorionic villi, cells of amniotic

fluid, placenta, blood lymphocytes). Therefore, chromosomal mosaicism, if present in other tissues, remains to be estimated. Notwithstanding, despite a number of uncertainties in our knowledge, studies of the incidence of chromosomal mosaicism throughout gestation provide indirect evidence that chromosomal mosaicism might be confined to a tissue with the possibility of affecting neuronal tissue.

C. Mosaic Forms of Numerical Chromosome Abnormalities in Postnatal Life

1. Somatic Chromosomal Mosaicism and Human Disease

Numerical chromosomal imbalances are assumed to be among the common causes of somatic mosaicism in humans. Although somatic chromosomal mosaicism is frequently overlooked, a number of pathogenic conditions are caused by mosaic forms of numerical chromosome abnormalities. Unstable clonal variants are consistently observed in chromosome instability syndromes, suggesting the failure of cellular processes that prevent mitotic non-disjunction as a cause (Youssoufian and Pyeritz, 2002). Another established source for delineating the contribution of mosaicism to human malformation is non-disjunction studies of common aneuploidy conditions. The latter, however, appears to be a challenge, as a critical value of causative abnormal clone content is not evident. Nevertheless, the contribution of mosaicism to the etiology of Down and Edwards syndromes is estimated to be 3–5% and 11–14%, respectively (Hassold and Hunt, 2001; Nicolaidis and Petersen, 1998). Since mosaic forms of aneuploidy may result in a diminished clinical appearance, the occurrence of chromosomal mosaicism is often not obvious. Currently, mosaic forms of autosomal aneuploidy, which have been described for all human chromosomes, can be divided into three groups, based on the number of corresponding reports in the available literature. These groups are defined as rare (fewer than 5–10 cases reported), relatively rare (over 15 cases reported), and frequent (mosaic autosomal aneuploidy forms that are consistently observed when cytogenetic analyses are carried out). Based on the literature, we have attributed mosaic aneuploidy of chromosomes 1, 2, 3, 4, 5, 6, 7, 10, 11, 12, 17, and 19 to rare mosaic autosomal aneuploidy; mosaic aneuploidy of chromosomes 14, 15, 16, and 20 to relatively rare mosaic autosomal aneuploidy; and mosaic aneuploidy of chromosomes 8, 9, 13, 18, 21, and 22 to frequent mosaic autosomal aneuploidy.

It is noteworthy that the overwhelming majority of cases of autosomal mosaicism were detected through cytogenetic evaluation of blood lymphocytes and skin fibroblasts. Therefore, tissue specificity was assessed by

comparing the incidence of chromosomal mosaicism in either lymphocytes or fibroblasts. It was shown that mosaic forms confined to blood lymphocytes or skin fibroblasts occur in a significant proportion of cases of autosomal mosaicism (Schinzel, 2001). Turner syndrome (monosomy of chromosome X) also seems to be an example of chromosomal mosaicism. As over 98% of 45,X conceptuses are spontaneously aborted, it was reasonable to suspect that livebirths with monosomy of chromosome X possessed cell lines with a normal female or male karyotype (Youssoufian and Pyeritz, 2002). The impact of mosaicism in terms of numerical abnormalities of sex chromosomes (except monosomy X) on human disease is hardly assessable in terms on nonapparent phenotypic manifestations in cases of low-level mosaicism. Nevertheless, a large number of abnormal sex chromosome mosaics have been described to date (Schinzel, 2001).

Diploidy/triploidy mosaicism associated with dysmorphology is considered a well-known chromosomal abnormality syndrome with strong evidence for tissue-specific patterns. Up to 75% of patients show a normal blood karyotype in contrast to cultured fibroblasts (van de Laar *et al*., 2002). Few data on tetraploidy/diploidy mosaics have been reported. However, during conventional cytogenetic analysis tetraploid metaphases may occasionally be detected in cultured lymphocytes of either affected or unaffected individuals (Schinzel, 2001). General observations show strong evidence for tissue-specific chromosome abnormality mosaicisms in humans. The best example of this phenomenon is acquired from reports on individuals with no apparent phenotypic abnormalities characterized by the presence of tissue-restricted chromosomal mosaicism. However, because of the lack of direct evidence suggesting the occurrence of this type of mosaicism, these case reports are unfortunately rare (Schinzel, 2001).

Additional knowledge concerning the contribution of mosaic aneuploidy to human disease may be acquired from analysis of supernumerary marker chromosomes. Although it is still being evaluated (Liehr *et al*., 2004a), the example of Pallister–Killian syndrome (an additional chromosome 12p) provides strong evidence that tissue-specific chromosomal mosaicism plays a role in the pathogenesis of human diseases associated with supernumerary marker chromosomes (Priest *et al*., 1992). Another extraordinary example of numerical chromosomal mosaicism has been given by studies of X-linked dominant neuropsychiatric diseases (Rett syndrome) in males. As these diseases have an increased intrauterine mortality rate for hemizygous males, the only possibility of Rett syndrome in males is either the presence of an additional X chromosome in the karyotype or somatic mosaicism for mutations of the corresponding gene (*MECP2*). The former was first shown to occur in mosaic form (47,XXY/46,XY) when a male with the clinical features of Rett syndrome was cytogenetically analyzed (Vorsanova *et al*., 1996).

Further investigation of Rett syndrome in males has indicated that the 47,XXY/46,XY mosaicism may be tissue–specific, suggesting that cytogenetic analysis of different tissues is the only way to thoroughly explain the occurrence of Rett syndrome in boys (Vorsanova *et al*., 2001). In conclusion, it should be noted that although there is still no clear understanding of the contribution of tissue-specific mosaicism to human disease, the investigation of this phenomenon has provided a firm base with which to launch studies targeted at estimating neuronal tissue-specific chromosomal mosaicism in humans.

2. Aneuploidy, Tumorigenesis, and Aging

Chromosomal mosaicism acquired during gestation is not the unique source of sporadic changes in chromosome complement that is observed in mammals. The two best studied biological processes associated with numerical chromosome imbalances are tumorigenesis and aging. Tumorigenesis is assumed to be related to aneuploidy, theorized to be the primary cause of genomic instability in neoplastic and preneoplastic cells (Duesberg *et al*., 2004; Lengauer *et al*., 1998). According to epidemiologic surveys, brain tumors are the second most common malignancy in children (Lacayo and Farmer, 1991) and are very frequent in adults, with an annual diagnosis rate ranging between 7.3 and 19.1 per 100,000 persons in the United States (DeAngelis, 2001). Brain tumors demonstrate aneuploid karyotypes in about 50% of cases, which is probably a significant underestimation (Binger *et al*., 1997; Yamada *et al*., 1994). The high frequency of brain tumors and the supposition that aneuploidy is a primary cause of neoplasia suggest that brain malignancy in children may be the result of the presence of aneuploidy in the newborn brain and adult brain tumors may be associated with clonal evolution of aneuploid cells in the brain during postnatal life (Fig. 2). However, sporadic aneuploidy in the postnatal brain may be related to brain tumors.

The variation of chromosome complement observed at the cytogenetic level as a feature of human aging has been well documented (Guttenbach *et al*., 1995; Jacobs and Brown, 1961; Nowinski *et al*., 1990). Later, this phenomenon was found to be likely explained by mitotic misregulation (Ly *et al*., 2000). Although tissue-specific chromosome complement variation in human aging is poorly understood, current data provide indirect evidence for acquired aneuploidy in numerous tissues. In addition, the CNS possesses parts in which long-term production of neurons occurs (Murray and Calof, 1999) and, therefore, low-level chromosomal mosaicism in the human brain may also contribute to aging processes either through mitotic errors or the onset of expression of age-related genes in aneuploid mature neurons (Fig. 2).

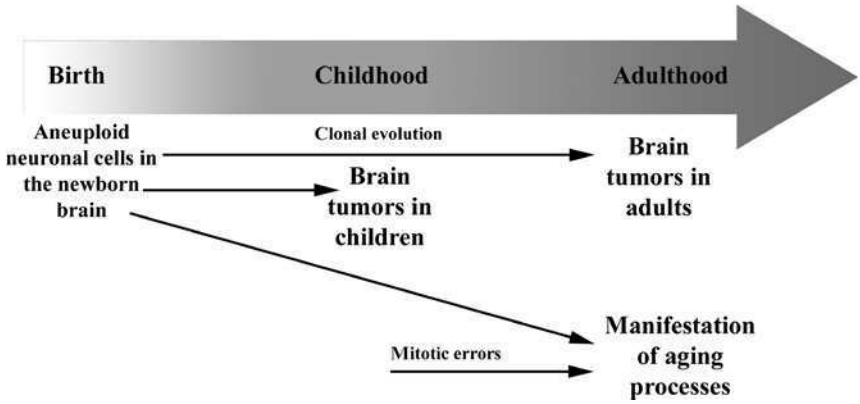

FIG. 2 Timeline describing the suggested contribution of brain-specific aneuploidy to tumorigenesis and aging processes. Aneuploid neuronal cells in the newborn brain have the potential to cause brain tumors in children. During early postnatal life the development of neuronal tissue is observed; therefore, the clonal evolution of aneuploid neuronal cells during childhood may result in brain tumors in adulthood. The persistence of aneuploid neuronal cells from birth until adulthood may be the cause of the brain aging process, probably through the onset of aging process-related gene expression. Another suggested brain aging mechanism is almost the same; the only exception is that aneuploid neuronal cells could be formed due to mitotic errors in the postnatal brain mainly during childhood.

IV. Somatic Chromosomal Mosaicism in Mammalian Neuronal Cells

A. Developing Mammalian Brain

The data described above provide indirect evidence for tissue-specific chromosomal mosaicism confined to the brain and become a fundamental base for studies targeted at proving experimentally chromosomal variations in neuronal cells. Since chromosome abnormalities are most commonly formed during gestation, it is of prime interest to assess the rate of chromosome imbalances in the developing mammalian brain. The period of neurogenesis in mice was found to be rather prone to error in terms of aneuploidy confined to neuroblasts. Lagging chromosomes were observed in proliferating cerebral cortical neuroblasts of mice, suggesting an increased rate of aneuploidy. The application of spectral karyotyping (SKY) for assessment of chromosomal imbalances has indicated that about one-third (33%) of metaphase spreads obtained from mice neuroblasts are aneuploid. Among them, 98% were associated with loss of either one or several chromosomes (hypoploidy). The remainder (about 2%) were found to have gained chromosomes

(hyperploidy). Between 1.6 and 8.4% of individual chromosomes were missing, with more frequent involvement of chromosomes 9 and 17 as well as the sex chromosomes. Hyperploidy involved sex chromosomes at a higher rate than autosomes. The results were then reconfirmed by interphase fluorescence *in situ* hybridization (FISH) using whole painting probes for sex chromosomes. Numerical chromosome abnormalities were confined to neuronal embryonic cells because the parents of embryos have not demonstrated an increased rate of aneuploidy in blood lymphocytes and the data obtained by different techniques were compatible (Rehen *et al.*, 2001). Additionally, this is unlikely to be explained by a sporadic chromosome mutation affecting all embryonic tissues, as the average rate of mitotic chromosome loss in mice is approximately 3% (Burns *et al.*, 1999). Therefore, it should be recognized that mice neuroblasts are characterized by an increased level of aneuploidy. The embryonic neuronal cells found to be aneuploid may be from a region lining the lateral ventricles of the cerebral hemispheres (ventricular zone). The region contains neuroblasts, from which postmitotic cortical neurons arise (Bayer and Altman, 1991). Thus, these findings raise questions concerning the fate of aneuploid neural embryonic cells in the context of brain development and functioning after birth.

Murine models have proven to be valuable in understanding the molecular processes underlying the etiology of brain diseases in humans (Watase and Zoghbi, 2003), but seem to be less convenient models for considerations concerning human chromosome abnormalities inasmuch as the incidence of meiotic errors differs between humans and mice in order of magnitude (Adler *et al.*, 1996; Glenister *et al.*, 1987; Hassold and Hunt, 2001). Consequently, the rate of chromosomal imbalance due to mitotic errors might be different as well. The human brain is indisputably more complex in terms of both structure and functions performed. Thus, the high number of aneuploid neuroblasts in the developing brain (as it is in mice) may result in nervous system development collapse. However, the developing human brain has demonstrated aneuploid karyotypes in 0.6–3.0% of cells studied. The study has been carried out through the application of multicolor interphase FISH using DNA probes for chromosomes 1, 13, 18, 21, X, and Y (Fig. 3A). Aneuploidy of chromosome X was found to be the most frequent. Interestingly, aneuploidy of chromosome 1, rarely observed in human conceptuses, was as frequent as aneuploidy of both chromosomes 13 and 21. Chromosome loss was only two-fold more frequent than chromosome gain in the human developing brain, suggesting another mechanism for neuronal tissue-specific aneuploidy formation as in the case of mice (Yurov *et al.*, 2005). The cumulative number of fetal neuronal cells with aneuploidy of chromosomes 1, 13, 18, 21, X, or Y in the developing human brain may be estimated at approximately 7%, which gives about 28% of aneuploid neuroblasts in terms of all 23 chromosome pairs. Although these considerations require

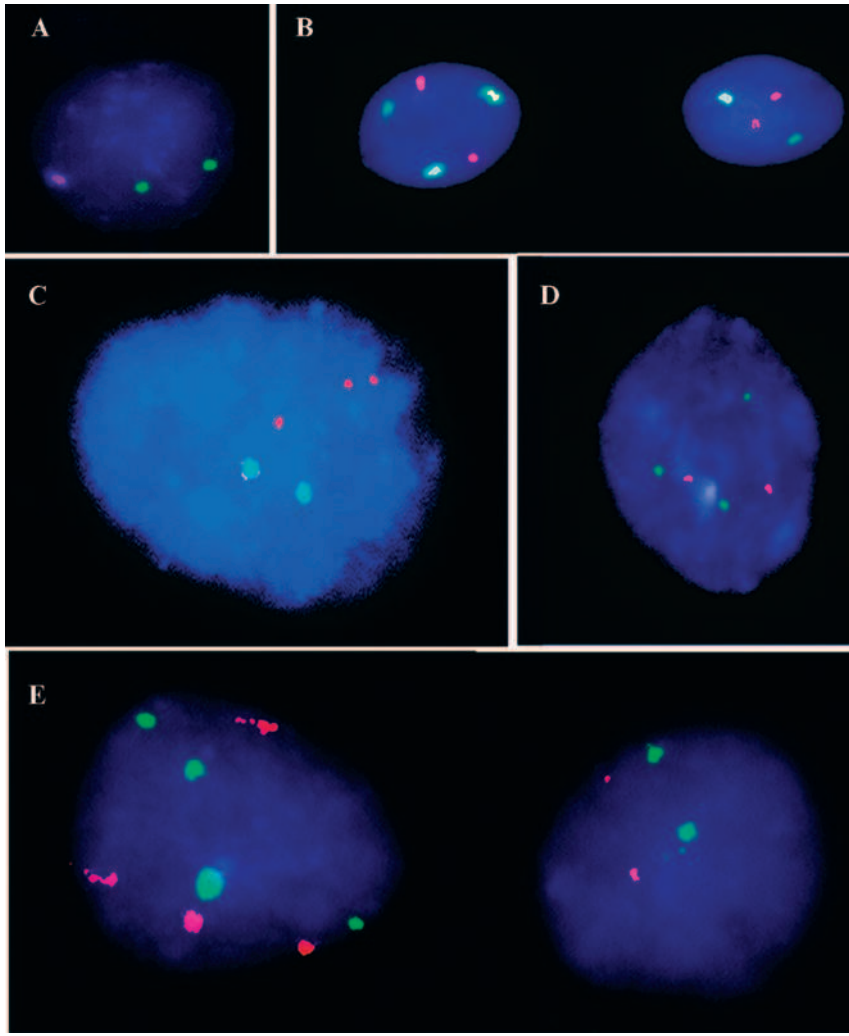

FIG. 3 Two-probe FISH assay on interphase nuclei of the human brain. (A) Nucleus of the normal developing brain (gestation age 10 weeks) after hybridization with a FluorX-labeled centromeric DNA probe for chromosome X (two green signals) and a Cy3-labeled centromeric DNA probe for chromosome Y (one red signal). Signal patterns show additional chromosome X in the nucleus. (B) Nuclei of organotypic culture of developing brain cells after hybridization with a biotin-labeled pericentromeric DNA probe for chromosome 1 (green signals) and a Cy3-labeled centromeric DNA probe for chromosome 18 (red signals). Signal patterns show additional chromosome 1 in the left nucleus in contrast to the normal right nucleus. (C) Nucleus of the normal adult brain (cerebral cortex) after hybridization with a FluorX-labeled centromeric DNA probe for chromosome X (green signals) and a Cy3-labeled centromeric DNA probe for chromosome 18 (red signals). Signal patterns show additional chromosome 18 in the nucleus. (D) Nucleus of the schizophrenia-affected adult brain (cerebral cortex) after hybridization with a FluorX-labeled

experimental proof, the rate of chromosomal mosaicism in humans seems to be approaching the rate in mice.

These studies indicate that mitotic errors are the main cause of neuronal tissue-specific chromosomal mosaicism in the developing mammalian brain. Since the mechanism of aneuploid cell generation is far from being established, chromosome segregation defects are the only appropriate consideration concerning formation of aneuploidy in neural cells. A common mechanism of postzygotic formation of aneuploidy is anaphase lagging, which is defined as the loss of chromosomes probably caused by defects in the kinetochore apparatus (Cleveland *et al.*, 2003). As a result, monosomy in aneuploid cells is observed. This type of error is a feature of human neoplastic and preimplantation embryo cells (Coonen *et al.*, 2004; Kirsch-Volders *et al.*, 2002; Lengauer *et al.*, 1998). Both monosomy and trisomy are supposed to form due to supernumerary centrosomes that produce either bipolar or multipolar divisions of a cell. The former is likely to be the cause of mosaicism with a larger monosomic clone content, in contrast to the latter, which is the cause of nearly equal monosomy/trisomy mosaicism (Brinkley, 2001). Mosaic trisomy is assumed to form through mitotic sister chromatid nondisjunction of an individual chromosome pair; similarly, tetraploidy is caused by nondisjunction of a diploid chromosome set. Direct investigation of defects in chromosome segregation by real-time imaging of neural progenitor cells has demonstrated 4.6% of mitoses harbor lagging chromosomes and 3.2% of nuclei undergo multipolar cell divisions (Yang *et al.*, 2003). This seems to be in accordance with the rate of aneuploidy in the murine developing brain (Rehen *et al.*, 2001). However, the percentage of aneuploid neuroblasts is higher than visualized defected mitoses, suggesting that other mechanisms are involved in already differentiated aneuploid cells of the murine embryonic brain. As to the human developing brain, as yet there are no direct studies of mitosis defects. Nevertheless, the patterns of chromosome imbalances observed in the developing human brain provide evidence that errors in mitotic divisions differ between humans and mice. The presence of a relatively small but significant proportion of trisomic neuroblasts in the human developing brain suggests that mitotic nondisjunction contributes to the formation of imbalances in the human fetal brain (Yurov *et al.*, 2005).

---

centromeric DNA probe for chromosome X (green signals) and a Cy3-labeled centromeric DNA probe for chromosome 18 (red signals). Signal patterns show additional chromosome X in the nucleus. (E) Nuclei of the schizophrenia-affected adult brain (cerebral cortex). Left nucleus: after hybridization with a biotin-labeled pericentromeric DNA probe for chromosome 1 (green signals) and a Cy3-labeled pericentromeric DNA probe for chromosome 9 (red signals). Right nucleus: after hybridization with a FluorX-labeled centromeric DNA probe for chromosome X (green signals) and a Cy3-labeled centromeric DNA probe for chromosome Y (red signals). Signal patterns show tetraploidy in both nuclei.

The latter correlates with molecular cytogenetic findings in spontaneous abortions of the same gestational age (Vorsanova *et al.*, 2005).

Another method used to uncover mechanisms of aneuploidy formation is the identification of chromosome imbalances in cultured developing brain cells. There are well-documented neuroblastoid mitogens that promote the growth of less differentiated cells (Ghosh and Greenberg, 1995). Culturing murine aneuploid neuroblasts with the mitogen demonstrated induced reduction of the rate of aneuploidy to 14%. Among lost cells were cells with multiple gained or lost chromosomes; subsequently, flow cytometric analysis showed a reduction in average DNA content by 2%, presumably achieved through the loss of aneuploid neuroblasts (Rehen *et al.*, 2001). Organotypic culture of fetal brain cells is performed for neuroscience research. The cultured cells are characterized by a high survival rate, well-preserved biochemical features, and a conserved shape. These types of neuroblast cultures allow analysis of the proliferation, differentiation, and migration of neural precursor cells (Gage, 2000; Suzuki *et al.*, 2004). Direct interphase FISH examination of organotypic cultured fetal brain cells (Fig. 3B) demonstrated an over 200% increase in aneuploidy rate (1.3–7%) as compared to uncultured cells (0.6–3%). The type of aneuploidy (contribution of monosomy or trisomy) has not significantly changed. Although cultivation-induced chromosome imbalances could not be excluded, these findings suggest that mitotic nondisjunction is an essential mechanism of aneuploidy formation in human fetal brain cells (Yurov *et al.*, 2003, 2005). Additionally, these results provide evidence for the persistence of aneuploid neural cells throughout human gestation following by differentiation into neurons after delivery. In conclusion, current data on chromosome complement in mammalian developing brain cells indicate that mitotic divisions of neuroblasts are prone to error with about one-third of the cells being aneuploid. Because such an increased rate of aneuploidy may diminish during gestation, chromosome complement in postnatal brain cells should be investigated.

B. Chromosomal Variations in the Normal Adult Brain

The mature brain of unaffected individuals was assumed to possess an identical number of chromosomes in all the cells. The mammalian adult brain is essentially composed of postmitotic neuronal cells that do not pass cell division and do not replicate chromosomal DNA. It employed interphase molecular cytogenetic studies as a unique way to prove or refute these initially unproven views. Pioneer interphase cytogenetic analyses of human CNS tissues had shown different patterns of chromosome nuclear organization in functionally distinct cell types, but no chromosome imbalances in the

human brain were noted (Manuelidis, 1984; Manuelidis and Borden, 1988). Additionally, large chromatin movements in neuronal cells were noted during differentiation (Manuelidis, 1990). Later investigations by means of *in situ* hybridization with DNA probes for satellite DNA sequences (pericentromeric and centromeric heterochromatin of chromosomes 1 and 17, respectively) provide evidence for the presence of interphase nuclei in the human brain containing either one or more than two hybridization signals. The former was attributed to a phenomenon known as somatic chromosome pairing, as the shape of these single signals was unusual (''not circular but more oval or figure-eight shaped'') compared to those in nuclei with two hybridization signals (considered diploid when *in situ* hybridization studies were performed). The presence of more than two signals was observed in a small proportion of nuclei and, therefore, was considered artifacts due to unequal hybridization (Arnoldus *et al.*, 1989, 1991). These data were then reconfirmed for chromosome 1 by a multicolor FISH study as well as a newly introduced quantitative FISH approach. Additionally, chromosomes 9 and 16 were also found to pair somatically by pericentromeric heterochromatic regions leading to difficulty in scoring the low content of monosomic cells in the human brain (Iourov *et al.*, 2005; Yurov *et al.*, 2001). It should be noted that somatic pairing of chromosomes in interphase refers to chromosome behavior in postmitotic cells but not chromosome abnormality. Somatic chromosome pairing is probably the least explored phenomenon of mammalian chromosome nuclear organization (Cook, 1997).

The first direct molecular cytogenetic studies targeted to reveal chromosome complement variations in the human brain were performed on postmortem brain samples of Alzheimer's disease (AD) and schizophrenia-affected patients. In these studies normal postmortem brain samples were used as a control and no significant proportions of aneuploid cells were detected (Yang *et al.*, 2001; Yurov *et al.*, 2001). This is not surprising, because even a moderate cell scoring—100 nuclei per sample per DNA probe as applied by Yang and associates (2001) and 200 nuclei per sample per DNA probe as applied by Yurov and associates (2001)—was able to offer evidence for numerical chromosome imbalances in postmortem brain cells of affected individuals (described later), suggesting that a significantly lower proportion of cells in the normal human brain was aneuploid. Further interphase FISH studies of the normal human brain yielded conflicting results. Thus, multicolor FISH analysis using centromeric DNA probes for chromosomes 1, 13/21, 18, X, and Y (Fig. 3C) demonstrated a total aneuploidy incidence of about 2.3% (Yurov *et al.*, 2005). However, a double-color FISH experiment using whole paint or ''FISH paint probe against of the whole q-arm of chromosome 21'' and site-specific DNA probes for chromosome 21 has shown an approximate rate of chromosome 21 aneuploidy in the human brain as high as 4% (Rehen *et al.*, 2005). Although the resolution of

this contradiction is certainly an aim of forthcoming investigations, some information about this discrepancy may already exist.

First, the application of whole chromosome paint probes on interphase nuclei shows nuclear organization specificity rather than chromosome complement, as the signals detected may present as multiple large spots in euploid nuclei, first depicted on human diploid fibroblasts by Zink and associates (1998). Therefore, whole paint probes, even with the application of site-specific probes taking into account the lack of any reproducible data on chromosome territories in the human brain, are not the ultimate probes for detection of mosaic aneuploidy. Second, the application of an alphoid DNA probe for both chromosomes 13 and 21 usually overestimates the level of aneuploidy for these chromosomes due to the possibility of hybridization with centromeres of other acrocentric chromosomes (Acar *et al.*, 2002). Hence, aneuploidy of both chromosomes 13 and 21 in the normal human brain affects probably less than 0.3% of cells as initially detected by FISH with an alphoid DNA probe (Yurov *et al.*, 2005).

Notwithstanding, the efficiency of diversified FISH studies with centromeric DNA probes for chromosomes 1, 18, 13/21, X, and Y has improved in the last 20 years because different human tissues studies avoid FISH artifact scoring (Iourov *et al.*, 2005; Soloviev *et al.*, 1995, 1998; Vorsanova *et al.*, 1986, 2001, 2005; Yurov *et al.*, 1996a,b). Therefore, experimental drawbacks are not likely to affect the results of multicolor FISH experiments with centromeric DNA probes in human brain studies. So, concluding that chromosome complement variations are probably different for each homologous chromosome pair present in the normal human brain should not be considered speculative.

Adult murine brain cells were shown to possess a little over 1% of cortical neurons with sex chromosome aneuploidy by an interphase FISH study. These data suggest the involvement of other chromosomes in aneuploidy of the adult murine brain probably at a higher rate. However, this rate of aneuploidy did not appear to differ significantly from the incidence of aneuploidy in murine blood lymphocytes (Rehen *et al.*, 2001). Since interphase molecular cytogenetic analysis is the only appropriate way to assess chromosome complement in postmitotic cells, it is difficult to come to any definite conclusion concerning chromosome variations in the adult murine brain. Another proposed analysis of chromosome complement in postnatal murine brain cells consisted of the application of SKY on metaphase spreads derived from cultured neural cells of the murine brain subventricular zone. This is the neurogenic area that remains active through postnatal life, and cells derived from this area are available for cultivation. The study has demonstrated that one-third (33%) of metaphase spreads have a deficient chromosome complement with a considerable prevalence of chromosome losses among aneuploid spreads. An interphase FISH experiment showed that up to 9% of

subventricular zone cells were characterized by either loss or gain of sex chromosomes. Importantly, control samples of liver cells and lymphocytes were found to be aneuploid in 10.4% and 3.4%, respectively, being statistically lower than in brain cells (Kaushal *et al.*, 2003). The development of animal cloning techniques has introduced nuclear transfer as an approach to the analysis of embryo neural cells, which retain all cellular peculiarities throughout the procedure (Yamazaki *et al.*, 2001). The technique was than applied for indirect chromatin and chromosome change assessment of reconstructed oocytes cloned from adult murine neuronal cells. The result of this study was rather sensational, as over 50% of metaphase spreads showed various aberrant chromosome constitutions manifested as nonspecific chromosome loss and undercondensed chromatin (Osada *et al.*, 2002). The latter, however, is not very relevant to the definition of chromosome imbalances in the adult mammalian brain, due to lack of apprehension of the causes and consequences of undercondensed chromatin observed in metaphase. Nevertheless, it provides evidence that a number of adult murine neural cells are genomically altered cells. Recent studies targeted to reveal the functional value of aneuploid murine neuronal cells have demonstrated that low-level mosaicism is present in all assayed areas of the brain. The analysis of aneuploid brain cell integration into brain circuitry showed these cells have distant axonal connections as well as the potential for functional activity (Kingsbury *et al.*, 2005). These data allow us to speculate that low-level chromosomal mosaicism in the normal mammalian brain is a feature of normal CNS organization and the larger increase in aneuploidy rate may lead to apparent changes in CNS organization.

Are there aneuploid neurons in the normal adult mammalian brain? Surely there are some. Does the rate of numerical chromosome abnormalities differ between the brain and other somatic tissues? This remains to be estimated. Notwithstanding, the complexity of the organization of the mammalian CNS suggests that even a low proportion of aneuploid neuronal cells contributes significantly to development, function, and neuronal diversity as compared to other somatic tissues. Thus, a difference in the content of genetic information in neuronal tissue represents a new mechanism for cellular diversity that is probably implicated in phenotypic diversity and neuropsychiatric disorders (Rehen *et al.*, 2002; Yurov *et al.*, 2001).

C. Somatic Chromosomal Mosaicism in the Mammalian Adult Brain and Disease

Estimates of chromosome imbalances in the normal human brain are of fundamental biological interest, but the application of biomedicine necessitates determining whether the increased aneuploidy or polyploidy rate in the

brain is relevant to human brain diseases. This forms the basis for the diagnosis, treatment, and care of affected individuals. Chromosome abnormalities identify the alterations in DNA sequence that cause these disorders. Neuropsychiatric diseases including cognition and behavioral deficits as well as mental retardation are consistently associated with chromosome aberrations either as case reports or as reproducible findings in case–control studies. Among the best explored in this context are schizophrenia and autism (Basset *et al.*, 2000; Castermans *et al.*, 2004). Alzheimer's disease (AD) is also associated with low-level trisomy 21 mosaicism in blood lymphocytes due to mitotic chromosome 21 malsegregation (Geller and Potter, 1999); it is probably the result of defective presenilin protein function frequently mutated in familial cases (Li *et al.*, 1997). It indicates that brain-specific chromosomal mosaicism might contribute to the etiology of these complex psychiatric disorders. The first attempt to analyze human chromosomes in brain tissue of affected individuals was based on analysis of chromatin arrangement. This study identified the specific movement of chromosome X within neuronal cell populations in epilepsy (Borden and Manuelidis, 1988). In the following decade there were no targeted studies of chromosomes in the diseased human brain, probably because molecular cytogenetic techniques were still not perfected. In 2001, AD and schizophrenia were the subject of the first two postmortem molecular cytogenetic studies of chromosomal mosaicism in the diseased human brain (Yang *et al.*, 2001; Yurov *et al.*, 2001).

The cause of AD, which is characterized by loss of neurons during adult life, remains uncertain (Mattson, 2000). Abnormal mitoses or chromosome complement might explain the death of neuronal cells that characterizes this devastating neurodegenerative disorder. This hypothesis was tested by combining molecular cytogenetic and histochemical techniques to assess the processes underlying neuronal cell death. A significant fraction of the hippocampal pyramidal and basal forebrain neurons was shown to possess cells with tetraploid chromosome complement (about 4%). Unaffected regions of postmortem brain samples of AD patients and nondemented age-matched controls have not demonstrated polyploid chromosome complement. The degenerative course in AD and the peculiarities of FISH experiments (the ability to identify the state of the nucleus when subjected to analysis) suggest underestimation of chromosomal mosaicism in AD neuronal cells. An additional intriguing finding was that a fraction of euploid as well as tetraploid nuclei demonstrated fully or partially replicated signals, leading to the conclusion that DNA replication preceded neuronal cell death in AD–affected individuals (Yang *et al.*, 2001). The data obtained represent new insight into the pathogenesis of AD. Polyploidy or the postreplicated state of a neuron is considered a signal for neuronal cell death. However, it is still unclear whether polyploidy persists throughout postnatal life up to the onset of

expression of genes implicated in aging processes (probably overexpressed in the AD brain) or if mutated genes in AD cause DNA replication lacking the following mitotic division.

The genetics of schizophrenia is probably the most enigmatic field of biological psychiatry. Numerous studies reported so far have indicated chromosome imbalances etiologically related to some phenotypic features of schizophrenia (Basset *et al*., 2000), supporting the contribution of brain-specific aneuploidy to the pathogenesis of this complex psychiatric disease. The initial studies proposed using multicolor FISH (three- and five-color FISH) with centromeric and site-specific DNA probes for chromosomes 1, 7, 8, 13, 16, 18, 21, 22, X, and Y. Six postmortem cerebral cortex brain samples (five female and one male) of schizophrenia-affected individuals as well as two age-matched control samples were subjected to molecular cytogenetic analysis. Although moderate cell scoring was applied (200 interphase nuclei per sample/DNA probe), the thoroughness of nucleus choice (i.e., nuclei with either two or three hybridization signals were scored only; only nuclei that were intact, undamaged, and free of cytoplasm were analyzed) was effective enough to provide evidence that two postmortem brain samples from schizophrenia patients possess trisomic cell populations. Thus, two out of five female postmortem brain samples have simultaneously demonstrated trisomy of chromosomes 18 and X. The abnormal clone content detected in two samples was 2.5% of trisomy 18 and 4% of trisomy X as well as 0.5% of trisomy 18 and 3% of trisomy X. Additionally, somatic pairing of homologous heterochromatic regions of chromosomes 1 and 16 was observed in a large fraction of cerebral cortex cells (Yurov *et al*., 2001). Examples of molecular cytogenetic studies of the schizophrenia-affected brain are depicted in Fig. 3D and E. These findings are rather impressive, as trisomy of chromosome 18 (Edwards' syndrome) is associated with conspicuous alterations in brain functioning and trisomy of chromosome X is a known aneuploidy condition associated with behavioral abnormalities (detailed above). Interestingly, structural abnormalities of chromosome 18 have been identified in at least six individuals with schizophrenia (Basset *et al*., 2000), and trisomy of chromosome X has been consistently described since early cytological and further cytogenetic studies of female schizophrenia individuals have been performed (Kaplan and Cotton, 1968; Kunugi *et al*., 1999). Molecular cytogenetic studies of the schizophrenic brain led to a new approach for identifying genetic causes of complex neuropsychiatric disorders. Even 1% represents about 10 billion out of a trillion neurons in the brain; additionally, one neuron forms over a thousand connections with other neurons (Lodish *et al*., 2000). Therefore, the incidence of aneuploidy in a fraction of neuronal cells may cause the functions of the brain to be seriously affected. Although these calculations may appear to be speculative, the deleterious effect of aneuploid neurons that populate the adult human brain should not be ignored.

A way to estimate induced chromosome imbalances in adult mammalian somatic tissues is to investigate murine models of chromosome instability syndromes (homozygous ataxia telangiectasia mutated gene $Atm^{-/-}$ knockout mice) and tumor suppressor or end-joining DNA repair knockout mice. The latter was achieved through breeding transformation-related protein 53 (encoding tumor suppressor protein 53) mutant mice ($Trp53^{-/-}$) as well as DNA repair-deficient $Xrcc5^{-/-}$ mutant mice. Assessment of aneuploidy of the murine knockout brain was performed by SKY on cerebral cortical hemispheres of murine embryo and interphase FISH using sex chromosome whole painting probes (McConnell *et al.*, 2004). The main purpose of the study was to test the previous hypothesis that the rate of karyotypically abnormal neural cells is dependent on the mutations affecting maintenance of chromosome stability (Allen *et al.*, 2001). Molecular cytogenetic studies of the mutants have demonstrated a 38% increase in the prevalence of sex chromosome aneuploidy in the adult $Atm^{-/-}$ cerebral cortex in contrast to the exceptional 78% and 43% decreases in aneuploidy in the $Trp53^{-/-}$ and $Xrcc5^{-/-}$ murine cerebral cortex, respectively (McConnell *et al.*, 2004). This provides evidence that the apoptotic clearance of neuronal cells previously observed in murine cortical development (Blaschke *et al.*, 1996) might be influenced by inherited mutations in genes implicated in the maintenance of chromosome stability. In addition, it also supports the hypothesis concerning the alteration of abnormal cell clearance observed throughout development followed by manifestations of age-related neurological disorders (McConnell *et al.*, 2004). Consequently, it suggests that aneuploid cells in the normal fetal brain should be cleared because a smaller rate of aneuploidy is detected in the adult normal brain. In contrast, the diseased brain, characterized by failure of clearance, possesses a more significant proportion of neuronal cells with an abnormal chromosome complement.

D. Summary of Data on Chromosomal Variations in Mammalian Neuronal Cells

To hypothesize and speculate further, we present a schematic summary of chromosomal variations in the mammalian brain (Fig. 4). Theoretically, two main types of studies of the molecular cytogenetics of the brain (normal brain and diseased brain) might be subdivided with respect to biomedical relevance. Thus, the observation that the rate of aneuploidy in the developing mammalian brain significantly decreases among adults (Fig. 4) (McConnell *et al.*, 2004; Rehen *et al.*, 2001; Yurov *et al.*, 2005) appears to be the basis for further developmental biological investigations with special regard to apoptotic pathways in fetal and adult neuronal cells. A second important finding was that AD and schizophrenia are characterized by the presence of significant

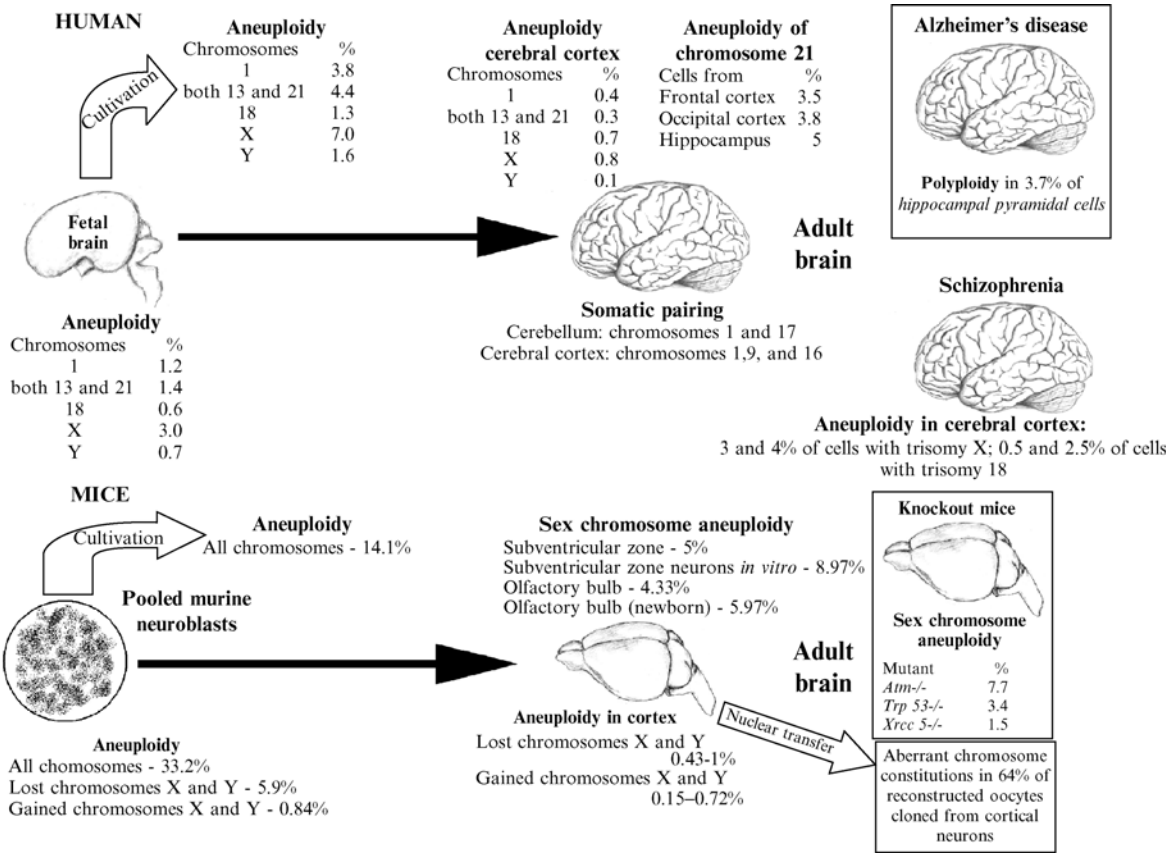

FIG. 4 Data on chromosomal variation in cells of the mammalian brain.

polyploid and aneuploid cell fractions in the affected brain (Yang *et al.*, 2001; Yurov *et al.*, 2001), opening new prospects for medical and psychiatric genetics. Third, the proven presence of aneuploidy in the mammalian brain, the alteration of gene expression by chromosome gain and loss in the brain, and aneuploid cell integration into the brain circuitry (Kaushal *et al.*, 2003; Kingsbury *et al.*, 2005; Rehen *et al.*, 2001; Yurov *et al.*, 2001, 2005) indicate that further epigenetic studies are needed to identify the role that brain-specific chromosomal mosaicism plays. Finally, the unexpectedly high level of fetal neuronal cells with an abnormal chromosome complement (Rehen *et al.*, 2001; Yurov *et al.*, 2003, 2005) must be taken into account when new medical approaches based on discoveries in stem biology are introduced. The delineation of these four directions in molecular cytogenetics of the brain has led us to propose the following four hypotheses.

V. Relevance of Chromosomal Variations in the Mammalian Brain

A. Numerical Chromosome Imbalance and Apoptosis in Neuronal Cells: First Hypothesis

Apoptosis, or programmed cell death, is one of the main processes needed to maintain proper function and constancy of tissue size in an organism. It is consistently observed in humans throughout both normal and abnormal intrauterine development as well as in genomic (chromosomal) instability (Hardy, 1999; Zhivotovski and Kroemer, 2004). Additionally, programmed neuronal cell death may underlie the phenotypic manifestations of numerous neurodegenerative diseases (Mattson, 2000). Apoptotic clearance has been previously noted in proliferative and postmitotic regions of the murine fetal cerebral cortex (Blaschke *et al.*, 1996). Although the causes and consequences of apoptosis in mammalian neuronal cells remain obscure, contemporary views of apoptosis allow us to hypothesize that there is a connection between chromosome imbalance and apoptosis in ontogenesis of normal and diseased CNS. Apoptosis in mammalian embryos and fetal neuronal tissue suggests that some signaling in a number of fetal cells is present (Blaschke *et al.*, 1996; Hardy, 1999). Taking into account problems associated with the fetal CNS in terms of chromosome imbalances as well as the devastating effect of aneuploidy and polyploidy, it seems reasonable to propose that both aneuploidy and polyploidy are a signal of neuronal cell apoptotic clearance, a feature of normal fetal CNS development (Fig. 5). However, alterations in the apoptosis machinery may result in a lack of abnormal neuronal cell clearance, leading, therefore, to neurodevelopmental abnormalities in childhood.

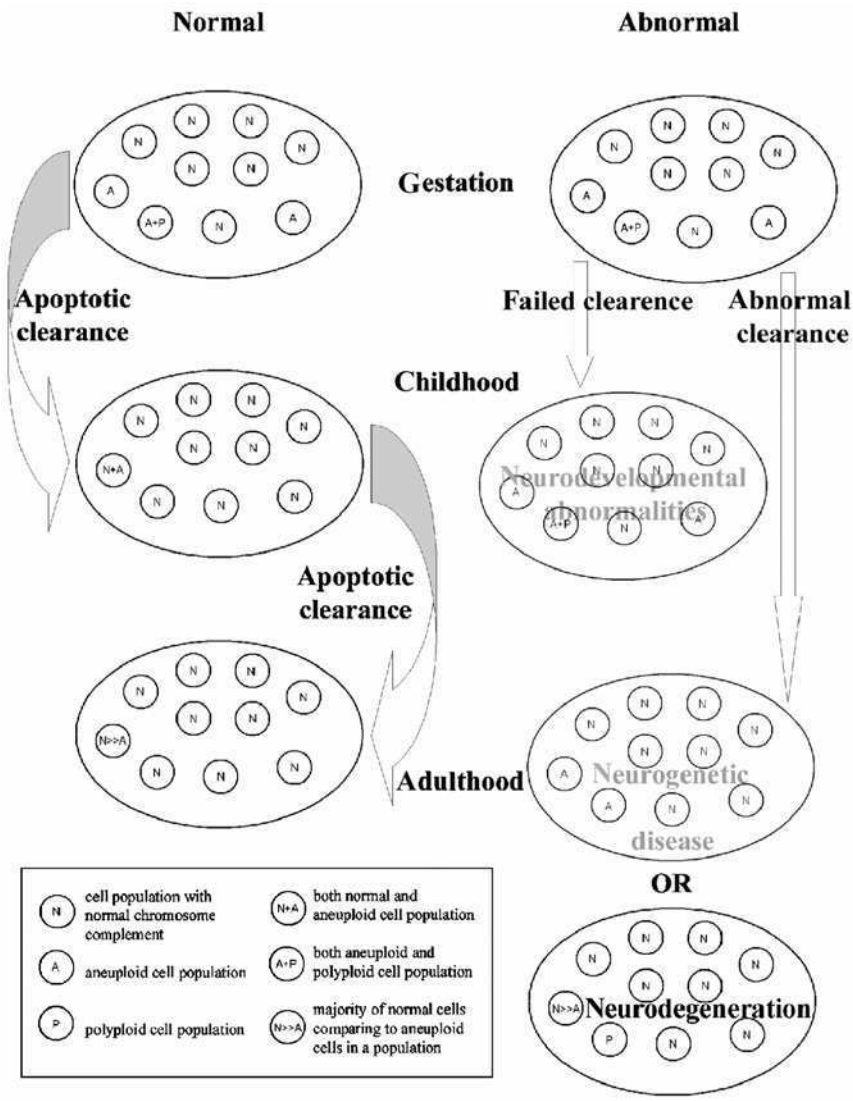

FIG. 5 Schematic representation of the hypothesis concerning the connection between apoptosis and chromosome imbalances in the brain. Normal CNS development: aneuploid and polyploid cells of the developing brain are cleared through apoptosis. As a result, the number of chromosome imbalances significantly decreases throughout postnatal life. Abnormal CNS development: failed clearance of aneuploid and polyploid cells occurring in the developing brain leads to neurodevelopmental abnormalities in childhood; abnormal clearance of both normal and abnormal cells occurring in the developing brain may not be apparent in childhood but has the potential to cause neurogenetic disease or neurodegeneration in adulthood.

Another problem in fetal neuronal cell apoptosis may be that both normal and abnormal cells are cleared regardless of the signaling. The latter is probably the cause of the persistence of genomic (chromosomal) instability in neuronal tissue throughout postnatal life. As genomic instability is the cause of the diseases termed "chromosome instability syndromes" and characterizes neoplastic cell populations (Youssoufian and Pyeritz, 2002; Zhivotovski and Kroemer, 2004), the second type of error in CNS cell apoptosis seems to be a candidate for processes underlying brain tumor formation (Fig. 2) and neurodegeneration. Because the onset of neuronal cell apoptosis is age dependent, the persistence of aneuploidy/polyploidy in the brain throughout postnatal life may be the cause of extensive apoptosis. Because extensive apoptotic clearance, if it exists, should disturb the maintenance of the established neuronal cell content in the adult brain, it may be considered a cause of late-onset neurodegenerative diseases. Another assumption based on postmortem brain molecular cytogenetic observations refers to the uneven apoptotic signaling potential, which depends on the type of chromosome imbalance. Thus, polyploidy seems to be more significantly involved in the neuronal cell death of postmortem brain samples from AD patients (Yang *et al.*, 2001), in contrast to the persistence of aneuploidy in the normal and schizophrenic brain (Yurov *et al.*, 2001, 2005). Therefore, each type of chromosome complement abnormality probably possesses a different propensity for apoptotic clearance (Fig. 5). Although the suggestions described here may appear speculative, the possibility of linking apoptosis, chromosomal variations in the brain, and both normal and abnormal CNS development is highly attractive.

B. Neurogenetic Diseases and Chromosomal Mosaicism in the Brain: Second Hypothesis

Despite evidence that numerous neuropsychiatric disorders are genetically based, no direct association has been proved. Additionally, for a broad spectrum of mental deficiency conditions improvidently termed "idiopathic mental retardation," there is little possibility of identifying the causative mutation. Hence, new theories drawn from basic biomedical studies have to be taken into account in delineating the complex genetic nature of these pathological conditions. Investigation of brain-specific chromosomal mosaicism appears to be one possibility. Few direct studies indicate that a number of cases of AD and schizophrenia are likely to be explained by chromosome imbalances in the brain (Yang *et al.*, 2001; Yurov *et al.*, 2001). It seems clear that some chromosome-specific patterns of brain aneuploidy/polyploidy cause neuropsychiatric diseases. Here, we hypothesize that chromosomal

mosaicism confined to the brain involves different chromosomes relevant to common brain disorders (not only AD and schizophrenia).

To extend the assumptions, we refer to conventional cytogenetic studies of the diseases. Thus, apart from mosaic trisomy 18 and X in the brain (Yurov *et al*., 2001), mosaic trisomy 8, and 45,X, 47,XXX (regular and mosaic), and 47,XXY conditions, multiple numerical chromosome abnormalities involving autosomes (chromosomes 8 and 21) and sex chromosomes were observed in patients with schizophrenia. Deletions and duplications (loss and gain of a specific chromosome region) of chromosomes 5, 9, 15, and 21 were documented, and deletion of chromosome 22q11.2 is consistently found in patients with schizophrenia (Basset *et al*., 2000). Therefore, the estimated brain-specific mosaic aneuploidy of the chromosomes mentioned might be implicated in the pathogenesis of schizophrenia as well (Fig. 6). As to studies of blood lymphocytes in patients with AD (Geller and Potter, 1999; Li *et al*., 1997), the aneuploidy of chromosome 21 can be added to ''the list of probable findings'' in the AD brain. Another common neurobehavioral disorder suspected of having a genetic background is autism. Current data suggest up to 15% of cases diagnosed as autism are associated with known

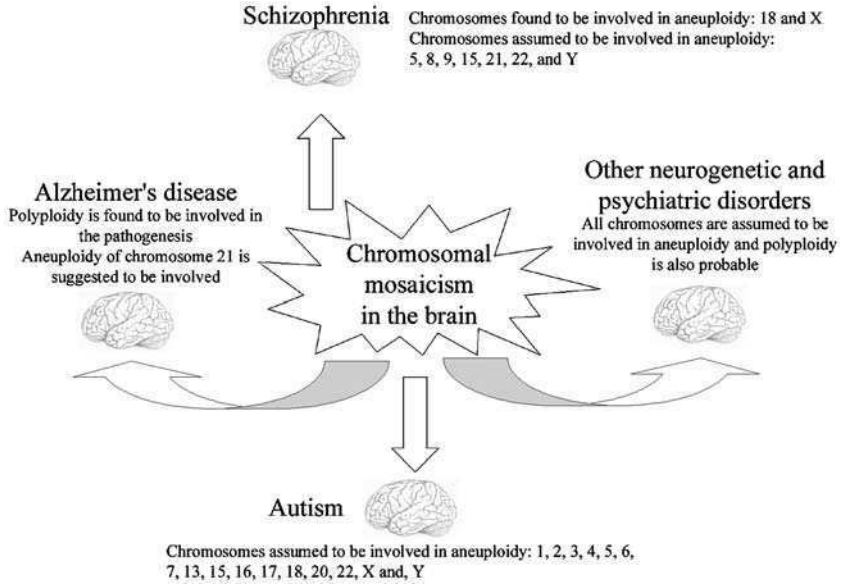

FIG. 6 Schematic representation of the hypothesis concerning major neuropsychiatric diseases and chromosomal mosaicism in the brain. Arrows are used to show the established and suggested relevance of chromosomal mosaicism in the brain to Alzheimer's disease, autism, schizophrenia, and other neurogenetic and psychiatric disorders.

genetic diseases (Fragile X syndrome, Rett syndrome, and tuberous sclerosis) as well as chromosome abnormalities (Jamain *et al.*, 2003). Structural chromosome abnormalities involving all autosomes were observed in autism with a larger part being deletions and duplications. Duplications of the long arm of chromosome 15q11–q13 are considered among the most frequent findings (Castermans *et al.*, 2004). In addition, the four-fold higher incidence of males compared to females among autistic individuals as well some case reports of structural abnormalities of sex chromosomes indicate the involvement of sex chromosomes in the etiology of autism. Although no direct proof of an association of autism with chromosomal mosaicism has yet been presented, the complex nature of the disease implies that brain-specific variations of chromosomes involved in deletions and duplications as well as sex chromosomes may contribute to its pathogenesis (Fig. 6). The neuropsychiatric diseases such as panic disorder, epilepsy, and idiopathic mental retardation are also assumed to be of genetic origin, being, therefore, a target for molecular cytogenetics of the brain (Fig. 6). In conclusion, we have to admit that although there is still little evidence, the analysis of chromosome complement in the brain may be a promising area of research in medical genetics.

C. Relation between Chromosomal Variations and Gene Expression Profiling in the Mammalian Brain: Third Hypothesis

It is difficult to find any field of biology that does not respect gene expression (epigenetic) studies. Data on different effects of gene expression in normal and pathogenic conditions suggest that related processes occur at all levels of tissue, genome, and chromatin organization (Birchler *et al.*, 2005). Relations between gene expression and aneuploidy can be defined as "double-sided." First, epigenetic silencing (changes in gene expression without mutational changes in DNA sequence) of genes encoding mitotic checkpoint proteins is considered a possible cause of mitotic errors (Cimini and Degrassi, 2005). However, the presence or lack of additional complete sets of genes of a chromosome impacts patterns of gene expression. Initial studies have shown that autosomal aneuploidy (mainly trisomy 21) has a primary gene–dosage effect. The latter is assumed to be manifested either as recognizable patterns of malformation at the whole organism level as in Down syndrome or as site- (tissue-) and stage-specific phenotypic features (Fitzpatrick, 2005). It appears to be intriguing in terms of brain-specific chromosome variations because an abnormal neuron content even as low as 0.1% has the potential to affect the brain because of the thousands of connections between neurons. The 10-fold increased variation (up to 1%) may possess more deleterious

effects, but the rate of aneuploidy found experimentally is significantly higher. Therefore, the potential of brain-specific large-scale genome variations to affect gene expression should be apparent.

Additionally, murine brain studies have indicated that chromosome loss alters gene expression in the postnatal brain (Kaushal *et al.*, 2003). The integration of aneuploid neurons into the brain circuitry in rodents (Kingsbury *et al.*, 2005) implies that the contribution of aneuploidy to the orchestrated activity of genes expressed in the brain exists. Although chromosomal variations may exceed current knowledge of gene expression in mammalian CNS beyond transcription and chromatin remodeling, it still remains questionable whether the incidence of low-level aneuploidy in somatic cells is a nonpathological condition. Nevertheless, due to the specificity of the CNS organization, the mammalian brain, shown to possess chromosomal mosaicism, has demonstrated a new mechanism of pathogenesis and diversity that should be exhibited through the orchestrated action of cellular epigenetic machinery.

Molecular cytogenetics of the brain can also offer insight on nuclear architecture. The latter remains the least explored phenomenon influencing gene expression (Cremer and Cremer, 2001). Additionally, defects in nuclear architecture may cause a number of diseases including cancer, mental retardation, neurodegeneration, and premature aging (Misteli, 2005). Investigations of human brain cells have indicated the extreme complexity of nuclear organization and the probability of an association between abnormal chromosome X behavior and epilepsy (Borden and Manuelidis, 1988; Manuelidis, 1990). Unfortunately, further extended studies of nuclear architecture in the brain involving the analysis of autosomes and chromosome Y have not been undertaken. Taking into account previous data on nuclear organization in humans (Cremer and Cremer, 2001; Misteli, 2005), molecular cytogenetics of the brain might be important in understanding both normal and abnormal CNS functioning at the cellular level.

D. Chromosomal Abnormalities in the Developing Human Brain: A Caution for Stem Cell Therapy: Fourth Hypothesis

Recent advances in molecular biology have suggested that transplantation of neural stem cells may be a nostrum for neurogenetic human diseases. Numerous investigations of human neural stem cell behavior in model organisms yielded positive results with respect to stem cell therapy (Ishibashi *et al.*, 2004; Kanemura *et al.*, 2002). In the future neural stem cell therapy may be used to cure human inherited neuropsychiatric diseases. As the source of neural stem cells is the developing brain (Gage, 2000), its characteristic features should be reevaluated. However, studies in the field do not

consider the increasing rate of chromosome imbalances in the mammalian developing brain. If a third part of fetal mammalian neuronal cells is aneuploid (Rehen *et al.*, 2001; Yurov *et al.*, 2005) and if an organotypic cultivation commonly used to increase the population of neural stem cells induces aneuploidy (Yurov *et al.*, 2003, 2005), injection of such a neural stem cell population may produce more deleterious effects than caused by the disease. This is further supported by the assumption that aneuploidy and polyploidy are assumed to be causative for human neoplasia (Duesberg *et al.*, 2004; Lengauer *et al.*, 1998). Therefore, it is important to conclude that transplantation therapy using cytogenetically unchecked neural stem cells is not a cure but may further damage already seriously affected health.

VI. Technical Aspects of Studies of Chromosomal Mosaicism in Mammalian Neuronal Cells

A. Molecular Cytogenetic Techniques

Looking through the broad spectrum of reviews describing molecular cytogenetic achievements and developments, we have come to the rueful conclusion that no studies are dedicated to the complex problem of chromosomal mosaicism. Our experience indicates that a number of peculiarities are associated with molecular cytogenetic analysis of the brain. This led us to conclude that a description of the technical aspects of studies of molecular cytogenetic chromosomal mosaicism in the brain would be pertinent.

The era of molecular cytogenetics in medical genetics began with the first reports on the applicability of the techniques to the diagnosis of chromosome abnormalities (Pinkel *et al.*, 1986; Vorsanova *et al.*, 1986). The next milestone in the development of molecular cytogenetic techniques for the identification of human chromosomes involves the introduction of multicolor FISH approaches (Schrock *et al.*, 1996; Speicher *et al.*, 1996; Yurov *et al.*, 1996b). Molecular cytogenetics now possesses highly effective approaches toward the identification of chromosome number in uncultured cells. Among them are numerous multicolor FISH-based techniques initially created to determine structural changes of metaphase chromosomes and now applicable to interphase chromosome analysis as well (Liehr *et al.*, 2004b). Additional multicolor FISH protocols using three or more ligands or fluorochromes for the specific labeling of chromosomal DNA are designed for simultaneous detection of several chromosomes in an interphase nucleus (Fig. 7A). The latter was found useful for identification of low-level chromosomal mosaicism (Vorsanova *et al.*, 2001, 2005; Yurov *et al.*, 1996b, 2001, 2005). An interesting alternative to FISH-based techniques for detection of mosaicism is primed

in situ chromosome labeling (PRINS) and peptide nucleic acid fluorescent *in situ* labeling (PNA). Multicolor PRINS and PNA approaches have been approved for the detection of chromosome abnormalities in human gametes and may be an additional powerful tool in studies of somatic tissue mosaicism (Pellestor *et al*., 1995, 2005). However, the applicability of PRINS and PNA for molecular cytogenetic studies of the brain still needs to be assessed experimentally. Since all known cytogenetic techniques used in the identification of chromosomal mosaicism have been mentioned, we will proceed to a description of their efficiency and a discussion of the pitfalls involved in studies of chromosomal mosaicism.

B. Identification of Low-Level Chromosomal Mosaicism in Neuronal Cells

To prepare metaphase spreads, human cytogenetics uses cell cultivation followed by chromosome banding such as GTG banding (G-bands by trypsin using Giemsa) as the gold standard for all routine cytogenetic studies. The most important restriction of these techniques for studies of mosaicism is the impossibility of scoring large cell populations. Another limitation arises from the possibility of failure of the cultivation procedure or the growth advantage of a normal cell population. In addition, the majority of mammalian somatic tissues including the adult brain possess, almost exclusively, postmitotic cells that cannot be subjected to either short- or long-term cultivation. Together, this suggests that molecular cytogenetic techniques are the most suitable for successful study of chromosome mosaicism.

FISH analysis is highly efficient in detecting chromosome abnormalities in prenatal and postnatal diagnosis and in studying chromosome aberrations of human germline cells, preimplantation embryos, and spontaneous abortions. However, despite apparent interest in improving and developing molecular cytogenetic approaches to the detection of mosaicism, all the difficulties have not been worked out. The most important complications seem to refer to defining a sample as mosaic and differentiating between chromosome abnormality and the peculiarities of FISH signal appearance in interphase.

The commonly applied benchmark for classifying a sample as mosaic is a 20% nuclei content with different signal patterns. This is used for scoring 50–100 nuclei per probe and is not applicable for studies of low-level mosaicism. However, the efficiency of hybridization and the relative simplicity of visual analysis allow significantly larger cell populations (over 1000 nuclei) to be scored. Unfortunately, to the best of our knowledge there are no guidelines for identifying chromosomal mosaicism in somatic tissues by molecular cytogenetic techniques. Nevertheless, detection of chromosomal mosaicism in spontaneous abortions targeted to reveal mosaics with more than 5%

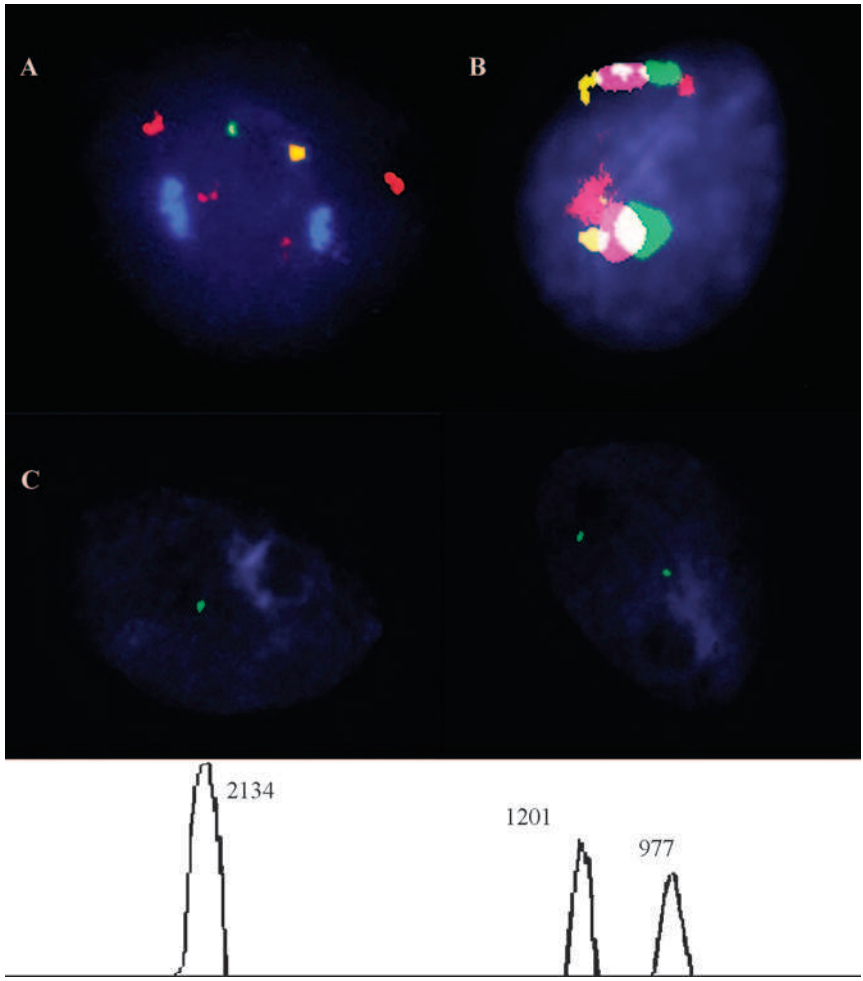

FIG. 7 State of the art in molecular cytogenetics of the human brain. (A) Multicolor FISH assay on interphase nuclei of the adult human brain. Pericentromeric diethylaminocoumarin-labeled DNA probe for chromosome 1 (two large oviform, i.e., replicated, blue signals); centromeric Spectrum Green-labeled DNA probe for chromosome X (one oviform-like or replicated green signal); centromeric Cy5-labeled DNA probe for chromosome Y (one oviform or replicated yellow signal); site-specific Spectrum Red-labeled DNA probe for chromosome 13q14 (two paired red replicated signals); site-specific Texas Red-labeled DNA probe for chromosome 21q22.1–22.2 (two paired magenta replicated signals). Signal patterns make it possible to suspect a tetraploid or replicated chromosome complement of neurons, which probably have not entered mitotic division after replication. (B) FISH assay on interphase nuclei of the adult brain using an MCB probe for chromosome 16. Spectrum Green signals correspond to 16p11.1–p13.1. Spectrum Orange signals correspond to 16p13.3–p21. Texas Red signals correspond to 16q11.1–q21 including the pericentromeric region (16qh). Cy5 signals

abnormal clone content demonstrated that scoring of 300–600 nuclei was efficient (Vorsanova *et al.*, 2005). Significantly, rather than a percentage of abnormal nuclei, the number of nuclei with a specific signal appearance was chosen as the benchmark for studies of mosaicism. Hence, if 10 nuclei with a characteristic signal pattern are, for instance, selected as a benchmark, scoring of 1000 nuclei per probe would permit the identification of 1% mosaicism. The number of nuclei selected as a benchmark may decrease to two as this provides for some reproducibility. Thus, scoring of 2000 nuclei will be applicable for detection of 0.1% mosaicism. Selection of two nuclei is rather risky, especially in the case of low-level mosaic studies. However, the analysis performed through identification of 5–10 nuclei characterized by different signal patterns from 5000–10,000 total nuclei scored can achieve 0.1% resolution. It is important to point out that all these calculations are based on the assumption that signal patterns detected in such a small number of nuclei are not a result of a FISH artifact. Consequently, low-level chromosomal studies of mosaicism seem to be highly sensitive to differentiation between "true abnormal" and "pseudoabnormal" patterns of signal appearance.

Molecular cytogenetics of the developing and adult mammalian brain meets all known types of artifacts referred to the specificity of the tissue, nuclear organization, and interphase FISH application. Because most brain cells are likely to be in interphase, the following discussion applies mainly to interphase molecular cytogenetics. The key point of any successful molecular cytogenetic analysis is a cautious selection of DNA probes. Current molecular cytogenetics possesses numerous FISH DNA probes sets for different kinds of applications (Liehr *et al.*, 2004b). Site-specific DNA probes hybridize with unique DNA sequences sized from 500 bp to 2–3 Mb along chromosome euchromatic regions. These are useful for precise determination of the structural chromosome abnormality breakpoint but are not very applicable to detection of chromosomal mosaicism. The latter is mainly explained by the relatively low efficiency of hybridization (40–80%) and the replication of chromosomal DNA (especially in the developing brain), which cause doubling of a signal (Soloviev *et al.*, 1995; Yurov *et al.*, 1996b, 2001). However, the application of site-specific DNA probes may be an issue for simultaneous use with other types of DNA probes. Apparently the most suitable probes for studies of chromosomal mosaicism are centromeric or chromosome

correspond to16q21–q24 (obtained through the collaboration of Dr. I. Y. Iourov and Dr. T. Liehr, Institute of Human Genetics and Anthropology, Jena, Germany). (C) Quantitative analysis of FISH signals in interphase nuclei of the adult brain using a pericentromeric DNA probe for chromosome 9. The left nucleus shows one signal possessing doubled intensity as compared to each signal of the right nucleus. This indicates the occurrence of somatic chromosome pairing.

enumerating DNA probes. Because of hybridization with large tandem repeated sequences, the efficiency of hybridization achieved is almost 100% (Soloviev *et al.*, 1998; Yurov *et al.*, 1996b). Despite this there is one important limitation to the use of a chromosome enumerating probe—the sharing of centromeric sequences between several chromosomes (chromosomes 5 and 19, 13 and 21, and 14 and 22). Additional large sets of FISH DNA probes are derived from chromosome microdissection libraries. Among them are whole chromosome paint (WCP) probes, part of a chromosome, the combination of 24 WCP probes for simultaneous visualization of all chromosome pairs, and probes that produce fluorescent GTG-like banding of chromosomes known as multicolor banding (MCB). Apart from MCB, all these probes are not useful for studies of interphase mosaicism due to the lack of reproducible signal patterns in interphase nucleus (Liehr *et al.*, 2004b). The MCB FISH assay based on simultaneous visualization of several chromosome regions (Fig. 7B) presented by Liehr and associates (2002) appears to be an interesting alternative to multiprobe FISH using either several chromosome enumerating probes or both site-specific and centromeric probes for one homologous chromosome pair. As interphase molecular cytogenetics of the brain requires differentiation between patterns of nuclear organization and chromosome abnormality, the possibility of visualizing all chromosome regions at the same time might be highly desirable for the detection of brain-specific chromosomal mosaicism.

General recommendations for avoiding artifact scoring suggest the analysis of intact and undamaged interphase nuclei free of cytoplasm (Yurov *et al.*, 2001, 2005). In other words, ''do not score the troublesome nuclei.'' It suggests that the opinion of the researcher is the ultimate interpretation. However, it is rather questionable whether it is possible to come to any definite decision concerning each nucleus, especially since 5000–10,000 nuclei are scored. This suggests that it is necessary to design additional tools targeted to defining of signal patterns. The difficulty in interphase studies of chromosomes in the human brain involves the phenomena of somatic chromosome pairing. This manifests as a large shaped signal characterized by doubled intensity to nuclei with two signals (Arnoldus *et al.*, 1989, 1991; Iourov *et al.*, 2005). Therefore, this signal pattern can be considered a false-positive monosomy. To solve the problem, an approach involving quantitative assessment of FISH signals was designed. The analysis of chromosomes 1, 9, and 16 indicated that up to 40% of adult brain nuclei possess only one signal instead of two (normal diploid chromosome complement). The quantification of these single signals has shown them to be of doubled intensity, representing, therefore, somatic pairing of pericentromeric regions but not a monosomy (Fig. 7C) (Iourov *et al.*, 2005). Consequently it can be concluded that signal quantification avoids the scoring of false-positive monosomic nuclei (''pseudomonosomy''). As to other types of FISH

artifacts caused by nuclear organization specificity of brain cells, the only more or less reliable recommendation may be that several site-specific (more than two) and centromeric/pericentromeric DNA probes each labeled by different fluorochromes or an MCB probe set (Fig. 7A and B) should be applied.

An additional common drawback of all neuroscience studies of postmortem samples is the increased level of background autofluorescence. Mammalian neuronal tissues are characterized by the presence of a fluorescent pigment lipofuscin that is accumulated with age in the cytoplasm of cells and may significantly affect the results of studies using fluorescent microscopy. Although numerous attempts toward the reduction of the lipofuscin-like autofluorescence were made (Neumann and Gabel, 2002; Schnell *et al.*, 1999), none of them seems to be applicable to molecular cytogenetics. This is explained by the fact that FISH signals are highly sensitive to histochemical reagents and that lipofuscin granules may cover the signals or appear as a false-positive hybridization signal. In conclusion, we note that although state-of-the-art molecular cytogenetic techniques are highly efficient, improvements in the molecular cytogenetic technology used for brain investigations are needed for further studies.

VII. Concluding Remarks

We recognize that initial sequencing and analysis of the human genome (International Human Genome Sequencing Consortium, 2001) have led to a more molecular approach to genetics. As a result, all types of cytogenetic investigations, referred to as the genetics of the past, are often considered to involve diagnostic issues only. However, we hope that this approach frequently encountered in genetic studies will soon be abandoned. In addition, the gaps in our knowledge about chromosome structure and function in the brain that were filled by molecular cytogenetic studies cannot be ignored. It is noteworthy that no experimentally proved hypothesis concerning the occurrence of chromosomal mosaicism and its relevance exists, especially when such complex systems as the CNS are involved. Finally, molecular cytogenetic studies of the brain have opened prospects for further investigations targeted at revealing the complex patterns of chromosome variations in the brain as well as delineating the role this phenomenon plays in the organization of the CNS.

Molecular cytogenetics of the brain has merged two immense parts of biology—neuroscience and genetics. It is noteworthy that the three reports that launched these studies of the brain (Rehen *et al.*, 2001; Yang *et al.*, 2001; Yurov *et al.*, 2001) were all published in 2001. Molecular cytogenetics of the

brain may therefore be considered a new direction in molecular biology in the twenty-first century. Additionally, to update the terminology of this bioscience, we would like to mention the term "neurocytogenetics," which was proposed by Osada and associates (2002) to describe their conventional cytogenetic studies of cloned murine neural cells. Here, we would like to extend this term to "molecular neurocytogenetics," which, in our opinion, is as appropriate as the former one, because the majority of the studies in the field involve molecular cytogenetics. Hence, "molecular neurocytogenetics" is a worthy term to replace "molecular cytogenetics of the brain."

Molecular neurocytogenetic findings have led to the theory that chromosomal variations manifesting as low-level chromosomal mosaicism are present in the normal developing mammalian brain (Rehen *et al.*, 2001; Yang *et al.*, 2003; Yurov *et al.*, 2003, 2005) followed by a decrease in order of magnitude in the postnatal adult mammalian brain (Kaushal *et al.*, 2003; Rehen *et al.*, 2001; Yurov *et al.*, 2005). The diseased adult human brain is characterized by an increased number of cells with an abnormal chromosome complement (Yang *et al.*, 2001; Yurov *et al.*, 2001). The model mice, lacking the gene encoding the chromosome stability maintenance protein, demonstrate a significant increase in brain-specific aneuploidy rate (McConnell *et al.*, 2004). Despite this, nuclear transfer shows an exceedingly high level of chromosome abnormality and abnormal chromatin behavior in cloned murine neuronal cells (Osada *et al.*, 2002). Molecular neurocytogenetic data depict stochastic aneuploidy as a new mechanism, not accounted for by Mendelian laws (classical genetics), that imparts neuronal diversity and neuropsychiatric pathogenesis (Rehen *et al.*, 2002; Yurov *et al.*, 2001). Finally, aneuploid neurons were found to be an integral part of the functioning of the murine CNS (Kingsbury *et al.*, 2005), making it difficult to ignore the presence of low-level chromosomal mosaicism in the mammalian brain.

The reasons for the formation of mosaic aneuploidy in the mammalian brain remain to be discovered. Current hypotheses suggest that aneuploidy forms not only through the occurrence of genomic mutations or mechanistic defects in mitotic machinery, but also through reduced gene expression and benign DNA sequence variations such as polymorphisms and allelic variants which slightly change the functional activity of proteins (Cimini and Degrassi, 2005). Interestingly, in the past decade related phenomena were found to influence behavior, neurodevelopment, abnormal neuropsychiatric phenotypes (schizophrenia), and mitotic missegregation (Cimini and Degrassi, 2005; O'Donovan *et al.*, 2003). This suggests a totally new direction in molecular neurogenetics, which can be roughly defined as the analysis of low-level chromosomal mosaicism in the brain and the coincidence with polymorphic DNA sequence variants affecting functional protein activity. The direction proposed possesses the potential for uncovering the complex

processes occurring in the brain of individuals affected by major psychiatric disorders.

Although the overall relevance of brain-specific chromosome imbalances is yet to be determined, the data obtained allow theorizing on future directions in the field. Thus, basic human molecular neurocytogenetic studies appear to require extended analysis of the normal developing and adult brain comprising all chromosomes (Yurov *et al*., 2005). Numerous human neuropsychiatric diseases should be considered a target for molecular neurocytogenetics. This also includes monogenic, neurogenetic, and chromatin remodeling diseases of known etiology, because the majority lack mechanisms able to explain their complex nature (Yurov *et al*., 2001). The suggested interactions among chromosome abnormalities, apoptosis, and gene expression profiling can be accounted for by diverse theories and create a firm basis for fundamental research in neuroscience and molecular cell biology. Neural stem cell biology, a rapidly developing field of applied neuroscience (Gage, 2000), demonstrates the possibility of treating devastating neurological diseases. However, the stochastic aneuploidy in the developing mammalian brain, which is persistent when multiplying neural stem cells (Rehen *et al*., 2001; Yurov *et al*., 2005), may be a significant hindrance to neural stem cell therapy. The murine model of chromosome instability syndromes shown to possess an increased level of brain-specific aneuploidy (McConnell *et al*., 2004) has defined the perspective of molecular neurocytogenetic analysis of the human brain in chromosome instability syndromes. To this end, we believe this review shows comprehensively the current achievements and potentials of molecular neurocytogenetics, which will certainly take a well-deserved place in biomedical science in the future.

Acknowledgments

The review is dedicated to Ilia V. Soloviev, who encouraged our studies in molecular cytogenetics. We would like to acknowledge Dr. V. Y. Voinova-Ulas for help in creating Figures 1, 4, and 6, as well as all the researchers in our laboratories who performed molecular cytogenetic studies of the human brain. Dr. T. Liehr is gratefully acknowledged for collaboration that allowed us to depict the MCB technique on postmortem human brain samples (Fig. 7B). The authors are supported by INTAS 03-51-4060, A-T Children's Project, and RGRF 030600447 (Russian Federation) projects.

REFERENCES

Acar, H., Yildrim, M. S., and Kaynak, M. (2002). Reliability and efficiency of interphase-FISH with alpha-satellite probe for detection of aneuploidy. *Genet. Counsel.* **13,** 11–17.

Adler, I. D., Bishop, J., Lowe, X., Schmid, T. E., Schriever-Schwemmer, G., Xu, W., and Wyrobek, A. J. (1996). Spontaneous rates of sex chromosomal aneuploidies in sperm and offspring of mice: A validation of the detection of aneuploid sperm by fluorescence *in situ* hybridization. *Mutat. Res.* **372,** 259–268.

Allen, D. M., van Praag, H., Ray, J., Weaver, Z., Winrow, C. J., Carter, T. A., Braquet, R., Harrington, E., Ried, T., Brown, K. D., Gage, F. H., and Barlow, C. (2001). Ataxia telangiectasia mutated is essential during adult neurogenesis. *Genes Dev.* **15,** 554–566.

Angell, R. R., Sandison, A., and Bain, A. D. (1984). Chromosome variation in perinatal mortality: A survey of 500 cases. *J. Med. Genet.* **21,** 39–44.

Antonarakis, S. E., Avramapoulos, D., Blouin, J. L., Talbot, C. C., Jr., and Schinzel, A. A. (1993). Mitotic errors in somatic cells cause trisomy 21 in about 4.5% of cases and are not associated with advanced maternal age. *Nat. Genet.* **3,** 146–150.

Arnoldus, E. P. J., Peters, A. C. B., Bots, G. T., Raap, A. K., and van der Ploeg, M. (1989). Somatic pairing of chromosome 1 centromeres in interphase nuclei of human cerebellum. *Hum. Genet.* **83,** 231–234.

Arnoldus, E. P. J., Noordermeer, I. A., Peters, A. C. B., Raap, A. K., and van der Ploeg, M. (1991). Interphase cytogenetics reveals somatic pairing of chromosome 17 centromeres in normal brain tissue, but no trisomy 7 or sex-chromosome loss. *Cytogenet. Cell Genet.* **56,** 214–216.

Basset, A. S., Chow, E. W. C., and Weksberg, R. (2000). Chromosomal abnormalities in schizophrenia. *Am. J. Med. Genet. (Semin. Med. Genet.)* **97,** 45–51.

Bayer, S. A., and Altaman, J. (1991). ''Neocortical Development.'' Raven, New York.

Bielanska, M., Tan, S. L., and Ao, A. (2002). Chromosomal mosaicism throughout preimplantation development *in vitro:* Incidence, type, and relevance to embryo outcome. *Hum. Reprod.* **17,** 413–419.

Binger, S. H., McLendon, R. E., Fuchs, H., McKeever, P. E., and Friedman, H. S. (1997). Chromosomal characteristics of childhood brain cancers. *Cancer Genet. Cytogenet.* **97,** 125–134.

Birchler, J. A., Riddle, N. C., Auger, D. L., and Veitia, R. A. (2005). Dosage balance in gene regulation: Biological implications. *Trends Genet.* **21,** 219–226.

Blaschke, A. J., Stanley, K., and Chun, J. (1996). Widespread programmed cell death in proliferative and postmitotic regions of the fetal cerebral cortex. *Development* **122,** 1165–1174.

Borden, J., and Manuelidis, L. (1988). Movement of chromosome X in epilepsy. *Science* **242,** 1687–1691.

Bregnard, A., Knusel, A., and Kuenzle, C. C. (1975). Are all the neuronal nuclei polyploid? *Histochemestry* **43,** 59–61.

Brinkley, B. R. (2001). Managing the centrosomes numbers game: From chaos to stability in cancer cell division. *Trends Cell Biol.* **11,** 18–21.

Bugge, M., Collins, A., Petersen, M. B., Fisher, J., Brandt, C., Hertz, J. M., Tranebjaerg, L., de Loizier-Blanchet, C., Nicolaidis, P., Brondum-Nielsen, K., Morton, N., and Mikkelsen, M. (1998). Non-disjunction of chromosome 18. *Hum. Mol. Genet.* **7,** 661–669.

Burns, E. M., Christopoulou, L., Corish, P., and Tyler-Smith, C. (1999). Quantitative measurement of mammalian chromosome mitotic loss rates using the green fluorescent protein. *J. Cell Sci.* **112,** 2705–2714.

Castermans, D., Wilquet, V., Steyaert, J., Van de Ven, W., Fryns, J. P., and Devriendt, K. (2004). Chromosomal abnormalities in individuals with autism. A strategy towards the identification of genes involved in autism. *Autism* **8,** 141–161.

Cimini, D., and Degrassi, F. (2005). Aneuploidy a matter of bad connections. *Trends Cell Biol.* **15,** 442–451.

Clarke, C. M., Edwards, J. H., and Smallpiece, V. (1961). 21-Trisomy/normal mosaicism in an intelligent child with some Mongoloid characteristics. *Lancet* **18,** 1028–1030.

Cleveland, D. W., Mao, Y., and Sullivan, K. F. (2003). Centromeres and kinetochores: From epigenetics to mitotic checkpoint signaling. *Cell* **112,** 407–421.

Cook, P. R. (1997). The transcriptional basis of chromosome pairing. *J. Cell Sci.* **110,** 1033–1040.

Coonen, E., Derhaag, J. G., Dumoulin, J. C., van Wissen, L. C., Bras, M., Janssen, M., Evers, J. L., and Graedts, J. P. (2004). Anaphase lagging mainly explains chromosomal mosaicism in human preimplantation embryos. *Hum. Reprod.* **19,** 316–324.

Cremer, T., and Cremer, C. (2001). Chromosome territories, nuclear architecture and gene regulation in mammalian cells. *Nat. Rev. Genet.* **2,** 292–301.

DeAngelis, L. M. (2001). Brain tumors. *N. Engl. J. Med.* **344,** 114–123.

de Moreira, L. M., San Juan, A., Pereira, P. S., and de Souza, C. S. (2000). A case of mosaic trisomy 21 with Down's syndrome signs and normal intelligent development. *J. Intellect. Dis. Res.* **44,** 91–96.

Delhanty, J. D., Harper, J. C., Ao, A., Handyside, A. H., and Winston, R. M. (1997). Multicolor FISH detects frequent chromosomal mosaicism and chaotic division in normal preimplantation embryos from fertile patients. *Hum. Genet.* **99,** 755–760.

Duesberg, P., Fabarius, A., and Hehlmann, R. (2004). Aneuploidy, the primary cause of the multilateral genomic instability of neoplastic and preneoplastic cells. *IUBMB Life* **56,** 65–81.

Elsheikh, M., Dunger, D. B., Conway, G. S., and Wass, J. A. H. (2002). Turner's syndrome in adulthood. *Endocr. Rev.* **23,** 120–140.

Engidawork, E., and Lubeck, G. (2003). Molecular changes in fetal Down syndrome brain. *J. Neurochem.* **84,** 895–904.

Fitzpatrick, D. R. (2005). Transcriptional consequences of autosomal trisomy: Primary gene dosage with complex downstream effects. *Trends Genet.* **21,** 249–253.

Ford, C. E., Miller, O. J., Polani, P. E., de Almeida, J. C., and Briggs, J. H. (1959). A sex-chromosome anomaly in a case of gonadal dysgenesis (Turner's syndrome). *Lancet* **I,** 711–713.

Forrester, M. B., and Merz, R. D. (1999). Trisomies 13 and 18: Prenatal diagnosis and epidemiologic studies in Hawaii, 1986–1997. *Genet. Test.* **3,** 335–340.

Gage, F. H. (2000). Mammalian neural stem cells. *Science* **287,** 1433–1438.

Geller, L. N., and Potter, H. (1999). Chromosome missegregation and trisomy 21 mosaicism in Alzheimer's disease. *Neurobiol. Dis.* **6,** 167–179.

Ghosh, A., and Greenberg, M. E. (1995). Distinct roles for bFGF and NT-3 in the regulation of cortical neurogenesis. *Neuron* **15,** 89–103.

Giraud, F., and Mattei, J. F. (1975). Aspects epidemiologiques de la trisomie 21. *J. Genet. Hum.* **23,** 1–30.

Glenister, P. H., Wood, M. J., Kirby, C., and Whittingham, D. G. (1987). Incidence of chromosome anomalies in first cleavage mouse embryos obtained from frozen-thawed oocytes fertilized *in vitro*. *Gamete Res.* **16,** 205–216.

Goldstein, H., and Nielsen, K. G. (1988). Rates and survival of individuals with trisomy 13 and 18: Data from a 10-year period in Denmark. *Clin. Genet.* **34,** 366–372.

Griffin, D. K. (1996). The incidence, origin and etiology of aneuploidy. *Int. Rev. Cytol.* **167,** 263–296.

Guttenbach, M., Koschorz, B., Bernthaler, U., Grimm, T., and Schmid, M. (1995). Sex chromosomes loss and aging: *In situ* hybridization studies on human interphase nuclei. *Am. J. Hum. Genet.* **57,** 1143–1150.

Hardy, K. (1999). Apoptosis in the human embryo. *Rev. Reprod.* **4,** 125–134.

Hassold, T. (1982). Mosaic trisomies in human spontaneous abortions. *Hum. Genet.* **61,** 31–35.

Hassold, T., and Hunt, P. (2001). To err (meiotically) is human: The genesis of human aneuploidy. *Nat. Rev. Genet.* **2,** 280–291.

Hook, E. B., and Warburton, D. (1983). The distribution of chromosomal genotypes associated with Turner's syndrome: Livebirth prevalence rates and severity in genotypes associated with structural X abnormalities of mosaicism. *Hum. Genet.* **64,** 24–27.

Horiushi, I., Hashimoto, T., Tsuji, Y., Shimaada, H., Furuyama, J., and Koyama, K. (1997). Direct assessment of triploid cells in mosaic human fetuses by fluorescence *in situ* hybridization. *Mol. Hum. Reprod.* **3,** 445–450.

Hsu, L. Y., and Perlis, T. E. (1984). United States survey on chromosome mosaicism and pseudomosaicism in prenatal diagnosis. *Prenat. Diagn.* **4,** 97–130.

International Human Genome Sequencing Consortium (2001). Initial sequencing and analysis of the human genome. *Nature* **409,** 860–921.

Iourov, I, Y., Soloviev, I. V., Vorsanova, S. G., Monakhov, V. V., and Yurov, Y. B. (2005). An approach for quantitative assessment of fluorescence *in situ* hybridization (FISH) signals for applied human molecular cytogenetics. *J. Histochem. Cytochem.* **53,** 401–408.

Ishibashi, S., Sakaguchi, M., Kuriowa, T., Yamasaki, M., Kanemura, Y., Shizuko, I., Shimazaki, T., Onodera, M., Okano, H., and Mizusawa, H. (2004). Human neural stem/progenitor cells, expanded in long-term neurosphere culture, promote functional recovery after focal ischemia in Mongolian gerbils. *J. Neurosci. Res.* **78,** 215–223.

Jacobs, P., Dalton, P., James, R., Mosse, K., Power, M., Robinson, D., and Skuse, D. (1997). Turner syndrome: A cytogenetic and molecular study. *Ann. Hum. Genet.* **61,** 471–483.

Jacobs, P. A., and Brown, C. W. (1961). Distribution of human chromosome count in relation to age. *Nature* **191,** 1178–1180.

Jacobs, P. A., and Strong, J. A. (1959). A case of human intersexuality having a possible XXY sex-determining mechanism. *Nature* **183,** 302–303.

Jacobs, P. A., Balkie, A. G., MacGregor, T. N., and Harnden, D. G. (1959). Evidence for the existence of the human "superfemale." *Lancet* **II,** 423–425.

Jacobs, P. A., Browne, C., Gregson, N., Joyce, C., and White, H. (1992). Estimates of the frequency of chromosome abnormalities detectable in unselected newborns using moderate levels of banding. *J. Med. Genet.* **29,** 103–108.

Jamain, S., Betancur, C., Giros, B., Leboyer, M., and Bourgeron, T. (2003). La genetique de l'autisme. *Med. Sci.* **19,** 1081–1090.

James, R. C., and Jacobs, P. A. (1996). Molecular studies of the aetiology of trisomy 8 in spontaneous abortions and the liveborn population. *Hum. Genet.* **97,** 283–286.

Jobanputra, V., Sobrino, A., Kinney, A., Kline, J., and Warburton, D. (2002). Multiplex interphase FISH as a screen for common aneuploidies in spontaneous abortions. *Hum. Reprod.* **17,** 1166–1170.

Kajii, T., Ohama, K., and Mikamo, K. (1978). Anatomic and chromosomal anomalies in 944 induced abortuses. *Hum. Genet.* **43,** 247–258.

Kalousek, D. K., and Vekemans, M. (1996). Confined placental mosaicism. *J. Med. Genet.* **33,** 529–533.

Kalousek, D. K., Barrett, I. J., and Gartner, A. B. (1992). Spontaneous abortion and confined chromosomal mosaicism. *Hum. Genet.* **88,** 642–646.

Kanemura, Y., Mori, H., Kobayashi, S., Islam, O., Kodama, E., Yamamoto, A., Nakanishi, Y., Arita, N., Yamasaki, M., Okano, H., Hara, M., and Miyake, J. (2002). Evaluation of *in vitro* proliferative activity of human fetal neural stem/progenitor cells using indirect measurements of viable cells based on cellular metabolic activity. *J. Neurosci. Res.* **69,** 869–879.

Kaplan, A. R., and Cotton, J. E. (1968). Chromosomal abnormalities in female schizophrenics. *J. Nerv. Ment. Dis.* **147,** 402–417.

Kaushal, D., Contos, J. J. A., Treuner, K., Yang, A. H., Kingsbury, M. A., Rehen, S. K., McConnell, M. J., Okabe, M., Barlow, C., and Chun, J. (2003). Alteration of gene expression by chromosome loss in the postnatal mouse brain. *J. Neurosci.* **23,** 5599–5606.

Kingsbury, M. A., Friedman, B., McConnell, M. J., Rehen, S. K., Yang, A. H., Kaushal, D., and Chun, J. (2005). Aneuploid neurons are functionally active and integrative into brain circuitry. *Proc. Natl. Acad. Sci. USA* **102,** 6143–6147.

Kirsch-Volders, M., Vanhauwaert, A., De Boeck, M., and Decordier, I. (2002). Importance of detecting numerical versus structural chromosome aberrations. *Mutat. Res.* **504,** 137–148.

Kunugi, H., Lee, K. B., and Nanko, S. (1999). Cytogenetic findings in 250 schizophrenics: Evidence confirming an excess of the X chromosome aneuploidies and pericentric inversion of chromosome 9. *Schizophr. Res.* **40,** 43–47.

Lacayo, A., and Farmer, P. M. (1991). Brain tumors in children: A review. *Ann. Clin. Lab. Sci.* **21,** 26–35.

Lanfranco, F., Kamischke, A., Zitzmann, M., and Nieschlag, E. (2004). Klinefelter's syndrome. *Lancet* **364,** 273–283.

Lejeune, J., Gautier, M., and Turpin, R. (1959). Etude des chromosomes somatiques de neuf enfants mongoliens. *C. R. Acad. Sci.* **248,** 1721–1722.

Lengauer, C., Kinzler, K. W., and Vogelstein, B. (1998). Genetic instabilities in human cancers. *Nature* **396,** 643–649.

Li, J., Xu, M., Zhou, H., Ma, J., and Potter, H. (1997). Alzheimer presenilins in the nuclear membrane, interphase kinetochores, and centrosomes suggest a role in chromosome segregation. *Cell* **90,** 917–927.

Liehr, T., Heller, A., Starke, H., Rubtsov, N., Trifonov, V., Mrasek, K., Weise, A., Kuechler, A., and Claussen, U. (2002). Microdissection based high resolution multicolor banding for all 24 human chromosomes. *Int. J. Mol. Med.* **9,** 335–339.

Liehr, T., Claussen, U., and Starke, H. (2004a). Small supernumerary marker chromosomes (sSMC) in humans. *Cytogenet. Genome Res.* **107,** 55–67.

Liehr, T., Starke, H., Weise, A., Lehrer, H., and Claussen, U. (2004b). Multicolor FISH probe sets and their applications. *Histol. Histopathol.* **19,** 229–237.

Lodish, H., Berk, A., Ziputsky, L., Matsudaria, P., Baltimore, D., and Darnell, J. (2000). ''Molecular Cell Biology,'' 4th ed. WRH. Freeman Publishers, New York.

Ly, D. H., Lockhart, D. J., Lerner, R. A., and Schultz, P. G. (2000). Mitotic misregulation and human aging. *Science* **287,** 2486–2492.

Manuelidis, L. (1984). Different central nervous system cell types display distinct and nonrandom arrangements of satellite DNA sequences. *Proc. Natl. Acad. Sci. USA* **81,** 3123–3127.

Manuelidis, L. (1990). A view of interphase chromosomes. *Science* **250,** 1533–1540.

Manuelidis, L., and Borden, J. (1988). Reproducible compartmentalization of individual chromosome domains in human CNS cells revealed by *in situ* hybridization and three-dimensional reconstruction. *Chromosoma* **96,** 397–410.

Mattson, M. P. (2000). Apoptosis in neurodegenerative disorders. *Nat. Rev. Mol. Cell Biol.* **1,** 120–129.

McConnell, M. J., Kaushal, D., Yang, A. H., Kingsbury, M. A., Rehen, S. K., Treuner, K., Helton, R., Annas, E. G., Chun, J., and Barlow, C. (2004). Failed clearance of aneuploidy embryonic neural progenitor cells leads to excess aneuploidy in the *Atm*-deficient but not the *Trp53*-deficient adult cerebral cortex. *J. Neurosci.* **24,** 8090–8096.

Misteli, T. (2005). Concepts in nuclear architecture. *Bioessays* **27,** 477–487.

Munne, S., and Cohen, J. (1998). Chromosome abnormalities in human embryos. *Hum. Reprod. Update* **4,** 842–855.

Munne, S., Weier, H. U. G., Grifo, J., and Cohen, J. (1994). Chromosome mosaicism in human embryos. *Biol. Reprod.* **51,** 373–379.

Murray, R. C., and Calof, A. L. (1999). Neuronal regeneration: Lessons from the olfactory system. *Sem. Cell Dev. Biol.* **10,** 421–431.

Neumann, M., and Gabel, D. (2002). Simple method for reduction of autofluorescence in fluorescence microscopy. *J. Histochem. Cytochem.* **50,** 437–439.

Nicolaidis, P., and Petersen, M. B. (1998). Origin and mechanisms of non-disjunction in human autosomal trisomies. *Hum. Reprod.* **13,** 313–319.

Nielsen, J., and Wohert, M. (1991). Chromosome abnormalities found among 34,910 newborn children: Results from a 13-year incidence study in Aarhus, Denmark. *Hum. Genet.* **87,** 81–83.

Nowinski, G. P., Van Dyke, D. L., Tilley, B. C., Jacobsen, G., Babu, V. R., Worsham, M. J., Wilson, G. N., and Weiss, L. (1990). The frequency of aneuploidy in cultured lymphocytes is correlated with age and gender but not with reproductive history. *Am. J. Hum. Genet.* **46,** 1101–1111.

O'Donovan, M., Williams, N. M., and Owen, M. J. (2003). Recent advances in the genetics of schizophrenia. *Hum. Mol. Genet.* **12**(Rev. Issue 2), 125–133.

Osada, T., Kusakabe, H., Akutsu, H., Yagi, T., and Yanagimachi, R. (2002). Adult murine neurons: Their chromatin and chromosome changes and failure to support embryonic development as revealed by nuclear transfer. *Cytogenet. Genome Res.* **97,** 7–12.

Patwardhan, A. J., Brown, W. E., Bender, B. G., Linden, M. C., Eliez, S., and Reiss, A. L. (2002). Reduced size of the amygdala in individuals with 47, XXY and 47, XXX karyotypes. *Am. J. Med. Genet.* **114,** 93–98.

Pellestor, F., Girardet, A., Lefort, G., Andreo, B., and Charlieu, J. P. (1995). Selection of chromosome-specific primers and their use in simple and double PRINS techniques for rapid *in situ* identification of human chromosomes. *Cytogenet. Cell Genet.* **70,** 138–142.

Pellestor, F., Andreo, B., Arnal, F., Humeau, C., and Demaille, J. (2003). Maternal aging and chromosomal abnormalities: New data drawn from *in vitro* unfertilized oocytes. *Hum. Genet.* **112,** 195–203.

Pellestor, F., Paulasova, P., Macek, M., and Hamamah, S. (2005). The use of peptide nucleic acids for *in situ* identification of human chromosomes. *J. Histochem. Cytochem.* **53,** 395–400.

Pflueger, S. M. V. (2005). Cytogenetics of spontaneous abortion. *In* "The Principles of Clinical Cytogenetics" (S. L. Gersen and M. B. Keagle, Eds.), 2nd ed., pp. 323–345. Humana Press, Totowa, NJ.

Pinkel, D., Straume, T., and Gray, J. W. (1986). Cytogenetic analysis using quantitative, high-sensitivity, fluorescent hybridization. *Proc. Natl. Acad. Sci. USA* **83,** 2934–2938.

Priest, J. H., Rust, J. M., and Fernhoff, P. M. (1992). Tissue specificity and stability of mosaicism in Pallister-Killian +i(12p) syndrome: Relevance for prenatal diagnosis. *Am. J. Med. Genet.* **42,** 820–824.

Rae, C., Joy, P., Harasty, J., Kemp, A., Kuan, S., Christodoulou, J., Cowell, C. T., and Coltheart, M. (2004). Enlarged temporal lobes in Turner syndrome: An X-chromosome effect? *Cereb. Cortex* **14,** 156–164.

Rajagopalan, H., and Lengauer, C. (2004). Aneuploidy and cancer. *Nature* **432,** 338–341.

Rehen, S. K., McConnell, M. J., Kaushal, D., Kingsbury, M. A., Yang, A. H., and Chun, J. (2001). Chromosomal variation in neurons of the developing and adult mammalian nervous system. *Proc. Natl. Acad. Sci. USA* **98,** 13361–13366.

Rehen, S. K., McConnell, M. J., Kaushal, D., Kingsbury, M. A., Yang, A. H., and Chun, J. (2002). Genetic mosaicism in the brain: A new paradigm for neuronal diversity. *Directions Sci.* **1,** 53–55.

Rehen, S. K., Yung, Y. C., McCreight, M. P., Kaushal, D., Yang, A. H., Almeida, B. S. V., Kingsbury, M. A., Cabral, K. M. S., McConnell, M. J., Anliker, B., Fontanoz, M., and

Chun, J. (2005). Constitutional aneuploidy in the normal human brain. *J. Neurosci.* **25,** 2176–2180.

Robinson, W. P., Binkert, I. J., Bernasconi, F., Lorda-Sanchez, I., Werder, E. A., and Schinzel, A. A. (1995). Molecular studies of chromosomal mosaicism: Relative frequency of chromosome gain or loss and possible role of cell selection. *Am. J. Hum. Genet.* **56,** 444–451.

Roizen, N. J., and Patterson, D. (2003). Down's syndrome. *Lancet* **361,** 1281–1289.

Rosenbusch, B. (2004). The incidence of aneuploidy in human oocytes assessed by conventional cytogenetic analysis. *Hereditas* **141,** 97–105.

Schinzel, A. (2001). "Catalogue of Unbalanced Chromosome Aberrations in Man," 2nd ed. Walter de Gruyter Inc., Berlin.

Schnell, S. A., Staines, W. A., and Wessendorf, M. W. (1999). Reduction of lipofuscin-like autofluorescence in fluorescently labeled tissue. *J. Histochem. Cytochem.* **47,** 719–730.

Schrock, E., du Manoir, S., Veldman, T., Schoell, B., Weinberg, J., Ferguson-Smith, M. A., Ning, Y., Ledbetter, D. H., Bar-Am, I., Soenksen, D., Garini, Y., and Ried, T. (1996). Multicolor spectral karyotyping of human chromosomes. *Science* **273,** 494–497.

Soloviev, I. V., Yurov, Y. B., Vorsanova, S. G., Fayet, F., Roizes, G., and Malet, P. (1995). Prenatal diagnosis of trisomy 21 using interphase fluorescence *in situ* hybridization of post-replicated cells with site-specific cosmid and cosmid contig probes. *Prenat. Diagn.* **15,** 237–248.

Soloviev, I. V., Yurov, Y. B., Vorsanova, S. G., Marcais, B., Rogaev, E. I., Kapanadze, B. I., Brodiansky, V. M., Yankovsky, N. K., and Roizes, G. (1998). Fluorescence *in situ* hybridization analysis of α-satellite DNA in cosmid libraries specific for human chromosomes 13, 21 and 22. *Rus. J. Genet.* **34,** 1247–1255.

Speicher, M. R., Ballard, G. S., and Ward, D. C. (1996). Karyotyping human chromosomes by combinatorial multi-fluor FISH. *Nat. Genet.* **12,** 368–375.

Stetten, G., Escallon, C. S., South, S. T., McMichael, J. L., Saul, D. O., and Blakemore, K. J. (2004). Reevaluating confined placental mosaicism. *Am. J. Med. Genet. A* **131,** 232–239.

Suzuki, M., Wright, L. S., Marwah, P., Lardy, H. A., and Svendsen, C. N. (2004). Mitotic and neurogenic effects of dehydroepiandrosterone (DHEA) on human neural stem cell cultures derived from the fetal cortex. *Proc. Natl. Acad. Sci. USA* **101,** 3202–3207.

Swartz, F. J., and Bhatnagar, K. P. (1981). Are CNA neurons polyploid? A critical analysis based upon cytophotometric study of the DNA content of cerebellar and olfactory bullar neurons of the bat. *Brain Res.* **208,** 267–281.

Szczygiet, M., and Kurpisz, M. (2001). Chromosomal anomalies in human gametes and pre-implantation embryos, and their potential effect on reproduction. *Andrologia* **33,** 249–265.

Thomas, N. S., Collins, A. R., Hassold, T., and Jacobs, P. A. (2000). A reinvestigation of non-disjunction resulting in 47,XXY males of paternal origin. *Eur. J. Hum. Genet.* **8,** 805–808.

Tjio, H. J., and Levan, A. (1956). The chromosome numbers of man. *Hereditas* **42,** 1–6.

Tsuji, K., and Nakano, R. (1978). Chromosome studies of embryos from induced abortions in pregnant women age 35 and over. *Obstet. Gynecol.* **52,** 542–544.

van de Laar, I., Rabelink, G., Hochstenbach, R., Tuerlings, J., Hoogeboom, J., and Giltay, J. (2002). Diploid/triploid mosaicism in dysmorphic patients. *Clin. Genet.* **62,** 376–382.

Vorsanova, S. G., Yurov, Y. B., Alexandrov, I. A., Demidova, I. A., Mitkevich, S. P., and Tirskaya, A. F. (1986). 18p-Syndrome: An unusual case and diagnosis by *in situ* hybridization with chromosome 18-specific alphoid DNA sequence. *Hum. Genet.* **72,** 185–187.

Vorsanova, S. G., Demidova, I. A., Ulas, V. Y., Soloviev, I. V., Kazantseva, L. Z., and Yurov, Y. B. (1996). Cytogenetic and molecular-cytogenetic investigation of Rett syndrome. Analysis of 31 cases. *Neuroreport* **7,** 187–189.

Vorsanova, S. G., Yurov, Y. B., Ulas, V. Y., Demidova, I. A., Kolotii, A. D., Gorbatchevskaia, N. L., Beresheva, A. K., and Soloviev, I. V. (2001). Cytogenetic and molecular-cytogenetic studies of Rett syndrome (RTT): A retrospective analysis of a Russian cohort of RTT patients (the investigation of 57 girls and three boys). *Brain Dev.* **23**(Suppl. 1), 196–201.

Vorsanova, S. G., Kolotii, A. D., Iourov, I. Y., Monakhov, V. V., Kirillova, E. A., Soloviev, I. V., and Yurov, Y. B. (2005). Evidence for high frequency of chromosomal mosaicism in spontaneous abortions revealed by interphase FISH analysis. *J. Histochem. Cytochem.* **53,** 375–380.

Warburton, D., Yu, C., Kline, J., and Stein, Z. (1978). Mosaic autosomal trisomy in cultures from spontaneous abortions. *Am. J. Hum. Genet.* **30,** 609–617.

Warburton, D., Byrne, J., and Canki, N. (1991). "Chromosome Anomalies and Prenatal Development: An Atlas," Oxford Monographs on Medical Genetics No. 21 Oxford University Press, New York.

Warwick, M. M., Doody, G. A., Lawrie, S. M., Kestelman, J. N., Best, J. J. K., and Johnstone, E. C. (1999). Volumetric magnetic resonance imaging study of the brain in subjects with sex chromosome aneuploidies. *J. Neurol. Neurosurg. Psychiatry* **66,** 628–632.

Watase, K., and Zoghbi, H. Y. (2003). Modeling brain diseases in mice: The challenges of design and analysis. *Nat. Rev. Genet.* **4,** 296–307.

Wolstenholme, J. (1996). Confined placental mosaicism for trisomies 2, 3, 7, 8, 9, 16, and 22: Their incidence, likely origins, and mechanisms for cell lineage compartmentalization. *Prenat. Diagn.* **16,** 511–524.

Yamada, K., Kasama, M., Kondo, T., Shinoura, N., and Yoshioka, M. (1994). Chromosome studies in 70 brain tumors with special attention to sex chromosome loss and single autosome aneuploidy. *Cancer Genet. Cytogenet.* **73,** 46–52.

Yamazaki, Y., Makino, H., Hamaguchi-Hamada, K., Hamada, S., Sugino, H., Kawase, E., Miyata, T., Ogawa, M., Yanagimachi, R., and Yagi, T. (2001). Assessment of the development totipotency of neural cells in the cerebral cortex of mouse embryos by nuclear transfer. *Proc. Natl. Acad. Sci. USA* **98,** 14022–14026.

Yang, A. H., Kaushal, D., Rehen, S. K., Kriedt, K., Kingsbury, M. A., McConnell, M. J., and Chun, J. (2003). Chromosome segregation defects contribute to aneuploidy in normal neural progenitor cells. *J. Neurosci.* **23,** 10454–10462.

Yang, Y., Geldmacher, D. S., and Herrup, K. (2001). DNA replication precedes neuronal cell death in Alzheimer's disease. *J. Neurosci.* **21,** 2661–2668.

Youssoufian, H., and Pyeritz, R. E. (2002). Mechanisms and consequences of somatic mosaicism in humans. *Nat. Rev. Genet.* **3,** 748–758.

Yurov, Y. B., Saias, M. J., Vorsanova, S. G., Erny, R., Soloviev, I. V., Sharonin, V. O., Guichaoua, M. R., and Luciani, J. M. (1996a). Rapid chromosomal analysis of germ-line cells by FISH: An investigation of an infertile male with large-headed spermatozoa. *Mol. Hum. Reprod.* **2,** 665–668.

Yurov, Y. B., Soloviev, I. V., Vorsanova, S. G., Marcais, B., Roizes, G., and Lewis, R. (1996b). High resolution fluorescence *in situ* hybridization using cyanine and fluorescein dyes: Ultra-rapid chromosome detection by directly fluorescently labeled alphoid DNA probes. *Hum. Genet.* **97,** 390–398.

Yurov, Y. B., Vostrikov, V. M., Vorsanova, S. G., Monakhov, V. V., and Iourov, I. Y. (2001). Multicolor fluorescent *in situ* hybridization on post–mortem brain in schizophrenia as an approach for identification of low-level chromosomal aneuploidy in neuropsychiatric diseases. *Brain Dev.* **23**(Suppl. 1), 186–190.

Yurov, Y. B., Vostrikov, V. M., Monakhov, V. V., Iourov, I. Y., and Vorsanova, S. G. (2003). Evidence for large scale chromosomal variations in neuronal cells of the fetal human brain. *Balkan J. Med. Genet.* **6,** 95–99.

Yurov, Y. B., Iourov, I. Y., Monakhov, V. V., Soloviev, I. V., Vostrikov, V. M., and Vorsanova, S. G. (2005). The variation of aneuploidy frequency in the developing and adult human brain revealed by an interphase FISH study. *J. Histochem. Cytochem.* **53,** 385–390.

Zaragoza, M. V., Milie, E., Redline, R. W., and Hassold, T. J. (1998). Studies of non-disjunction in trisomies 2, 7, 15, and 22: Does the parental origin of trisomy influence placental morphology? *J. Med. Genet.* **35,** 924–931.

Zhivotovski, B., and Kroemer, G. (2004). Apoptosis and genomic instability. *Nat. Rev. Mol. Cell. Biol.* **5,** 752–762.

Zink, D., Cremer, T., Saffrich, R., Fischer, R., Trendelenburg, M. F., Ansorge, W., and Seltzer, E. H. K. (1998). Structure and dynamics of human interphase chromosome territories *in vivo*. *Hum. Genet.* **102,** 241–251.

This page intentionally left blank

Automated Interpretation of Protein Subcellular Location Patterns

Xiang Chen* and Robert F. Murphy*†
*Department of Biological Sciences, Center for Automated Learning and Discovery and Center for Bioimage Informatics
Carnegie Mellon University, Pittsburgh, Pennsylvania 15213
†Department of Biomedical Engineering, Carnegie Mellon University
Pittsburgh, Pennsylvania 15213

Proteomics is a major current focus of biomedical research, and location proteomics is the important branch of proteomics that systematically studies the subcellular distributions for all proteins expressed in a given cell type. Fluorescence microscopy of labeled proteins is currently the main methodology to obtain location information. Traditionally, microscope images are analyzed by visual inspection, which suffers from inefficiency and inconsistency. Automated and objective interpretation approaches are therefore needed for location proteomics. In this article, we briefly review recent advances in automated imaging interpretation tools, including supervised classification (which assigns location pattern labels to previously unseen images), unsupervised clustering (which groups proteins based on the similarity among their subcellular distributions), and additional statistical tools that can aid cell and molecular biologists who use microscopy in their work.

KEY WORDS: Location proteomics, Subcellular location features, Fluorescence microscopy, Cluster analysis, Protein distribution comparison, CD-tagging, Systems biology.

0074-7696/06 $35.00
DOI: 10.1016/S0074-7696(06)49004-5

I. Introduction

With the development of high-throughput analysis techniques, the approaches used for biological and biomedical research have been fundamentally changed. The completion of sequencing for dozens of genomes has revolutionized the way we think about acquiring biological data. We can now imagine projects to acquire comprehensive data in a reasonable time frame for a specific characteristic (sequence, structure, function, interaction, etc.) for a complete set of molecules (DNA, RNA, protein, lipids, etc.) in a given organism.

Although DNA contains all of the genetic information for an organism, it is largely protein expression that differentiates cell types within that organism. Therefore, the focus of biological research has shifted from genomics, which mainly studies sequence information, to proteomics, where the central goal is to characterize protein functionality.

Proteomics systematically characterizes different properties of all proteins in a given cell type or tissue, including their sequences, expression levels, structures, functions, regulations, interactions, and location patterns. Knowledge of the location pattern of a protein is necessary for a complete understanding of its function. There are a number of ways in which this is true. First, location pattern changes often correlate with activity changes. For example, it has been shown that activation of the *rgr* oncogene is partially associated with a change of its location pattern from the endomembrane network to the plasma membrane, which facilitates interaction with RAS and activates the RAS downstream pathways (Hernandez-Munoz *et al.*, 2003). Activity of p53 is also regulated by its location (O'Brate and Giannakakou, 2003). The protective effects of extracellular signal-regulated kinase 2 (ERK2) against apoptogenic stimuli are also dependent on the cellular location of ERK activation (Ajenjo *et al.*, 2004). Second, protein mislocalization is often associated with disease. For example, while lamin B receptors (LBR) are located in the inner nuclear membrane in normal cells, they are largely distributed in the cytoplasm in cells carrying a mutation that causes an autosomal-dominant form of Emery–Dreifuss muscular dystrophy (Reichart *et al.*, 2004). Third, the relationship between two proteins' locations can be used to support (or question) protein interaction results found in other experiments (such as those from yeast two-hybrid screening) since components of a single protein complex may be expected to have the same distribution pattern. We have coined the term location proteomics to describe the systematic study of protein location patterns (Chen *et al.*, 2003). It requires (1) methods to either experimentally determine or predict location patterns for all proteins, and (2) methods to systematically organize the set of possible locations where a protein can be found. This chapter reviews work

focused on automated experimental determination and discovery of protein location patterns.

II. Subcellular Location of Proteins

A. Description, Prediction, and Determination

1. Gene Ontology

Currently the most systematic approach to define and organize the set of all possible location patterns is the set of terms for "cellular component" in the Gene Ontology (GO) (Harris *et al.*, 2004). Cellular component is one of the three general categories defined in the GO database, describing locations at subcellular structure (such as plasma membrane) and macromolecular complex (such as the ubiquitin ligase complex) levels. The "cell" term (GO:0005623) in GO describes all components within and including plasma membrane as well as extracellular structures. The cellular component ontology is represented as a directed acyclic graph (DAG) in which location terms are grouped into higher order structures. A DAG differs from a tree-structured hierarchy in that a child can have multiple parents (i.e., multiple paths from the root to a specific node). For example, two GO codes are found for mouse Atp5a1 protein (ATP synthase, H^+ transporting, mitochondrial F1 complex, α subunit, isoform 1): GO:0005739 (mitochondrion) and GO:0005615 (extracellular space). A portion of the cellular component ontology leading to GO:0005739 (mitochondrion) is shown in Fig. 1.

2. Overview of Current Methodology for Protein Location Prediction and Determination

Genome sequencing projects have produced large numbers of putative amino acid sequences that are often largely unannotated. To learn protein functions in the context of their subcellular organelle, it is crucial either to experimentally determine their location pattern or to predict their subcellular location from a sequence.

a. Protein Subcellular Location Prediction In the past decade, many efforts have been made to develop location prediction methods using different approaches. One category of approaches is based on protein sequence similarity, such as LOCKey (Nair and Rost, 2002) and Proteome Analyst (Lu *et al.*, 2004). A protein sequence is searched against a set of experimentally annotated sequences, and text features are extracted from homologs and

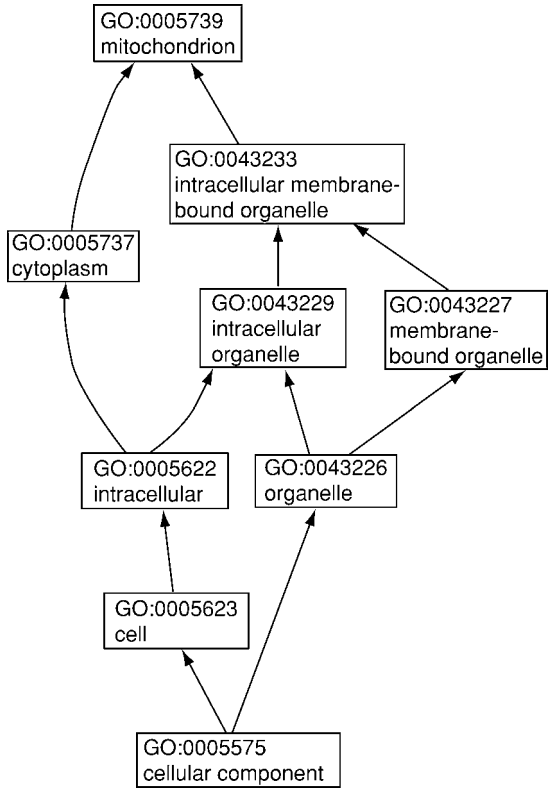

FIG. 1 Portion of cellular component ontology for GO:0005739 (mitochondrion).

used to predict the location pattern. However, this approach suffers when there is no significant match between the query protein and proteins in the training set. The second set of approaches is based on amino acid composition (or its variations), and includes NNPSL (Reinhardt and Hubbard, 1998) and SubLoc (Hua and Sun, 2001). Information about amino acid compositions and the correlation between amino acids is used as features for prediction. Although these approaches utilize general information of proteins, it is not clear whether they can capture enough information to distinguish the difference between some slightly different patterns (such as endosome and lysosome). A third category is based on motif finding, such as TargetP (Emanuelsson *et al.*, 2000). This approach tries to identify motifs that are important for localization (such as signal peptides) in the target sequence and use this information for prediction. The major limitations for this approach are (1) not all proteins in the same subcellular location have the same motif and (2) many genes in automatically annotated genomes have

unreliable 5′ sequences. Most current methods, such as PSORT (Nakai and Horton, 1999; Nakai and Kanehisa, 1992), LOC3D (Nair and Rost, 2003), and LOCtarget (Nair and Rost, 2004) use a mixture of these approaches to achieve better performance. Current research in this area focuses on (1) design of more discriminating sequence descriptors, (2) improvement of classification algorithms, and (3) incorporation of Gene Ontology information into the classification scheme.

Even with recent improvements, current prediction algorithms still suffer from two major limitations: (1) unsatisfactory prediction accuracy, especially for some organelles (such as mitochondria), and (2) limited coverage, both for the number of location patterns and for the number of taxonomic categories covered in prediction.

b. Protein Subcellular Location Determination Protein subcellular location prediction algorithms require a large database of proteins with experimentally determined locations. Without major improvement in automated determination of protein location patterns, the prediction methods will inevitably suffer from limited prediction accuracies and limited coverage. For example, many similar but still statistically different location patterns exhibited by different proteins in the same organelle or compartment cannot be distinguished by predictive schemes until there are sensitive and consistent methods to identify and systematically describe these slight differences in the first place.

Different approaches can be employed to determine protein location patterns. For example, differential centrifugation separation can be used to obtain subcellular fractions (Hardonk *et al.*, 1977) and proteins contained in each fraction can be identified by two-dimensional polyacrylamide gel electrophoresis, enzymatic digestion of separated protein spots, and mass spectrometry analysis. This approach is usually labor-intensive, and the resolution of differential centrifugation separation is limited. Recently, efforts have been made to create a high-throughput protocol for this approach (Jiang *et al.*, 2004).

Different microscopy technologies can also be employed for protein location study. For example, electron microscopy (Subramaniam and Milne, 2004), which provides ultrahigh resolution of the specimen, can be used to achieve precise localization information (Lujan, 2004). Because electron microscopy cannot be carried out on live cells, fluorescence microscopy has become the most commonly used technique to study protein distribution within a cell and the relationships between different proteins (i.e., colocalization of two proteins) (Brelie *et al.*, 2002).

Traditionally protein locations are determined from images by visual inspection. For large-scale, systematic location proteomics, however, visual inspection is no longer feasible since it is labor-intensive and can be highly

subjective. Unfortunately, while the determination of sequence, expression, and even structure has been automated and large-scale high-throughput projects have been initiated (Macbeath, 2002; Norin and Sundstrom, 2002), the automated determination of protein location patterns has just begun. Here we review current achievements for automated interpretation of protein subcellular location patterns from fluorescence microscopy images.

B. Fluorescent Labeling of Proteins

Modern fluorescence microscopy combines high-performance optical components with digital image acquisition components and computerized control to allow imaging of cells and tissues with a combination of temporal and spatial resolution and sensitivity achievable by no other method. Confocal approaches use spatial filtering to reduce or eliminate out-of-focus light and permit images of thin optical slices to be acquired. This provides confocal microscopy with the ability to collect a series of image sections in a thick specimen, and has led to the tremendous popularity of confocal microscopy (and its cousin, two-photon microscopy) in recent years.

While cells have some intrinsic fluorescence, little information can be obtained by fluorescence microscopy of unstained cells. The coupling of fluorophores and target proteins is therefore the key step in preparation for a fluorescence microscopy experiment. In general, there are two types of techniques used for this purpose.

The first method, commonly referred to as *immunofluorescence*, relies on delivering *external* fluorescent molecules into cells (Fujiwara and Pollard, 1976). Cells are first *fixed* by adding a substance (e.g., paraformaldehyde) that cross-links proteins in the cell, essentially immobilizing all cellular components. This prevents the contents of the cells from washing away when the cells are *permeabilized*; i.e., when a detergent is used to fully or partially dissolve the cell membrane. With the membrane barrier out of the way it is possible to introduce desired molecules into the cell—for example, antibodies conjugated to fluorescent dyes. An alternative to using antibodies is to use other substances known to bind to a particular protein. For example, the compound phalloidin binds to F-actin, the polymerized protein that forms part of the cytoskeleton. Therefore dye-conjugated phalloidin can be used to label the actin cytoskeleton. The use of such probes is not strictly *immuno*fluorescence, but, if the probes are specific and require permeabilization for entry, it is functionally identical. There are several limitations to immunofluorescent labeling, including dependence on the existence of specific antibodies or probes that are known to bind to the protein of interest and an inability to image live cells due to the need for fixation and permeabilization (which may also disrupt cellular structures). Vital fluorescent

probes, such as probes that equilibrate preferentially into an organelle, address the latter limitation but not the former.

The second method therefore is to have fluorescent molecules *internally* generated in the cells. DNA sequences coding for a naturally fluorescent protein (such as the green fluorescent protein, GFP) can be joined to either cDNA or genomic DNA to produce a fluorescent chimeric protein. If a genomic approach is used, either a specific gene or a random location in the genome can be tagged. There have been several examples of this approach (Habeler *et al.*, 2002; Jarvik *et al.*, 1996; Rolls *et al.*, 1999; Telmer *et al.*, 2002). Random tagging of proteins can also be done with the use of small epitopes (essentially short sections of a protein) instead of fluorescent proteins (Kumar *et al.*, 2000, 2002). In this case either a fluorescent antibody against the epitope tag (which requires fixation and permeabilization) or a cell-permeant fluorescent probe that binds to specific epitopes can be used (Griffin *et al.*, 1998). Epitope tags can be much smaller than fluorescent proteins and are less likely to disrupt the function of the protein to which they are attached.

When random-tagging experiments are repeated enough times, eventually most (or possibly all) proteins in a given cell type can be labeled. Combined with fluorescence microscopy, random tagging allows comprehensive libraries of images depicting the location patterns of proteins in a given cell type to be generated.

Assuming that a (large) collection of digital images has been acquired by one or more of the above methods, the next step is to automate extraction of information.

III. Subcellular Location Patterns of Proteins

A. Automated Classification

The first basic task to be carried out by automated interpretation is to assign a location pattern label to a previously unseen image. This task can be formalized as

> Given a set of images I_{known} and corresponding labels Y_{known}, learn a mapping function f between I_{known} and Y_{known}, such that when a new image $i \notin I_{\text{known}}$ is presented the label $y = f(i)$ that is assigned is optimal according to some criteria.

Such a system is termed a classifier.

Different approaches can be used for this task. Either raw images or characteristics (termed *features*) extracted from raw images can be used as input into a classifier. Most work in the area of subcellular analysis has

utilized the latter approach (Boland and Murphy, 2001; Boland *et al.*, 1998; Chen and Murphy, 2004; Conrad *et al.*, 2004; Huang and Murphy, 2004b; Murphy *et al.*, 2000; Steckling *et al.*, 2004), although a successful application of the first approach has been reported (Danckaert *et al.*, 2002). The reason for this preference is obvious: cells vary greatly in their size, shape, intensity, position, and orientation in fluorescent images, and as a result, raw pixel intensity values in general are not very useful in location pattern recognition. Consequently, the feature-based approach is the focus of this review.

The core of the feature-based approaches is the development of sets of numerical features to represent patterns that are not overly sensitive to changes in intensity, rotation, and position of a cell (Boland and Murphy, 2001; Murphy *et al.*, 2000). Several categories of features have been used for this purpose, including morphological, Zernike moment, Harlick texture, and wavelet features. A standard nomenclature for referring to specific features and sets of features has been introduced, in which the prefix SLF (for subcellular location feature) is followed by either the number of a set of features (e.g., SLF1) or a number and a subindex for a specific feature (e.g., SLF7.3). Tables I and II summarize all SLFs developed so far for two-dimensional (2D) and three-dimensional (3D) images, respectively.

Experience gained from the work described below indicates that calculation of a large number of features (dozens, even hundreds) from a number of different categories can benefit a classifier, since they may contain different types of information. However, this potential advantage comes at a cost: the automated classifier becomes more complicated when more input features are included. Computational learning theory (Mitchell, 1997) points out that the number of training samples required is linear with the complexity. Therefore, a large set of input features can be used only when sufficient training images are available. Unfortunately, even with the newly developed automated techniques, image collection can still be a slow process and often only limited training samples are available. In this situation, more features do not guarantee better performance. Therefore, reducing the size of the feature set by eliminating redundant or uninformative features is desirable in many machine learning applications. In addition to helping with classification problems, using fewer features is preferred for applications involving retrieval of images from databases using image content.

Different feature reduction methods have been tried for this problem, including both feature recombination and feature selection methods. Feature selection methods were observed to achieve better performance than feature recombination methods in the context of subcellular pattern analysis (Huang *et al.*, 2003). Among feature selection methods, stepwise discriminant analysis (SDA) and genetic algorithms have been observed to achieve the best overall classification accuracy, and SDA is preferred since it is much more

TABLE I
Subcellular Location Feature Sets for 2D Images

Feature set name	Number of features	Feature selection	Feature categories[a]									Reference
			M	E	C	S	D	Z	H	W	G	
SLF1	16	Unselected	8	6	2							Boland and Murphy (2001)
SLF2	22	Unselected	8	6	2		6					Boland and Murphy (2001)
SLF3	78	Unselected	8	6	2			49	13			Boland and Murphy (2001)
SLF4	84	Unselected	8	6	2		6	49	13			Boland and Murphy (2001)
SLF5	37	Selected from SLF4	8	2	1		3	11	12			Boland and Murphy (2001)
SLF6	65	Unselected	8	6	2			49				
SLF7	84	Unselected	9	6	2	5		49	13			Murphy *et al*. (2002)
SLF8	32	Selected from SLF7	8	3		3		7	11			Murphy *et al*. (2002)
SLF12	8	The first eight features from SLF8	2	1				2	3			Huang *et al*. (2003)
SLF13	31	Selected from SLF7 and six DNA features	6	3		3	3	7	9			Murphy *et al*. (2003)
SLF15	44	Selected	6	4	2	2		12	7	2	12	Huang and Murphy (2004b)
SLF16	47	Selected	5	4	2	2	3	12	7	4	11	Huang and Murphy (2004b)

[a]The feature categories are M, morphological features; E, edge features; C, convex hull features; S, object skeleton features; D, DNA features; Z, Zernike moment features; H, Haralick texture features; W, Daubechies D4 wavelet features; G, Gabor features.

TABLE II
Subcellular Location Feature Sets for 3D Images

Feature set name	Parallel DNA requirement	Number of features	Short description	Reference
3D-SLF9	Yes	28	Unselected morphological features	Velliste and Murphy (2002)
3D-SLF10	Yes	9	SDA selected features from 3D-SLF9	N/A
3D-SLF11	No	42	Unselected morphological, edge and Haralick texture features	Chen *et al*. (2003)
3D-SLF14	No	14	Subset of 3D-SLF9 which does not require DNA image	N/A
3D-SLF17	No	7	The first seven SDA selected features from 3D-SLF11 on 3D HeLa set[a]	Chen and Murphy (2004)
3D-SLF18	No	34	The first 34 SDA selected features from 3D-SLF11 on 3D 3T3 set[b]	Chen and Murphy (2005)
3D-SLF19	Yes	56	3D-SLF11 and 14 DNA features from 3D- SLF9	Nair *et al*. (2005)
3D-SLF20	Yes	52	SDA selected features from 3D- SLF19	Nair *et al*. (2005)

[a]The 3D Haralick texture features were calculated at 0.4 μm pixel resolution and 256 gray levels. This feature set achieved 98% overall classification on the 3D HeLa dataset.

[b]The 3D Haralick texture features were calculated at 0.5 μm pixel resolution and 64 gray levels. This feature set is used for clustering the 3D 3T3 dataset.

computationally efficient (i.e., it requires less computer time to find a good subset of features).

1. Classification Based on Cell Level Features

Studies of protein subcellular location patterns are most easily understood in the context of a single cell. Consequently, automated classification of protein location patterns was initially carried out on single cell images.

However, many acquired images contain multiple cells per field. To properly calculate features at the level of each cell, regions of each image corresponding to a single cell need to be defined. This *cell segmentation* can be done either manually (by drawing a polygon for each cell) (Boland and Murphy, 2001) or automatically (i.e., with balloon or watershed algorithms) (De Solorzano *et al.*, 2001; Nair *et al.*, 2005; Velliste and Murphy, 2002). The automated methods usually utilize either total protein staining (so that each cell appears as a contiguous region) or surface protein staining (so that the cell boundary is visible).

a. Classification of Major Subcellular Location Patterns in HeLa Cells Using 2D Images To test the feasibility of using automated classification to determine protein subcellular location patterns, a 2D image dataset that covers all major location patterns was first generated in HeLa cells (Boland and Murphy, 2001). Nine proteins were fluorescently labeled, eight using antibodies against proteins in the endoplasmic reticulum (ER), Golgi (giantin and gpp130), lysosomes (LAMP2), endosomes (transferrin receptor), mitochondria, nucleoli (nucleolin), and microtubules (tubulin), and one using phalloidin that binds to microfilaments (actin). DNA was simultaneously labeled with a fluorescent probe (DAPI) that could be separately detected. Two Golgi proteins (giantin and gpp130) were intentionally included to test the distinguishing power of automated classifiers. These two proteins are almost indistinguishable by human visual inspection (Murphy *et al.*, 2003). The dataset contains 78–98 single cell images per class and 862 images in total. Figure 2 shows representative images for this dataset.

i. Optimizing Classification Accuracy A steady improvement in the accuracy of classification of this dataset has been achieved over the past few years. With the implementation of new features and the choice of more robust classifiers, the overall classification accuracy improved from 84% with a set of 37 features and a neural network classifier (Boland and Murphy, 2001) to the current best accuracy of 92.3% with 47 features and a majority-voting ensemble classifier (Huang and Murphy, 2004b). The performance of the current best classifier is presented in Table III in the form of a confusion matrix. The diagonal numbers of the confusion matrix show the accuracies for each individual class and the off-diagonal numbers represent the

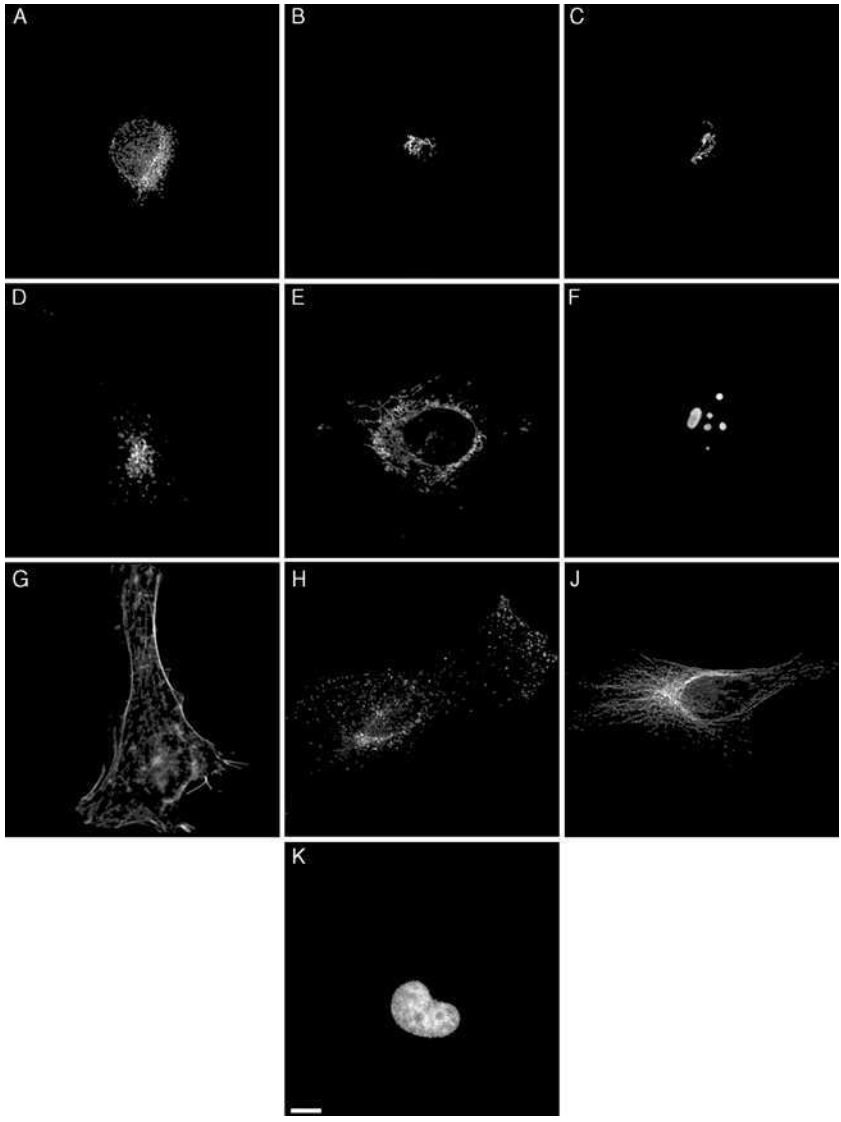

FIG. 2 Typical images from the 2D HeLa image dataset. Images are shown for cells labeled with antibodies against an ER protein (A), the Golgi protein giantin (B), the Golgi protein gpp130 (C), the lysosomal protein LAMP2 (D), a mitochondrial protein (E), the nucleolar protein nucleolin (F), the endosomal protein transferrin receptor (H), and the cytoskeletal protein tubulin (J). Filamentous actin was labeled with rhodamine-phalloidin (G) and DNA was labeled with DAPI (K). Scale bar = 10 μ. (From Boland and Murphy, 2001.)

TABLE III
Confusion Matrix for a Majority Voting Ensemble Classifier with SLF16 for the 2D HeLa Dataset[a]

	Output of the classifier									
True class	DNA	ER	Gia	GPP	LAM	Mit	Nuc	Act	TfR	Tub
DNA	99	1	0	0	0	0	0	0	0	0
ER	0	97	0	0	0	2	0	0	0	1
Giantin	0	0	91	7	0	0	0	0	2	0
GPP130	0	0	14	82	0	0	2	0	1	0
LAMP2	0	0	1	0	88	1	0	0	10	0
Mitochondria	0	3	0	0	0	92	0	0	3	3
Nucleolin	0	0	0	0	0	0	99	0	1	0
Actin	0	0	0	0	0	0	0	100	0	0
TfR	0	1	0	0	12	2	0	1	81	2
Tubulin	1	2	0	0	0	1	0	0	1	95

[a]The values shown are the percentage of images from the class shown in the row heading that were classified as being in the class shown by the column heading. The overall accuracy is 92.3%. From Huang and Murphy (2004).

percentage of test samples of each ''True'' class (row heading) misclassified as the ''Predicted'' class (column heading). We can interpret the classifier's performance on each individual class from the confusion matrix. For example, the classifier shown in Table III correctly classified 88% of LAMP2 classes and mistakenly classified 1% of LAMP2 as giantin, 1% as mitochondria, and 10% as tubulin. Due to rounding errors, the sum for a row is not necessarily 100%.

ii. Tradeoff between Classification Accuracy and Computation Cost of the Feature Set The features (SLF16) used to achieve the best accuracy of 92.3% were SDA selected from a mixture of 180 features of various types (including wavelet features). Since wavelet feature calculation involves rotating each image to a common frame of reference and then decomposing it with different scale filters, the computation cost (CPU time per image) is significantly higher than for the other features (Huang and Murphy, 2004b). When the computation cost is a concern, a feature set (SLF13) with 31 features selected by SDA from all features except the wavelet features achieved a 90.7% classification accuracy with one-sixth of the average CPU time for feature calculation (Huang and Murphy, 2004b).

iii. Classification without Parallel DNA Images A parallel DNA channel provides information on nuclear location, which serves as a reference point for the cell center. Several features were designed to capture protein

distribution information relative to the nucleus and these features were included in the input feature sets above that give the best overall classification accuracy. However, not all imaging protocols require or permit the acquisition of the parallel DNA channel. A feature set with no DNA information is preferred for those cases.

A feature subset (SLF15) with 44 features SDA selected from a mixture of features that does not require DNA information achieved 91.5% overall classification accuracy (Huang and Murphy, 2004b), which indicates that while not having DNA features degrades classification performance slightly, satisfactory performance can still be achieved without them. An overall classification accuracy of 89.7% is achieved by a similar classifier trained on SDA-selected features (SLF8 with 32 features) when computation-costly wavelet features are removed (Huang and Murphy, 2004b). These results suggest that when using numerical features, the protein subcellular location pattern can be automatically determined in a reasonable time scale from fluorescence microscope images acquired using standard protocols that do not require collection of DNA images.

iv. Classification of Sets of Images When evaluating a protein's location, a cell biologist will usually not make a decision based on an image of a single cell. Instead, a set of images is viewed and a final conclusion is based on an overall impression. The same rationale can be used for automated classifiers. By considering sets of cells as small as 10 and choosing the label that has the most images assigned to it, an overall classification accuracy of 98% could be obtained with a classifier that had an average accuracy of only 83% on single cells (Boland and Murphy, 2001).

b. Classification of Two Proteins with Visually Similar Patterns in CSO-1 Cells Using 2D Images A similar feature-based approach was use to distinguish two visually similar proteins (Huntingtin and GIT) in CSO-1 cells (Steckling *et al.*, 2004). For this task, seven features, mostly defined in the previous section, were used to train a maximum likelihood classification scheme to separate the two proteins. In this experiment, 87% of the test images were correctly classified. This independent research confirms that the location pattern of previously unknown proteins could be automatically identified by feature-based approaches.

c. Classification of Images from Automated Microscopy An alternative to genomic tagging that is suitable for automated acquisition and analysis is the creation of a cell array in which each spot in the array contains a different GFP-tagged cDNA (Ziauddin and Sabatini, 2001). This approach has been combined with automated microscopy to demonstrate the feasibility of classifying images from automated acquisition (Conrad *et al.*, 2004). In this

study, images for 11 cDNAs showing different subcellular location patterns were captured automatically. An SVM classifier achieved an 82.2% overall classification with 25 SDA-selected features drawn from a large number of features (448) extracted from different feature categories (such as object, edge, texture, moments, wavelets). Achieving this accuracy required training of the system to recognize an "artifact" category; approximately half of the images were found to be in this category. Even with this step, the observed accuracies for two of the categories (ER and microtubules) were below 50%. The results are encouraging for the application of the methods described in this chapter to images obtained by automated microscopy.

d. Classification of Major Subcellular Location Patterns in HeLa Cells Using 3D Images With the development of optical sectioning techniques (i.e., confocal microscopy), it has become increasingly common to collect 3D images when visualizing protein distributions. A 3D image is simply a stack of 2D images taken at different focal planes. Compared to their 2D counterparts, 3D fluorescence images provide an opportunity to achieve better classification accuracy since we can expect that 3D images contain more information content than 2D images. Indistinguishable location patterns in a 2D slice could be potentially separated by their distribution along the third dimension. This is obvious for polarized cells where the protein composition of the apical surface is different from that of the basal and lateral surface. In this case, the protein distribution is different among three dimensions. Even for an unpolarized cell, the protein distribution on the third dimension still provides extra information that may help in distinguishing different patterns. For example, F-actin in HeLa cells is preferentially located above the nucleus while tubulin is more concentrated near the bottom of the cell.

A 3D HeLa cell image dataset was collected using the same labeling techniques as for the 2D HeLa dataset to determine whether an improved classification accuracy could be obtained (Velliste and Murphy, 2002). This dataset contains 50–52 single cell images per class and 502 imaged cells in total. Figure 3 shows the representative images of this dataset.

Most 3D features [morphological (Velliste and Murphy, 2002), edge (Chen *et al.*, 2003), and Haralick texture features (Chen *et al.*, 2003)] were natural extensions of their 2D versions. Some new features were also implemented to capture characteristics of protein fluorescence distribution along the z axis.

An overall classification accuracy of 98% was achieved using 3D-SLF17, an SDA-selected feature subset of seven features. Table IV shows the confusion matrix for this case. The results suggest that the classifier is near optimal, since cells were imaged randomly and inevitably a small fraction of "abnormal" cells, such as mitotic or dying cells, would be expected to be included. Protein location patterns in these cells are likely different from those

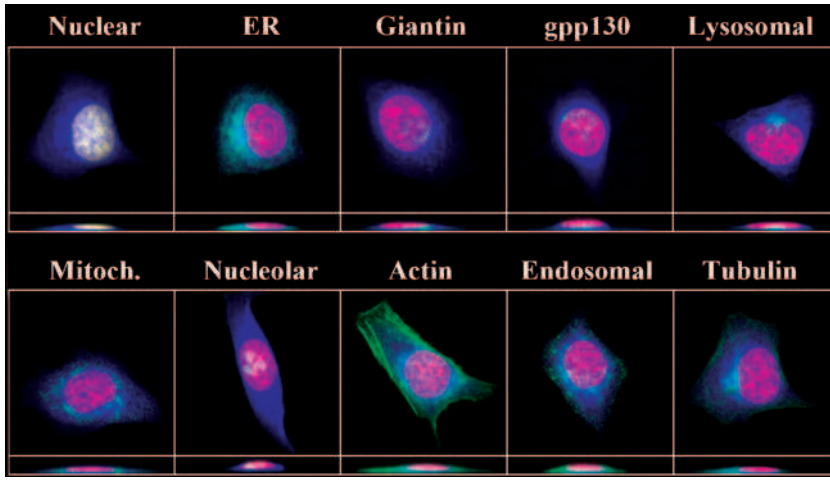

FIG. 3 Typical images from the 3D HeLa image dataset. Red, blue, and green colors represent DNA staining, total protein staining, and target protein fluorescence. Projections on the X–Y (top) and the X–Z (bottom) planes are shown. The proteins labeled are the same as those in the 2D HeLa image dataset (Fig. 2). (Reprinted by permission of Carnegie Mellon University.)

TABLE IV
Confusion Matrix for a Neural Network Classifier with 3D-SLF17 for the 3D HeLa Dataset[a]

	Output of the classifier									
True class	DNA	ER	Gia	Gpp	LAM	Mit	Nuc	Act	TfR	Tub
DNA	98	2	0	0	0	0	0	0	0	0
ER	0	100	0	0	0	0	0	0	0	0
Giantin	0	0	100	0	0	0	0	0	0	0
Gpp130	0	0	0	96	4	0	0	0	0	0
LAMP2	0	0	0	4	95	0	0	0	0	2
Mitochondria	0	0	2	0	0	96	0	2	0	0
Nucleolin	0	0	0	0	0	0	100	0	0	0
Actin	0	0	0	0	0	0	0	100	0	0
TfR	0	0	0	0	2	0	0	0	96	2
Tubulin	0	2	0	0	0	0	0	0	0	98

[a]The values shown are the percent of images from the class shown in the row heading that were classified as being in the class shown by the column heading. The overall accuracy is 98%. From Chen and Murphy (2004).

observed in normal cells and could account for the small classification errors. It is also worth noting that the 3D classifier is the first that is able to distinguish giantin and gpp130, two proteins known to be located in slightly different parts of the Golgi apparatus, with over 95% accuracy at the single cell level.

3D-SLF17 consists of at least one feature from each category (morphological, edge, and Haralick texture for 3D images), suggesting that different feature categories capture different information in the image and an optimal classifier should be trained from a combination of features from different categories. 3D-SLF17 can be calculated efficiently, as the time-consuming wavelet features are not included. Another important advantage of 3D-SLF17 is that it does not require a parallel DNA image. It confirms that for 3D images, even without the reference DNA information, an optimal classifier could be trained to learn major subcellular location patterns, a crucial step in extending the feature-based approach toward general usage for biological and biomedical researchers.

The already impressive performance can be improved further by classifying sets of images. Trained classifiers (using either neural networks or support vector machines) achieved above 99% classification accuracy with a set size of 3 and 99.9% with a set size of 5 (data not shown).

2. Classification Using Field Level Features

As discussed above, classifiers trained on SLFs are capable of automatically labeling protein subcellular location patterns in previously unseen images in a single cell setting. However, typically a field containing multiple cells is imaged. Partial cells on the boundary of imaged fields are also frequently observed. Since current SLFs are designed to capture protein spatial distributions in a single cell setting, their use on multiple cells (either intact or partial) would not necessarily give appropriate results. SLF1.1, the number of objects inside the cell (an object is defined as a set of connected above-threshold pixels in the image), is a good example. It is a very useful feature to distinguish the nuclear or nucleolar patterns (with one to a few objects) from the mitochondrial or lysosomal patterns (with hundreds of objects). However, this feature is meaningless if an image contains multiple cells (unless it is known that all images have the same number of cells!). As discussed above, a few automated segmentation algorithms have been described for identifying regions corresponding to a single cell in a multicell field. Unfortunately, they either require extra labeling (such as nucleus, total cellular protein, or plasma membrane protein labeling) or assume specific models (Sclaroff and Liu, 2001), which makes them difficult to be generalized to arbitrary protein fluorescence images. An alternative solution would be a set of features that is not sensitive to the number of cells in a field.

Such a feature set was created by selecting features that meet this requirement from previous SLFs. This approach was tested by building an SVM classifier to recognize images with multiple cells (Huang and Murphy, 2004a). So that the label of each cell in a multicell image could be known with certainty, synthetic multicell images were created by combining single cell images whose location patterns were known. A confusion matrix for this classifier is shown in Table V, and the overall classification accuracy of 94.8% was even higher than for the single cell counterpart. This "surprising" improvement in performance could be partially explained by so-called "majority voting" effects where the effect of abnormal cells in a class is diluted in multicell images so that the classifier makes the correct prediction based on the majority type of cells in a field.

Although experiments classifying 3D multicell images have not yet been carried out, higher accuracy is expected as well since most features in the best 3D feature set (3D-SLF17) are edge and texture features, which are insensitive to the number of cells in the field. The only morphological feature in SLF17 is 3D-SLF9.4, the standard deviation of object volumes, and since it does not depend on the number of cells, it is also a potential field level feature.

3. Classification of Mixed Patterns Using Object Level Features

Previous sections show that a classifier can be trained to distinguish a set of predefined patterns with high accuracy. However, protein localization is a complicated process, and proteins are not restricted to being in a single

TABLE V

Confusion Matrix for an SVM Classifier with Entire 2D Field Level Features for the Multicell Image Dataset[a]

	Output of the classifier									
True class	DNA	ER	Gia	GPP	LAM	Mit	Nuc	Act	TfR	Tub
DNA	100	0	0	0	0	0	0	0	0	0
ER	0	96	0	0	0	0	0	0	4	0
Giantin	0	0	100	0	0	0	0	0	0	0
GPP130	1	0	2	98	0	0	0	0	0	0
LAMP2	0	0	0	4	94	0	0	0	2	0
Mitochondria	0	4	0	2	0	96	0	0	2	0
Nucleolin	0	0	0	0	0	0	100	0	0	0
Actin	0	0	0	0	0	0	0	100	0	0
TfR	0	4	0	0	2	4	4	0	82	4
Tubulin	0	4	0	0	2	4	0	0	8	82

[a]The overall accuracy was 94.8%. From Huang and Murphy (2004a).

organelle. For example, the human mannose 6-phosphate uncovering enzyme (UCE) cycles between the *trans*-Golgi network (TGN) and the plasma membrane (Rohrer and Kornfeld, 2001). In this case, the steady-state pattern of UCE is a mixture of two fundamental location patterns (TGN and plasma membrane) and the feature values for the UCE location pattern would be different from the typical values for either of those fundamental patterns. Consequently, a classifier trained to recognize the two fundamental patterns would fail to recognize this mixed pattern.

A straightforward solution would be to train a classifier to distinguish each possible combination of fundamental location patterns. However, the large number of possible combinations (exponential in the number of fundamental patterns) makes this approach prohibitive. The problem is even more complicated because different mixture ratios would be expected to yield different combined patterns. For example, a Y488A mutation in UCE slows down its traffic from the plasma membrane back to the TGN and consequently the mutant protein has a much higher plasma membrane distribution. The location patterns for wild-type and Y488A-mutant UCE are distinguishable by both human visual inspection and automated machine learning algorithms although they are both mixed from TGN and plasma membrane patterns.

A more suitable approach would be to apply a machine learning algorithm that is capable of recognizing mixtures composed of varying amounts of independent fundamental patterns. An initial approach to this problem has been presented (Zhao *et al.*, 2005). It is based on the principle that each fundamental pattern has a distinguishable (but stochastic) combination of object types. Object types were learned by cluster analysis and then classifiers trained to recognize each type. The distribution of object types within each fundamental pattern was also modeled. The decomposition of an arbitrary mixed image into its component patterns was then carried out by a two-step process. Each object in the image was assigned a type and then the mixture fractions that would most likely have led this distribution of object types were found.

For the training phase of this system, the individual objects in images of known fundamental patterns were first identified and a set of subcellular object features (SOF1, shown in Table VI) was calculated for each. These features for all objects in the dataset were then used to perform cluster analysis to determine the types of objects that exist in the dataset. A classifier was then trained to recognize each object type from its SOFs. Each fundamental pattern (whether for a training image or a test image) could then be represented by the number of objects of each type or the fraction of fluorescence in each object type (or both). This allows the object type vector for a mixture pattern to be considered as a linear combination of object type vectors of component fundamental patterns. The mixture fractions could

TABLE VI

Subcellular Object Features (SOF1) Used to Cluster Objects to Learn Object Types and to Train Classifiers to Recognize Them[a]

Feature ID	Description
SOF1.1	Number of pixels in object
SOF1.2	Distance between object center of fluorescence (COF) and DNA COF
SOF1.3	Fraction of object pixels overlapping with DNA
SOF1.4	A measure of eccentricity of the object
SOF1.5	Euler number of the object
SOF1.6	A measure of roundness of the object
SOF1.7	The length of the object's skeleton
SOF1.8	The ratio of skeleton length to the area of the convex hull of the skeleton
SOF1.9	The fraction of object pixels contained within the skeleton
SOF1.10	The fraction of object fluorescence contained within the skeleton
SOF1.11	The ratio of the number of branch points in the skeleton to the length of the skeleton

[a]From Zhao *et al.* (2005).

then be found by solving a set of linear equations or maximizing the likelihood of a multinomial model.

Using this approach on test images synthesized by creating random mixtures of up to eight subcellular patterns, an average of 83% accuracy in determining the mixture proportions was achieved (Zhao *et al.*, 2005). While further work on this important problem will clearly be required, these initial results suggest that decomposition of complex mixture patterns is feasible.

B. Objective Clustering

It has been shown in the previous section that a classifier trained on SLFs could assign a set of predefined location pattern labels to previously unseen images with high accuracy. However, it remains an open question as to how many location patterns exist in a specific proteome. Ideally, we would like to collect images of all proteins and learn the number of statistically distinguishable location patterns and the identity of each pattern in a proteome. This becomes a typical unsupervised learning problem, addressable by methods of cluster analysis.

Central to unsupervised clustering is the notion of the degree of similarity (or dissimilarity) between individual data points (cell images). A major

advantage of using SLFs to represent images is that the distance between two data points can be easily defined. This measures the dissimilarity between two points, e.g., a larger distance means two points are less similar to each other. Common distance functions include Euclidean distance [2-norm (Qian *et al.*, 2004)], Manhattan distance [1-norm (Batchelor, 1978)], Chebyshev distance [infinity-norm (Diday, 1974)], Mahanlanobis distance (Nadler and Smith, 1993), cosine angle distance (Qian *et al.*, 2004), and Hamming distance [suitable for binary features (Exoo, 2003)].

1. Dendrogram Analysis of the 2D HeLa Dataset

As an initial demonstration of the cluster analysis approach to subcellular patterns, hierarchical clustering was performed on the 10 class 2D HeLa dataset (Murphy *et al.*, 2002). Although many techniques that could improve the quality of the clustering were not used in this simple experiment, the resulting dendrogram (Fig. 4) still revealed that (1) similar location patterns were grouped first (the two Golgi proteins, and the lysosomal and endosomal proteins), and (2) it was consistent with the biological understanding of these organelle patterns. This first result suggested the utility of clustering approaches using SLFs to reveal the intrinsic relationships among subcellular patterns displayed in a dataset.

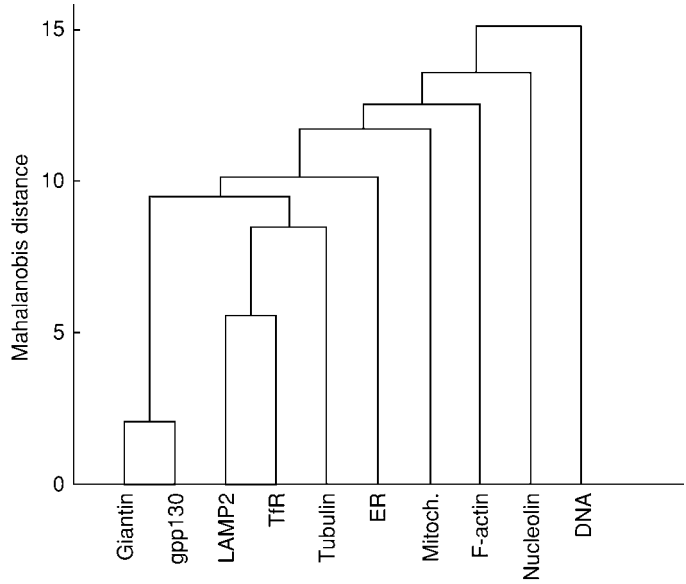

FIG. 4 Subcellular location tree created from the 2D HeLa dataset using SLF8 and hierarchical clustering with a Mahalanobis distance function. (From Murphy *et al.*, 2002. Copyright © 2002, IEEE.)

2. Clustering of the 3D 3T3 Dataset

One of the ultimate goals for location proteomics is to determine which proteins share the same location pattern. In other words, given a set of proteins, each with multiple image representations, we need to find a partitioning so that proteins in one partition share a single location pattern. Ideally, this approach would be applied to images of all proteins expressed in a given cell type. Methods are therefore needed to collect images of the distributions of large numbers of (or all) proteins.

As discussed in Section II.B , this can be done by creating GFP fusions for many different cDNAs and expressing them by carrying out individual transfections. The advantage is that the tagged gene is known in each transfection, but the disadvantage is that the protein is expressed under the control of an exogenous promoter that may lead to overexpression and mislocalization.

An alternative is to create random GFP fusions, make clonal lines, and then determine the tagged gene in each line. Although more work is required to identify the tagged gene, the advantage is that the protein is expressed in its normal genomic context with all transcriptional and posttranscriptional controls intact. One variation on this approach, CD-tagging, is particularly powerful because tags may be inserted at a number of sites on each protein (Jarvik *et al.*, 1996). The CD-tagging method employs an engineered retroviral vector to randomly insert into the target genome a CD-cassette, flanked by splicing acceptor and donor sequences. If the viral vector is inserted into a genomic intron, the CD-cassette will be transcribed as a guest exon. This approach was used in the laboratories of Drs. Jonathan Jarvik and Peter Berget to create a collection of 3T3 cell clones each of which expresses a different tagged protein (Jarvik *et al.*, 2002). The CD-cassette used for this collection contains a GFP coding sequence, thus permitting the tagged proteins to be visualized in live cells. To date, over 90 randomly tagged clones expressing GFP chimera proteins have been isolated. To acquire live cells images with a minimum of blur due to organelle movement, spinning disk confocal microscopy (Kozubek *et al.*, 2004; Nakano, 2002) was used to collect a large number of images of each clone (Chen *et al.*, 2003). The 3D 3T3 dataset obtained to date contains 8–33 single cell images per clone and 1554 images in total. Figure 5 shows representative images of example clones.

Three machine learning algorithms have been applied to the dataset, including k-means clustering of individual cells, hierarchical clustering of mean feature vectors for each clone, and an *ad hoc* clustering algorithm based on a confusion matrix from a classifier trying to identify each individual clone (Chen and Murphy, 2005). Both standardized (z-scored) Euclidean (where each feature is normalized to have unit variance) and Mahalanobis (where the correlation between features is taken into consideration) distance

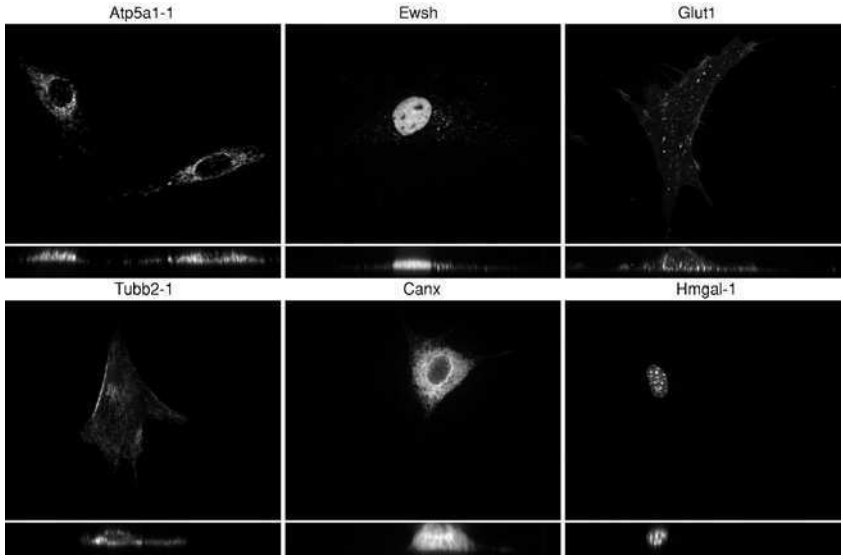

FIG. 5 Selected images from the 3D 3T3 image dataset. Tagged protein names are shown with a hyphen followed by a clone number if the same protein was tagged in more than one clone in the dataset. Projections on the X–Y (top) and the X–Z (bottom) planes are shown. (From Chen and Murphy, 2005.)

functions were evaluated. The performance of machine clustering algorithms was also compared to a grouping based on visual inspection.

A traditional difficulty in machine clustering approaches is to find the number of clusters in a dataset. For example, k-means approaches require the number of clusters to be directly specified in the program. For hierarchical clustering, it is also critical to know which branches represent identical classes. This can be achieved by finding a distance under which the separation is not statistically significant. The distance threshold identified also indirectly determines the number of clusters since data points connected at the threshold belong to the same cluster. In some specific problems, outside information can be used to determine the number of clusters. When this information is not available, a set of trials with different numbers of clusters can be performed and evaluated by some criterion that measures the goodness of the clustering results. There is no prior information suggesting the proper number of clusters for the 3D 3T3 dataset, although a reasonable assumption is that the cells from the same protein clone should belong to a single cluster. Therefore, the goodness of various clustering models was assessed by the Akaike information criterion (AIC) (Ichimura, 1997) for different numbers

of clusters (from two to the number of clones in the dataset) (Chen and Murphy, 2005).

Evaluation of the clustering results using different clustering algorithms and/or different distance functions is an equally difficult task since the actual partition of the dataset is unknown for any real problem setting. Nevertheless, it is reasonable to assume that a good distance function would achieve better agreement among different clustering algorithms. Cohen's κ statistic (Cook, 1998) can be used to measure the agreement between two partitionings. This statistic measures the portion of agreement beyond random and it has a value of 1 if two partitionings are in total agreement and an expected value of 0 if the two partitionings are mutually independent.

Table VII summarizes the comparison of the κ statistic using different clustering algorithms and distance functions. It clearly indicates that the standardized Euclidean distance function achieved better agreement compared to Mahalanobis distance. It also revealed that machine learning clustering algorithms (k-means/AIC, consensus analysis and clustering based on confusion matrix) achieved much higher agreement compared to pairs between a machine algorithm and clustering by visual inspection. The consistency displayed further suggested the value of automated clustering approaches in location proteomics.

When standardized Euclidean distance was used in the k-means/AIC algorithm to cluster the 3D 3T3 dataset, the optimal number of clusters was 30. However, 13 of these clusters contained only outlier images (outliers of a clone were those distributed to any cluster except the one with the most images for that clone). Therefore, these clusters were ignored, leaving 17

TABLE VII
Comparison of Clustering Methods and Distance Functions[a,b]

	Standardized Euclidean distance	Mahalanobis distance
	(κ)	(κ)
k-means/AIC vs. consensus	1	0.5397
k-means/AIC vs. ConfMat	0.4171	0.3634
Consensus vs. ConfMat	0.4171	0.1977
k-means/AIC vs. visual	0.2055	0.1854
Consensus vs. visual	0.2055	0.1156

[a]The agreement between the sets of clusters resulting from the four clustering methods described in the text was measured using the κ test. A value of 1 represents perfect agreement between the clusters formed by the two methods. From Chen and Murphy (2005).

[b]The standard deviations of the statistic under the null hypothesis were estimated to range between 0.014 and 0.023 from multiple simulations.

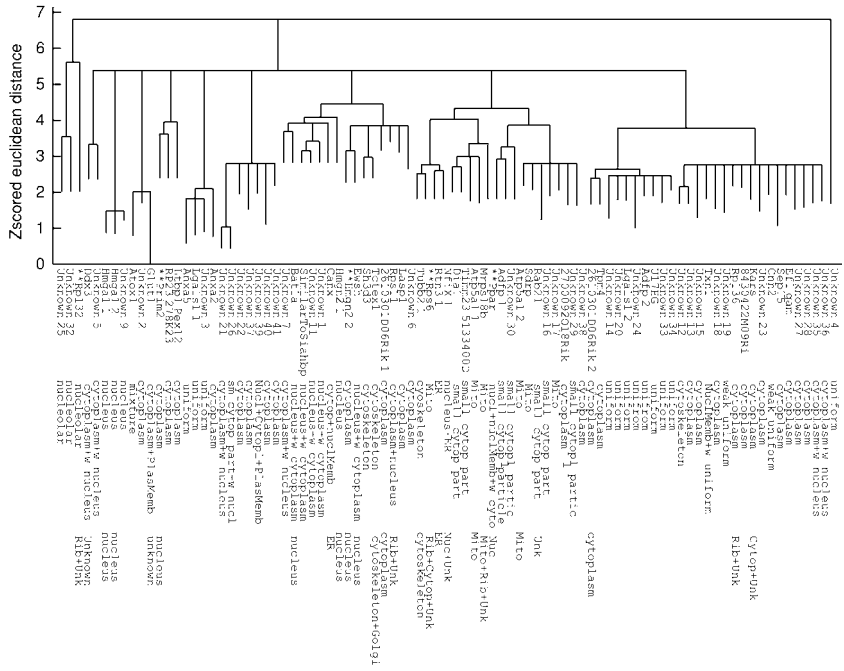

FIG. 6 A consensus subcellular location tree generated for the 3D 3T3 image dataset using 3D-SLF18 features. The columns to the right of the tree show the protein names (if known), descriptions of the subcellular location from visual inspections of the images, and subcellular location inferred from Gene Ontology (GO) annotations (if any). The sum of the lengths of horizontal edges connecting two proteins represents the distance between them in the feature space. Proteins for which the location described by human observation differs significantly from that inferred from GO annotations are marked (**). (From Chen and Murphy, 2005.)

clusters containing the major patterns in the dataset. The consensus tree from hierarchical clustering is displayed in Fig. 6 (this tree and the representative images for each protein clone are available in an interactive web interface: http://murphylab.web.cmu.edu/services/PSLID/tree.html). The same 17 clusters were identified in both the consensus clustering and AIC analysis.

A natural question is whether the clusters obtained from unsupervised learning could be used for supervised training of a classifier to recognize this new set of patterns. When this test was performed, an average accuracy of 87% was achieved. This classifier is able to recognize the largest number of subcellular patterns reported to date.

As at least a partial confirmation of the validity of the results obtained by clustering, we can observe that the tree shows visually similar location

patterns being grouped together. For example, the three nucleolar proteins in the dataset were combined in a distinct cluster. Also, two groups of nuclear proteins were found in the dataset. Close inspection of the images from both groups confirmed that there are differences between them, one with exclusive nucleus distribution and the other with weak cytoplasmic distribution as well (Chen *et al.*, 2003).

3. Cluster Analysis of Location Patterns in UCE Mutants

The clustering results above had the goal of clustering *proteins* with similar patterns. An analogous goal would be to cluster *mutant* versions of a single protein to determine which share the same location. Mutagenesis of suspected targeting sequences is often used to identify important residues in that sequence. To illustrate the value of the clustering approach in this context, we applied it to images of a set of mutants obtained by the laboratory of Dr. Jack Rohrer.

The trafficking of UCE, a key enzyme in lysosome biogenesis, has been discussed briefly above. UCE uncovers the mannose 6-phosphate recognition tag on lysosomal enzymes, a step necessary for mannose 6-phosphate receptors to recognize these enzymes and ensure their sorting to lysosomes. UCE is localized to the TGN in steady state and cycles between the TGN and plasma membrane. It requires targeting information both for exit from the TGN and for return from the plasma membrane. It has been determined that the Y^{488} residue is required for traffic from the plasma membrane back to the TGN since a Y^{488}-A mutant has impaired internalization from the plasma membrane. To locate the sequence that mediates exit from the TGN, the subcellular distributions of a set of mutants created by site-directed mutagenesis of a GFP-tagged UCE were studied by imaging and cluster analysis (Nair *et al.*, 2005).

In an initial experiment, adjacent pairs of residues suspected of being part of the targeting signal were mutagenized. When images of these mutants were clustered, the dendrogram (Fig. 7A, the dendrogram and representative images from each clone are available online at http://murphylab.web.cmu.edu/services/PSLID/HeLa_UCE/Figure4A.html) suggested that mutating the QE or MN residues of the cytoplasmic tail created an intermediate location pattern between wild-type UCE (which exhibited mostly TGN staining) and the Y^{488} mutant (which had a strong plasma membrane distribution). It was therefore postulated that one or more of the Q^{492}EMN residues could be responsible for the traffic from the TGN to the plasma membrane. Mutants with single residue mutation were consequently generated and studied together with the double mutants. The clusters formed by the single and double mutants are shown in Fig. 7B (available online at http://murphylab.web.cmu.edu/services/PSLID/HeLa_UCE/Figure4B.html). The

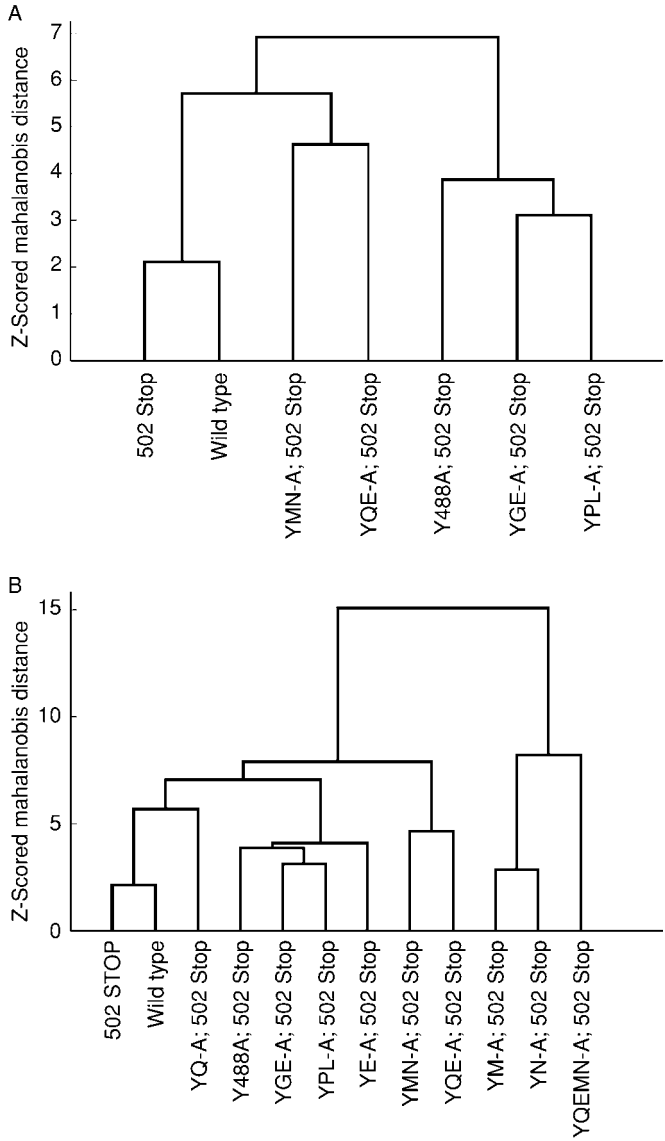

FIG. 7 Subcellular location tree using 3D-SLF20 and Mahalanobis distance showing grouping of various GFP constructs of the uncovering enzyme (UCE) by similarity in localization. (A) Results for the GFP-UCE wild-type, GFP-UCE 502 Stop (which truncates the cytoplasmic tail but does not affect targeting), GFP-UCE Y^{488}-A/502 Stop (which is not internalized from the plasma membrane), and mutant constructs with pairs of the Q^{492}EMNGEPL residues in the cytoplasmic tail of UCE converted to alanine. (B) Results for those mutants plus a mutant with all four of the Q^{492}EMN residues converted to alanine plus single mutants in those four residues. (From Nair *et al.*, 2005.)

largest cluster contained the Y^{488} mutant and three mutants that do not appear to affect TGN exit significantly. A second cluster contained wild-type UCE, a mutant with a truncated cytoplasmic tail that does not affect tracking, and a mutant in which both the Y^{488} and Q^{492} residues were replaced by alanines. The important conclusion is that the first mutation stops return to the TGN but the second mutation compensates for it by preventing exit from the TGN. However, additional conclusions not obvious on visual inspection could also be drawn from the remaining clusters. These are that mutations in the M, N, and E residues, while not blocking TGN exit, conferred a distinct phenotype on the enzyme. The results suggest that yet another step in the traffic process involves those residues.

This experiment indicated that coupled with prior biological knowledge and proper experimental design, an automated interpretation approach could yield new biological knowledge.

4. Clustering Drugs by Their Affects on Location Patterns

The work described above involved clustering of proteins (or mutant proteins) by their location patterns reflected in fluorescence microscope images. Clustering using features derived from analysis of fluorescence microscope images has also been described to group drugs by their mechanism of action on cultured cells (Perlman *et al.*, 2004). In this study, automated microscopy was used to collect 10 images for cells stained in parallel for 10 different marker proteins (plus DNA) upon treatment with one of 100 different drugs. The DNA fluorescence image was used to find nuclear regions, and then a 14-pixel-wide cytoplasmic annulus surrounding each nucleus was created. These regions were used to calculate a total of 93 descriptors from all of the marker images for a given drug. The descriptors mainly measured nuclear size, shape, and intensity, and the average intensities of the 10 marker proteins in the nuclear region and in the cytoplasmic annulus. For each drug, each descriptor for each marker was converted into a score reflecting how much the distribution of that descriptor changed from the control case. The drugs were then clustered using this vector of scores. Drugs with known mechanisms of action were observed to be clustered, validating the approach for determining mechanisms of action for unknown drugs.

C. Other Statistical Analyses

Results from classification and clustering analysis clearly show that SLFs capture the essential characteristics of protein fluorescence images. This suggests that they can also be used as a foundation for other kinds of

statistical analysis. Two approaches that address commonly encountered problems in cell biology studies are described below.

1. Objective Selection of Typical Images from an Image Set

Due to space limitations, only a small portion of the images in a dataset can be used for communicating results in papers or presentations. Selecting typical images from an image set is therefore a routine task for many researchers, especially for cell biologists. Similar to location pattern determination, visual inspection is the traditional and most commonly used approach for this task. Consequently, criteria for the selection are largely subjective and this approach suffers from inconsistency (i.e., for the same image set, two independent researchers are unlikely to choose the same image or set of images as representative).

The shortcomings of selection by visual inspection can be avoided by developing an automated system using SLFs that make objective selections of representative images based on statistical models. As in clustering, distance (or dissimilarity) is the core concept here. When each image is reduced to a feature vector, the distances from each vector to the mean feature vector of the image set can be used to reflect the dissimilarity between the corresponding image and the set as a whole. Therefore the inverse of this distance can be used to rank images in order of their typicality (Markey *et al.*, 1999). This approach was experimentally validated using 2D images of subcellular patterns in Chinese hamster ovary cells. Figure 8 shows the

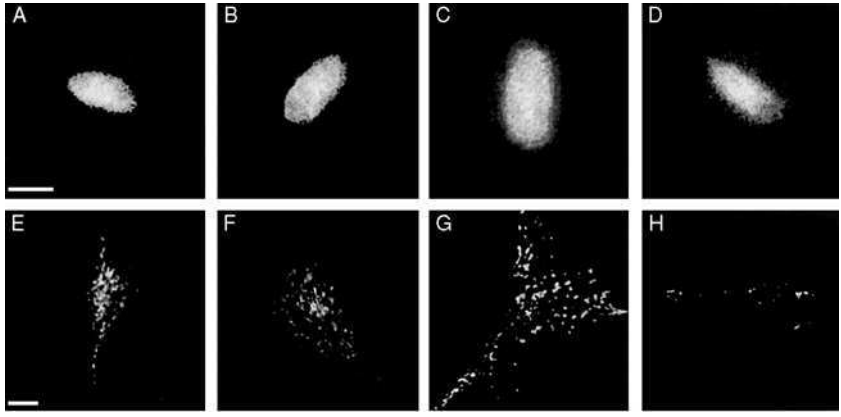

FIG. 8 The most (A, B, E, and F) and least (C, D, G, and H) typical DNA (A–D) and LAMP2 (E–H) images selected by the TypIC program from the 2D CHO dataset. Scale bar = 10 μm. (After Markey *et al.*, 1999.)

most and least representative images selected for DNA (A–D) and lysosomal protein (E–H) patterns. The most typical images (A and B) selected for the DNA pattern show a clear boundary between nucleus and cytoplasm while the least typical images (C and D) exhibit a weak but distinguishable punctuate pattern extending from the nucleus, which suggests either a poor fixation or perhaps that the nuclear membrane had been compromised before fixation. For the lysosomal protein pattern, the most typical images (E and F) showed some lysosomes concentrated in the perinuclear region and some distributed peripherally. In contrast, the least typical images showed a much more peripheral distribution (G), or an apparent reduction in the number of lysosomes (H).

A program for implementing this algorithm, TypIC (for *Typ*ical *I*mage *C*hooser), was originally implemented as a web service and is now included in the PSLID database service described below.

2. Objective Comparison of Two Image Sets

Another frequent question asked by biologists using fluorescence microscopy is whether two image sets represent different location patterns. For instance, there could be interest in whether expression of a mutated or engineered gene changes the location pattern of the targeted protein. Pharmaceutical researchers could be interested in determining whether a certain drug treatment significantly changes the location pattern of a protein of interest. As is the case for the task of selecting typical images, the conventional approach to comparing sets of patterns is visual inspection. The same limitation applies: two different researchers could possibly reach the opposite conclusion for the same two sets.

This problem can be avoided by using the automated and objective approach of statistical hypothesis tests, such as the Hotelling T^2 test, to compare two feature matrices (Roques and Murphy, 2002). When the Hotelling T^2 test (a multivariate version of the Student's t test) is employed, two image sets would be concluded to be different at a given confidence level if the resulting F value is greater than a critical F value calculated for that confidence level. By this method, all pairs of classes in the 2D HeLa dataset were shown to be statistically different at the 95% confidence level, which is consistent with the finding that a trained classifier could distinguish all 10 classes with relatively high accuracy. On the other hand, when two sets of images of giantin labeled with different antibodies were compared, the sets were found to be indistinguishable at that confidence level. This supports the utility of this approach for detecting meaningful differences without being overly sensitive to experimental variations.

A program for implementing this algorithm, SImEC (for *S*tatistical *Im*aging *E*xperiment *C*omparator) is also available in the PSLID system described below.

D. Protein Subcellular Location Image Database

As for other biological entities, there is a need for large scale online databases to organize biological images from different sources as well as to exchange and manage these images. A number of approaches to creating such databases have been described (Andrews *et al.*, 2002; Gonzalez-Couto *et al.*, 2001; Huang *et al.*, 2002). A critical requirement for such databases is integration of well-designed numerical features for describing each image into the database. The SLFs described above provide excellent discrimination between subcellular location patterns to create a database to capture large numbers of fluorescence microscope images depicting protein location (Huang *et al.*, 2002). This Protein Subcellular Location Image Database (PSLID) uses a publicly available database schema (Fluorescence Microscope Annotation Schema, http://murphylab.web.cmu.edu/services/FMAS), and permits query via text annotation of sample preparation and image collection.

PSLID is built using public domain database and web server software (Postgres and Apache). It contains a Java Server Page (JSP) web interface that permits the different tasks described in this chapter (i.e., classification, clustering, SImEC, and TypIC) as well as text and feature-based query to be carried out on large sets of images. The current PSLID database (containing the 2D and 3D images for HeLa and 3T3 cells described above) can be accessed at http://murphylab.web.cmu.edu/services/PSLID, and the open source software can also be downloaded to create additional local databases. One goal of the current work is focused on providing tools for federating such local databases to create a global but distributed database (Singh *et al.*, 2004).

IV. Concluding Remarks

Current advances in automated interpretation of protein subcellular location distributions were briefly discussed in this review. The studies summarized here have shown that protein subcellular location patterns can be interpreted automatically and objectively by feature-based approaches, and usually outperform visual inspection.

The core of the automated interpretation approaches is the development of features capturing essential characteristics of protein subcellular distributions while not being overly sensitive to experimental variations, such as the cell location, orientation, and absolute intensity. Even for unpolarized cells, 3D images have higher pattern information content than 2D images. Consequently, classifiers trained on 3D images achieved better performance.

Although the current methods are still far from perfect, they can be expected to form the foundation of future research in location proteomics.

For example, better performance could be achieved by continuously improving feature design (more complete coverage of information contained), better feature implementation (increased computational efficiency), and developing algorithms for using images with higher dimension (e.g., time series images).

Combined with advances in random tagging and high-throughput imaging techniques, automated interpretation tools can generate a complete view of the location patterns for most, if not all, proteins expressed in an arbitrary cell type. We are only at the threshold of discovering what new insights location proteomics can contribute to biological and biomedical research.

Acknowledgments

The work from our research group could not have been accomplished without the help of Drs. David Casasent, Jonathan Jarvik, Peter Berget, Simon Watkins, and our colleagues in the Center for Automated Learning and Discovery and the Center for Bioimage Informatics. That work was supported in part by NIH Grant R01 GM068845, NSF Grant EF-0331657, and Research Grant 017393 from the Commonwealth of Pennsylvania Tobacco Settlement Fund. X. Chen was supported by a Graduate Fellowship from the Merck Computational Biology and Chemistry Program at Carnegie Mellon University founded by the Merck Company Foundation.

REFERENCES

Ajenjo, N., Canon, E., Sanchez-Perez, I., Matallanas, D., Leon, J., Perona, R., and Crespo, P. (2004). Subcellular localization determines the protective effects of activated ERK2 against distinct apoptogenic stimuli in myeloid leukemia cells. *J. Biol. Chem.* **279,** 32813–32823.

Andrews, P., Harper, I., and Swedlow, J. (2002). To 5D and beyond: Quantitative fluorescence microscopy in the postgenomic era. *Traffic* **3,** 29–36.

Batchelor, B. G. (1978). "Pattern Recognition: Ideas in Practice." Plenum Press, New York. 71–72.

Boland, M. V., and Murphy, R. F. (2001). A neural network classifier capable of recognizing the patterns of all major subcellular structures in fluorescence microscope images of HeLa cells. *Bioinformatics* **17,** 1213–1223.

Boland, M. V., Markey, M. K., and Murphy, R. F. (1998). Automated recognition of patterns characteristic of subcellular structures in fluorescence microscopy images. *Cytometry* **33,** 366–375.

Brelie, T. C., Wessendorf, M. W., and Sorenson, R. L. (2002). Multicolor laser scanning confocal immunofluorescence microscopy: Practical application and limitations. *Methods Cell Biol.* **70,** 165–244.

Chen, X., and Murphy, R. F. (2004). Robust classification of subcellular location patterns in high resolution 3D fluorescence microscope images. Proc. 26th Annual Intl. Conf. IEEE Eng. Med. Biol. Soc., pp. 1632–1635.

Chen, X., and Murphy, R. F. (2005). Objective clustering of proteins based on subcellular location patterns. *J. Biomed. Biotechnol.* **2005,** 87–95.

Chen, X., Velliste, M., Weinstein, S., Jarvik, J. W., and Murphy, R. F. (2003). Location proteomics – building subcellular location trees from high resolution 3D fluorescence microscope images of randomly-tagged proteins. *Proc. SPIE* **4962,** 298–306.

Conrad, C., Erfle, H., Warnat, P., Daigle, N., Lorch, T., Ellenberg, J., Pepperkok, R., and Eils, R. (2004). Automatic identification of subcellular phenotypes on human cell arrays. *Genome Res.* **14,** 1130–1136.

Cook, R. (1998). Kappa. *In* "The Encyclopedia of Biostatistics" (P. Armitage and T. Colton, Eds.), pp. 2160–2166. John Wiley & Sons Inc., New York.

Danckaert, A., Gonzalez-Couto, E., Bollondi, L., Thompson, N., and Hayes, B. (2002). Automated recognition of intracellular organelles in confocal microscope images. *Traffic* **3,** 66–73.

De Solorzano, C. O., Malladi, R., Lelievre, S. A., and Lockett, S. J. (2001). Segmentation of nuclei and cells using membrane related protein markers. *J. Microsc.* **201,** 404–415.

Diday, E. (1974). Recent progress in distance and similarity measures in pattern recognition. Proc. 2nd. Intl. Joint Conf. Pattern Recog., pp. 534–539.

Emanuelsson, O., Nielsen, H., Brunak, S., and von Heijne, G. (2000). Predicting subcellular localization of proteins based on their N-terminal amino acid sequence. *J. Mol. Biol.* **300,** 1005–1016.

Exoo, G. (2003). A Euclidean Ramsey problem. *Discrete Comput. Geom.* **29,** 223–227.

Fujiwara, K., and Pollard, T. D. (1976). Fluorescent antibody localization of myosin in the cytoplasm, cleavage furrow, and mitotic spindle of human cells. *J. Cell Biol.* **71,** 848–875.

Gonzalez-Couto, E., Hayes, B., and Danckaert, A. (2001). The life sciences Global Image Database (GID). *Nucleic Acids Res.* **29,** 336–339.

Griffin, B. A., Adams, S. R., and Tsien, R. Y. (1998). Specific covalent labeling of recombinant protein molecules inside live cells. *Science* **281,** 269–272.

Habeler, G., Natter, K., Thallinger, G. G., Crawford, M. E., Kohlwein, S. D., and Trajanoski, Z. (2002). YPL.db: The Yeast Protein Localization database. *Nucleic Acids Res.* **30,** 80–83.

Hardonk, M. J., Dijkhuis, F. W., Haarsma, T. J., Koudstaal, J., and Huijbers, W. A. (1977). Application of enzyme histochemical methods to isolated subcellular fractions and to sucrose-Ficoll density gradients. A contribution to the comparison of histochemical and biochemical data. *Histochemistry* **53,** 165–181.

Harris, M. A., Clark, J., Ireland, A., Lomax, J., Ashburner, M., Foulger, R., Eilbeck, K., Lewis, S., Marshall, B., Mungall, C., Richter, J., Rubin, G. M., Blake, J. A., Bult, C., Dolan, M., Drabkin, H., Eppig, J. T., Hill, D. P., Ni, L., Ringwald, M., Balakrishnan, R., Cherry, J. M., Christie, K. R., Costanzo, M. C., Dwight, S. S., Engel, S., Fisk, D. G., Hirschman, J. E., Hong, E. L., Nash, R. S., Sethuraman, A., Theesfeld, C. L., Botstein, D., Dolinski, K., Feierbach, B., Berardini, T., Mundodi, S., Rhee, S. Y., Apweiler, R., Barrell, D., Camon, E., Dimmer, E., Lee, V., Chisholm, R., Gaudet, P., Kibbe, W., Kishore, R., Schwarz, E. M., Sternberg, P., Gwinn, M., Hannick, L., Wortman, J., Berriman, M., Wood, V., De la Cruz, N., Tonatello, P., Jaiswal, P., Seigfried, T., and White, R. (2004). The Gene Ontology (GO) database and informatics resource. *Nucleic Acids Res.* **32,** D258–D261.

Hernandez-Munoz, I., Benet, M., Calero, M., Jimenez, M., Diaz, R., and Pellicer, A. (2003). rgr oncogene: Activation by elimination of translational controls and mislocalization. *Cancer Res.* **63,** 4188–4195.

Hua, S., and Sun, Z. (2001). Support vector machine approach for protein subcellular localization prediction. *Bioinformatics* **17,** 721–728.

Huang, K., and Murphy, R. F. (2004a). Automated classification of subcellular patterns in multicell images without segmentation into single cells. Proc. 2002 IEEE Intl. Symp. Biomed. Imaging (ISBI 2004), pp. 1139–1142.

Huang, K., and Murphy, R. F. (2004b). Boosting accuracy of automated classification of fluorescence microscope images for location proteomics. *BMC Bioinformatics* **5,** 78.

Huang, K., Lin, J., Gajnak, J. A., and Murphy, R. F. (2002). Image content-based retrieval and automated interpretation of fluorescence microscope images via the protein subcellular location image database. Proc. 2002 IEEE Intl. Symp. Biomed. Imaging (ISBI 2002), pp. 325–328.

Huang, K., Velliste, M., and Murphy, R. F. (2003). Feature reduction for improved recognition of subcellular location patterns in fluorescence microscope images. *Proc. SPIE* **4962,** 307–318.

Ichimura, N. (1997). Robust clustering based on a maximum-likelihood method for estimating a suitable number of clusters. *Syst. Comput. Jpn.* **28,** 10–23.

Jarvik, J. W., Adler, S. A., Telmer, C. A., Subramaniam, V., and Lopez, A. J. (1996). CD-tagging: A new approach to gene and protein discovery and analysis. *BioTechniques* **20,** 896–904.

Jarvik, J. W., Fisher, G. W., Shi, C., Hennen, L., Hauser, C., Adler, S., and Berget, P. B. (2002). *In vivo* functional proteomics: Mammalian genome annotation using CD-tagging. *BioTechniques* **33,** 852–867.

Jiang, X. S., Zhou, H., Zhang, L., Sheng, Q. H., Li, S. J., Hao, P., Li, Y. X., Xia, Q. C., Wu, J. R., and Zeng, R. (2004). A high-throughput approach for subcellular proteome: Identification of rat liver proteins using subcellular fractionation coupled with two-dimensional liquid chromatography tandem mass spectrometry and bioinformatic analysis. *Mol. Cell. Proteom.* **3,** 441–455.

Kozubek, M., Matula, P., Matula, P., and Kozubek, S. (2004). Automated acquisition and processing of multidimensional image data in confocal *in vivo* microscopy. *Microsc. Res. Tech.* **64,** 164–175.

Kumar, A., Cheung, K.-H., Ross-Macdonald, P., Coelho, P. S. R., Miller, P., and Snyder, M. (2000). TRIPLES: A database of gene function in Saccharomyces cerevisiae. *Nucleic Acids Res.* **28,** 81–84.

Kumar, A., Agarwal, S., Heyman, J. A., Matson, S., Heidtman, M., Piccirillo, S., Umansky, L., Drawid, A., Jansen, R., and Liu, Y. (2002). Subcellular localization of the yeast proteome. *Genes Dev.* **16,** 707–719.

Lu, Z., Szafron, D., Greiner, R., Lu, P., Wishart, D. S., Poulin, B., and Anvik, J. (2004). Predicting subcellular localization of proteins using machine-learned classifiers. *Bioinformatics* **20,** 547–556.

Lujan, R. (2004). Electron microscopic studies of receptor localization. *Methods Mol. Biol.* **259,** 123–136.

Macbeath, G. (2002). Protein microarrays and proteomics. *Nat. Genet.* **32,** 526–532.

Markey, M. K., Boland, M. V., and Murphy, R. F. (1999). Towards objective selection of representative microscope images. *Biophys. J.* **76,** 2230–2237.

Mitchell, T. M. (1997). "Machine Learning." WCB/McGraw-Hill, New York.

Murphy, R. F., Boland, M. V., and Velliste, M. (2000). Towards a systematics for protein subcellular location: Quantitative description of protein localization patterns and automated analysis of fluorescence microscope images. *Proc. Int. Conf. Intell. Syst. Mol. Biol.* **8,** 251–259.

Murphy, R. F., Velliste, M., and Porreca, G. (2002). Robust classification of subcellular location patterns in fluorescence microscope images. Proc. 2002 IEEE Intl. Workshop Neural Networks Sig. Proc. (NNSP '03), pp. 67–76.

Murphy, R. F., Velliste, M., and Porreca, G. (2003). Robust numerical features for description and classification of subcellular location patterns in fluorescence microscope images. *J. VLSI Sig. Proc.* **35,** 311–321.

Nadler, M., and Smith, E. P. (1993). "Pattern Recognition Engineering." John Wiley & Sons, Inc., New York.

Nair, P., Schaub, B. E., Huang, K., Chen, X., Murphy, R. F., Griffith, J. M., Geuze, H. J., and Rohrer, J. (2005). Characterization of the TGN exit signal of the human mannose 6-phosphate uncovering enzyme. *J. Cell Sci.* **118,** 2949–2956.

Nair, R., and Rost, B. (2002). Inferring sub-cellular localization through automated lexical analysis. *Bioinformatics* **18,** S78–S86.

Nair, R., and Rost, B. (2003). LOC3D: Annotate sub-cellular localization for protein structures. *Nucleic Acids Res.* **31,** 3337–3340.

Nair, R., and Rost, B. (2004). LOCnet and LOCtarget: Sub-cellular localization for structural genomics tar. *Nucleic Acids Res.* **32,** W517–W521.

Nakai, K., and Horton, P. (1999). PSORT: A program for detecting sorting signals in proteins and predicting their subcellular localization. *Trends Biochem. Sci.* **24,** 34–35.

Nakai, K., and Kanehisa, M. (1992). A knowledge base for predicting protein localization sites in eukaryotic cells. *Genomics* **14,** 897–911.

Nakano, A. (2002). Spinning-disk confocal microscopy—a cutting-edge tool for imaging of membrane traffic. *Cell Struct. Funct.* **27,** 349–355.

Norin, M., and Sundstrom, M. (2002). Structural proteomics: Developments in structure-to-function predictions. *Trends Biotechnol.* **20,** 79–84.

O'Brate, A., and Giannakakou, P. (2003). The importance of p53 location: Nuclear or cytoplasmic zip code? *Drug Resist. Updates* **6,** 313–322.

Perlman, Z. E., Slack, M. D., Feng, Y., Mitchison, T. J., Wu, L. F., and Altschuler, S. J. (2004). Multidimensional drug profiling by automated microscopy. *Science* **306,** 1194–1198.

Qian, G., Sural, S., Gu, Y., and Pramanik, S. (2004). Similarity between Euclidean and cosine angle distance for nearest neighbor queries. Proc. 2004 ACM Symp. Applied Comput., pp. 1232–1237.

Reichart, B., Klafke, R., Dreger, C., Kruger, E., Motsch, I., Ewald, A., Schafer, J., Reichmann, H., Muller, C. R., and Dabauvalle, M.-C. (2004). Expression and localization of nuclear proteins in autosomal-dominant Emery-Dreifuss muscular dystrophy with LMNA R377H mutation. *BMC Cell Biol.* **5,** 12.

Reinhardt, A., and Hubbard, T. (1998). Using neural networks for prediction of the subcellular location of proteins. *Nucleic Acids Res.* **26,** 2230–2236.

Rohrer, J., and Kornfeld, R. (2001). Lysosomal hydrolase mannose 6-phosphate uncovering enzyme resides in the trans-Golgi network. *Mol. Biol. Cell* **12,** 1623–1631.

Rolls, M. M., Stein, P. A., Taylor, S. S., Ha, E., McKeon, F., and Rapoport, T. A. (1999). A visual screen of a GFP-fusion library identifies a new type of nuclear envelope membrane protein. *J. Cell Biol.* **146,** 29–44.

Roques, E. J. S., and Murphy, R. F. (2002). Objective evaluation of differences in protein subcellular distribution. *Traffic* **3,** 61–65.

Sclaroff, S., and Liu, L. (2001). Deformable shape detection and description via model-based region grouping. *IEEE Trans. Pattern Anal. Machine Intell.* **23,** 475–489.

Singh, A. K., Manjunath, B. S., and Murphy, R. F. (2004). Design of a distributed database for biomolecular images. *SIGMOD Rec.* **33,** 65–71.

Steckling, T., Hellwich, O., Wälter, S., and Wanker, E. (2004). Protein classification by analysis of confocal microscopic images of single cells. Proc. XXth ISPRS Congress, pp. 302–305.

Subramaniam, S., and Milne, J. L. (2004). Three-dimensional electron microscopy at molecular resolution. *Annu. Rev. Biophys. Biomol. Struct.* **33,** 141–155.

Telmer, C. A., Berget, P. B., Ballou, B., Murphy, R. F., and Jarvik, J. W. (2002). Epitope tagging genomic DNA using a CD-tagging Tn10 minitransposon. *BioTechniques* **32,** 422–430.

Velliste, M., and Murphy, R. F. (2002). Automated determination of protein subcellular locations from 3D fluorescence microscope images. Proc. 2002 IEEE Intl. Symp. Biomed, Imaging (ISBI 2002), pp. 867–870.

This page intentionally left blank

Cell and Molecular Biology of Human Lacrimal Gland and Nasolacrimal Duct Mucins

Friedrich Paulsen
Department of Anatomy and Cell Biology, Martin Luther University, Halle-Wittenberg, 06097 Halle, Germany

The old concept that the lacrimal gland is only a serous gland has been superseded by the finding that lacrimal acinar cells are able to produce mucins—high-molecular-weight proteins—the major mass being carbohydrates with the common feature of tandem repeats of amino acids rich in serine, threonine, and proline in the central domain of the mucin core peptide. At the ocular surface, maintenance of the tear film, lubrication, and provision of a pathogen barrier on the epithelia, conjunctiva, and cornea have been shown to be facilitated by mucins that are present in membrane-anchored (lining epithelial cells) or secreted (goblet cells) form. Also in the lacrimal gland, both membrane-anchored (MUCs 1, 4, and 16) and secreted (MUCs 5B and 7) mucins have been identified. The lacrimal gland is the main contributor to the aqueous portion of the tear film. It is part of the lacrimal apparatus that comprises, together with the lacrimal gland, the paired lacrimal canaliculi, the lacrimal sac, and the nasolacrimal duct, which collects the tear fluid and conveys it into the nasal cavity. In this review, the latest information regarding mucin function in the human lacrimal gland and the human efferent tear ducts is summarized with regard to mucous epithelia integrity, rheological and antimicrobial properties of the tear film and tear outflow, age-related changes, and certain disease states such as the pathogenesis of dry eye, dacryostenosis, and dacryolith formation.

KEY WORDS: Lacrimal gland, Nasolacrimal ducts, Mucin, MUC, Tear film, Tear outflow, Dry eye.

0074-7696/06 $35.00
DOI: 10.1016/S0074-7696(06)49005-7

I. Introduction

For decades, medical students have been taught that the human lacrimal gland is a tubuloalveolar gland of the *serous* type. This statement is based on light microscopic findings in which exocrine glands of the mucous membranes are classified according to the products produced by serous secretory cells, mucous secretory cells, or both cell types.

Serous secretory cells have central nuclei and eosinophilic secretory storage granules in their cytoplasm. They secrete a thin secretion rich in glycoproteins that also contains enzymes. They are therefore generally basophilic. Zymogen granules— material from which secretion is produced—can often be seen in the vicinity of the Golgi apparatus near the apex of the cell. Mucous secretory cells feature a frothy cytoplasm and basal, flattened nuclei. They produce a viscous acid secretion mainly composed of mucins, glycoproteins of high-polymer structure. They stain strongly with metachromatic stains and periodic acid–Schiff (PAS) methods that detect carbohydrate residues. However, in general (i.e., nonspecific) histological preparations they are weakly stained because much of their water content in the mucin is extracted by the processing procedures.

The human lacrimal gland as seen under the light microscope consists only of serous secretory cells and therefore has been termed a gland of the pure serous type. However, even though it does not contain mucous secretory cells, microscopic results obtained in the 1960s and 1970s suggested that the lacrimal gland might also be a source of ocular mucins. A high sialic acid content in lacrimal tissue and fluid (Jensen *et al.*, 1969) and positivity for acidic and neutral glycoprotein stains (Allen *et al.*, 1972; Ito and Shibasaki, 1964; Kühnel, 1968; Millar *et al.*, 1996), suggestive of glycoprotein synthesis, were recently complemented by evidence of mucin synthesis in rodents (Arango *et al.*, 2001) and human lacrimal glands (Jumblatt *et al.*, 2003; Paulsen *et al.*, 2004a; Schäfer *et al.*, 2005).

This review will provide a general overview of the great impact of mucins on the integrity of epithelia and on their rheological and antimicrobial properties in the lacrimal system under healthy conditions and in the presence of certain diseases, with the main focus on the cell and molecular biology of human lacrimal gland mucins and mucins of the efferent tear duct system required to transport ''old, used'' tear fluid into the inferior meatus of the nose.

II. Anatomy of the Lacrimal System

The lacrimal apparatus consists of the lacrimal gland, which secretes a complex fluid (tears) and whose excretory ducts convey fluid to the surface

of the eye where the fluid forms part of the tear film, the paired lacrimal canaliculi, the lacrimal sac, and the nasolacrimal duct, which collects the fluid and conveys it into the nasal cavity.

A. The Lacrimal Gland

The main lacrimal gland forms from invaginations of the ectoderm at the superolateral angles of the conjunctival sac that do not mature until about 6 weeks after birth. After maturing it is localized anteriorly in the superolateral region of the orbit, and is divided into two parts by the levator palpebrae superioris muscle. The orbital part has nearly the size and shape of an almond and lodges in the lacrimal fossa on the medial aspect of the zygomatic process of the frontal bone, just within the orbital margin. The smaller palpebral part (nearly one-third of the orbital part) is inferior to the levator palpebrae superioris in the superolateral part of the eyelid. Functionally, it synthesizes, stores, and secretes a bulk of different proteins and peptides, water, and electrolytes that are released into the tears and, via the excretory duct system of the lacrimal gland, onto the surface of the eye as part of the tear film. Similar to the salivary glands and the pancreas, the lacrimal gland is a multilobed, tubuloalveolar gland of serous type. The tubules discharge without any characteristic excretory duct system (histological distinction from serous salivary glands) into the interlobular excretory ducts. In contrast to rat and rabbit with only one single excretory duct, in the human lacrimal gland 8–10 main excretory ducts then open onto the surface of the eye in front of the lateral portion of the superior conjunctival fornix. In cross sections, the secretory units of the gland appear as a ring-like structure, the so called acinus. An acinus is composed of secretory cells, the acinar cells (shaped like a bunch of grapes). Since several secretory units open into one secretory duct, the lacrimal gland is termed ''branched.'' Acinar cells comprise about 80% of the mass of the lacrimal gland. Although the lacrimal gland has no characteristic excretory duct system (compared to the salivary glands), the ductal cells are able to modify the secretory product of the acinar cells.

Lacrimal gland acinar cells are polarized secretory cells that secrete their proteins unidirectionally. This is enabled by a dense ring of tight junctions that surrounds the cells at the lumen dividing the plasma membrane into apical (luminal) and basolateral (blood-related) membranes. Receptors for neurotransmitters and neuropeptides are located at the basolateral membrane of the acinar cells. The transmitters and peptides are released by the nerves in close proximity to the membranes. The nerves comprise a dense innervation of the lacrimal gland (for review see Hodges and Dartt, 2003). Moreover, the basolateral membranes also contain several transport proteins

and ionic channels necessary for electrolyte and water secretion (for review see Hodges and Dartt, 2003; Takata *et al.*, 2004). Acinar cells have prominent endoplasmic reticulum and Golgi apparatus. Both cell organelles are situated together with the nucleus, mainly in the basal portion of the cells, while the apical portion of the cell has numerous protein-containing secretory granules. Acinar cells have been shown to be influenced by various hormones, e.g., androgens, estrogens, glucocorticoids, mineralocorticoids, retinoic acid, prolactin, α-melanocyte-stimulating hormone, adrenocorticotropic hormone, luteinizing hormone, follicle-stimulating hormone, growth hormone, thyroid-stimulating hormone, arginine vasopressin, oxytocin, thyroxine, parathyroid hormone, insulin, glucagons, melatonin, human chorionic gonadotropin, cholecystokinin (for review see Sullivan, 2004), and, as indicated recently by our own unpublished results, somatostatin.

Excretory lacrimal gland ducts are lined by one (beginning of ducts) to two (most parts of ducts) layers of cuboidal cells. Comparable to the acinar cells, the superficial lining cells of the excretory duct system contain luminally tight junctions creating polarized cells, whereas superficial and basal cells of the ducts are connected by gap junctions creating a syncytium. Also in the lining cells, the nucleus is in the basal portion of the cell while the endoplasmic reticulum and Golgi apparatus are located more apically. The cells have been shown to secrete mainly water and electrolytes, but a limited protein secretion potential has also been demonstrated. For example, basal epithelial cells of lacrimal gland ducts secrete bactericidal permeability-increasing protein (BPI), which occurs in a relatively high concentration in tears and plays a substantial antibacterial role in human tears (Peuravuori *et al.*, 2005). The main excretory ducts often contain single goblet cells or groups of goblet cells forming intraepithelial glands near their transition into the conjunctival fornix.

Basally, acinar and ductal cells are surrounded by myoepithelial cells. Comparable to the salivary glands, the myoepithelial cells are thought to contribute to transport of secretions. They express receptors for several neurotransmitters that are known to stimulate protein secretion from acinar cells (Hodges *et al.*, 1997; Lemullois *et al.*, 1996). Moreover, it has been hypothesized that myoepithelial cells play a structural role in helping the gland maintain its shape.

From the viewpoint of mucosal immunology the lacrimal gland is thought to be an integral part of the ocular mucosal immune system. It contains similar cell populations of lymphocytes, plasma cells [expressing all immunoglobulins (A, G, E, M, D)], mast cells, macrophages, and dendritic cells. More than 50% of the mononuclear cells are plasma cells and most of them secrete IgA—a critical component of the ocular mucosal immune system (for review see Knop *et al.*, 2005; Pflugfelder and Stern, 2005; Stern and Pflugfelder, 2004).

B. The Nasolacrimal Ducts

Tear fluid is drained by the nasolacrimal ducts (also termed efferent tear ducts or lacrimal passage) into the inferior meatus of the nose. The lacrimal passage consists of a bony passage and a membranous lacrimal passage (Duke-Elder, 1961). The bony passage is formed anteriorly by the frontal process of the maxilla and posteriorly by the lacrimal bone. The membranous lacrimal passages include the lacrimal canaliculi, the lacrimal sac, and the nasolacrimal duct (for review see Paulsen, 2003; Paulsen *et al.*, 2003a).

The upper and lower canaliculus are lined by a pseudostratified/stratified columnar epithelium and are surrounded by a dense ring of connective tissue as well as by muscle fibers of Horner's muscle (the lacrimal portion of the orbicularis oculi muscle; Halben, 1904). The lacrimal sac and the nasolacrimal duct are lined by a double-layered epithelium revealing a superficial columnar layer and a deep, flattened layer of basal cells (Duke-Elder, 1961; Tsuda, 1952). Both layers sometimes appear as a pseudostratified epithelium. Superficial epithelial cells contain numerous secretory vesicles in their cytoplasm (Paulsen *et al.*, 1998) and have been shown to secrete many different antimicrobial proteins and peptides (Paulsen *et al.*, 2001a, 2002a). In addition to epithelial cells, goblet cells are integrated in the epithelium as single cells or, more often, in a characteristic arrangement forming intraepithelial mucous glands (Paulsen *et al.*, 1998; Werncke, 1905). Moreover, kinociliae (motile ciliae) have been described as a common finding in some epithelial cells (Radnot, 1977; Radnot and Bölcs, 1971). Most epithelial cells are, however, lined by microvilli (for review see Paulsen, 2003a). Rivas *et al.* (1991) described small serous glands in the lamina propria, especially in the fundus of the lacrimal sac.

The wall of the lacrimal sac and the nasolacrimal duct are made up of a helical system of different connective tissue fibers. Wide luminal plexi with specialized blood vessels are embedded in this helical system, which functions as a cavernous body (Ayub *et al.*, 2003; Paulsen *et al.*, 2000a). Caudally, the vascular system is connected to the cavernous body of the inferior turbinate. With lid closure the system distends and may be "wrung out" due to its medial attachment and helically arranged fibrillar structures, whereby tear fluid is drained distally (Thale *et al.*, 1998). The embedded blood vessels as well as the epithelial layer are under vegetative control. This was emphasized by a high density of nerve fibers as well as the presence of various neuropeptides (Paulsen *et al.*, 2000b). By means of its innervation, the specialized blood vessels permit regulation of blood flow by opening and subsidence of the cavernous body, at the same time regulating tear outflow. Related functions, such as a role in the occurrence of epiphora related to emotional responses, are relevant.

Also, the nasolacrimal ducts are an integral part of the ocular mucosal immune system. In most cases there is a diffuse infiltrate of variable intensity within the lamina propria, consisting predominantly of T lymphocytes with scattered CD20- and CD45RA-positive B cells as well as many plasma cells, most of them immunoglobulin A (IgA) positive. Aggregated follicles are present in nearly one-third of nasolacrimal ducts, fulfilling the criteria for designation as mucosa-associated lymphoid tissue (MALT) or tear duct-associated lymphoid tissue (TALT) (for review see Paulsen, 2003; Paulsen *et al.*, 2000c, 2002b, 2003a, 2006).

As a draining and secretory system, the nasolacrimal ducts play a role in tear transport and nonspecific immune defense. Moreover, components of tear fluid are absorbed in the nasolacrimal passage and are transported into the surrounding vascular system (Paulsen *et al.*, 2002d).

It has been suggested that under normal conditions, tear fluid components are constantly absorbed into the blood vessels of the surrounding cavernous body. These vessels are connected to the blood vessels of the outer eye and could act as a feedback signal for tear fluid production, which ceases if these tear components are not absorbed (Paulsen *et al.*, 2001a, 2002c).

III. Properties of Mucins

A. Classification and General Properties of Mucins

1. Nomenclature and Classification

Mucus protects, moisturizes, and lubricates mucosal surfaces. Not long ago, mucus was still thought to be exclusively a product of goblet cells and glandular mucous cells. Today, with general acceptance of the molecular characterization of mucins, it is generally believed that mucus is primarily composed of mucins as well as inorganic salts suspended in water. Mucins are a family of high-molecular-weight glycoproteins with at least half of their mass in the form of O-linked carbohydrates and consist of tandem repeats of amino acids rich in serine, threonine, and proline in the central domain of the mucin core peptide (Gendler and Spicer, 1995; Moniaux *et al.*, 2001). The core peptide is *apomucin*. Mucins can be distinguished from each other by the number of amino acids per tandem repeat (for review see Gipson and Argüeso, 2003). Moreover, the numbers of tandem repeats per allele often vary. The molecular weights of mucins can therefore vary within an individual (Swallow *et al.*, 1987). Alleles of different sizes are codominantly expressed (Fowler *et al.*, 2001; Vinall *et al.*, 1998), and some mucins can exhibit splice variants (Ligtenberg *et al.*, 1990; Moniaux *et al.*, 2000) leading,

together with genetic and tissue variation after posttranslational processing of mucins (as does glycosylation), to mucin types of different sizes and characters both intraindividually and interindividually (Gipson and Argüeso, 2003).

To date, human genome mapping has identified 19 mucin genes (MUC1–MUC20, including 3A, 3B, 5AC, 5B and excluding 10, 14, and 18 that do not appear in the HUGO gene nomenclature; http://www.gene.ucl.AC.UK/egi-bin/nomenclature/searchgenes), numbered chronologically in the order of reported cloning (Table I). Human mucins are abbreviated *MUC*, mouse homologues are designated *Muc,* and rat mucins *rMuc*. Mucins are classified as either membrane-anchored or secreted. However, several mucins have not yet been completely characterized. Secreted mucins are further subclassified as gel-forming or soluble, based on their ability to produce polymers (Table I).

2. Membrane-Anchored Mucins

As stated above, not long ago all mucins were still assumed to be secreted. However, several mucins have now been well characterized as having hydrophobic membrane-spanning domains near their carboxyl-terminal region (Fig. 1) that anchor them to the apical surface of wet-surfaced epithelia (both simple and stratified) and as constituting a major portion of the glycocalyx (for review see Carraway *et al.*, 2000; Gendler, 2001; Table I). The extracellular domain of some mucins rises 200–500 nm above the 10-nm glycocalyx (Bramwell *et al.*, 1986; Gum, 1995; Hilkens *et al.*, 1995) leading to protective *disadhesive* properties preventing cell–cell and cell–matrix interactions and so adhesion of macromolecules (Komatsu *et al.*, 1997). On the other hand, there is also evidence for effects on cell adhesion from studies showing that MUC1 binds ß-catenin by means of a motif similar to those found in E-cadherin and the adenomatous polyposis coli proteins, at the SAGNGGSSL sequence (Yamamoto *et al.*, 1997). Moreover, there is growing evidence that the cytoplasmic domains of membrane-anchored mucins interact with cytoplasmic proteins such as actin to facilitate and activate signal transduction (Parry *et al.*, 1990; Yamamoto *et al.*, 1997). It has been demonstrated that tyrosine residues in the cytoplasmic domains of MUC1 can be phosphorylated and interact with SH2 domain-containing proteins. This interaction is believed to contribute to signal transduction mediating cell cycle and apoptosis (Li *et al.*, 2003; Zrihan-Licht *et al.*, 1994). Further studies have shown that MUC1 binds Grb2/SOS, which are signaling mediators of a number of receptor kinases (Pandey *et al.*, 1995). Further functions such as cytokine-like functions will be mentioned later. Interestingly, genes of four of them (MUCs 3A, 3B, 12, 17) are clustered on chromosome 7q22 (Gum *et al.*, 2002; Pratt *et al.*, 2000; Williams *et al.*, 1999). Membrane-anchored mucins are free of cysteine-rich domains and do not form multimers.

TABLE I

Human Mucin Protein Superfamily[a]

Mucin	Type if sequenced	Chromosomal mapping	Amino acids in VNTR	cDNA source	Reference
MUC1	Membrane-anchored	1q21-q23	20	Mammary/pancreatic tumor	Gendler *et al.* (1987); Lan *et al.* (1990)
MUC2	Secreted/gel-forming	11p15	23	Intestine	Gum *et al.* (1989)
MUC3A	Membrane-anchored	7q22	17	Intestine	Gum *et al.* (1990)
MUC3B	Membrane-anchored	7q22	17	Intestine	Pratt *et al.* (2000)
MUC4	Membrane-anchored	3q29	16	Trachea	Porchet *et al.* (1991)
MUC5AC	Secreted/gel-forming	11p15	8	Trachea	Guyonnet Duperat *et al.* (1995); Meerzaman *et al.* (1994)
MUC5B	Secreted/gel-forming	11p15	29	Trachea	Dufosse *et al.* (1993)
MUC6	Secreted/gel-forming	11p15	169	Stomach	Toribara *et al.* (1993)
MUC7	Secreted/soluble monomer	4q13-q21	23	Salivary gland	Bobek *et al.* (1993)
MUC8	Secreted	12q24.3	26	Trachea	Shankar *et al.* (1994)
MUC9	Secreted	1p13	15	Fallopian tube	Arias *et al.* (1994)
MUC11	Membrane-anchored	7q22	28	Intestine	Williams *et al.* (1999)
MUC12	Membrane-anchored	7q22	28	Intestine	Williams *et al.* (1999)
MUC13	Membrane-anchored	3q13.3	15	Intestine, trachea	Williams *et al.* (2001)
MUC15	Membrane-anchored	11p14.3	None	Mammary gland	Pallesen *et al.* (2002)
MUC16	Membrane-anchored	19p13.2	156	OVCAR-3 cells	Yin and Lloyd (2001)
MUC17	Membrane-anchored	7q22	59	Intestine	Gum *et al.* (2002)
MUC19	Secreted	12q12		Genomic database	Chen *et al.* (2004)
MUC20	Membrane-anchored	3q29	19	Kidney	Higuchi *et al.* (2004)

[a]For more information see Gipson and Argüeso (2003), Gipson *et al.* (2004), and HUGO gene nomenclature website: http://www.gene.ucl.AC.UK/egi-bin/nomenclature/searchgenes.

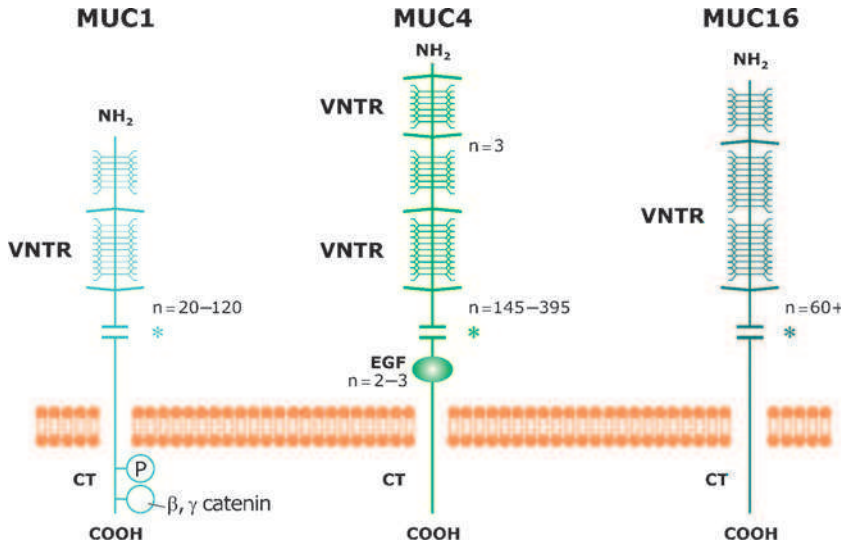

FIG. 1 Diagram demonstrating structural features of membrane-anchored mucins (MUC) expressed by lacrimal gland acinar cells, ocular surface epithelia, and nasolacrimal duct epithelia. All mucins have variable numbers of tandem repeats (VNTR) of amino acids in their protein backbone that are rich in serine and threonine, which are O-glycosylated. Repeats of VNTRs vary in individuals and alleles. MUCs 1, 4, and 16 are expressed by corneal and conjunctival epithelia. The cytoplasmic tail of MUC1 has seven tyrosine residues that can be phosphorylated (P) and participate in signal transduction, as well as sites of association with ß and γ catenin, which link to the cytoskeleton. MUC4 has EGF-like domains extracellularly. All membrane-anchored mucins have cleavage sites (*) associated with shedding of the ectodomain from the surface of the cell. (Modified from Gipson *et al.*, 2004.)

Mucins identified as membrane-anchored include MUCs 1, 3A, 3B, 4, 12, 13, 16, 17, and 20 (Table I). Of these the most knowledge has been obtained about MUCs 1 and 4 (Carraway *et al.*, 2002; Gendler, 2001). Gene clustering for membrane-anchored mucins is present on chromosome 7q22 (MUCs 3A, 3B, 12, 17) and chromosome 3q29 (MUCs 4 and 20) (Gum *et al.*, 2002; Higuchi *et al.*, 2004; Pratt *et al.*, 2000; Williams *et al.*, 1999).

Several of these mucins (MUCs 1, 4, 16, 20) can occur in both membrane-anchored as well as soluble form (Carraway *et al.*, 2003; Higuchi *et al.*, 2004; Ligtenberg *et al.*, 1992). Most likely, the soluble form is a result of alternative splicing in which the membrane-anchored domain is split off posttranscriptionally (Gendler, 2001; Higuchi *et al.*, 2004; Moniaux *et al.*, 2001). Just recently, it was demonstrated that even novel proteins can derive from mucin genes by alternative splicing and frameshifting as demonstrated for MUC1 (Levitin *et al.*, 2005). However, cleavage of the exodomain (α domain) of the mucin from the cellular surface has also been shown (Rossi *et al.*, 1996). In

this process, MUCs 1, 4, and 16 all appear to be shed from the epithelial surface (Auersperg *et al.*, 1999; Ligtenberg *et al.*, 1992; Sheng *et al.*, 1990), although the mechanism is unclear. Finally, there are also hints of intracellular proteolysis (Komatsu *et al.*, 2002). These studies provide evidence that Muc4 (sialomucin complex, SMC) is produced by proteolytic cleavage before substantial O-glycosylation takes place, near the time of transit from the endoplasmic reticulum to the Golgi complex (although Muc4 is translated as a membrane protein, it is produced as a soluble form in many epithelia).

3. Secreted Mucins

To date, two different types of secreted mucins have been designated: gel-forming mucins and soluble mucins (for review see Gendler and Spicer, 1995; Gipson and Argüeso, 2003; Moniaux *et al.*, 2001; Table I and Fig. 2).

a. Gel-Forming Mucins The large gel-forming mucins MUCs 2, 5AC, 5B, and 6 are clustered on chromosome 11p15.5, and the recently discovered MUC19 is located on chromosome 12q12. According to Sellers *et al.* (1991),

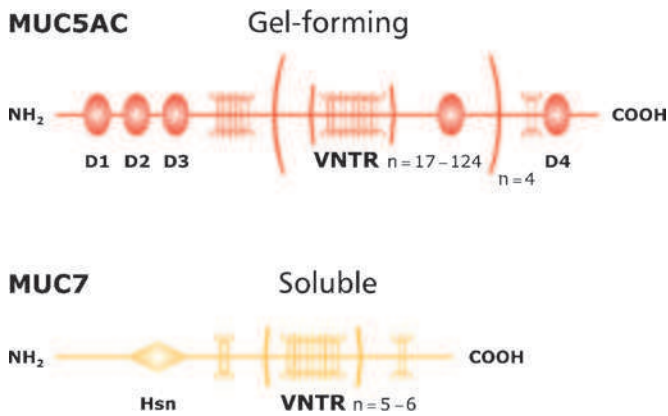

FIG. 2 Diagram demonstrating structural features of secreted mucins (MUC) expressed by lacrimal gland acinar cells, ocular surface epithelia, and nasolacrimal duct epithelia. All mucins have variable numbers of tandem repeats (VNTR) of amino acids in their protein backbone that are rich in serine and threonine, which are O-glycosylated. Repeats of NTRs vary in individuals and alleles. Of the secreted-type mucins, MUC5AC, expressed by goblet cells of the ocular surface and nasolacrimal ducts, is a large gel-forming mucin, with D domains that are rich in cysteines and that provide disulfide cross-linking sites for polymerization of these mucins to form the mucous network that gives mucus its rheologic properties. The small soluble mucin MUC7, expressed by acinar cells of the lacrimal gland as well as columnar cells of the nasolacrimal ducts, has a histatin-like domain (HSM) in the amino terminal region and does not form disulfide linkages. (Modified from Gipson *et al.,* 2004.)

gel-forming mucins are the largest glycoproteins discovered so far and are responsible for the rheological properties of mucus. The molecular size of these proteins is nearly 600 kDa; the cDNAs range between 15.7 and 17 kb (Moniaux *et al.*, 2001). In between they share several structural motifs. Each contains a large, central, tandem repeat domain flanked by cysteine-rich domains showing high levels of homology to the D domains of von Willebrand factor. Three cysteine-rich D domains are present on the amino-terminal side, with one on the carboxy-terminal side (except MUC6, which has D domains only at the amino-terminus). The D domains allow multimerization of individual mucin molecules through disulfide bond formation beginning in the endoplasmic reticulum, and further multimeric processing in the Golgi apparatus (Godl *et al.*, 2002; Peres-Vilar and Hill, 1999; for review see Gipson *et al.*, 2003). Subsequent glycosylation occurs, producing huge macromolecules with estimated molecular weights of up to 40,000 Da (Peres-Vilar and Hill, 1999). It is not clear so far whether individual gel-forming mucins multimerize in different ways by forming networks or linear associations. Both processes have been demonstrated (Godl *et al.*, 2002; Sheehan *et al.*, 2000; for review see Gipson *et al.*, 2004).

The gel-forming mucins share common structural motifs and are thought to evolve from a common ancestral gene (Desseyn *et al.*, 1998, 2000). These are the mucins that are secreted by cells classically known to secrete mucus, i.e., goblet cells and mucus cells of the respiratory, gastrointestinal, endocervical, and ocular surface epithelia as well as the salivary glands and submucosal glands associated with the epithelia mentioned above. The recently characterized MUC19 is no exception (Chen *et al.*, 2004). However, the gel-forming mucins reveal a tissue- and cell-specific expression and distribution pattern in these organ systems (for review see Gipson and Argüeso, 2003).

b. Small Soluble Mucins MUCs 7 and 9 have been categorized as soluble mucins (Table I and Fig. 2). They have been cloned from salivary gland (MUC7) and hamster oviduct (MUC9) and are the smallest mucins known, composed primarily of tandem repeats of amino acids. They lack cysteine-rich D domains and are present predominantly as monomers. MUC7 has a histatin-like domain on the N-terminal side of the tandem repeat. Its size is 39 kDa (Bobek *et al.*, 1993). MUC7 is secreted by serous cells rather than mucus cells of salivary glands (Nielsen *et al.*, 1997), submucosal glands of bronchial airways (Sharma *et al.*, 1998), as well as by acinar cells of the lacrimal gland and columnar cells of the nasolacrimal ducts (see below, and Jumblatt *et al.*, 2003; Paulsen *et al.*, 2003b, 2004a; for review see Schäfer *et al.*, 2005). MUC9 (oviductin) has so far been demonstrably expressed only in the fallopian tube (Lapensee *et al.*, 1997) and under pathological conditions in middle ear effusions of patients with otitis media (Takeuchi *et al.*, 2003). The apomucin of MUC9 has a size of 72 kDa (Arias *et al.*, 1994).

B. Preocular Tear Film and Its Mucins

Early studies described the tear film as a trilaminar structure, consisting predominantly of a superficial coating of lipid, a watery aqueous phase, and a thin mucous layer overlying the epithelium (Holly and Lemp, 1977; Wolff, 1946). Today it is generally accepted that the precorneal tear film contains three components: a lipid component, an aqueous component, and a mucous component (Fig. 3). The lipid component is secreted by the Meibomian glands in the eyelid. The aqueous component is secreted by the main lacrimal gland and the accessory lacrimal glands (glands of Krause; glands of Wolfring) of the lids. The mucus component is the product of conjunctival goblet and epithelial cells, corneal epithelial cells, acinar cells, and excretory duct cells of the lacrimal gland, and probably also of acinar cells of the accessory lacrimal glands (for review see Paulsen *et al.*, 2003a). Tear film thickness is still a matter of debate. Recent studies using cryofixation with freeze substitution electron microscopy, measurement of tear film

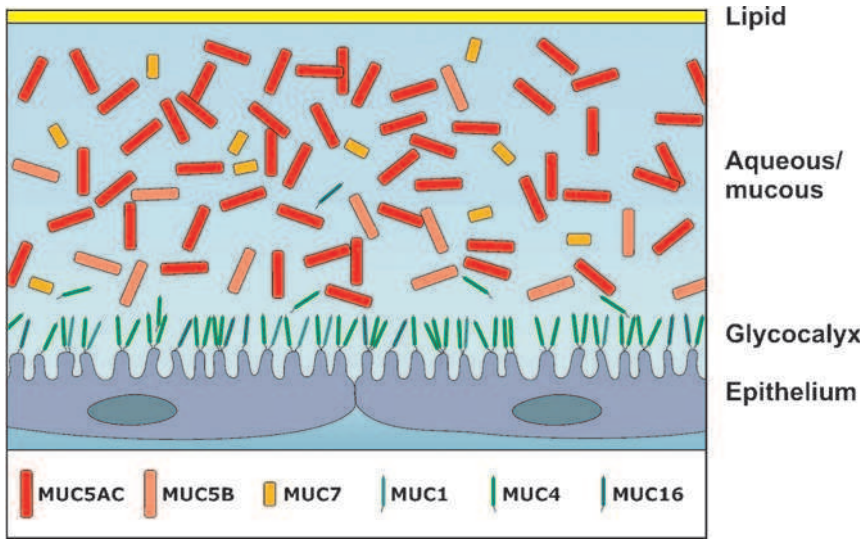

FIG. 3 Diagram demonstrating a hypothetical model of the tear fluid composition. Membrane-anchored mucins MUC1, MUC4, and MUC16 form part of the glycocalyx and are bound at the tips of epithelial cell microplicae. They may be shed into the overlying aqueous/mucous component of the tear film. Moreover, the diagram shows mucins MUC5AC (from conjunctival goblet cells) as well as MUC5B and MUC7 (both from acinar cells of the lacrimal gland) forming multimers in solution in the tear fluid. Negative charges on the mucins prevent their direct association and allow movement of gel-forming mucins over the surface of the eye for its janitorial duties of collecting and removing debris and harmful pathogens. (Modified from Gipson and Argüeso, 2003.)

electrical profile, examination of reflectance spectra, or optical coherence tomography suggest that the human tear film is approximately 3 μm thick (King-Smith *et al.*, 2000; Wang *et al.*, 2003) whereas in mice it is an average of 7 μm (Tran *et al.*, 2003) and in rats it is 2–6 μm (Chen *et al.*, 1997; for review see Johnson and Murphy, 2004).

These differing results for rodents and humans underline the fact that it is very difficult to apply results from animal models to humans. Most animals used to determine the structure of the tear film have markedly greater tear stability and a much lower blink rate (Duke-Elder and Gloster, 1968). It is well known, for example, that the rabbit has a very low eye-blink rate, with an average of one blink every 20–30 min (Gormezano *et al.*, 1962), and can also manage for long periods without drinking water (Denton *et al.*, 1985; Tarjan *et al.*, 1984), suggesting special enabling mechanisms. Moreover, in contrast to humans, many animals commonly used in laboratory research have a large gland filling the posterior part of the orbit and surrounding the optic nerve, called the Harderian gland, the function of which is still poorly understood but which certainly contributes to tear film thickness. Therefore, studies by Chen *et al.* (1997) and Tran *et al.* (2003), who observed a homogeneous, fine network-like structure throughout the tear film in rodents warrant caution.

The whole epithelium covering the ocular surface (cornea; bulbar, fornical, and palpebral conjunctiva) produces mucins, and as will be reviewed later, lacrimal gland acinar and ductal cells also produce mucins that contribute to maintenance of the tear film (Fig. 3). However, the pattern of expression and type of mucin production in the different structures of the ocular surface vary, attributing diverse functions to each zone.

Since several very good review articles have recently been published (Gipson, 2004; Gipson and Argüeso, 2003; Gipson *et al.*, 2004; Watanabe, 2002) dealing with mucins of the conjunctival and corneal epithelia, these data are mentioned only briefly here.

1. Membrane-Anchored Mucins

Conjunctival and corneal epithelial cells express at least the three membrane-anchored mucins MUCs 1, 4, and 16 (Argüeso and Gipson, 2001; Argüeso *et al.*, 2003; Berry *et al.*, 2000; Inatomi *et al.*, 1995). As measured by real-time polymerase chain reaction (PCR), MUC4 reveals the highest relative expression of these three mucins (Gipson and Argüeso, 2003). In contrast to MUC1, MUC4 shows regional variation of distribution with higher levels in conjunctiva and limbal epithelia and a noted decrease toward the central cornea (Pflugfelder *et al.*, 2004). It seems that there is an association between MUC4 and type 1 growth factor receptors (ErbB2–4). They are present as a complex in rat rMuc4 and ErbB2 (Swan *et al.*, 2002). The

membrane-anchored mucins have been shown to extend from the microplicae of corneal and conjunctival superficial epithelial cells, and the actin cytoskeleton to which their cytoplasmic tails may interact are clearly seen extending into the microplicae (for review see Gipson, 2004; Gipson and Argüeso, 2003; Gipson *et al.*, 2003). There is some evidence that the extracellular domains of all three mucins MUCs 1, 4, and 16 are shed into the tear film (Hori *et al.*, 2004a; Pflugfelder *et al.*, 2000; Spurr-Michaud *et al.*, 2004). In addition to these three membrane-anchored mucins, low expression levels of MUC11 have also been found by PCR methods (Argüeso and Gipson, unpublished data), in which the MUC15 message reportedly occurs as well (Jiang and Jumblatt, 2003). However, neither immunolocalization nor *in situ* hybridization verifying the source of the RNA has been reported so far for these two mucins. It can be expected that additional membrane-anchored mucins will be detected in the near future, indicative of their importance in the hydration and protection of these epithelia.

2. Secreted Mucins

MUC5AC has been shown to be the major gel-forming mucin of the tear film and is secreted by conjunctival goblet cells (Berry *et al.*, 1996; Corfield *et al.*, 1997; Ellingham *et al.*, 1999; Inatomi *et al.*, 1995, 1996; Jumblatt *et al.*, 1999). According to Gipson *et al.* (2003), all conjunctival goblet cells appear to secrete MUC5AC, but there have been no systematic studies to date of all zones of the human conjunctiva or of the goblet cell crypts located in the fornical region of the human conjunctiva (Kessing, 1968). In addition to MUC5AC, MUC2 has also been reported to be produced by conjunctival goblet cells, but at levels about 5600 times lower than MUC5AC (Inatomi *et al.*, 1997; McKenzie *et al.*, 2000). It is suggested that MUC2 is secreted by a subset of conjunctival goblet cells, as has been reported in the intestine (Podolsky *et al.*, 1986) and respiratory tract (Buisine *et al.*, 1999). Recently, MUC2 has also been demonstrated at the protein level in conjunctival samples (Berry *et al.*, 2004a). PCR has also detected MUC5B message in the conjunctiva, but neither the message nor protein has been demonstrated in goblet cells (Jumblatt *et al.*, 2003). Recently, transcripts of MUCs 13, 15, and 17 have also been detected in the conjunctiva (Corrales *et al.*, 2003).

Before secreted mucins of the conjunctiva become functionally active, they are stored densely packed and dry in the granules of goblet cells. Since the large gel-forming mucins can have molecular weights as high as 40,000 kDa, packaging in goblet cells requires considerable condensation. The space-occupying features of the molecules are probably the highly negatively charged carbohydrate chains, which are extraordinarily hydrophilic (Verdugo, 1991). To package mucins, intracytoplasmatic goblet cells shield the anionic charges on the mucins. The cationic shielding has been

hypothesized to be provided by calcium ions that are three times higher than outside the secretory vesicles (Verdugo *et al.*, 1987a,b). Upon secretion, mucin molecules hydrate, thereby increasing thousands of times in volume (Gerken *et al.*, 1992; Shogren *et al.*, 1989). Secretion is associated with a decrease in calcium, allowing the mucins to become hydrated and thus swell. Support for this theory comes from vitamin D receptor knockout mice that suffer not only from hypocalcemia but also reveal altered mucin packaging and decreased mucin content in conjunctival goblet cells (Paz *et al.*, 2003).

Following secretion, a polymeric mucin is built by a linear concatenation of subunits linked by disulfide bonds. Mucin function is associated with both peptide core and glycosylation characteristics. It has been shown that conjunctival surface mucins are predominantly smaller than intracellular species. This reduction in surface mucin size indicates postsecretory cleavage (Berry *et al.*, 2004b). Alterations in mucin structure reflect the condition of the ocular surface because they occur without clinically detectable signs (Berry *et al.*, 2004b).

IV. Lacrimal Gland Mucins

Supported by older studies (Allen *et al.*, 1972; Ito and Shibasaki, 1964; Jensen *et al.*, 1969; Kühnel, 1968; Millar *et al.*, 1996) and the finding that rat lacrimal glands synthesize rMuc4 (Arango *et al.*, 2001), recent studies have demonstrated mucin expression and protein synthesis of a spectrum of mucins (Jumblatt *et al.*, 2003; Paulsen *et al.*, 2004a; Table II).

A. Membrane-Anchored Mucins

1. MUC1

MUC1 mRNA and protein have been demonstrated in specimens of human lacrimal gland tissue. MUC1 reveals intense membrane-bound reactivity at the luminal lining of acinar epithelial cells (Paulsen *et al.*, 2004a). Its specific localization on the apical surface of epithelial cells has been suggested to function in signaling and may be important as a sensor mechanism in response to invasion or damage of epithelia (Ren and Kufe, 2002).

2. MUC4

Membrane-bound mucins, MUC1 and MUC4, reveal marked differences in expression and production in the lacrimal gland. Both have been shown to provide steric protection of epithelial surfaces. MUC4 has been detected as a

TABLE II
Mucins in the Lacrimal Gland

Mucin[a]	Expression in lacrimal gland	Localization in lacrimal gland	Changes in dry eye
MUC1	Positive	Membrane bound at the luminal lining of acinar epithelial cells	No
MUC2	Negative	Not present	No
MUC4	Sporadic	If present, membrane bound and cytoplasmic in acinar cells	Yes
MUC5AC	Positive	Goblet cells of larger excretory ducts	Yes
MUC5B	Positive	Cytoplasmic in many acinar cells	Yes
MUC6	Sporadic	Not present	No
MUC7	Positive	Cytoplasmic in many acinar cells and columnar epithelial cells of excretory ducts	Yes
MUC8	ND[b]	Not present	ND
MUC16	Positive	Supranuclear in the Golgi in single groups of acinar cells	ND

[a]No data exist about MUCs 3A, 3B, 9, 11, 12, 13, 15, 17, 19, and 20.
[b]ND, not determined.

main mucin of the rat lacrimal gland (Arango *et al.*, 2001). Human lacrimal gland message for MUC4 is present in only some lacrimal glands (Paulsen *et al.*, 2004a). MUC4 protein has been detected, but only in specimens aged 87 years or older, and was not detectable in samples aged less than 87 years regardless of the presence of MUC4 mRNA (Paulsen *et al.*, 2004a). When present, MUC4 is not only membrane-associated but also cytoplasmic in acinar cells, with single acinar cells revealing intense cytoplasmic staining (Fig. 4).

The low detection rate of MUC4 might be due to the fact that localization of MUC4 and indeed of all mucins in tissue sections has been fraught with problems of antibody specificity. As a result of mucins being heavily O-glycosylated, access of antibodies to the protein core is restricted. MUC4 is especially difficult to immunolocalize because the serine and threonine residues, which represent potential O-linked glycosylation sites, always present into the extracellular domain from their positions at the amino-terminus. It has been hypothesized that the most specific of the MUC4 antibodies are those directed to the so-called ASGP2 or ß-subunit, and the membrane-associated/cytoplasmic domain, since it lacks the heavy O-glycosylated regions found in the mucin ectodomain (Pflugfelder *et al.*, 2000). Our experience supports this, revealing that MUC4 is better detectable

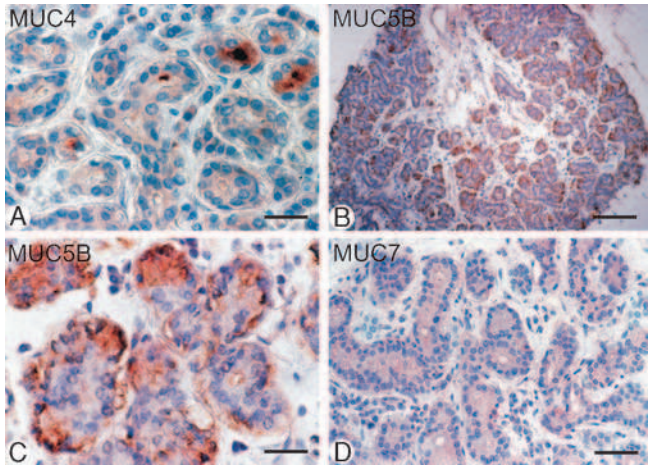

FIG. 4 Distribution of single mucins in human lacrimal gland. (A) MUC4 (brown) in the lacrimal gland of a woman who was treated with artificial tears. (B) MUC5B (brown) in a lobule of the lacrimal gland. (C) MUC5B (brown) in the lacrimal gland acinar cells. (D) MUC7 (red) in acinar cells of the lacrimal gland. Counterstains: hemalum. Scale bars: (A, C) 38 μm; (B) 330 μm; (D) 82.5 μm; Fig. 4C, see Paulsen *et al.* (2004a).

in paraffin-embedded tissue sections if an antibody directed to the membrane-binding domain is used.

As is the case in several other membrane-anchored mucins (e.g., MUCs 3A, 3B, 12, 13, 17), MUC4 also has two (or more) epidermal growth factor (EGF)-like domains between the tandem repeat region and the membrane-associated domain (Carraway *et al.*, 2000; Gum *et al.*, 2002; Pratt *et al.*, 2000; Williams *et al.*, 2001). Hints that the EGF-like domains play a role in the regulation of epithelial growth in the lacrimal gland come from studies by rMuc4 (Carraway *et al.*, 2002). rMuc4 is capable of triggering a specific phosphorylation of the receptor tyrosine kinase ErbB2 (Jepson *et al.*, 2002) and potentiates neuroregulin activation of the ErbB3 receptor. The receptor interactions suggest that rMuc4 has the potential to be involved in regulation of epithelial cell growth. Moreover, recent evidence indicates that ErbB2 can activate T lymphocytes (Fisk *et al.*, 1997; Kuerer *et al.*, 2002). Activation of T lymphocytes is a common feature in some lacrimal gland and ocular surface pathologies (i.e., in dry-eye syndromes), leading to abnormal apoptosis in terminally differentiated acinar epithelial cells of the lacrimal gland (Gao *et al.*, 1998). Arango *et al.* (2001) and Carraway *et al.* (2002) showed that rMuc4 and ErbB2 interact in the healthy lacrimal gland, while Z. Liu *et al.* (2000) found increased expression of ErbB2 and ErbB3 in the conjunctival epithelium of patients with non-Sjögren keratoconjunctivitis sicca. These

results point to the possibility that lacrimal gland MUC4 contributes to T cell activation.

3. MUC16

MUC16 is a high-molecular-weight glycoprotein (Yin and Lloyd, 2001), initially known as the CA125 antigen, that was initially detected in ovarian carcinoma cell lines of epithelial origin and in the luminal surface of tumor tissues taken from patients with ovarian cancer (Bast *et al.*, 1981). Today, MUC16 domains provide novel opportunities to develop new assays and refine current tools to improve the sensitivity and specificity of CA125 for population-based screening guidelines (McLemore and Aouizerat, 2005). In addition to its function as a tumor marker, studies have also revealed the presence of CA125 antigen in a number of normal tissues such as endocervical epithelium, endometrium, pleura, pericardium, and peritoneum (Kabawat *et al.*, 1983), in seminal plasma (Halila, 1985), milk secretions (Hanisch *et al.*, 1985), and cervical mucus (Halila, 1985; Hanisch *et al.*, 1985; Kabawat *et al.*, 1983), and just recently also in human ocular surface epithelia (Argüeso *et al.*, 2003). With regard to conjuctival epithelial cells (a telomerase-immortalized human conjunctival epithelial cell line was used), Hori *et al.* (2004b) showed that the expression pattern of MUC16 transcripts is different from that of the protein, suggesting that the regulation of MUC16 in human conjunctival epithelial cells may occur posttranscriptionally*.

To date, neither MUC16 expression nor protein has been detected in the human lacrimal gland. However, our own unpublished observations indicate production of MUC16 mRNA and protein in the lacrimal gland. In contrast to MUC1, which is membrane-anchored in the lacrimal gland, and to MUC4, which shows both membrane-associated and cytoplasmic occurrence in acinar cells (see above), MUC16 is immunohistochemically visible in intracytoplasmic organelles localized mainly above the nucleus, suggesting a synthesis and secretion mechanism as shown for soluble Muc4 (SMC, Komatsu *et al.*, 2002); i.e., two subunits may be produced by proteolytic cleavage prior to substantial O-glycosylation, near the time of transit from the endoplasmic reticulum to the Golgi. Our unpublished immunohistochemical results indicate that only a soluble form of MUC16 is produced by acinar cells, but no membrane-anchored MUC16. MUC16-positive acinar cells are very rare in the lacrimal gland, with numbers varying among individual specimens (own unpublished results). Immunodot blot analysis of tears from healthy volunteers indicates that they are positive for a secreted

*Moreover, the same group demonstrated just recently that MUC16 has a role in the protection of ocular surface epithelia (Argüeso *et al.*, 2006).

form of MUC16 (own unpublished observations). However, it is not clear at present whether the detected MUC16 is a product (soluble form of MUC16) of the lacrimal gland or originates from conjunctival and corneal epithelial cells (shed MUC16), or both.

B. Secreted Mucins

1. MUC5AC

MUC5AC is demonstrably present in the excretory duct system of the human lacrimal gland (Paulsen *et al.*, 2004a), where it is associated with single goblet cells of larger excretory ducts. It seems that the MUC5AC-positive goblet cells are goblet cells that immigrated from the fornical conjunctiva and do not belong to the lacrimal gland. However, and this will be discussed later, acinar cells of the lacrimal gland also seem to be able to produce MUC5AC. We observed MUC5AC production in lacrimal glands of elderly women who received treatment for dry eyes (Paulsen *et al.*, 2004a).

2. MUC5B

As already indicated by the study of one specimen with PCR, there is message for MUC5B in the lacrimal gland (Jumblatt *et al.*, 2003). Our own results indicated that message for MUC5B is nearly always present in the lacrimal gland, and that there is also protein production (Paulsen *et al.*, 2004a). MUC5B is produced by many acinar cells of lacrimal gland lobules, but there are also areas in the lacrimal gland that are completely free of MUC5B (Paulsen *et al.*, 2004a; Fig. 4). MUC5B has been shown to participate in bacterial adhesion (Baughan *et al.*, 2000; Thomsson *et al.*, 2002). Secretion by the lacrimal gland might be a necessary event in ocular surface protection because of lack of secretion by the ocular surface epithelia. MUC5B secretion is also well known from serous cells of salivary glands (Nielsen et al., 1997), although the secretory activities of the lacrimal gland are not unlike those of serous cells of salivary glands.

3. MUC7

Recent studies by Jumblatt *et al.* (2003) have demonstrated MUC7 mRNA and protein in four of six specimens of human lacrimal tissue RNA. By *in situ* hybridization they demonstrated the presence of message in some of the acinar cells of the gland. Protein for the small soluble MUC7 has also been detected in cellular extracts of lacrimal gland by immunoblot, but was

not detectable in tear samples assayed by immunoblot (Jumblatt *et al.*, 2003). Our own investigations confirmed message for MUC7, and immunohistochemistry revealed the cytoplasmic presence of MUC7 by some, but not all, acinar cells as well as columnar epithelial cells of excretory ducts of the lacrimal gland (Fig. 4). The lack of detection of MUC7 in tears, reported by Jumblatt *et al.* (2003), is likely to be due to its low concentration. Like MUC5B, MUC7 has been shown to participate in bacterial adhesion (B. Liu *et al.*, 2000; Situ and Bobek, 2000) as well as to have antifungal activity (Wei and Bobek, 2004, 2005). Moreover, MUC7 has a lubricative function in saliva (Gururaja *et al.*, 1998, 1999) and may have a similar role at the ocular surface after secretion from the lacrimal gland.

4. MUC2, MUC6, MUC8

Message and protein for mucins MUC2 and MUC8 have been demonstrated to be absent in human lacrimal gland (Paulsen *et al.*, 2004a, and unpublished observations). MUC6 mucin, however, was not detected, although message for this mucin was present in half of the samples analyzed (Paulsen *et al.*, 2004a).

C. Changes in the Mucin Composition Related to Age (Presence of Dry Eye Pathology)

1. Age-Related Dry Eye

The term "dry eye" (synonymously termed sicca syndrome or keratoconjunctivitis sicca) or the so-called dry eye syndrome (DES) refers to a common but highly heterogeneous group of ocular surface disorders (Dana and Hamrah, 2002; Schaumberg *et al.*, 2002). Nearly 11 million people suffer from dry eye in Germany (source: Professional Federation of German Ophthalmologists), and a larger number suffer from dry eye in the United States (source: National Eye Institute; 2.5:1 women to men). Approximately 2% of all dry eye cases are a consequence of Sjögren's syndrome. People wearing contact lenses or undergoing LASIK surgery are also at greater risk for developing dry eye. In the meantime, dry eye accounts for the largest group of patients seeing an ophthalmologist. Precise determination of the prevalence of dry eye is hampered by the lack of agreed diagnostic criteria, due in part to the wide spectrum of conditions the term encompasses, the wide variation in disease severity, the nonspecificity of its associated symptoms and clinical signs, and, last but not least (at least in Germany), the amount of time required for extensive and useful diagnostics. Despite these limitations, most large studies, based on a variety of definitions, have estimated the prevalence of "significant" dry eye to be about 10–20% in the adult

population (Bandeen-Roche *et al.*, 1997; Begley *et al.*, 2002; Bjerrum, 1997; Caffery *et al.*, 1998; Chia *et al.*, 2003; Doughty *et al.*, 1997; Hikichi *et al.*, 1995; Lin *et al.*, 2003; McCarty *et al.*, 1998; Moss *et al.*, 2000; Schaumberg *et al.*, 2003; Schein *et al.*, 1999). At any rate, severe dry eye is less frequent. Most of the cases result from normal aging of the glands and epithelia in the eye, although the condition can occur at any age. An estimated 20% of people over the age of 45 years will experience dry eye syndrome. Clearly, cumulative prevalence will climb as the elderly bracket of the population increases. The most frequent case, the "typical" case, in the ophthalmological practice is an elderly (postmenopausal) female patient who complains of ocular discomfort and is diagnosed with "age-related dry eye" [although—as stated above—there are also younger (premenopausal) as well as male patients, albeit in lower numbers]. This diagnosis is based on subjective symptoms, results of ophthalmic examination, and Schirmer I testing (normally no serologic testing is done to rule out Sjögren's syndrome if the patient reports no history of connective tissue disorders or xerostomia, which would be associated with this autoimmune disease). Such patients are typically treated with artificial tears for periods lasting from months to years. It is expected that in the near future, the DEWS (Dry Eye Workshop Study Group), which involves leading academics and opthalmologists, will define internationally agreed-upon criteria for differential diagnoses of the various conditions covered by the generic term "dry eye."

2. Lacrimal Gland Mucins Related to Age

Recently, we analyzed aging of the lacrimal gland with regard to mucin production (Paulsen *et al.*, 2004a; Table II). Membrane-bound mucins, MUC1 and MUC4, revealed marked differences in expression and production in the human lacrimal gland. As stated above, MUC1 was detectable in all of the lacrimal glands analyzed at the luminal lining of acinar epithelial cells. Its specific localization in relation to the apical surface of epithelial cells has been suggested to function in signaling and may be important as a sensor mechanism in response to invasion or damage of epithelia (Ren and Kufe, 2002). Interestingly, dry eye is also associated with epithelial damage of the ocular surface and/or the lacrimal gland. However, no change in MUC1 related to age or to cases treated with artificial tears was observed, suggesting that MUC1 is not involved in the processes occurring in dry eye.

MUC4 protein has been detected in lacrimal gland samples of women who were treated with artificial tears and in specimens aged 87 years or older but was not detectable in samples aged less than 87 years regardless of the presence of MUC4 mRNA (Paulsen *et al.*, 2004a; Figs. 1 and 2). When present, MUC4 is not only membrane-associated but also cytoplasmic in acinar cells, with single acinar cells revealing intense cytoplasmic staining. As

stated above, MUC4 functions in activation of T lymphocytes in the lacrimal gland via Erb receptors. Such activation is a common feature in dry eye syndromes, leading to abnormal apoptosis in terminally differentiated acinar epithelial cells of the lacrimal gland (Gao *et al.*, 1998). On the other hand, it has been shown that rMUC4 acts as an antiapoptotic agent (Komatsu *et al.*, 2001). Thus, as production of MUC4 in membrane-bound and soluble form in acinar cells of the human lacrimal gland is seen only in the advanced age group (Paulsen *et al.*, 2004a), it has been speculated that MUC4 is involved in providing a protective mechanism to retard loss of acinar cells as well as in T cell activation. Whether MUC4 occurs in reaction to the one or the other function, or both, whether the functions depend on each other, and whether MUC4 acts only in the lacrimal gland or also at the ocular surface epithelia after it is secreted into the tear film is not clear at present.

Zhao *et al.* (2001) quantified levels of MUC5AC in tears of healthy subjects and in dry eye patients. No correlation between the amount of MUC5AC and age or gender in the healthy population was found. However, decreased levels of the mucin in tears of patients with dry eye were observed. A similar finding was obtained by Argüeso *et al.* (2002), who demonstrated decreased levels of MUC5AC in tears of patients with Sjögren's syndrome. From these results a deficiency of MUC5AC mucin in tears was proposed to be one of the mechanisms responsible for tear film instability in Sjögren's syndrome. In the lacrimal gland, a strong increase in immunodot blot staining intensity of MUCs 4, 5AC, and 5B was observed in lacrimal glands of elderly women who received treatment for dry eyes (Paulsen *et al.*, 2004a;

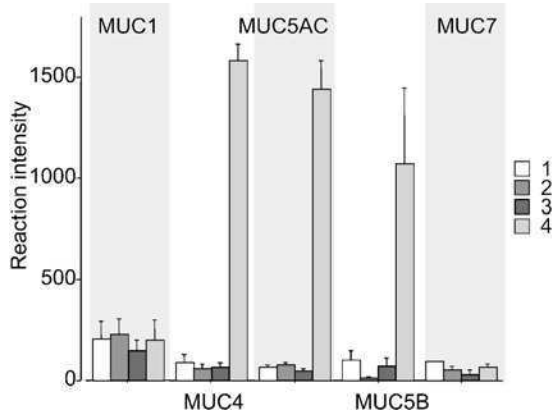

FIG. 5 Densitometry of a dot-blot analysis for MUCs 1, 4, 5AC, 5B, and 7 in human lacrimal gland samples divided into four different groups (group 1, male, 25–59 years; group 2, male, 82–87 years; group 3, female, 53–78 years; group 4, age-related changes group, female, 80–96 years). (Paulsen *et al.,* 2004).

Fig. 5). In such cases, MUC5AC is not only produced by goblet cells of excretory ducts under "healthy" (normal) conditions but also by some acinar cells of the lacrimal gland. The induction of MUC5AC production in acinar cells might be explained as an attempt at partial compensation for the loss of MUC5AC production in the conjunctiva. However, mucin degradation by means of yet unknown pathological processes in dry eye might also be an explanation for the findings. Mucin degradation could lead to the increased staining observed.

The latter explanation could also be suggested for MUC5B in the lacrimal gland. As previously stated, MUC5B is produced by acinar cells of the healthy lacrimal gland (Paulsen *et al.*, 2004a; Fig. 5). Immunodot blot staining intensity has been observed to be strongly increased in lacrimal glands of elderly women who were treated with artificial tears (Paulsen *et al.*, 2004a). The findings suggest that the increased staining intensity is not due to inflammatory mediators, growth factors, or microbial colonization, because only MUC5AC has been shown to be up-regulated by such substances and not MUC5B (Almstahl *et al.*, 2001; Borchers *et al.*, 1999; Leikauf *et al.*, 2002; Perrais *et al.*, 2002; Smirnova *et al.*, 2001).

3. Hormonal Regulation of Lacrimal Gland Mucins

Regulation of MUC5B seems to depend on hormonal regulation, as shown recently for the endocervical cycle (Gipson *et al.*, 2001). There is little information in the literature regarding hormonal regulation of mucin expression other than the membrane-spanning mucins. Recent studies show that expression of the SMC (rMuc4; the rat homologue of MUC4) in the rat uterus is down-regulated by progesterone (McNeer *et al.*, 1998), as is the case of MUC5B in the human endocervix (Gipson *et al.*, 2001). Thus, postmenopausal down-regulation of progesterone could account for changes in MUC4 and MUC5B production in age-related dry eye. Moreover, androgens regulate both lacrimal and Meibomian gland function, and androgen deficiency correlates with the occurrence of dry eye (Sullivan *et al.*, 1999). However, with the exception of MUC1 (Mitchell *et al.*, 2002), no data exist regarding androgen-dependent regulation of mucins, and recent results obtained by our group (Paulsen *et al.*, 2004a) indicate that MUC1 production by the lacrimal gland is unaffected in cases of age-related dry eye.

4. Mucin Secretion due to Neuronal Stimuli in the Lacrimal Gland

It has been shown that acinar cells of the lacrimal gland are densely supplied by nervous tissue and peptidergic nerve fibers (Seifert *et al.*, 1996; for review see Hodges and Dartt, 2003). This innervation pattern has been suggested to be part of the "functional ocular surface-central nervous system-lacrimal

gland sensory-autonomic neural network'' that maintains ocular surface health and homeostasis (Song *et al.*, 2003). This ''lacrimal functional unit'' encompasses the ocular surface tissues (cornea and conjunctiva, including goblet cells and Meibomian glands), the lacrimal glands [main and accessory (Krause and Wolfring)], and their interconnecting sensory (CN V) and autonomic (CN VII) innervation (Stern *et al.*, 1998; Stern and Pflugfelder, 2004).

As reviewed recently by Hodges and Dartt (2003), activation of parasympathetic and sympathetic nerves that surround lacrimal gland acini causes the release of their classic and peptide neurotransmitters, which then bind to their specific receptors on myoepithelial and acinar cells and lead to regulated protein secretion. Of the three types of nerves, parasympathetic, sympathetic, and sensory, that innervate the lacrimal gland, only parasympathetic and sympathetic nerves are major stimulators of lacrimal gland protein secretion. The parasympathetic neurotransmitters acetylcholine and vasoactive intestinal peptide and the sympathetic neurotransmitter norepinephrine are potent stimuli of lacrimal gland secretion, whereas others have minor stimulatory or no effects (for review see Hodges and Dartt, 2003). Acetylcholine released from parasympathetic nerves activates the M_3 (glandular subtype receptor, the only one of the five muscarinic receptor subtypes present in human lacrimal gland). M_3 is located on the basolateral membranes of acinar and the plasma membranes of myoepithelial cells (for review see Hodges and Dartt, 2003) and has obtained attention as a marker of Sjögren's syndrome (Bacman *et al.*, 2001; Gao *et al.*, 2004).

To date, no data exist with regard to lacrimal gland innervation and mucin secretion. However, it may be hypothesized that lacrimal gland mucin production depends on stimuli from the nerves innervating the lacrimal gland. In a murine model of Sjögren's syndrome it has been shown that activation of nerves of lacrimal glands infiltrated with lymphocytes does not increase the release of neurotransmitters, which results in impaired secretion from these glands (Zoukhri and Kublin, 2000). In another model it was demonstrated that mice with a deficiency of neuturin—a neurotrophic factor for parasympathetic neurons—develop defective parasympathetic innvervation of their lacrimal glands, leading to symptoms of dry eye (Song *et al.*, 2003). Finally, Nguyen *et al.* (2004) demonstrated in the rat lacrimal gland that following the loss of parasympathetic control, tear secretion was significantly reduced and corneal ulcers developed in all experimental eyes. Light microscopy showed breakdown of the acinar structure of the lacrimal gland, and DNA microarray analysis revealed down-regulation of genes associated with the endoplasmic reticulum and Golgi, including genes involved in protein folding and processing. Conversely, transcripts for cytoskeleton and extracellular matrix components, inflammation, and apoptosis

were up-regulated (Nguyen *et al.*, 2004). It might be hypothesized from these findings that mucin production by the lacrimal gland is also altered with loss of neuronal control. However, this connection requires further elucidation.

5. Interaction of Lacrimal Gland Mucins with Trefoil Factor Family Peptides

It has been demonstrated that distinct mucins (MUC2 and MUC5AC) are able to interact directly with trefoil factor family peptides (trefoil peptides, TFF peptides) (Thim *et al.*, 2002; Tomasetto *et al.*, 2000; for review see Hoffmann and Jagla, 2001). TFF peptides have recently been shown to be secreted by porcine and human conjunctival goblet cells (Jagla *et al.*, 1999; Langer *et al.*, 1999). Three TFF peptides have been characterized in mammals, including humans: TFF1 (formerly pS2), TFF2 (formerly hSP), and TFF3 (formerly hP1.B/hITF). They are characterized by the TFF motif, a three-looped structure held tightly together by disulfide bonds based on six cysteine residues. One such motif is found in TFF1 and TFF3, whereas TFF2 possesses two TFF domains. In addition to their occurrence as major secretory products of many mucin-producing cells (Hoffmann and Jagla, 2001; Hoffmann *et al.*, 2001), they have been detected in the brain (Jagla *et al.*, 2000). TFF peptides have multiple physiological functions such as promotion of epithelial cell migration, antiapoptotic properties, induction of cell scattering, epithelial restitution, function as neuropeptides (for review see Hoffmann and Jagla, 2001; Hoffmann *et al.*, 2001), as well as their impact on the rheological properties, especially in the tear film (Jagla *et al.*, 1999; Langer *et al.*, 1999). At the ocular surface, Langer *et al.* (1999) showed that TFF1 and TFF3, but not TFF2, are secreted by conjunctival goblet cells under healthy conditions. Healthy cornea does not produce TFF peptides, although message for TFF3 is also present (Steven *et al.*, 2004). Under certain disease states such as keratoconus and Fuch's dystrophy, however, there is production of TFF3 protein by corneal epithelial, stromal, and endothelial cells. In cases of herpetic keratitis, TFF3 is produced by healthy corneal epithelial and stromal cells that surround the herpetic lesions, suggesting that TFF3 may be induced as a result of structural damage (Steven *et al.*, 2004).

The production of TFF peptides by the lacrimal gland is unclear at present. Our own unpublished observations demonstrated message for TFF1 in only approximately 30% of the investigated samples, whereas TFF3 was present in all of them (Paulsen *et al.*, 2004b). TFF2 was not detectable. Immunohistological localization reveals weak cytoplasmic staining of acinar cells as well as strong staining of some single cells between lacrimal acini that are not lymphocytes or CD68-positive macrophages

(unpublished observations). Western blot analysis shows that the detected protein is only about half the size of normal TFF3 protein (Paulsen *et al.*, 2004b). The detected "half-sized" protein may reflect protein degradation of normal TFF3 due to use of postmortem material from human lacrimal glands. Whether TFF3 is secreted by acinar cells and whether it has a function in acinar cell physiology are yet to be determined.

D. Accessory Lacrimal Gland Mucins

Accessory lacrimal glands were first described by Carl Friedrich Krause from Hanover in the conjunctival fornix and at the edge of the upper tarsus (Krause, 1842). These latter glands at the edge of the upper tarsus were described again by Wilhelm Johann Krause from Göttingen (Krause, 1876) as well as by Emil von Wolfring from Warsaw (Wolfring, 1872), who seems to have been unaware of the original publication by C. F. Krause (Krause, 1842). Ever since, the glands in the fornix have been referred to as the glands of Krause and the glands of Wolfring. Although the accessory lacrimal glands participate in the aqueous phase of tear secretion and are believed to play an important role in the pathogenesis of dry eye, there are only a few publications on the structure of the glandular elements, their blood vessels, and their neural supply (Seifert *et al.*, 1993, 1994a, 1997). Histologically, they appear to be a mixed population of cells—very similar to the main lacrimal gland—with both serous and mucus types of secretory vesicles—with an appearance much like that of other submucosal glands (Seifert *et al.*, 1994b). Presumably, these glands also produce mucins, but they have not been examined for mucin production to date.

E. Relationship of Lacrimal Gland Mucins to the Tear Film

Actual models of tear film distribution suggest that the secreted mucins are mixed within the aqueous tear fluid (for review see Gipson, 2004; Gipson and Argüeso, 2003; Gipson *et al.*, 2004). The amount of secreted mucin at any one position on the ocular surface may depend on the eyelid position. It has been suggested that as the eyelids move toward closure, the mucin layer may increase in depth and be moved toward the nasal puncta for elimination. A system can be envisioned whereby the secreted mucins move about over the ocular surface with the blink to trap and remove debris and cellular components from the surface of the epithelium (Gipson, 2004). In this model system, mucins are constitutively secreted and removed, and represent a sort of cleaning rag or janitorial service. The secreted gel-forming mucins form networks of entangled linear polymers responsible for the

non-Newtonian thixotropic or viscoelastic properties of mucin gels that help avoid shearing damage during rapid relative movements of the lids and globe (Carlstedt *et al.*, 1985; Corfield *et al.*, 1997). Whether these secreted gel-forming mucins are only MUC5AC from conjunctival goblet cells or also MUC5B from the lacrimal gland needs to be determined (Fig. 3). The secreted mucins must move easily and freely over the membrane-anchored mucins of the thick glycocalyx. Membrane-anchored and secreted mucins are highly glycosylated, so they carry negative charges, and also hydrophilic, facilitating a "wet repulsion" that allows movement of the mucins secreted by the goblet cells over the membrane-associated mucins of the surfaces of cornea and conjunctiva (Gipson, 2004). The same character would allow smooth movement of the lids over the eye to prevent epithelial–epithelial adherence. Adhesionless gliding of gels over each other may act in tandem with shear thinning of preocular fluid during blink to protect underlying epithelia from being dislodged and to prevent sensory nerve activation (Berry *et al.*, 2001). A lack of adhesion between mucins (Sharma, 1993) allows spreading of the tear film, and prevents microtrauma to the ocular surface by reducing transmitted shear during blinking (Corfield *et al.*, 1997). Lack of adhesion might also account for the persistence of foreign material (trapped in a mucin gel) in the same position through a number of blinks (Berry *et al.*, 2001). Loss of ocular surface material into the surrounding aqueous tears seems to be prevented or at least decreased by polymeric mucins linked by disulfide bonds (Berry *et al.*, 2004a). These mucin features may help explain the physiological observations of tear film stability. In dry eye, mucins dehydrate and lose their polar properties. This results in mucin binding to itself and to epithelium, causing the hydrophilic mucin gel to collapse into hydrophobic aggregates and the formation of filaments (Danjo *et al.*, 1998; Sharma, 1993). Whether the secreted mucins of lacrimal glands MUC5B, MUC7, and possibly also secreted MUC16 play a role in tear film stability is not known and needs to be determined.

F. Function of Lacrimal Gland Mucins in Antimicrobial Defense

Mucin production is an evolutionary defense strategy. In addition to lubrication of the mucosa and waterproofing to regulate epithelial cell hydration, mucus protects mucosal surfaces against potentially harmful substances such as particles, aggressive chemical agents, digestive enzymes, food lectins, toxins, and bacterial and other infectious agents (Faillard and Schauer, 1972; Forstner, 1978; Hutch, 1970; Reuter *et al.*, 1992; Schauer, 1992; Walker, 1976). It has long been assumed that mucus protects mucosal surfaces from infective agents and noxious substances. Intestinal mucus has been observed

to carry away bacteria (Florey, 1933). Moreover, it has been shown that mucus possesses structures mimicking the receptor sites for microorganisms on epithelial cells that facilitate trapping and subsequent disposal of bacteria (Abraham and Beachey, 1985) and viruses (Reuter *et al.*, 1988). A variety of oral and intestinal bacteria have been revealed to produce neuraminidase (sialidase), an enzyme that can degrade mucins by the removal of sialic acid (Corfield, 1992). In addition, oral, intestinal, and female reproductive tract bacteria synthesize an array of other glycosidases, proteases, and sulfatases (so-called mucinases), enzymes that are capable of degrading mucins (Schauer, 1997; Wiggins *et al.*, 2001).

Also at the ocular surface, mucus more commonly binds with potential harmful tear contaminants and acts as a debris removal system. Mucin secretion together with the secretion of other antibacterial proteins is expected to diminish bacterial, viral, and fungal colonization. Antibacterials are secreted by the ocular surface epithelia and to a great extent by the lacrimal gland. The antibacterials secreted are lysozyme, lactoferrin, betalysin, lipoglycans, immunoglobulins A, G, and E, complement (for review see Milder and Weil, 1983), lipocalin (Fluckinger *et al.*, 2004), surfactant proteins D (SP-D, Ni *et al.*, 2005) and A (SP-A, Kindler *et al.*, 2005), as well as various antimicrobial peptides (for review see McDermott, 2004) such as ß-defensins 1–4, psoriasin (unpublished observations), human cationic antimicrobial protein (hCAP-18, LL37, Lysenko *et al.*, 2000), angiogenin (Sack *et al.*, 2005), bactericidal/permeability-increasing protein (Peuravuori *et al.*, 2005), and liver-expressed antimicrobial peptide 1 (heptcidin, LEAP1) and 2 (LEAP2, McIntosh *et al.*, 2005). The antibacterials, presumably together with mucins of the tear film, maintain bacteria at such low levels that 40% of ocular surfaces are culture negative (Willcox and Stapleton, 1996). It has been demonstrated that mucin decreases bacterial adherence to the cornea (Fleiszig *et al.*, 1994). The diversity of tear mucin-linked oligosaccharide epitopes creates an enormous repertoire of potential binding sites (Thomsson *et al.*, 2002).

The additional secretion of lacrimal gland mucins (MUC5B, MUC7, and secreted MUC16) may potentiate this effect. Both MUC5B and MUC7 have been shown to participate in bacterial adhesion (Baughan *et al.*, 2000; B. Liu *et al.*, 2000; Situ and Bobek, 2000; Thomsson *et al.*, 2002). Soluble MUC7 may, as occurs at the oral surface, associate with histatins, which are known to be produced by the ocular surface and the lacrimal gland (Steele and Jumblatt, 2001), and help protect against microbial colonization (B. Liu *et al.*, 2000; Situ and Bobek, 2000). Until now, no data are available regarding antimicrobial protection by secreted MUC16. Steady renewal of tear film mucins is necessary, since it has been shown that commensal bacteria in the healthy ocular surface possess mucinolytic activity on both intact and

surface-processed mucins, targeted to discrete sites in the mucin molecule and leading to mucin degradation. Inhibition of bacterial growth by ocular mucins can be seen as part of the system of mucosal control of microbiota (Berry *et al.*, 2002).

The innate immune system in the form of the local ocular environment with its antimicrobial substances, including mucins, exchanges signals with the adaptive immune system (McNamara, 2003; Thakur and Willcox, 1998; Willcox *et al.*, 1997). Although leukocytes are rarely seen in normal open-eye tear fluid (McNamara, 2003; Norn, 1989; Thakur and Willcox, 1998; Willcox *et al.*, 1997), they are numerous in the tear film under closed lids (Sack *et al.*, 1992, 2000; Sakata *et al.*, 1997). Interactions between mucins and neutrophils have been shown in a number of mucosae. For example, MUC7 from salivary glands has been associated with neutrophils from the oral cavity (Prakobphol *et al.*, 1999). Neutrophil products such as elastase and cathepsin G can, in turn, release mucin secretion (Dwyer and Farley, 2000; Fischer and Voynow, 2002; Fischer *et al.*, 2003; Kim *et al.*, 1987, 2003; Kohri *et al.*, 2002; Pettersen and Adler, 2002; Shim *et al.*, 2001). Neutrophil defensins, in particular, show an ability to enhance MUC5AC and MUC5B gene expression in cultured epithelial cell lines (Aarbiou *et al.*, 2004). On the other hand, it has been demonstrated that normal mucin glycosylation and conformation are important for neutrophil activation at mucosal surfaces (Aknin *et al.*, 2004).

The findings also suggest interactions between the lacrimal gland mucins MUC5B and MUC7 and neutrophils in the lacrimal gland and in tear film that still require elucidation. Whether there are also interactions between lacrimal gland mucins and other defense cells such as macrophages, mast cells, or lymphocytes also awaits clarification.

V. Mucins of the Nasolacrimal Ducts

Although the physiology of lacrimal drainage has been under study for more than a century, the forces that cause tear flow are not completely understood. Various mechanisms have been proposed to explain the drainage of tears. These include an active lacrimal pump mechanism that functions by contraction of the orbicularis eye muscle (Amrith *et al.*, 2005; Jones, 1958; Kakizaki *et al.*, 2005; Pavlidis *et al.*, 2005); a "wrung-out mechanism," governed by a system of helically arranged fibrillar structures (Thale *et al.*, 1998); and the action of a cavernous body surrounding the lacrimal sac and the nasolacrimal duct (Ayub *et al.*, 2003; Paulsen *et al.*, 2000a). Physical factors such as capillarity, gravity, respiration, evaporation, and reabsorption of tear fluid through the lining epithelium of the efferent tear ducts have also been

invoked (for review see Paulsen, 2003; Paulsen *et al.*, 2002d, 2003a). Both the upper and lower canaliculus are lined by a thick, noncornified, stratified epithelium (Paulsen *et al.*, 1998). To date, no data are available on mucins in the canaliculi, although such information would be very interesting with regard to tear flow through the canaliculi. At the transition from the canaliculi into the lacrimal sac the stratified epithelium produces a double-layered epithelial area that is rich in goblet cells and intraepithelial mucous glands (Paulsen *et al.*, 1998). The epithelial lining of the lacrimal sac and the nasolacrimal duct consists of pseudostratified, columnar epithelia rich in goblet cells. Major secretory products of the epithelial cells are mucins, together with TFF peptides (Paulsen *et al.*, 2002d,e, 2003a,b, 2004c). In addition to epithelial and goblet cells, small serous glands are situated subepithelially in some lacrimal systems (Paulsen *et al.*, 1998).

A. Membrane-Anchored Mucins

The membrane-anchored mucins MUC1 and MUC4 have not been detected in the lacrimal sac and nasolacrimal duct, although message has been found to be present in all nasolacrimal ducts, though not in all lacrimal sacs (Paulsen *et al.*, 2003b). Comparable results were obtained by Lin *et al.* (2001), who were also unable to detect membrane-bound mucins in the mucosa of the middle ear, although the mucosa of the auditory tube was positive for MUCs 1 and 4. An explanation for the negative immunohistochemistry would be that the antibodies used were raised to epitopes within the VNTR region of the peptide core. These antibodies are likely to have varying reactivities, depending on the glycosylation of the mucins in the tissues under study. Mature mucins, with dense glycosylation, may not react with antibodies directed toward tandem repeat epitopes of the peptide core, since these regions support maximum glycosylation density. Different glycosylation patterns may explain reactivity in positive control samples. Use of an antibody (1G8) to the membrane-binding domain of MUC4 revealed membrane-bound as well as cytoplasmically present MUC4 in high columnar epithelial cells of the lacrimal sac and nasolacrimal duct (unpublished observations; Fig. 6 and Table III). As stated above, MUC1, if present, and MUC4 may function in signaling and may be important as a sensor mechanism in response to invasion or damage of epithelia as well as in T cell activation.

MUC16 has not yet been described in the nasolacrimal ducts. However, our unpublished observations indicate the presence of mRNA and MUC16 protein in nasolacrimal ducts (Table III). Immunohistochemistry reveals perinuclear reactivity in the cells of the double-layered epithelium of the lacrimal sac and nasolacrimal duct. Perinuclear reactivity coincides with

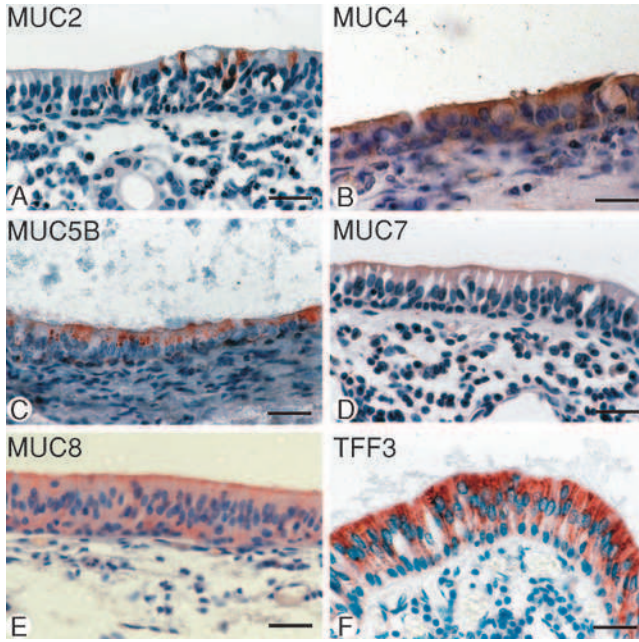

FIG. 6 Distribution of single mucins and trefoil factor family peptide 3 (TFF3) in human nasolacrimal ducts. (A) MUC2 (red) in single goblet cells of the nasolacrimal duct. (B) MUC4 (red) in high columnar epithelial cells of the nasolacrimal duct. (C) MUC5B in goblet cells and intraepithelial mucous glands of the nasolacrimal duct. (D) MUC7 in high columnar epithelial cells of the nasolacrimal duct. (E) MUC 8 in high columnar epithelial cells of the nasolacrimal duct. (F) TFF3 in high columnar epithelial cells of the nasolacrimal duct. Counterstains: hemalum. Scale bars: (A–E) 38 μm.

immature, lightly glycosylated mucins still in the Golgi apparatus. Reactivity for MUC16 is absent in goblet cells and intraepithelial mucous glands but is also present in the serous parts and secretion products of subepithelial serous glands of the nasolacrimal ducts (unpublished observations), indicating that MUC16 has a function as secreted mucin, and not as membrane-anchored mucin, in the nasolacrimal passage.

B. Secreted Mucins

The epithelia of the lacrimal sac and nasolacrimal duct produce MUC5B and MUC7 and, to a lesser extent, MUC5AC and MUC2. MUC2, MUC5AC, and MUC5B are produced by single goblet cells and goblet cells forming intraepithelial mucous glands, but not columnar epithelial cells (Paulsen

TABLE III
Mucins in the Nasolacrimal Ducts[a]

Mucin[b]	Expression in nasolacrimal ducts	Localization in nasolacrimal ducts	Changes in PANDO[c]
MUC1	Positive	Not present	No
MUC2	Positive	Single goblet cells and intraepithelial mucous glands	Yes
MUC4	Positive	Cytoplasmic in acinar cells	No
MUC5AC	Positive	Single goblet cells and intraepithelial mucous glands	Yes
MUC5B	Positive	Single goblet cells and intraepithelial mucous glands	Yes
MUC6	Sporadic	Not present	No
MUC7	Positive	Cytoplasmic in all high columnar epithelial cells	No
MUC8	Positive	Cytoplasmic in all high columnar epithelial cells	ND[d]
MUC16	Positive	Supranuclear in the Golgi in all high columnar epithelial cells and single basal cells as well as serous cells of subepithelial glands	ND

[a]The mucin distribution is based on investigations of the epithelia of the lacrimal sac and nasolacrimal duct. No data are available regarding mucins of the canaliculi.
[b]No data exist about MUCs 3A, 3B, 9, 11, 12, 13, 15, 17, 19, and 20.
[c]PANDO, primary acquired nasolacrimal duct obstruction.
[d]ND, not determined.

et al., 2003b; Fig. 6 and Table III). The low-molecular-weight, non-gel-forming mucin MUC7 is produced by columnar epithelial cells of the lacrimal sac and nasolacrimal duct, similar to its distribution in the submandibular and lacrimal glands, where MUC7 is the secretory product of salivary and lacrimal serous cells (Paulsen *et al.*, 2004c; Tabak, 1995). MUC7 has a lubricating effect (Gururaja *et al.*, 1998, 1999) in addition to the antimicrobial function already described (Baughan *et al.*, 2000; B. Liu *et al.*, 2000; Situ and Bobek, 2000) in saliva and may have a similar role at the epithelial surface of the nasolacrimal ducts. MUC6 mucin is not present, although message for this mucin was observed in half of the samples (Paulsen *et al.*, 2003b).

Unpublished results reveal that the columnar epithelial cells of the lacrimal sac and the nasolacrimal duct also produce MUC8 and secrete it into the lacrimal passage. MUC8 has been demonstrated in particular as a ciliated cell marker in human nasal epithelium and the epithelium of the paranasal sinuses (Jung *et al.*, 2000; Kim *et al.*, 2005; Yoon *et al.*, 1999) and is

up-regulated by proinflammatory cytokines and under chronic inflammatory conditions (Jung *et al.*, 2000; Kim *et al.*, 2005; Yoon *et al.*, 1999).

C. Comparison of Mucins of the Nasolacrimal Ducts with Mucins of Tear Film

The lacrimal sac and nasolacrimal duct have a mucin gene expression pattern that is comparable in quality to the mucins in the tear film, though it differs in quantity. Conjunctiva mainly express MUC5AC, and, at much lower levels, MUC2 (McKenzie *et al.*, 2000; Table IV). In addition to these mucins, MUC7, as well as probably MUC5B and MUC16, are present in the tear film originating from the lacrimal gland and (at least) from the ocular surface epithelia (Argüeso *et al.*, 2003; Hori *et al.*, 2004b; Jumblatt *et al.*, 2003; Paulsen *et al.*, 2004a; unpublished observations; Table IV). The epithelia of the lacrimal sac and nasolacrimal duct produce mainly MUC5B and MUC7 as well as MUC5AC and MUC2 (Paulsen *et al.*, 2003a). MUC16 and MUC8 are also secreted (unpublished results). Whether the ocular surface epithelia also produce MUC8 has not been assessed as yet. The lacrimal gland, at any rate, does not. MUC8 in the nasolacrimal ducts could be interpreted as a transition mucin making the change from ocular surface mucin production to the nasal mucosa that produces MUC8 as a main mucin. In addition to MUC8, the nasal mucosa has been shown to produce MUCs 4, 5AC, 5B, and 7. MUC2 and MUC6 are not present (Jung *et al.*, 2000; Yoon *et al.*, 1999; Table IV). However, quantitative comparisons of mucins in the different regions—ocular surface, nasolacrimal ducts, and nasal mucosa—are lacking, as is a comparative localization study.

D. Influence of Efferent Tear Duct Mucins on Tear Outflow

A distinct regional distribution of secretory mucins in the lacrimal sac and nasolacrimal duct may significantly influence the rheology and thus the flow of tears through the efferent tear passages. At the ocular surface, mucin composition, distribution, and function are influenced by shear forces generated during blinking (for review see Corfield *et al.*, 1997). In the nasolacrimal ducts, such forces are absent, and other mechanisms are necessary to ease the flow of tears.

Each mucin-producing cell type has been shown to secrete a characteristic TFF peptide–mucin combination (Hoffmann and Jagla, 2001; Hoffmann *et al.*, 2001). Based on the cosecretion of TFF peptides with mucins—as stated above—it is postulated that TFF peptides interact with mucins as link peptides, influencing the rheological properties of these complex viscous

TABLE IV
Comparative Mucin and TFF Peptide Distribution in the Lacrimal System and the Ocular Surface

Mucin[a]	Lacrimal gland	Conjunctiva	Cornea	Nasolacrimal ducts
MUC1	Yes	Yes	Yes	No
MUC2	No	Yes	No	Yes
MUC4	Yes/sporadic	Yes	Yes	Yes
MUC5AC	Yes/goblet cells of excretory ducts	Yes	No	Yes
MUC5B	Yes	No	No	Yes
MUC6	No	No	No	No
MUC7	Yes	No	No	Yes
MUC8	No	ND	ND	Yes
MUC16	Yes	Yes	Yes	Yes
TFF1	No	Yes	No	Yes
TFF2	No	No	No	No/inducible under pathological conditions
TFF3	Unclear	Yes	No/inducible under pathological conditions	Yes

[a]No data are available on MUCs 3A, 3B, 9, 11, 12, 13, 15, 17, 19, and 20.

biopolymers (Hauser *et al.*, 1993). The precise nature of the interaction between TFF peptides and mucins is currently not known. However, recent studies show that TFF1 interacts with the von Willebrand factor (vWBF) C-terminal domains of MUC2 and MUC5AC, indicating that the protective effect of TFF peptides may operate by organizing the complex mucus layer (Tomasetto *et al.*, 2000). The epithelium of the nasolacrimal ducts has been shown to synthesize TFF3, and in some cases TFF1 as well (Paulsen *et al.*, 2002e). In contrast to the human conjunctiva, in which TFF3 is detectable only in goblet cells, TFF3 from the lacrimal sac and nasolacrimal duct is produced in large amounts by epithelial cells as well as by serous glands, but not—or only in small amounts—by goblet cells (Paulsen *et al.*, 2002e; Fig. 6). This is comparable to localization of TFF3 in the major salivary glands (Nielsen *et al.*, 1996, 1997). TFF3 may thus have a special function in tear transport through the lacrimal passage comparable to its function on the ocular surface, because the peptide, together with TFF1, may contribute to the rheological properties of the tear film by way of interaction with the mucins of the nasolacrimal ducts.

E. Mucin Changes in Diseases of the Nasolacrimal Ducts

In common with all mucosae, the surfaces of the lacrimal sac and the nasolacrimal duct are in constant interaction with environmental microorganisms and hence are vulnerable to infection. Previous studies have shown that the efferent tear duct mucosa has developed a variety of anti-infection strategies to prevent colonization by microorganisms. These are required to thwart attacks from microorganisms leading to dacryocystitis, the most frequent disease of the nasolacrimal ducts (Knop and Knop, 2001; Paulsen *et al.*, 1998, 2000c, 2001a, 2002a, 2003; Perra *et al.*, 1995; Sirigu *et al.*, 2000). MUC5B and MUC7 support these antimicrobial mechanisms, having been shown to participate in bacterial adhesion (Baughan *et al.*, 2000; B. Liu *et al.*, 2000; Situ and Bobek, 2000).

Idiopathic or primary acquired dacryostenosis, synonymous with primary acquired nasolacrimal duct obstruction (PANDO), is a syndrome of unknown etiology that accounts for most nontraumatic cases observed in adults. Pathologic investigations indicate that it results from fibrous obstruction secondary to chronic inflammation (Busse and Müller, 1977; Linberg and McCormick, 1986; Mauriello *et al.*, 1992). However, the pathophysiology of functional dacryostenosis (i.e., patients with epiphora despite patent lacrimal passages on syringing) is yet to be understood. The pathologic condition in the epithelia is characterized by squamous metaplasia with loss of goblet cells (Paulsen *et al.*, 2001b). Consistent with the condition, a marked reduction of message for goblet cell-associated mucins MUC2, MUC5AC, and MUC5B has been observed in PANDO specimens (Paulsen *et al.*, 2003b; Table III). No change has been detected for MUC7 expression, despite metaplasia of the columnar cells. Unchanged production of the antimicrobial mucin MUC7 could help explain why dacryocystitis never develops in some patients with epiphora due to postsaccal stenosis (Paulsen *et al.*, 2003b; Table III). Reduced levels of mRNA of secretory mucins in functional dacryostenosis support the assumption that mucins ease tear flow through the efferent ducts.

Dacryoliths (lacrimal stones, calculi) are commonly observed by lacrimal surgeons during dacryocystorhinostomy (DCR). They are one of the causes of PANDO. Although the history of dacryolith studies is long, our understanding of the pathophysiology involved is still in the Dark Ages according to Linberg (2001). It has recently been demonstrated that dacryoliths consist partly of secreted mucins comparable with the mucin spectrum of the epithelium of healthy nasolacrimal ducts (Paulsen *et al.*, 2006). Moreover, TFF1 and TFF3 appear to be augmented in dacryoliths and TFF2, which is not present under healthy conditions, is additionally induced and secreted in cases of dacryolithiasis. It has been hypothesized that because of their rheological properties, mucins and TFF peptides may play a functional role in

dacryolith formation (Paulsen *et al.*, 2006). However, it is not clear from these findings whether mucins and TFF peptides per se influence dacryolith formation or whether their secretion is merely a secondary phenomenon.

VI. Conclusions and Perspectives

Both the human lacrimal gland and the epithelial structures of the nasolacrimal ducts synthesize a special spectrum of mucins. The diversity of mucins in the lacrimal gland can be linked to cell signaling, tear film rheology, and antimicrobial defense at the ocular surface; the production of mucins in the healthy lacrimal sac and nasolacrimal duct is associated with enhanced tear transport and antimicrobial defense. Some lacrimal gland mucins may be correlated with age. Reduced levels of mucin mRNA in nonfunctioning though patent segments of the lacrimal passage, associated with epiphora, suggest that mucins ease tear flow through the efferent tear ducts.

A full understanding of the molecular function of lacrimal gland mucins as well as mucins at the mucosal surface of the efferent tear duct passage will provide further insight into the pathophysiology of dry eye, ocular surface infections, and dacryocystitis, which can lead to residual functional impairment of the lacrimal system with ocular discomfort or problems in the medial canthal region. The factors controlling the production of lacrimal gland-associated mucins or efferent tear duct-associated mucins are unknown at present, but it seems that old age, changes in hormonal status (postmenopausal women), or immunodeficiency are associated with changes in lacrimal gland and/or efferent tear duct mucin production. It has been suggested that the normally constant flow of tears ensures mucin production through a feedback control and that this production comes to a halt if tears are not drained into the nose (Paulsen, 2003; Paulsen *et al.*, 2002d, 2003a).

There has been tremendous progress in the cloning and characterization of mucin structure and function in health and disease, as well as at the ocular surface. However, specific functions of each of the membrane-anchored mucins, the nature and function of glycosylation, their regulation, particularly as related to goblet cell differentiation, their interaction with other tear constituents, their possible involvement in bacterial biofilm formation (Zegans *et al.*, 2005), and their contribution to disease states need to be determined in the future. To obtain deeper insight into these features and functions of the human lacrimal gland and nasolacrimal ducts will be particularly challenging, since cell culture models or cell lines of lacrimal gland or epithelia of the efferent tear ducts are very difficult to realize. Results of animal models, as already discussed, are difficult to apply to humans, especially with regard to the tear film. However, such investigations will be of

great relevance, as the number of patients with dry eye is still increasing, as is the number of contact lens wearers and surgical ocular surface manipulations, all of which affect normal mucin function. Future improvements in our capacity to analyze the mucus secretory apparatus will hopefully suggest novel therapies beneficial in the fight against diseases of the lacrimal apparatus and ocular surface.

Acknowledgments

This work was supported by the Deutsche Farschungsgemeinschaft (DFG), Bonn, Germany (program grants PA738/1–2; 1–3; 1–4; and 1–5) as well as the BMBF- Wilhelm Roux Program, Halle, Germany (FK) 9/18 and 12/08).

REFERENCES

Aarbiou, J., Verhoosel, R. M., Van Wetering, S., De Boer, W. I., Van Krieken, J., Litvinov, S. V., Rabe, K. F., and Hiemstra, P. S. (2004). Neutrophil defensins enhance lung epithelial wound closure and mucin gene expression *in vitro*. *Am. J. Respir. Cell Mol Biol.* **30,** 193–201.

Abraham, S. N., and Beachey, E. H. (1985). Host defenses against adhesion of bacteria to mucosal surfaces. *In* "Advances in Host Defense Mechanisms" (J. F. Gallin and A. S. Fauci, Eds.), Vol. 4, pp. 63–88. Raven Press, New York.

Aknin, M.-L. R., Berry, M., Dick, A. D., and Khan-Lim, D. (2004). Normal but not altered mucins activate neutrophils. *Cell Tissue Res.* **318,** 545–551.

Allen, M., Wright, P., and Reid, L. (1972). The human lacrimal gland. A histochemical and organ culture study of the secretory cells. *Arch. Ophthalmol.* **88,** 493–497.

Almstahl, A., Wikstrom, M., and Groenink, J. (2001). Lactoferrin, amylase and mucin MUC5B and their relation to the oral microflora in hyposalivation of different origins. *Oral Microbiol. Immunol.* **16,** 345–352.

Amrith, S., Goh, P. S., and Wang, S.-C. (2005). Tear flow dynamics in the human nasolacrimal ducts—a pilot study using dynamic magnetic resonance imaging. *Graefe's Arch. Clin. Exp. Ophthalmol.* **243,** 127–131.

Arango, M. E., Li, P., Komatsu, M., Montes, C., Carraway, C. A., and Carraway, K. L. (2001). Production and localization of Muc4/sialomucin complex and its receptor tyrosine kinase erbB2 in the rat lacrimal gland. *Invest. Ophthalmol. Vis. Sci.* **42,** 2749–2756.

Argüeso, P., and Gipson, I. K. (2001). Epithelial mucins of the ocular surface: Structure, biosynthesis and function. *Exp. Eye Res.* **73,** 281–289.

Argüeso, P., Balaram, M., Spurr-Michaud, S., Keutmann, H. T., Reza Dana, M., and Gipson, I. K. (2002). Decreased levels of the goblet cell mucin MUC5AC in tears of patients with Sjogren syndrome. *Invest. Ophthalmol. Vis. Sci.* **43,** 1004–1011.

Argüeso, P., Spurr-Michaud, S., Russo, C. L., Tisdale, A., and Gipson, I. K. (2003). MUC16 mucin is expressed by the human ocular surface epithelia and carries the H185 carbohydrate epitope. *Invest. Ophthalmol. Vis. Sci.* **44,** 2487–2495.

Argüeso, P., Tisdale, A., Spurr-Michaud, S., Sumiyoshi, M., and Gipson, I. K. (2006). Mucin characteristics of human corneal-limbal epithelial cells that exclude the rose Bengal anionic dye. *Invest. Opthalmol. Vis. Sci.* **47,** 113–119.

Arias, E. B., Verhage, H. G., and Jaffe, R. C. (1994). Complementary deoxyribonucleic acid cloning and molecular characterization of an estrogen-dependent human oviductal glycoprotein. *Biol. Reprod.* **51,** 685–694.

Auersperg, N., Pan, J., Grove, B. D., Peterson, T., Fischer, J., Maines-Bandiera, S., Somasiri, A., and Roskelley, C. D. (1999). E-cadherin induces mesenchymal-to-epithelial transition in human ovarian surface epithelium. *Proc. Natl. Acad. Sci. USA* **96,** 6249–6254.

Ayub, M., Thale, A., Hedderich, J., Tillmann, B., and Paulsen, F. (2003). The cavernous body of the human efferent tear ducts functions in regulation of tear outflow. *Invest. Ophthalmol. Vis. Sci.* **44,** 4900–4907.

Bacman, S., Berra, A., Sterin-Borda, L., and Borda, E. (2001). Muscarinic acetylcholine receptor antibodies as a new marker of dry eye Sjögren's syndrome. *Invest. Ophthalmol. Vis. Sci.* **42,** 321–327.

Bandeen-Roche, K., Munoz, B., Tielsch, J. M., West, S. K., and Schein, O. D. (1997). Self-reported assessment of dry eye in a population-based setting. *Invest. Ophthalmol. Vis. Sci.* **38,** 2469–2475.

Bast, R. C., Jr., Feenay, M., Lazarus, H., Nadler, L. M., Colvin, R. B., and Knapp, R. C. (1981). Reactivity of a monoclonal antibody with human ovarian carcinoma. *J. Clin. Invest.* **68,** 1331–1337.

Baughan, L. W., Robertello, F. J., Sarrett, D. C., Denny, P. A., and Denny, P. C. (2000). Salivary mucin as related to oral Streptococcus mutans in elderly people. *Oral. Microbiol. Immunol.* **15,** 10–14.

Begley, C. G., Caffery, B., Nichols, K., Mitchell, G. L., and Chalmers, R. (2002). DREI study group. Results of a dry eye questionnaire from optometric practices in North America. *Adv. Exp. Med. Biol.* **506**(Pt B), 1009–1016.

Berry, M., Ellingham, R. B., and Corfield, A. P. (1996). Polydispersity of normal human conjunctival mucins. *Invest. Ophthalmol. Vis. Sci.* **37,** 2559–2571.

Berry, M., Ellingham, R. B., and Corfield, A. P. (2000). Membrane-associated mucins in normal human conjunctiva. *Invest. Ophthalmol. Vis. Sci.* **41,** 398–403.

Berry, M., McMaster, T. J., Corfield, A. P., and Miles, M. J. (2001). Exploring the molecular adhesion of ocular mucins. *Biomacromolecules* **2,** 498–503.

Berry, M., Harris, A., Lumb, R., and Powell, K. (2002). Commensal ocular bacteria degrade mucins. *Br. J. Ophthalmol.* **86,** 1412–1416.

Berry, M., Ellingham, R. B., and Corfield, A. P. (2004a). Human preocular mucins reflect changes in surface physiology. *Br. J. Ophthalmol.* **88,** 377–383.

Berry, M., Brayshaw, D., and McMaster, T. J. (2004b). Dynamic molecular resolution imaging of preocular fluid impressions. *Br. J. Ophthalmol.* **88,** 1460–1466.

Bjerrum, K. B. (1997). Keratoconjunctivitis sicca and primary Sjogren's syndrome in a Danish population aged 30–60 years. *Acta Ophthalmol. Scand.* **75,** 281–286.

Bobek, L. A., Tsai, H., Biesbrock, A. R., and Levine, M. J. (1993). Molecular cloning, sequence, and specificity of expression of the gene encoding the low molecular weight human salivary mucin (MUC7). *J. Biol. Chem.* **268,** 20563–20569.

Borchers, M. T., Carty, M. P., and Leikauf, G. D. (1999). Regulation of human airway mucins by acrolein and inflammatory mediators. *Am. J. Physiol.* **276,** L549–L555.

Bramwell, M. E., Wiseman, G., and Shotton, D. M. (1986). Electron-microscopic studies of the CA antigen, epitectin. *J. Cell Sci.* **86,** 249–261.

Buisine, M. P., Devisme, L., Copin, M. C., Durand-Reville, M., Gosselin, B., Aubert, J. P., and Porchet, N. (1999). Developmental mucin gene expression in the human respiratory tract. *Am. J. Respir. Cell. Mol.* **20,** 209–218.

Busse, H., and Müller, K. (1977). Zur Enstehung der idiopathischen Dakryostenose. *Klin. Monatsbl. Augenheilkd.* **170,** 627–632.

Caffery, B. E., Richter, D., Simpson, T., Fonn, D., Doughty, M., and Gordon, K. (1998). CANDEES. The Canadian Dry Eye Epidemiology Study. *Adv. Exp. Med. Biol.* **438,** 805–806.

Carlstedt, I., Sheenan, J. K., Corfield, A. P., and Gallagher, J. T. (1985). Mucous glycoproteins: A gel of a problem. *Essays Biochem.* **20,** 40–76.

Carraway, K. L., Price-Schiavi, S. A., Komatsu, M., Idris, N., Perez, A., Li, P., Jepson, S., Zhu, X., Carvajal, M. E., and Carraway, C. A. (2000). Multiple facets of sialomucin complex/MUC4, a membrane mucin and erbb2 ligand, in tumors and tissues (Y2K update). *Front. Biosci.* **5,** D95–D107.

Carraway, K. L., Perez, A., Idris, N., Jepson, S., Arango, M., Komatsu, M., Haq, B., Price-Schiavi, S. A., Zhang, J., and Carraway, C. A. (2002). Muc4/sialomucin complex, the intramembrane ErbB2 ligand, in cancer and epithelia: To protect and to survive. *Prog. Nucleic Acid Res. Mol. Biol.* **71,** 149–185.

Carraway, K. L., Ramsauer, V. P., Haq, B., and Carothers Carraway, C. A. (2003). Cell signaling through membrane mucins. *Bioessays* **25,** 66–71.

Chen, H. B., Yamabayashi, S., Ou, B., Tanaka, Y., Ohno, S., and Tsukahara, S. (1997). Structure and composition of rat precorneal tear film. A study by an *in vivo* cryofixation. *Invest. Ophthalmol. Vis. Sci.* **38,** 381–387.

Chen, Y., Zhao, A. H., Kalaslavadi, T. B., Hamati, E., Nehrke, K., Le, A. D., Ann, D. K., and Wu, R. (2004). Genome-wide search and identification of a novel gel-forming mucin MUC19/Muc19 in glandular tissues. *Am. J. Respir. Cell. Mol. Biol.* **30,** 155–165.

Chia, E. M., Mitchell, P., Rochtchina, E., Lee, A. J., Maroun, R., and Wang, J. J. (2003). Prevalence and associations of dry eye syndrome in an older population: The Blue Mountains Eye Study. *Clin. Exp. Ophthalmol.* **31,** 229–232.

Corfield, A. P., Carrington, S. D., Hicks, S. J., Berry, M., and Ellingham, R. (1997). Ocular mucins: Purification, metabolism and functions. *Prog. Retinal. Eye Res.* **16,** 627–656.

Corfield, T. (1992). Bacterial sialidases—roles in pathogenicity and nutrition. *Glycobiology* **2,** 509–521.

Corrales, R. M., Galarreta, D. J., Herreras, J. M., Calonge, M., and Chaves, F. J. (2003). Normal human conjunctival epithelium expresses muc, MUC13, MUC15, MUC16 and MUC17 mucin genes. *Arch. Soc. Esp. Ophthamol.* **78,** 375–382.

Dana, M. R., and Hamrah, P. (2002). Role of immunity and inflammation in corneal and ocular surface disease associated with dry eye. *Adv. Exp. Med. Biol.* **506**(Pt B), 729–738.

Danjo, Y., Watanabe, H., Tisdale, A. S., George, M., Tsumura, T., Abelson, M. B., and Gipson, I. K. (1998). Alteration of mucin in human conjunctival epithelia in dry eye. *Invest. Ophthalmol. Vis. Sci.* **39,** 2602–2609.

Denton, D. A., Nelson, J. F., and Tarjan, E. (1985). Water and salt intake of wild rabbits (Oryctolagus cuniculus (L)) following dipsogenic stimuli. *J. Physiol.* **326,** 285–301.

Desseyn, J. L., Buisine, M.-P., Porchet, N., Aubert, J.-P., Degand, P., and Laine, A. (1998). Evolutionary history of the 11p15 human mucin gene family. *J. Mol. Evol.* **46,** 102–106.

Desseyn, J. L., Aubert, J. P., Porchet, N., and Laine, A. (2000). Evolution of the large secreted gel-forming mucins. *Mol. Biol. Evol.* **17,** 1175–1184.

Doughty, M. J., Fonn, D., Richter, D., Simpson, T., Caffery, B., and Gordon, K. (1997). A patient questionnaire approach to estimating the prevalence of dry eye symptoms in patients presenting to optometric practices across Canada. *Optom. Vis. Sci.* **74,** 624–631.

Dufosse, J., Porchet, N., Audie, J. P., Guyonnet-Duperat, V., Laine, A., Van-Seuningen, I., Marranchi, S., Degand, P., and Aubert, J. P. (1993). Degenerate 87-base-pair tandem repeats create hydrophilic/hydrophobic alternating domains in human mucin peptides mapped to 11p15. *Biochem. J.* **293,** 329–337.

Duke-Elder, S. (1961). Trachoma and allied infections. *Trans. Ophthalmol. Soc. UK* **81,** 343–349.

Duke-Elder, S. S., and Gloster, J. (1968). The protective mechanism. The movements of the eyelids. *In* "System of Ophthalmology. The Physiology of the Eye and of Vision" (S. S. Duke-Elder, Ed.), Vol. 4, pp. 414–419. Henry Kimpton, London.

Dwyer, T. M., and Farley, J. M. (2000). Human neutrophil elastase releases two pools of mucinlike glycoconjugate from tracheal submucosal gland cells. *Am. J. Physiol. Lung Cell Mol. Physiol.* **278,** L675–L682.

Ellingham, R. B., Berry, M., Stevenson, D., and Corfield, A. P. (1999). Secreted human conjunctival mucus contains MUC5AC glycoforms. *Glycobiology* **9,** 1181–1189.

Faillard, H., and Schauer, R. (1972). Glycoproteins as lubricants, protective agents, carriers, structural proteins and as participants in other functions. *In* "Their Composition, Structure, and Function" (A. Gottschalk, Ed.), 2nd ed., part B, pp. 1246–1267. Elsevier, Amsterdam.

Fischer, B. M., and Voynow, J. A. (2002). Neutrophil elastase induces MUC5AC gene expression in airway epithelium via a pathway involving reactive oxygen species. *Am. J. Respir. Cell Mol. Biol.* **26,** 447–452.

Fischer, B. M., Cuellar, J. G., Diehl, M. L., deFreytas, A. M., Zhang, J., Carraway, K. L., and Voynow, J. A. (2003). Neutrophil elastase increases MUC4 expression in normal human bronchial epithelial cells. *Am. J. Physiol. Lung Cell Mol. Physiol.* **284,** L671–L679.

Fisk, B., Hudson, J. M., Kavanagh, J., Wharton, J. T., Murray, J. L., Ioannides, C. G., and Kudelka, A. P. (1997). Existent proliferative responses of peripheral blood mononuclear cells from healthy donors and ovarian cancer patients to HER-2 peptides. *Anticancer Res.* **17,** 45–53.

Fleiszig, S. M. J., Zaidi, T. S., Ramphal, R., and Pier, G. B. (1994). Modulation of Pseudomonas aeruginosa adherence to the corneal surface by mucus. *Infect. Immun.* **62,** 1799–1804.

Florey, H. W. (1933). Observations on the functions of mucus and the early stages of bacterial invasion of the intestinal mucosa. *J. Pathol. Bacteriol.* **37,** 283–289.

Fluckinger, M., Haas, H., Merschak, P., Glasgow, B. J., and Redl, B. (2004). Human tear lipocalin exhibits antimicrobial activity by scavenging microbial siderophores. *Antimicrob. Agents Chem.* **48,** 3367–3372.

Forstner, J. F. (1978). Intestinal mucins in health and disease. *Digestion* **17,** 234–263.

Fowler, J., Vinall, L., and Swallow, D. (2001). Polymorphism of the human muc genes. *Front. Biosci.* **6,** D1207–D1215.

Gao, J., Schwalb, T. A., Adedeo, J. V., Ghosn, C. R., and Stern, M. E. (1998). The role of apoptosis in the pathogenesis of canine keratoconjunctivitis sicca: The effect of topical cyclosporin A therapy. *Cornea* **17,** 654–663.

Gao, J., Cha, S., Jonsson, R., Opalko, J., and Peck, A. B. (2004). Detection anti-type 3 muscarinic acetylcholine receptor autoantibodies in the sera of Sjögrens's syndrome patients by use of a transfected cell line assay. *Arthritis Rheum.* **50,** 2615–2621.

Gendler, S. J. (2001). MUC1, the renaissance molecule. *J. Mamm. Gland. Biol. Neoplasia* **6,** 339–353.

Gendler, S. J., and Spicer, A. P. (1995). Epithelial mucin genes. *Annu. Rev. Physiol.* **57,** 607–634.

Gendler, S. J., Burchell, J. M., Duhig, T., Lamport, D., White, R., Parker, M., and Taylor-Papadimitriou, J. (1987). Cloning of partial cDNA encoding differentiation and tumor-associated mucin glycoproteins expressed by human mammary epithelium. *Proc. Natl. Acad. Sci. USA* **84,** 6060–6064.

Gerken, T. A., Gupta, R., and Jentoft, N. (1992). A novel approach for chemically deglycosylating O-linked glycoproteins. The deglycosylation of submaxillary and respiratory mucins. *Biochemistry* **31,** 639–648.

Gipson, I. K. (2004). Distribution of mucins at the ocular surface. *Exp. Eye Res.* **78,** 379–388.

Gipson, I. K., and Argüeso, P. (2003). Role of mucins in the function of the corneal and conjunctival epithelia. *Int. Rev. Cytol.* **231,** 1–49.

Gipson, I. K., Moccia, R., Spurr-Michaud, S., Argüeso, P., Gargiulo, A. R., Hill, J. A., 3rd, Offner, G. D., and Keutmann, H. T. (2001). The amount of MUC5B mucin in cervical mucus peaks at midcycle. *J. Clin. Endocrinol. Metab.* **86,** 594–600.

Gipson, I. K., Spurr-Michaud, S. J., Argüesco, P., Tisdale, A., Ng, T. F., and Russo, C. L. (2003). Mucin gene expression in immortalized human corneal-limbal and conjunctival epithelial cell lines. *Invest. Ophthalmol. Vis. Sci.* **44,** 2496–2506.

Gipson, I. K., Hori, Y., and Argüeso, P. (2004). Character of ocular surface mucins and their alterations in dry eye disease. *Ocular Surf.* **2,** 131–148.

Godl, K., Johansson, M. E. V., Lidell, M. E., Mörgelin, M., Karlsson, H., Olson, F. J., Gum, J. R., Jr., Kim, Y. S., and Hansson, G. C. (2002). The N terminus of the MUC2 mucin forms trimers that are held together within a trypsin-resistant core fragment. *J. Biol. Chem.* **277,** 47248–47256.

Gormezano, I., Schneiderman, N., Deaux, E., and Fuentes, I. (1962). Nictitating membrane: Classical conditioning and extinction in the albino rabbit. *Science* **138,** 33–34.

Gum, J. R. (1995). Human mucin glycoproteins: Varied structures predict diverse properties and specific functions. *Biochem. Soc. T.* **23,** 795–799.

Gum, J. R., Byrd, J. C., Hicks, J. W., Toribara, N. W., Lamport, D. T. A., and Kim, Y. S. (1989). Molecular cloning of human intestinal mucin cDNAs. Sequence analysis and evidence for genetic polymorphism. *J. Biol. Chem.* **264,** 6480–6487.

Gum, J. R., Hicks, J. W., Swallow, D. M., Lagace, R. L., Byrd, J. C., Lamport, D. T. A., Siddiki, B., and Kim, Y. S. (1990). Molecular cloning of cDNAs derived from a novel human intestinal mucin gene. *Biochem. Biophys. Res. Commun.* **171,** 407–415.

Gum, J. R., Jr., Crawley, S. C., Hicks, J. W., Szymkowski, D. E., and Kim, Y. S. (2002). MUC17, a novel membrane-tethered mucin. *Biochem. Biophys. Res. Commun.* **291,** 466–475.

Gururaja, T. L., Ramasubbu, N., Venugopalan, P., Reddy, M. S., Ramalingam, L., and Levine, M. J. (1998). Structural features of the human salivary mucin, MUC7. *Glycoconj. J.* **15,** 457–467.

Gururaja, T. L., Levine, J. H., Tran, D. T., Naganagowda, G. A., Ramalingam, K., Ramasubbu, N., and Levine, M. J. (1999). Candidacidal activity prompted by N-terminus histatin-like domain of human salivary mucin (MUC7). *Biochim. Biophys. Acta* **1431,** 107–119.

Guyonnet Duperat, V., Audie, J.-P., Debailleul, V., Leine, A., Buisine, M.-P., Galiegue-Zouitina, S., Pigny, P., Degand, P., Aubert, J.-P., and Porchet, N. (1995). Characterization of the human mucin gene MUC5AC: A consensus cysteine-rich domain for 11p15 mucin genes? *Biochem. J.* **305,** 211–219.

Halben, R. (1904). Beiträge zur Anatomie der Tränenwege. *Albrecht von Graefes Arch. Klin. Exp. Ophthalmol.* **57,** 61–92.

Halila, M. (1985). Detection of ovarian cancer marker CA 125 in human seminal plasma. *Tumour Biol.* **6,** 207–212.

Hanisch, F. G., Uhlenbruck, G., Dienst, C., Stottrop, M., and Hippauf, E. (1985). Ca 125 and Ca 19-9: Two cancer-associated sialylsaccharide antigens on a mucus glycoprotein from human milk. *Eur. J. Biochem.* **149,** 323–330.

Hauser, F., Poulson, R., Chinery, R., Rogers, L. A., Handby, A. M., Wright, N. A., and Hoffmann, W. (1993). hP1.B, a human P-domain peptide homologous with rat intestinal trefoil factor, is expressed also in the ulcer-associated cell lineage and the uterus. *Proc. Natl. Acad. Sci. USA* **90,** 6961–6965.

Higuchi, T., Orita, T., Nakanishi, S., Katsuya, K., Watanabe, H., Yamasaki, Y., Waga, I., Nanayama, T., Yamamoto, Y., Munger, W., Sun, H. W., Falk, R. J., Jennette, J. C., Alcorta, D. A., Li, H., Yamamoto, T., Saito, Y., and Nakamura, M. (2004). Molecular cloning, genomic structure, and expression analysis of MUC20, a novel mucin protein, up-regulated in injured kidney. *J. Biol. Chem.* **279,** 1968–1979.

Hikichi, T., Yoshida, A., Fukui, Y., Hamano, T., Ri, M., Araki, K., Horimoto, K., Takamura, E., Kitagawa, K., Oyama, M., Danjo, Y., Kondo, S., Fujishima, K., Toda, I., and Tsubota, K. (1995). Prevalence of dry eye in Japanese eye centers. *Graefes Arch. Clin. Exp. Ophthalmol.* **233,** 555–558.

Hilkens, J., Wesseling, J., Vos, H. L., Storm, J., Boer, B., van der Walk, S. W., and Maas, M. C. E. (1995). Involvement of the cell surface-bound mucin, episialin MUC1, in progression of human carcinomas. *Biochem. Soc. T.* **23,** 822–826.

Hodges, R. R., and Dartt, D. A. (2003). Regulatory pathways in lacrimal gland epithelium. *Int. Rev. Cytol.* **231,** 129–200.

Hodges, R. R., Zoukhri, D., Sergheraert, C., Zieske, J. D., and Dartt, D. A. (1997). Identification of vasoactive intestinal peptide receptor subtypes in the lacrimal gland and their signal-transducing components. *Invest. Ophthalmol. Vis. Sci.* **38,** 610–619.

Hoffmann, W., and Jagla, W. (2001). Cell type specific expression of secretory TFF peptides: Colocalization with mucins and synthesis in the brain. *Int. Rev. Cytol.* **213,** 147–181.

Hoffmann, W., Jagla, W., and Wiede, A. (2001). Molecular medicine of TFF-peptides: From gut to brain. *Histol. Histopathol.* **16,** 319–334.

Holly, F. J., and Lemp, M. A. (1977). Tear physiology and dry eyes. *Surv. Ophthalmol.* **22,** 69–87.

Hori, Y., Spurr-Michaud, S., Argüeso, P., Gulati, A., Dana, M. R., and Gipson, I. K. (2004a). The expression of mucin mRNA and protein on the ocular surface in tolerant contact lens wearers. *ARVO 2004,* p. 64, No. 1567.

Hori, Y., Spurr-Michaud, S., Russo, C. L., Argüeso, P., and Gipson, I. K. (2004b). Differential regulation of membrane-associated mucins in the human ocular surface epithelium. *Invest. Ophthalmol. Vis. Sci.* **45,** 114–122.

Hutch, J. A. (1970). The role of urethral mucus in the bladder defense mechanism. *J. Urol.* **103,** 165–167.

Inatomi, T., Spurr-Michaud, S., Tisdale, A. S., and Gipson, I. K. (1995). Human corneal and conjunctival epithelia express MUC1 mucin. *Invest. Ophthalmol. Vis. Sci.* **36,** 1818–1827.

Inatomi, T., Spurr-Michaud, S., Tisdale, A. S., Zhan, Q., Feldman, S. T., and Gipson, I. K. (1996). Expression of secretory mucin genes by human conjunctival epithelia. *Invest. Ophthalmol. Vis. Sci.* **37,** 1684–1692.

Inatomi, T., Tisdale, A. S., Zhank, Q., Spurr-Michaud, S., and Gipson, I. K. (1997). Cloning of rat Muc5AC mucin gene: Comparison of its structure and tissue distribution to that of human and mouse homologues. *Biochem. Biophys. Res. Commun.* **236,** 789–797.

Ito, T., and Shibasaki, S. (1964). Lichtmikroskopische Untersuchungen über die Glandula lacrimalis des Menschen. *Arch. Histol. Jpn.* **25,** 117–144.

Jagla, W., Wiede, A., Dietzmann, K., Gulicher, D., Gerlach, K. L., and Hoffmann, W. (1999). Secretion of TFF-peptides by human salivary glands. *Cell Tissue Res.* **298**(1), 161–166.

Jagla, W., Wiede, A., Dietzmann, K., Rutkowski, K., and Hoffmann, W. (2000). Co-localization of TFF3 peptide and oxytocin in the human hypothalamus. *FASEB J.* **14,** 1126–1131.

Jensen, O. A., Falbe-Hansen, I., Jacobsen, T., and Michelsen, A. (1969). Mucosubstances of the acini of the human lacrimal gland (orbital part). I. Histochemical identification. *Acta Ophthalmol. (Copenh.)* **47,** 605–619.

Jepson, S., Komatsu, M., Haq, B., Arango, M. E., Huang, D., Carraway, C. A., and Carraway, K. L. (2002). Muc4/sialomucin complex, the intramembrane ErbB2 ligand, induces specific phosphorylation of ErbB2 and enhances expression of p27(kip), but does not activate mitogen-activated kinase or protein kinaseB/Akt pathways. *Oncogene* **21,** 7524–7532.

Jiang, T., and Jumblatt, J. E. (2003). Expression of membrane-associated mucins in human cornea and conjunctiva. *ARVO Program Summary Book.* **837**(Abstract), 34.

Johnson, M. E., and Murphy, P. J. (2004). Changes in the tear film and ocular surface from dry eye syndrome. *Prog. Retin. Eye Res.* **23**(4), 449–474.

Jones, L. T. (1958). Practical fundamental of anatomy and physiology. *Trans. Am. Acad. Ophthalmol. Otolaryngol.* **62,** 669–687.

Jumblatt, M. M., McKenzie, R. W., and Jumblatt, J. E. (1999). MUC5AC mucin is a component of the human precorneal tear film. *Invest. Ophthalmol. Vis. Sci.* **40,** 43–49.

Jumblatt, M. M., McKenzie, R. W., Steele, P. S., Emberts, C. G., and Jumblatt, J. E. (2003). MUC7 Expression in the human lacrimal gland and conjunctiva. *Cornea* **22,** 41–45.

Jung, H. H., Lee, J. H., Kim, Y. T., Lee, S. D., and Park, J. H. (2000). Expression of mucin genes in chronic ethmoiditis. *Am. J. Rhino.* **14,** 163–170.

Kabawat, S. E., Bast, R. C., Jr., Bhan, A. K., Welch, W. R., and Knapp, R. C. (1983). Tissue distribution of a coelomic-epithelium-related antigen recognized by the monoclonal antibody OC125. *Int. J. Gynecol. Pathol.* **2,** 275–285.

Kakizaki, H., Zako, M., Miyaishi, O., Nakano, T., Asamoto, K., and Iwaki, M. (2005). The lacrimal canaliculus and sac bordered by the Horner's muscle form the functional lacrimal drainage system. *Ophthalmology* **112,** 710–716.

Kessing, S. (1968). Mucous gland system of the conjunctiva: A quantitative normal anatomical study. *Acta Ophthalmol.* **95**(Suppl.), 1–133.

Kim, C. H., Kim, H. J., Song, K. S., Seong, J. K., Kim, K. S., Lee, J. G., and Yoon, J. H. (2005). MUC8 as a ciliated cell marker in human nasal epithelium. *Acta Otolaryngol.* **125,** 76–81.

Kim, K. C., Wasano, K., Niles, R. M., Schuster, J. E., Stone, P. J., and Brody, J. S. (1987). Human neutrophil elastase releases cell surface mucins from primary cultures of hamster tracheal epithelial cells. *Proc. Natl. Acad. Sci. USA* **84,** 9304–9308.

Kim, K. C., Lee, B. C., Pou, S., and Ciccolella, D. (2003). Effects of activation of polymorphonuclear leukocytes on airway goblet cell mucin release in a co-culture system. *Inflamm. Res.* **52,** 258–262.

Kindler, C., Recker, K., Ehrich, D., Sel., and Paulsen, F. (2005). Structural and functional aspects of collectins SP-A and SP-D in the lacrimal system and in ocular surface epithelia. *Ann. Anat.* **187**(Suppl.), 46.

King-Smith, P. E., Fink, B. A., Fogot, N., Nichols, K. K., Hill, R. M., and Wilson, G. S. (2000). The thickness of the human precorneal tear film: Evidence from reflection spectra. *Invest. Ophthalmol. Vis. Sci.* **41,** 3348–3359.

Knop, E., and Knop, N. (2001). Lacrimal drainage-associated lymphoid tissue (LDALT): A part of the human mucosal immune system. *Invest. Ophthalmol. Vis. Sci.* **42,** 566–574.

Knop, E., Knop, N., and Pleyer, U. (2005). Clinical aspects of MALT. *In* "Uveitis and Immunological Disorders" (G. K. Kriegelstein and R. N. Weinreb, Eds.), pp. 67–87. Springer, Berlin.

Kohri, K., Ueki, I. F., and Nadel, J. A. (2002). Neutrophil elastase induces mucin production by ligand-dependent epidermal growth factor receptor activation. *Am. J. Physiol. Lung Cell Mol. Physiol.* **283,** L531–L540.

Komatsu, M., Carraway, C. A., Fregien, N. L., and Carraway, K. L. (1997). Reversible disruption of cell-matrix and cell-cell interactions by overexpression of sialomucin complex. *J. Biol. Chem.* **272,** 33245–33254.

Komatsu, M., Jepson, S., Arango, M. E., Carothers Carraway, C. A., and Carraway, K. L. (2001). Muc4/sialomucin complex, an intramembrane modulator of ErbB2/HER2/Neu, potentiates primary tumor growth and suppresses apoptosis in a xenotransplanted tumor. *Oncogene* **20,** 461–470.

Komatsu, M., Arango, M. E., and Carraway, K. L. (2002). Synthesis and secretion of Muc4/sialomucin complex: Implication of intracellular proteolysis. *Biochem. J.* **368,** 41–48.

Krause, C. F. T. (1842)."Handbuch der menschlichen Anatomie," 2nd ed., Vol. 1, Part 2, pp. 514–519. Hahn, Hannover.

Krause, W. J. (1876). Hilfsorgane des Auges. *In* "Allgemeine und Microscopische Anatomie" (W. J. Krause, Ed.), pp. 138–140. Hahn, Hannover.

Kuerer, H. M., Peoples, G. E., Sahin, A. A., Murray, J. L., Singletary, S. E., Castilleja, A., Hunt, K. K., Gershenson, D. M., and Ioannides, C. G. (2002). Axillary lymph node cellular immune response to HER-2/neu peptides in patients with carcinoma of the breast. *J. Interferon Cytokine* **22,** 583–592.

Kühnel, W. (1968). Vergleichende histologische, histochemische und elektronen-mikroskopische Untersuchungen an Tränendrüsen. *Z. Zellforsch.* **89,** 550–572.

Lan, M. S., Batra, S. K., Qi, W. N., Metzgar, R. S., and Hollingsworth, M. A. (1990). Cloning and sequencing of a human pancreatic tumor mucin cDNA. *J. Biol. Chem.* **265,** 15294–15299.

Langer, G., Jagla, W., Behrens-Baumann, W., Walters, S., and Hoffmann, W. (1999). Secretory peptides TFF1 and TFF3 synthesized in human conjunctival goblet cells. *Invest. Ophthalmol. Vis. Sci.* **40,** 2220–2224.

Lapensee, L., Paquette, Y., and Bleau, G. (1997). Allelic polymorphism and chromosomal localization of the human oviductin gene (MUC9). *Fertil. Steril.* **68,** 702–708.

Leikauf, G. D., Borchers, M. T., Prows, D. R., and Simpson, L. G. (2002). Mucin apoprotein expression in COPD. *Chest* **121**(5 Suppl.), 166S–182S.

Lemp, M. A. (1995). Report of the National Eye Institute/Industry workshop on clinical trials in dry eyes. *CLAO J.* **21,** 221–232.

Lemullois, M., Rossignol, B., and Maudit, P. (1996). Immunolocalization of myoepithelial cells in isolated acini of rat exorbital lacrimal gland: Cellular distribution of muscarinic receptors. *Biol. Cell* **86,** 175–181.

Levitin, F., Baruch, A., Weiss, M., Stiegman, K., Hartmann, M. L., Yoeli-Lerner, M., Ziv, R., Zrihan-Licht, S., Shina, S., Gat, A., Lifschitz, B., Simha, M., Stadler, Y., Cholostoy, A., Gil, B., Greaves, D., Keydar, I., Zaretsky, J., Smorodinsky, N., and Wreschner, D. H. (2005). A novel protein derived from the MUC1 gene by alternative splicing and frameshifting. *J. Biol. Chem.* **280,** 10655–10663.

Li, Y., Liu, D., Chen, D., Kharbanda, S., and Kufe, D. (2003). Human DF3/MUC1 carcinoma-associated protein functions as an oncogene. *Oncogene* **22,** 6107–6110.

Ligtenberg, M., Vos, H. L., Gennisen, A., and Hilkens, J. (1990). Episialin, a carcinoma-associated mucin, is generated by a polymorphic gene encoding splice variants with alternate amino termini. *J. Biol. Chem.* **265,** 5573–5578.

Ligtenberg, M. J. L., Kruijshaar, L., Buijs, F., Meijer, M. V., Litvinov, S. V., and Hilkens, J. (1992). Cell-associated episalin is a complex containing two proteins derived from a common precursor. *J. Biol. Chem.* **267,** 6171–6177.

Lin, J., Tsuprun, V., Kawano, H., Paparella, M. M., Zhang, Z., Anway, R., and Ho, S. B. (2001). Characterization of mucins in human middle ear and Eustachian tube. *Am. J. Physiol. Lung Cell Mol. Physiol.* **280,** L1157–L1167.

Lin, P. Y., Tsai, S. Y., Cheng, C. Y., Liu, J. H., Chou, P., and Hsu, W. M. (2003). Prevalence of dry eye among an elderly Chinese population in Taiwan: The Shihpai Eye Study. *Ophthalmology* **110,** 1096–1101.

Linberg, J. V. (2001). Discussion of lacrimal sac daryoliths. *Ophthalmology* **108,** 1312.

Linberg, J. V., and McCormick, S. A. (1986). Primary acquired nasolacrimal duct obstruction. A clinicopathologic report and biopsy technique. *Ophthalmology* **93,** 1055–1063.

Liu, B., Rayment, S. A., Gyurko, C., Oppenheim, F. G., Offner, G. D., and Troxler, R. F. (2000). The recombinant N-terminal region of human salivary mucin MG2 (MUC7) contains a binding domain for oral Streptococci and exhibits candidacidal activity. *Biochem. J.* **345,** 557–564.

Liu, Z., Carvajal, M., Carothers Carraway, C. A., Carraway, K. L., and Pflugfelder, S. C. (2000). Increased expression of the type 1 growth factor receptor family in the conjunctival epithelium of patients with keratoconjunctivitis sicca. *Am. J. Ophthalmol.* **129,** 472–480.

Lysenko, E. S., Gould, J., Bals, R., Wilson, J. M., and Weiser, J. N. (2000). Bacterial phosphorylcholine decreases susceptibility of the antimicrobial peptide Ll-37/hCAP18 expressed in the upper respiratory tract. *Infect. Immun.* **68,** 1664–1671.

Mauriello, J. A., Jr., Palydowycz, S., and DeLuca, J. (1992). Clinicopathologic study of lacrimal sac and nasal mucosa in 44 patients with complete acquired nasolacrimal duct obstruction. *Ophthal. Plast. Reconstr. Surg.* **8,** 13–21.

McCarty, C. A., Bansal, A. K., Livingston, P. M., Stanislavsky, Y. L., and Taylor, H. R. (1998). The epidemiology of dry eye in Melbourne, Australia. *Ophthalmology* **105,** 1114–1119.

McDermott, A. M. (2004). Defensins and other antimicrobial peptides at the ocular surface. *Ocular Surf.* **2,** 229–247.

McIntosh, R. S., Cade, J. E., Al-Abed, M., Shanmuganathan, V., Gupta, R., Bhan, A., Tighe, P. J., and Dua, H. S. (2005). The spectrum of antimicrobial Peptide expression at the ocular surface. *Invest. Ophthalmol. Vis. Sci.* **46,** 1379–1385.

McKenzie, R. W., Jumblatt, J. E., and Jumblatt, M. M. (2000). Quantification of MUC2 and MUC5AC transcripts in human conjunctiva. *Invest. Ophthalmol. Vis. Sci.* **41,** 703–708.

McLemore, M. R., and Aouizerat, B. (2005). Introducing the MUC16 gene: Implications for prevention and early detection in epithelial ovarian cancer. *Biol. Res. Nurs.* **6,** 262–267.

McNamara, N. A. (2003). Innate defense of the ocular surface. *Eye Contact Lens* **29**(1 Suppl.), S10–3; discussion S26–9, S192–4.

McNeer, R. R., Carraway, C. A., Fregien, N. L., and Carraway, K. L. (1998). Characterization of the expression and steroid hormone control of sialomucin complex in the rat uterus: Implications for uterine receptivity. *J. Cell Physiol.* **176,** 110–119.

Meerzaman, D., Charles, P., Daskal, E., Polymeropoulos, M. H., Martin, B. M., and Rose, M. C. (1994). Cloning and analysis of cDNA encoding a major airway glycoprotein, human tracheobronchial mucin (MUC5). *J. Biol. Chem.* **269,** 12932–12939.

Milder, B., and Weil, B. A. (1983). Composition of tear fluid. *In* "The Lacrimal System" (B. Milder and B. A. Weil, Eds.), pp. 35–48. Appleton-Century-Crofts, Norwalk, CT.

Millar, T. J., Herok, G., Koutavas, H., Martin, D. K., and Anderton, P. J. (1996). Immunohistochemical and histochemical characterization of epithelial cells of rabbit lacrimal glands in tissue sections and cell cultures. *Tissue Cell* **28,** 301–312.

Mitchell, S., Abel, P., Madaan, S., Jeffs, J., Chaudhary, K., Stamp, G., and Lalani, el-N. (2002). Androgen-dependent regulation of human MUC1 mucin expression. *Neoplasia* **4,** 9–18.

Moniaux, N., Escande, F., Batra, S. K., Porchet, N., Laine, A., and Aubert, J. P. (2000). Alternative splicing generates a family of putative secreted and membrane-associated MUC4 mucins. *Eur. J. Biochem.* **267,** 4536–4544.

Moniaux, N., Escande, F., Porchet, N., Aubert, J. P., and Batra, S. K. (2001). Structural organization and classification of the human mucin genes. *Front. Biosci.* **6,** D1192–D1206.

Moss, S. E., Klein, R., and Klein, B. E. (2000). Prevalence of and risk factors for dry eye syndrome. *Arch. Ophthalmol.* **118,** 1264–1268.

Nguyen, D. H., Toshida, H., Schurr, J., and Beuermann, R. W. (2004). Microarray analysis of the rat lacrimal gland following the loss of parasympathetic control of secretion. *Physiol. Genom.* **18,** 108–118.

Ni, M., Evans, D. J., Hawgood, S., Anders, E. M., Sack, R. A., and Fleiszig, S. M. (2005). Surfactant protein D is present in human tear fluid and the cornea and inhibits epithelial cell invasion by Pseudomonas aeruginosa. *Infect. Immun.* **73,** 2147–2156.

Nielsen, P. A., Mandel, U., Therkildsen, M. H., and Clausen, H. (1996). Differential expression of human high-molecular-weight salivary mucin (MG1) and low-molecular-weight salivary mucin (MG2). *J. Dent. Res.* **75,** 1820–1826.

Nielsen, P. A., Bennett, E. P., Wandall, H. H., Therkildsen, M. H., Hannibal, J., and Clausen, H. (1997). Identification of a major human high molecular weight salivary mucin (MG1) as tracheobronchial mucin MUC5B. *Glycobiology* **7,** 413–419.

Norn, M. (1989). Tear stix tests for leucocyte-esterase, nitrite, haemoglobin, and albumin in normals and in a clinical series. *Acta Ophthalmol. (Copenh.)* **67,** 192–198.

Pallesen, L. T., Berglund, L., Rasmussen, L. K., Petersen, T. E., and Rasmussen, J. T. (2002). Isolation and characterization of MUC15, a novel cell membrane-associated mucin. *Eur. J. Biochem.* **269,** 2755–2763.

Pandey, P., Kharbanda, S., and Kufe, D. (1995). Association of the DF3/MUC1 breast cancer antigen with Grb2 and the Sos/Ras exchange protein. *Cancer Res.* **55,** 4000–4003.

Parry, G., Beck, J. C., Moss, L., Bartley, J., and Ojakian, G. K. (1990). Determination of apical membrane polarity in mammary epithelial cell cultures: The role of cell-cell, cell-substratum, and membrane-cytoskeleton interactions. *Exp. Cell. Res.* **188,** 302–311.

Paulsen, F. (2003). The human nasolacrimal ducts. *Adv. Anat. Embryol. Cell Biol.* **170,** 1–106.

Paulsen, F., and Nölle, B. (2006). Functional anatomy and immunological interactions of ocular surface and adnexa. *In* "Surgery for the Dry Eye" (G. Geerling and H. Brewitt, Eds.). Developments in Ophthalmology. Karger, Basel.

Paulsen, F., Thale, A., Kohla, G., Schauer, R., Rochels, R., Parwaresch, R., and Tillmann, B. (1998). Functional anatomy of human lacrimal duct epithelium. *Anat. Embryol. (Berl.)* **198,** 1–12.

Paulsen, F., Thale, A., Hallmann, U., Schaudig, U., and Tillmann, B. (2000a). The cavernous body of the human efferent tear ducts—function in tear outflow mechanism. *Invest. Ophthalmol. Vis. Sci.* **41,** 965–970.

Paulsen, F., Hallmann, U., Paulsen, J., and Thale, A. (2000b). Innervation of the cavernous body of the human efferent tear ducts and function in tear outflow mechanism. *J. Anat.* **197,** 373–381.

Paulsen, F., Paulsen, J., Thale, A., and Tillmann, B. (2000c). Mucosa-associated lymphoid tissue (MALT) in the human efferent tear ducts. *Virchows Arch.* **437,** 185–189.

Paulsen, F., Pufe, T., Schaudig, U., Held-Feindt, J., Lehmann, J., Schröder, J.-M., and Tillmann, B. (2001a). Detection of natural peptide antibiotics in human nasolacrimal ducts. *Invest. Ophthalmol. Vis. Sci.* **42,** 2157–2163.

Paulsen, F., Thale, A., Maune, S., and Tillmann, B. (2001b). Primary acquired dacryostenosis—histopathology and pathophysiology. *Ophthalmology* **108,** 2329–2336.

Paulsen, F., Pufe, T., Schaudig, U., Held-Feindt, J., Lehmann, J., Thale, A., and Tillmann, B. (2002a). Protection of human efferent tear ducts by antimicrobial peptides. *Adv. Exp. Med. Biol.* **506,** 547–553.

Paulsen, F., Paulsen, J., Thale, A., Schaudig, U., and Tillmann, B. (2002b). Organized mucosa associated lymphoid tissue in human nasolacrimal ducts. *Adv. Exp. Med. Biol.* **506,** 873–876.

Paulsen, F., Föge, M., Thale, A., Tillmann, B., and Mentlein, R. (2002c). Absorption of lipophilic substances from tear fluid by the epithelium of the nasolacrimal ducts. *Invest. Ophthalmol. Vis. Sci.* **43,** 3137–3143.

Paulsen, F., Thale, A., and Schaudig, U. (2002d). Ableitende Tränenwege und Trockenes Auge. *Ophthalmologe* **99,** 566–574.

Paulsen, F. P., Hinz, M., Schaudig, U., Thale, A. B., and Hoffmann, W. (2002e). TFF-peptides in the human efferent tear ducts. *Invest. Ophthalmol. Vis. Sci.* **43,** 3359–3364.

Paulsen, F., Schaudig, U., and Thale, A. (2003a). Drainage of tears—impact on the ocular surface and lacrimal system. *Ocular Surf.* **1,** 180–191.

Paulsen, F., Corfield, A., Hinz, M., Hoffmann, W., Schaudig, U., Thale, A., and Berry, M. (2003b). Characterization of mucins in human lacrimal sac and nasolacrimal duct. *Invest. Ophthalmol. Vis. Sci.* **44,** 1807–1813.

Paulsen, F., Langer, G., Hoffmann, W., and Berry, M. (2004a). Human lacrimal gland mucins. *Cell Tissue Res.* **316,** 167–177.

Paulsen, F., Langer, G., Hoffmann, W., and Berry, M. (2004b). Mucin production by the human lacrimal gland. *Ann. Anat.* **186**(Suppl.), 268.

Paulsen, F., Corfield, A., Hinz, M., Hoffmann, W., Schaudig, U., Thale, A., and Berry, M. (2004c). Tränenabfluss—Bedeutung von Muzinen und TFF-Peptiden. *Ophthalmologe* **101,** 19–24.

Paulsen, F., Varoga, D., Steven, P., and Pufe, T. (2005). Antimicrobial peptides at the ocular surface. *In* "Immunology of Lacrimal Gland and Tear Film" (M. Zierhut, M. E. Stern, and D. A. Sullivan, Eds.), pp. 97–104. Taylor & Francis, London.

Paulsen, F., Schaudig, U., Fabian, A., Ehrich, D., and Sel, S. (2006). Production of TFF peptides and single mucins is augmented in dacryolithiasis. *Graefe's Arch. Clin. Exp. Ophthalmol.* (in press).

Pavlidis, M., Stupp, T., Grenebach, U., Busse, H., and Thanos, S. (2005). Ultrasonic visualization of the effect of blinking on the lacrimal pump mechanism. *Graefe's Arch. Clin. Exp. Ophthalmol.* **243,** 228–234.

Paz, H. B., Tisdale, A. S., Danjo, Y., Spurr-Michaud, S. J., Argüeso, P., and Gipson, I. K. (2003). Location and clonal analysis of stem cells and their differentiated progeny in the human ocular surface. *J. Cell Biol.* **145,** 769–782.

Peres-Vilar, J., and Hill, R. L. (1999). The structure and assembly of secreted mucins. *J. Biol. Chem.* **274,** 31751–31754.

Perra, M. T., Serra, A., Sirigu, P., and Turno, F. (1995). A histochemical and immunohistochemical study of certain defense mechanisms in the human lacrimal sac epithelium. *Arch. Histol. Cytol.* **58,** 517–522.

Perrais, M., Pigny, P., Copin, M. C., Aubert, J. P., and Van Seuningen, I. (2002). Induction of MUC2 and MUC5AC mucins by factors of the epidermal growth factor (EGF) family is mediated by EGF receptor/Ras/Raf/extracellular signal-regulated kinase cascade and Sp1. *J. Biol. Chem.* **277,** 32258–32267.

Pettersen, C. A., and Adler, K. B. (2002). Airways inflammation and COPD: Epithelial-neutrophil interactions. *Chest* **121**(5 Suppl.), 142S–150S.

Peuravuori, H., Aho, V. V., Aho, H. J., Collan, Y., and Saari, K. M. (2005). Bactericidal/permeability-increasing protein in lacrimal gland and in tears of healthy subjects. *Graefes Arch. Clin. Exp. Ophthalmol.* **26,** 1–6.

Pflugfelder, S. C., and Stern, M. E. (2005). Dry eye: Inflammation of the lacrimal functional unit. *In* "Uveitis and Immunological Disorders" (G. K. Kriegelstein and R. N. Weinreb, Eds.), pp. 11–22. Springer, Berlin.

Pflugfelder, S. C., Liu, Z., Monroy, D., Li, D.-Q., Carvajal, M., Price-Schiavi, S. A., Idris, N., Solomon, A., Perez, A., and Carraway, K. L. (2000). Detection of sialomucin complex (MUC4) in human ocular surface epithelium and tear fluid. *Invest. Ophthalmol. Vis. Sci.* **41,** 1316–1326.

Pflugfelder, S. C., Stern, M. E., and Beuermann, R. W. (2004). Dysfunction of the integrated functional unit and its impact on tear film stability and composition. *In* "Dry Eye and the Ocular Surface—a United Approach" (S. C. Pflugfelder, M. E. Stern, and R. W. Beuermann, Eds.), pp. 63–88. Marcel Dekker, New York.

Podolsky, D. K., Fournier, D. A., and Lynch, K. E. (1986). Human colonic goblet cells. Demonstration of distinct subpopulations defined by mucin-specific monoclonal antibodies. *J. Clin. Invest.* **77,** 1263–1271.

Porchert, N., van Cong, N., Duffosse, J., Audie, J. P., Guyonnet-Duperat, V., Gross, M. S., Denis, C., Degand, P., Bernheim, A., and Aubert, J. P. (1991). Molecular cloning and chromosomal localization of a novel human tracheo-bronchial mucin cDNA containing tandemly repeated sequences of 48 base pairs. *Biochem. Biophys. Res. Commun.* **175,** 414–422.

Prakobphol, A., Tangemann, K., Rosen, S. D., Hoover, C. I., Leffler, H., and Fischer, S. J. (1999). Separate oligosaccharide determinants mediate interactions of the low-molecular-weight salivary mucin with neutrophils and bacteria. *Biochemistry* **38,** 6817–6825.

Pratt, W. S., Crawley, S., Hicks, J., Ho, J., Nash, M., Kim, Y. S., Gum, J. R., and Swallow, D. M. (2000). Multiple transcripts of MUC3: Evidence for two genes, MUC3A and MUC3B. *Biochem. Biophys. Res. Commun.* **275,** 916–923.

Radnot, M. (1977). Die Flimmerhaare des Tränensackepithels. *Klin. Monatsbl. Augenheilkd.* **170,** 428–432.

Radnot, M., and Bölcs, S. (1971). Fine structure of the epithelial cell surfaces in the lacrimal sac. *Klin. Monatsbl. Augenheilkd.* **159,** 158–164.

Ren, J., Li, Y., and Kufe, D. (2002). Protein kinase C delta regulates function of the DF3/MUC1 carcinoma antigen in beta-catenin signaling. *J. Biol. Chem.* **277,** 17616–17622.

Reuter, G., Schauer, R., and Bumm, P. (1988). Sialic acids of human nasal mucin, possible targets of influenza C viruses. *In* "Sialic Acids" (R. Schauer and T. Yamakawa, Eds.), Proceedings of the Japanese-German Symposium on Sialic Acids, pp. 259–260. Berbel-Mendel, Kiel.

Reuter, G., Struwe, R., Feige, J., Brede, R., Bumm, P., and Schauer, R. (1992). Analysis of carbohydrate composition and sialidase activity in oral secretions of patients with tumors in the upper aerodigestive tract. *Eur. Arch. Otorhinolaryngol.* **249,** 5–11.

Rivas, L., Rodriguez, J. J., and Murube, J. (1991). Glandulas seosas en el saco lagrimal. *Arch. Soc. Esp. Oftal.* **60,** 173–176.

Rossi, E. A., McNeer, R. R., Price-Schiavi, S. A., Van den Brand, J. M. H., Komatsu, M., Thompson, J. F., Carraway, C. A., Fregien, N. L., and Carraway, K. L. (1996). Sialomucin complex, a heterodimeric glycoprotein complex. *J. Biol. Chem.* **271,** 33476–33485.

Sack, R. A., Tan, K. O., and Tan, A. (1992). Diurnal tear cycle: Evidence for a nocturnal inflammatory constitutive tear fluid. *Invest. Ophthalmol. Vis. Sci.* **33,** 626–640.

Sack, R. A., Beaton, A., Sathe, S., Morris, C., Willcox, M., and Bogart, B. (2000). Towards a closed eye model of the pre-ocular tear layer. *Prog. Retin. Eye Res.* **19,** 649–668.

Sack, R. A., Conradi, L., Krumholz, D., Beaton, A., Sathe, S., and Morris, C. (2005). Membrane array characterization of 80 chemokines, cytokines, and growth factors in open- and closed-eye tears: Angiogenin and other defense system constituents. *Invest. Ophthalmol. Vis. Sci.* **45,** 1228–1238.

Sakata, M., Sack, R. A., Sathe, S., Holden, B., and Beaton, A. R. (1997). Polymorphonuclear leukocyte cells and elastase in tears. *Curr. Eye Res.* **16,** 810–819.

Schäfer, G., Hoffmann, W., Berry, M., and Paulsen, F. (2005). Altersabhängige Produktion Tränendrüsen-assoziierte Muzine—Rolle in der Pathophysiologie des Trockenen Auges. *Ophthalmologe* **102,** 175–183.

Schauer, R. (1992). Sialinsäurereiche Schleime als bioaktive Schmierstoffe. *Nachr. Chem. Tech. Lab.* **40,** 1227–1231.

Schauer, R. (1997). Enzyme als Werkzeuge für die Analyse der Struktur und Funktion von sialylierten Glykokonjugaten. *BIO-forum.* **20,** 541–544.

Schaumberg, D. A., Sullivan, D. A., and Dana, M. R. (2002). Epidemiology of dry eye syndrome. *Adv. Exp. Med. Biol.* **506,** 989–998.

Schaumberg, D. A., Sullivan, D. A., Buring, J. E., and Dana, M. R. (2003). Prevalence of dry eye syndrome among US women. *Am. J. Ophthalmol.* **136,** 318–326.

Schein, O. D., Hochberg, M. C., Munoz, B., Tielsch, J. M., Bandee-Roche, K., Provost, T., Anhalt, G. J., and West, S. (1999). Dry eye and dry mouth in the elderly: A population-based assessment. *Arch. Intern. Med.* **159,** 1359–1363.

Seifert, P., and Spitznas, M. (1994). Demonstration of nerve fibres in human accessory lacrimal glands. *Graefes Arch. Clin. Exp. Ophthalmol.* **232,** 107–114.

Seifert, P., Spitznas, M., Koch, F., and Cusumano, A. (1993). The architecture of human accessory lacrimal glands. *Ger. J. Ophthalmol.* **2,** 444–454.

Seifert, P., Spitznas, M., Koch, F., and Cusumano, A. (1994a). Light and electron microscopic morphology of accessory lacrimal glands. *In* "Lacrimal Gland, Tear Film, and Dry Eye Syndromes: Basic Science and Clinical Relevance" (D. A. Sullivan, Ed.), pp. 19–23. Plenum Press, New York.

Seifert, P., Stuppi, S., Spitznas, M., and Weihe, E. (1996). Differential distribution of neuronal markers and neuropeptides in the human lacrimal gland. *Graefe's Arch. Clin. Exp. Ophthalmol.* **234,** 232–240.

Seifert, P., Stuppi, S., and Spitznas, M. (1997). Distribution pattern of nervous tissue and peptidergic nerve fibres in accessory lacrimal glands. *Curr. Eye Res.* **16,** 298–302.

Sellers, L. A., Allen, A., Morris, E. R., and Ross-Murphy, S. B. (1991). The rheology of pig small intestinal and colonic mucus: Weakening of gel structure by non-mucin components. *Biochim. Biophys. Acta* **1115,** 174–179.

Shankar, V., Gilmore, M. S., Elkins, R. C., and Sachdev, G. P. (1994). A novel human airway mucin cDNA encodes a protein with unique tandem-repeat organization. *Biochem. J.* **300,** 295–298.

Sharma, A. (1993). Energetics of corneal epithelial cell-ocular mucus-tear film interactions: Some surface-chemical pathways of corneal defense. *Biophys. Chem.* **47,** 87–99.

Sharma, P., Dudus, L., Nielsen, P. A., Clausen, H., Yankaskas, J. R., Hollingsworth, M. A., and Engelhardt, J. F. (1998). MUC5B and MUC7 are differentially expressed in mucous and serous cells of submucosal glands in human bronchial airways. *Am. J. Respir. Cell Mol. Biol.* **19,** 30–37.

Sheehan, J. K., Brazeau, C., Kutay, S., Pigeon, H., Kirkham, S., Howard, M., and Thornton, D. J. (2000). Physical characterization of the MUC5AC mucin: A highly oligometric glycoprotein whether isolated from cell culture or *in vivo* from respiratory mucous secretion. *Biochem. J.* **347**(Pt 1), 37–44.

Sheng, Z., Hull, S. R., and Carraway, K. L. (1990). Biosynthesis of the cell surface sialomucin complex of ascites 13762 rat mammary adenocarcinoma cells from a high molecular weight precursor. *J. Biol. Chem.* **265,** 8505–8510.

Shim, J. J., Dabbagh, K., Ueki, I. F., Dao-Pick, T., Burgel, P. R., Takeyama, K., Tam, D. C. W., and Nadel, J. A. (2001). IL-13 induces mucin production by stimulating epidermal growth factor receptors and by activating neutrophils. *Am. J. Physiol. Lung Cell Mol. Physiol.* **280,** L134–L140.

Sirigu, P., Maxia, C., Puxeddu, R., Zuca, I., Piras, F., and Perra, M. T. (2000). The presence of a local immune system in the upper blind and lower part of the human nasolacrimal duct. *Arch. Histol. Cytol.* **63,** 431–439.

Situ, H., and Bobek, L. (2000). *In vitro* assessment of antifungal therapeutic potential of salivary histatin-5, two variants of histatin 5, and salivary mucin (MUC7) domain 1. *Antimicrob. Agents Chemother.* **44,** 1485–1493.

Smirnova, M. G., Kiselev, S. L., Birchall, J. P., and Pearson, J. P. (2001). Up-regulation of mucin secretion in HT29-MTX cells by the pro-inflammatory cytokines tumor necrosis factor-alpha and interleukin-6. *Eur. Cytokine Netw.* **12,** 119–125.

Song, X. J., Li, D. Q., Farley, W., Luo, L. H., Heuckeroth, R. O., Milbrandt, J., and Pflugfelder, S. C. (2003). Neuturin-deficient mice develop dry eye and keratoconjunctivitis sicca. *Invest. Ophthalmol. Vis. Sci.* **44,** 4223–4229.

Spurr-Michaud, S., Argüeso, P., and Gipson, I. K. (2004). Detection of multiple mucin species in human tear film samples. *ARVO 2004*, p.162, No. 3883.

Steele, P. J., and Jumblatt, M. M. (2001). Identification of histatins 1 and 3 in normal human lacrimal glands. *Invest. Ophthalmol. Vis. Sci.* **42**(ARVO Suppl.), 263.

Stern, M. E., and Pflugfelder, S. C. (2004). Inflammation in dry eye. *Ocular Surf.* **2,** 124–130.

Stern, M. E., Beuermann, R. W., Fox, R. I., Gao, J., Mircheff, A. K., and Pflugfelder, S. C. (1998). The pathology of dry eye: The interaction between the ocular surface and lacrimal glands. *Cornea* **17,** 584–589.

Steven, P., Schäfer, G., Nolle, B., Hinz, M., Hoffmann, W., and Paulsen, F. (2004). Distribution of TFF peptides in corneal disease and pterygium. *Peptides* **25,** 819–825.

Sullivan, D. A. (2004). Tearful relationships? Sex, hormones, the lacrimal gland, and aqueous-deficient dry eye. *Ocular Surf.* **2,** 92–123.

Sullivan, D. A., Wickham, L. A., Rocha, E., Krenzer, K. L., Sullivan, B. D., Steagall, R., Cermak, J. M., Dana, M. R., Ullman, M. D., Sato, E. H., Gao, J., Rocha, F. J., Ono, M., Silveira, L. A., Lampert, R. W., Kelleher, R. S., Tolls, D. B., and Toda, I. (1999). Androgens and dry eye in Sjogren's syndrome. *Ann. NY Acad. Sci.* **876,** 312–324.

Swallow, D. M., Gendler, S., Griffiths, B., Corney, G., Taylor-Papadimitrou, J., and Bramwell, M. E. (1987). The human tumour-associated epithelial mucins are coded by an expressed hypervariable gene locus PUM. *Nature* **328,** 82–84.

Swan, J. S., Arango, M. E., Carothers-Carraway, C. A., and Carraway, K. L. (2002). An ErbB2-Muc4 complex in rat ocular surface epithelia. *Curr. Eye Res.* **24,** 397–402.

Tabak, L. A. (1995). In defense of the oral cavity: Structure, biosynthesis, and function of salivary mucins. *Annu. Rev. Physiol.* **57,** 547–564.

Takata, K., Matzusaki, T., and Tajika, Y. (2004). Aquaporins: Water channel proteins of the cell membrane. *Prog. Histochem. Cytochem.* **39,** 1–83.

Takeuchi, K., Yagawa, M., Ishinaga, H., Kishioka, C., Harada, T., and Majima, Y. (2003). Mucin gene expression in the effusions of otitis media with effusion. *Int. J. Pediatr. Otorhinolaryngol.* **67,** 53–58.

Tarjan, E., Denton, D. A., McKinley, M. J., Nelson, J. F., and Weisinger, R. S. (1984). What makes wild rabbits drink? *J. Physiol. (Paris)* **79,** 466–470.

Thakur, A., and Willcox, M. D. P. (1998). Chemotactic activity of tears and bacteria isolated during adverse responses. *Exp. Eye Res.* **66,** 129–137.

Thale, A., Paulsen, F., Rochels, R., and Tillmann, B. (1998). Functional anatomy of human efferent tear ducts—a new theory of tear outflow. *Graefe's Arch. Clin. Exp. Ophthalmol.* **236,** 674–678.

Thim, L., Madsen, F., and Poulsen, S. S. (2002). Effect of trefoil factors on the viscoelastic properties of mucus bels. *Eur. J. Clin. Invest.* **32,** 519–527.

Thomsson, K. A., Prakobphol, A., Leffler, H., Reddy, M. S., Levine, M. J., Fischer, S. J., and Hansson, G. C. (2002). The salivary mucin MG1 (MUC5B) carries a repertoire of unique oligosaccharides that is large and diverse. *Glycobiology* **12,** 1–14.

Tomasetto, C., Masson, R., Linaires, J. L., Wendling, C., Lefebvre, O., Chenard, M. P., and Rio, M. C. (2000). pS2/TFF1 interacts directly with the VWFC cysteine-rich domains of mucins. *Gastroenterology* **118,** 70–80.

Toribara, N. W., Robertson, A. M., Ho, S. B., Kuo, W. L., Gum, E., Siddiki, B., and Kim, Y. S. (1993). Human gastric mucin: Identification of a unique species by expression cloning. *J. Biol. Chem.* **268,** 5879–5885.

Tran, C. H., Routledge, C., Miller, F., and Hodson, S. A. (2003). Examination of murine tear film. *Invest. Ophthalmol Vis. Sci.* **44,** 3520–3525.

Tsuda, K. (1952). On the histology of ductulus lacrimalis in adult, especially on its innervation. *Tohoku J. Exp. Med.* **56,** 233–243.

Verdugo, P. (1991). Mucin exocytosis. *Am. Rev. Respir. Dis.* **144,** S33–S37.

Verdugo, P., Aitken, M., Langley, L., and Villalon, M. J. (1987a). Molecular mechanism of product storage and release in mucin secretion. II. The role of extracellular Ca^{++}. *Biorheology* **24,** 625–633.

Verdugo, P., Deyrup-Olsen, I., Aitken, M., Villalon, M., and Johnson, D. (1987b). Molecular mechanism of mucin secretion: I. The role of intragranular charge shielding. *J. Dent. Res.* **66,** 506–508.

Vinall, L. E., Hill, A. S., Pigny, P., Pratt, W. S., Toribara, N., Gum, J. R., Kim, Y. S., Porchet, N., Aubert, J.-P., and Swallow, D. M. (1998). Variable number tandem repeat polymorphism of the mucin genes located in the complex on 11p15.5. *Hum. Genet.* **102,** 357–366.

Walker, W. A. (1976). Host defense mechanisms in the gastrointestinal tract. *Pediatrics* **57,** 901–916.

Wang, J., Fonn, D., Simpson, T. L., and Jones, L. (2003). Precorneal and pre- and postlens tear film thickness measured indirectly with optical coherence tomography. *Invest. Ophthalmol. Vis. Sci.* **44,** 2524–2528.

Watanabe, H. (2002). Significance of mucin on the ocular surface. *Cornea* **21**(2 Suppl. 1), S17–S22.

Wei, G. X., and Bobek, L. A. (2004). *In vitro* synergic antifungal effect of MUC7 12-mer with histatin-5 12-mer or miconazole. *J. Antimicrob. Chemother.* **53,** 750–758.

Wei, G. X., and Bobek, L. A. (2005). Human salivary mucin MUC7 12-mer-L and 12-mer-D peptides: Antifungal activity in saliva, enhancement of activity with protease inhibitor cocktail or EDTA, and cytotoxicity to human cells. *Antimicrob. Agents Chemother.* **49,** 2336–2342.

Werncke, T. (1905). Ein Beitrag zur Anatomie des Tränensackes, speziell zur Frage der Tränensackdrüsen. *Klin. Monatsbl. Augenheilkd.* **43,** 191–205.

Wiggins, R., Hicks, S., Soothill, P. W., Millar, M. R., and Corfield, A. P. (2001). Mucinases and sialidases: Their role in the pathogenesis of sexually transmitted infections in the female genital tract. *Sex Transm. Inf.* **77,** 402–408.

Willcox, M. C. P., and Stapleton, F. (1996). Ocular bacteriology. *Med. Microbio. Rev.* **7,** 123–131.

Willcox, M. D., Morris, C. A., Thakur, A., Sack, R. A., Wickson, J., and Boey, W. (1997). Complement and complement regulatory proteins in human tears. *Invest. Ophthalmol. Vis. Sci.* **38,** 1–8.

Williams, S. J., McGuckin, M. A., Gotley, D. C., Eyre, H. J., Sutherland, G. R., and Antalis, T. M. (1999). Two novel mucin genes down-regulated in colorectal cancer identified by differential display. *Cancer Res.* **59,** 4083–4089.

Williams, S. J., Wreschner, D. H., Tran, M., Eyre, H. J., Sutherland, G. R., and McGuckin, M. A. (2001). Muc13, a novel human cell surface mucin expressed by epithelial and hemopoietic cells. *J. Biol. Chem.* **276,** 18327–18336.

Wolff, E. (1946). The muco-cutaneous junction of the lid margin and the distribution of the tear fluid. *Trans. Ophthalmol. Soc. UK* **66,** 291–308.

Wolfring, E.von (1872). Untersuchungen über die Drüsen der Bindehaut des Auges. *Centrbl. Med. Wiss.* **10,** 852–854.

Yamamoto, M., Bharti, A., Li, Y., and Kufe, D. (1997). Interaction of the DF3/MUC1 breast carcinoma-associated antigen and beta-catenin in cell adhesion. *J. Biol. Chem.* **272,** 12492–12494.

Yin, B. W., and Lloyd, K. O. (2001). Molecular cloning of the CA125 ovarian cancer antigen: Identification as a new mucin, MUC16. *J. Biol. Chem.* **276,** 27371–27375.

Yoon, J. H., Kim, K. S., Kim, H. U., Linton, J. A., and Lee, J. G. (1999). Effects of TNF-alpha and IL-1 beta on mucin, lysozyme, IL-6 and IL-8 in passage-2 normal human nasal epithelial cells. *Acta Otolaryngol.* **119,** 905–910.

Zegans, M. E., Shanks, R. M. Q., and O'Toole, G. A. (2005). Bacterial biofilms and ocular infections. *Ocular Surf.* **3,** 73–80.

Zhao, H., Jumblatt, J. E., Wood, T. O., and Jumblatt, M. M. (2001). Quantification of MUC5AC protein in human tears. *Cornea* **20,** 873–877.

This page intentionally left blank

INDEX

D

E

F

G

H

N

O

P

R

S

T

U

V

Z